MASARYKOVA UNIVERZITA
Přírodovědecká fakulta
Ústav experimentální biologie
Oddělení genetiky a molekulární biologie

Molekulární podstata nových terapeutických přístupů v léčbě solidních nádorů dětského věku

Habilitační práce

Obor: Molekulární biologie a genetika

RNDr. Jakub Neradil, Ph.D.

Brno 2017

PODĚKOVÁNÍ

Na tomto místě bych rád poděkoval prof. Renatě Veselské za možnost podílet se na práci a výzkumu v rámci Laboratoře nádorové biologie a za vytrvalý mentoring. Dr. Janu Škodovi patří mé díky za grafickou editaci této práce a všem ostatním členům laboratoře za vytvoření přátelského kolektivu. Prof. Jaroslavu Štěrbovi děkuji za příležitost nahlédnout do problematiky dětské onkologie z klinické stránky.

Tato práce by nevznikla bez podpory mé manželky Evy a celé rodiny.

OBSAH

SEZNAM ZKRATEK

ABC	ATP- vázající kazeta (ATP-binding cassette)
AICAR	5-aminoimidazol-4-karboxamidribonukleosid
ALDH	aldehyddehydrogenáza
ALK	kináza anaplastického lymfomu (anaplastic lymphoma kinase)
APL	akutní promyelocytární leukémie
ATIC	AICAR transformyláza
ATRA	kyselina all-*trans*-retinová
BAA	BODIPY aminoacetát
BAAA	BODIPY aminoacetaldehyd
CD	cluster of differentiation
CFU	colony-forming unit
COX	cyklooxygenáza
CRABP	buněčný protein vázající kyselinu retinovou (cellular retinoic acid-binding protein)
CRBP	buněčný protein vázající retinol (cellular retinol-binding protein)
CSCs	nádorové kmenové buňky (cancer stem cells)
DHFR	dihydrofolátreduktáza
DR	přímá repetice (direct repeat)
dTMP	deoxythymidinmonofosfát
dTTP	deoxythymidintrifosfát
dUMP	deoxyuridinmonofosfát
dUTP	deoxyuridintrifosfát
EGFR	receptor pro epidermalní růstový faktor (epidermal growth factor receptor)
ErbB	erythroblastic leukemia viral oncogene homolog
ERK1/2	extracelulárním signálem aktivovaná kináza (extracellular signal-regulated kinase)
FAK	kináza kokální adheze (focal adhesion kinase)

FFPE	formalínem fixované do parafínu zalité (formalin-fixed paraffin embedded)
FGF	fibroblastový růstový faktor (fibroblast growth factor)
FGFR	receptor pro fibroblastový růstový faktor (fibroblast growth factor receptor)
GAR	glycinamidribonukleotid
GART	GAR transformyláza
GSH	redukovaná forma glutationu
GSK3	glykogen syntáza kináza (glycogen synthase kinase-3)
GSSG	oxidovaný dimer glutationu
HDACi	inhibitor histondeacetyláz
HD-MTX	vysokodávkový MTX (high-dose MTX)
IGF	inzulinu podobný růstový faktor (insulin like growth factor)
IGFBP-3	protein vázající inzulinu podobný růstový faktor 3 (insulin like growth factor binding protein 3)
IGF-IR	receptor pro inzulinu podobný růstový faktor 1 (insulin like growth factor 1 receptor)
JNK	c-Jun N-terminal kinase
LD-MTX	nízkodávkový MTX (low-dose MTX)
LOX	lipoxygenáza
MAPK	MAP kináza, mitogenem aktivovaná proteinkináza
MAPKK	MAP2 kináza
MAPKKK	MAP3 kináza
MAT	methionin S-adenosyltransferáza
Mdm2	mouse double minute 2
MDR1	protein mnoholékové rezistence 1 (multidrug resistence protein1)
mTOR	mammalian target of rapamycin
MTX	metotrexát
NADPH	nikotinamidadenindinukleotidfosfát
NBT	nitro blue tetrazolium
NCOA	koaktivátor jaderného receptoru (nuclear receptor coactivator)

NCOR	korepresor jaderného receptoru (nuclear receptor corepressor)
NOD/SCID	non-obese diabetic/severe combined immunodeficiency
NOG	NOD/ShiJic-scid/IL2Rγnull
NSG	NOD/ShiLtSz-scid/IL2Rγnull
PDAC	duktální karcinom pankreatu (pancreatic ductal adenocarcinoma)
PDGF	růstový faktor krevních destiček (platelet-derived growth factor)
PDGFR	receptor pro růstový faktor krevních destiček (platelet-derived growth factor receptor)
PDK	phosphoinositide-dependent kinase
Pgp	P-glykoprotein
PH	pleckstrin homology
PI3K	fosfatidylinositol-3 kináza
PIP_2	fosfatidylinositol (3,4)-bisfosfát
PIP_3	fosfatidylinositol (3,4,5)-trifosfát
PLCγ	fosfolipáza γ
PPARγ	receptor aktivovaný peroxizomovým proliferátorem γ (peroxisomal proliferator activated receptor)
PRC2	polycomb represivní komplex 2 (polycomb repressive complex 2)
PTEN	phosphatase and tensin homolog
RA	kyselina retinová
RAF	rapidly accelerated fibrosarcoma
RAR	receptor kyseliny retinové (retinoic acid receptor)
RARE	responzivní elementy kyseliny retinové (retinoic acid responsive elements)
RAS	rat sarcoma
RTK	receptorová tyrozinkináza
RXR	receptor retinoidu X (retinoid X receptor)
SAH	S-adenosylhomocystein
SAHA	kyselina suberoylanilid hydroxamová
SAM	S-adenosylmethionin

SH2	src-homology 2
SHH	Sonic Hedgehog
SP	vedlejší populace (side population)
STAT	signal transducer and activator of transcription
SÚKL	Státní ústav pro kontrolu léčiv
TGFα	transformující růstový faktor α (transforming growth factor α)
THF	tetrahydrofolát
TR	receptor pro tyroidní hormon
TS	thymidylátsyntáza
TSA	trichostatin A
VDR	receptor pro vitamin D
VEGFR	receptor pro vaskulární endotelový růstový faktor (vascular endothelial growth factor receptor)

1. ÚVOD

Tato práce a publikace s ní spojené vznikly v rámci výzkumných aktivit Laboratoře nádorové biologie (Laboratory of Tumor Biology, LTB), která je společným pracovištěm Ústavu experimentální biologie PřF MU a Kliniky dětské onkologie LF MU a FN Brno. Činnost naší laboratoře je zaměřena především na problematiku nádorů dětského věku, ale v průběhu minulých let jsme se zabývali i jinými typy nádorových onemocnění. Od roku 2015 zastřešuje naše aktivity na poli laboratorního translačního výzkumu Mezinárodní centrum klinického výzkumu (ICRC) Fakultní nemocnice u sv. Anny v Brně.

V rámci našeho výzkumu spolupracujeme i s dalšími partnerskými pracovišti, která se podílejí na řešení jednotlivých projektů. Jedním z nich je Regionální centrum aplikované a molekulární onkologie (RECAMO) Masarykova onkologického ústavu, s nímž se společně zabýváme mechanismy konvenční i kombinované protinádorové terapie. Další spolupracující institucí je I. patologicko-anatomický ústav Fakultní nemocnice u sv. Anny v Brně, kde se provádějí histologické a imunohistochemické analýzy vzorků nádorové tkáně, především v oblasti studia nádorových kmenových buněk. Na aplikovaném výzkumu při identifikaci terapeutických cílů u vysoce rizikových refrakterních solidních nádorů dětského věku spolupracujeme s výzkumnou skupinou Molekulární onkologie II - solidní nádory v rámci Středoevropského technologického institutu (CEITEC).

Naší snahou je řešit aktuální vědecké otázky a témata spojená s nádorovou biologií, která však mají úzkou vazbu na klinickou praxi. Cílem je odhalování a popis biologických vlastností především solidních nádorů dětského věku a zejména pochopení molekulárních a buněčných mechanismů vzniku a vývoje těchto nádorových onemocnění. Hlavním účelem získaných výsledků je pak jejich uplatnění při zpřesnění diagnózy či prognózy u jednotlivých pacientů, popřípadě využití těchto poznatků pro nalezení nejvhodnějšího způsobu léčby.

Předkládaná habilitační práce je zaměřena na čtyři konkrétní oblasti nádorové biologie, které přímo souvisí s protinádorovou terapií u dětských pacientů a pokrývají většinu výzkumného zaměření naší laboratoře. První část práce je věnována konvenční chemoterapii a konkrétně jednomu z nejdéle používaných chemoterapeutik – metotrexátu, u něhož jsou popsány vedle desítky let známého vlivu na folátový metabolismus i nově objevené účinky nezávislé na inhibici DHFR. Druhá část práce je zaměřena na mechanismy diferenciační terapie, konkrétně na využití kyseliny retinové a její kombinace s inhibitory metabolismu kyseliny arachidonové. Třetí část práce popisuje roli signálních drah receptorových

tyrozinkináz v nádorových buňkách a možnost aplikace nízkomolekulárních inhibitorů těchto drah v terapii. V poslední části práce jsou charakterizovány nádorové kmenové buňky z hlediska svého fenotypu a funkčních vlastností, dále je popsána jejich úloha v tumorigenezi a jejich význam jako možných cílů protinádorové léčby.

2. KONVENČNÍ CHEMOTERAPIE: METOTREXÁT A JEHO ÚČINKY

Historie konvenční chemoterapie

Počátek moderní éry konvenční protinádorové chemoterapie lze datovat do roku 1942, kdy byl poprvé využit dusíkatý yperit (angl. nitrogen mustard) k léčbě pacienta s non-Hodgkinovým lymfomem. Dusíkatý yperit je svou molekulární strukturou podobný yperitu, což je alkylační látka di-(2-chloroethylsulfid), která byla za I. světové války používána jako bojový plyn. Právě pitvy padlých vojáků přinesly poznatek, že zasažení trpěli vedle primárního zpuchýřujícího účinku také lymfoidní hypoplazií a vykazovali známky myelosuprese. K podobným závěrům dospěli lékaři vyšetřující v roce 1943 vojáky a civilní obyvatele zasažené dusíkatým yperitem v blízkosti italského přístavu Bari po výbuchu lodi John Harvey, která převážela náklad chemických zbraní. Po ověření protinádorových účinků na zvířecím modelu byl proto dusíkatý yperit aplikován pacientovi s non-Hodgkinovým lymfomem, což vedlo k několikatýdenní remisi. I když byl protinádorový efekt v tomto případě krátkodobý, použití dusíkatého yperitu znamenalo průlom v onkologické léčbě a otevřelo možnost systematického zavedení různých typů chemických látek do léčebných protokolů. Později bylo prokázáno, že konkrétně molekuly dusíkatého yperitu se kovalentně váží na DNA, především na purinové báze, a díky dvěma reaktivním alkylovým skupinám způsobují vytváření křížových vazeb mezi řetězci DNA, což ve svém důsledku vede ke spuštění procesu buněčné smrti (Chabner et Roberts 2005).

Dalším milníkem v protinádorové chemoterapii byla ve 40. letech 20. století syntéza a následná aplikace aminopterinu a amethopterinu (metotrexát) jakožto analogů kyseliny listové. Těchto antagonistů folátového metabolismu bylo využito k léčbě dětí s akutní lymfoblastickou leukémií, přičemž i tentokrát bylo výsledkem dosažení remise, i když opět krátkodobé. Metotrexát byl později použit také pro léčbu choriokarcinomu, což je vysoce zhoubný germinální tumor pocházející z buněk trofoblastu, a v tomto případě šlo o první lidský solidní nádor, který byl za použití chemoterapie úspěšně vyléčen (Bertino 2009).

V 50. a 60. letech 20. století se pozornost vědců studujících nové protinádorové léky zaměřila mimo jiné i na látky přírodního původu, z nichž nejvýznamnější a dosud klinicky používané jsou vinca alkaloidy a taxany, popřípadě jejich deriváty. Mezi nejznámější vinca alkaloidy patří vinblastin a vincristin; obě sloučeniny byly izolovány z barvínku lékařského (*Vinca rosea*) a jejich primárním účinkem je inhibice polymerace mikrotubulů a následně

zástava buněčného dělení. Naopak inhibici depolymerace mikrotubulů způsobují taxany, tj. alkaloidy derivované z tisu (*Taxus sp.*), jež se v současnosti vyrábějí polosynteticky (např. paclitaxel a docetaxel).

Rozmach vývoje nových protinádorových látek s sebou přinesl i zvýšené požadavky na toxikologické testování a klinické hodnocení nových chemoterapeutik. Postupně byly zavedeny standardizované metody *in vivo* pro stanovení cytotoxicity, byla prováděna analýza kinetiky nádorového růstu na zvířecích modelech včetně xenograftů solidních nádorů a začaly se používat první leukemické buněčné linie pro testování *in vitro*. Výsledky experimentů ukazovaly, že cytotoxicita nových sloučenin je přímo závislá na koncentraci, což otevřelo dveře tzv. vysokodávkové chemoterapii (angl. high-dose chemotherapy). Současně se rozvíjel i trend kombinované chemoterapie, která u pacientů zabraňovala vniku tzv. získané lékové rezistence.

Rozdělení chemoterapeutik v závislosti na mechanismu účinku

Podle typu molekulárního mechanismu, který indukuje cytotoxický účinek protinádorových chemoterapeutik, lze tyto látky rozdělit do několika hlavních skupin (dle Klener et Klener 2013):

- Antimetabolity – látky inhibující klíčové enzymy metabolismu DNA
  (např. metotrexát, merkaptopurin, fluoruracil, azacytidin, aj.)
- Genotoxická cytostatika – látky inhibující replikaci a transkripci
  (např. cyklofosfamid, temozolomid, cisplatina, doxorubicin, aj.)
- Zesilovače účinku genotoxických cytostatik – látky inhibující opravy DNA
  (např. bleomycin, irinotekan, etopozid, aj.)
- Antimitotika – látky inhibující průchod buněčného dělení
  (např. vinkristin, vinblastin, paklitaxel, aj.)
- Inhibitory proteosyntézy a degradace proteinů
  (např. L-asparagináza, bortezomib)
- Ostatní mechanismy účinku
  (např. syntetické alkylfosfolipidy)

V poslední době je však čím dál více zřejmé, že použití této klasické, resp. konvenční chemoterapie dosáhlo svého limitu. Je to především z toho důvodu, že konvenční cytostatika působí primárně na proliferující buňky, a to nespecificky. Proto při léčbě cytostatiky dochází také k poškození dělících se buněk zdravých tkání, jako jsou např. hematopoetické buňky kostní dřeně či epiteliální buňky trávicího traktu, což s sebou nese řadu závažných vedlejších účinků. Druhou významnou nevýhodou konvenční chemoterapie je fakt, že jejímu působení často unikají tzv. nádorové kmenové buňky (cancer stem cells; CSCs), mezi jejichž vlastnosti patří nízký proliferační index a exprese specifických membránových transportérů, které společně zaručují rezistenci k různým xenobiotikům včetně konvenčních cytostatik.

Metotrexát jako inhibitor biosyntézy nukleotidů: klasické využití v léčbě nádorů

I přes popsané nevýhody představují konvenční chemoterapeutika v léčbě nádorových onemocnění stále zásadní strategii. I nadále jsou proto studovány jejich účinky na různé typy nádorových buněk, kdy se vedle původního molekulárního cíle může objevit nový mechanismus působení, který rozšíří aplikační potenciál daného léku. Jedním z příkladů může být metotrexát (MTX), který je nejčastěji a nejdéle používaným antifolátem v protinádorové léčbě. MTX se využívá pro léčbu hematologických malignit, karcinomu prsu, kolorektálního karcinomu, nádorů hlavy a krku, lymfomu, osteogenních sarkomů nebo choriokarcinomu, ale také pro terapii některých nenádorových onemocnění, například lupénky či revmatoidní artritidy (Huang et al. 2005).

Primárním místem zásahu MTX v rámci folátového metabolismu je dihydrofolátreduktáza (DHFR), tedy klíčový enzym, který ve dvou krocích katalyzuje redukci folátu na tetrahydrofolát (THF). THF je dále metabolizován a účastní se významných buněčných metabolických procesů: hladina folátových metabolitů v buňce zásadně ovlivňuje syntézu purinů a pyrimidinů (především thymidinu), ale také přeměnu homocysteinu na metionin, který slouží jako výchozí molekula pro metylaci DNA a proteinů (Obr. 1).

Nedostatečné množství 5,10-methylen-THF, které je způsobeno inhibicí DHFR, vede ke snížení možnosti syntézy pyrimidinových prekurzorů, protože thymidylátsyntáza (TS) nemůže bez tohoto folátového metabolitu katalyzovat metylaci dUMP na dTMP. Navíc TS je přímo blokována MTX a nemetabolizovaným dihydrofolátem (Genestier et al. 2000). Podobně je také blokována syntéza purinových prekurzorů, a to opět přímo nemetabolizovaným dihydrofolátem nebo nepřímo nedostatkem folátového kofaktoru

10-formyl-THF. MTX navíc inhibuje aktivitu dvou klíčových enzymů nutných pro syntézu purinových prekurzorů, kterými jsou AICAR transformyláza (Chan et Cronstein 2013) a GAR transformyláza (Baggott et al. 1994).

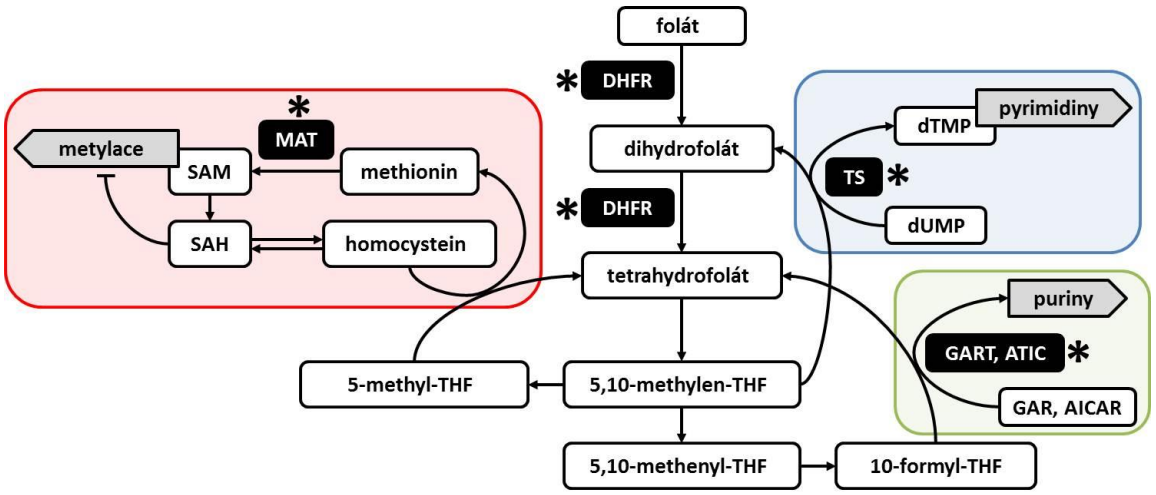

Obr. 1. Folátový metabolismus. Schematické znázornění tří metabolických drah využívajících folátové metabolity: metylace biomolekul (červený rámeček), syntéza thymidylátu (modrý rámeček) a syntéza purinů (zelený rámeček). Místa účinku MTX označena hvězdičkou. Zkratky použité v obrázku: AICAR – 5-aminoimidazol-4-karboxamidribonukleosid; ATIC – AICAR transformyláza; DHFR – dihydrofolátreduktáza; GAR – glycinamidribonukleotid; GART – GAR transformyláza; MAT – methionin S-adenosyltransferáza; SAM – S-adenosylmethionin; SAH – S-adenosylhomocystein; THF – tetrahydrofolát; TS – thymidylátsyntáza. Převzato a upraveno z Neradil et al. 2012.

Následkem deplece purinových a pyrimidinových prekurzorů je nejčastěji indukce buněčné smrti v důsledku nesprávného začleňování dUTP místo dTTP v nově syntetizovaných molekulách DNA během S-fáze buněčného cyklu. Následné mechanismy excizní reparace nemohou bez dostatku dTTP správně probíhat, což vede ke spuštění apoptózy (Webley et al. 2001).

Ačkoliv je MTX součástí mnoha léčebných protokolů pro různé typy nádorových onemocnění, jeho toxicita pro buňky normálních tkání je limitující, obzvláště v rámci dětské onkologie, kde se často setkáváme s nežádoucími pozdními následky protinádorové léčby. Cytotoxický efekt vysokodávkového MTX (high-dose MTX; HD-MTX) na normální buňky je možné redukovat použitím antidota leukovorinu. Leukovorin je transportován do buněk stejnými mechanismy jako MTX. U nádorových buněk však mohou být mechanismy transportu pro foláty (leukovorin) i antifolika (MTX) porušené, a proto do těchto buněk

proniká MTX až při vysokých koncentracích difuzí, zatímco koncentrace leukovorinu není pro průnik dostatečná. Do normálních buněk s neporušenými transportními mechanismy leukovorin vstupuje i při poměrně nízké extracelulární koncentraci a potlačuje účinek MTX. V případě aplikace chemoterapie s použitím HD-MTX je však na místě obava ze získání rezistence, která může léčebný efekt MTX snížit (Wang et Li 2014). V současnosti standardní protokoly protinádorové léčby pomocí MTX obsahují aplikaci HD-MTX (tj. dávky vyšší než 1 g/m^2 povrchu těla) v kombinaci s leukovorinem, který je podáván vždy se zpožděním 24–48 hodin (Holmboe et al. 2012, Cohen et Wolff 2014) Jinou možností je opakované podávání nízkodávkového MTX (low-dose MTX; LD-MTX) bez leukovorinu (Sterba et al. 2006).

V rámci našich experimentů jsme analyzovali účinky MTX na buněčné linie derivované z osteosarkomu a meduloblastomu za použití koncentrací MTX, kterých je možné dosáhnout v plazmě pacientů léčených LD-MTX i HD-MTX. Výsledky ukázaly, že MTX výrazně snižuje proliferační aktivitu buněk, zastavuje buněčný cyklus v S-fázi a indukuje apoptózu u referenčních sbírkových linií Saos-2 a Daoy. U obou těchto senzitivních linií jsme zaznamenali stejný efekt MTX v rozmezí koncentrací 1–40 μM. Tyto experimenty ukázaly, že srovnatelného účinku může být u senzitivních buněk dosaženo řádově nižšími koncentracemi MTX, než odpovídá plazmatickým koncentracím při aplikaci HD-MTX. Při zařazení leukovorinu aplikovaného 42 hodin po MTX jsme nezaznamenali žádný efekt vzhledem k účinku MTX ve stejném rozmezí koncentrací, tedy 1–40 μM. Naproti tomu tzv. pacientské linie – a to jak osteosarkomové, tak meduloblastomové – které byly derivovány na našem pracovišti ze vzorků nádorové tkáně po provedení diagnostické biopsie, vykazovaly nižší proliferační potenciál a současně výraznou rezistenci k MTX: při maximální použité koncentraci 100 μM MTX nebylo dosaženo ani hodnot IC_{50} (Neradil et al. 2015, Sramek et al. 2016).

Vedle cytostatického, popřípadě cytotoxického účinku MTX byl však nově popsán i efekt diferenciační, a to na několika různých modelech včetně myších i lidských embryonálních kmenových buněk. Mechanismus tohoto účinku není zcela objasněn, ale opět se předpokládá, že vlastním induktorem diferenciace by mohl být nedostatek prekurzorů nukleotidů (Neradil et al. 2012, Sramek et al. 2017). Výsledky našeho výzkumu na osteosarkomových liniích potvrdily schopnost MTX měnit expresi genů, které jsou spojeny s diferenciací: především se jednalo o geny, jejichž produkty jsou zapojeny do metabolismu retinoidů (Sramek et al. 2016).

Metotrexát jako inhibitor metylace biomolekul

Dalším z důležitých folátových metabolitů je 5-metyl THF, který je donorem metylové skupiny a podílí se na endogenní syntéze metioninu z homocysteinu. V následujícím kroku metylační dráhy metionin reaguje s ATP za vzniku S-adenosylmetioninu (SAM), který je výchozí molekulou pro metylaci proteinů (včetně histonů), cytosinových bází na DNA (CpG ostrovy), neurotransmiterů, fosfolipidů a dalších malých molekul (Stover 2009). Vedle nepřímé inhibice folátových metabolitů MTX blokuje také enzym methionin S-adenosyltranferázu (Wang et Chiang 2012), která je nezbytná pro katalýzu syntézy SAM a tím ovlivňuje celý metylační proces.

Příkladem demetylačního účinku MTX může být např. jeho působení na buňky kožního T-buněčného lymfomu, jež mají vysoce metylovaný promotor genu kódujícího receptor Fas. V těchto buňkách MTX snížil metylaci CpG ostrovů v promotoru genu *Fas*, což vedlo k zesílené expresi proteinu a zvýšené senzitivitě vůči apoptóze spouštěné touto signální dráhou (Wu et Wood. 2011). Podobně jsme v našich experimentech detekovali pokles celkové metylace DNA v buňkách osteosarkomových linií po aplikaci MTX. Především po aplikaci 40 μM MTX byl zaznamenán pokles metylace až o 25 % vůči kontrolním buňkám, přičemž tento účinek se vyrovnal výsledku působení 5-aza-2′-deoxycytidinu, který se používá v léčbě některých hematoonkologických malignit jako hypometylační agens (Sramek et al. 2016).

Obecně lze snížení metylace DNA po aplikaci MTX očekávat u rychle proliferujících buněk, například ve fyziologických procesech hematopoézy či obnovy epitelů, ale také u buněk transformovaných. Při nedostatečné intracelulární zásobě metylových donorů vzniknou v DNA po mitotickém dělení hemimetylovaná místa a v následném buněčném cyklu již budou chybět metylové templáty na obou řetězcích DNA dceřiných buněk. Tento proces může vést ke ztrátě metylačních vzorců v DNA a následně ke změně genové exprese (Salbaum et Kappen 2012).

Z výše uvedených důvodů lze o MTX uvažovat jako o metylačním inhibitoru, který by mohl mít uplatnění při léčbě nádorových onemocnění vykazujících specifickou metylaci DNA. Hypermetylované CpG ostrovy v oblasti genů (a/nebo jejich promotorů), které regulují vývoj tkání, diferenciaci a tumorigenezi, byly popsány například u rabdomyosarkomu (Mahoney et al. 2012), meduloblastomu (Diede et al. 2010), různých typů gliomů (Rostrepo et al. 2011, Hill et al. 2011) a dalších nádorových onemocnění (Esteller 2002).

Metotrexát jako inhibitor histondeacetyláz

Na základě podobnosti struktury MTX (Obr. 2a) a funkčních skupin některých inhibitorů histondeacetyláz (HDACi) bylo predikováno, že by MTX mohl mít i schopnost inhibovat HDAC (Yang et al. 2010). Některé ze známých HDACi, například trichostatin A (TSA, Obr. 2d) nebo kyselina suberoylanilid hydroxamová (SAHA, Obr. 2c), obsahují ve své molekule hydrofobní skupinu (benzyl) připojenou krátkým alifatickým řetězcem k funkční skupině (hydroxamová kyselina). Ta působí jako chelátor zinkových iontů v aktivním místě zinek-dependentních HDAC (Xu et al. 2007, Marks et Xu 2009). Oproti tomu molekula butyrátu sodného (Obr. 2b), nejmenšího HDACi, se skládá z tříuhlíkatého řetězce navazujícího na karboxylovou skupinu.

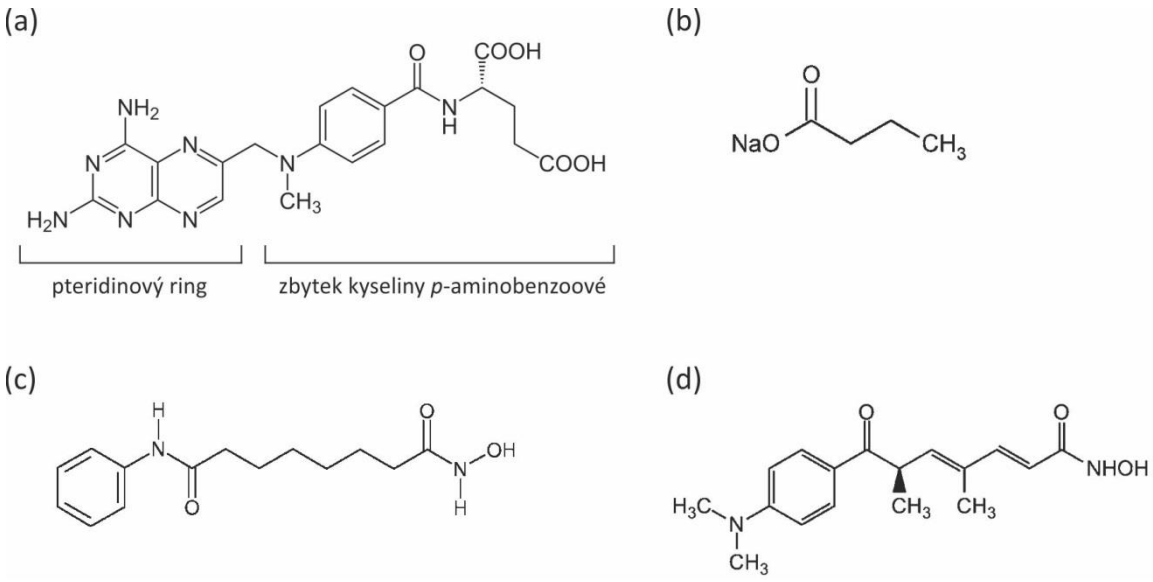

Obr. 2. Srovnání struktury MTX a dalších inhibitorů histondeacetyláz. (a) metotrexát, (b) butyrát sodný, (c) kyselina suberoylanilid hydroxamová, (d) trichostatin A.

V molekule MTX je hydrofobní skupinou pteridinový ring, přičemž zbytek kyseliny *para*-aminobenzoové je strukturně podobný TSA i SAHA a navíc na konci molekuly obsahuje zbytek butyrátu. Metodou počítačového modelování byla prokázána schopnost vazby MTX na homolog HDAC (tzv. HDAC-like protein) do jeho cílového místa a interakce s iontem zinku i okolními strukturami proteinu. Inhibice HDAC byla poté ověřena v podmínkách *in vitro* na buněčných liniích derivovaných z karcinomu plic, karcinomu děložního čípku či karcinomu žaludku, přičemž docházelo k nárůstu acetylace histonu H3

(Yang et al. 2010). Také v rámci našich experimentů jsme prokázali zvýšení celkové acetylace histonu H3 po aplikaci MTX u osteosarkomové pacientské linie OSA-06. Výsledný efekt byl srovnatelný s účinky butyrátu sodného a valproátu sodného, tedy dvou známých HDACi, které v experimentech sloužily jako pozitivní kontrola (Sramek et al. 2016)

Vedle acetylace histonu H3 byla u buněk linie karcinomu plic A549 prokázána schopnost MTX indukovat acetylaci proteinu p53 v místě zbytků aminokyselin Lys373/382 (Huang et al. 2011). Tato posttranslační změna však nebyla zaznamenána v případě aplikace jiných HDACi. Současně s acetylací p53 indukoval MTX i fosforylaci v místě Ser15. MTX těmito změnami navozoval akumulaci a větší stabilitu proteinu p53, protože acetylovaná místa slouží také pro ubikvitinaci, která vede k degradaci proteinu proteasomovým systémem.

Inhibiční aktivita MTX vůči HDAC se projevila snížením exprese metyltransferázy EZH2, což je klíčový enzym, který zprostředkovává umlčení tumor supresorových genů pomocí metylace histonu H3 (Chang et Hung 2012). Epigenetické potlačení exprese EZH2 vlivem MTX vedlo k zesílení exprese E-kadherinu, který se podílí na snížení buněčné migrace a omezuje možnost transformace epiteliálních buněk (Huang et al. 2011).

Přestože aplikace HDACi patří mezi nadějné strategie, jak čelit epigenetickým změnám spojených s tumorigenezí (Bolden et al. 2006, Dell´Aversana et al. 2012), jejich kombinace s MTX vykazuje rozdílné účinky v závislosti na zvoleném inhibitoru. Například u buněčných linií derivovaných z akutní lymfoblastické leukémie se jako vhodné HDACi pro kombinaci s MTX jeví SAHA a butyrát sodný. Tyto inhibitory zvyšují cytotoxicitu MTX a indukci apoptózy modulací exprese enzymů zapojených do folátového metabolismu. Jedním z nich je folylpoly-γ-glutamát syntetáza (Leclerc et al. 2010), která připojuje glutamátové zbytky k MTX, čímž je zabráněno jeho vyloučení z buňky a tím navozeno prodloužení účinnosti (Assaraf 2007). V případě kombinace HDACi a MTX se však klíčovým problémem jeví sekvence podávání těchto látek, neboť výsledný efekt na buněčné úrovni může být opačný v případě obráceného pořadí jejich aplikace (Einsiedel et al. 2006, Bastian et al. 2011). Jak bylo prokázáno na myších liniích derivovaných z karcinomu choroidního plexu, některé z HDACi – např. valproát nebo MS275 – mohou dokonce zvyšovat rezistenci buněk k MTX, a to zvýšením exprese thymidylátsyntázy (Prasad et al. 2009).

Metotrexát jako inhibitor glyoxalázového systému

Dalším místem působení MTX v buněčném metabolismu je glyoxalázový systém (Obr. 3). V této třístupňové metabolické dráze dochází v cytoplazmě k odbourávání

metylglyoxalu jako vedlejšího produktu peroxidace lipidů a glykolýzy na D-laktát. Glyoxalázový systém zahrnuje dva enzymy – glyoxalázu 1 a glyoxalázu 2 – a katalytické množství redukovaného glutationu (Thornalley et Rabbani 2011).

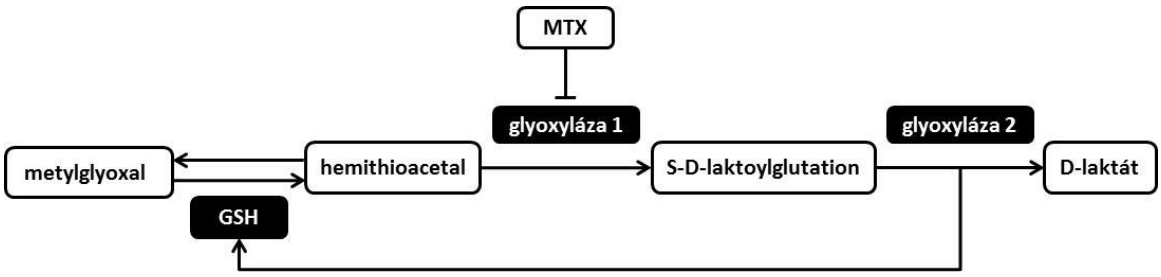

Obr. 3. Schéma glyoxalázového cyklu. MTX inhibicí glyoxalázy 1 blokuje metabolickou přeměnu metylglyoxalu na D-latát za vzniku glutationu. Převzato a upraveno z Bartyik et al. (2004).

Zvýšení aktivity nebo exprese glyoxalázy 1 bylo popsáno jako marker řady nádorových onemocnění. Tyto změny byly asociovány se zvýšenou invazivitou nádorů, metastázováním a rezistencí k chemoterapeutikům (Thornalley et Rabbani 2011). Navíc u některých typů primárních tumorů byla identifikována amplifikace genu kódující glyoxalázu 1 (Santarius et al. 2010).

Bartyik et al. (2004) prokázali *in vitro*, že MTX inhibuje glyoxalázu 1, a to jak na modelu lyzátu z lidských erytrocytů, tak s použitím glyoxalázy 1 izolované z kvasinek. V případě léčby pomocí MTX se u pacientů s akutní lymfoblastickou leukémií jeho inhibiční účinky na glyoxalázový systém projevily snížením koncentrace laktátu v plazmě. Současně inhibice glyoxalázy 1 vede na buněčné úrovni ke zvýšení intracelulární koncentrace metylglyoxalu, který následně způsobuje glykaci biomolekul (Suji et Sivakami 2007, Pepper et al. 2010), produkci reaktivních kyslíkových radikálů či genotoxicitu (Kalapos 2008, Koizumi et al. 2011), což může vést k zesílení protinádorové aktivity MTX. Glyoxalázový systém, konkrétně glyoxaláza1, tedy představuje další terč protinádorového působení MTX a tím rozšiřuje spektrum jeho účinků.

Metotrexát jako induktor oxidativního stresu

Jak bylo prokázáno v několika studiích, součástí cytotoxického působení MTX je rovněž indukce oxidativního stresu (Uzar et al. 2006, Miketova et al. 2005, Jahovic et al. 2003). MTX je schopen inhibovat některé z NAD(P)H-dependentních dehydrogenáz, jako

jsou např. 2-oxoglutarátdehydrogenáza, isocitrátdehydrogenáza, malátdehydrogenáza a pyruvátdehydrogenáza (Caetano et al. 1997), inhibice těchto enzymů následně může vést ke snížení dostupnosti NADPH (nikotinamidadenindinukleotidfosfát) v buňkách. NADPH slouží jako donor elektronu pro redukci oxidovaného dimeru glutationu (GSSG) na redukovanou formu (GSH). GSH je významným antioxidantem podílejícím se na komplexním antioxidačním systému organismu, přičemž efektivita tohoto systému může být po aplikaci MTX snížena právě z důvodu poklesu hladiny GSH (Babiak et al. 1998). Vardi et al. (2012) prokázali, že na tkáňové úrovni, konkrétně v krysím mozečku, byl po aplikaci MTX zaznamenán kromě poklesu koncentrace GSH také pokles aktivity superoxiddismutázy a katalázy. Na buněčné úrovni byla popsána tvorba reaktivních kyslíkových radikálů vlivem MTX u buněk leukemických linií a v mononukleárních buňkách periferní krve. Zvýšená hladina těchto radikálů vedla k aktivaci JNK kinázy, zesílení exprese pro-apoptotických genů a indukci apoptózy mitochondriální dráhou (Huang et al. 2005, Spurlock et al. 2011).

Vlastní publikace vztahující se k tématu

- Sramek M, **Neradil J**, Veselska R. Much more than you expected: The non-DHFR-mediated effects of methotrexate. Biochimica et Biophysica Acta 1861: 499-503, 2017.
- Sramek M, **Neradil J**, Sterba J, Veselska R. Non-DHFR-mediated effects of methotrexate in osteosarcoma cell lines: epigenetic alterations and enhanced cell differentiation. Cancer Cell International 16: 14, 2016.
- **Neradil J,** Pavlasova G, Sramek M, Kyr M, Veselska R, Sterba J. DHFR-mediated effects of methotrexate in medulloblastoma and osteosarcoma cells: the same outcome of treatment with different doses in sensitive cell lines. Oncology Reports 33: 2169-2175, 2015.
- **Neradil J,** Pavlasova G, Veselska R. New mechanisms for an old drug; DHFR- and non-DHFR-mediated effects of methotrexate in cancer cells. Klinicka Onkologie 25 (Suppl 2): 2S87-92, 2012.

3. DIFERENCIAČNÍ TERAPIE

Předchozí kapitoly byly věnovány konvenčním chemoterapeutikům, jejichž účinek je především cytotoxický a je cílen na rychle proliferující buňky nádorové masy. Od 70. let 20. století se ale v léčbě solidních nádorů i hematologických malignit začínají prosazovat nové přístupy založené na indukované diferenciaci nádorových buněk, které – už ze své podstaty – nejsou terminálně diferencované. Podstatou diferenciační terapie je reaktivace endogenního diferenciačního programu nádorových buněk s následnou maturací a ztrátou nádorového fenotypu (Cruz et Matushansky 2012). Jako induktory buněčné diferenciace se při této léčbě nejčastěji využívají retinoidy (deriváty vitamínu A), deltanoidy (deriváty vitamínu D) a antagonisté PPARγ (peroxisome proliferator-activated receptor γ). Objevují se však i nové přístupy založené na regulaci transkripce za využití specifických transkripčních faktorů, dále na regulaci epigenetických změn či na cílené diferenciaci nádorových kmenových buněk.

Retinoidy a jejich molekulární účinky

Retinoidy představují skupinu přírodních a syntetických derivátů vitamínu A (all-*trans*-retinol), které regulují významné buněčné procesy: v rámci embryonálního vývoje zastávají funkci morfogenů a diferenciačních agens, postnatálně jsou potřebné pro vidění, růst, imunitní funkce, reprodukci a regulaci homeostázy v různých tkáních (Alizadeh et al. 2014, Cunningham et Duester 2015). Přirozené zdroje prekursorů vitamínu A jsou dvojí - v potravě živočišného původu (např. vejce, maso, ryby, aj.) jsou obsaženy retinyl estery, v ovoci a zelenině se pak nachází provitamín A ve formě karotenů a kryptoxantinu. Retinol je v organismu metabolizován retinoldehydrogenázou na all-*trans*-retinaldehyd a ten následně retinaldehyddehydrogenázou na kyselinu all-*trans*-retinovou (ATRA) (di Masi et al. 2015). ATRA je tedy typickým zástupcem přírodních retinoidů, stejně jako její neenzymaticky konvertované izoformy: 9-*cis*-retinová kyselina a 13-*cis*-retinová kyselina (Obr. 4).

Z chemického hlediska jsou retinoidy definovány jako skupina chemických sloučenin, obsahujících čtyři lineárně navazující izoprenoidové podjednotky. V rámci každé molekuly lze rozlišit hydrofobní část, centrální spojovací část tvořenou nenasyceným uhlovodíkovým řetězcem a polární oblast, nejčastěji v podobě karboxylové skupiny. Syntetické retinoidy jsou primárně vytvářeny modifikací hydrofobní a centrální části molekuly, což jim dodává zvýšenou stabilitu (di Masi et al. 2015). U některých retinoidů se centrální část podílí na

tvorbě dalších cyklických struktur, které přispívají k nižší konformační flexibilitě zvyšující schopnost vazby na retinoidové receptory. Vedle toho mohou být součástí cyklických struktur heteroatomy, které významně snižují toxicitu syntetických retinoidů (Benbrook 2002).

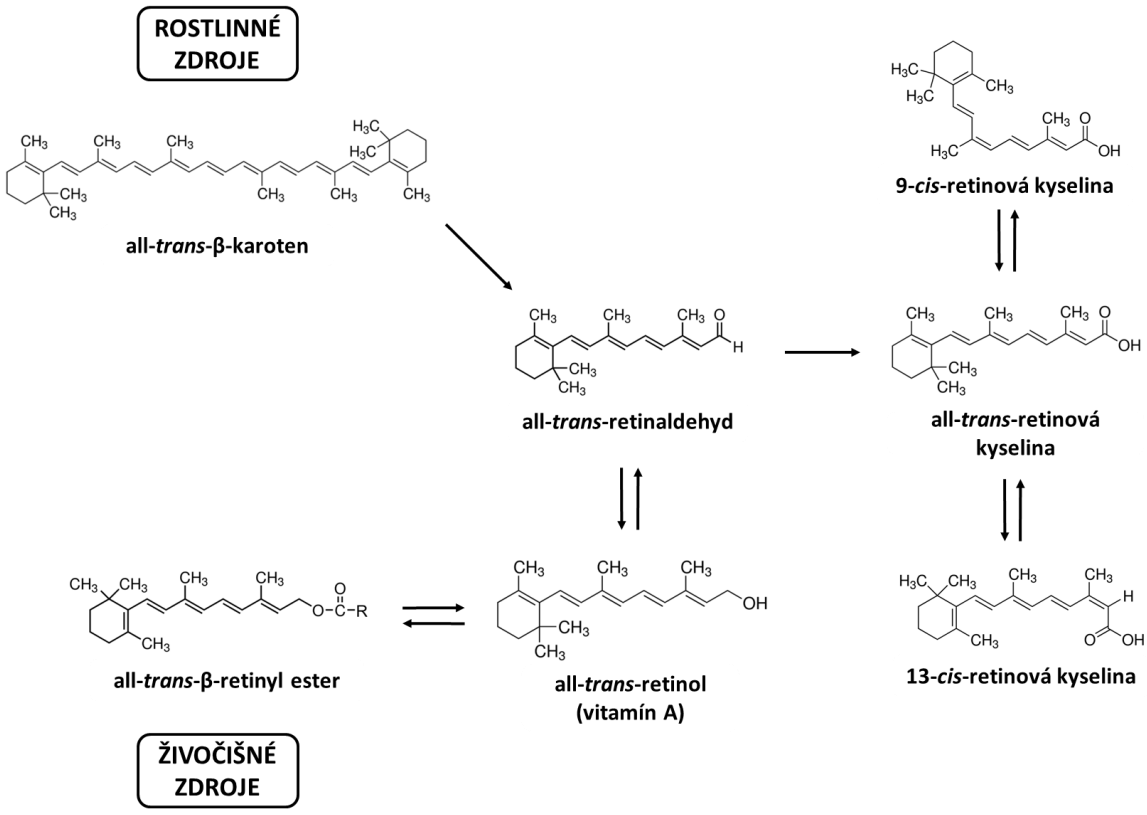

Obr. 4. Metabolismus retinoidů. Zdroje živočišných i rostlinných prekurzorů vitamínu A jsou enzymaticky metabolizovány na vitamín A (all-*trans*-retinol), přes meziprodukt all-*trans*-retinaldehyd vzniká kyselina all-*trans*-retinová, která může být neenzymaticky konvertovaná na izoformy 9-*cis*-retinovou a 13-*cis*-retinovou kyselinu. Převzato a upraveno z di Masi et al. (2015).

V současné době jsou popsány tři generace klinicky používaných retinoidů. První generace obsahuje přírodní retinoidy (retinol, retinaldehyd a izoformy kyseliny retinové), do druhé generace patří etretinát a jeho metabolit acitretin, třetí generace je zastoupena tazarotenem, bexarotenem a adapalenem (Alizadeh et al. 2014).

Molekuly kyseliny retinové (RA), stejně jako ostatní retinoidy, vykazují lipofilní charakter, díky kterému snadno pronikají přes plazmatickou membránu do buňky. V cytoplazmě jsou all-*trans*-retinol a jeho oxidační produkt all-*trans*-retinal asociovány s různými izoformami retinol-vázajícího proteinu (CRBP, cellular retinol-binding protein), zatímco ATRA se váže na izoformy proteinu CRABP (cellular retinoic acid-binding protein).

Protože proteiny CRABP byly detekovány i v buněčném jádře, předpokládá se, že slouží k transportu molekul RA do jádra, kde následně tvoří komplexy se specifickými jadernými receptory, které vykazují funkci inducibilních transkripčních faktorů (Bushue et Wan 2010). Zatím bylo popsáno šest retinoidových receptorů (RARα, -β, -γ a RXRα, -β, -γ), které vykazují podobnou strukturu včetně konzervované DNA vazebné domény a více variabilní ligand vázající domény na C-konci molekuly. ATRA se přednostně váže na receptory RAR, zatímco její 9-*cis* izomer vykazuje afinitu k oběma skupinám receptorů. Retinoidové receptory při vazbě na DNA dimerizují: RAR vytvářejí heterodimery s RXR, zatímco RXR heterodimerizují s dalšími jadernými receptory, např. s receptorem pro tyroidní hormon (TR), receptorem pro vitamin D (VDR) nebo s PPARγ (peroxisomal proliferator activated receptor γ) (Ortiz et al. 2002). RAR/RXR heterodimery v rámci DNA rozpoznávají a vážou se na úseky RARE (retinoic acid responsive elements), které jsou typické přítomností dvou hexamerních sekvencí (A/G)G(G/T)TCA se stejnou orientací (direct repeat, DR) oddělených dvěma nebo pěti nukleotidy (DR2, resp. DR5) (Cunningham et Duester 2015).

Sekvence RARE se nacházejí v oblasti promotorů většiny RA-responzivních genů. V nepřítomnosti odpovídajícího ligandu retinoidové receptory potlačují expresi cílových genů prostřednictvím navázání korepresorových proteinů NCOR1 a NCOR2 (nuclear receptor corepressor 1, resp. 2). Korepresorové proteiny dále vážou histon deacetylázové komplexy a polycomb represivní komplex 2 (PRC2), které způsobují trimetylaci lysinu Lys^{27} na histonu H3, kondenzaci chromatinu a následně blokování exprese cílových genů. Po vazbě RA na RAR/RXR podléhá heterodimer retinoidových receptorů konformačním změnám, v jejichž důsledku se uvolňují korepresorové proteiny a jsou nahrazeny koaktivátory NCOA1, 2 a 3 (nuclear receptor co-activator). Na tyto koaktivátory se váže řada proteinů regulujících epigenetické a strukturální modifikace chromatinu, které umožňují aktivaci transkripčního aparátu a transaktivaci cílových genů (Ablain et The 2011, diMasi et al. 2015, Cuningham et Duester 2015)

Model diferenciační terapie

Modelovým příkladem diferenciační terapie (Obr. 5) je využití ATRA jako induktoru diferenciace při léčbě akutní promyelocytární leukémie (APL), což v kombinaci s následnou chemoterapií vede ke kompletní remisi až u 90 % pacientů (Massard et al. 2006). Klinická remise je u pacientů s APL podmíněna indukcí diferenciace nezralých leukemických blastů do terminálně diferencovaných granulocytů. Tyto blasty jsou u většiny pacientů charakteristické

přítomností chromosomální translokace t(15;17)(q24;q21), jejímž výsledkem je fúzní gen *PML-RARA*, který kóduje transkripční faktor PML a receptor RARα. Fúzní protein PML-RARα může dimerizovat nebo vytvářet heterodimery s receptorem RXR a následně se vázat na sekvenci RARE v promotorech cílových genů. V případě, že není na receptor navázán ligand – tedy kyselina retinová – fúzní protein váže řadu korepresorů včetně molekul HDAC a celý komplex vyvolá transkripční i epigenetickou represi (Ablain et The 2011).

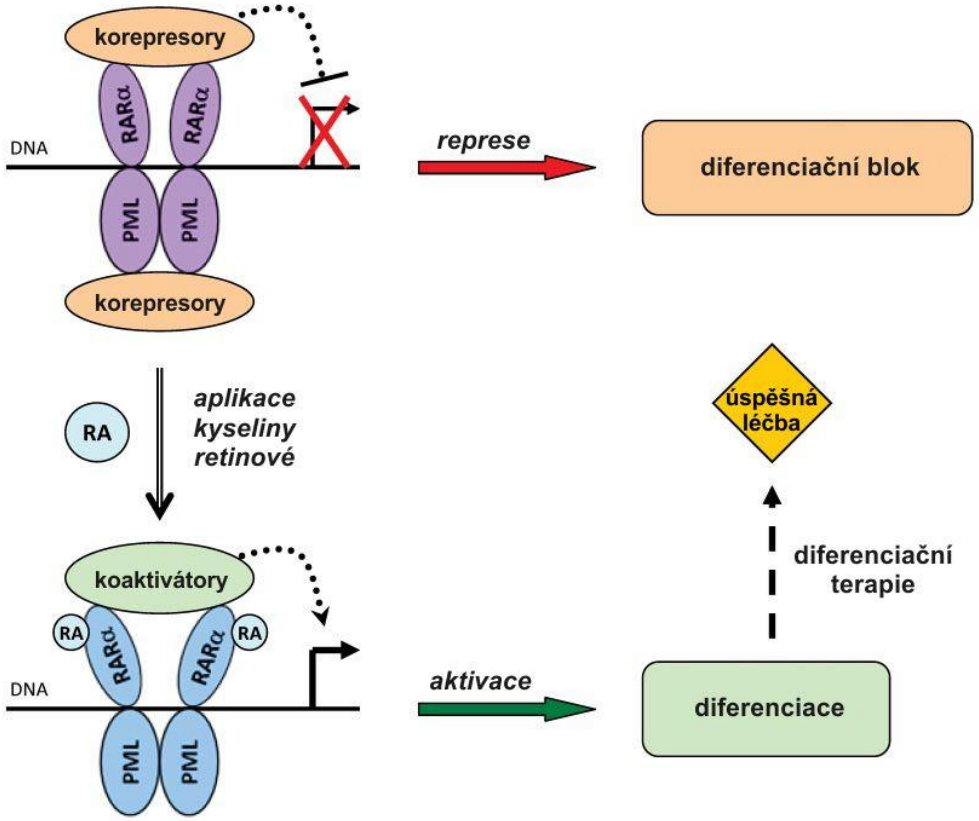

Obr. 5. Tradiční model diferenciační terapie pomocí retinoidů na modelu akutní promyelocytární leukémie. Fúzní receptor PML-RARα s navázaným korepresorovým komplexem blokuje expresi cílových genů a tím i diferenciaci. Po aplikaci farmakologické dávky kyseliny retinové jsou korepresory nahrazeny koaktivátory a je spuštěn diferenciační program, což vede k remisi onemocnění. Převzato a upraveno z Ablain et The (2011).

Blokování transkripce cílových genů je způsobeno především deacetylací histonů, což vede ke konformačním změnám molekuly DNA, které následně omezují vazbu transkripčních faktorů i RNA polymerázy. V normálních blastech aktivují fyziologické koncentrace ATRA (v rozmezí 10^{-9} – 10^{-8} M) disociaci korepresorových proteinů, navázání koaktivátorů s histonacetyltransferázovou aktivitou a spuštění transkripce cílových genů, a to následně

vede k procesu diferenciace. U APL blastů však zmíněné koncentrace ATRA nestačí k disociaci korepresorových proteinů z fúzního receptoru, což způsobuje zablokování diferenciační dráhy a zmožení blastů ve stádiu promyelocytů. Až řádově vyšší terapeutické koncentrace ATRA (v rozmezí 10^{-7} – 10^{-6} M) uvolní korepresorový komplex z fúzního proteinu PML-RARα a tím spustí diferenciační program (Siddikuzzaman et al. 2011).

Vedle represe genů regulujících diferenciaci aktivuje fúzní protein PML-RARα transkripci genů zahrnutých do signálních drah Wnt a Jagged1/Notch, které podporují schopnost sebeobnovy kmenových buněk a tím napomáhají udržení maligního fenotypu APL blastů (Braekeleer at al. 2014).

Koncept tohoto historicky prvního příkladu použití diferenciační terapie a svým způsobem i terapie založené na změně regulace transkripce podléhá v poslední době revizi. U pacientů léčených monoterapií pomocí ATRA bývá zaznamenána pouze přechodná remise a teprve v kombinaci s konvenční chemoterapií nebo oxidem arsenitým dochází k celkovému bezpříznakovému vyléčení (Ablain et The 2011).

Vzhledem k tomu, že se diferenciační terapie s využitím retinoidů experimentálně osvědčila k potlačení různých typů nádorů na zvířecích modelech, mohla být následně testována i v humánní medicíně. Do současné doby proběhla řada klinických studií s přírodními i syntetickými retinoidy testovanými pro léčbu mnoha typů nádorových onemocnění (přehledně Di Masi et al. 2015). I když v některých případech byla aplikace retinoidů úspěšná, část klinických studií prokázala negativní vedlejší účinky této terapie, které jsou spojené především s toxicitou retinoidů (de Oliveira 2015). Použití retinoidů v rámci monoterapie, zvláště ve vysokých dávkách, se proto nejeví jako optimální.

Naopak kombinace retinoidů s některými dalšími sloučeninami může vykazovat synergický vliv na regulaci proliferace a indukci apoptózy, čímž při snížené koncentraci retinoidů zůstává zachován jejich terapeutický efekt a současně jsou potlačeny nežádoucí vedlejší účinky. Jednou skupinou molekul vhodných pro kombinovanou terapii s retinoidy jsou inhibitory enzymů účastnících se epigenetické regulace genové exprese (např. DNA metyltransferázy, histondeacetylázy, histonmetyltransferázy aj.). Tyto enzymy mohou negativně, ale reverzibilně modifikovat cílové geny retinoidů nebo jejich promotory, čímž omezují jejich transkripci v nádorových buňkách. Po aplikaci inhibitorů dochází ke zvýšení citlivosti k retinoidům a aktivaci transkripce RA-responzivních genů (Di Masi et al. 2015).

Modulace diferenciace – kombinovaná léčba

Dalším možným způsobem, jak snížit terapeutickou koncentraci retinoidů při současném zachování nebo prodloužení jejich účinku, je regulace metabolismu retinoidů, konkrétně inhibice enzymů, které se podílejí na intracelulární degradaci retinoidů. Mezi tyto enzymy patří lipoxygenázy (LOX) a cyklooxygenázy (COX), které jsou součástí metabolismu kyseliny arachidonové, neboť některé finální produkty tohoto metabolismu, především prostaglandiny a leukotrieny, se také mohou účastnit katabolismu kyseliny retinové - a to buď přímo její degradací nebo nepřímo regulací aktivity retinoidových receptorů (Krzyzankova et al. 2014). V případě kombinace inhibitoru cyklooxygenázy-2 a syntetického retinoidu N-(4-hydroxyphenyl) retinamidu byl také popsán synergický efekt při potlačení aktivace signální dráhy PI3K/AKT a při indukci mitochondriální apoptotické dráhy (Schroeder et al. 2006).

V rámci experimentů *in vitro* jsme se v naší laboratoři zabývali antineoplastickými účinky ATRA v kombinaci s kyselinou kávovou, která je inhibitorem 5-lipoxygenázy, nebo s celecoxibem, jenž inhibuje cyklooxygenázu-2. Primární modelovou linií, na které jsme prokázali modulaci diferenciačního účinku ATRA pomocí kyseliny kávové, byla promyelocytární leukemická linie HL-60. Na tomto modelu kyselina kávová v kombinované aplikaci výrazně zesilovala ATRA-indukovanou granulocytární diferenciaci buněk, což bylo prokázáno jak významným nárůstem populace CD66b-pozitivních buněk, tak zvýšenými hodnotami NBT (nitro blue tetrazolium) testu, jehož podstatou je cytochemická detekce granulocytů (Veselska et al. 2004). V další fázi výzkumu jsme se zaměřili na modely solidních nádorů dětského věku - konkrétně na neurogenní nádory (neuroblastom a meduloblastom) a na sarkomy (osteosarkom).

Na dvou sbírkových neuroblastomových liniích (SK-N-BE(2) a SH-SY5Y) byly detailně studovány změny morfologie, exprese diferenciačních markerů, proliferační aktivita, buněčný cyklus a indukce apoptózy po kombinované aplikaci ATRA s LOX/COX inhibitory. Výsledky prokázaly schopnost kyseliny kávové zesilovat ATRA-indukovanou diferenciaci u testovaných linií, zatímco celecoxib samotný i v kombinaci s ATRA, vykazoval spíše cytotoxický účinek (Redova et al. 2010). Expresním profilováním 440 genů asociovaných s tumorigenezí byly u takto experimentálně ovlivněných neuroblastomových linií popsány dávkově závislé změny v expresi genů, které se účastní neuronální diferenciace a remodelace cytoskeletu. Některé změny v genové expresi byly detekovány v obou liniích a nezávisle na použitém inhibitoru, což naznačuje obecný mechanismus zesílení ATRA-indukované diferenciace pomocí LOX/COX inhibitorů (Chlapek et al. 2010).

Předchozí výsledky účinků kombinované aplikace ATRA s LOX/COX inhibitory byly následně ověřovány na dvou sbírkových meduloblastomových liniích (Daoy a D283 Med). I tato studie potvrdila, že diferenciační potenciál ATRA lze zesílit její kombinovanou aplikací s kyselinou kávovou nebo celecoxibem. Tento efekt byl zaznamenán u obou meduloblastomových linií pomocí expresního profilování, kdy byla popsána zvýšená hladina exprese genů účastnících se indukované diferenciace, změn cytoskeletu, regulace buněčného cyklu a degradace proteinů (Chlapek et al. 2014).

Naše další studie pak ověřovala účinky kombinované aplikace ATRA s LOX/COX inhibitory na osteosarkomových liniích Saos-2 a OSA-01. Výsledky potvrdily schopnost kyseliny kávové a celecoxibu zvyšovat antiproliferativní účinek ATRA, stejně jako zesilovat mineralizaci extracelulární matrix obou buněčných linií a zvyšovat expresi vybraných markerů osteogenní diferenciace. Popsané výsledky jednoznačně demonstrují schopnost inhibitorů LOX/COX zesilovat diferenciační účinek ATRA u buněk osteosarkomových linií, i když některé ze sledovaných procesů vykazovaly u jednotlivých linií odlišnosti (Krzyzankova et al. 2014).

Výše popsané výsledky, které byly získány na modelových buněčných liniích derivovaných ze solidních nádorů dětského věku, navazují na předchozí studie popisující pozitivní léčebnou odpověď na metronomickou léčbu pediatrických pacientů trpících různými druhy relabujících solidních nádorů s velmi špatnou prognózou (Sterba et al. 2006, Zapletalova et al. 2012). Protokoly metronomické terapie jsou založeny na dlouhodobém podávání nízkých dávek (low-dose) cytotoxických a antiangiogenních léčiv. V některých protokolech se konkrétně jedná o podávání retinoidů v kombinaci s celecoxibem a dalšími chemoterapeutiky (např. etoposid, temozolomid, cyklofosfamid). Z tohoto pohledu naše výsledky získané *in vitro*, které jsou založené především na expresním profilování na úrovni mRNA a na hodnocení exprese diferenciačních markerů na úrovni proteinů, podporují terapeutické použití retinoidů zejména v kombinaci s celecoxibem jakožto inhibitorem COX-2. Na zesílení průběhu buněčné diferenciace indukované retinoidy se pak může podílet i příjem potravy obsahující přírodní fenolické sloučeniny včetně kyseliny kávové – například med, jablečná šťáva, hrozny a některé druhy zeleniny (Chlapek et al. 2010).

Vlastní publikace vztahující se k tématu

- Chlapek P, **Neradil J**, Redova M, Zitterbart K, Sterba J, Veselska R. The ATRA-induced differentiation of medulloblastoma cells is enhanced with LOX/COX inhibitors: an analysis of gene expression. Cancer Cell International 14: 51, 2014.
- Krzyzankova M, Chovanova S, Chlapek P, Radsetoulal M, **Neradil J**, Zitterbart K, Sterba J, Veselska R. LOX/COX inhibitors enhance the antineoplastic effects of all-trans retinoic acid in osteosarcoma cell lines. Tumour Biology 35: 7617-7627, 2014.
- Veselska R, Zitterbart K, Auer J, **Neradil J.** Differentiation of HL-60 myeloid leukemia cells induced by all-trans retinoic acid is enhanced in combination with caffeic acid. International Journal of Molecular Medicine 14: 305-310, 2004.

4. CÍLENÁ MOLEKULÁRNÍ BIOLOGICKÁ LÉČBA

Výše popsaná diferenciační léčba je založena na biologických vlastnostech určitého typu nádoru a je obecně vhodná zejména pro leukémie a embryonální nádory s nízkým stupněm diferenciace (blastomy). Aktuálním trendem v onkologii je však personalizovaná medicína, která vychází z informací o konkrétním nádoru u konkrétního pacienta. Personalizovaná medicína je obecně založena na individuální léčbě daného pacienta, kterému je poskytnuta správná péče, v pravý čas a v odpovídajícím množství, přičemž tato léčba povede jednak k prokazatelnému zlepšení jeho zdravotního stavu, ale také k racionálnímu vynaložení finančních prostředků. V oblasti nádorových onemocnění je personalizovaný přístup v první řadě podložen využitím různých typů tzv. biomarkerů, které lze rozdělit dle vztahu k diagnóze a léčbě na diagnostické, prognostické, prediktivní a biomarkery časné odpovědi. Dalším krokem je správná stratifikace pacientů do kategorií rizika, což je jeden ze zásadních postupů vedoucích k volbě vhodné léčby pro konkrétního pacienta. Z těchto důvodů tedy cílená a individualizovaná medicína nahrazuje tradiční přístup jednoho druhu léčby pro všechny, tzv. one-size-fits-all medicine (Kalia 2013).

Jak bylo uvedeno výše, základním východiskem pro nové a efektivní terapeutické strategie je detailní molekulární charakteristika daného nádoru. Aktuální výzkumné studie prokazují, že určité onemocnění může zahrnovat více klinicky a biologicky odlišných subtypů, jak lze vidět na příkladu meduloblastomu, který představuje nejčastější typ zhoubného mozkového nádoru u dětí (Northcott et al. 2012). Právě identifikace rozdílů na molekulární úrovni - ať už jsou analyzovány nukleové kyseliny nebo proteiny - ve vzorku nádorové tkáně odebrané pacientovi představuje cestu k nalezení vhodných terapeutických cílů. Přestože jsou známy klinické i biologické rozdíly mezi nádorovými onemocněními u dětí a u dospělých, aplikace nízkomolekulárních inhibitorů a monoklonálních protilátek proti různým cílům v nádorových buňkách, zejména zaměřených na inhibici signálních drah, je stále častěji součástí personalizované protinádorové léčby pacientů obou věkových kategorií na základě využití mechanismu účinku těchto látek (Rossig et al. 2011, Zhou et al. 2014, Pearson et al. 2016).

Receptorové tyrozinkinázy

Jedna ze slibných strategií personalizované protinádorové léčby je založena na narušení nebo přímo blokování signálních drah v buňkách nádoru. Signální dráhy se u živočišných organismů vyvinuly a zakonzervovaly na základě potřeby integrovat a koordinovat mnoho složitých buněčných procesů, jakými jsou např. pohyb, proliferace, diferenciace a buněčná smrt. Mnohé buněčné signální dráhy jsou založeny na principu přenosu signálu, který je vyvolán vazbou externího stimulu (typicky růstového faktoru) na odpovídající receptory, které jsou lokalizovány na povrchu cílových buněk. V dalším kroku přenosu signálu z těchto membránových receptorů dovnitř buňky mohou být aktivní různé systémy: konformační změny v iontových kanálech vedou k depolarizaci plazmatické membrány, přenos signálu je zprostředkován pomocí malých molekul, tzv. „druhých poslů“, nebo se mechanismem fosforylace aktivují proteinové kinázy, které následně tvoří signální kaskády, v nichž je signál ve formě fosforylace přenášen z jedné kinázy na další.

Jednou z nejvýznamnějších skupin přenašečů signálu je rodina receptorových tyrozinkináz (RTK). V lidském genomu bylo dosud identifikováno 90 funkčních genů a 5 pseudogenů kódujících tyrozinkinázy, z nichž 58 je receptorového typu - jak lze predikovat dle přítomnosti transmembránové domény v kódovaném proteinu. Lidské RTK (Obr. 6) jsou kategorizovány do 20 skupin, založených na sekvenční podobnosti kinázové domény (Robinson et al. 2000).

Všechny RTK mají podobnou molekulární strukturu: extracelulární doména obsahuje ligand-vazebnou část, skrze plazmatickou membránu prochází α-helix motiv, cytoplazmatická část proteinu obsahuje juxtamembránový region, tyrozinkinázovou doménu a je zakončena C-terminální oblastí. V rámci extracelulární domény RTK nacházíme největší strukturní variabilitu, zatímco cytoplazmatická část je primárně tvořena evolučně konzervovanou tyrozinkinázovou doménou, která se skládá ze dvou podjednotek (Lemmon et Schlessinger 2010).

Po vazbě odpovídajícího ligandu na extracelulární doménu dochází k dimerizaci (popř. oligomerizaci) a stabilizaci receptorů, což vyvolá vzájemnou fosforylaci tyrozinových zbytků cytoplazmatické domény. Následné konformační změny cytoplazmatické části receptoru odhalí vazebná místa pro adaptorové, ukotvující či dokovací proteiny, které vytvářejí signální komplex umožňující přenos signálu na další molekuly v cytoplazmě. Specifické vzájemné interakce těchto proteinů, které obsahují různé katalytické a vazebné domény, určují směr signální dráhy (Bache et al. 2004).

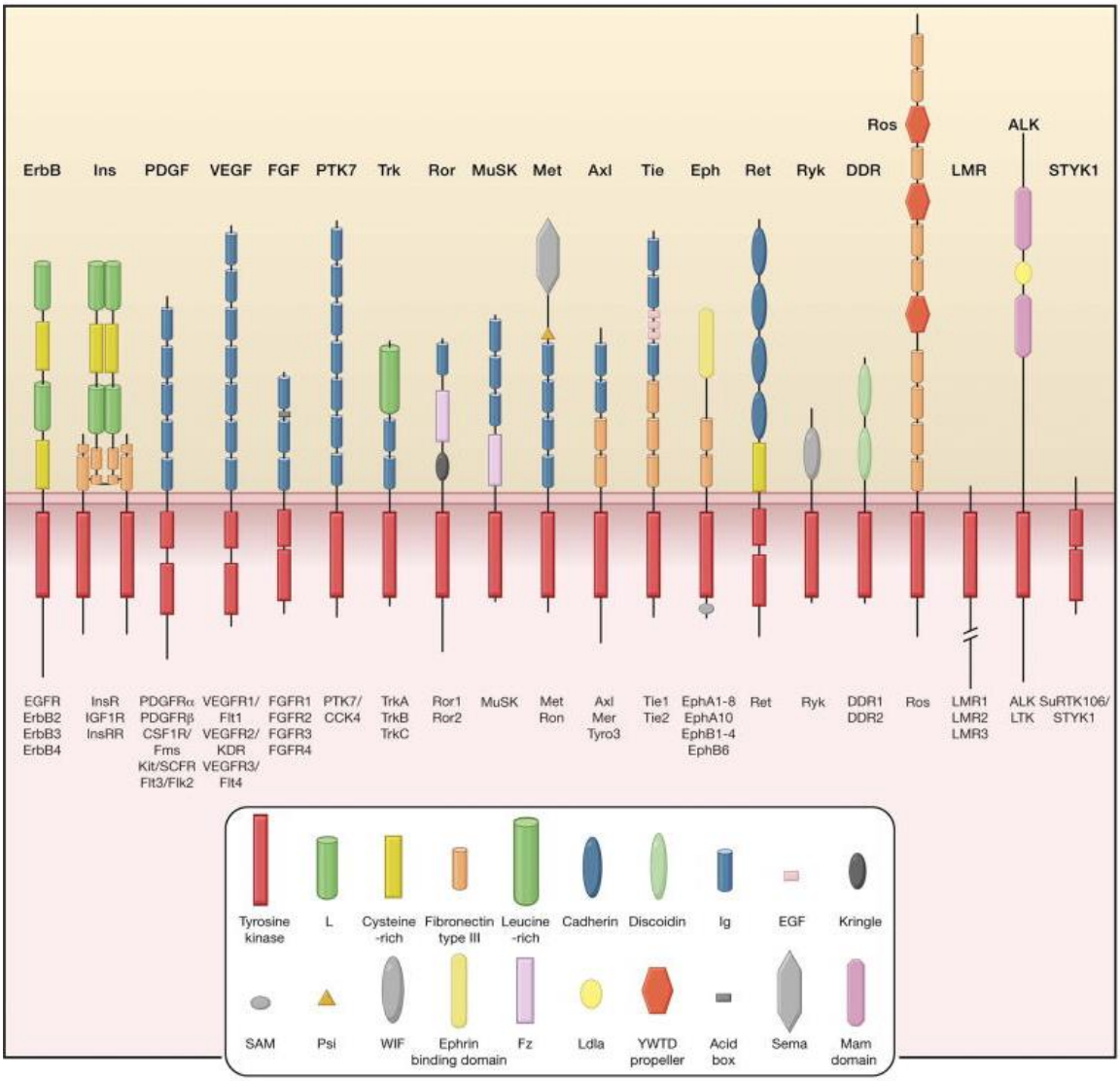

Obr. 6. Přehled 20 rodin receptorových tyrozinkináz u člověka. V bílém rámečku jsou schematicky znázorněny jednotlivé typy strukturních domén. Převzato z Lemon et Schlessinger (2010).

Signální dráha pak představuje přenos signálu, který je amplifikován a integrován prostřednictvím řady proteinů, až k cílovým molekulám, jež vyvolají příslušnou biologickou odpověď. Zásadní mezičlánky v mnoha signálních drahách reprezentují proteinkinázy, především mitogenem aktivované proteinkinázy (MAP kinázy) a serin/treoninové AKT kinázy. Tyto kinázy jsou primárně součástí signálních drah odpovídajících na mitogenní a stresové stimuly, ale regulují i další děje včetně buněčného dělení, apoptózy, genové exprese, motility a metabolismu (Gerits et al. 2007, Mundi et al. 2016). Uvedené buněčné procesy jsou však také regulovány i dalšími drahami, kdy přenašečem signálu mohou být

např. fosfolipáza γ (PLCγ), proteiny STAT (signal transducer and activator of transcription) či FAK kináza (focal adhesion kinase) (Lemmon et Schlessinger 2010).

Navazující signální dráhy

Obecně je MAP kinázová dráha sestavena z kaskády tří na sebe navazujících druhů kináz (Obr. 7), přičemž MAP3 kináza (MAPKKK) fosforyluje a aktivuje MAP2 kinázu (MAPKK), která následně fosforyluje MAP kinázu (MAPK). MAP kinázy pak mohou fosforylovat cílový protein (typicky transkripční faktor po transferu do jádra) nebo jinou kinázu (Gerits et al. 2007). Mezi MAP kinázy nejčastěji aktivované prostřednictvím RTK patří především ERK1/2 (extracellular signal-regulated kinase), JNK1-3 (c-Jun N-terminal kinase) a čtyři izoformy proteinu p38 (α, β, γ, δ).

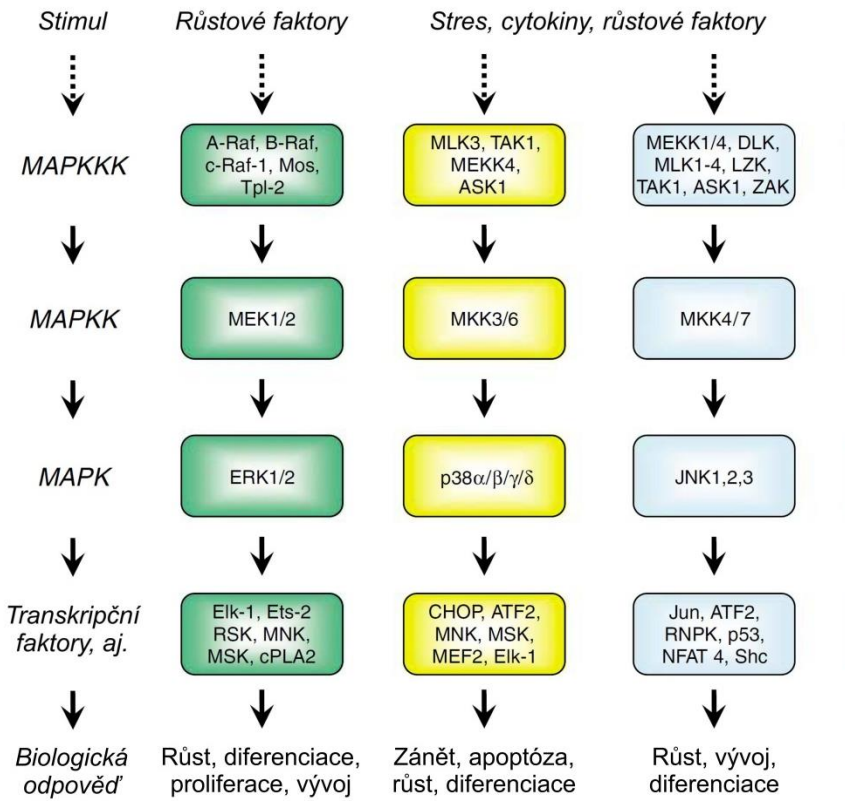

Obr. 7. MAP kinázové signální dráhy. V levém sloupci je znázorněno obecné schéma MAPK signalizace, dále jsou uvedeny tři příklady konkrétních signálních drah. Převzato a upraveno z Roberts et Der (2007).

Serin/treoninové proteinkinázy ERK1/2 jsou považovány za kanonické MAP kinázy regulující základní biologické procesy. ERK 1/2 se aktivují fosforylací MAP2 kináz MEK1/2, jež jsou tyrozin/treoninovými proteinkinázami esenciálními pro vývoj a proliferaci buněk. Serin/treoninové proteinkinázy z rodiny RAF (RAF-1, B-RAF a A-RAF) patří do skupiny MAP3 kináz a fosforylují MEK1/2. Signální osa RAF/MEK/ERK je iniciována malým G-proteinem RAS, který je lokalizován na vnitřní straně plazmatické membrány a aktivuje se po kontaktu se signálním komplexem (obsahujícím Grb2/SOS proteiny) navázaným na cytoplazmatickou část fosforylované RTK (Cristea et Sage 2016).

Druhou z významných signálních drah aktivovaných prakticky všemi RTK je signální dráha PI3K/AKT. Fosfatidylinositol-3 kinázy (PI3K) tvoří soubor kooperujících signálních proteinů, které lze na základě molekulární struktury rozdělit do tří tříd. Třída I PI3 kináz je tvořena heterodimery sestavenými z katalytických a regulačních podjednotek. V rámci podskupiny IA se mohou kombinovat katalytické podjednotky p110α, p110β a p110δ s regulačními podjednotkami p85α, p85β a p55γ, podskupina IB obsahuje jen jeden komplex sestavený z katalytické podjednotky p110γ a regulační podjednotky p101 (Blachly et Baiocchi 2014). Aktivované fosfo-tyrozinové zbytky cytoplazmatické domény RTK interagují s SH2 (src-homology 2) doménou regulační podjednotky PI3K. Poté, co je regulační podjednotka aktivována – ať už RTK nebo G-proteinem spřaženým s receptorem – katalytická podjednotka PI3K katalyzuje konverzi fosfatidylinositol (3,4)-bisfosfátu (PIP_2) na molekuly tzv. „druhého posla“, kterým je fosfatidylinositol (3,4,5)-trifosfát (PIP_3). Molekuly PIP_3 jsou lokalizovány na vnitřní straně plazmatické membrány a mohou aktivovat množství proteinů, které ve své struktuře obsahují PH (pleckstrin homology) doménu, např. PDK (phosphoinositide-dependent kinase), AKT a další serin/treoninové kinázy. AKT následně fosforyluje - a tím aktivuje nebo inhibuje - velké množství cílových proteinů. Mezi hlavní substráty AKT patří zejména mTOR (mammalian target of rapamycin), IκB kináza, Mdm2 homolog (mouse double minute 2), Bad, p27, GSK3 (glycogen synthase kinase-3) a transkripční faktory FOXO1 a FOXO4. Spektrum procesů regulovaných signální dráhou PI3K/AKT je široké, ale mezi nejdůležitější z nich patří proliferace, regulace buněčné smrti a glukózový metabolismus (Mundi et al. 2016).

Onkogenní role receptorových tyrozin kináz

Klíčová role RTK v řízení buněčných procesů je zřejmá zejména ze skutečnosti, že tyto mitogenní receptory patří do skupiny proteinových tyrozin kináz, což je největší skupina

dominantních onkogenů, která vykazuje strukturní homologii (Blume-Jensen et Hunter 2001). Současně bylo prokázáno, že přibližně 30 % RTK je mutováno nebo dysregulováno v různých typech malignit (Amit et al. 2007). Podle jedné z uznávaných teorií je vznik a maligní růst nádorů asociován s určitými molekulárními a biologickými vlastnostmi nádorově transformovaných buněk (Hanahan et Weinberg 2000), přičemž některé z těchto charakteristik (indukce angiogeneze, schopnost metastázování, odolnost vůči apoptotickým signálům) jsou přímo regulovány prostřednictvím RTK. Rovněž nezávislost nádorově transformovaných buněk na externích růstových faktorech je možná díky autokrinním smyčkám, kdy pro vlastní produkci růstových faktorů je nutná aktivace MAP kináz. Podobně může být vyšší proliferační aktivita nádorových buněk způsobena aktivační mutací v genech kódujících RTK nebo jiné signální proteiny. Tyto onkogenní mutace jsou detekovány v molekulách regulujících jak signální dráhu RAS/RAF/MAPK (typicky v genech pro RAS a B-RAF), tak signální dráhu PI3K/AKT, kde jsou časté mutace v katalytické podjednotce PI3K nebo v genu pro tumor-supresorový protein PTEN (phosphatase and tensin homolog), který je hlavní negativním regulátorem této signální dráhy (Amit et al. 2007).

Deregulace RTK signalizace u vybraných solidních nádorů dětského věku

Nejčastějšími solidními nádory u dětí a mladých dospělých (do 19 let věku) jsou v České republice neurogenní nádory s téměř 30 % z celkového počtu případů, přičemž většinu z nich tvoří nádory CNS a ostatní intrakraniální a intraspinální neoplazie (http://detskaonkologie.registry.cz/). U meduloblastomu, což je histogeneticky embryonální neuroektodermální nádor mozečku a obecně představuje nejrozšířenější nádor mozku u dětí, bylo identifikováno mnoho signálních drah spojených s tvorbou a růstem nádoru, včetně vývojových signálních drah (např. Hedgehog, Notch a Wnt), drah aktivovaných RTK (c-Met, ErbB2, IGF-R a TrkC) a onkoproteinu Myc (Guessous et al. 2008). Za vysokou malignitu tohoto onemocnění je patrně zodpovědná signální dráha IGF/IGF-IR (insulin like growth factor 1 receptor), která se podílí především na patogenezi podskupiny SHH (Sonic Hedgehog). Signální dráha IGF/IGF-IR aktivuje PI3K, což vede k potlačení degradace n-Myc, přičemž zvýšená transkripce genu *MYCN* koreluje se sníženým přežitím pacientů. Jednou ze strategií léčby meduloblastomu je proto použití inhibitorů PI3K. Vedle aktivace PI3K/AKT dráhy dále dochází i k aktivaci RAS/MAPK signálních drah. Jednou z příčin může být nadměrná exprese receptorů PDGFR β (platelet-derived growth factor receptor β) nebo

ErbB2, jehož exprese byla prokázána v přibližně 80 % vzorků nádorové tkáně odebraných od pacientů trpících meduloblastomem se špatnou prognózou (Sümer-Turanligil et al. 2013).

Podobně u neuroblastomu, což je embryonální tumor vzniklý z nediferencovaných buněk neurální lišty, byla popsána deregulace signálních drah umožňující přežití nádorově transformovaných buněk. Například fosforylace AKT kinázy korelovala se stupněm onemocnění, nepříznivou histologií a s amplifikací onkogenu *MYCN*. Z rodiny RTK podporuje přežívání neuroblastomových buněk kináza ALK (anaplastic lymphoma kinase), která se fyziologicky podílí na buněčném růstu a vývoji nervových tkání, ale její nadměrná exprese byla detekována ve více než 90 % vzorků neuroblastomu současně s mutacemi genu *ALK*. Dalšími receptory, jejichž zvýšená exprese je popisována v souvislosti s neuroblastomem, jsou např. IGF-R, PDGFR, VEGFR a EGFR, který je také signifikantně více exprimován v neuroblastomových liniích s rezistencí vůči chemoterapeutikům (Megison et al. 2013).

Role RTK a navazujících signálních drah byla rovněž zkoumána u high-grade gliomů v souvislosti se zásadními procesy tumorigeneze, kterými jsou iniciace a progrese nádoru a angiogeneze. Významnou roli zde hrají receptory EGFR, PDGFR a VEGFR rodiny a navazující signální dráhy RAS/RAF/MAPK a PI3K/AKT/mTOR, které jsou potenciálním cílem protinádorové léčby (Ren et al. 2007). Deregulovaná signalizace prostřednictvím RTK vede u gliomů k maligní progresi a může být vyvolána aktivačními mutacemi v genech *EGFR* a *MET*, nadměrnou expresí růstových faktorů a odpovídajících receptorů (např. FGF/FGFR a PDGF/PDGFR) nebo přílišnou aktivací autokrinní smyčky TGFα/EGFR (Kapoor et O'Rourke 2003, Mellinghoff et al. 2012, Skoda et al. 2014). Vedle toho může mutantní forma EGFR transaktivovat další receptory, což společně vede ke konstitutivní aktivaci navazujících signálních drah (Kalman et al. 2013). V rámci signální dráhy RAS/RAF/MAPK se na patogenezi gliomů také podílejí poruchy v genu *BRAF*, a to jak mutace, tak fúze s jinými geny (Louis et al. 2016).

Další skupinou nádorů, u nichž se intenzivně studují signální dráhy, jsou sarkomy, které představují třetí nejčastější skupinu solidních nádorů dětského věku a lze je rozdělit na dvě hlavní kategorie: sarkomy kostí (osteosarkom, Ewingův sarkom, aj.) a sarkomy měkkých tkání (rabdomyosarkom, fibrosarkom, leiomyosarkom, liposarkom, synoviální sarkom, aj.) (Spector et al. 2006). U Ewingova sarkomu, který je typický několika chromosomálními aberacemi – až 85% případů je postiženo translokací t(11;22) za vzniku fúzního proteinu EWS-FLI1 – byly popsány dysregulace různých signálních drah včetně RTK. V některých případech byla zaznamenána aktivace signální dráhy IGF/IGF-IR fúzním proteinem

EWS-FLI1, který přímo inhibuje promotor genu *IGFBP-3* (insulin like growth factor binding protein 3), čímž dojde ke zvýšení dostupnosti IGF-I a následné podpoře proliferace nádorových buněk (Wagner et Maki 2013). V souvislosti s patogenezí Ewingova sarkomu jsou však v literatuře zmiňovány téměř všechny významné rodiny RTK. Receptory spadající do rodiny ErbB vykazovaly vyšší expresi v nádorové tkáni i derivovaných buněčných liniích (Fleuren et al. 2014, Mendoza-Naranjo et al. 2013), podobně jako VEGF - ligand VEGF receptorů (Kreuter et al. 2006, Ackermann et al. 2012). Mezi další aktivní signální dráhy popsané u Ewingova sarkomu patří dráha FGF2/FGFR1, která v kostním mikroprostředí hraje významnou roli v procesech invazivity a metastázování nádoru (Kamura et al. 2010), a dále aktivované receptory rodiny PDGFR, jejichž fosforylace však není v nádorových buňkách Ewingova sarkomu způsobena aktivační mutací (Bozzi et al. 2007). Podle současných výzkumů se na patogenezi Ewingova sarkomu také podílejí receptory c-KIT a MET včetně odpovídajících ligandů a jejich signalizace přispívá k regulaci buněčného růstu, přežívání a schopnosti metastázovat (Mora et al. 2012, Fleuren et al. 2013).

Také u rabdomyosarkomu, který je nejčastějším typem sarkomů měkkých tkání, byly zaznamenány změny v regulaci signálních drah aktivovaných RTK. Jednou ze dvou základních variant rabdomyosarkomu je alveolární rabdomyosarkom, který je charakteristický přítomností translokace t(2;13) a následným vznikem fúzního proteinu PAX3-FOXO1 (Barr et al. 1996). Tento fúzní protein je schopen zvyšovat transkripci genů kódujících receptory IGF-IR, PDGFRα a FGFR4 (Cao et al. 2010, Blandford et al. 2006, Crose et Linardic 2011). Popsaná zvýšená exprese IGF-IR, ale i receptorů VEGF a jejich ligandů ve tkáni rabdomyosarkomu naznačuje, že nádorové buňky jsou nezávislé na externích růstových faktorech a signalizace podporující proliferaci a angiogenezi nádorů je regulována autokrinní smyčkou (Cao et al. 2010, Gee at al. 2005). Rozdíly mezi jednotlivými variantami rabdomyosarkomu lze najít u exprese receptorů rodiny ErbB: pro embryonální typ je charakteristickým znakem zvýšená exprese EGFR, zatímco ErbB2 je častěji detekován u alveolárního typu rabdomyosarkomu (Ganti et al. 2006). Aktuálně byla u rabdomyosarkomu popsaná nadměrně zvýšená exprese MET, kdy deregulace tohoto receptoru se jeví jako klíčový prvek metastatického potenciálu konkrétního nádoru, přičemž hyperaktivace MET koreluje se schopností metastázovat i u jiných typů nádorů (Miekus et al. 2013).

RTK signalizace jako cíl protinádorové léčby

Současné terapeutické přístupy pro léčbu vysoce rizikových solidních nádorů dětského věku jsou primárně založeny na chirurgickém odstranění nádoru, různě intenzivních protokolech chemoterapie a popřípadě na aplikaci radioterapie, ale s poměrně malým zastoupením cílené léčby. Celkové přežití ve skupině pacientů trpících metastatickými sarkomy a dalšími refrakterními solidními nádory je nízké (např. 10 – 30 % pro sarkomy) a konvenční léčbu navíc doprovázejí závažné časné i pozdní vedlejší účinky. Z toho vyplývá potřeba zavedení efektivních léčebných přístupů založených na principech personalizované medicíny (Quesada et Amato 2012, Hegde et al. 2015).

Inhibice vybraných signálních drah, ať už s použitím monoklonálních protilátek nebo nízkomolekulárních inhibitorů, je v současné době jednou z perspektivně se vyvíjejících strategií v cílené léčbě nádorových onemocnění. Povrchové RTK a na ně navazující kinázy, které zprostředkovávají intracelulární signalizaci indukovanou zejména růstovými faktory, představují ideální cíle pro tento druh terapie. Kromě látek již schválených pro klinické použití existuje celá řada dalších nových inhibitorů v různých fázích klinického testování (Fleuren et al. 2014). Přehled dostupných nízkomolekulárních inhibitorů a monoklonálních protilátek proti RTK, popřípadě jejich ligandům či dalším kinázám, které jsou registrovány jako léky v České republice u Státního ústavu pro kontrolu léčiv (SÚKL), je uveden v tabulce 1, respektive 2.

Tab. 1. Přehled nízkomolekulárních inhibitorů proteinkináz registrovaných jako léčiva v České republice u Státního ústavu pro kontrolu léčiv.

Název inhibitoru	Název léku v ČR	Molekulární cíle inhibitoru
Afatinib	Giotrif	EGFR; ErbB2
Alektinib	-	ALK
Axitinib	Inlyta	VEGFR1/2/3; PDGFRβ; c-Kit
dBosutinib	Bosulif	Src; Abl
Cabozantinib	Cometriq	VEGFR2; c-Met; Ret; c-Kit; VEGFR1/3; FLK2; Tie2; AXL
Cediranib	-	VEGFR1/2/3; PDGFRβ; c-Kit
Ceritinib	Zykadia	ALK
Dabrafenib	Tafinlar	B-Raf (mut. V600)
Dasatinib	Sprycel	Abl; Src; c-Kit,
Erlotinib	Tarceva	EGFR
Everolimus	Afinitor, Votubia	mTOR
Gefitinib	Iressa	EGFR
Ibrutinib	Imbruvica	Btk
Imatinib	Glivec, Imakrebin, Imanitec, Latib, Meaxi	v-Abl; c-Kit; PDGFR
Kobimetinib	Cotellic	MEK1

Tab. 1. Pokračování

Název inhibitoru	Název léku v ČR	Molekulární cíle inhibitoru
Krizotinib	Xalkori	c-Met; ALK
Lapatinib	Tyverb	EGFR; ErbB2
Lenvatinib	Lenvima	VEGFR1, 2, 3
Masitinib	-	c-Kit; PDGFRα/β
Midostaurin	-	PKCα/β/γ; Syk; Flk-1; Akt; PKA; c-Kit; c-Fgr; c-Src; FLT3; PDFRβ, VEGFR1/2
Nilotinib	Tasigna	Bcr-Abl
Nintedanib	Ofev, Vargatef	VEGFR1/2/3; PDGFRα/β; FGFR1/2/3
Osimertinib	-	EGFR
Palbociklib	-	CDK4/6
Pazopanib	Votrient	VEGFR1/2/3; PDGFR; FGFR; c-Kit; CSF-1R
Ponatinib	Iclusig	Abl; PDGFRα; VEGFR2; FGFR1; Src
Regorafenib	Stivarga	VEGFR1/2/3; PDGFRβ; c-Kit; RET; Raf-1
Ridaforolimus	-	mTOR
Rociletinib	-	EGFR
Ruxolitinib	Jakavi	JAK1/2
Sorafenib	Nexavar	Raf-1; B-Raf; VEGFR-2
Sunitinib	Sutent	VEGFR2; PDGFRβ; c-Kit
Temsirolimus	Torisel	mTOR
Tivozanib	-	VEGFR1/2/3; PDGFR; c-Kit
Trametinib	Mekinist	MEK1/2
Vandetanib	Caprelsa	VEGFR2
Vemurafenib	Zelboraf	B- Raf (mut. V600E)

Tab. 2. Přehled monoklonálních protilátek proti receptorovým tyrozinkinázám a jejich ligandům registrovaných jako léčiva v České republice u Státního ústavu pro kontrolu léčiv.

Název protilátky	Název léku v ČR	Molekulární cíl inhibitoru
Bevacizumab	Avastin	VEGF-A
Cetuximab	Erbitux	EGFR
Necitumumab	Portrazza	EGFR
Panitumumab	Vectibix	EGFR
Pertuzumab	Perjeta	ErbB2 (HER2/neu)
Ramucirumab	Cyramza	VEGFR2
Trastuzumab	Herceptin	ErbB2 (HER2/neu)
Trastuzumab emtansin	Kadcyla	ErbB2 (HER2/neu)

Nevýhodu v aplikaci některých nízkomolekulárních inhibitorů může představovat jejich nespecificita a nejednotný pohled na strategii jejich klinického použití – nabízí se možnost cílené léčby jedinou látkou, kombinací několika inhibitorů nebo použití inhibitorů jako součásti standardního léčebného protokolu zahrnujícího i chemoterapii a/nebo radioterapii. V každém případě je však základním krokem personalizovaného přístupu k léčbě založené na použití nízkomolekulárních inhibitorů kináz i monoklonálních protilátek proti

RTK či jich ligandům důkladná charakterizace konkrétního nádoru z hlediska exprese a aktivace RTK, stejně jako aktivity navazujících signálních drah.

Většina studií citovaných v této kapitole popisuje souvislost expresní hladiny mRNA nebo celkového obsahu vybraného proteinu s patogenezí určitého typu nádoru, a to převážně ve FFPE (formalin-fixed paraffin embedded) vzorcích. Nicméně plošný screening fosforylace RTK poskytuje celkový přehled o aktivovaných signálních drahách daného nádoru a fosforylační profil kináz v příslušném nádoru tak může být vodítkem k výběru vhodného léčebného postupu (Fleuren et al. 2014). Ačkoliv byly proteinové arrays pro detekci fosforylace RTK v praxi několikrát použity pro charakterizaci vybraných nádorů u dospělých pacientů (Yu et al. 2008, Dewaele et al. 2010, Ströbel et al. 2010, Chen et al. 2010, Montero et al. 2014), využití stejného metodického přístupu u pediatrických nádorů je však dosud stále výjimečné (Sikkema et al. 2009, Melicharkova et al. 2015, Mudry et al. 2017).

Jedna z mála prací, ve které byly využity proteinové arrays pro detekci fosforylace signálních proteinů k vyhledání potenciálních cílů v rámci personalizované terapie u dítěte, byla publikována v rámci našeho výzkumu (Melicharkova et al. 2015). V této případové studii je popsán klinický průběh onemocnění u pacientky trpící Maffucciho syndromem, jenž je typický výskytem mnohočetných enchondromů a progredujících hemangiomů, které u pacientky způsobovaly různé zdravotní komplikace (např. omezení hybnosti, poruchy růstu, bolesti, fluidothorax nebo ascites). Dosavadní zvolené způsoby konvenční léčby vedly ke smíšené odpovědi, popřípadě k zachování stacionárního stavu s periodickou potřebou odstranění ascitu a fluidothoraxu. Po vyšetření fosforylačního profilu RTK, MAP kináz a dalších signálních proteinů se jako jeden z možných cílů jevila signální dráha PDGFR/ERK. Ve vyšetřené tkáni byla detekována zvýšená fosforylace obou forem PDGFR (α i β), stejně jako ERK1 a ERK2. Nově byl proto do léčebného schématu přidán sunitinib, což je nízkomolekulární inhibitor primárně zasahující receptory pro růstový faktor krevních destiček (PDGFR-α a PDGFR-β) a receptory pro vaskulární endoteliální růstový faktor (VEGFR-1, VEGFR-2 a VEGFR-3). Tato změna v léčbě vedla ke klinicky významné odpovědi trvající šest měsíců.

V druhé případové studii, kde jsme použili analýzu fosforylačního profilu kináz, byl vyšetřen pacient trpící infantilní myofibromatózou (Mudry et al. 2017). Onemocnění patří do skupiny sarkomů měkkých tkání, ale v tomto případě postihovalo měkké tkáně i kosti, přičemž léze byly nalezeny také intrakraniálně. Po aplikaci několika cyklů chemoterapie byla u pacienta zaznamenána pouze částečná odpověď doprovázená negativními vedlejšími účinky léčby. Následně byla ve vzorku bioptované nádorové tkáně provedena analýza fosforylace 49

RTK, přičemž relativně nejvyšší fosforylace byla detekována u PDGFRβ. Navíc sekvenace genu *PDGFRB* odhalila zárodečnou heterozygotní mutaci c.1681C>T (p.Arg561Cys), která je asociovaná s infantilní myofibromatózou (Arts et al. 2016). Na základě získaných poznatků byla aplikována cílená léčba sunitinibem v kombinaci s nízkodávkovým vinblastinem, která vedla k přetrvávající pozitivní odpovědi bez toxicity doprovázející předchozí léčbu.

Z pohledu výše zmíněných kazuistik se metoda detekce fosforylačních profilů RTK a navazujících signálních proteinů jeví jako vhodný prostředek pro identifikaci cílů na úrovni proteinů a signálních drah. Navíc tím, že RTK mají zásadní vliv na mnoho buněčných procesů, které jsou deregulované v nádorových buňkách, může inhibice jedné RTK postihnout více dějů, než jen buněčnou proliferaci (Crose et Linardic 2011). Na druhou stranu volba správného cíle předpokládá důkladnou znalost genetického pozadí aktivace specifických signálních drah. Mutační screening jednotlivých RTK a analýza navazujících signálních drah tak může představovat optimální strategii pro volbu vhodného léčebného postupu. Cílená molekulární biologická terapie tedy díky potlačení specifických signálních drah může zlepšit výsledky léčby, snížit u pacienta množství komplikací a celkově redukovat náklady na léčbu vlastního onemocnění (Kalia 2013).

Vlastní publikace vztahující se k tématu

- Mudry P, Slaby O, **Neradil J**, Soukalova J, Melicharkova K, Rohleder O, Jezova M, Seehofnerova A, Michu E, Veselska R, Sterba J. Case report: rapid and durable response to PDGFR targeted therapy in a child with refractory multiple infantile myofibromatosis and a heterozygous germline mutation of the PDGFRB gene. BMC Cancer 17: 119, 2017.
- Melichárková K, **Neradil J**, Múdry P, Zitterbart K, Obermannová R, Skotáková J, Veselská R, Štěrba J. Profil aktivace receptorových tyrozinkináz a mitogenem aktivovaných proteinkináz v terapii Maffucciho syndrome. Klinická Onkologie 28 (Suppl 2): 2S47-51, 2015.
- Skoda J, **Neradil J,** Zitterbart K, Sterba J, Veselska R. EGFR signaling in the HGG-02 glioblastoma cell line with an unusual loss of EGFR gene copy. Oncology Reports 31: 480-7, 2014.

5. NÁDOROVÉ KMENOVÉ BUŇKY A JEJICH ROLE V PROTINÁDOROVÉ LÉČBĚ

Buněčná heterogenita je obvyklým rysem celého spektra lidských malignit – jak solidních, tak hematologických – přičemž tato heterogenita představuje zásadní komplikaci v protinádorové léčbě (Visvader et Lindeman 2008). Podobně jako tomu je u normálních tkání, mnoho solidních nádorů vykazuje hierarchické uspořádání, kdy tumorigenní nádorové kmenové buňky (cancer stem cells, CSCs) diferencují do různých buněčných typů, které původní schopnost tumorigenity ztrácejí. Mnoho studií potvrdilo, že ačkoliv CSCs a z nich derivované netumorigenní nádorové buňky mohou vykazovat stejný genotyp, tyto dvě skupiny buněk se odlišují na úrovni epigenetické regulace, což se fenotypově odráží především v aktivaci různých signálních drah. Jak bylo popsáno v předchozí kapitole, tyto dráhy regulují buněčnou adaptaci na stresové podněty včetně zánětu, hypoxie, nízkého pH a metabolické starvace, ale také protinádorové terapie (Cojoc et al. 2015). Detailní studium CSCs izolovaných z různých typů nádorů ukazuje, že právě CSCs mohou být hlavní příčinou selhání konvenční protinádorové terapie. Ta je zaměřena na rychle proliferující buňky nádorové masy, které však již nemají schopnost tumorigeneze, zatímco CSCs s nízkou proliferační aktivitou a účinnými reparačními mechanismy (např. DNA reparační aktivita, transmembránové pumpy) působení záření a chemoterapeutik unikají. Proto identifikace CSCs a terapie cílená právě na tyto buňky jsou jedním z hlavních směrů současné experimentální onkologie. Za nejslibnější strategii ve vývoji efektivních protokolů protinádorové léčby je pak považována kombinace konvenční terapie postihující nádorovou masu a cílené terapie proti CSCs (Chen et al. 2016).

Nádorové kmenové buňky a jejich funkce v karcinogenezi

CSCs jsou popisovány jako klíčová komponenta heterogenní nádorové buněčné masy, která si zachovává schopnost sebeobnovy a leží na vrcholu hierarchického uspořádání všech typů buněk v rámci nádoru. Jinými slovy, CSCs tedy představují diferenciační prekurzory všech buněčných populaci v rámci nádoru. Mnoho studií obecně definuje CSCs na základě jejich schopnosti iniciovat vznik nádoru, což lze experimentálně ověřit funkčním testem tumorigenity v imunodeficientních myších. U některých typů malignit, např. u leukémií nebo karcinomů prsu, plic a střeva je množství buněk schopných iniciovat vznik nádoru relativně

malé a podobá se zastoupení „normálních“ (tedy nenádorových) adultních kmenových buněk ve většině tkání, které je obvykle nižší než 1 % z celkového počtu buněk v příslušné tkáni. Oproti tomu se vyskytují i nádory (typicky např. melanom), u nichž většina nádorových buněk nese totožnou schopnost tumorigeneze, což by naznačovalo, že specifická a početně omezená subpopulace CSCs u těchto nádorů nemusí existovat. Obecně však lze shrnout, že jednotlivé subpopulace buněk v rámci konkrétního nádoru se mohou lišit mírou schopností sebeobnovy a tumorigeneze a také svým diferenciačním potenciálem, přičemž na základě změn v těchto schopnostech lze definovat fenotypovou plasticitu, která umožňuje dynamický přechod mezi „kmenovým“ a „nekmenovým“ fenotypem nádorových buněk (Ravasio et al. 2016).

Další charakteristickou vlastností CSCs je rezistence vůči konvenční radioterapii a chemoterapii. Vysvětlení rezistence vůči xenobiotikům spočívá v expresi ABC (ATP-binding cassette) transportérů, která se u CSCs zvyšuje po aplikaci chemoterapie. Mezi nejlépe charakterizované transportéry, které jsou v lidském genomu kódovány 49 geny, patří především ABCB1 (známý též jako P-glykoprotein, Pgp nebo také multidrug resistence protein, MDR1), dále ABCB5, ABCC1 či ABCG2. Například nadměrná exprese ABCB1 zvyšuje rezistenci nádorových buněk vůči chemoterapeutikům, jako jsou kolchicin, doxorubicin, etoposid, vinblastin a paclitaxel, které způsobují poškození DNA, inhibici funkce cytoskeletálních komponent nebo tvorbu kyslíkových radikálů (Carnero et al. 2016). Základními mechanismy radiorezistence CSCs je spuštění reparačních procesů po poškození DNA a vyšší aktivita mechanismů neutralizujících reaktivní kyslíkové radikály, které záření může indukovat (Beck et Blanpain 2013).

Chování a vlastnosti nádorových buněk významně ovlivňují jejich vzájemné interakce, stejně jako interakce s buňkami původem z okolních tkání, přičemž všechny tyto buňky společně vytvářejí nádorové mikroprostředí. Nádorové mikroprostředí je tedy komplexní buněčná struktura nejčastěji tvořená lymfocyty, myeloidními buňkami, endotelovými buňkami a fibroblasty, která ovlivňuje invazivitu nádorových buněk, angiogenezi, hypoxii, epiteliálně-mezenchymální tranzici a rezistenci k chemoterapii (Boesch et al. 2016, Carnero et al. 2016). CSCs – podobně jako jiné kmenové buňky – jsou pak lokalizovány ve specifickém mikroprostředí zvaném niche, které je řízeno především mezibuněčnou komunikací, adherencí na extracelulární matrix, parakrinní, juxtakrinní a hormonální signalizací, přičemž všechny zmíněné faktory regulují přežívání, sebeobnovu a diferenciaci CSCs (Carnero et al. 2016).

Teorií o hierarchickém uspořádání nádoru, regulaci jeho růstu a buněčně heterogenitě různých populací v rámci nádoru existuje několik (Obr. 8). V historicky původním, tzv.

stochastickém modelu se předpokládá, že všechny nádorové buňky mají stejný tumorigenní potenciál, přičemž náhodně část buněk proliferuje a jiná část podléhá diferenciaci. Druhý, tzv. CSC model, popisuje nádor jako hierarchickou strukturu organizovanou podobně jako normální zdravé tkáně, kde pouze specifická část buněčné populace (kmenové buňky) má schopnost sebeobnovy, přičemž více diferencované progenitory mají růstový potenciál omezený. Analogicky ke tkáňově-specifickým adultním kmenovým buňkám, které jsou zodpovědné za obnovu tkání v organismu, se předpokládá, že CSCs vykazují schopnost dlouhodobé proliferace a sebeobnovy a jsou zodpovědné za zachování nádoru i za vznik ostatních více diferencovaných buněčných typů. V rámci obou modelů však může docházet ke klonální evoluci, kdy se v některých nádorových buňkách akumulují nové somatické mutace, které mohou přinášet selektivní výhody zvyšující jejich schopnost proliferace a přežití (Beck et Blanpain 2013, Akbari-Birgani et al. 2016).

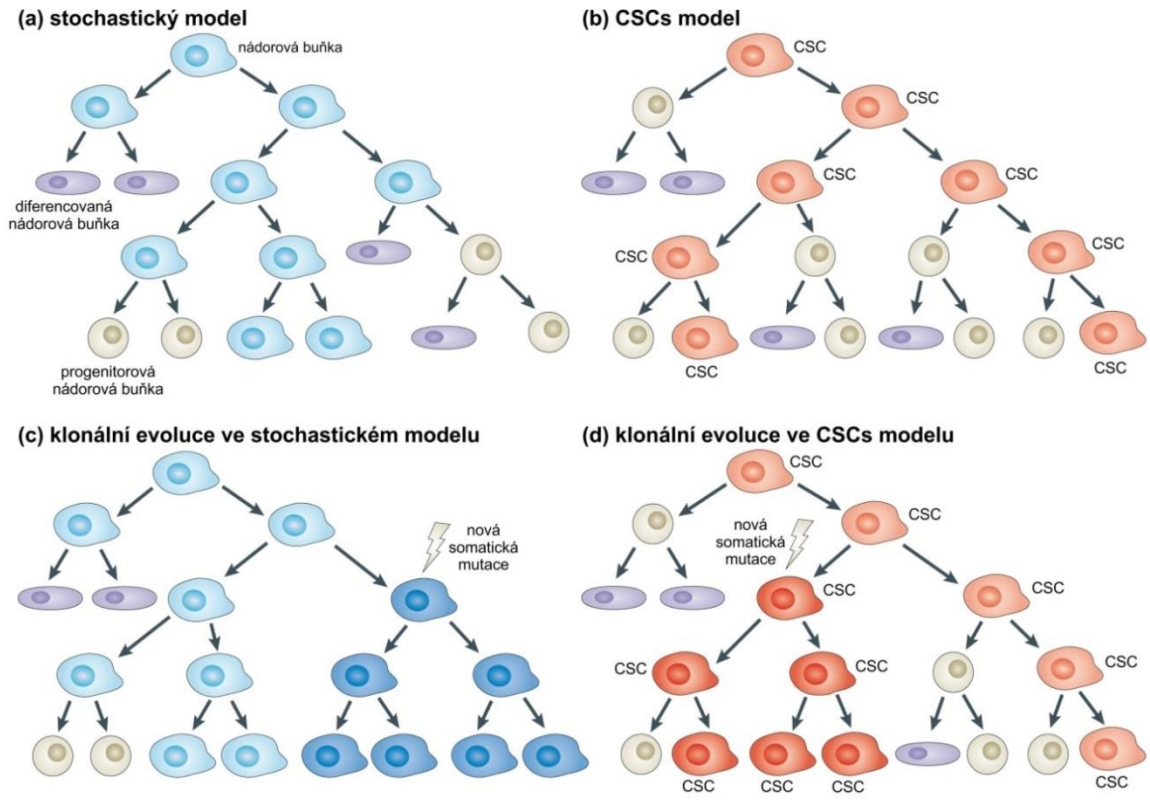

Obr. 8. Modely nádorového růstu. (a) Stochastický model, (b) CSCs model, (c) klonální evoluce ve stochastickém modelu, (d) klonální evoluce v CSCs modelu. Převzato a upraveno dle Beck et Blanpain (2013).

Teorie vzniku nádorových kmenových buněk

Výše zmíněný CSC model popisuje úlohu CSCs v udržování a růstu nádoru, samotný způsob vzniku a původ CSCs však zatím není zcela objasněn. Jednou z hypotéz je vznik CSC z tkáňově specifické adultní kmenové buňky (Obr. 9), která nese velmi podobné fenotypové znaky, tj. zejména schopnost sebeobnovy a diferenciace. Tuto hypotézu podporuje fakt, že CSCs vykazují podobně primitivní fenotyp a exprimují markery typické pro adultní kmenové buňky v příslušné zdravé tkáni. Navíc adultní kmenové buňky mohou během poměrně dlouhého přežívání ve tkáni akumulovat mutace iniciující nádorovou transformaci (Foreman et al. 2009, McDonald et al. 2009).

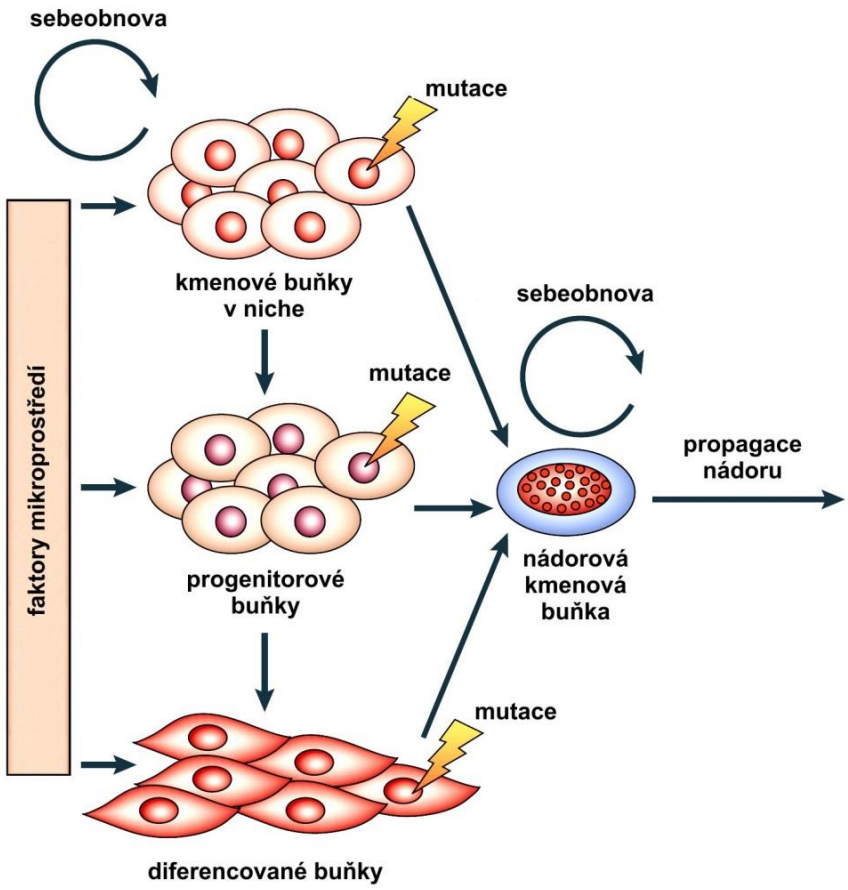

Obr. 9. Hypotézy vzniku CSCs. CSCs se podle různých hypotéz mohou vyvinout z adultních kmenových buněk, progenitorových či diferencovaných buněk na základě somatických mutací. Významnou roli v iniciaci nádoru však hraje mikroprostředí a faktory v něm obsažené. Převzato a upraveno dle Bjerkvig et al. (2005).

Podle další z hypotéz proces nádorové transformace vyvíjí silný selekční tlak na diferencované buňky, který umožňuje přežití takové buněčné populace, u níž proběhly epigenetické změny vedoucí k obnovení fenotypu kmenových buněk. Tato hypotéza předpokládá, že znovunabytí schopnosti sebeobnovy je součástí transformačního procesu. Jedná se v podstatě o modifikovaný klasický model nádorové transformace, v němž porucha diferenciace a růstové regulace je výsledkem selekčního procesu v populaci geneticky nestabilních buněk (Foreman et al. 2009).

Třetí hypotéza předpokládá vznik CSCs z omezeného množství buněčných populací zahrnujících adultní kmenové buňky i nezralé progenitorové buňky, které jsou v diferenciační hierarchii níže a jsou schopné omezené sebeobnovy. Experimentálně byla tato teorie podpořena několika studiemi, kdy zavedení a exprese onkogenního fúzního genu do hematopoetických progenitorových buněk vedlo na myším modelu k rozvoji akutní myeloidní leukémie (Foreman et al. 2009).

Detekce nádorových kmenových buněk

Jak bylo popsáno výše, základními a typickými vlastnostmi CSCs jsou tedy schopnost tumorigeneze, sebeobnovy a diferenciační potenciál pro vznik různých buněčných populací tvořících nádorovou masu. Další vlastnosti CSCs v různých typech nádorů se však mohou vzájemně lišit. Během poslední dekády proto byly vyvinuty různé metody pro ověření zejména schopností sebeobnovy a iniciace vzniku nádoru, kterými lze v podmínkách *in vitro* nebo *in vivo* potvrdit fenotyp CSCs (Skoda et al. 2014, Akbari-Birgani et al. 2016).

Za „zlatý standard“ detekčních testů fenotypu CSCs se považuje test tumorigenity *in vivo* (Clarke et al. 2006). Jeho podstatou je ověření schopnosti sebeobnovy nádorových buněk a schopnosti tvořit nádor po injikaci testovaných buněk do imunodeficientního zvířete. Nejčastěji se používá kmen myší NOD/SCID (non-obese diabetic/severe combined immunodeficiency), popřípadě odvozené kmeny NSG a NOG (McDermot et al. 2010). Tumorigenita je poté stanovena podílem zvířat s nádorem k celkovému počtu injikovaných zvířat. Pokud se srovnává více buněčných frakcí či populací, mohou být dalšími kritérii jejich hodnocení např. velikost vytvořeného nádoru, doba od injikace do vytvoření nádoru o určité velikosti nebo množství injikovaných buněk. Schopnost sebeobnovy testovaných buněk je následně nutné ověřit sériovou transplantací, tzn. izolováním CSCs z nádoru vytvořeného v myši a opakovanou injikací těchto buněk další sérii imunodeficientních zvířat (O´Brien et al. 2010).

Z důvodu rychlejšího provedení (a také nižší finanční náročnosti) lze ověřit fenotyp CSCs pomocí různých testů *in vitro*, které rovněž mají dostatečnou citlivost pro detekci řídce zastoupené populace CSCs a umožňují i kvantitativní zhodnocení experimentu. Mezi nejčastější testy patří metody založené na detekci tvorby kolonií z jediné buňky (colony-forming unit [CFU] assay), detekci tvorby buněčných sfér (sphere assay), detekci schopnosti zadržení detekční značky v buňce (label-retention assay), stanovení vedlejší populace (side population analysis) a na hodnocení aktivity aldehyddehydrogenázy (ALDH assay).

CFU assay zvaná též clonogenic assay (test klonogenity) ověřuje schopnost jednotlivých adherentních buněk tvořit kolonie. Po vysetí suspenze jednotlivých buněk na kultivační misku, která může být případně ošetřena přípravkem Matrigel™, se hodnotí vznik a nárůst kolonií, které je možno opakovaně pasážovat (Clarke et al. 2006, Cao et al. 2011). Kultivace v tomto případě probíhá v dvourozměrných podmínkách a v médiu s přídavkem séra. Třírozměrnou alternativou tohoto testu je kultivace buněk v bezsérovém tekutém nebo semisolidním médiu s definovaným obsahem růstových faktorů, kdy je při vzniku kolonie z jediné buňky potvrzena vedle schopností sebeobnovy a klonogenity i nezávislost buněk na substrátu (Tirino et al. 2008). Kulovité kolonie jsou označovány jako sféry a pro potvrzení úspěšnosti testu je nutné jednotlivé sféry enzymaticky rozvolnit na buněčnou suspenzi. Po převedení takto získané buněčné suspenze do vhodných podmínek se pak v případě úspěšné verifikace z jednotlivých buněk opět vytvoří nové sféry.

Výsledkem label-retention assay je rozlišení populací s rozdílnou délkou buněčného cyklu v rámci testované buněčné suspenze. Využití této metody používané pro detekci CSCs je založeno na předpokladu, že kmenové buňky se od ostatních buněčných typů odlišují prodlouženým buněčným cyklem. Vlastní metoda se skládá ze dvou navazujících fází. V první z nich se do buněk inkorporuje značka, která se může vázat na DNA (např. bromodeoxyuridin nebo H^3-thymidin), fosfolipidy membrán (např. DiI nebo PKH26) či po enzymatickém štěpení esterázami na intracelulární proteiny (např. carboxyfluorescein diacetát succinimidyl ester). Ve druhé fázi pak dochází ke snižování obsahu značky přímo úměrně rychlosti buněčného dělení: pomaleji se dělící buňky vykazují silnější signál, na jehož základě je lze odlišit, případně separovat (Moore et al. 2012, Skoda et al. 2014). Novou modifikací tohoto testu je použití histonu H2B spojeného s fluorescenčním proteinem pod kontrolou tetracyklinového responsivního elementu, kdy v přítomnosti doxycyklinu je u rychle se dělících buněk fluorescenční histon nahrazen nefluorescenčním, zatímco pomalu se dělící buňky udržují fluorescenční histon navázaný na DNA. (Hsu et Fuchs 2012).

Jak bylo popsáno výše, další z typických vlastností CSCs je zvýšená rezistence k různým xenobiotikům z důvodu exprese a aktivity membránových ABC transportérů (Richard et al. 2013). Testem pro stanovení jejich přítomnosti a funkce je detekce tzv. vedlejší populace (side population, SP), která je definovaná schopností vyloučit z cytoplazmy fluorochrom Hoechst 33342, který se váže na DNA. Test je koncipován pro využití průtokové cytometrie, kdy je při současné detekci v modré i červené části spektra (odpovídající emisním maximům volného i navázaného fluorochromu) lokalizována populace s nízkým fluorescenčním signálem posunutým směrem k modré části spektra. Pro ověření specificity a přesnosti označení vedlejší populace je vždy nutné provádět kontrolní experiment s aplikací vhodného inhibitoru transportérů ABC (Hoe et al. 2014).

Pro kmenové buňky včetně nádorových je rovněž typická exprese enzymů rodiny aldehyddehydrogenáz (ALDH), u nichž bylo popsáno 19 izoforem a které se podílejí na metabolické obraně buňky před negativními účinky aldehydů a reaktivních kyslíkových radikálů. Enzymy rodiny ALDH proto hrají významnou úlohu v chemorezistenci CSCs (Xu et al. 2015). Funkční test aktivity ALDH v CSCs je založen na intracelulárním štěpení substrátu BAAA (BODIPY aminoacetaldehyd), který volně difunduje z kultivačního média do buněk. Po vzniku fluorescenčního produktu BAA (BODIPY amino acetate) je v buňkách s aktivní ALDH detekována fluorescence, kterou lze kvantifikovat s použitím průtokové cytometrie. Současně je vhodné provést kontrolní experiment s aplikací specifického inhibitoru ALDH (např. diethylaminobenzaldehyd) sloužící pro stanovení intenzity fluorescence pozadí.

Přes výše zmíněné výhody testů *in vitro* je vždy vhodné a žádoucí získané výsledky ověřit testem tumorigenity *in vivo*, protože testy *in vitro* nemohou zcela napodobit podmínky tumorigeneze v živém organismu.

Markery nádorových kmenových buněk

Identifikace a profilování exprese specifických markerů v populaci nádorových buněk patří mezi významné a často používané metody detekce, selekce a charakterizace CSCs (Akbari-Birgani et al. 2016). Vedle detekce jednoho nebo kombinace několika membránových proteinů (CD markerů) je možné využít i identifikaci CSCs na základě exprese cytoplazmatických nebo jaderných proteinů. S použitím protilátek konjugovaných s fluorochromy proti povrchovým markerům lze pomocí metod průtokové cytometrie a sortrování izolovat buněčné populace exprimující sledovaný fenotyp CSCs. Přehled

markerů, které byly identifikovány u buněk s fenotypem CSCs v různých typech nádorových onemocnění, je uveden v tabulce 3.

Tab. 3. Přehled membránových markerů CSCs. Převzato a upraveno dle Akbari-Birgani et al. (2016), Boesch et al. (2016), Schmohl et Vallera (2016), Hadjimichael et al. (2015), Neradil et Veselska (2015), Veselska et al. (2012) a Ding et al. (2010).

Membránový marker	Typ nádoru
ABCB5	karcinom kolorekta, melanom
ABCG2	karcinom plic, hepatocelulární karcinom, adenokarcinom pankreatu, retinoblastom, melanom
CD13	hepatocelulární karcinom
CD15 (SSEA1)	gliom
CD17	karcinom ovarií
CD19	akutní lymfoblastická leukémie
CD20	melanom
CD24	karcinomy prsu, kolorekta, ovarií, adenokarcinom pankreatu, hepatocelulární karcinom
CD26	karcinom kolorekta, chronická myeloidní leukémie
CD27	Hodgkinův lymfom
CD29	karcinom kolorekta
CD34	akutní myeloblastická leukémie, akutní lymfoblastická leukémie, chronická myeloidní leukémie
CD38	akutní myeloblastická leukémie
CD44	karcinomy prsu, kolorekta, žaludku, močového měchýře, plic, prostaty, ovarií, pankreatu, hepatocelulární karcinom, sarkomy kostí
CD47	karcinom prsu, močového měchýře
CD90	karcinom plic, hepatocelulární karcinom, chronická myeloidní leukémie
CD105	sarkomy kostí, karcinom ledvin
CD117	karcinom ovarií, plic
CD133	karcinomy prsu, kolorekta, plic, prostaty, ovarií, adenokarcinom pankreatu, hepatocelulární karcinom, gliom, melanom, sarkomy kostí a měkkých tkání, meduloblastom
CD166	karcinomy kolorekta, prostaty
CD271	melanom
c-Met	adenokarcinom pankreatu
CXCR4	karcinomy prsu, plic, adenokarcinom pankreatu, gliomy
EpCAM	karcinomy kolorekta, prsu, hepatocelulární karcinom
ErbB2	karcinomy prsu, ovarií
LGR5	karcinom kolorekta
Trop-2	karcinom prostaty
α2β1 integrin	karcinom prostaty
α6 integrin	karcinom prsu, gliomy
β-catenin	karcinom kolorekta
Cytoplazmatický marker	
26s proteasom	nemalobuněčný karcinom plic
ALDH1	karcinomy prsu, plic, ovarií, kolorekta, adenokarcinom pankreatu, prostaty, melanom, Hodgkinův lymfom

Tab. 3. Pokračování

Cytoplazmatický marker	Typ nádoru
Hedgehog-Gli	karcinom prsu
Krt19	karcinom kolorekta
Nestin	gliomy, meduloblastom, ependymom, sarkomy kostí a měkkých tkání, karcinomy prostaty, prsu, ovarií, kolorekta, žaludku, plic, močového měchýře, adenokarcinom pankreatu
Nodal-Activin	adenokarcinom pankreatu
Stro-1	sarkomy kostí
Jaderný marker	
Nanog	karcinomy prsu, ovarií, plic, gliom
Klf4	karcinomy prsu, kolorekta, gliom
Sox2	meduloblastom, gliom, adenokarcinom pankreatu, karcinomy prostaty, ovárií, plic, melanom
Oct4	karcinomy ovarií, melanom

V rámci našeho výzkumu jsme se zaměřili na detekci buněk s fenotypem CSCs především u sarkomů dětského věku - a to jak v původní nádorové tkáni, tak v odpovídajících buněčných liniích derivovaných z těchto vzorků nádorové tkáně. V deseti tkáňových vzorcích od sedmi pacientů s rabdomyosarkomem jsme detekovali vysoké zastoupení buněk exprimujících nestin a sporadické zastoupení buněk exprimujících CD133. V pěti liniích derivovaných z těchto nádorů byly nalezeny buňky exprimující oba detekované CSC markery a u sledovaných linií byla navíc potvrzena exprese genů typicky exprimovaných v kmenových buňkách (Oct3/4, nucleostemin). Z toho důvodu byly provedeny funkční testy detekce CSCs *in vitro* a *in vivo*, které u buněk linie NSTS-11 potvrdily schopnost klonogenity a tumorigenity (Sana et al. 2011).

Výše zmíněný membránový glykoprotein CD133 (prominin-1) je jedním z nejčastěji uváděných markerů, které jsou využívány pro identifikaci kmenových buněk obecně, a jeho glykosylovaná forma s epitopem označovaným jako AC133 se považuje za marker vhodný pro identifikaci CSCs v různých typech nádorů. Při studiu exprese CD133 u pediatrických sarkomů jsme jako první zaznamenali a detailně popsali atypickou lokalizaci CD133 v jádrech buněk celkem 5 linií derivovaných z rabdomyosarkomů. Incidence jaderné lokalizace CD133 se u jednotlivých linií pohybovala od 3 do 8 % a nezávisela na typu použité protilátky. Výsledky byly následně verifikovány konfokální a transmisní elektronovou mikroskopií se třemi různými specifickými protilátkami, dále byla provedena separace jader a ověření intracelulární lokalizace CD133 pomocí imunoblotingu (Nunukova et al. 2015).

V podrobné studii na modelu nejčastěji se vyskytujících sarkomů u dětí (tj. Ewingův sarkomu, osteosarkomu a rabdomyosarkomu) jsme analyzovali expresi tří kandidátních

markerů CSCs, které jsou v literatuře zmiňovány právě v souvislosti se sarkomy. Proteiny ABCG2, CD133 a nestin jsme detekovali jak v nádorové tkáni, tak v buněčných liniích derivovaných z této tkáně a byla porovnávána exprese jednotlivých markerů vždy v původním nádoru a v odpovídající buněčné linii. Obecně byla vyšší frekvence buněk exprimujících ABCG2 a CD133 zaznamenána v derivovaných buněčných liniích ve srovnání s původní nádorovou tkání, což by mohlo souviset se selekční výhodou buněk s tímto fenotypem v prostředí *in vitro*. Naproti tomu funkční test *in vivo* v imunodeficientních NGS myších prokázal, že tumorigenní potenciál nádorových buněk není asociován s expresí vysoké hladiny ABCG2 a CD133. Následnou analýzou exprese markerů buněčné sebeobnovy jsme prokázali přímou souvislost mezi tumorigenezí nádorových buněk a zvýšenou expresí Sox2. Nejvyšší exprese tohoto transkripčního faktoru byla zaznamenána právě u buněčných linií, které byly schopny po injikaci do imunodeficientní myši vytvářet nádory. Následně byla přítomnost Sox2-pozitivních buněk zpětně prokázána i v odpovídajících primárních nádorech a dále ve všech xenograftových nádorech vzniklých z těchto buněčných linií, kde navíc jejich četnost byla mnohem vyšší než v původní nádorové tkáni. Z uvedených výsledků je tedy zřejmé, že bez ohledu na míru exprese ABCG2, CD133 nebo nestinu pouze buňky se zvýšenou expresí Sox2 mají schopnost iniciovat vznik nádoru, a tudíž se shodují s fenotypem nádorových kmenových buněk (Skoda et al. 2016a).

Vedle studia solidních nádorů u dětí jsme se rovněž zabývali i jedním vysoce maligním typem nádoru, který typicky postihuje dospělou populaci a patří k nádorovým onemocněním s nejvyšší mortalitou – duktálním karcinomem pankreatu (pancreatic ductal adenocarcinoma, PDAC). Horší prognóza se při tomto onemocnění přičítá pozdní diagnostice z důvodu absence časných symptomů, typického rozšíření metastáz a vysoké rezistence primárního tumoru na chemoterapii i radioterapii (Seufferlein et al. 2012). Podobně jako u jiných solidních nádorů, i u PDAC byly popsány CSCs, pro jejichž identifikaci se využívá specifická kombinace markerů, kterou však publikované studie definují rozdílně (Li et al. 2007, Hermann et al. 2007). Zabývali jsme se proto – jako vůbec první – společnou expresí markerů CD24, CD44, EpCAM a CD133 a naše výsledky prokázaly přítomnost CD24/CD44/EpCAM/CD133-pozitivní subpopulace buněk ve třech buněčných liniích derivovaných ze vzorků nádorové tkáně PDAC. Buněčná linie P28B, v níž zastoupení této subpopulace přesahovalo 70 %, byla derivována ze vzorku nádoru pacienta, který vykazoval nejkratší dobu přežití, a expresní profilování navíc potvrdilo u této buněčné linie zvýšenou expresi protumorigenních genů oproti ostatním zkoumaným liniím (Skoda et al. 2016b).

Terapie cílená na nádorové kmenové buňky

Klinický význam přítomnosti populace CSCs v solidních nádorech spočívá ve dvou zásadních vlastnostech CSCs. Jednak bylo prokázáno, že CSCs jsou schopné indukovat tumorigenezi v imunodeficientních myších, což vede k domněnce, že CSCs jsou v organismu zodpovědné za tvorbu metastáz. U některé typů CSCs je jejich fenotyp navíc ovlivňován geny asociovanými s epiteliálně-mezenchymální tranzicí (Beck et Blanpain 2013, Mani et al. 2008). Vedle toho vykazují CSCs i rezistenci vůči různým cytotoxickým látkám i vůči radioterapii, čímž snižují účinnost konvenční protinádorové léčby a mohou být zodpovědné za relaps onemocnění. Tyto hypotézy jsou v souladu s dosud publikovanými studiemi, které ukazují, že stavy remise nebo minimální reziduální nemoci, které často uniknou klinické diagnostice, jsou zapříčiněny CSCs, které odolaly původní léčbě. Navíc během chemoterapie pravděpodobně dochází k vyselektování buněčné populace s vysokým zastoupením CSCs a relabující nádory tak obsahují více CSCs než nádory primární. Dále bylo prokázáno, že u různých nádorových onemocnění koreluje četnost buněk exprimujících specifické markery CSCs s horší klinickou prognózou a rovněž predikuje horší odpověď vůči protinádorové terapii (Boesch et al. 2016).

Vedle aktivních obranných mechanismů, kterými jsou exprese ABC transportérů a aktivita ALDH, přispívá k celkové chemorezistenci CSCs také jejich schopnost dormance, tedy zástavy buněčného cyklu, popřípadě jeho prodloužení, což snižuje citlivost CSCs k chemoterapeutikům a inhibitorům tyrozinkináz, které primárně cílí na proliferující nádorové buňky (Visvader et Lindeman 2008, Li et Bhatia 2011). Tento terapeutický problém lze vyřešit aktivací buněčného cyklu dormantních CSCs např. pomocí As_2O_3 nebo interferonu-α a následnou aplikací konvenční protinádorové léčby. Další možností je použití epigenetických modulátorů - např. HDACi - v kombinaci s tyrozinkinázovými inhibitory, což se osvědčilo při eradikaci dormantních leukemických kmenových buněk (Trumpp et al. 2010, Zhang et al. 2010).

Dalšími přístupy v hledání látek a postupů vhodných pro terapii cílenou na CSCs je „high-throughput screening“ potenciálně účinných molekul, nebo kombinace známých léčiv se syntetickými protilátkami, oligonukleotidy či rekombinantními proteiny. U nově popsaných, ale i u konvenčních chemoterapeutik pravděpodobně existují zatím neprozkoumané tzv. „off-target“ účinky, které by se mohly v protinádorové terapii také uplatňovat. V současné době se rovněž rozvíjí terapie s použitím nanotechnologií, založená

především na snaze dopravit účinnou látku přímo k cílovým buňkám, tedy k CSCs (Carnero et al. 2016).

Vlastní publikace vztahující se k tématu

- Skoda J, Hermanova M, Loja T, Nemec P, **Neradil J**, Karasek P, Veselska R. Co-Expression of Cancer Stem Cell Markers Corresponds to a Pro-Tumorigenic Expression Profile in Pancreatic Adenocarcinoma. PLoS One 11: e0159255, 2016.
- Skoda J, Nunukova A, Loja T, Zambo I, **Neradil J**, Mudry P, Zitterbart K, Hermanova M, Hampl A, Sterba J, Veselska R. Cancer stem cell markers in pediatric sarcomas: Sox2 is associated with tumorigenicity in immunodeficient mice. Tumor Biology 37: 9535-9548, 2016.
- Nunukova A, **Neradil J**, Skoda J, Jaros J, Hampl A, Sterba J, Veselska R. Atypical nuclear localization of CD133 plasma membrane glycoprotein in rhabdomyosarcoma cell lines. International Journal of Molecular Medicine 36: 65-72, 2015.
- **Neradil J**, Veselska R. Nestin as a marker of cancer stem cells. Cancer Science 106: 803-811, 2015.
- Skoda J, **Neradil J**, Veselská R. Funkční testy pro detekci nádorových kmenových buněk. Klinická Onkologie 27 (Suppl 1): S42-47, 2014.
- Veselska R, Skoda J, **Neradil J**. Detection of cancer stem cell markers in sarcomas. Klinická Onkologie 25 (Suppl 2): 2S16-20, 2012.
- Sana J, Zambo I, Skoda J, **Neradil J**, Chlapek P, Hermanova M, Mudry P, Vasikova A, Zitterbart K, Hampl A, Sterba J, Veselska R. CD133 expression and identification of CD133/nestin positive cells in rhabdomyosarcomas and rhabdomyosarcoma cell lines. Analytical Cellular Pathology 34: 303-318, 2011.
- Krupkova O Jr, Loja T, Redova M, **Neradil J**, Zitterbart K, Sterba J, Veselska R. Analysis of nuclear nestin localization in cell lines derived from neurogenic tumors. Tumour Biology 32: 631-639, 2011.
- Veselska R, Kuglik P, Cejpek P, Svachova H, **Neradil J**, Loja T, Relichova J. Nestin expression in the cell lines derived from glioblastoma multiforme. BMC Cancer 6: 32, 2006.

6. ZÁVĚR

I přes neustálou snahu o vyvíjení efektivních terapeutických přístupů a režimů v léčbě mnoha typů malignit dětského věku, zůstávají nádorová onemocnění druhým nejčastějším důvodem úmrtí (po úrazech) u dětí mladších 15 let, přičemž významné procento přežívajících trpí pozdními následky protinádorové léčby. Z tohoto důvodu je jedním z hlavních cílů dětské onkologie porozumění biologickým vlastnostem nádorových onemocnění, která se typicky vyskytují v tomto věkovém období, protože rychlá a přesná diagnóza následovaná vhodnou a efektivní léčbou může vést k vyléčení nebo alespoň k významnému prodloužení doby přežití pacientů a současně může snížit terapeutickou zátěž, která s sebou často přináší riziko pozdních následků léčby (Smith et Reaman 2015).

Současná průměrná míra přežití nádorového onemocnění dosahuje u dětí a adolescentů přibližně 80 % za použití multimodální terapie včetně konvenčních chemoterapeutik. U mnoha malignit však bylo dosaženo jistého maxima a současná léčba nepřináší další zlepšení (Rossig et al. 2011). Některá nádorová onemocnění (např. akutní lymfoblastická leukémie, Wilmsův tumor, některé typy lymfomů aj.) se daří léčit s vysokou úspěšností, kdy pětiletého přežití dosahuje 90 % pacientů, ale u jiných (např. high-grade gliomy, rabdomyosarkom, osteosarkom, Ewingův sarkom) je pokrok v léčbě omezen především z důvodu rozvinutí rezistence vůči použité léčbě a omezenému množství klinických studií na dětských pacientech (Pui et al. 2011, Smith et Reaman 2015).

Aktuálně se jako velmi perspektivní přístup jeví personalizovaná terapie, jejímž cílem je zvyšování efektivity a snižování toxicity léčby jejím specifickým zacílením na nádorové buňky nebo okolní podpůrné stroma. Cílená terapie vychází z předpokladů, že jsou popsány specifické markery nebo biologické vlastnosti, které odlišují maligní buňky od buněk zdravé tkáně. Podařilo se identifikovat signální dráhy, které jsou výrazně aktivní v nádorových tkáních, a některé z nich hrají významnou roli v mnoha typech nádorů nezávisle na věku pacienta. Určité povrchové markery jsou relativně specifické pro maligní buňky a tím pádem jsou i vhodnými kandidáty na tzv. tumor-associated antigens, jež lze využít jako cíle v personalizované protinádorové terapii. Je však třeba podotknout, že nádorová onemocnění v dětském věku často vykazují odlišné histologické vlastnosti oproti stejnému typu onemocnění v dospělosti, podobně se může lišit toxicita léčby v závislosti na věku. Na druhou stranu vzrůstající množství znalostí o biologické podstatě nádorů a zjištění, že protinádorová

léčiva určená pro dospělé zasahují stejné cíle (dráhy) i u dětí a adolescentů, mohou urychlit vývoj cílené terapie i pro tuto skupinu pacientů (Bernstein 2011).

U některých druhů nádorových onemocnění byly zaznamenány dědičné predispozice a specifické germinální mutace, které výrazně zvyšují riziko vzniku těchto nemocí (např. karcinom prsu, familiární adenomatózní polypóza aj.). V posledních dekádách byla odhalena genetická podstata několika nádorových onemocnění a návazně byly spuštěny diagnostické a screeningové programy zaměřené na mutace rizikových genů (např. *BRCA1*, *BRCA2*, *PTEN*, *APC*). Mutační analýza vybraných genů je proto důležitá pro genetické poradenství, neboť pomáhá zvyšovat pravděpodobnost přežívání, upřesňuje prognózu u přenašečů a umožňuje volbu vhodného preventivního opatření (Kamps et al. 2017).

Současně se zvyšuje množství testovaných látek se slibnými výsledky pro cílenou terapii různých malignit u dětí i dospělých, přičemž zásadní význam spočívá v molekulární charakterizaci nádoru každého pacienta. Vývoj nových cílených léčiv by neměl vést pouze ke zvýšení přežívání pacientů, ale také ke snížení léčebných dávek a tím k omezení vedlejších účinků cytotoxické chemoterapie. Významným úkolem je také optimální kombinace cílených léčiv s konvenčními chemoterapeutiky (Macy et al. 2008). Otázkou však zůstává, jak správně sestavit a zavést klinické studie, které odhalí efektivní strategie ke zlepšení výsledků léčby u skupiny rezistentních malignit vykazujících genetické změny. Narůstající množství nových cílených léčiv vyžaduje vetší mezinárodní spolupráci v testování těchto látek a v případných modifikacích terapie. Navíc individuální rozdíly ve farmakodynamice protinádorových léčiv, které mohou být ovlivněny prostředím či podmíněny geneticky, vedou k rozdílům v účinnosti a toxicitě léčby (Pui et al. 2011).

Výzkum biologických vlastností solidních nádorů u dětí tak představuje základní východisko k získávání poznatků o specifických odlišnostech od nádorů dospělých a může přispívat k vyvíjení inovovaných postupů, které zlepší účinnost současné protinádorové léčby.

7. LITERATURA

Ablain J, de The H. Revisiting the differentiation paradigm in acute promyelocytic leukemia. Blood 117: 5795-5802, 2011.

Ackermann M, Morse BA, Delventhal V, Carvajal IM, Konerding MA. Anti-VEGFR2 and anti-IGF-1R-Adnectins inhibit Ewing's sarcoma A673-xenograft growth and normalize tumor vascular architecture. Angiogenesis 15: 685-695, 2012.

Akbari-Birgani S, Paranjothy T, Zuse A, Janikowski T, Cieslar-Pobuda A, Likus W, Urasinska E, Schweizer F, Ghavami S, Klonisch T, Los MJ. Cancer stem cells, cancer-initiating cells and methods for their detection. Drug Discovery Today 21: 836-842, 2016.

Alizadeh F, Bolhassani A, Khavari A, Bathaie SZ, Naji T, Bidgoli SA. Retinoids and their biological effects against cancer. International Immunopharmacology 18: 43-49, 2014.

Amit I, Wides R, Yarden Y. Evolvable signaling networks of receptor tyrosine kinases: relevance of robustness to malignancy and to cancer therapy. Molecular Systems Biology 3: 151, 2007.

Arts FA, Chand D, Pecquet C, Velghe AI, Constantinescu S, Hallberg B, Demoulin JB. PDGFRB mutants found in patients with familial infantile myofibromatosis or overgrowth syndrome are oncogenic and sensitive to imatinib. Oncogene 35: 3239-3248, 2016.

Assaraf YG. Molecular basis of antifolate resistance. Cancer Metastasis Reviews 26: 153-181, 2007.

Babiak RM, Campello AP, Carnieri EG, Oliveira MB. Methotrexate: pentose cycle and oxidative stress. Cell Biochemistry and Function 16: 283-293, 1998.

Bache KG, Slagsvold T, Stenmark H. Defective downregulation of receptor tyrosine kinases in cancer. EMBO Journal 23: 2707-2712, 2004.

Baggott JE, Morgan SL, Vaughn WH. Differences in methotrexate and 7-hydroxymethotrexate inhibition of folate-dependent enzymes of purine nucleotide biosynthesis. The Biochemical Journal 300 (Pt 3): 627-629, 1994.

Barr FG, Nauta LE, Davis RJ, Schafer BW, Nycum LM, Biegel JA. In vivo amplification of the PAX3-FKHR and PAX7-FKHR fusion genes in alveolar rhabdomyosarcoma. Human Molecular Genetics 5: 15-21, 1996.

Bartyik K, Turi S, Orosz F, Karg E. Methotrexate inhibits the glyoxalase system in vivo in children with acute lymphoid leukaemia. European Journal of Cancer 40: 2287-2292, 2004.

Bastian L, Einsiedel HG, Henze G, Seeger K, Shalapour S. The sequence of application of methotrexate and histone deacetylase inhibitors determines either a synergistic or an antagonistic response in childhood acute lymphoblastic leukemia cells. Leukemia 25: 359-361, 2011.

Beck B, Blanpain C. Unravelling cancer stem cell potential. Nature Reviews Cancer 13:727-738, 2013.

Benbrook DM. Refining retinoids with heteroatoms. Mini Reviews in Medicinal Chemistry 2: 277-283, 2002.

Bernstein ML. Targeted therapy in pediatric and adolescent oncology. Cancer 117: 2268-2274, 2011.

Bertino JR. Cancer research: from folate antagonism to molecular targets. Best practice & research Clinical haematology 22: 577-582, 2009.

Bjerkvig R, Tysnes BB, Aboody KS, Najbauer J, Terzis AJ. Opinion: the origin of the cancer stem cell: current controversies and new insights. Nature Reviews. Cancer 5: 899-904, 2005.

Blachly JS, Baiocchi RA. Targeting PI3-kinase (PI3K), AKT and mTOR axis in lymphoma. British Journal of Haematology 167: 19-32, 2014.

Blandford MC, Barr FG, Lynch JC, Randall RL, Qualman SJ, Keller C. Rhabdomyosarcomas utilize developmental, myogenic growth factors for disease advantage: a report from the Children's Oncology Group. Pediatric Blood and Cancer 46: 329-338, 2006.

Blume-Jensen P, Hunter T. Oncogenic kinase signalling. Nature 411: 355-365, 2001.

Boesch M, Sopper S, Zeimet AG, Reimer D, Gastl G, Ludewig B, Wolf D. Heterogeneity of Cancer Stem Cells: Rationale for Targeting the Stem Cell Niche. Biochimica et Biophysica Acta 1866: 276-289, 2016.

Bolden JE, Peart MJ, Johnstone RW. Anticancer activities of histone deacetylase inhibitors. Nature Reviews Drug Discovery 5: 769-784, 2006.

Bozzi F, Tamborini E, Negri T, Pastore E, Ferrari A, Luksch R, Casanova M, Pierotti MA, Bellani FF, Pilotti S. Evidence for activation of KIT, PDGFRalpha, and PDGFRbeta receptors in the Ewing sarcoma family of tumors. Cancer 109: 1638-1645, 2007.

Bushue N, Wan YJ. Retinoid pathway and cancer therapeutics. Advanced Drug Delivery Reviews 62: 1285-1298, 2010.

Caetano NN, Campello AP, Carnieri EG, Kluppel ML, Oliveira MB. Effect of methotrexate (MTX) on NAD(P)+ dehydrogenases of HeLa cells: malic enzyme, 2-oxoglutarate and isocitrate dehydrogenases. Cell Biochemistry and Function 15: 259-264, 1997.

Cao L, Yu Y, Bilke S, Walker RL, Mayeenuddin LH, Azorsa DO, Yang F, Pineda M, Helman LJ, Meltzer PS. Genome-wide identification of PAX3-FKHR binding sites in rhabdomyosarcoma reveals candidate target genes important for development and cancer. Cancer Research 70: 6497-6508, 2010.

Cao L, Zhou Y, Zhai B, Liao J, Xu W, Zhang R, Li J, Zhang Y, Chen L, Qian H, Wu M, Yin Z. Sphere-forming cell subpopulations with cancer stem cell properties in human hepatoma cell lines. BMC Gastroenterology 11: 71, 2011.

Carnero A, Garcia-Mayea Y, Mir C, Lorente J, Rubio IT, ME LL. The cancer stem-cell signaling network and resistance to therapy. Cancer Treatment Reviews 49: 25-36, 2016.

Carrasco MP, Enyedy EA, Krupenko NI, Krupenko SA, Nuti E, Tuccinardi T, Santamaria S, Rossello A, Martinelli A, Santos MA. Novel folate-hydroxamate based antimetabolites: synthesis and biological evaluation. Medicinal Chemistry 7: 265-274, 2011.

Chabner BA, Roberts TG, Jr. Timeline: Chemotherapy and the war on cancer. Nature Reviews Cancer 5: 65-72, 2005.

Chan ES, Cronstein BN. Mechanisms of action of methotrexate. Bulletin of the Hospital for Joint Disease 71 (Suppl 1): S5-8, 2013.

Chang CJ, Hung MC. The role of EZH2 in tumour progression. British Journal of Cancer 106: 243-247, 2012.

Chen GJ, Karajannis MA, Newcomb EW, Zagzag D. Overexpression and activation of epidermal growth factor receptor in hemangioblastomas. Journal of Neurooncology 99: 195-200, 2010.

Chen W, Dong J, Haiech J, Kilhoffer MC, Zeniou M. Cancer Stem Cell Quiescence and Plasticity as Major Challenges in Cancer Therapy. Stem Cells International 2016: 1740936, 2016.

Chlapek P, Neradil J, Redova M, Zitterbart K, Sterba J, Veselska R. The ATRA-induced differentiation of medulloblastoma cells is enhanced with LOX/COX inhibitors: an analysis of gene expression. Cancer Cell International 14: 51, 2014.

Chlapek P, Redova M, Zitterbart K, Hermanova M, Sterba J, Veselska R. Enhancement of ATRA-induced differentiation of neuroblastoma cells with LOX/COX inhibitors: an expression profiling study. Journal of Experimental and Clinical Cancer Research 29: 45, 2010.

Clarke MF, Dick JE, Dirks PB, Eaves CJ, Jamieson CH, Jones DL, Visvader J, Weissman IL, Wahl GM. Cancer stem cells--perspectives on current status and future directions: AACR Workshop on cancer stem cells. Cancer Research 66: 9339-9344, 2006.

Cohen IJ, Wolff JE. How long can folinic acid rescue be delayed after high-dose methotrexate without toxicity? Pediatric Blood and Cancer 61: 7-10, 2014.

Cojoc M, Mabert K, Muders MH, Dubrovska A. A role for cancer stem cells in therapy resistance: cellular and molecular mechanisms. Seminars in Cancer Biology 31: 16-27, 2015.

Cristea S, Sage J. Is the Canonical RAF/MEK/ERK Signaling Pathway a Therapeutic Target in SCLC? Journal of Thoracic Oncologyl 11: 1233-1241, 2016.

Crose LE, Linardic CM. Receptor tyrosine kinases as therapeutic targets in rhabdomyosarcoma. Sarcoma 2011: 756982, 2011.

Cruz FD, Matushansky I. Solid tumor differentiation therapy - is it possible? Oncotarget 3: 559-567, 2012.

Cunningham TJ, Duester G. Mechanisms of retinoic acid signalling and its roles in organ and limb development. Nature Reviews Molecular Cell Biology 16: 110-123, 2015.

De Braekeleer E, Douet-Guilbert N, De Braekeleer M. RARA fusion genes in acute promyelocytic leukemia: a review. Expert Review of Hematology 7: 347-357, 2014.

de Oliveira MR. Vitamin A and Retinoids as Mitochondrial Toxicants. Oxidative Medicine and Cellular Longevity 2015: 140267, 2015.

Dell'Aversana C, Lepore I, Altucci L. HDAC modulation and cell death in the clinic. Experimental Cell Research 318: 1229-1244, 2012.

Dewaele B, Floris G, Finalet-Ferreiro J, Fletcher CD, Coindre JM, Guillou L, Hogendoorn PC, Wozniak A, Vanspauwen V, Schoffski P, Marynen P, Vandenberghe P, Sciot R, Debiec-Rychter M. Coactivated platelet-derived growth factor receptor α and epidermal growth factor receptor are potential therapeutic targets in intimal sarcoma. Cancer Research 70: 7304-7314, 2010.

di Masi A, Leboffe L, De Marinis E, Pagano F, Cicconi L, Rochette-Egly C, Lo-Coco F, Ascenzi P, Nervi C. Retinoic acid receptors: from molecular mechanisms to cancer therapy. Molecular Aspects of Medicine 41: 1-115, 2015.

Diede SJ, Guenthoer J, Geng LN, Mahoney SE, Marotta M, Olson JM, Tanaka H, Tapscott SJ. DNA methylation of developmental genes in pediatric medulloblastomas identified by denaturation analysis of methylation differences. Proceedings of the National Academy of Sciences of the USA 107: 234-239, 2010.

Ding XW, Wu JH, Jiang CP. ABCG2: a potential marker of stem cells and novel target in stem cell and cancer therapy. Life Sciences 86: 631-637, 2010.

Einsiedel HG, Kawan L, Eckert C, Witt O, Fichtner I, Henze G, Seeger K. Histone deacetylase inhibitors have antitumor activity in two NOD/SCID mouse models of B-cell precursor childhood acute lymphoblastic leukemia. Leukemia 20: 1435-1436, 2006.

Esteller M. CpG island hypermethylation and tumor suppressor genes: a booming present, a brighter future. Oncogene 21: 5427-5440, 2002.

Fleuren ED, Roeffen MH, Leenders WP, Flucke UE, Vlenterie M, Schreuder HW, Boerman OC, van der Graaf WT, Versleijen-Jonkers YM. Expression and clinical relevance of MET and ALK in Ewing sarcomas. International Journal of Cancer 133: 427-436, 2013.

Fleuren ED, Versleijen-Jonkers YM, Boerman OC, van der Graaf WT. Targeting receptor tyrosine kinases in osteosarcoma and Ewing sarcoma: current hurdles and future perspectives. Biochimica et Biophysica Acta 1845: 266-276, 2014.

Foreman KE, Rizzo P, Osipo C, Miele L. The Cancer Stem Cell Hypothesis. In: Stem Cells and Cancer, edited by Bagley R and Teicher B: Humana Press, 3-14, 2009.

Freemantle SJ, Spinella MJ, Dmitrovsky E. Retinoids in cancer therapy and chemoprevention: promise meets resistance. Oncogene 22: 7305-7315, 2003.

Ganti R, Skapek SX, Zhang J, Fuller CE, Wu J, Billups CA, Breitfeld PP, Dalton JD, Meyer WH, Khoury JD. Expression and genomic status of EGFR and ErbB-2 in alveolar and embryonal rhabdomyosarcoma. Modern Pathology 19: 1213-1220, 2006.

Gee MF, Tsuchida R, Eichler-Jonsson C, Das B, Baruchel S, Malkin D. Vascular endothelial growth factor acts in an autocrine manner in rhabdomyosarcoma cell lines and can be inhibited with all-trans-retinoic acid. Oncogene 24: 8025-8037, 2005.

Genestier L, Paillot R, Quemeneur L, Izeradjene K, Revillard JP. Mechanisms of action of methotrexate. Immunopharmacology 47: 247-257, 2000.

Gerits N, Kostenko S, and Moens U. In vivo functions of mitogen-activated protein kinases: conclusions from knock-in and knock-out mice. Transgenic Research 16: 281-314, 2007.

Guessous F, Li Y, Abounader R. Signaling pathways in medulloblastoma. Journal of Cellular Physiology 217: 577-583, 2008.

Hadjimichael C, Chanoumidou K, Papadopoulou N, Arampatzi P, Papamatheakis J, Kretsovali A. Common stemness regulators of embryonic and cancer stem cells. World Journal of Stem Cells7: 1150-84, 2015.

Hanahan D, Weinberg RA. The hallmarks of cancer. Cell 100: 57-70, 2000.

Hegde M, Moll AJ, Byrd TT, Louis CU, Ahmed N. Cellular immunotherapy for pediatric solid tumors. Cytotherapy 17: 3-17, 2015.

Hermann PC, Huber SL, Herrler T, Aicher A, Ellwart JW, Guba M, Bruns CJ, Heeschen C. Distinct populations of cancer stem cells determine tumor growth and metastatic activity in human pancreatic cancer. Cell Stem Cell 1: 313-323, 2007.

Hill VK, Underhill-Day N, Krex D, Robel K, Sangan CB, Summersgill HR, Morris M, Gentle D, Chalmers AD, Maher ER, Latif F. Epigenetic inactivation of the RASSF10 candidate tumor suppressor gene is a frequent and an early event in gliomagenesis. Oncogene 30: 978-989, 2011.

Hoe SL, Tan LP, Jamal J, Peh SC, Ng CC, Zhang WC, Ahmad M, Khoo AS. Evaluation of stem-like side population cells in a recurrent nasopharyngeal carcinoma cell line. Cancer Cell International 14: 101, 2014.

Holmboe L, Andersen AM, Morkrid L, Slordal L, Hall KS. High dose methotrexate chemotherapy: pharmacokinetics, folate and toxicity in osteosarcoma patients. British Journal of Clinical Pharmacology 73: 106-114, 2012.

Hsu YC, Fuchs E. A family business: stem cell progeny join the niche to regulate homeostasis. Nature Reviews Molecular Cell Biology 13: 103-114, 2012.

Huang C, Hsu P, Hung Y, Liao Y, Liu C, Hour C, Kao M, Tsay GJ, Hung H, Liu GY. Ornithine decarboxylase prevents methotrexate-induced apoptosis by reducing intracellular reactive oxygen species production. Apoptosis 10: 895-907, 2005.

Huang WY, Yang PM, Chang YF, Marquez VE, Chen CC. Methotrexate induces apoptosis through p53/p21-dependent pathway and increases E-cadherin expression through downregulation of HDAC/EZH2. Biochemical Pharmacology 81: 510-517, 2011.

Jahovic N, Cevik H, Sehirli AO, Yegen BC, Sener G. Melatonin prevents methotrexate-induced hepatorenal oxidative injury in rats. Journal of Pineal Research 34: 282-287, 2003.

Kalapos MP. The tandem of free radicals and methylglyoxal. Chemico-Biological Interactions 171: 251-271, 2008.

Kalia M. Personalized oncology: recent advances and future challenges. Metabolism: Clinical and Experimental 62 (Suppl 1): S11-14, 2013.

Kalman B, Szep E, Garzuly F, Post DE. Epidermal growth factor receptor as a therapeutic target in glioblastoma. Neuromolecular Medicine 15: 420-434, 2013.

Kamps R, Brandao RD, Bosch BJ, Paulussen AD, Xanthoulea S, Blok MJ, Romano A. Next-Generation Sequencing in Oncology: Genetic Diagnosis, Risk Prediction and Cancer Classification. International Journal of Molecular Sciences 18: 308, 2017.

Kamura S, Matsumoto Y, Fukushi JI, Fujiwara T, Iida K, Okada Y, Iwamoto Y. Basic fibroblast growth factor in the bone microenvironment enhances cell motility and invasion of Ewing's sarcoma family of tumours by activating the FGFR1-PI3K-Rac1 pathway. British Journal of Cancer 103: 370-381, 2010.

Kapoor GS, O'Rourke DM. Receptor tyrosine kinase signaling in gliomagenesis: pathobiology and therapeutic approaches. Cancer Biology and Therapy 2: 330-342, 2003.

Klener P jr, Klener P. Principy systémové protinádorové léčby: Grada, 2013.

Koizumi K, Nakayama M, Zhu WJ, Ito S. Characteristic effects of methylglyoxal and its degraded product formate on viability of human histiocytes: a possible detoxification pathway of methylglyoxal. Biochemical and Biophysical Research Communications 407: 426-431, 2011.

Kreuter M, Paulussen M, Boeckeler J, Gerss J, Buerger H, Liebscher C, Kessler T, Jurgens H, Berdel WE, Mesters RM. Clinical significance of Vascular Endothelial Growth Factor-A expression in Ewing's sarcoma. European Journal of Cancer 42: 1904-1911, 2006.

Krupkova O jr, Loja T, Redova M, Neradil J, Zitterbart K, Sterba J, Veselska R. Analysis of nuclear nestin localization in cell lines derived from neurogenic tumors. Tumour Biology 32: 631-639, 2011.

Krzyzankova M, Chovanova S, Chlapek P, Radsetoulal M, Neradil J, Zitterbart K, Sterba J, Veselska R. LOX/COX inhibitors enhance the antineoplastic effects of all-trans retinoic acid in osteosarcoma cell lines. Tumour Biology 35: 7617-7627, 2014.

Leclerc GJ, Mou C, Leclerc GM, Mian AM, Barredo JC. Histone deacetylase inhibitors induce FPGS mRNA expression and intracellular accumulation of long-chain methotrexate polyglutamates in childhood acute lymphoblastic leukemia: implications for combination therapy. Leukemia 24: 552-562, 2010.

Lemmon MA, Schlessinger J. Cell signaling by receptor tyrosine kinases. Cell 141: 1117-1134, 2010.

Li C, Heidt DG, Dalerba P, Burant CF, Zhang L, Adsay V, Wicha M, Clarke MF, Simeone DM. Identification of pancreatic cancer stem cells. Cancer Research 67: 1030-1037, 2007.

Li L, Bhatia R. Stem cell quiescence. Clinical Cancer Research 17: 4936-4941, 2011.

Louis DN, Perry A, Reifenberger G, von Deimling A, Figarella-Branger D, Cavenee WK, Ohgaki H, Wiestler OD, Kleihues P, Ellison DW. The 2016 World Health Organization Classification of Tumors of the Central Nervous System: a summary. Acta Neuropathologica 131: 803-820, 2016.

Macy ME, Sawczyn KK, Garrington TP, Graham DK, Gore L. Pediatric developmental therapies: interesting new drugs now in early-stage clinical trials. Current Oncology Reports 10: 477-490, 2008.

Mahoney SE, Yao Z, Keyes CC, Tapscott SJ, Diede SJ. Genome-wide DNA methylation studies suggest distinct DNA methylation patterns in pediatric embryonal and alveolar rhabdomyosarcomas. Epigenetics 7: 400-408, 2012.

Mani SA, Guo W, Liao MJ, Eaton EN, Ayyanan A, Zhou AY, Brooks M, Reinhard F, Zhang CC, Shipitsin M, Campbell LL, Polyak K, Brisken C, Yang J, Weinberg RA. The epithelial-mesenchymal transition generates cells with properties of stem cells. Cell 133: 704-715, 2008.

Marks PA, Xu WS. Histone deacetylase inhibitors: Potential in cancer therapy. Journal of Cellular Biochemistry 107: 600-608, 2009.

Massard C, Deutsch E, Soria JC. Tumour stem cell-targeted treatment: elimination or differentiation. Annals of Oncology 17: 1620-1624, 2006.

McDermott SP, Eppert K, Lechman ER, Doedens M, Dick JE. Comparison of human cord blood engraftment between immunocompromised mouse strains. Blood 116: 193-200, 2010.

McDonald SA, Graham TA, Schier S, Wright NA, Alison MR. Stem cells and solid cancers. Virchows Archiv 455: 1-13, 2009.

Megison ML, Gillory LA, Beierle EA. Cell survival signaling in neuroblastoma. Anticancer Agents in Medicinal Chemistry 13: 563-575, 2013.

Melicharkova K, Neradil J, Mudry P, Zitterbart K, Obermannova R, Skotakova J, Veselska R, Sterba J. Profil aktivace receptorových tyrozinkináz a mitogenem aktivovaných proteinkináz v terapii Maffucciho syndromu. Klinická Onkologie 28 (Suppl 2): 2S47-51, 2015.

Mellinghoff IK, Schultz N, Mischel PS, Cloughesy TF. Will kinase inhibitors make it as glioblastoma drugs? Current Topics in Microbiology and Immunology 355: 135-169, 2012.

Mendoza-Naranjo A, El-Naggar A, Wai DH, Mistry P, Lazic N, Ayala FR, da Cunha IW, Rodriguez-Viciana P, Cheng H, Tavares Guerreiro Fregnani JH, Reynolds P, Arceci RJ, Nicholson A, Triche TJ, Soares FA, Flanagan AM, Wang YZ, Strauss SJ, Sorensen PH. ERBB4 confers metastatic capacity in Ewing sarcoma. EMBO Molecular Medicine 5: 1087-1102, 2013.

Miekus K, Lukasiewicz E, Jarocha D, Sekula M, Drabik G, Majka M. The decreased metastatic potential of rhabdomyosarcoma cells obtained through MET receptor downregulation and the induction of differentiation. Cell Death and Disease 4: e459, 2013.

Miketova P, Kaemingk K, Hockenberry M, Pasvogel A, Hutter J, Krull K, Moore IM. Oxidative changes in cerebral spinal fluid phosphatidylcholine during treatment for acute lymphoblastic leukemia. Biological Research for Nursing 6: 187-195, 2005.

Montero JC, Esparis-Ogando A, Re-Louhau MF, Seoane S, Abad M, Calero R, Ocana A, Pandiella A. Active kinase profiling, genetic and pharmacological data define mTOR as an important common target in triple-negative breast cancer. Oncogene 33: 148-156, 2014.

Moore N, Houghton J, Lyle S. Slow-cycling therapy-resistant cancer cells. Stem Cells and Development 21: 1822-1830, 2012.

Mora J, Rodriguez E, de Torres C, Cardesa T, Rios J, Hernandez T, Cardesa A, de Alava E. Activated growth signaling pathway expression in Ewing sarcoma and clinical outcome. Pediatric Blood and Cancer 58: 532-538, 2012.

Mudry P, Slaby O, Neradil J, Soukalova J, Melicharkova K, Rohleder O, Jezova M, Seehofnerova A, Michu E, Veselska R, Sterba J. Case report: rapid and durable response to PDGFR targeted therapy in a child with refractory multiple infantile myofibromatosis and a heterozygous germline mutation of the PDGFRB gene. BMC Cancer 17: 119, 2017.

Mundi PS, Sachdev J, McCourt C, Kalinsky K. AKT in cancer: new molecular insights and advances in drug development. British Journal of Clinical Pharmacology 82: 943-956, 2016.

Neradil J, Pavlasova G, Veselska R. New mechanisms for an old drug; DHFR- and non-DHFR-mediated effects of methotrexate in cancer cells. Klinická Onkologie 25 (Suppl 2): 2S87-92, 2012.

Neradil J, Pavlasova G, Sramek M, Kyr M, Veselska R, Sterba J. DHFR-mediated effects of methotrexate in medulloblastoma and osteosarcoma cells: the same outcome of treatment with different doses in sensitive cell lines. Oncology Reports 33: 2169-2175, 2015.

Neradil J, Veselska R. Nestin as a marker of cancer stem cells. Cancer Science 106: 803-811, 2015.

Northcott PA, Dubuc AM, Pfister S, Taylor MD. Molecular subgroups of medulloblastoma. Expert Review of Neurotherapeutics 12: 871-884, 2012.

Nunukova A, Neradil J, Skoda J, Jaros J, Hampl A, Sterba J, Veselska R. Atypical nuclear localization of CD133 plasma membrane glycoprotein in rhabdomyosarcoma cell lines. International Journal of Molecular Medicine 36: 65-72, 2015.

O'Brien CA, Kreso A, Jamieson CH. Cancer stem cells and self-renewal. Clinical Cancer Research 16: 3113-3120, 2010.

Ortiz MA, Bayon Y, Lopez-Hernandez FJ, Piedrafita FJ. Retinoids in combination therapies for the treatment of cancer: mechanisms and perspectives. Drug Resistance Updates 5: 162-175, 2002.

Pearson AD, Herold R, Rousseau R, Copland C, Bradley-Garelik B, Binner D, Capdeville R, Caron H, Carleer J, Chesler L, Geoerger B, Kearns P, Marshall LV, Pfister SM, Schleiermacher G, Skolnik J, Spadoni C, Sterba J, van den Berg H, Uttenreuther-Fischer M, Witt O, Norga K, Vassal G. Implementation of mechanism of action biology-driven early drug development for children with cancer. European Journal of Cancer 62: 124-131, 2016.

Pepper ED, Farrell MJ, Nord G, Finkel SE. Antiglycation effects of carnosine and other compounds on the long-term survival of Escherichia coli. Applied and Environmental Microbiology 76: 7925-7930, 2010.

Prasad P, Vasquez H, Das CM, Gopalakrishnan V, Wolff JE. Histone acetylation resulting in resistance to methotrexate in choroid plexus cells. Journal of Neuro-oncology 91: 279-286, 2009.

Pui CH, Gajjar AJ, Kane JR, Qaddoumi IA, Pappo AS. Challenging issues in pediatric oncology. Nature Reviews Clinical Oncology 8: 540-549, 2011.

Quesada J, Amato R. The molecular biology of soft-tissue sarcomas and current trends in therapy. Sarcoma 2012: 849456, 2012.

Ravasio R, Ceccacci E, Minucci S. Self-renewal of tumor cells: epigenetic determinants of the cancer stem cell phenotype. Current Opinion in Genetics & Development 36: 92-99, 2016.

Redova M, Chlapek P, Loja T, Zitterbart K, Hermanova M, Sterba J, Veselska R. Influence of LOX/COX inhibitors on cell differentiation induced by all-trans retinoic acid in neuroblastoma cell lines. International Journal of Molecular Medicine 25: 271-280, 2010.

Ren H, Yang BF, Rainov NG. Receptor tyrosine kinases as therapeutic targets in malignant glioma. Reviews on Recent Clinical Trials 2: 87-101, 2007.

Restrepo A, Smith CA, Agnihotri S, Shekarforoush M, Kongkham PN, Seol HJ, Northcott P, Rutka JT. Epigenetic regulation of glial fibrillary acidic protein by DNA methylation in human malignant gliomas. Neuro-Oncology 13: 42-50, 2011.

Richard V, Nair MG, Santhosh Kumar TR, Pillai MR. Side population cells as prototype of chemoresistant, tumor-initiating cells. BioMed Research International 2013: 517237, 2013.

Roberts PJ, Der CJ. Targeting the Raf-MEK-ERK mitogen-activated protein kinase cascade for the treatment of cancer. Oncogene 26: 3291-3310, 2007.

Robinson DR, Wu YM, Lin SF. The protein tyrosine kinase family of the human genome. Oncogene 19: 5548-5557, 2000.

Rossig C, Juergens H, Berdel WE. New targets and targeted drugs for the treatment of cancer: an outlook to pediatric oncology. Pediatric Hematology and Oncology 28: 539-555, 2011.

Salbaum JM, Kappen C. Genetic and epigenomic footprints of folate. Progress in Molecular Biology and Translational Science 108: 129-158, 2012.

Sana J, Zambo I, Skoda J, Neradil J, Chlapek P, Hermanova M, Mudry P, Vasikova A, Zitterbart K, Hampl A, Sterba J, Veselska R. CD133 expression and identification of CD133/nestin positive cells in rhabdomyosarcomas and rhabdomyosarcoma cell lines. Analytical Cellular Pathology 34: 303-318, 2011.

Santarius T, Bignell GR, Greenman CD, Widaa S, Chen L, Mahoney CL, Butler A, Edkins S, Waris S, Thornalley PJ, Futreal PA, Stratton MR. GLO1-A novel amplified gene in human cancer. Genes, Chromosomes and Cancer 49: 711-725, 2010.

Schmohl JU, Vallera DA. CD133, Selectively Targeting the Root of Cancer. Toxins 8: 165, 2016.

Schroeder CP, Kadara H, Lotan D, Woo JK, Lee HY, Hong WK, Lotan R. Involvement of mitochondrial and Akt signaling pathways in augmented apoptosis induced by a combination of low doses of celecoxib and N-(4-hydroxyphenyl) retinamide in premalignant human bronchial epithelial cells. Cancer Research 66: 9762-9770, 2006.

Seufferlein T, Bachet JB, Van Cutsem E, Rougier P. Pancreatic adenocarcinoma: ESMO-ESDO Clinical Practice Guidelines for diagnosis, treatment and follow-up. Annals of Oncology 23 (Suppl 7): vii33-40, 2012.

Siddikuzzaman, Guruvayoorappan C, Berlin Grace VM. All trans retinoic acid and cancer. Immunopharmacology and Immunotoxicology 33: 241-249, 2011.

Sikkema AH, Diks SH, den Dunnen WF, ter Elst A, Scherpen FJ, Hoving EW, Ruijtenbeek R, Boender PJ, de Wijn R, Kamps WA, Peppelenbosch MP, de Bont ES. Kinome profiling in pediatric brain tumors as a new approach for target discovery. Cancer Research 69: 5987-5995, 2009.

Skoda J, Neradil J, Veselska R. Funkční testy pro detekci nádorových kmenových buněk. Klinická Onkologie 27 (Suppl 1): S42-47, 2014.

Skoda J, Nunukova A, Loja T, Zambo I, Neradil J, Mudry P, Zitterbart K, Hermanova M, Hampl A, Sterba J, Veselska R. Cancer stem cell markers in pediatric sarcomas: Sox2 is associated with tumorigenicity in immunodeficient mice. Tumour Biology 37: 9535-9548, 2016a.

Skoda J, Hermanova M, Loja T, Nemec P, Neradil J, Karasek P, Veselska R. Co-Expression of Cancer Stem Cell Markers Corresponds to a Pro-Tumorigenic Expression Profile in Pancreatic Adenocarcinoma. PLoS One 11: e0159255, 2016b.

Smith MA, Reaman GH. Remaining challenges in childhood cancer and newer targeted therapeutics. Pediatric Clinics of North America 62: 301-312, 2015.

Spector L, Ross JA, Nagarajan R. Epidemiology of Bone and Soft Tissue Sarcomas. In: Pediatric Bone and Soft Tissue Sarcomas, edited by A P: Springer Berlin Heidelberg, 2006, p. 1-11.

Spurlock CF, 3rd, Aune ZT, Tossberg JT, Collins PL, Aune JP, Huston JW, 3rd, Crooke PS, Olsen NJ, Aune TM. Increased sensitivity to apoptosis induced by methotrexate is mediated by JNK. Arthritis and Rheumatism 63: 2606-2616, 2011.

Sramek M, Neradil J, Sterba J, Veselska R. Non-DHFR-mediated effects of methotrexate in osteosarcoma cell lines: epigenetic alterations and enhanced cell differentiation. Cancer Cell International 16: 14, 2016.

Sramek M, Neradil J, Veselska R. Much more than you expected: The non-DHFR-mediated effects of methotrexate. Biochimica et Biophysica Acta 1861: 499-503, 2017.

Sterba J, Dusek L, Demlova R, Valik D. Pretreatment plasma folate modulates the pharmacodynamic effect of high-dose methotrexate in children with acute lymphoblastic leukemia and non-Hodgkin lymphoma: "folate overrescue" concept revisited. Clinical Chemistry 52: 692-700, 2006.

Sterba J, Valik D, Mudry P, Kepak T, Pavelka Z, Bajciova V, Zitterbart K, Kadlecova V, Mazanek P. Combined biodifferentiating and antiangiogenic oral metronomic therapy is feasible and effective in relapsed solid tumors in children: single-center pilot study. Onkologie 29: 308-313, 2006.

Stover PJ. One-carbon metabolism-genome interactions in folate-associated pathologies. Journal of Nutrition 139: 2402-2405, 2009.

Strobel P, Bargou R, Wolff A, Spitzer D, Manegold C, Dimitrakopoulou-Strauss A, Strauss L, Sauer C, Mayer F, Hohenberger P, Marx A. Sunitinib in metastatic thymic carcinomas: laboratory findings and initial clinical experience. British Journal of Cancer 103: 196-200, 2010.

Suji G, Sivakami S. DNA damage during glycation of lysine by methylglyoxal: assessment of vitamins in preventing damage. Amino Acids 33: 615-621, 2007.

Sumer-Turanligil NC, Cetin EO, Uyanikgil Y. A contemporary review of molecular candidates for the development and treatment of childhood medulloblastoma. Child's Nervous System 29: 381-388, 2013.

Thornalley PJ, Rabbani N. Glyoxalase in tumourigenesis and multidrug resistance. Seminars in Cell and Developmental Biology 22: 318-325, 2011.

Tirino V, Desiderio V, d'Aquino R, De Francesco F, Pirozzi G, Graziano A, Galderisi U, Cavaliere C, De Rosa A, Papaccio G, Giordano A. Detection and characterization of CD133+ cancer stem cells in human solid tumours. PLoS One 3: e3469, 2008.

Trumpp A, Essers M, Wilson A. Awakening dormant haematopoietic stem cells. In: Nature Reviews. Immunology. England2010, p. 201-209.

Uzar E, Koyuncuoglu HR, Uz E, Yilmaz HR, Kutluhan S, Kilbas S, Gultekin F. The activities of antioxidant enzymes and the level of malondialdehyde in cerebellum of rats subjected to methotrexate: protective effect of caffeic acid phenethyl ester. Molecular and Cellular Biochemistry 291: 63-68, 2006.

Vardi N, Parlakpinar H, Ates B. Beneficial effects of chlorogenic acid on methotrexate-induced cerebellar Purkinje cell damage in rats. Journal of Chemical Neuroanatomy 43: 43-47, 2012.

Veselska R, Zitterbart K, Auer J, Neradil J. Differentiation of HL-60 myeloid leukemia cells induced by all-trans retinoic acid is enhanced in combination with caffeic acid. International Journal of Molecular Medicine 14: 305-310, 2004.

Veselska R, Kuglik P, Cejpek P, Svachova H, Neradil J, Loja T, Relichova J. Nestin expression in the cell lines derived from glioblastoma multiforme. BMC Cancer 6: 32, 2006.

Veselska R, Skoda J, Neradil J. Detection of cancer stem cell markers in sarcomas. Klinická Onkologie 25 (Suppl 2): 2S16-20, 2012.

Visvader JE, Lindeman GJ. Cancer stem cells in solid tumours: accumulating evidence and unresolved questions. Nature Reviews Cancer 8: 755-768, 2008.

Wagner MJ, Maki RG. Type 1 insulin-like growth factor receptor targeted therapies in pediatric cancer. Frontiers in Oncology 3: 9, 2013.

Wang JJ, Li GJ. Relationship between RFC gene expression and intracellular drug concentration in methotrexate-resistant osteosarcoma cells. Genetics and Molecular Research 13: 5313-5321, 2014.

Wang YC, Chiang EP. Low-dose methotrexate inhibits methionine S-adenosyltransferase in vitro and in vivo. Molecular Medicine 18: 423-432, 2012.

Webley SD, Welsh SJ, Jackman AL, Aherne GW. The ability to accumulate deoxyuridine triphosphate and cellular response to thymidylate synthase (TS) inhibition. British Journal of Cancer 85: 446-452, 2001.

Wu J, Wood GS. Reduction of Fas/CD95 promoter methylation, upregulation of Fas protein, and enhancement of sensitivity to apoptosis in cutaneous T-cell lymphoma. Archives of Dermatology 147: 443-449, 2011.

Xu WS, Parmigiani RB, Marks PA. Histone deacetylase inhibitors: molecular mechanisms of action. Oncogene 26: 5541-5552, 2007.

Xu X, Chai S, Wang P, Zhang C, Yang Y, Wang K. Aldehyde dehydrogenases and cancer stem cells. Cancer Letters 369: 50-57, 2015.

Yang PM, Lin JH, Huang WY, Lin YC, Yeh SH, Chen CC. Inhibition of histone deacetylase activity is a novel function of the antifolate drug methotrexate. Biochemical and Biophysical Research Communications 391: 1396-1399, 2010.

Yu L, Saile K, Swartz CD, He H, Zheng X, Kissling GE, Di X, Lucas S, Robboy SJ, Dixon D. Differential expression of receptor tyrosine kinases (RTKs) and IGF-I pathway activation in human uterine leiomyomas. Molecular Medicine 14: 264-275, 2008.

Zapletalova D, Andre N, Deak L, Kyr M, Bajciova V, Mudry P, Dubska L, Demlova R, Pavelka Z, Zitterbart K, Skotakova J, Husek K, Martincekova A, Mazanek P, Kepak T, Doubek M, Kutnikova L, Valik D, Sterba J. Metronomic chemotherapy with the COMBAT regimen in advanced pediatric malignancies: a multicenter experience. Oncology 82: 249-260, 2012.

Zhang B, Strauss AC, Chu S, Li M, Ho Y, Shiang KD, Snyder DS, Huettner CS, Shultz L, Holyoake T, Bhatia R. Effective targeting of quiescent chronic myelogenous leukemia stem cells by histone deacetylase inhibitors in combination with imatinib mesylate. Cancer Cell 17: 427-442, 2010.

Zhou L, Xu N, Sun Y, Liu XM. Targeted biopharmaceuticals for cancer treatment. Cancer Letters 352: 145-151, 2014.

Internetové zdroje

http://detskaonkologie.registry.cz/

8. PŘÍLOHY

1. Mudry P, Slaby O, Neradil J, Soukalova J, Melicharkova K, Rohleder O, Jezova M, Seehofnerova A, Michu E, Veselska R, Sterba J. Case report: rapid and durable response to PDGFR targeted therapy in a child with refractory multiple infantile myofibromatosis and a heterozygous germline mutation of the PDGFRB gene. BMC Cancer 17: 119, 2017.

2. Sramek M, Neradil J, Veselska R. Much more than you expected: The non-DHFR-mediated effects of methotrexate. Biochimica et Biophysica Acta 1861: 499-503, 2017.

3. Skoda J, Hermanova M, Loja T, Nemec P, Neradil J, Karasek P, Veselska R. Co-Expression of Cancer Stem Cell Markers Corresponds to a Pro-Tumorigenic Expression Profile in Pancreatic Adenocarcinoma. PLoS One 11: e0159255, 2016.

4. Sramek M, Neradil J, Sterba J, Veselska R. Non-DHFR-mediated effects of methotrexate in osteosarcoma cell lines: epigenetic alterations and enhanced cell differentiation. Cancer Cell International 16: 14, 2016.

5. Skoda J, Nunukova A, Loja T, Zambo I, Neradil J, Mudry P, Zitterbart K, Hermanova M, Hampl A, Sterba J, Veselska R. Cancer stem cell markers in pediatric sarcomas: Sox2 is associated with tumorigenicity in immunodeficient mice. Tumor Biology 37: 9535-9548, 2016.

6. Melichárková K, Neradil J, Múdry P, Zitterbart K, Obermannová R, Skotáková J, Veselská R, Štěrba J. Profil aktivace receptorových tyrozinkináz a mitogenem aktivovaných proteinkináz v terapii Maffucciho syndrome. Klinická Onkologie 28 (Suppl 2): 2S47-51, 2015.

7. Nunukova A, Neradil J, Skoda J, Jaros J, Hampl A, Sterba J, Veselska R. Atypical nuclear localization of CD133 plasma membrane glycoprotein in rhabdomyosarcoma cell lines. International Journal of Molecular Medicine 36: 65-72, 2015.

8. Neradil J, Veselska R. Nestin as a marker of cancer stem cells. Cancer Science 106: 803-811, 2015.

9. Neradil J, Pavlasova G, Sramek M, Kyr M, Veselska R, Sterba J. DHFR-mediated effects of methotrexate in medulloblastoma and osteosarcoma cells: the same outcome of treatment with different doses in sensitive cell lines. Oncology Reports 33: 2169-2175, 2015.

10. Chlapek P, Neradil J, Redova M, Zitterbart K, Sterba J, Veselska R. The ATRA-induced differentiation of medulloblastoma cells is enhanced with LOX/COX inhibitors: an analysis of gene expression. Cancer Cell International 14: 51, 2014.

11. Skoda J, Neradil J, Veselská R. Funkční testy pro detekci nádorových kmenových buněk. Klinická Onkologie 27 (Suppl 1): S42-47, 2014.

12. Krzyzankova M, Chovanova S, Chlapek P, Radsetoulal M, Neradil J, Zitterbart K, Sterba J, Veselska R. LOX/COX inhibitors enhance the antineoplastic effects of all-trans retinoic acid in osteosarcoma cell lines. Tumour Biology 35: 7617-7627, 2014.

13. Skoda J, Neradil J, Zitterbart K, Sterba J, Veselska R. EGFR signaling in the HGG-02 glioblastoma cell line with an unusual loss of EGFR gene copy. Oncology Reports 31: 480-487, 2014.

14. Neradil J, Pavlasova G, Veselska R. New mechanisms for an old drug; DHFR- and non-DHFR-mediated effects of methotrexate in cancer cells. Klinicka Onkologie 25 (Suppl 2): 2S87-92, 2012.

15. Veselska R, Skoda J, Neradil J. Detection of cancer stem cell markers in sarcomas. Klinická Onkologie 25 (Suppl 2): 2S16-20, 2012.

16. Sana J, Zambo I, Skoda J, Neradil J, Chlapek P, Hermanova M, Mudry P, Vasikova A, Zitterbart K, Hampl A, Sterba J, Veselska R. CD133 expression and identification of CD133/nestin positive cells in rhabdomyosarcomas and rhabdomyosarcoma cell lines. Analytical Cellular Pathology 34: 303-318, 2011.

17. Krupkova O Jr, Loja T, Redova M, Neradil J, Zitterbart K, Sterba J, Veselska R. Analysis of nuclear nestin localization in cell lines derived from neurogenic tumors. Tumour Biology 32: 631-639, 2011.

18. Veselska R, Kuglik P, Cejpek P, Svachova H, Neradil J, Loja T, Relichova J. Nestin expression in the cell lines derived from glioblastoma multiforme. BMC Cancer 6: 32, 2006.

19. Veselska R, Zitterbart K, Auer J, Neradil J. Differentiation of HL-60 myeloid leukemia cells induced by all-trans retinoic acid is enhanced in combination with caffeic acid. International Journal of Molecular Medicine 14: 305-310, 2004.

Mudry et al. BMC Cancer (2017) 17:119
DOI 10.1186/s12885-017-3115-x

BMC Cancer

CASE REPORT Open Access

Case report: rapid and durable response to PDGFR targeted therapy in a child with refractory multiple infantile myofibromatosis and a heterozygous germline mutation of the *PDGFRB* gene

Peter Mudry[1*], Ondrej Slaby[2], Jakub Neradil[3,1,7], Jana Soukalova[4], Kristyna Melicharkova[1,7], Ondrej Rohleder[1], Marta Jezova[5], Anna Seehofnerova[6], Elleni Michu[2], Renata Veselska[3,1,7] and Jaroslav Sterba[1,7]

Abstract

Background: Infantile myofibromatosis belongs to a family of soft tissue tumors. The majority of these tumors have benign behavior but resistant and malignant courses are known, namely in tumors with visceral involvement. The standard of care is surgical resection. Observations suggest that low dose chemotherapy is beneficial. The treatment of resistant or relapsed patients with multifocal disease remains challenging. Patients that harbor an actionable mutation in the kinase domain are potential subjects for targeted tyrosine kinase inhibitor therapy.

Case presentation: An infant boy with inborn generalized infantile myofibromatosis that included bone, intracranial, soft tissue and visceral involvement was treated according to recent recommendations with low dose chemotherapy. The presence of a partial but temporary response led to a second line of treatment with six cycles of chemotherapy, which achieved a partial response again but was followed by severe toxicity. The generalized progression of the disease was observed later. Genetic analyses were performed and revealed a *PDGFRB* gene c. 1681C>A missense heterozygous germline mutation, high PDGFRβ phosphokinase activity within the tumor and the heterozygous germline Slavic Nijmegen breakage syndrome 657del5 mutation in the *NBN* gene. Targeted treatment with sunitinib, the PDGFRβ inhibitor, plus low dose vinblastine led to an unexpected and durable response without toxicities or limitations to daily life activities. The presence of the Slavic *NBN* gene mutation limited standard chemotherapy dosing due to severe toxicities. Sister of the patient suffred from skull base tumor with same genotype and histology. The same targeted therapy led to similar quick and durable response.

Conclusion: Progressive and resistant incurable infantile myofibromatosis can be successfully treated with the new approach described herein. Detailed insights into the biology of the patient's tumor and genome are necessary to understand the mechanisms of activity of less toxic and effective drugs except for up to date population-based chemotherapy regimens.

Keywords: Infantile myofibromatosis, Tyrosine kinase inhibitor, PDGFR, Chemotherapy, Theranostics, Case report

* Correspondence: pmudry@fnbrno.cz
[1]Department of Pediatric Oncology, University Hospital Brno and School of Medicine, Masaryk University, Cernopolni 9, Brno 613 00, Czech Republic
Full list of author information is available at the end of the article

Background

The family of fibroblastic-myofibroblastic tumors consists of more than 30 distinguished entities, such as inflammatory myofibroblastic tumor (IMT), aggressive fibromatosis and infantile myofibromatosis (IM). These tumors have uncertain biologic behaviors that range from low grade, locally aggressive and rarely metastasizing to a highly aggressive course that eventually evolves to a true high-grade sarcoma after recurrences. IM is a rare tumor that affects infants with a median age of 3 months; approximately 100 solitary lesion cases have been published in the literature during the past decade [1]. Soft tissue lesions of IM can arise at any time during life and, intriguingly, can regress spontaneously. However, visceral lesions are associated with high morbidity and mortality. The standard of care is the surgical resection of a single lesion. Multiple lesions and surgically unresectable lesions could be treated with anti-inflammatory drugs, interferon alpha, or distinct chemotherapeutic regimens that are based on low dose metronomic or maximum tolerated doses (MTD) of chemotherapeutics, such as the vinca alkaloids vincristine, vinorelbine and vinblastine; the alkylating agents cyclophosphamide and ifosfamide; or others, such as actinomycine D, doxorubicin or methotrexate [2–4]. The results of such treatments are under investigation in ongoing observational clinical trials of cooperative groups, such as European Soft Tissue Sarcoma Study Group (EpSSG) or Children's Oncology Group (COG). Several studies of desmoid-type fibromatosis with response rates of 33–49% were reviewed elsewhere [4]. Nevertheless, the treatment of resistant patients, particularly those with visceral involvement, remains challenging.

For patients with progressive disease after MTD based chemotherapy, there are no established standards of care, and these patients are, thus, subjected to experimental treatments. One of the most promising agents with proven activity for IMT is the ALK tyrosine kinase inhibitor crizotinib [5]. Patients with ALK rearrangement are reportedly rapidly responding to crizotinib, but those without the detected fusion are not [5]. A recent work by Lovly et al. on IMTs revealed multiple fusion partners of ALK, and newly reported ROS1 and PDGFRβ fusions with projected TKI sensitivity were demonstrated in a patient with an ROS1 fusion [6]. Similar to IMTs, IMs may harbor missense mutations in the PDGFRβ kinase that constitutively alter PDGFR activity. Moreover, in several families, the c.1681C>T (p.Arg561Cys) mutation in the *PDGFRB* gene was found to cause familial infantile myofibromatosis [7]. A phase II study of sunitinib in 19 patients with aggressive fibromatosis has been published and described a 26.3% overall response, but the analysis of the kinase pathway was lacking [8]. A case report of aggressive fibromatosis that favored the PDGFRβ inhibitor sunitinib against imatinib was published that described a good response with sunitinib which was interrupted after 13 months and substituted by imatinib. But reactivation of painful lesions occurred within several days and re-growth of aggressive fibromatosis led to successful re-treatment with sunitinib [9].

Herein, we report the case of a patient with refractory multiple infantile myofibromatosis who was confirmed to harbor the *PDGFRB* germline mutation and who responded well to treatment with the PDGFRβ tyrosine kinase inhibitor sunitinib.

Case presentation

The newborn boy with microtia and meatal atresia and with family history of two spontaneous missed abortions and myofibroblastic lesions with spontaneous regression in his older sister and father, was diagnosed with generalized myofibromatosis that affected the calva and radius bones, the spleen and subcutaneous tissue of face, the head, inguina and arm. Histopathology, with regard to the family history, revealed the presence of infantile familial myofibromatosis. Immunohistochemistry (ICH) and FISH did not reveal any pathological staining for ALK. The patient was treated according to the EpSSG 2005 observational trial recommendation with the metronomic vinblastine/methotrexate combination, which was expected to be less toxic than MTD based regimens. Despite this, severe neutropenia had been observed; therefore, a dose reduction was necessary down to 10%/30% of the original doses of vinblastine/methotrexate, respectively. The therapy was stopped after 8 weeks due to clearly progressive disease in the soft tissues and in the spleen and with the appearance of new FDG PET positive lesions in the bones. Thereafter, the standard MTD based therapy with vincristine/actinomycine D/cyclophosphamide – the "VAC" regimen with doses based on body weight (vincristine 0.05 mg/kg, actinomycine D 0.05 mg/kg, cyclophosphamide 50 mg/kg) had been initiated. Such treatment after the second course (the first course was given with a 75% reduction of cyclophosphamide) had led to severe febrile neutropenia, gastrointestinal toxicity with gastric palsy, subileus and bilateral bronchopneumonia. However, a reassessment after those 2 cycles revealed a partial response. Due to the previous toxicity, we decided to substitute vincristine with vinblastine at 10% of the recommended dose and cyclophosphamide at 75% of the recommended dose. The patient received the treatment without dose limiting toxicities up to six cycles and continued to respond. The patient was still in partial remission according to CT and MRI images and the FDG PET of the remaining measurable lesions was negative. Unfortunately, the first follow-up re-assessment confirmed the presence of progressive disease just 3 months

after the last chemotherapy dose and several new lesions were detected in the humerus, head, lungs and skin, and all were FDG-PET positive.

A new biopsy was carried out to obtain tumor tissue for phosphoproteomic analysis of the new lesion. The Human Phospho-RTK Array Kit was used to determine the relative levels of tyrosine phosphorylation of 49 different RTKs. The analysis was performed as previously described [10]. In addition to the antibodies (spotted in duplicate) against individual RTKs, each membrane contained three positive reference double spots and one negative control that was also spotted in duplicate and contained phosphate-buffered saline only. Furthermore, we also performed the following negative control experiment in each run: the membrane treated with lysis buffer only (without protein lysate) to ensure the specificity of the spotted antibodies. In such a design, a healthy control sample is not necessary for the determination of the RTK phosphorylation profile of the examined tumor tissue [11–13]. The phosphorylation profile of receptor tyrosine kinases showed that PDGFRβ kinase exhibited the highest level of activity and less intense positivity was observed for EGFR, M-SCFR, Axl and PDGFRα (Fig. 1). Targeted DNA analysis of the *PDGFRB* gene and next generation sequencing (NGS) were performed on genomic DNA from peripheral blood samples. We performed Sanger sequencing of the two *PDGFRB* regions to detect the presence of the c.1978C>A (p.Pro660Thr) and c.1681C>T (p.Arg561Cys) mutations [6] and uncovered a germ-line heterozygous c.1681C>A missense mutation that had previously been shown to be an IM causing mutation [14, 15]. To obtain the complex picture of the genetic background of the case we performed DNA analysis from peripheral blood with the Illumina TruSight Cancer panel, which enabled the sequencing of the hotspots in 94 predisposition cancer genes, according to the standard Illumina protocol (Illumina Inc., USA) and identified the heterozygous Slavic mutation 657del5 in the *NBN* gene of the NBS.

In the meantime, and based on parental request, the patient was observed for the next 4 months. He was doing very well clinically, with a Lansky performance status of 90% and with respect to his treatment history with toxicities after chemotherapy; we did not initiate another chemotherapy regimen but were awaiting the results of genetic analyses, which have revealed potential therapeutic targets. Further follow-up confirmed that the disease continued to progress; several new lesions were detected within the head and the left orbit, a new one was detected in the spine, and the spleen lesion had increased in size.

Due to clear clinical and radiologic progression and new molecular genetic findings, and with respect to the history of the disease, we initiated the single agent *off-label* treatment with sunitinib 12.5 mg once a day. This dose corresponded to 2/3 of the recommended adult dose. An unexpected and dramatic reduction of the palpable soft tissue and bony lesions on the head was observed during the 4 weeks of treatment with the single agent sunitinib. An MR scan confirmed the regression of intracranial and intraorbital lesions as well (Figs. 2, 3 and 4). However, this dosing schedule led to grade 3–4 neutropenia, and the drug was stopped for 4 days. After only 4 days, we could observe the reactivation of the skin and soft tissue lesions; therefore, the sunitinib was given at the same dose every other day. Reactivated reddish swollen and painful sentinel lesions responded again to lower doses of sunitinib, but three more weeks of reduced doses of the single agent sunitinib did not lead to any further regression of the regressed but still palpable skin lesions. A low dose of vinblastine was added to the sunitinib. The starting vinblastine dose was 2 mg/m^2; however, based on the further hematological

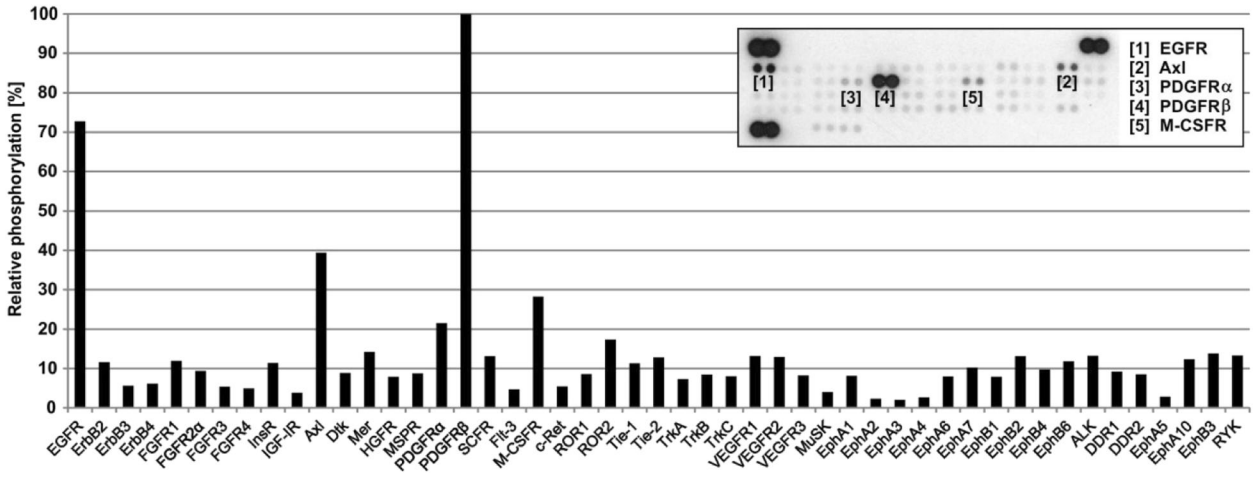

Fig. 1 The relative phosphorylation of kinases in the tumor tissue sample

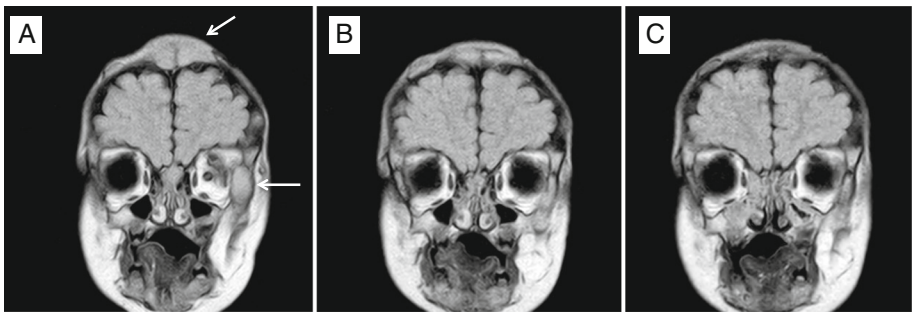

Fig. 2 MRI Frontal view (seq. eFLAIR_long_TR_CLEAR). Two lesions of the left orbit and the skull in the fronto-parietal region (*bars*). **a** Before sunitinib treatment. **b** Day + 56 of sunitinib. **c** Day + 156 of sunitinib

toxicity, the dose was tapered down to a 0.4 mg/m^2 dose once weekly.

An unexpected toxicity of sunitinib occurred after 4 months of treatment when accidental hypoglycemia led to a coma and the patient had to be admitted for glycemia corrections. Thereafter, the parents were educated on regular feeding before sunitinib administration. Further episodes of hypoglycemia were not noted. The patient remained on the treatment paradigm with a marked continuing response with no disease activity 1 year after the initiation of the treatment and without any dose limiting toxicities.

Interestingly, the 8 year old sister of the patient, who had a history of spontaneous regression of subcutaneous lesions, suffered from the symptomatic re-activation of the disease when the patient was receiving treatment. She presented with tumor size of 29 × 24 × 16 mm on the skull base with night pain. Histopathological and detailed mutation analyses found the same IM histopathology and the same genotype in the *PDGFB* and *NBN* genes. As with the index case, the sister is doing well on sunitinib and vinblastine treatment and has exhibited a rapid response. The nigh pain relieved after 2 weeks on sunitinib + vinblastine. Initial tumor volume shrinked by 44% after 97 days of combined treatment without any adverse events requiring reduction of doses. Timeline of both cases is shown on Additional file 1.

Discussion and conclusions

Despite the finding that the patient exhibited a partial response to systemic VAC treatment, the disease continued to progress; moreover, the patient experienced severe, life threatening dose-limiting toxicities.

Inflammatory myofibroblastic tumors that harbor an ALK/ROS1 or PDGFRβ kinase fusion are potentially targetable with TKIs due to the presence of a constitutively active kinase domain that drives cellular proliferation [6, 16]. A response to the ALK inhibitor crizotinib is reported in tumors that harbor any of the ALK kinase fusions. Patients with IMT and ALK negative rearrangements are unlikely to respond to such targeted treatment.

PDGFRB mutations are reported to be involved in the pathogenesis of infantile myofibromatosis in a proposed autosomal dominant pattern with incomplete penetrance and variable expressivity [7]. The missense *PDGFRB* c.1681C>T (R681C) mutation is located in exon 12 and is predicted to decrease the autoinhibition of the JM domain (an autoinhibitory domain that masks the catalytic cleft when the receptor is not bound by its ligand) at baseline, which leads to increased kinase firing and promotes the formation of myofibromas in tissues with high PDGFRβ signaling activity. More recently, it was demonstrated in a cell culture model that the R561C mutation activates signaling pathways that are normally

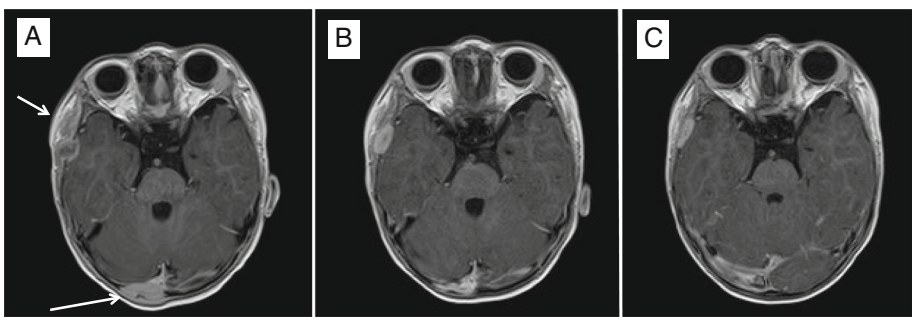

Fig. 3 MRI Axial view (seq. esT1W_3S_FFE post-contrast). Intracranial lesions of the right temporal and right parieto-occipital regions (*bars*). **a** Before sunitinib treatment. **b** Day + 56 of sunitinib. **c** Day + 156 of sunitinib

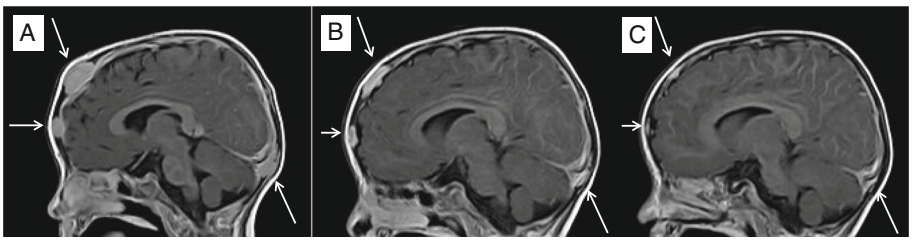

Fig. 4 MRI Sagittal view (seq. esT1W_3S_FFE post-contrast). Frontal and parieto-occipital lesion (*bars*). **a** Before sunitinib treatment. **b** Day + 56 of sunitinib. **c** Day + 156 of sunitinib

activated by the stimulated wild-type PDGFRβ receptor in the absence of PDGF [14]. PDGFR is the immediate NOTCH3 target gene [17]. If these two signaling pathways are linked and the IM disease-causing mutations in either *PDGFRB* or *NOTCH3* are demonstrated to be activating, theoretically, the inhibition of *PDGFRB* or *NOTCH3* would result in a targeted therapeutic strategy [7]. Our case report shows the clinical efficacy of such an approach. Targeted therapy against altered PDGFRβ with a TKIs inhibitor can overcome tumor growth and can lead to tumor shrinkage. Compared to the toxicity of conventional chemotherapy, treatment with sunitinib was tolerated well except for the occurrence of asymptomatic granulocytopenia and one episode of symptomatic hypoglycemia. However, the cessation of the drug lead to increased tumor activity and a decreased drug dose of the single agent sunitinib led to a stable disease only.

The analysis of tumor tissue or a patient's samples and the use of a subsequent results driven treatment provide a new opportunity for personalized medicine as opposed to a population based study. Such treatments are supported by new insights into the molecular pathology of rare diseases, such as IM. A similar strategy would at least justify the *off-label* use of new drugs when the individual tumor biology and data about the safety of such drugs is well defined. TKIs could be an example, as these drugs are not available to orphan disease patients because of the absence of appropriate clinical trials. The careful management and regular observation of the patient is mandatory, however, in situations where standard approaches are either exploited or ineffective or absent, the prudent use of targeted agents based on the mechanism of action might lead to impressive results.

The rapid tumor re-growth that occurred when the patient was off of the sunitinib during the induction treatment indicates that metronomic dosing should be maintained at a lower dose with limited toxicity rather than being interrupted. The successful use of low dose vinblastine that is described here, together with the use of sunitinib at a dose of approximately 1/3 of the usually recommended dose per kg or m^2 in adults, could be at least in part explained by the fact that targeted agents could act as biology response modifiers and lower doses of biological agents and chemotherapy could be nontoxic and advantageous [18, 19]. This theory is supported by our observation of the clear disease progression when sunitinib therapy was interrupted. Regular observations of the patient and preemptive measures such as the after-feeding dosing of sunitinib should be considered during treatment.

The finding of the Slavic mutation of the NBS was noted as accidental during NGS sequencing and the relevance for the disease course is unknown. The toxicity of chemotherapy might be at least in part conditioned by the NBS mutation As known, the intensity of chemotherapy in NBS patients must be adapted to individual risk factors and tolerance. The use of radiomimetics, alkylating agents, and epipodophyllotoxins should be avoided, and the dose of methotrexate should be limited [20].

However, the overall duration of such clinically effective treatment remains speculative, especially in patients with germline mutations. Different approaches that consider cancer to be a chronic disease, such as diabetes, should be considered in instances in which pathogenic germline mutations are in place. Should such targeted agents be maintained for a very long time, e.g., maintenance therapies in childhood acute leukemia, where other mechanisms of action, not only the cytostatic effect are in place? [21]. Should some pulses of targeted agents be considered?

These are only a few of the new questions that arose by the increased availability of diagnostic methods, such as NGS and functional proteomics.

The patients with an orphan disease like IM could benefit from detailed insights into the biology of their tumor and genome. Such approach is necessary to better understand the molecular pattern of disease and mechanisms of action of less toxic and effective drugs except for up to date population-based chemotherapy regimens. Morover, an unexpected finding of germline mutation can be important for treatment decisions. Progressive and resistant incurable infantile myofibromatosis can be successfully treated with the new approach described herein.

Additional file

Additional file 1: Timeline. This file shows timeline of both described cases. (PDF 466 kb)

Abbreviations

ALK: Anaplastic lymphoma kinase; COG: Children's oncology group; EpSSG: European Soft Tissue Sarcoma Study Group; FDG PET: Fluorodeoxyglucose positron emission tomography; FISH: Fluorescent in situ hybridization; IHC: Immunohistochemistry; IM: Infantile myofibromatosis; IMT: Inflammatory myofibroblastic tumor; IVA: Ifosfamide/vincristine/actinomycine D; MRI: Magnetic resonance imaging; MTD: Maximum tolerated doses; MTX: Methotrexate; NBS: Nijmegen breakage syndrome; NGS: Next generation sequencing; PDGFR: Platelet derived growth factor receptor; PDGFRB: Platelet derived growth factor receptor gene B; PDGFRβ: Platelet derived growth factor receptor beta; TKI: Tyrosine kinase inhibitor; VAC: Vincristine/actinomycine D/cyclophosphamide; VBL: Vinblastine

Acknowledgements

The authors thank Drs. Eva Machackova and Lenka Foretova from Masaryk Memorial Cancer Institute for helpful comments and NGS gene analysis. Martina Svobodova has substantially contributed to the resolution of administrative issues of the treatments including insurance coverage.

Funding

This study was supported by projects No. 16-34083A and No. 16-33209A from the Ministry of Healthcare of the Czech Republic, by project No. LQ1605 from the National Program of Sustainability II (MEYS CR). The funders had no role in the study design, data collection and analysis, decision to publish, or preparation of the manuscript.

Availability of data and materials

The datasets and/or the analyzed current case report are available from the corresponding author upon reasonable request.

Authors' contributions

PM performed the review of the literature and wrote the draft of the manuscript. OS and EM performed the DNA analysis of the *PDGFRB* gene. JN and RV designed and performed the phosphoproteomic analysis. JSo proposed to perform the NGS analysis and participated as clinical geneticist. KM took care of the patient and participated in the writing of the manuscript. OR took care of the patient and participated in the writing of the manuscript. MJ performed the histopathological analysis. AS performed the radiological evaluation and managed the MRI images. JSt proposed the study of molecular biology details of the case with a theranostic aim. All of the authors read and approved the final manuscript.

Competing interests

The authors declare that they have no competing interests.

Consent for publication

Written informed consent for the publication of their clinical details and/or clinical images was obtained from the parents of the patient. A copy of the consent form is available for review by the Editor of this journal.

Ethics approval and consent to participate

The study was approved by both the Ethics Committee of the University Hospital Brno on 9.6.2015 and the Ethics Committee of the School of Medicine Masaryk University on 23.6.2015, reference number 30/2015. All of the research described herein was conducted according to the Declaration of Helsinki. Written informed consent for the tissue and blood analysis and the *off-label* treatment of the child with the tyrosine kinase inhibitor was obtained from parents.

Author details

[1]Department of Pediatric Oncology, University Hospital Brno and School of Medicine, Masaryk University, Cernopolni 9, Brno 613 00, Czech Republic. [2]Central European Institute of Technology, Masaryk University, Kamenice 753/5, Brno 625 00, Czech Republic. [3]Laboratory of Tumor Biology, Department of Experimental Biology, School of Science, Masaryk University, Kotlarska 2, Brno 611 37, Czech Republic. [4]Division of Medical Genetics, Department of Biology, University Hospital Brno and School of Medicine, Masaryk University, Cernopolni 9, Brno 613 00, Czech Republic. [5]Department of Pathology, University Hospital Brno and School of Medicine, Masaryk University, Cernopolni 9, Brno 613 00, Czech Republic. [6]Department of Pediatric Radiology, University Hospital Brno and School of Medicine, Masaryk University, Cernopolni 9, Brno 613 00, Czech Republic. [7]International Clinical Research Center, St. Anne's University Hospital Brno, Pekarska 53, Brno 656 91, Czech Republic.

Received: 2 August 2016 Accepted: 4 February 2017
Published online: 10 February 2017

References

1. Levine E, Fréneaux P, Schleiermacher G, Brisse H, Pannier S, Teissier N, et al. Risk-adapted therapy for infantile myofibromatosis in children. Pediatr Blood Cancer. 2012;59:115–20.
2. Johnson K, Notrica DM, Carpentieri D, Jaroszewski D, Henry MM. Successful treatment of recurrent pediatric inflammatory myofibroblastic tumor in a single patient with a novel chemotherapeutic regimen containing celecoxib. J Pediatr Hematol Oncol. 2013;35:414–6.
3. Auriti C, Kieran MW, Deb G, Devito R, Pasquini L, Danhaive O. Remission of infantile generalized myofibromatosis after interferon alpha therapy. J Pediatr Hematol Oncol. 2008;30:179–81.
4. Ferrari A, Alaggio R, Meazza C, Chiaravalli S, de Pava MV, Casanova M, et al. Fibroblastic tumors of intermediate malignancy in childhood. Expert Rev Anticancer Ther. 2013;13:225–36.
5. Butrynski JE, D'Adamo DR, Hornick JL, Dal Cin P, Antonescu CR, Jhanwar SC, et al. Crizotinib in *ALK* -rearranged inflammatory myofibroblastic tumor. N Engl J Med. 2010;363:1727–33.
6. Lovly CM, Gupta A, Lipson D, Otto G, Brennan T, Chung CT, et al. Inflammatory myofibroblastic tumors harbor multiple potentially actionable kinase fusions. Cancer Discov. 2014;4:889–95.
7. Martignetti JA, Tian L, Li D, Ramirez MCM, Camacho-Vanegas O, Camacho SC, et al. Mutations in PDGFRB cause autosomal-dominant infantile myofibromatosis. Am J Hum Genet. 2013;92:1001–7.
8. Jo J-C, Hong YS, Kim K-P, Lee J-L, Lee J, Park YS, et al. A prospective multicenter phase II study of sunitinib in patients with advanced aggressive fibromatosis. Invest New Drugs. 2014;32:369–76.
9. Skubitz KM, Manivel JC, Clohisy DR, Frolich JW. Response of imatinib-resistant extra-abdominal aggressive fibromatosis to sunitinib: case report and review of the literature on response to tyrosine kinase inhibitors. Cancer Chemother Pharmacol. 2009;64:635–40.
10. Skoda J, Neradil J, Zitterbart K, Sterba J, Veselska R. EGFR signaling in the HGG-02 glioblastoma cell line with an unusual loss of EGFR gene copy. Oncol Rep. 2014;31:480–7.
11. Dewaele B, Floris G, Finalet-Ferreiro J, Fletcher CD, Coindre J-M, Guillou L, et al. Coactivated platelet-derived growth factor receptor and epidermal growth factor receptor are potential therapeutic targets in intimal sarcoma. Cancer Res. 2010;70:7304–14.
12. Ströbel P, Bargou R, Wolff A, Spitzer D, Manegold C, Dimitrakopoulou-Strauss A, et al. Sunitinib in metastatic thymic carcinomas: laboratory findings and initial clinical experience. Br J Cancer. 2010;103:196–200.
13. Zhang Y-X, van Oosterwijk JG, Sicinska E, Moss S, Remillard SP, van Wezel T, et al. Functional profiling of receptor tyrosine kinases and downstream signaling in human chondrosarcomas identifies pathways for rational targeted therapy. Clin Cancer Res. 2013;19:3796–807.
14. Arts FA, Chand D, Pecquet C, Velghe AI, Constantinescu S, Hallberg B, et al. PDGFRB mutants found in patients with familial infantile myofibromatosis or overgrowth syndrome are oncogenic and sensitive to imatinib. Oncogene. 2015. doi:10.1038/onc.2015.383.
15. Cheung YH, Gayden T, Campeau PM, LeDuc CA, Russo D, Nguyen V-H, et al. A recurrent PDGFRB mutation causes familial infantile myofibromatosis. Am J Hum Genet. 2013;92:996–1000.
16. Davies KD, Doebele RC. Molecular pathways: ROS1 fusion proteins in cancer. Clin Cancer Res. 2013;19:4040–5.
17. Jin S, Hansson EM, Tikka S, Lanner F, Sahlgren C, Farnebo F, et al. Notch signaling regulates platelet-derived growth factor receptor-beta expression in vascular smooth muscle cells. Circ Res. 2008;102:1483–91.

18. Reynolds AR. Potential relevance of bell-shaped and u-shaped dose-responses for the therapeutic targeting of angiogenesis in cancer. Dose-response Publ Int Hormesis Soc. 2009;8:253–84.
19. Reynolds AR, Hart IR, Watson AR, Welti JC, Silva RG, Robinson SD, et al. Stimulation of tumor growth and angiogenesis by low concentrations of RGD-mimetic integrin inhibitors. Nat Med. 2009;15:392–400.
20. Chrzanowska K. Nijmegen Breakage Syndrome Treatment & Management. 2016. http://emedicine.medscape.com/article/1116869-treatment. Accessed 09 Jan 2016
21. Andre N, Cointe S, Barlogis V, Arnaud L, Lacroix R, Pasquier E, et al. Maintenance chemotherapy in children with ALL exerts metronomic-like thrombospondin-1 associated anti-endothelial effect. Oncotarget. 2015;6:23008–14.

Biochimica et Biophysica Acta 1861 (2017) 499–503

Contents lists available at ScienceDirect

Biochimica et Biophysica Acta

journal homepage: www.elsevier.com/locate/bbagen

Review

Much more than you expected: The non-DHFR-mediated effects of methotrexate

Martin Sramek, Jakub Neradil, Renata Veselska *

International Clinical Research Center, St. Anne's University Hospital Brno, Pekarska 53, Brno 656 91, Czech Republic

ARTICLE INFO

Article history:
Received 24 October 2016
Received in revised form 10 December 2016
Accepted 15 December 2016
Available online 16 December 2016

Keywords:
Methotrexate
Oxidative stress
Cell differentiation
Epigenetic regulation
DNA methylation
Histone acetylation

ABSTRACT

Background: For decades, methotrexate (MTX; amethopterin) has been known as an antifolate inhibitor of dihydrofolate reductase (DHFR), and it is widely used for the treatment of various malignancies and autoimmune diseases. Although the inclusion of MTX in various therapeutic regimens is based on its ability to inhibit DHFR and consequently to suppress the synthesis of pyrimidine and purine precursors, recent studies have shown that MTX is also able to target other intracellular pathways that are independent of folate metabolism.
Scope of review: The main aim of this review is to summarize the most important, up-to-date findings of studies regarding the non-DHFR-mediated mechanisms of MTX action.
Major conclusions: The effectiveness of MTX is undoubtedly caused by its capability to affect various intracellular pathways at many levels. Although the most important therapeutic mechanism of MTX is strongly based on the inhibition of DHFR, many other effects of this compound have been described and new studies bring new insights into the pharmacology of MTX every year.
General significance: Identification of these new targets for MTX is especially important for a better understanding of MTX action in new protocols of combination therapy.

1. Introduction

Mammalian cells cannot synthesize folates *de novo* and are dependent on a supply of fully reduced folates to drive a series of 1-carbon reactions. Folates are hydrophilic anionic molecules that do not cross biological membranes by diffusion. The best-characterized folate transporter is the ubiquitously expressed reduced folate carrier (RFC) [25]. Importantly, in addition to its role in transporting folates, RFC is a major transporter of antifolate drugs used for cancer chemotherapy, such as MTX [24].

Intracellular folates are predominantly long-chain polyglutamate derivatives. Inside the cell, folylpolyglutamate synthetase (FPGS) adds glutamate molecules to folate, which is important for the retention of folates in cells [57]. The same mechanism is involved in MTX conversion to active methotrexate polyglutamates (MTXPGs) by FPGS [47]. Catabolism of MTXPGs is dependent on the rate of entry of polyglutamates into lysosomes and hydrolysis by the lysosomal enzyme gamma-glutamyl hydrolase. Effective intracellular levels of MTX are reduced by various transport mechanisms, including ABC transporters such as ABCB1, ABCG2 [46] and many others [20].

MTX and MTXPGs block the activity of the key enzyme DHFR (Fig. 1), which converts folates to their active forms – dihydrofolate (DHF) and tetrahydrofolate (THF). MTXPGs also potently inhibit thymidylate synthase (TS). Furthermore, during dTMP synthesis, TS utilizes the cofactor 5,10-methylene THF, which serves as a donor of the -CH_2OH group. As a result of this reaction, 5,10-methylene THF is oxidized to DHF, which cannot be reduced back to THF due to the inhibition of DHFR [21]. In addition, MTXPGs and DHF polyglutamates that are accumulated after DHFR inhibition exert an inhibitory effect on GAR transformylase (GART). MTXPGs further inhibit 5-aminoimidazole-4-carboxamide ribonucleotide (AICAR) transformylase (ATIC). The inhibition of ATIC promotes the accumulation of AICAR, a potent inhibitor of adenosine deaminase (ADA) [7].

Overall, it is well known that MTX interferes with purine and pyrimidine synthesis, which is required for DNA replication and cell

Abbreviations: ADA, adenosine deaminase; AICAR, 5-aminoimidazole-4-carboxamide ribonucleotide; ALL, acute lymphoblastic leukemia; ATIC, AICAR transformylase; ATRA, all-*trans* retinoic acid; DHF, dihydrofolate; DHFR, dihydrofolate reductase; E2F1, E2F transcription factor 1; FAICAR, 5-formaminoimidazole-4-carboxamide ribonucleotide; FGAR, formylglycinamide ribonucleotide; FPGS, folylpolyglutamate synthetase; GAR, glycinamide ribonucleotide; GART, GAR transformylase; Glo1, glyoxalase I; HATs, histone acetyltransferases; HDACi, histone deacetylase inhibitor; HDACis, histone deacetylase inhibitors; HDACs, histone deacetylases; MAT, methionine adenosyltransferase; MITF, microphthalmia-associated transcription factor; MTHFR, methylenetetrahydrofolate reductase; MTX, methotrexate; MTXPGs, methotrexate polyglutamates; PP2A, protein phosphatase-2A; RFC, reduced folate carrier; ROS, reactive oxygen species; SAH, S-adenosylhomocysteine; SAHA, suberoylanilide hydroxamic acid; SAM, S-adenosylmethionine; THF, tetrahydrofolate; TMECG, 3-O-(3,4,5-trimethoxybenzoyl)-(-)-epicatechin; TS, thymidylate synthase.

* Corresponding author.
E-mail address: veselska@sci.muni.cz (R. Veselska).

http://dx.doi.org/10.1016/j.bbagen.2016.12.014
0304-4165/

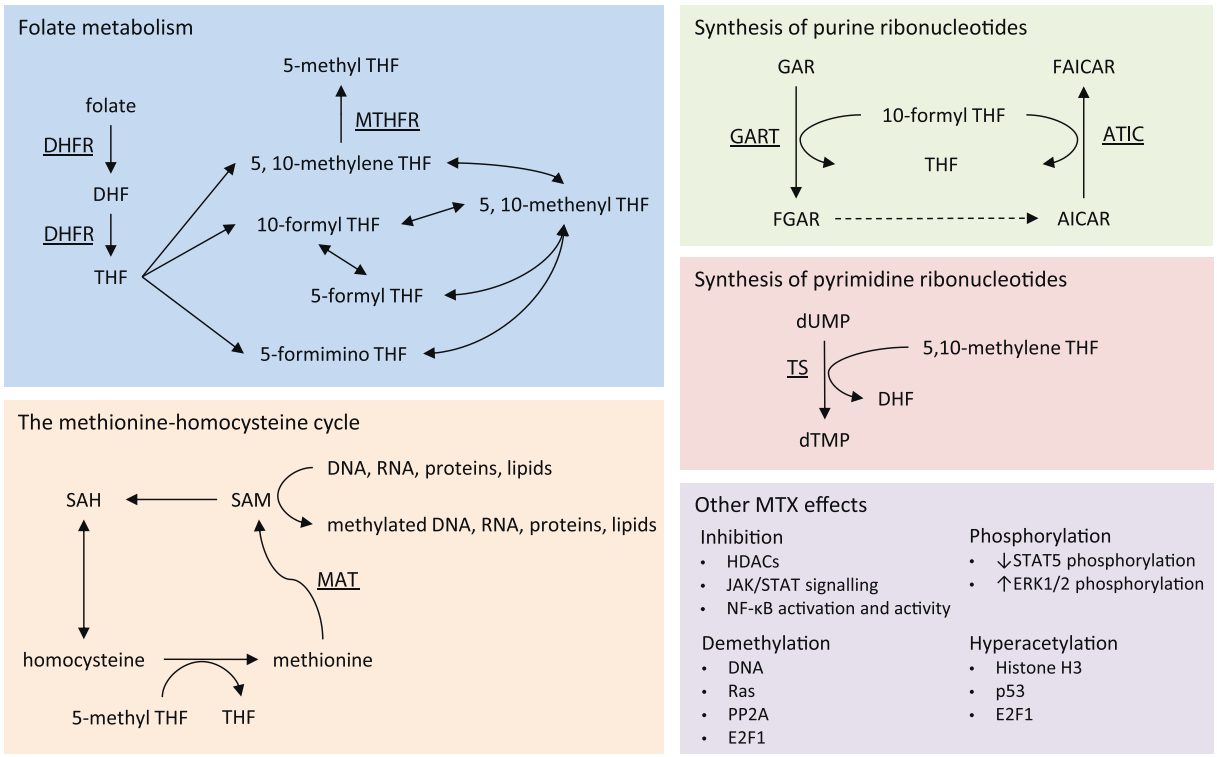

Fig. 1. Overview of MTX effects. The enzymes that are inhibited by MTX/MTXPGs are in bold and underlined. Dashed line - multiple enzymatic steps. Abbreviations: AICAR - 5-aminoimidazole-4-carboxamide ribonucleotide; ATIC - AICAR transformylase; DHF - dihydrofolate; DHFR - dihydrofolate reductase; E2F1 - E2F transcription factor 1; FAICAR - 5-formaminoimidazole-4-carboxamide ribonucleotide; FGAR - formylglycinamide ribonucleotide; GAR - glycinamide ribonucleotide; GART - GAR transformylase; HDACs - histone deacetylases; MAT - methionine adenosyltransferase; MTHFR - methylenetetrahydrofolate reductase; PP2A - protein phosphatase-2A; SAH - S-adenosylhomocysteine; SAM - S-adenosylmethionine THF - tetrahydrofolate; TS - thymidylate synthase.

proliferation [30]. The inhibition of DHFR and other enzymes by MTX results in the depletion of reduced forms of DHF and nucleotides, which strongly affects the proliferation of treated cell populations and also induces cell death [33,35]. However, there are also many non-DHFR-mediated effects of MTX (Fig. 1), which are discussed below.

2. Oxidative stress

Although the cytotoxic effects of MTX are often induced by nucleotide depletion, non-DHFR-mediated effects of MTX are also important, as MTX can interfere with glyoxalase and antioxidant systems. It has been shown that MTX affects α-oxoaldehyde metabolism. The inhibition of glyoxalase I (Glo1) by MTX leads to the accumulation of methylglyoxal, a highly reactive α-oxoaldehyde, which causes glycation of biomolecules. This action contributes to the anticancer activity and toxicity of MTX [4]. Regarding oxidative stress, some reports show that MTX-induced anti-proliferation and pro-apoptotic effects depend on alterations of the intracellular reactive oxygen species (ROS) levels [13,34]. Indirect evidence for MTX-induced actions through increased ROS production was demonstrated by studying the role of ornithine decarboxylase. The proposed mechanism of action is that MTX indirectly inhibits polyamine-producing enzymes. As a consequence, decreased polyamine production leads to increased intracellular ROS levels [51]. Furthermore, MTX is able to induce both apoptosis, through oxidative stress by reducing NO and increasing caspase-3 levels [8], and oxidative DNA damage, which can be lethal to tumor cells with defects in the *MSH2* DNA mismatch repair gene [23].

3. Cell differentiation

It has also been described that MTX acts as a strong differentiation factor for immature and undifferentiated monocytic cells [39] and is able to induce differentiation in human keratinocytes [38]. Moreover, MTX has the ability to trigger cellular differentiation in tumor cells, including human and rat choriocarcinoma cells, HL-60 human promyelocytic cells and other human leukemia cell lines, LA-N-1 human neuroblastoma cells, HT29 colon cancer cells and A549 human lung adenocarcinoma cells [30]. Recently, it has been described that in human melanoma cells, MTX promotes differentiation and prevents invasion [37], whereas it also induces differentiation of human osteosarcoma cells [44].

These effects of MTX may be caused by the depletion of thymine deoxyribonucleotides [38] or by the depletion of purines [42]. Although a reduction of nucleotides seems to be a clear explanation of this effect, it is hard to distinguish the precise mechanisms by which induced differentiation is achieved. Non-DHFR-mediated mechanisms of MTX can also be involved in the differentiation process. For example, MTX can induce a decrease of S-adenosylmethionine (SAM) by multiple mechanisms, and reduction in SAM concentrations may contribute to the decrease in cell proliferation as well as to the induction of differentiation by MTX [42]. Interestingly, it has been found that SAM is a key regulator for maintaining undifferentiated pluripotent stem cells and regulates their differentiation [41]. An important feature of MTX is its ability to affect the expression of genes or proteins that are directly or indirectly involved in the differentiation process [15,44]. To be more specific, some differentiation markers of epithelial cells, e.g., E-cadherin, involucrin, and filaggrin, are selectively induced by MTX in human squamous cell carcinoma cell lines [2]. MTX also promotes E-cadherin expression in the SW620 colorectal adenocarcinoma cell line and in the SK-MEL-28 melanoma cell line [15]. Another study showed that MTX upregulates the mRNA and protein expression of *MITF* (microphthalmia-associated transcription factor), which prevents the invasion of human melanoma cells. Importantly, through this effect of MTX, human melanoma cells are further sensitized to a tyrosinase-processed antifolate pro-drug 3-

O-(3,4,5-trimethoxybenzoyl)-(-)-epicatechin (TMECG), which inhibits DHFR; thus, an MTX and TMECG combination treatment effectively induces apoptosis in human melanoma cells [37]. In human osteosarcoma cell lines, MTX affects the expression of genes involved in all-*trans* retinoic acid (ATRA) metabolism and in the regulation of gene expression. The combined treatment of osteosarcoma cells with MTX and ATRA subsequently enhances matrix mineralization, which is considered a marker of osteogenic differentiation [44].

4. Anti-inflammatory effects of MTX

In addition to cytotoxic and cytostatic effects, the anti-inflammatory activity of MTX was also described by several studies. Inhibition of ATIC by MTX has been found to result in the accumulation of 5-aminoimidazole-4-carboxamide-1-β-d-ribofuranosyl 5′-monophosphate and its metabolites, which inhibit ADA and adenosine monophosphate deaminase, resulting in an increase in adenosine and adenine nucleotide levels. Elevated levels of extracellular adenosine through adenosine receptor activation result in a reduction of inflammation [9]. Other important regulators of inflammation are cytokines, and there is evidence that their biosynthesis is also influenced by MTX. For example, MTX inhibits the production of cytokines induced by activation of T-cells: the inhibition of IL-4, IL-13, IFNγ, TNFα, granulocyte-macrophage colony-stimulating factor and other cytokines was previously described [10]. Furthermore, MTX reduces the production of the proinflammatory IL-6 cytokine in patients with juvenile rheumatoid arthritis [1]. Patients suffering from rheumatoid arthritis with good or excellent responses to MTX treatment had a lower ratio of IL-1ra/IL-1β cytokines constitutively produced by peripheral blood mononuclear cells [11]. In contrast, another research group described that MTX can promote inflammation by influencing cytokine production, demonstrating that in the U937 monocyte cell line, MTX upregulates the production of the proinflammatory cytokines IL-1, IL-6 and TNFα, which may explain the mechanisms of some MTX side effects, such as mucositis and pneumonitis [32].

5. DNA and protein demethylation

As reviewed above, MTX and MTXPGs not only block DHFR but also inhibit a number of other enzymes. Some of these enzymes are involved in the metabolism of SAM, which plays a pivotal role as the universal methyl donor in many metabolic pathways and regulation mechanisms including methylation of proteins, lipids, and nucleic acids.

Regarding SAM metabolism, both DHFR- and non-DHFR-mediated effects of MTX can be involved. On one hand, inhibition of DHFR decreases THF levels. This can affect SAM metabolism since the reduced derivative of 5,10-methylene THF, 5-methyl THF, provides the methyl group to regenerate methionine from homocysteine. On the other hand, MTXPGs and DHF polyglutamates have an inhibitory effect on methylenetetrahydrofolate reductase (MTHFR), which catalyzes the conversion of 5,10-methylene THF to 5-methyl THF [5]. Moreover, MTX inhibits methionine adenosyltransferase (MAT) expression and MAT enzyme activity. MAT is a key enzyme for SAM metabolism, as it catalyzes the synthesis of SAM from methionine and ATP [50].

Several studies showed that MTX also affects DNA methylation. Folate deficiency is associated with hypomethylated DNA in rat liver cells [3]. In mice, the total level of DNA methylation showed a significant reduction compared to the control group when different doses of MTX were used [12]. In zebrafish embryos, treatment with MTX reduced overall methylation levels and altered gene-specific methylation patterns [26]. In humans, administration of MTX is unable to induce genomic DNA hypomethylation in patients with inflammatory arthritis, but this disease is associated with a significant degree of systemic DNA hypomethylation [18]. In cutaneous T-cell lymphoma cells, MTX treatment significantly reduces SAM levels, and this effect is accompanied by reduction in promoter methylation at CpG islands and by an increase in the expression of Fas protein [54]. Treatment with MTX also decreases global DNA methylation in A549 human lung carcinoma cells [19] and reduces the *FAS* promoter methylation in melanoma cell lines, which is associated with increased levels of Fas protein [31]. In patients suffering with rheumatoid arthritis, treatment with MTX restores defective Treg cell function through demethylation of the *FOXP3* locus, leading to the subsequent increase in FoxP3 expression [6]. Very recently, MTX was shown to decrease global DNA methylation in several osteosarcoma cell lines [44].

Methylation of DNA is not the only situation in which MTX can change the methylation status of biomolecules. For example, MTX inhibits Ras carboxyl methylation. Ras is a prototypic GTPase that functions as a molecular switch to control cell growth and differentiation. After MTX treatment of DKOB8 cells, Ras methylation is decreased by almost 90%. This hypomethylation is accompanied by mislocalization of Ras to the cytoplasm and a substantial decrease in the activation of p44 mitogen-activated protein kinase and Akt [53]. Another example is the methylation of phosphatase-2A (PP2A). MTX reduces the levels of methylated PP2A in primary rat neurons. This effect is accompanied by an increase in phosphorylation of Tau-protein because methylated PP2A is the active form of PP2A [56]. There is also evidence that MTX is able to promote demethylation of the transcription factor E2F1 [36].

6. Protein acetylation

Several reports show that MTX is able to induce acetylation of histones and other proteins. Extensive studies have established that histone acetylation is primarily associated with gene activation. Acetylation occurs at lysine residues on the amino-terminal tail of the protein molecule. This process is highly dynamic and is regulated by the opposing action of two enzyme families, histone acetyltransferases (HATs) and histone deacetylases (HDACs). Numerous correlative studies have demonstrated aberrant expression of HDACs in human tumors, and histone deacetylase inhibitors (HDACis) are used for treatment of many cancer diseases, such as thymoma, melanoma, B cell malignancies, various solid tumors, and cutaneous T-cell lymphoma [52].

Molecular modeling suggests that MTX is a potential histone deacetylase inhibitor (HDACi). The MTX molecule consists of a hydrophobic pteridine ring and a carboxylate-containing *para*-aminobenzoic acid tail similar to the structure of well-known HDACis such as trichostatin A, suberoylanilide hydroxamic acid (SAHA) and butyrate. This prediction was later confirmed, as MTX was shown to inhibit HDAC activity and to induce acetylation of histone H3 in A549 human lung carcinoma cells and in HeLa cervical carcinoma cells [55]. Moreover, MTX is able to increase the expression of E-cadherin through the downregulation of HDACs. This effect is associated with an inhibition of the expression of the methyltransferase enzyme enhancer of zeste homolog 2: this inhibitory effect was the same as observed after the treatment with SAHA [17]. In addition, MTX can have a positive impact on the accumulation of acetylated histone H3 in osteosarcoma cells [44].

Considering the acetylation of non-histone proteins, MTX induces an increase in p53 acetylation, and this effect is correlated with higher nuclear accumulation and stability of p53 [17]. Another study showed that treatment with MTX induces hyperacetylation of the transcription factor E2F1 in melanoma cells [36].

7. Effects of MTX on other proteins

Although many molecular mechanisms and targets of MTX have been identified so far, many others have yet to be revealed. Several recently published studies showed that MTX can even influence some protein kinases and other signaling proteins. For instance, MTX suppresses human JAK/STAT signaling without affecting other phosphorylation-dependent pathways. MTX significantly reduces STAT5 phosphorylation in cells expressing JAK2 V617F, a mutation associated with most human myeloproliferative neoplasms [48]. Another study

showed that in human T-cell lines, MTX inhibits the activation of NF-κB via depletion of tetrahydrobiopterin and increases Jun-N-terminal kinase-dependent p53 activity. MTX also inhibits NF-κB activity in fibroblast-like synoviocytes via the release of adenosine and adenosine receptor activation [43]. In human skin fibroblasts, MTX induces an increase in phosphorylation of ERK1/2 and expression of MMP-1 through the ERK1/2 pathway [27]. These effects are not limited to human cells. Treatment of mice with MTX leads to the phosphorylation of AMP-activated protein kinase α, the induction of manganese superoxide dismutase in the aorta and the subsequently reduced expression of cell adhesion molecules [49]. Very recently, MTX was shown to induce post-translational nitrosative modification of proteins; however, it is not known which target proteins are involved in this process [28].

8. Dose effects of MTX treatment

The diverse effects of MTX described above are apparently concentration-dependent. The non-DHFR effects summarized in this review are achievable using MTX concentrations detectable in human plasma during the treatment of oncologic patients, particularly the high-dose MTX treatment, which is defined as a dose >1 g/m^2 of body surface and contributes to high plasma concentrations of MTX. It has been shown that concentrations of MTX of approximately 40 μM are reached during high-dose MTX treatments of pediatric solid tumors [29,45], and MTX concentrations of 100 μM or higher can be achieved in human plasma several hours after the administration of MTX in osteosarcoma patients [16]. However, the situation varies for other diseases as well as for low-dose MTX treatment [14]. For example, low-dose MTX is a standard regimen for the treatment of rheumatoid arthritis, and the maximum plasma concentration of MTX in rheumatoid arthritis patients who take an average MTX dosage of 7.2 mg/week ranges from 0.04 to 0.38 μM [40]. Therefore, it is important to reflect the concentrations of MTX that are needed to achieve a desired effect.

For example, 200 nM MTX markedly stimulates the differentiation of the monocytic U937 cells [39], but only 10 nM MTX is sufficient for the inhibition of clonogenicity in the ALL and APL cell lines [22]. Furthermore, an even lower concentration of MTX (2 nM) selectively induces the expression of p27 and E-cadherin, which are markers of growth arrest and differentiation, in SCC13 and HEK1 carcinoma cell lines [2]. In contrast, 50 μM MTX induces the expression of E-cadherin in A549 cells [17].

In addition to cell differentiation, other non-DHFR-mediated effects were also observed at various concentrations that can easily be achieved in human plasma. For example, 50 nM MTX inhibits the activity of MAT in hepatocellular carcinoma Hep G2 cells [50], 1 μM MTX induces demethylation and hyperacetylation of E2F1 in melanoma cells [36] and 50 μM MTX induces histone H3 acetylation in A549 cells [55]. Regarding DNA methylation, treating CD4+ T cells with 50 nM MTX leads to demethylation of the FoxP3 upstream enhancer [6], whereas 40 μM MTX induces hypomethylation of DNA in osteosarcoma cells, although 1 μM MTX is sufficient to decrease DNA methylation in osteosarcoma cells [44]. In contrast, a high concentration of MTX is needed to inhibit the glyoxalase system. The mean IC_{50} value of 125 μM MTX was determined for Glo1 [4]. Altogether, it is obvious that some of the non-DHFR-mediated effects of MTX can be relevant *in vivo* only when patients are treated with high-dose MTX.

9. Conclusion

In human medicine, MTX has been used as a potent folate antagonist for almost 70 years, especially for treating cancer diseases and autoimmune disorders. As described above, the effectiveness of MTX is undoubtedly caused by its capability to affect various intracellular pathways at many levels. Although the most important therapeutic mechanism of MTX is strongly based on the inhibition of DHFR, many other effects of this compound have been described and new studies bring new insights into the pharmacology of MTX every year. Identification of these new targets for MTX is especially important for a better understanding of MTX action in new protocols of combination therapy.

Transparency document

The Transparency document associated with this article can be found, in the online version.

Acknowledgements

Supported by the project no. LQ1605 from the National Program of Sustainability II (MEYS CR) and by the project FNUSA-ICRC no. CZ.1.05/1.1.00/02.0123 (OP VaVpI).

References

[1] A. Aggarwal, R. Misra, Methotrexate inhibits interleukin-6 production in patients with juvenile rheumatoid arthritis, Rheumatol. Int. 23 (2003) 134–137.
[2] S. Anand, G. Honari, T. Hasan, P. Elson, E.V. Maytin, Low-dose methotrexate enhances aminolevulinate-based photodynamic therapy in skin carcinoma cells in-vitro and in-vivo, Clin. Cancer Res. 15 (2009) 3333–3343.
[3] M. Balaghi, C. Wagner, DNA methylation in folate deficiency: use of CpG methylase, Biochem. Biophys. Res. Commun. 1933 (1993) 1184–1190.
[4] K. Bartyik, S. Turi, F. Orosz, E. Karg, Methotrexate inhibits the glyoxalase system in vivo in children with acute lymphoid leukaemia, Eur. J. Cancer 40 (2004) 2287–2292.
[5] M. Blits, G. Jansen, Y.G. Assaraf, M.A. van de Wiel, W.F. Lems, M.T. Nurmohamed, D. van Schaardenburg, A.E. Voskuyl, G.J. Wolbink, S. Vosslamber, C.L. Verweij, Methotrexate normalizes up-regulated folate pathway genes in rheumatoid arthritis, Arthritis Rheum. 65 (2013) 2791–2802.
[6] A.P. Cribbs, A. Kennedy, H. Penn, P. Amjadi, P. Green, J.E. Read, F. Brennan, B. Gregory, R.O. Williams, Methotrexate restores regulatory t cell function through demethylation of the FoxP3 upstream enhancer in patients with rheumatoid arthritis, Arthritis Rheum. 67 (2015) 1182–1192.
[7] T. Dervieux, D. Furst, D.O. Lein, R. Capps, K. Smith, M. Walsh, J. Kremer, Polyglutamation of methotrexate with common polymorphisms in reduced folate carrier, aminoimidazole carboxamide ribonucleotide transformylase, and thymidylate synthase are associated with methotrexate effects in rheumatoid arthritis, Arthritis Rheum. 9 (2004) 2766–2774.
[8] T. Elango, H. Dayalan, P. Gnanaraj, H. Malligarjunan, S. Subramanian, Impact of methotrexate on oxidative stress and apoptosis markers in psoriatic patients, Clin. Exp. Med. 14 (2014) 431–437.
[9] R.S. Funk, L. van Haandel, M.L. Becker, J.L. Leeder, Low-dose methotrexate results in the selective accumulation of aminoimidazole carboxamide ribotide in an erythroblastoid cell line, J. Pharmacol. Exp. Ther. 347 (2013) 154–163.
[10] A.H. Gerards, S. de Lathouder, E.R. de Groot, B.A. Dijkmans, L.A. Aarden, Inhibition of cytokine production by methotrexate. Studies in healthy volunteers and patients with rheumatoid arthritis, Rheumatology (Oxford) 42 (2003) 1189–1196.
[11] K.I. Halilova, E.E. Brown, S.L. Morgan, S.L. Bridges Jr., M.-H. Hwang, D.K. Arnett, M.I. Danila, Markers of treatment response to methotrexate in rheumatoid arthritis: where do we stand? Int. J. Rheumatol. 2012 (2012) 978396.
[12] S.M. Hanafy, T. Salem, A. El-Aziz, B. El-Fiky, M. Shokair, Influence OF anticancer drugs on DNA methylation in liver of female mice, Am. J. Mol. Biol. 1 (2011) 62–69.
[13] S. Herman, N. Zurgil, M. Deutsch, Low dose methotrexate induces apoptosis with reactive oxygen species involvement in T lymphocytic cell lines to a greater extent than in monocytic lines, Inflamm. Res. 54 (2005) 273–280.
[14] Y. Hiraga, Y. Yuhki, K. Itoh, K. Tadano, Y. Takahashi, M. Mukai, Pharmacokinetics and efficacy of low-dose methotrexate in patients with rheumatoid arthritis, Mod. Rheumatol. 14 (2004) 135–142.
[15] T. Hirano, R. Satow, A. Kato, M. Tamura, Y. Murayama, H. Saya, H. Kojima, T. Nagano, T. Okabe, K. Fukami, Identification of novel small compounds that restore E-cadherin expression and inhibit tumor cell motility and invasiveness, Biochem. Pharmacol. 86 (2013) 1419–1429.
[16] L. Holmboe, A.M. Andersen, L. Mørkrid, L. Slørdal, K.S. Hall, High dose methotrexate chemotherapy: pharmacokinetics, folate and toxicity in osteosarcoma patients, Br. J. Clin. Pharmacol. 73 (2012) 106–114.
[17] W.Y. Huang, P.M. Yang, Y.F. Chang, V.E. Marquez, C.C. Chen, Methotrexate induces apoptosis through p53/p21-dependent pathway and increases E-cadherin expression through downregulation of HDAC/EZH2, Biochem. Pharmacol. 81 (2011) 510–517.
[18] Y.I. Kim, J.W. Logan, J.B. Mason, R. Roubenoff, DNA hypomethylation in inflammatory arthritis: reversal with methotrexate, J. Lab. Clin. Med. 128 (1996) 165–172.
[19] M. Li, S.L. Hu, Z.J. Shen, X.D. He, S.N. Tao, L. Dong, Y.Y. Zhu, High-performance capillary electrophoretic method for the quantification of global DNA methylation: application to methotrexate-resistant cells, Anal. Biochem. 387 (2009) 71–75.
[20] A. Lima, M. Bernardes, R. Azevedo, J. Monteiro, H. Sousa, R. Medeiros, V. Seabra, SLC19A1, SLC46A1 and SLCO1B1 polymorphisms as predictors of methotrexate-related toxicity in Portuguese rheumatoid arthritis patients, Toxicol. Sci. 142 (2014) 196–209.

[21] A. Lima, V. Seabra, M. Bernardes, R. Azevedo, H. Sousa, R. Medeiros, Role of key TYMS polymorphisms on methotrexate therapeutic outcome in portuguese rheumatoid arthritis patients, PLoS One 9 (2014) e108165.
[22] T.L. Lin, M.S. Vala, J.P. Barber, J.E. Karp, B.D. Smith, W. Matsui, R.J. Jones, Induction of acute lymphocytic leukemia differentiation by maintenance therapy, Leukemia 21 (2007) 1915–1920.
[23] S.A. Martin, A. McCarthy, L.J. Barber, D.J. Burgess, S. Parry, C.J. Lord, A. Ashworth, Methotrexate induces oxidative DNA damage and is selectively lethal to tumour cells with defects in the DNA mismatch repair gene MSH2, EMBO Mol. Med. 1 (2009) 323–337.
[24] L.H. Matherly, Z. Hou, Structure and function of the reduced folate carrier: a paradigm of a major facilitator superfamily mammalian nutrient transporter, Vitam. Horm. 79 (2008) 145–184.
[25] L.H. Matherly, Z. Hou, Y. Deng, Human reduced folate carrier: translation of basic biology to cancer etiology and therapy, Cancer Metastasis Rev. 26 (2007) 111–128.
[26] D.M. McGaughey, H.O. Abaan, R.M. Miller, P.A. Kropp, L.C. Brody, Genomics of CpG methylation in developing and developed zebrafish, G3 (Bethesda) 4 (2014) 861–869.
[27] L. Nabai, R.T. Kilani, F. Aminuddin, Y. Li, A. Ghahary, Methotrexate modulates the expression of MMP-1 and type 1 collagen in dermal fibroblast, Mol. Cell. Biochem. 409 (2015) 213–224.
[28] K. Natarajan, P. Abraham, Methotrexate administration induces differential and selective protein tyrosine nitration and cysteine nitrosylation in the subcellular organelles of the small intestinal mucosa of rats, Chem. Biol. Interact. 251 (2016) 45–59.
[29] J. Neradil, G. Pavlasova, M. Sramek, M. Kyr, R. Veselska, J. Sterba, DHFR-mediated effects of methotrexate in medulloblastoma and osteosarcoma cells: the same outcome of treatment with different doses in sensitive cell lines, Oncol. Rep. 33 (2015) 2169–2175.
[30] J. Neradil, G. Pavlasova, R. Veselska, New mechanisms for an old drug; DHFR- and non-DHFR-mediated effects of methotrexate in cancer cells, Klin. Onkol. 2 (2012) 2S87-2S92.
[31] M. Nihal, J. Wu, G.S. Wood, Methotrexate inhibits the viability of human melanoma cell lines and enhances Fas/Fas-ligand expression, apoptosis and response to interferon-alpha: rationale for its use in combination therapy, Arch. Biochem. Biophys. 563 (2014) 101–107.
[32] N.J. Olsen, C.F. Spurlock, T.M. Aune, Methotrexate induces production of IL-1 and IL-6 in the monocytic cell line U937, Arthritis Res. Ther. 16 (2014) R17.
[33] A. Ongaro, M. De Mattei, M.G. Della Porta, G. Rigolin, C. Ambrosio, F. di Raimondo, A. Pellati, F.F. Masieri, A. Caruso, L. Catozzi, D. Gemmati, Gene polymorphisms in folate metabolizing enzymes in adult acute lymphoblastic leukemia: effects on methotrexate-related toxicity and survival, Haematologica 94 (2009) 1391–1398.
[34] D.C. Phillips, K.J. Woollard, H.R. Griffiths, The anti-inflammatory actions of methotrexate are critically dependent upon the production of reactive oxygen species, Br. J. Pharmacol. 138 (2003) 501–511.
[35] L. Quéméneur, L.M. Gerland, M. Flacher, M. Ffrench, J.P. Revillard, L. Genestier, Differential control of cell cycle, proliferation, and survival of primary T lymphocytes by purine and pyrimidine nucleotides, J. Immunol. 170 (2003) 4986–4995.
[36] M. Sáez-Ayala, M.P. Fernández-Pérez, M.F. Montenegro, L. Sánchez-del-Campo, S. Chazarra, A. Piñero-Madrona, J. Cabezas-Herrera, J.N. Rodríguez-López, Melanoma coordinates general and cell-specific mechanisms to promote methotrexate resistance, Exp. Cell Res. 318 (2012) 1146–1159.
[37] M. Sáez-Ayala, M.F. Montenegro, L. Sánchez-Del-Campo, M.P. Fernández-Pérez, S. Chazarra, R. Freter, M. Middleton, A. Piñero-Madrona, J. Cabezas-Herrera, C.R. Goding, J.N. Rodríguez-López, Directed phenotype switching as an effective antimelanoma strategy, Cancer Cell 24 (2013) 105–119.
[38] P.M. Schwartz, S.K. Barnett, E.S. Atillasoy, L.M. Milstone, Methotrexate induces differentiation of human keratinocytes, Proc. Natl. Acad. Sci. U. S. A. 89 (1992) 594–598.
[39] M. Seitz, M. Zwicker, P. Loetscher, Effects of methotrexate on differentiation of monocytes and production of cytokine inhibitors by monocytes, Arthritis Rheum. 41 (1998) 2032–2038.
[40] H. Shoda, S. Inokuma, N. Yajima, Y. Tanaka, T. Oobayashi, K. Setoguchi, Higher maximal serum concentration of methotrexate predicts the incidence of adverse reactions in Japanese rheumatoid arthritis patients, Mod. Rheumatol. 17 (2007) 311–316.
[41] N. Shiraki, Y. Shiraki, T. Tsuyama, F. Obata, M. Miura, G. Nagae, H. Aburatani, K. Kume, F. Endo, S. Kume, Methionine metabolism regulates maintenance and differentiation of human pluripotent stem cells, Cell Metab. 19 (2014) 780–794.
[42] R. Singh, A.A. Fouladi-Nashta, D. Li, N. Halliday, D.A. Barrett, K.D. Sinclair, Methotrexate induced differentiation in colon cancer cells is primarily due to purine deprivation, J. Cell. Biochem. 99 (2006) 146–155.
[43] C.F. Spurlock, H.M. Gass, C.J. Bryant, B.C. Wells, N.J. Olsen, T.M. Aune, Methotrexate-mediated inhibition of nuclear factor κB activation by distinct pathways in T cells and fibroblast-like synoviocytes, Rheumatology (Oxford) 54 (2015) 178–187.
[44] M. Sramek, J. Neradil, J. Sterba, R. Veselska, Non-DHFR-mediated effects of methotrexate in osteosarcoma cell lines: epigenetic alterations and enhanced cell differentiation, Cancer Cell Int. 16 (2016) 14.
[45] J. Sterba, L. Dusek, R. Demlova, D. Valik, Pretreatment plasma folate modulates the pharmacodynamic effect of high-dose methotrexate in children with acute lymphoblastic leukemia and non-Hodgkin lymphoma: "folate overrescue" concept revisited, Clin. Chem. 52 (2006) 692–700.
[46] S. Suthandiram, G.G. Gan, S.M. Zain, P.C. Bee, L.H. Lian, K.M. Chang, T.C. Ong, Z. Mohamed, Effect of polymorphisms within methotrexate pathway genes on methotrexate toxicity and plasma levels in adults with hematological malignancies, Pharmacogenomics 15 (2014) 1479–1494.
[47] H. Tian, B.N. Cronstein, Understanding the mechanisms of action of methotrexate: implications for the treatment of rheumatoid arthritis, Bull. NYU Hosp. Jt. Dis. 65 (2007) 168–173.
[48] S. Thomas, K.H. Fisher, J.A. Snowden, S.J. Danson, S. Brown, M.P. Zeidler, I. Methotrexate, A JAK/STAT pathway inhibitor, PLoS One 10 (2015) e0130078.
[49] C.C. Thornton, F. Al-Rashed, D. Calay, G.M. Birdsey, A. Bauer, H. Mylroie, B.J. Morley, A.M. Randi, D.O. Haskard, J.J. Boyle, J.C. Mason, Methotrexate-mediated activation of an AMPK-CREB-dependent pathway: a novel mechanism for vascular protection in chronic systemic inflammation, Ann. Rheum. Dis. 75 (2015) 439–448.
[50] Y.C. Wang, E.P. Chiang, Low-dose methotrexate inhibits methionine S-adenosyltransferase in vitro and in vivo, Mol. Med. 18 (2012) 423–432.
[51] J.A. Wessels, T.W. Huizinga, H.J. Guchelaar, Recent insights in the pharmacological actions of methotrexate in the treatment of rheumatoid arthritis, Rheumatology (Oxford) 47 (2008) 249–255.
[52] A.C. West, R.W. Johnstone, New and emerging HDAC inhibitors for cancer treatment, J. Clin. Invest. 124 (2014) 30–39.
[53] A.M. Winter-Vann, B.A. Kamen, M.O. Bergo, S.G. Young, S. Melnyk, S.J. James, P.J. Casey, Targeting Ras signaling through inhibition of carboxyl methylation: an unexpected property of methotrexate, Proc. Natl. Acad. Sci. U. S. A. 100 (2003) 6529–6534.
[54] J. Wu, G.S. Wood, Reduction of Fas/CD95 promoter methylation, upregulation of Fas protein, and enhancement of sensitivity to apoptosis in cutaneous T-cell lymphoma, Arch. Dermatol. 147 (2011) 443–449.
[55] P.M. Yang, J.H. Lin, W.Y. Huang, Y.C. Lin, S.H. Yeh, C.C. Chen, Inhibition of histone deacetylase activity is a novel function of the antifolate drug methotrexate, Biochem. Biophys. Res. Commun. 391 (2010) 1396–1399.
[56] S.Y. Yoon, H.I. Choi, J.E. Choi, C.A. Sul, J.M. Choi, D.H. Kim, Methotrexate decreases PP2A methylation and increases tau phosphorylation in neuron, Biochem. Biophys. Res. Commun. 363 (2007) 811–816.
[57] R. Zhao, I.D. Goldman, Resistance to antifolates, Oncogene 22 (2003) 7431–7457.

PLOS ONE

RESEARCH ARTICLE

Co-Expression of Cancer Stem Cell Markers Corresponds to a Pro-Tumorigenic Expression Profile in Pancreatic Adenocarcinoma

Jan Skoda[1,2,3], Marketa Hermanova[4], Tomas Loja[1], Pavel Nemec[1], Jakub Neradil[1,2,3], Petr Karasek[5], Renata Veselska[1,2,3]*

1 Laboratory of Tumor Biology, Department of Experimental Biology, Faculty of Science, Masaryk University, Brno, Czech Republic, **2** Department of Pediatric Oncology, University Hospital Brno and Faculty of Medicine, Masaryk University, Brno, Czech Republic, **3** International Clinical Research Center, St. Anne's University Hospital and Faculty of Medicine, Masaryk University, Brno, Czech Republic, **4** 1st Department of Pathological Anatomy, St. Anne's University Hospital and Faculty of Medicine, Masaryk University, Brno, Czech Republic, **5** Department of Complex Oncology Care, Masaryk Memorial Cancer Institute, Brno, Czech Republic

* veselska@sci.muni.cz

Citation: Skoda J, Hermanova M, Loja T, Nemec P, Neradil J, Karasek P, et al. (2016) Co-Expression of Cancer Stem Cell Markers Corresponds to a Pro-Tumorigenic Expression Profile in Pancreatic Adenocarcinoma. PLoS ONE 11(7): e0159255. doi:10.1371/journal.pone.0159255

Editor: Daotai Nie, Southern Illinois University School of Medicine, UNITED STATES

Received: December 2, 2015

Accepted: June 29, 2016

Published: July 14, 2016

Data Availability Statement: Raw microarray data are available in the ArrayExpress database (www.ebi.ac.uk/arrayexpress) under accession number E-MTAB-4055.

Funding: This study was supported by grants from the European Regional Development Fund - Projects FNUSA-ICRC (No. CZ.1.05/1.1.00/02.0123) and CEB (No. CZ.1.07/ 2.3.00/ 20.0183), and by National Program of Sustainability II - Project Translational Medicine LQ1605. The funders had no role in study design, data collection and analysis, decision to publish, or preparation of the manuscript.

Abstract

Pancreatic ductal adenocarcinoma (PDAC) remains one of the most lethal malignancies. Its dismal prognosis is often attributed to the presence of cancer stem cells (CSCs) that have been identified in PDAC using various markers. However, the co-expression of all of these markers has not yet been evaluated. Furthermore, studies that compare the expression levels of CSC markers in PDAC tumor samples and in cell lines derived directly from those tumors are lacking. Here, we analyzed the expression of putative CSC markers—CD24, CD44, epithelial cell adhesion molecule (EpCAM), CD133, and nestin—by immunofluorescence, flow cytometry and quantitative PCR in 3 PDAC-derived cell lines and by immunohistochemistry in 3 corresponding tumor samples. We showed high expression of the examined CSC markers among all of the cell lines and tumor samples, with the exception of CD24 and CD44, which were enriched under *in vitro* conditions compared with tumor tissues. The proportions of cells positive for the remaining markers were comparable to those detected in the corresponding tumors. Co-expression analysis using flow cytometry revealed that $CD24^+/CD44^+/EpCAM^+/CD133^+$ cells represented a significant population of the cells (range, 43 to 72%) among the cell lines. The highest proportion of $CD24^+/CD44^+/EpCAM^+/CD133^+$ cells was detected in the cell line derived from the tumor of a patient with the shortest survival. Using gene expression profiling, we further identified the specific pro-tumorigenic expression profile of this cell line compared with the profiles of the other two cell lines. Together, $CD24^+/CD44^+/EpCAM^+/CD133^+$ cells are present in PDAC cell lines derived from primary tumors, and their increased proportion corresponds with a pro-tumorigenic gene expression profile.

Competing Interests: The authors have declared that no competing interests exist.

Introduction

Pancreatic ductal adenocarcinoma (PDAC) is a highly lethal malignancy that represents the fourth leading cause of cancer-related deaths in Western countries [1]. PDAC has no early warning signs or symptoms; therefore, most patients present with advanced disease. The dismal prognosis of PDAC is primarily due to its late diagnosis, which is often accompanied by metastatic disease and high resistance of the primary tumor to chemotherapy and radiotherapy [2]. Despite recent advances in the diagnosis and treatment of pancreatic cancer, its incidence almost equals its mortality rate, and the 5-year survival rate does not generally reach 5% [1].

PDAC is a type of solid tumor in which transformed cells with stemness properties, termed cancer stem cells (CSCs), have been identified [3–5]. CSCs represent a subpopulation of tumor cells that can self-renew and undergo multilineage differentiation and that possess high tumorigenic potential *in vivo*. CSCs are highly resistant to conventional chemotherapy and radiotherapy and are considered a cause of tumor relapse after eradication of the tumor bulk.

The first evidence for the existence of CSCs in PDAC was reported by two groups in 2007 [3,4]. First, Li *et al.* demonstrated that the combination of cell surface markers CD44, CD24, and epithelial cell adhesion molecule (EpCAM; epithelial-specific antigen, ESA) identified a highly tumorigenic subpopulation of PDAC cells with stem cell properties [3]. Later, Hermann *et al.* reported pancreatic CSCs that were defined by the expression of prominin-1 (CD133) [4]. Since then, other putative markers of pancreatic CSCs have been found, including nestin, CXCR4, c-Met, and aldehyde dehydrogenase 1 [1, 6]. Some of these putative markers were also tested in combination with those first described. For example, c-Met^{high} cells were found to be more tumorigenic if they co-expressed CD44 [7]. CD133$^+$/CXCR4$^+$ cells were reported to have increased migration ability *in vitro*, and they also demonstrated metastatic potential in a mouse model [4]. However, a comprehensive study that has evaluated the co-expression of CD44, CD24, EpCAM and CD133 has not yet been conducted. Although Hermann *et al.* noted a 14% overlap among CD44$^+$/CD24$^+$/EpCAM$^+$ and CD133$^+$ cell populations in their pioneering study, this result was obtained in only one pancreatic cell line that was derived from a metastatic tumor and not from a primary tumor [4]. Similar to other combinations of CSC markers, the CD24$^+$/CD44$^+$/EpCAM$^+$/CD133$^+$ phenotype might more accurately identify true pancreatic CSCs. Thus, in the first step, the possible overlap among CD24$^+$/CD44$^+$/EpCAM$^+$ and CD133$^+$ cell populations in cell lines derived from primary PDAC should be determined. Additionally, it remains unknown to what extent the expression levels of CSC markers change under *in vitro* conditions because no study has compared the expression levels of CSC markers in PDAC tumor samples and in cell lines derived directly from those tumors.

Therefore, we performed a detailed expression analysis of the most frequently discussed putative markers of CSCs in PDAC (i.e., CD24, CD44, EpCAM, CD133, and nestin) in both human primary tumor samples and in the respective cell lines derived from those tumors. For the first time, we also examined the co-expression of CD24, CD44, EpCAM, and CD133 in cell lines derived from primary PDACs. Furthermore, these cell lines were subjected to expression profiling analysis to identify genes, the functions of which may correlate with the presence of CSC markers. We found that CD24$^+$/CD44$^+$/EpCAM$^+$/CD133$^+$ cells represented a significant subpopulation in these cell lines, and their increased proportion corresponded to a pro-tumorigenic gene expression profile.

Materials and Methods

Primary cell lines and tumor samples

Three PDAC primary cell lines were included in this study: P6B, P28B and P34B. These cell lines were derived from tissue samples of corresponding primary tumors. These tumor samples

Table 1. Description of patient cohort and derived cell lines.

Tumor sample	Gender	Age	Diagnosis	Localization	Grade	Stage	OS	PFS	Cell line
P6	M	66	PDAC	Head	3	pT3N1M0	33	21	P6B
P28	M	49	PDAC	Head	3	pT3N0M0	9	9	P28B
P34	F	62	PDAC	Body	2	pT3N1M0	21	11	P34B

Gender: M, male; F, female. Age at the time of diagnosis: years. Localization: Head, head of the pancreas; Body, body of the pancreas. Grade: 2, moderately differentiated; 3, poorly differentiated. OS, overall-free survival: months. PFS, progression free survival: months.

doi:10.1371/journal.pone.0159255.t001

were obtained from patients undergoing pancreatic resection surgery as a part of standard diagnostic therapeutic procedures for PDAC, and they were de-identified to comply with the Czech legal and ethical regulations governing the use of human biological material for research purposes (Act No. 372/2011 Coll. on Health Services, paragraph 81, article 4, letter a). The patients signed a written consent containing information on this issue. Resection specimens were routinely processed at the department of pathology and during the gross inspection, the pathologist (MH) obtained the tumor tissue samples for a derivation of cell lines. For immunohistochemical (IHC) analysis, formalin-fixed, paraffin-embedded (FFPE) tumor tissue samples primarily taken for diagnostic purposes were used and selected by the pathologist (MH) who also performed the standard histopathological diagnostic procedures. A previously described protocol was used to generate the primary cultures [8]. A description of the cohort is provided in Table 1.

Cell cultures

The cell lines were cultured in DMEM supplemented with 20% fetal calf serum, 2 mM glutamine, 100 IU/ml penicillin, and 100 μg/ml streptomycin (all purchased from GE Healthcare Europe GmbH, Freiburg, Germany). The cells were maintained under standard conditions at 37°C in an atmosphere containing 5% CO_2 and were subcultured one or two times per week.

Immunohistochemistry

IHC detection was performed on FFPE samples of primary tumors, as mentioned above. Sections that were cut at a thickness of 4 μm were applied to positively charged slides, deparaffinized in xylene and rehydrated through a graded alcohol series. Antigen retrieval was performed in a calibrated pressure chamber Pascal (Dako, Glostrup, Denmark) for each antibody as follows: for nestin and CD133, the sections were heated in Tris/EDTA buffer (Dako) at pH 9.0 for 40 min at 97°C; for CD24, CD44 and EpCAM, the sections were heated in citrate buffer (Dako) at pH 6.1 for 4 min at 117°C. Endogenous peroxidase activity was quenched with 3% hydrogen peroxide in methanol for 20 min, followed by incubation at room temperature (RT) with the primary antibody (S1 Table). For nestin, the Vectastain Elite ABC kit using a streptavidin-biotin horseradish peroxidase (HRP) detection method was used (Vector Laboratories, Burlingame, CA, USA). For CD133 and EpCAM, the EnVision+ Dual Link system-HRP without avidin or biotin was used for detection (Dako). The expression of CD44 was visualized using an EXPOSE Rabbit-specific HRP/DAB detection kit (Abcam, Cambridge, UK), while the expression of CD24 was visualized using an ImmunoCruz ABC Staining system (Santa Cruz Biotechnology, Inc., Dallas, TX, USA). 3,3′-diaminobenzidine (DAB) (Dako) was used as the chromogen. Samples that were incubated without the primary antibodies served as negative controls. CD133- and nestin-positive endothelial cells in the tumor tissue samples served as internal positive controls, while glioblastoma multiforme tissue served as an external

positive control for nestin. For EpCAM, CD44 and CD24, colon carcinoma, urinary bladder tissue and lymph node tissue, respectively, served as the positive controls. An evaluation of all IHC results was performed using an Olympus BX51 microscope and an Olympus DP72 camera with uniform settings. All immunostained slides were evaluated at 400× magnification.

Immunofluorescence

Indirect immunofluorescence (IF) was performed as previously described [9]. The primary and secondary antibodies that were used in these experiments are listed in S1 Table; a mouse monoclonal anti-α-tubulin served as the positive control. An Olympus BX-51 microscope was used for sample evaluation; micrographs were captured using an Olympus DP72 CCD camera and were analyzed using the Cell^P imaging system (Olympus, Tokyo, Japan).

Flow cytometry

Flow cytometry was performed on either fixed or live cells. Briefly, cells were detached from the culture flask with Accutase (Life Technologies, Carlsbad, CA, USA) and were washed in PBS. Regarding cell surface labeling, live cells were incubated in 3% BSA for 10 minutes. For both cell surface and intracellular labeling, cells were fixed in 3% paraformaldehyde (Sigma) for 30 minutes, washed twice in PBS and incubated in 3% BSA for 10 minutes. All subsequent labeling was performed at 37°C for fixed cells or at 4°C for live cells. Each sample was divided into two, and in the parallel sample, the respective isotype controls were used instead of the primary antibodies. A list of antibodies used in this study is provided in S1 Table. Briefly, the sample was washed twice with 3% BSA, incubated with the mouse monoclonal CD133 antibody for 30 minutes, and washed twice in 3% BSA. A secondary donkey anti-mouse Alexa488-conjugated antibody was applied in the same manner. After two additional washes, primary conjugated antibodies against CD24, CD44 and EpCAM were added to the sample and incubated for 30 minutes. Finally, the sample was washed four times with PBS and was subjected to analysis using FACSVerse (BD Biosciences, San Jose, CA, USA). Side scatter and forward scatter profiles were used to eliminate cell doublets. At least 10,000 events were collected per sample, and the data were analyzed using FlowJo X software (Tree Star, Inc., Ashland, OR, USA). Positive cells were evaluated relative to the respective isotype control; Boolean gating was applied to determine the cells that co-expressed the CSC markers.

Real-Time Quantitative Reverse Transcription PCR (qRT-PCR)

Regarding qRT-PCR of PDAC cell lines, total RNA was extracted and reverse transcribed as previously described [10]. Quantitative PCR was performed in a volume of 10 μl using the KAPA SYBR® FAST qPCR Kit (Kapa Biosystems, Wilmington, MA, USA) and 7500 Fast Real-Time PCR System (Applied Biosystems, Foster City, CA, USA). At least three technical replicates were analyzed for each sample. For microarray validation experiments, three biological replicates (different cell passages) of each cell line were used. The data were analyzed by 7500 Software v. 2.0.6 (Applied Biosystems) and relative quantification (RQ) of gene expression was calculated using $2^{-\Delta\Delta CT}$ method [11]; heat shock protein gene (*HSP90AB1*) was used as the endogenous reference control. The primer sequences used are listed in S2 Table.

Gene expression profiling

Total RNA was extracted using the GenElute™ Mammalian Total RNA Miniprep Kit (Sigma-Aldrich; St. Louis, MO, USA). Total RNA with a purity ratio of 260/280>1.7 and an integrity (RIN)>7.5 (as measured by an Agilent 2010 Bioanalyzer; Agilent Technologies, Santa Clara,

CA, USA) was transcribed into cDNA (Ambion WT Expression Kit), labeled and hybridized to the Affymetrix GeneChip® Human Gene ST 1.0 array and processed through a complete Affymetrix workflow (all from Affymetrix, Santa Clara, CA, USA). Raw microarray data are available in the ArrayExpress database (www.ebi.ac.uk/arrayexpress) under accession number E-MTAB-4055. Affymetrix power tools were used to normalize raw CEL files at the gene level. Robust multiarray averaging (RMA) normalization and complete annotation files were selected. Gene ontology analysis was performed using the GOTERM_BP_FAT database in the DAVID functional annotation tool [12, 13]. Cytoscape v. 3.1.1 [14] with the Reactome Functional Interaction (FI) plug-in was used for functional protein interaction network analysis. The Reactome FI plug-in gene set analysis tool was selected to include interactions from the Reactome FI network 2013 version and FI annotations.

Statistical analysis

The qRT-PCR validation data were analyzed using one-tailed Mann-Whitney U test. $P < 0.01$ was considered statistically significant.

Results

CSC markers were highly expressed in PDAC-derived cell lines compared with PDAC tumor tissues

To address the expression of the putative CSC markers CD24, CD44, EpCAM, CD133, and nestin in pancreatic cancer, we used three cell lines (P6B, P28B, and P34B) derived from PDAC tumor tissues and three corresponding FFPE tumor samples (Table 1). Initially, the expression of individual CSC markers in the cell lines was assessed by IF (Fig 1). Using this method, the expression of all of the examined CSC markers was determined in all three cell lines. The observed pattern of expression of each marker was in accordance with the expected cellular localization of these molecules (Fig 1). Subsequently, the exact quantification of the proportion of cells that were positive for these markers was performed solely by flow cytometry (see below), with the exception of nestin. This was because approximately 95% of the cells in all

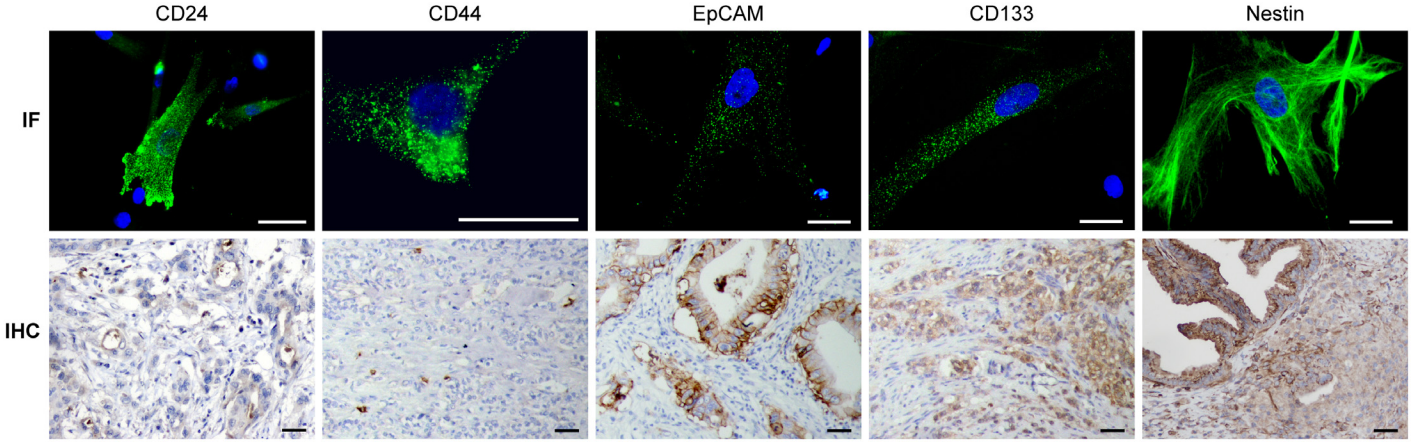

Fig 1. IF and IHC analysis of CSC marker expression in PDAC cell lines and corresponding tumors. Representative images of immunofluorescence (IF) and immunohistochemical (IHC) detection of CD24, CD44, EpCAM, CD133, and nestin expression are shown. For IF analysis, the cells of each PDAC cell line were stained with the appropriate antibodies against the CSC markers (green) and were counterstained with DAPI (blue) to visualize the nuclei. IHC was performed on tumor samples with antibodies that recognize specific markers; positive cells were visualized by DAB staining. Scale bars, 40 μm.

doi:10.1371/journal.pone.0159255.g001

Table 2. IHC analysis of CSC marker expression in PDAC tumor samples.

	Positive cells[a]			Localization of marker expression		
	P6	P28	P34	P6	P28	P34
CD24	++	+	-	apical cytoplasmic, luminal	apical cytoplasmic	–
CD44	-	+/-	-	–	poorly differentiated component	–
EpCAM	+++	+++	+++	membranous	membranous	membranous
Nestin	+++	+++	+++	cytoplasmic	cytoplasmic	cytoplasmic
CD133	++	+++	+	cytoplasmic	cytoplasmic, rarely membranous	cytoplasmic

[a]The percentage of positive tumor cells was categorized into five levels:—(0%), +/- (1–5%), + (6–20%), ++ (21–60%), and +++ (61–100%).

doi:10.1371/journal.pone.0159255.t002

three cell lines were nestin-positive as detected by IF; thus, nestin was omitted from the flow cytometric analysis. IHC was used to evaluate the expression levels of the CSC markers in the corresponding FFPE tumor samples (Fig 1; Table 2). IHC revealed a high percentage of tumor cells that expressed nestin and EpCAM in all of the tumor samples. In addition, CD133 was highly expressed in P6 and P28 tumors, although only a small number of positive cells was identified in P34 tumor tissue. Similarly, CD24 was expressed solely in P6 and P28 tumors. By contrast, $CD44^+$ cells were identified in a poorly differentiated component of P28 tumor tissue but not in the other two tumor samples. Based on the IHC results, the P28 tumor was the only one that expressed all of the tested CSC markers.

Next, multicolor flow cytometry was used to evaluate the percentage of cells that were positive for CD24, CD44, EpCAM, CD133, and their combinations in three tumor-derived cell lines (Fig 2; Table 3). For multicolor flow cytometry, we used both live cells and cells fixed in paraformaldehyde. Surprisingly, using the fixed cells, we detected very high percentages of $CD24^+$, $CD44^+$, $EpCAM^+$, and $CD133^+$ cells in all of the cell lines examined (Table 3). Additionally, cells that were positive for the combinations of these markers were very common. The $CD24^+/CD44^+/CD133^+$ phenotype was present in approximately 80% of the cells irrespective of the cell line. The percentages of $CD24^+/CD44^+/EpCAM^+$ and $CD24^+/CD44^+/CD133^+/EpCAM^+$ cells varied more among the cell lines, but the percentages of each ranged from 43 to 72%. Compared with their respective tumor tissues, the cell lines were markedly enriched for $CD24^+$ and $CD44^+$ cells. In accordance with the IHC results, the highest frequency of the cells that expressed CD24, CD44, EpCAM, and CD133 was found in the P28B cell line.

Live cells differed greatly from fixed cells with respect to positivity for CSC markers

Due to the surprising prevalence of cells in the PDAC cell lines that were positive for CSC markers, we next used live cells for subsequent flow cytometric analyses. Because fixation itself can permeabilize the cell membranes, this approach enabled us to evaluate the expression of CSC markers only on the cell surface. Using live cells for flow cytometric analyses of the expression of CD24, CD44, EpCAM, and CD133 in the PDAC cell lines, we observed a marked decrease in positivity for these markers in compared with fixed cells (Fig 2; Table 3). In the samples of live cells, CD44 was the only marker that was detected at levels that were similar to those in fixed cell samples. However, the proportions of $CD24^+/CD44^+/EpCAM^+$ and $CD24^+/CD44^+/CD133^+$ cells were markedly lower and ranged from 0.4 to 1.14% and from 0 to 1.43%, respectively. $CD24^+/CD44^+/CD133^+/EpCAM^+$ cells were detected only in the P34B cell line.

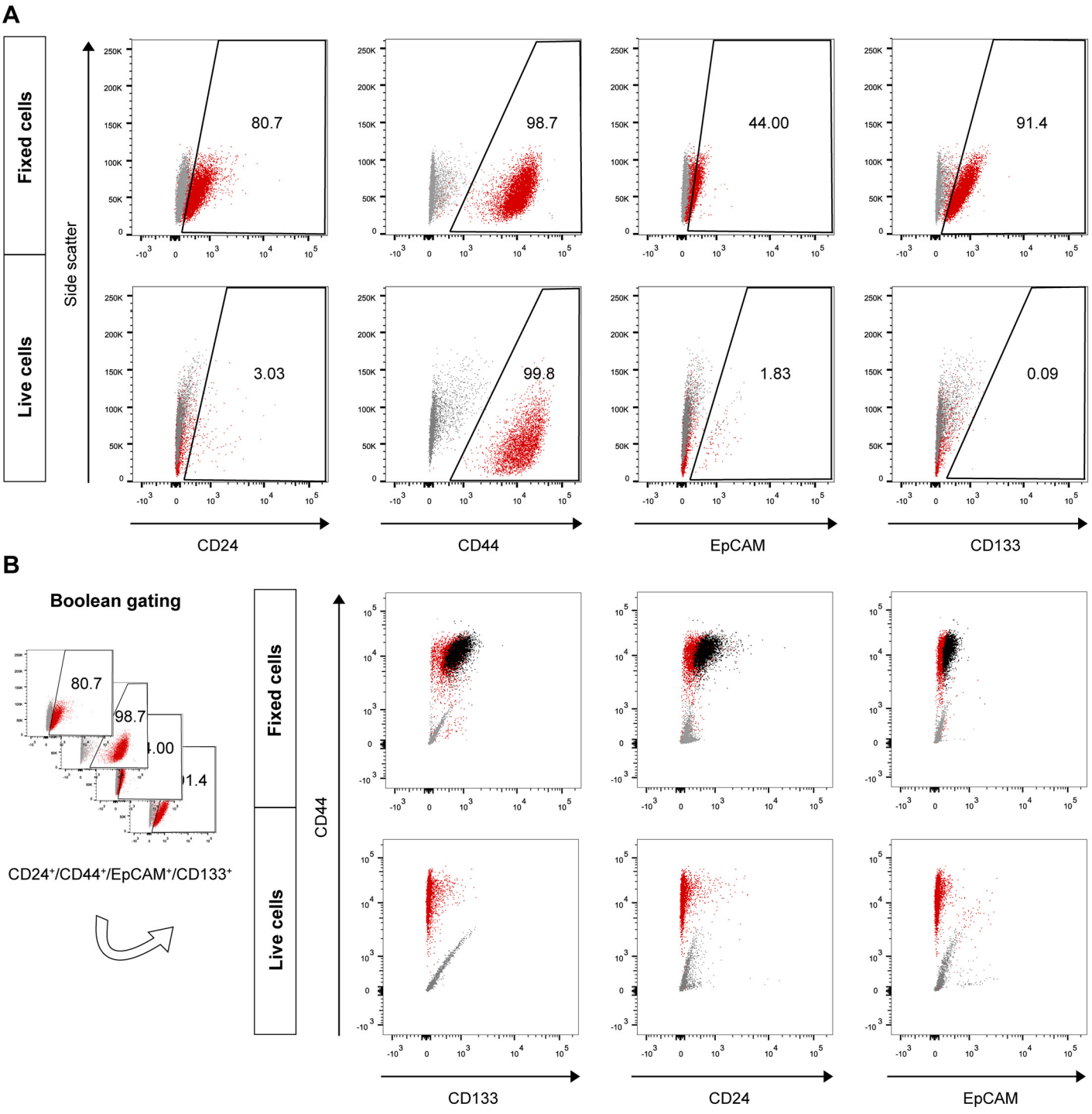

Fig 2. Flow cytometric analysis of the expression of CSC markers in fixed and live PDAC cells. (A) Dot plot diagrams depict the differences in CSC marker expression in PDAC cells when fixed or live cells were used in the flow cytometric analysis. The percentages of cells that were positive for specific markers are marked by numbers in the gated areas. (B) A Boolean gating approach was used to determine the proportion of cells that co-expressed CSC markers. An illustrative Boolean gate of the $CD24^+/CD44^+/EpCAM^+/CD133^+$ population (black) is shown in the dot plot diagrams. Cells stained with matched isotype control antibodies (gray) were used as controls for each CSC marker antibody (red) in both experimental designs (fixed cells and live cells). Representative data for the P6B cell line are shown. For detailed results of CSC marker expression, see Table 3.

doi:10.1371/journal.pone.0159255.g002

Table 3. Flow cytometric analysis of CSC marker expression in PDAC cell lines.

Marker	Fixed cells[a]			Live cells[a]		
	P6B	P28B	P34B	P6B	P28B	P34B
$CD24^+$	80.70	79.10	79.10	3.03	13.00	2.52
$CD44^+$	98.70	96.10	96.70	99.80	98.50	98.20
$EpCAM^+$	44.00	78.60	57.50	1.83	4.08	2.28
$CD133^+$	91.40	94.90	89.60	0.09	0	6.70
$CD24^+/CD44^+/EpCAM^+$	43.20	72.10	55.10	0.40	0.76	1.14
$CD24^+/CD44^+/CD133^+$	79.70	78.10	78.00	0.06	0	1.43
$CD24^+/CD44^+/CD133^+/EpCAM^+$	43.20	71.90	55.00	0	0	1.14

[a]Proportions of cells positive for expression of individual CSC marker or combination of markers are indicated as percentages.

doi:10.1371/journal.pone.0159255.t003

Gene expression profiling identified a pro-tumorigenic profile of the P28B cell line that highly co-expressed CSC markers

To verify the expression of CSC markers observed at the protein level and investigate possible differences among the PDAC cell lines, we next evaluated gene expression at the mRNA level. In the first step, we performed qRT-PCR for the genes that encode the CSC markers (Fig 3). qRT-PCR revealed upregulated mRNA expression of the proteins CD24, CD44, and EpCAM in P28B cells. As clinical data show, the P28B cell line was derived from the tumor of the patient with the shortest overall survival (P28, Table 1). IHC, flow cytometry and qRT-PCR results all revealed that P28B cells also expressed the highest levels of CSC markers among the tested cell lines. To investigate this phenomenon more thoroughly, we employed gene expression profile analysis. Using this method, we detected 344 genes that were upregulated (fold-change ≥ 2), and 258 genes that were downregulated (fold-change ≤ 0.5) in the P28B cells compared with the expression profiles of P6B and P34B cell lines.

To analyze the biological functions of the differentially expressed genes in P28B cells, we performed gene ontology analysis (Table 4; S3 Table). Most of the upregulated genes were found to be associated with cell surface receptor signaling (18.8% of the upregulated genes) or

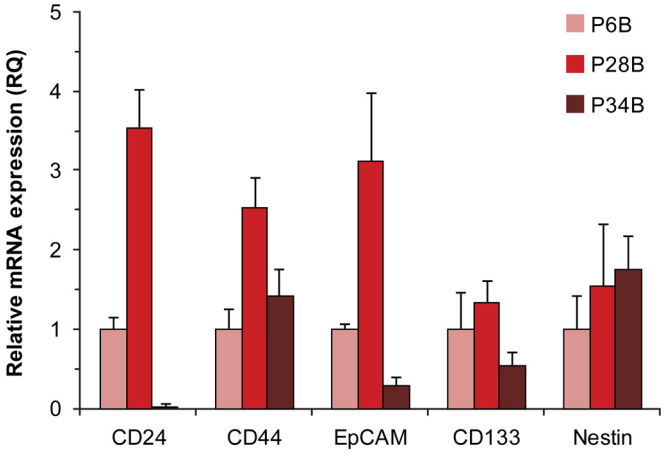

Fig 3. qRT-PCR analysis of CSC marker expression. P6B cell line served as the arbitrary calibrator of the gene expression. The error bars indicate the calculated maximum (RQMax) and minimum (RQMin) expression levels that represent the standard error of the mean expression level (RQ value).

doi:10.1371/journal.pone.0159255.g003

Table 4. Gene ontology analysis of genes differentially expressed in P28B cells.

Biological process	Number of genes	P value
Upregulated genes (fold-change ≥ 2)		
Cell surface receptor linked signal transduction	65	< 0.001
Cell adhesion	32	< 0.001
G-protein coupled receptor protein signaling pathway	30	0.049
Ion transport	29	< 0.001
Cell-cell signaling	28	< 0.001
Regulation of cell proliferation	26	0.007
Response to wounding	22	0.001
Immune response	20	0.061
Cell motion	16	0.034
Downregulated genes (fold-change ≤ 0.5)		
Regulation of cell proliferation	29	< 0.001
Cell motion	20	< 0.001
Regulation of apoptosis	18	0.039
Immune response	17	0.022
Cell adhesion	17	0.024
Mitotic cell cycle	11	0.026
Vasculature development	10	0.006

Upregulated (fold-change ≥ 2) and downregulated (fold-change ≤ 0.5) genes in P28B cells compared with P6B and P34B cells were analyzed for gene ontology. Gene ontology analysis was performed using GOTERM_BP_FAT database in DAVID functional annotation tool.

doi:10.1371/journal.pone.0159255.t004

cell adhesion (9.3%). Downregulated genes were linked to the regulation of cell proliferation (11.2% of the downregulated genes), cell motility (7.6%) or regulation of apoptosis (7%). Furthermore, a review of the literature revealed that the vast majority of the upregulated genes have been reported to have pro-tumorigenic potential, whereas about one-third of the downregulated genes were found to suppress tumorigenesis (Table 5; S4 Table). To validate the results obtained by expression profiling, we performed qRT-PCR analysis of five pro-tumorigenic and five anti-tumorigenic genes in samples from three different passages of each cell line (Fig 4). In agreement with the microarray data, all selected anti-tumorigenic genes were significantly ($P < 0.001$) downregulated in P28B cells, whereas the expression of pro-tumorigenic genes was significantly ($P < 0.001$) upregulated compared with that of P6B and P34B cells. Taken together, these analyses revealed a specific pro-tumorigenic profile of the P28B cell line that was highly enriched in cells that co-expressed CSC markers. By contrast, the lower expression of CSC markers in the P6B and P34B cell lines reflected differences in the expression profiles of these cell lines compared with the profile of P28B cells.

To further analyze the expression profile of P28B cells compared with that of P6B and P34B cells, we performed a functional protein interaction network analysis of the differentially expressed genes. Using Cytoscape software with the Reactome FI plug-in, we created an interaction network that enabled us to visualize expression profiling data combined with information on the interactions of the proteins encoded by the respective genes (Fig 5). This approach clearly showed the most prominent genes whose expression was upregulated or downregulated in P28B cells compared with the other two cell lines. Downregulated genes included *FYN*, *RAC2*, *GNG2*, *PLK1* and *MET*. Of the upregulated genes, *LYN*, *WNT2*, *KIT*, *TEK* (*TIE2*) and *ARRB1* were identified.

Table 5. Differentially expressed genes in P28B cells grouped by their role in tumorigenesis.

Role in cancer	Number of genes	Genes
Upregulated genes (fold-change ≥ 2)		
Pro-tumorigenic	62	ABCC4, ADAMTS7, ADM, ANO1, BAMBI, CD24, CP, CSF1, CXCL14, CXCR7, CYP1A1, EDN1, ELMO1, ENTPD1, EPHA6, F3, FGFR4, FZD6, FZD7, GFRA1, GPR183, GPR56, GPR65, GRIA4, CHRM3, IL6R, ITGB3, JAM2, KIT, LAMA3, LPAR3, LYN, MCAM, MITF, NCAM2, NLK, NOG, NOX4, P2RY1, PMP22, PREX2, PTGER4, PTHLH, RPS6KA5, SCN5A, SEMA4D, SEMA6A, SHC3, SLC4A4, SMAD9, SORT1, TEK, TFAP2C, TRPA1, TRPC3, TRPC6, TRPV2, UCP2, VTN, WFDC1, WNT2, WNT2B
Anti-tumorigenic	10	DSC2, DSC3, FOXF1, GBP2, PENK, PPAP2A, RELN, RGS6, TNFSF10, TXNIP
Mixed	9	ADAMTS8, CD9, DSG2, F11R, CHL1, ITGA8, NPY, SMURF2, UNC5C
Downregulated genes (fold-change ≤ 0.5)		
Pro-tumorigenic	28	ADRA2A, ARHGEF2, BGN, CENPF, CTSS, DLGAP5, ENPP2, GLI3, HORMAD1, CHST11, IL1A, IL1B, IL6, JAG1, KCNMA1, MET, MSX2, NFIB, NRP1, PLAUR, PLK1, PTX3, SEMA3C, SERPINE1, SPOCK1, TPBG, VASH2, VCAN
Anti-tumorigenic	18	CCND2, CDH13, CLDN11, EMILIN2, EPHB2, GAS1, CHST11, KLF4, KYNU, NEFL, PCDH10, PLA2G4A, RARB, SERPINB2, SLIT2, SRPX, TGFBR3, UNC5B
Mixed	16	ASPM, BUB1B, CD74, CDC6, CDKN3, CLU, CTH, ENPEP, FYN, ITGA2, ITGA3, POSTN, PRRX1, RAC2, TOP2A, UACA

The role of individual genes in tumorigenesis was determined based on the literature review (S4 Table).

doi:10.1371/journal.pone.0159255.t005

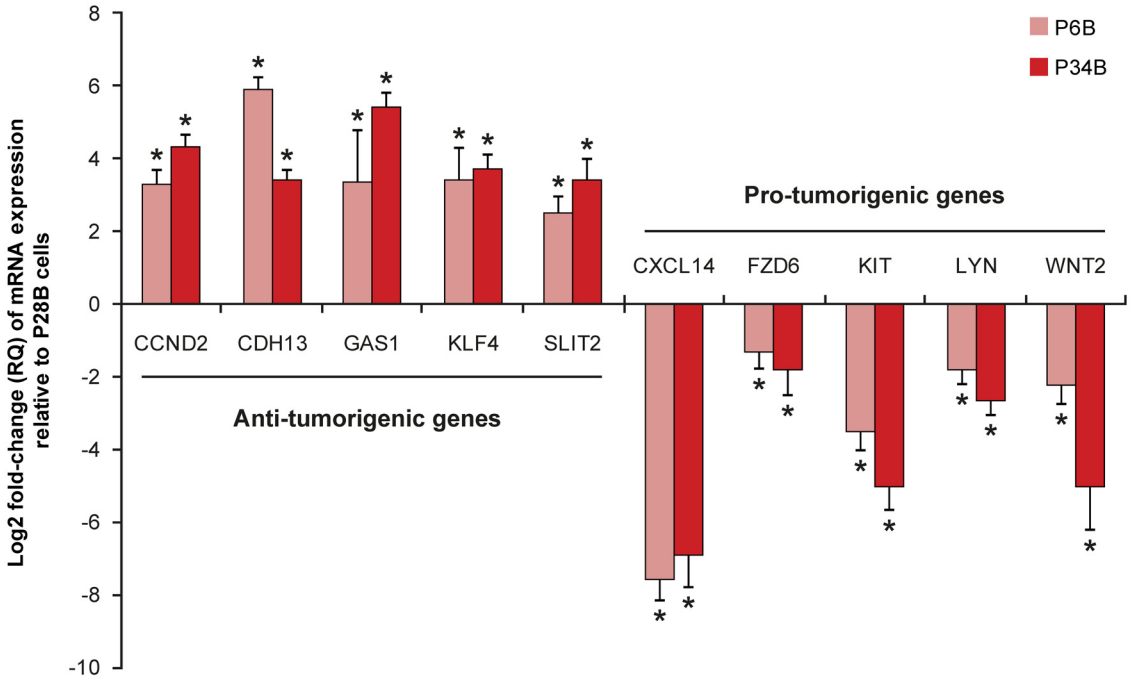

Fig 4. Validation of pro-tumorigenic expression profile of P28B cells by qRT-PCR. Five anti-tumorigenic and five pro-tumorigenic genes were selected based on the microarray data and their expression was validated by qRT-PCR. The graph shows the expression levels of the respective genes in P6B and P34B cells relative to that in P28B cell line, which served as the arbitrary calibrator. The bars represent the mean expression level (RQ value) of three biological replicates; the data are presented in log2 scale. The calculated maximum (RQMax) and minimum (RQMin) expression levels are indicated by error bars. *$P < 0.001$, indicates significant differences from P28B cell line.

doi:10.1371/journal.pone.0159255.g004

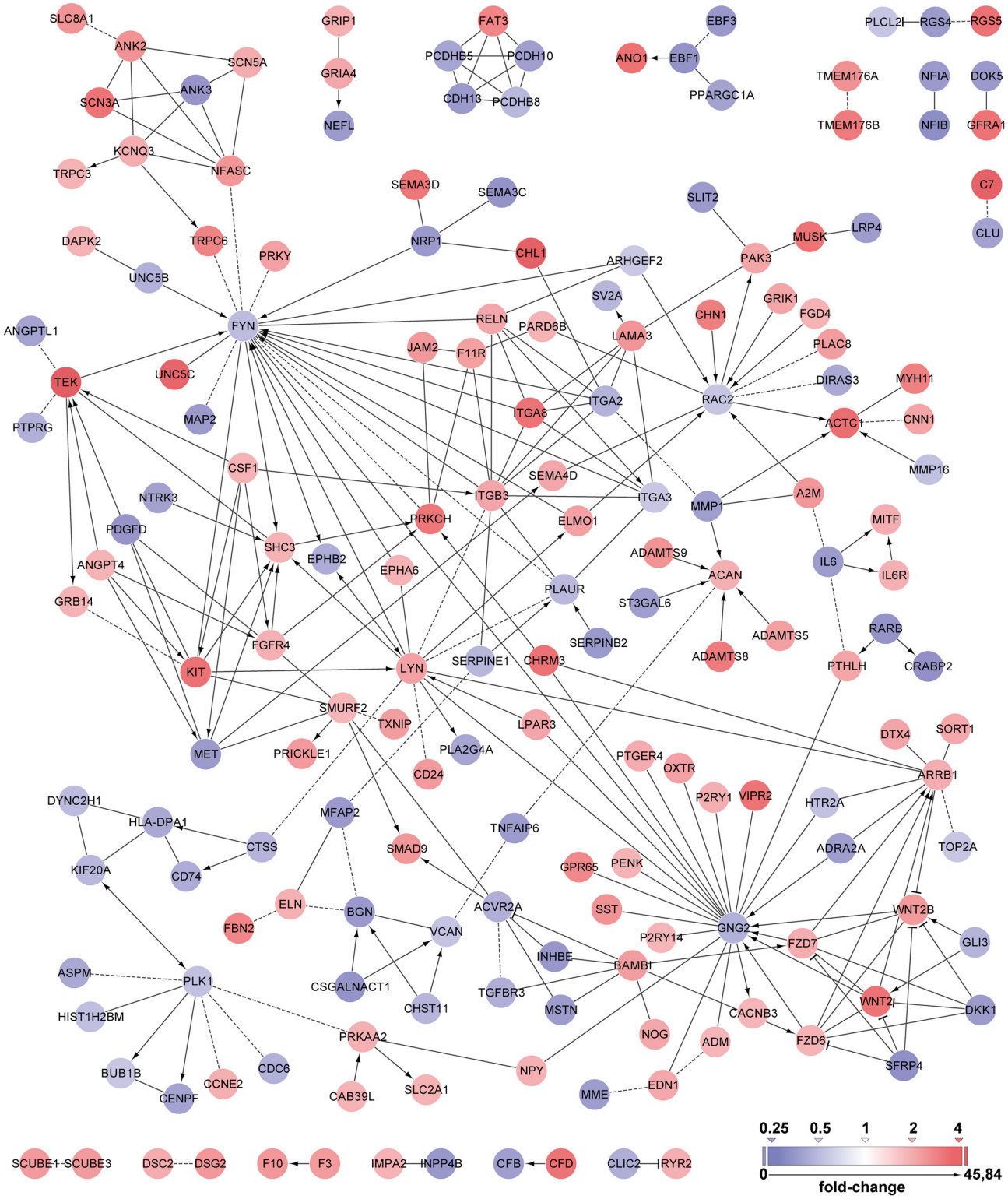

Fig 5. Functional protein network analysis based on a set of differentially expressed genes in P28B cells. A set of upregulated (fold-change ≥ 2) and downregulated (fold-change ≤ 0.5) genes in P28B cells compared with P6B and P34B cells was visualized with Cytoscape. A Reactome FI plug-in was used to analyze the functional network of proteins that are encoded by the respective genes. The fold-change values of gene expression are depicted as tints of blue (downregulated genes) or red (upregulated genes) color.

doi:10.1371/journal.pone.0159255.g005

Together, our results indicated that a high proportion of cells that expressed CSC markers corresponded with a pro-tumorigenic expression profile. In addition, the highest expression of CSC markers was found in the tumor sample taken from the patient with the shortest survival and also in the P28B cell line that was derived from this tumor.

Discussion

Although pancreatic CSCs were described nearly ten years ago as $CD44^+$/ $CD24^+$/$EpCAM^+$ cells [3] or $CD133^+$ cells [4], no study has determined the co-expression of all of these markers in PDAC either directly in the tumor samples or in the human PDAC cell lines derived from primary tumors. Therefore, the present study was focused on a detailed analysis of the expression of putative CSC markers (CD24, CD44, EpCAM, CD133 and nestin) in 3 pairs of matched primary PDAC tissue samples and derived cell lines.

We detected the expression of all of the examined markers in each tumor cell line. Markedly high levels of nestin were detected in all cell lines and corresponding tumors. Because nestin was expressed in most of the cells, these results suggest that nestin is not suitable as a CSC marker in PDAC, a finding that is in accordance with the results of our previous study [15]. Therefore, we omitted nestin from further flow cytometric co-expression analyses. In the cell lines, flow cytometric analysis of fixed cells revealed a high proportion of cells that expressed CSC markers. IHC confirmed that the expression patterns of the CSC markers were similar in the corresponding tumor tissues, although CD24 and CD44 expression levels were considerably lower. An increased proportion of $CD24^+$ and $CD44^+$ cells in PDAC cell lines compared with the original tumor tissues might indicate that these cells had a selective advantage in cell culture. This finding is in agreement with other studies that reported high percentages of $CD44^+$ cells in pancreatic cell lines compared with PDAC tumor tissues [16, 17]. However, in these studies, the cell lines that were used were not derived from the examined tumors; therefore, it is difficult to determine the baseline expression levels of these markers in the original tumor tissues for comparison. Our study is the first to show that the proportion of $CD44^+$ and/or $CD24^+$ cells increases in PDAC-derived cell lines compared with the corresponding tumor tissues. This phenomenon should be considered when performing *in vitro* studies of CSCs in PDAC.

Surprisingly, flow cytometric analysis of fixed cells showed that CD24, CD44, CD133, or EpCAM, as evaluated separately, are expressed in more than 80% of cells irrespective of the cell line and marker (except EpCAM in P6B and P34B cells). These values are much higher than those that have been previously reported [16, 17]. However, when live cells were used in the flow cytometry experiments, we detected a significant decrease in the proportion of $CD24^+$, $CD133^+$ and $EpCAM^+$ cells (Table 3). Using this approach, the levels of positivity for each of these markers were comparable to those in the aforementioned studies [16, 17]. Only CD44 expression in live cells was detected at the same level as in fixed cells (Table 3). Nevertheless, the reason for this discrepancy is obvious. It is widely known that fixation with paraformaldehyde permeabilizes the cell membranes and therefore enables the antibody to bind to the proteins that are localized within the cell. By contrast, live cells have intact membranes, and antibodies can bind only to extracellular epitopes of the proteins. This means that when fixed cells were used for flow cytometry, we could also detect cells that expressed the CSC markers within the cell.

It was previously thought that most CSC marker proteins performed their functions at the cell surface. However, growing evidence has indicated that the subcellular localization of CSC markers can vary greatly, possibly leading to completely different effects of these proteins on cell signaling, proliferation, invasiveness, and metastatic potential. Therefore, the distinct

subcellular localization of CSC markers may result in different patient outcomes. For example, several studies have reported cytoplasmic localization of CD24 in PDAC [18, 19] as well as in other tumor types [20–27]. Cytoplasmic CD24 expression has been identified as a marker of poor prognosis in gastric cancer [25], colorectal cancer [22, 23], ovarian cancer [20, 21] and malignant neoplasms of the salivary glands [26]. However, little is known concerning the functional role of CD24 within the cell. It has been reported that intracellular CD24 may inhibit the invasiveness of PDAC cells [19]. Nevertheless, a recently published study showed that intracellular CD24 promotes the growth of prostate cancer cells through the inhibition of p14ARF, resulting in decreased levels of p53 and p21 [27]. In that study, the authors also reported that CD24 positivity increased substantially when detection was performed with fixed cells. Recently, very similar findings have also been shown in breast cancer [28]. These observations are in agreement with our results and indicate that a significant amount of CD24 protein may be located in the cytoplasm of PDAC cells.

CD133 is another marker that we examined, and the cell surface immunoreactivity of this protein was significantly lower than the intracellular immunoreactivity. Originally, CD133 was introduced as a marker of pancreatic CSCs that is expressed in approximately 2% of PDAC cells [4]. Several flow cytometric studies then reported a similar low proportion of $CD133^+$ cells (0–28%) in PDAC [16, 17]. However, these results are in contrast with the high (up to 100%) CD133 positivity of cells detected by IHC even in the aforementioned studies [16, 17, 29]. IHC analysis also demonstrated that a significant amount of CD133 was localized within the cytoplasm of PDAC cells [29], a finding that is in agreement with our results (Tables 2 and 3). We and other groups have recently shown that membranous localization of CD133 may be altered in tumor cells and that intracellular CD133 may be involved in cell signaling pathways [9, 30–33]. Furthermore, the correlation of high intracellular CD133 expression with poor prognosis has been found in different types of tumors [33–36]. The results of the present study note the need for better understanding of the role of the intracellular expression of CSC markers in PDAC. Considering that flow cytometric analyses in previously published studies were typically performed to detect cell surface expression in live cells, these studies might have significantly underestimated the expression levels of CD24 (a maximum of 30% $CD24^+$ cells were reported [3, 16, 17]) and CD133 in PDAC cells, which may lead to misinterpretation of the results as discussed by other authors [37].

In the present study, we showed for the first time that cells co-expressing CD24, CD44, EpCAM, and CD133 are present in human PDAC cell lines derived from primary tumors. Moreover, $CD24^+/CD44^+/EpCAM^+/CD133^+$ cells represented a significant population of cells (range, 43.2 to 71.9%) among the cell lines. By contrast, the proportion of cells that co-expressed these markers at the cell surface was very limited (range, 0 to 1.43%) as indicated by flow cytometry with live cells (Table 3). These differences in subcellular localization represent a practical restriction in the isolation of CD24/CD44/EpCAM/CD133-positive and -negative cell populations. Sorting the cells based on cell surface labeling alone could be problematic because a large proportion of cells that express CSC markers within the cell would be sorted into negative fractions, likely compromising the results of further experiments. In a recent comprehensive study, Huang *et al.* reported that both CSC marker-positive (CSC^+) and -negative (CSC^-) populations of cells could initiate tumors in immunodeficient mice [38]. For various tumor types, they showed that not only were CSC^+ cells able to produce CSC^-cells but CSC^-cells could produce CSC^+ cells over long-term period in culture. These results suggested that tumorigenic cells might not be able to be distinguished by common CSC markers due to the phenotypic plasticity of tumor cells. However, the expression of CSC markers was evaluated only by flow cytometry followed by cell sorting. Because the authors used only live (non-permeabilized) cells in their experiments, they might have overlooked the cells that expressed CSC

markers localized in the cytoplasm or cell nucleus. This might also explain why the expression of CSC markers was detected in CSC^-cells by PCR. We speculate that the shift of CSC marker proteins from the cytoplasm to the plasma membrane and vice versa could, to a certain extent, explain the phenotypic plasticity of the FACS-sorted cells observed by Huang *et al.* and other groups [38–40]. Nevertheless, we suggest that the detection of CSC markers located within the cell should be included in future studies to validate and extend the data that are based solely on cell surface expression.

Our results revealed that the proportion of $CD24^+/CD44^+/EpCAM^+/CD133^+$ cells differed among the cell lines and that the highest number of cells that co-expressed all of these markers was detected in the P28B cell line, which was derived from the tumor of the patient with the shortest overall survival. Therefore, we decided to further analyze the differences among the cell lines using gene expression profiling to identify genes that may be associated with high expression levels of CSC markers. For this reason, the expression profile of P28B cells was compared with the profiles of P6B and P34B cells. Gene ontology analysis and a review of the literature revealed a specific pro-tumorigenic expression profile of P28B cells (Table 5; S4 Table). As high tumorigenic potential is a widely accepted hallmark of CSCs, this result clearly corresponds to the increased proportion of cells that co-express CSC markers in the P28B cell line. However, it should be noted that the pro-tumorigenic expression profile of P28B cells does not imply stemness of $CD24^+/CD44^+/EpCAM^+/CD133^+$ cells and subsequent functional *in vivo* assays are needed to determine whether $CD24^+/CD44^+/EpCAM^+/CD133^+$ phenotype specifically identifies PDAC cells which fulfill all the criteria defining CSCs. Of the 602 differentially expressed genes in P28B cells, the 10 most prominent genes were identified using functional protein network analysis. These genes could represent potential targets in PDAC because their expression was associated with the co-expression of CSC markers.

Fyn and Lyn are non-receptor tyrosine kinases that belong to the Src family. It has been reported that *LYN* expression is downregulated during embryonic stem cell differentiation, whereas *FYN* expression remains constant [41]. Lyn facilitates glioblastoma cell survival [42], and *LYN* expression is associated with migration and invasion in breast cancer [43]. In a study on pancreatic cancer, the downregulation of Lyn kinase activity reduced invasiveness and migration of the cells [44]. In the present study, we found that *LYN* expression was notably upregulated in P28B cells. In a colorectal cancer study, Su *et al.* reported that the overexpression of CD24 promoted cancer cell invasion through the activation of Lyn and its interaction with Erk1/2 [45]. Patients whose tumors had a lower expression of CD24 or Lyn had a higher survival rate. In accordance with these results, we showed the upregulation of *CD24* and *LYN* in P28B cells, which were derived from the tumors of patient with the shortest overall survival. This indicates that the overexpression of the CD24/Lyn axis might also play a role in PDAC. By contrast, the expression of Fyn kinase was downregulated in P28B cells. The overexpression of Fyn has been detected in various cancers, but its role in cancer is controversial [46–48]. Fyn has been reported to correlate with the metastasis of PDAC, while the inhibition of Fyn decreased liver metastasis in nude mice [47]. By contrast, the expression of Fyn kinase induces the differentiation and growth arrest of neuroblastoma cells [46]. Moreover, Fyn is downregulated in advanced tumor stages, and its downregulation predicts the short-term survival of patients with neuroblastoma. This is in agreement with our results where the downregulation of Fyn was observed in the P28B cell line. However, the exact role of Fyn kinase in PDAC has yet to be determined.

Of the other downregulated genes in P28B cells, *GNG2* was the most prominent. This gene encodes the Gγ2 subunit that forms Gβγ dimers of heterotrimeric G proteins [49]. Although it was reported that the overexpression of GNG2 inhibits the migration and invasiveness of melanoma cells [50], little is known about the function of *GNG2* in PDAC or in other tumor types.

Our study presents the first evidence that the downregulation of *GNG2* is associated with $CD24^+/CD44^+/EpCAM^+/CD133^+$ cells and might indicate a poor prognosis in patients with PDAC.

Recently, Yu *et al*. published a study that analyzed the expression profiles of circulating pancreatic tumor cells [51]. They determined that the expression of *WNT2* was upregulated in these cells. Their additional functional experiments showed that Wnt2 promotes anchorage-independent cell survival and the metastatic potential of pancreatic cancer cells. These results are in accordance with our findings as follows: *WNT2* was overexpressed in the P28B cell line, which contains the highest proportion of cells that express CSC markers and is derived from the tumor of the patient with the shortest overall survival. Moreover, expression profiling revealed that inhibitors of Wnt (i.e., DKK1 [52] and SFRP4 [53]) were downregulated in P28B cells compared with the other two cell lines. We also showed the upregulation of WNT2B, FZD7 and FZD6, which are other components of the Wnt signaling pathway. Recently, WNT2B was found to correlate with poor prognosis in PDAC [54], FZD6 expression was reported to be a marker of tumorigenic stem-like cells [55], and FZD7 was required for the maintenance of an undifferentiated phenotype of embryonic stem cells [56]. The upregulation of these genes in P28B cells indicates that the Wnt pathway was activated in cells that were highly positive for CSC markers. These results support the hypothesis that Wnt pathway signaling is of high importance in PDAC tumorigenesis [57].

Conclusions

Our study showed that putative CSC markers (i.e., CD24, CD44, EpCAM, CD133, and nestin) are highly expressed in PDAC. Although the expression of these markers was enhanced in PDAC-derived cell lines, the expression pattern of each individual cell line corresponded to that of the original corresponding tumor specimen. We demonstrated that a large proportion of cells expressed some typically membranous CSC markers (i.e., CD24, EpCAM and CD133) solely within the cell. Thus, these proteins may also play other currently unknown roles in the cytoplasm of PDAC cells, and further research is necessary to determine the biological significance of this finding. Most importantly, our study is the first to show that $CD24^+/CD44^+/EpCAM^+/CD133^+$ cells are present in human PDAC cell lines derived from primary tumors. Although $CD24^+/CD44^+/EpCAM^+/CD133^+$ cells were common under *in vitro* conditions, we showed that a higher proportion of these cells in the PDAC cell line corresponded with a protumorigenic gene expression profile. Upregulated Wnt signaling, upregulated expression of *LYN*, and downregulation of *FYN* expression were primarily associated with the proportion of cells that co-expressed CSC markers. In summary, these results suggest that $CD24^+/CD44^+/EpCAM^+/CD133^+$ cells may be of further interest in the research of PDAC and emphasize the need for further studies that would investigate whether $CD24^+/CD44^+/EpCAM^+/CD133^+$ phenotype specifically identifies pancreatic CSCs.

Supporting Information

S1 Table. Primary, conjugated primary and secondary antibodies used in this study.
(PDF)

S2 Table. Primer sequences used for qRT-PCR.
(PDF)

S3 Table. List of upregulated and downregulated genes in P28B cells according to the gene ontology analysis.
(PDF)

S4 Table. The role of differentially expressed genes in tumorigenesis—review of literature.
(PDF)

Acknowledgments

The authors thank Johana Maresova and Martin Sramek for their skillful technical assistance.

Author Contributions

Conceived and designed the experiments: JS RV. Performed the experiments: JS MH TL PN. Analyzed the data: JS RV JN. Wrote the paper: JS RV MH JN. Provided the patients' clinical data: PK. Participated in the collection of the human tissue samples: MH.

References

1. Balic A, Dorado J, Alonso-Gomez M, Heeschen C. Stem cells as the root of pancreatic ductal adenocarcinoma. Exp Cell Res. 2012; 318(6): 691–704. doi: 10.1016/j.yexcr.2011.11.007 PMID: 22119145
2. Seufferlein T, Bachet JB, Van Cutsem E, Rougier P. Pancreatic adenocarcinoma: ESMO-ESDO Clinical Practice Guidelines for diagnosis, treatment and follow-up. Ann Oncol. 2012; 23 Suppl 7: vii33–40. PMID: 22997452
3. Li C, Heidt DG, Dalerba P, Burant CF, Zhang L, Adsay V, et al. Identification of pancreatic cancer stem cells. Cancer Res. 2007; 67(3): 1030–7. PMID: 17283135
4. Hermann PC, Huber SL, Herrler T, Aicher A, Ellwart JW, Guba M, et al. Distinct populations of cancer stem cells determine tumor growth and metastatic activity in human pancreatic cancer. Cell Stem Cell. 2007; 1(3): 313–23. doi: 10.1016/j.stem.2007.06.002 PMID: 18371365
5. Lee CJ, Li C, Simeone DM. Human pancreatic cancer stem cells: implications for how we treat pancreatic cancer. Transl Oncol. 2008; 1(1): 14–8. PMID: 18607507
6. Matsuda Y, Kure S, Ishiwata T. Nestin and other putative cancer stem cell markers in pancreatic cancer. Med Mol Morphol. 2012; 45(2): 59–65. doi: 10.1007/s00795-012-0571-x PMID: 22718289
7. Li C, Wu JJ, Hynes M, Dosch J, Sarkar B, Welling TH, et al. c-Met is a marker of pancreatic cancer stem cells and therapeutic target. Gastroenterology. 2011; 141(6): 2218–27.e5. doi: 10.1053/j.gastro.2011.08.009 PMID: 21864475
8. Veselska R, Kuglik P, Cejpek P, Svachova H, Neradil J, Loja T, et al. Nestin expression in the cell lines derived from glioblastoma multiforme. BMC Cancer. 2006; 6: 32. PMID: 16457706
9. Nunukova A, Neradil J, Skoda J, Jaros J, Hampl A, Sterba J, et al. Atypical nuclear localization of CD133 plasma membrane glycoprotein in rhabdomyosarcoma cell lines. Int J Mol Med. 2015; 36(1): 65–72. doi: 10.3892/ijmm.2015.2210 PMID: 25977066
10. Skoda J, Neradil J, Zitterbart K, Sterba J, Veselska R. EGFR signaling in the HGG-02 glioblastoma cell line with an unusual loss of EGFR gene copy. Oncol Rep. 2014; 31(1): 480–7. doi: 10.3892/or.2013.2864 PMID: 24270553
11. Livak KJ, Schmittgen TD. Analysis of relative gene expression data using real-time quantitative PCR and the $2^{-\Delta\Delta}$CT method. Methods. 2001; 25: 402–8. PMID: 11846609
12. Huang da W, Sherman BT, Lempicki RA. Bioinformatics enrichment tools: paths toward the comprehensive functional analysis of large gene lists. Nucleic Acids Res. 2009; 37(1): 1–13. doi: 10.1093/nar/gkn923 PMID: 19033363
13. Huang da W, Sherman BT, Lempicki RA. Systematic and integrative analysis of large gene lists using DAVID bioinformatics resources. Nat Protoc. 2009; 4(1): 44–57. doi: 10.1038/nprot.2008.211 PMID: 19131956
14. Shannon P, Markiel A, Ozier O, Baliga NS, Wang JT, Ramage D, et al. Cytoscape: a software environment for integrated models of biomolecular interaction networks. Genome Res. 2003; 13(11): 2498–504. PMID: 14597658
15. Lenz J, Karasek P, Jarkovsky J, Muckova K, Dite P, Kala Z, et al. Clinicopathological correlations of nestin expression in surgically resectable pancreatic cancer including an analysis of perineural invasion. J Gastrointestin Liver Dis. 2011; 20(4): 389–96. PMID: 22187705
16. Kure S, Matsuda Y, Hagio M, Ueda J, Naito Z, Ishiwata T. Expression of cancer stem cell markers in pancreatic intraepithelial neoplasias and pancreatic ductal adenocarcinomas. Int J Oncol. 2012; 41(4): 1314–24. doi: 10.3892/ijo.2012.1565 PMID: 22824809

17. Bunger S, Barow M, Thorns C, Freitag-Wolf S, Danner S, Tiede S, et al. Pancreatic carcinoma cell lines reflect frequency and variability of cancer stem cell markers in clinical tissue. Eur Surg Res. 2012; 49 (2): 88–98. doi: 10.1159/000341669 PMID: 22948659

18. Jacob J, Bellach J, Grutzmann R, Alldinger I, Pilarsky C, Dietel M, et al. Expression of CD24 in adenocarcinomas of the pancreas correlates with higher tumor grades. Pancreatology. 2004; 4(5): 454–60. PMID: 15256807

19. Taniuchi K, Nishimori I, Hollingsworth MA. Intracellular CD24 inhibits cell invasion by posttranscriptional regulation of BART through interaction with G3BP. Cancer Res. 2011; 71(3): 895–905. doi: 10.1158/0008-5472.CAN-10-2743 PMID: 21266361

20. Kristiansen G, Denkert C, Schluns K, Dahl E, Pilarsky C, Hauptmann S. CD24 is expressed in ovarian cancer and is a new independent prognostic marker of patient survival. Am J Pathol. 2002; 161(4): 1215–21. PMID: 12368195

21. Choi YL, Kim SH, Shin YK, Hong YC, Lee SJ, Kang SY, et al. Cytoplasmic CD24 expression in advanced ovarian serous borderline tumors. Gynecol Oncol. 2005; 97(2): 379–86. PMID: 15863133

22. Weichert W, Denkert C, Burkhardt M, Gansukh T, Bellach J, Altevogt P, et al. Cytoplasmic CD24 expression in colorectal cancer independently correlates with shortened patient survival. Clin Cancer Res. 2005; 11(18): 6574–81. PMID: 16166435

23. Choi YL, Xuan YH, Lee SJ, Park SM, Kim WJ, Kim HJ, et al. Enhanced CD24 Expression in Colorectal Cancer Correlates with Prognostic Factors. Korean J Pathol. 2006; 40: 103–11.

24. Bircan S, Kapucuoglu N, Baspinar S, Inan G, Candir O. CD24 expression in ductal carcinoma in situ and invasive ductal carcinoma of breast: an immunohistochemistry-based pilot study. Pathol Res Pract. 2006; 202(8): 569–76. PMID: 16828238

25. Chou YY, Jeng YM, Lee TT, Hu FC, Kao HL, Lin WC, et al. Cytoplasmic CD24 expression is a novel prognostic factor in diffuse-type gastric adenocarcinoma. Ann Surg Oncol. 2007; 14(10): 2748–58. PMID: 17680316

26. Soave DF, Oliveira da Costa JP, da Silveira GG, Ianez RC, de Oliveira LR, Lourenco SV, et al. CD44/CD24 immunophenotypes on clinicopathologic features of salivary glands malignant neoplasms. Diagn Pathol. 2013; 8: 29. doi: 10.1186/1746-1596-8-29 PMID: 23419168

27. Wang L, Liu R, Ye P, Wong C, Chen GY, Zhou P, et al. Intracellular CD24 disrupts the ARF-NPM interaction and enables mutational and viral oncogene-mediated p53 inactivation. Nat Commun. 2015; 6: 5909. doi: 10.1038/ncomms6909 PMID: 25600590

28. Rostoker R, Abelson S, Genkin I, Ben-Shmuel S, Sachidanandam R, Scheinman EJ, et al. CD24(+) cells fuel rapid tumor growth and display high metastatic capacity. Breast Cancer Res. 2015; 17: 78. doi: 10.1186/s13058-015-0589-9 PMID: 26040280

29. Kim HS, Yoo SY, Kim KT, Park JT, Kim HJ, Kim JC. Expression of the stem cell markers CD133 and nestin in pancreatic ductal adenocarcinoma and clinical relevance. Int J Clin Exp Pathol. 2012; 5(8): 754–61. PMID: 23071857

30. Skoda J, Nunukova A, Loja T, Zambo I, Neradil J, Mudry P, et al. Cancer stem cell markers in pediatric sarcomas: Sox2 is associated with tumorigenicity in immunodeficient mice. Tumor Biol. 2016; doi: 10.1007/s13277-016-4837-0

31. Chen H, Luo Z, Dong L, Tan Y, Yang J, Feng G, et al. CD133/prominin-1-mediated autophagy and glucose uptake beneficial for hepatoma cell survival. PLoS One. 2013; 8(2): e56878. doi: 10.1371/journal.pone.0056878 PMID: 23437259

32. Shimozato O, Waraya M, Nakashima K, Souda H, Takiguchi N, Yamamoto H, et al. Receptor-type protein tyrosine phosphatase kappa directly dephosphorylates CD133 and regulates downstream AKT activation. Oncogene. 2015; 34(15): 1949–60. doi: 10.1038/onc.2014.141 PMID: 24882578

33. Huang M, Zhu H, Feng J, Ni S, Huang J. High CD133 expression in the nucleus and cytoplasm predicts poor prognosis in non-small cell lung cancer. Dis Markers. 2015; 2015: 986095. doi: 10.1155/2015/986095 PMID: 25691807

34. Sasaki A, Kamiyama T, Yokoo H, Nakanishi K, Kubota K, Haga H, et al. Cytoplasmic expression of CD133 is an important risk factor for overall survival in hepatocellular carcinoma. Oncol Rep. 2010; 24 (2): 537–46. PMID: 20596644

35. Jao SW, Chen SF, Lin YS, Chang YC, Lee TY, Wu CC, et al. Cytoplasmic CD133 expression is a reliable prognostic indicator of tumor regression after neoadjuvant concurrent chemoradiotherapy in patients with rectal cancer. Ann Surg Oncol. 2012; 19(11): 3432–40. doi: 10.1245/s10434-012-2394-3 PMID: 22739652

36. Hashimoto K, Aoyagi K, Isobe T, Kouhuji K, Shirouzu K. Expression of CD133 in the cytoplasm is associated with cancer progression and poor prognosis in gastric cancer. Gastric Cancer. 2014; 17(1): 97–106. doi: 10.1007/s10120-013-0255-9 PMID: 23558457

37. Kristiansen G, Machado E, Bretz N, Rupp C, Winzer KJ, Konig AK, et al. Molecular and clinical dissection of CD24 antibody specificity by a comprehensive comparative analysis. Lab Invest. 2010; 90(7): 1102–16. doi: 10.1038/labinvest.2010.70 PMID: 20351695

38. Huang SD, Yuan Y, Tang H, Liu XH, Fu CG, Cheng HZ, et al. Tumor cells positive and negative for the common cancer stem cell markers are capable of initiating tumor growth and generating both progenies. PLoS One. 2013; 8(1): e54579. doi: 10.1371/journal.pone.0054579 PMID: 23349932

39. Meyer MJ, Fleming JM, Ali MA, Pesesky MW, Ginsburg E, Vonderhaar BK. Dynamic regulation of CD24 and the invasive, CD44posCD24neg phenotype in breast cancer cell lines. Breast Cancer Res. 2009; 11(6): R82. doi: 10.1186/bcr2449 PMID: 19906290

40. Botchkina IL, Rowehl RA, Rivadeneira DE, Karpeh MS Jr, Crawford H, Dufour A, et al. Phenotypic subpopulations of metastatic colon cancer stem cells: genomic analysis. Cancer Genomics Proteomics. 2009; 6(1): 19–29. PMID: 19451087

41. Zhang X, Simerly C, Hartnett C, Schatten G, Smithgall TE. Src-family tyrosine kinase activities are essential for differentiation of human embryonic stem cells. Stem Cell Res. 2014; 13(3 Pt A): 379–89. doi: 10.1016/j.scr.2014.09.007 PMID: 25305536

42. Liu WM, Huang P, Kar N, Burgett M, Muller-Greven G, Nowacki AS, et al. Lyn facilitates glioblastoma cell survival under conditions of nutrient deprivation by promoting autophagy. PLoS One. 2013; 8(8): e70804. doi: 10.1371/journal.pone.0070804 PMID: 23936469

43. Choi YL, Bocanegra M, Kwon MJ, Shin YK, Nam SJ, Yang JH, et al. LYN is a mediator of epithelial-mesenchymal transition and a target of dasatinib in breast cancer. Cancer Res. 2010; 70(6): 2296–306. doi: 10.1158/0008-5472.CAN-09-3141 PMID: 20215510

44. Fu Y, Zagozdzon R, Avraham R, Avraham HK. CHK negatively regulates Lyn kinase and suppresses pancreatic cancer cell invasion. Int J Oncol. 2006; 29(6): 1453–8. PMID: 17088984

45. Su N, Peng L, Xia B, Zhao Y, Xu A, Wang J, et al. Lyn is involved in CD24-induced ERK1/2 activation in colorectal cancer. Mol Cancer. 2012; 11:43. doi: 10.1186/1476-4598-11-43 PMID: 22731636

46. Berwanger B, Hartmann O, Bergmann E, Bernard S, Nielsen D, Krause M, et al. Loss of a FYN-regulated differentiation and growth arrest pathway in advanced stage neuroblastoma. Cancer Cell. 2002; 2 (5): 377–86. PMID: 12450793

47. Chen ZY, Cai L, Bie P, Wang SG, Jiang Y, Dong JH, et al. Roles of Fyn in pancreatic cancer metastasis. J Gastroenterol Hepatol. 2010; 25(2): 293–301. doi: 10.1111/j.1440-1746.2009.06021.x PMID: 19968749

48. Saito YD, Jensen AR, Salgia R, Posadas EM. Fyn: a novel molecular target in cancer. Cancer. 2010; 116(7): 1629–37. doi: 10.1002/cncr.24879 PMID: 20151426

49. Modarressi MH, Taylor KE, Wolfe J. Cloning, characterization, and mapping of the gene encoding the human G protein gamma 2 subunit. Biochem Biophys Res Commun. 2000; 272(2): 610–5. PMID: 10833460

50. Yajima I, Kumasaka MY, Yamanoshita O, Zou C, Li X, Ohgami N, et al. GNG2 inhibits invasion of human malignant melanoma cells with decreased FAK activity. Am J Cancer Res. 2014; 4(2): 182–8. PMID: 24660107

51. Yu M, Ting DT, Stott SL, Wittner BS, Ozsolak F, Paul S, et al. RNA sequencing of pancreatic circulating tumour cells implicates WNT signalling in metastasis. Nature. 2012; 487(7408): 510–3. doi: 10.1038/nature11217 PMID: 22763454

52. Niida A, Hiroko T, Kasai M, Furukawa Y, Nakamura Y, Suzuki Y, et al. DKK1, a negative regulator of Wnt signaling, is a target of the beta-catenin/TCF pathway. Oncogene. 2004; 23(52): 8520–6. PMID: 15378020

53. Ford CE, Jary E, Ma SS, Nixdorf S, Heinzelmann-Schwarz VA, Ward RL. The Wnt gatekeeper SFRP4 modulates EMT, cell migration and downstream Wnt signalling in serous ovarian cancer cells. PLoS One. 2013; 8(1): e54362. doi: 10.1371/journal.pone.0054362 PMID: 23326605

54. Jiang H, Li F, He C, Wang X, Li Q, Gao H. Expression of Gli1 and Wnt2B correlates with progression and clinical outcome of pancreatic cancer. Int J Clin Exp Pathol. 2014; 7(7): 4531–8. PMID: 25120849

55. Cantilena S, Pastorino F, Pezzolo A, Chayka O, Pistoia V, Ponzoni M, et al. Frizzled receptor 6 marks rare, highly tumourigenic stem-like cells in mouse and human neuroblastomas. Oncotarget. 2011; 2 (12): 976–83. PMID: 22249030

56. Fernandez A, Huggins IJ, Perna L, Brafman D, Lu D, Yao S, et al. The WNT receptor FZD7 is required for maintenance of the pluripotent state in human embryonic stem cells. Proc Natl Acad Sci U S A. 2014; 111(4): 1409–14. doi: 10.1073/pnas.1323697111 PMID: 24474766

57. Vaz A, Ponnusamy M, Seshacharyulu P, Batra S. A concise review on the current understanding of pancreatic cancer stem cells. Journal of Cancer Stem Cell Research. 2014; 2: e1004. PMID: 26451384

Sramek *et al. Cancer Cell Int (2016) 16:14*
DOI 10.1186/s12935-016-0289-2

Cancer Cell International

PRIMARY RESEARCH

Open Access

Non-DHFR-mediated effects of methotrexate in osteosarcoma cell lines: epigenetic alterations and enhanced cell differentiation

Martin Sramek[1,2], Jakub Neradil[1,2], Jaroslav Sterba[2] and Renata Veselska[1,2*]

Abstract

Background: Methotrexate is an important chemotherapeutic drug widely known as an inhibitor of dihydrofolate reductase (DHFR) which inhibits the reduction of folic acid. DHFR-mediated effects are apparently responsible for its primary antineoplastic action. However, other non-DHFR-mediated effects of methotrexate have been recently discovered, which might be very useful in the development of new strategies for the treatment of pediatric malignancies. The principal goal of this study was to analyze the possible impact of clinically achievable methotrexate levels on cell proliferation, mechanisms of epigenetic regulation (DNA methylation and histone acetylation), induced differentiation and the expression of differentiation-related genes in six osteosarcoma cell lines.

Methods: The Saos-2 reference cell line and five other patient-derived osteosarcoma cell lines were chosen for this study. The MTT assay was used to assess cell proliferation, DNA methylation and histone acetylation were detected using ELISA, and western blotting was used for a detailed analysis of histone acetylation. The expression of differentiation-related genes was quantified using RT-qPCR and the course of cell differentiation was evaluated using Alizarin Red S staining, which detects the level of extracellular matrix mineralization.

Results: Methotrexate significantly decreased the proliferation of Saos-2 cells exclusively, suggesting that this reference cell line was sensitive to the DHFR-mediated effects of methotrexate. In contrast, other results indicated non-DHFR-mediated effects in patient-derived cell lines. Methotrexate-induced DNA demethylation was detected in almost all of them; methotrexate was able to lower the level of 5-methylcytosine in treated cells, and this effect was similar to the effect of 5-aza-2′-deoxycytidine. Furthermore, methotrexate increased the level of acetylated histone H3 in the OSA-06 cell line. Methotrexate also enhanced all-*trans* retinoic acid-induced cell differentiation in three patient-derived osteosarcoma cell lines, and the modulation of expression of the differentiation-related genes was also shown.

Conclusions: Overall non-DHFR-mediated effects of methotrexate were detected in the patient-derived osteosarcoma cell lines. Methotrexate acts as an epigenetic modifier and has a potential impact on cell differentiation and the expression of related genes. Furthermore, the combination of methotrexate and all-*trans* retinoic acid can be effective as a differentiation therapy for osteosarcoma.

Keywords: Methotrexate, Osteosarcoma, Epigenetic regulation, DNA methylation, Histone acetylation, All-*trans* retinoic acid, Osteogenic differentiation

*Correspondence: veselska@sci.muni.cz
[1] Laboratory of Tumor Biology, Department of Experimental Biology, Faculty of Science, Masaryk University, Kotlarska 2, 611 37 Brno, Czech Republic
Full list of author information is available at the end of the article

Background

Methotrexate (MTX; amethopterin; 4-amino-10-methylfolic acid), a structural analogue of folic acid, is a chemotherapeutic drug which is still very frequently used as a treatment of osteosarcomas—the most common primary malignant bone tumors affecting both children and adults [1]. MTX has been included in therapeutic protocols for many years, but its dosage and administration schedules are still being optimized [2, 3].

MTX enters the cell through an active transport mechanism and by facilitated diffusion, and once inside, it is converted into polyglutamate MTX by folylpolyglutamyl synthase [4–6]. Polyglutamate MTX reversibly inhibits dihydrofolate reductase (DHFR) but also inhibits other enzymes, for example, phosphoribosylaminoimidazolecarboxamide formyltransferase (AICAR transformylase) or thymidylate synthase (TS). Inhibition of DHFR affects the reduction of folic acid and consequently leads to a lack of 5,10-methylenetetrahydrofolate, which is used as a coenzyme in the biosynthesis of thymidine. Moreover, TS is directly blocked by MTX and by unmetabolized dihydrofolate. Purine precursor biosynthesis is also affected by the deficiency of another folate co-factor, 10-formyltetrahydrofolate and by MTX inhibition of AICAR transformylase. The inhibition of dTMP and purine synthesis causes MTX-induced cell death [7].

Although MTX is able to inhibit proliferation and/or induce apoptosis in neoplastic cells, there is also evidence that it induces differentiation. MTX was able to induce differentiation in colon cancer cells primarily due to the intracellular depletion of purines [8], in immature and undifferentiated monocytic cells [9] and in rat choriocarcinoma cells [10]. Overall, cytostatic, cytotoxic and differentiation effects are mediated by the functional suppression of DHFR and nucleotide biosynthesis.

In addition to the cytostatic and differentiation effects of MTX, non-DHFR-mediated effects concerning the modulation of important epigenetics determinants have also been described, such as DNA methylation [11] and histone acetylation [12]. The mechanism of the methylation of biomolecules is not always clear because both the DHFR- and non-DHFR-mediated effects of MTX can contribute to the decreased methylation of molecules in the cell. On one hand, inhibition of folate metabolism as described above can affect the intracellular levels of 5-methyltetrahydrofolate which transfers methyl groups to methionine synthase to generate methionine from homocysteine [13]. Methionine can be utilized for the synthesis of the universal methyl donor S-adenosylmethionine (SAM) which plays a pivotal role in the generation of 5-methylcytosine. On the other hand, MTX directly inhibits methionine adenosyltransferase (MAT) mRNA expression and reduces MAT protein levels which significantly decreases MAT activity [13]. This is of particular importance because MAT is a key enzyme that catalyzes the only reaction that produces SAM. Moreover, MAT expression and activity can be inhibited even by a very low concentration of MTX (50 nmol). Regarding histone acetylation, molecular modeling suggested that MTX is a potential histone deacetylase inhibitor due to its shared structural similarity with some histone deacetylase inhibitors (e.g., butyrate or trichostatin A), and it has been shown that MTX directly inhibits histone deacetylase activity and induces histone H3 acetylation in vitro [12].

It has been shown that the induced differentiation of tumor cells is a promising strategy in cancer therapy [14]. Especially, all-*trans* retinoic acid (ATRA) and its derivatives are widely used differentiation drugs that can induce the osteogenic differentiation of osteosarcoma cells [15]. The main disadvantage of retinoid usage is the occurrence of resistance [16]. On one hand, DNA methylation has a significant role in preventing normal differentiation in pediatric cancers [17], and on the other hand, DNA demethylation can contribute to cell differentiation; for example, the expression of the retinoic acid receptor beta (*RARB*) can be activated by the hypomethylating action of 5-aza-2′-deoxycytidine [18]. Histones are involved in the regulation of chromatin structure and gene expression as well as in DNA methylation. Histone H3 acetylation is also associated with gene expression. Therefore, due to its impact on nucleotide synthesis, as well as DNA methylation and histone acetylation, MTX could modulate gene expression and enhance the ATRA-induced differentiation of osteosarcoma cells.

In the present study, we focused on MTX action in six cell lines derived from osteosarcomas. The MTX effect on DNA methylation was compared with the effect of the known DNA methyltransferase inhibitor 5-aza-2′-deoxycytidine (5AZA), and the accumulation of acetyl histone H3 after MTX treatment was compared with the effects of the known histone deacetylase inhibitors sodium butyrate (BUT) and sodium valproate (VAL). We also studied the MTX impact on the expression of selected genes related to cell differentiation, and we assessed cell differentiation induced by MTX, ATRA or a combination of the two. Therefore, our work represents the first complex study of the non-DHFR-mediated effects of MTX in cancer cells with special attention to the modulation of epigenetic information in terms of DNA methylation and histone acetylation.

Results

Our results showed that the non-DHFR mediated effects of MTX were detectable, especially in patient-derived cell lines and that MTX act as an epigenetic modifier with an impact both on DNA demethylation and the accumulation

of acetylated histones. Moreover, the combination of MTX and ATRA may represent a new therapeutic option in the differentiation therapy of osteosarcoma.

Patient-derived cell lines are more resistant to MTX than Saos-2 cell line

Using the MTT assay, an analysis of proliferation activity was performed on day 6 of MTX treatment at concentrations from 0.0001 to 100 μM. Significant differences in the sensitivity of cell lines used in this study (Fig. 1) were noted. On one hand, MTX showed a strong cytotoxic effect on the Saos-2 reference cell line at concentrations ranging from 0.1 to 100 μM. On the other hand, all five patient-derived OSA cell lines were significantly more resistant to MTX action, and even the very high concentration of 100 μM was not sufficient to reach the IC_{50}.

MTX induces DNA demethylation in a majority of osteosarcoma cell lines

Despite the mild effect of MTX on cell proliferation, we continued to study the non-DHFR-mediated effects of MTX on DNA methylation. Significant DNA demethylation was observed in Saos-2, OSA-03, OSA-05, OSA-06 and OSA-08 cells at day 3 of the MTX treatment, especially at a concentration of 40 μM (Fig. 2). The MTX-induced DNA demethylation was most obvious in the OSA-06 cells–the level of 5-methylcytosine decreased to 86 % at 1 μM MTX and to 76 % at 40 μM MTX in comparison with untreated control cells. As expected, the positive control 5AZA induced DNA demethylation in Saos-2, OSA-03, OSA-05, OSA-06 and OSA-08. Surprisingly in Saos-2, OSA-03, OSA-05 and OSA-06 cells, 40 μM MTX induced DNA demethylation comparable to the effect of 5AZA at the same concentration. We did not observe any changes in DNA methylation in OSA-02 cells.

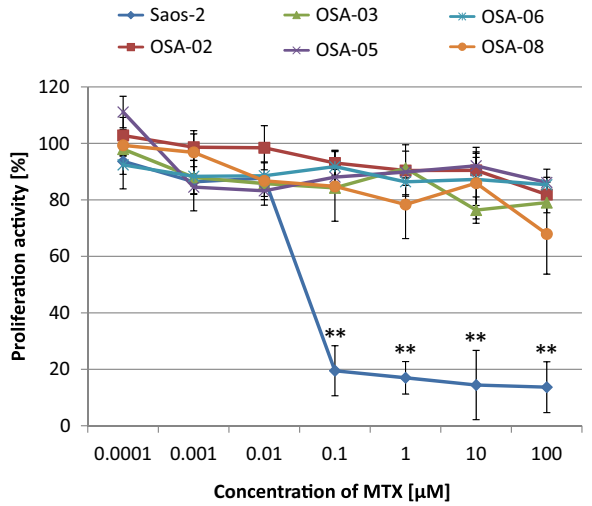

Fig. 1 Proliferation activity of osteosarcoma cell lines after treatment with MTX. Proliferation activity was measured using MTT assay at day 6 of incubation with various concentrations of MTX and compared with those of untreated control cells. Untreated controls were set as 100 %. The data represent the mean ± SD. Experiments were repeated three times in duplicates. $^{**}P < 0.01$, indicates significant differences from the respective cell lines

MTX increases the global histone H3 acetylation in OSA-06 cells

Given that MTX is a possible histone deacetylase inhibitor, we determined whether MTX could increase histone H3 acetylation. Treatment with BUT and VAL served as a positive controls and, in some cases, treated cells showed the significant accumulation of acetylated histone H3 in comparison with an untreated control (Fig. 3). We did not detect an increase in the global acetylation of histone H3 at day 3 of the MTX treatment in Saos-2, OSA-02, OSA-03, OSA-05 and OSA-08 cells (Fig. 3a–d, f); however, we observed an increase of histone H3 acetylation in OSA-06 cells (Fig. 3e), and therefore, this cell line was further analyzed using western blotting. Cells were incubated with MTX, VAL or BUT, and the nuclear protein fractions were harvested and immunoblotted on day 3 of the treatment (Fig. 4). Our data demonstrated that MTX increased histone H3 acetylation in OSA-06 cells in a concentration-dependent manner.

MTX alters the expression of differentiation-related genes

To further explore the importance of epigenetic alterations induced by MTX, we decided to assess the MTX impact on the expression of selected genes involved in cell differentiation. The expression of genes encoding known markers of osteogenic differentiation (*COLLI*, *ALPL*) as well as genes involved in ATRA metabolism and the regulation of gene expression were evaluated using RT-qPCR on day 3 of MTX treatment at concentrations of 1 μM and 40 μM (Fig. 5). In Saos-2 cells, we observed a significant increase in the expression of *RARA*, *CRBP1* and *CRABP2*. Interestingly, the expression of *CRABP2* was increased approximately ten-fold, but the expression of *RARB* and *ALPL* was significantly lower (Fig. 5a). In OSA-02 cells, MTX at both concentrations significantly increased the expression of *RARA* and also the expression of *COLLI* at 40 μM. In contrast, the expression of *CRBP1* was at a very low level (Fig. 5b). In OSA-03 cells, *COLLI* expression was significantly higher after treatment with 40 μM MTX, but the same concentration of MTX significantly decreased the expression of *CRABP2* and *ALPL* (Fig. 5c). In OSA-05 cells, 1 μM MTX significantly increased the expression of *RARA*, *RARB* and *RXRA* (Fig. 5d). In OSA-06 cells, MTX significantly

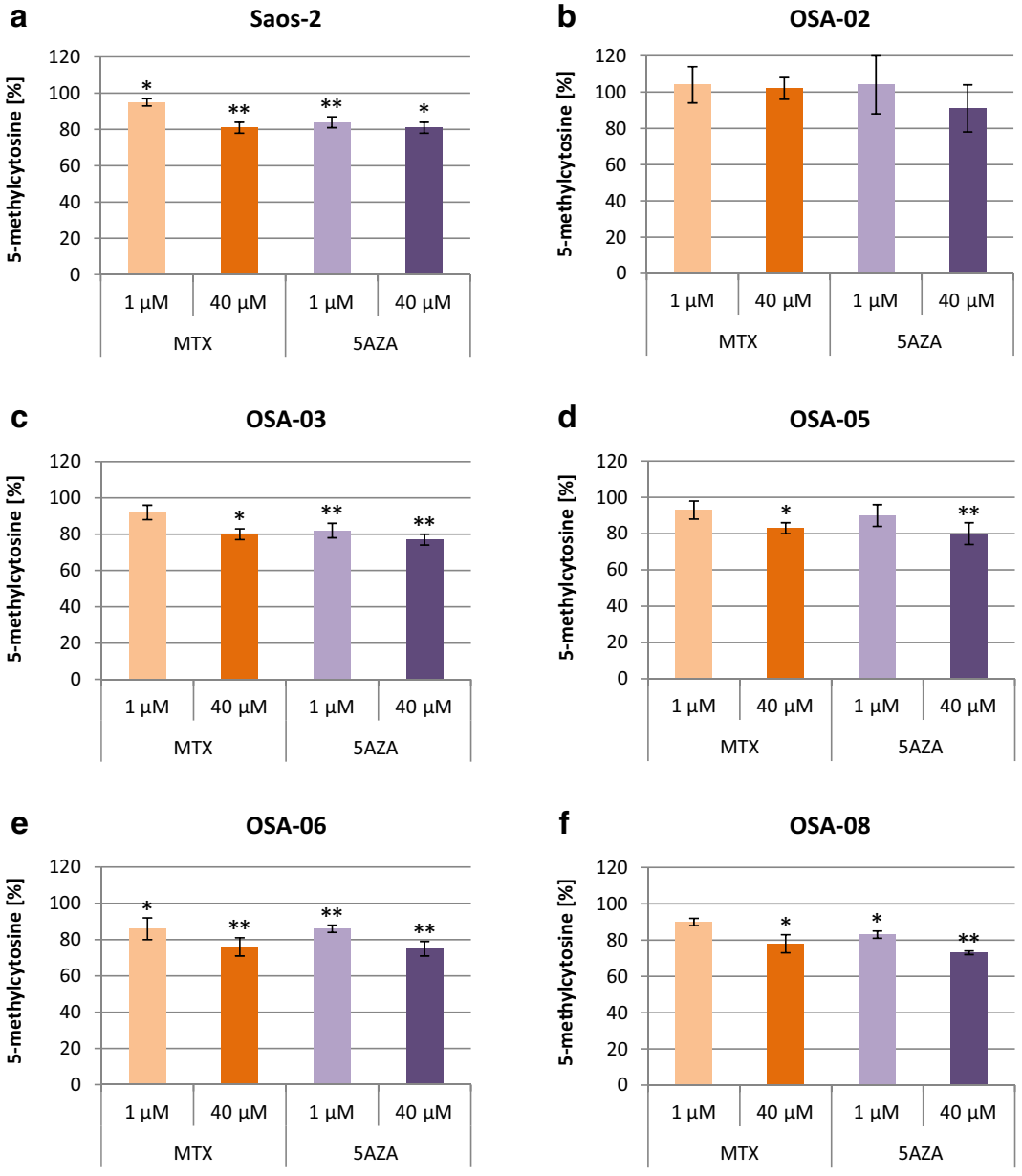

Fig. 2 Changes in DNA methylation in osteosarcoma cell lines after treatment with MTX. Levels of 5-methylcytosine in Saos-2 (**a**), OSA-02 (**b**), OSA-03 (**c**), OSA-05 (**d**), OSA-06 (**e**) and OSA-08 (**f**) cells as measured using an ELISA assay at day 3 of incubation. The levels of 5-methylcytosine are presented as a percentage change compared to the levels found in untreated control cells. Untreated controls were set as 100 %. The data represent the mean ± SD. Experiments were repeated three times. *$P < 0.05$, **$P < 0.01$, indicate significant differences from the respective control groups

decreased the expression of *CRABP2* only (Fig. 5e). In OSA-08 cells, the expression of *RARA* and *CRBP1* was significantly increased after MTX treatment (Fig. 5f).

Osteogenic differentiation is enhanced by combined treatment with MTX and ATRA

As indicated by the previous analyses, MTX treatment significantly increased the expression of some genes involved in ATRA metabolism and the regulation of gene expression. This observation led us to explore whether MTX could enhance ATRA-induced differentiation. After 21 days of cultivation, all cell lines formed calcium-positive nodules in control cell populations as well as under all experimental conditions. In the Saos-2 cell line, MTX significantly enhanced the extent of this mineralization (Fig. 6a), but MTX-induced mineralization was less apparent in all five OSA cell lines (Fig. 6b–f). ATRA significantly enhanced the mineralization in Saos-2 cells in a manner

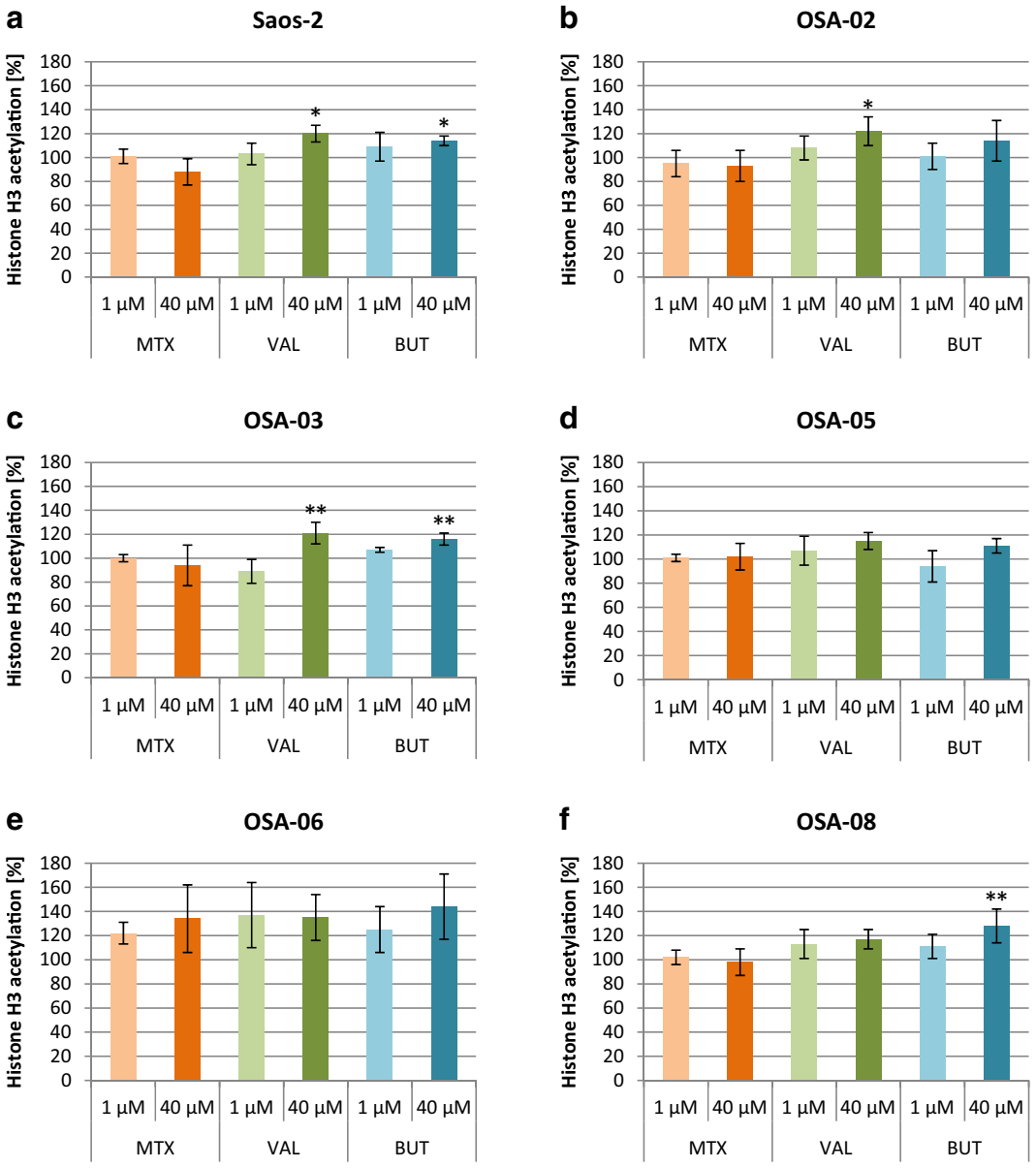

Fig. 3 Changes in global histone H3 acetylation in osteosarcoma cell lines after treatment with MTX. Levels of global histone H3 acetylation in Saos-2 (**a**), OSA-02 (**b**), OSA-03 (**c**), OSA-05 (**d**), OSA-06 (**e**) and OSA-08 (**f**) cells as measured using ELISA assay at day 3 of incubation. The levels of global histone H3 acetylation are presented as a percentage change compared to the levels found in untreated control cells. Untreated controls were set as 100 %. The data represent the mean ± SD. Experiments were repeated three times. *$P < 0.05$, **$P < 0.01$, indicate significant differences from the respective control groups

similar to MTX. In all OSA cell lines ATRA was always more effective in enhancing mineralization than MTX and in all cases significantly enhanced the extent of the mineralization. The combination of ATRA (0.1 or 1 μM) and MTX (1 or 40 μM) did not have an additional effect on the amount of calcium sediments in Saos-2, OSA-02 and OSA-08 cell lines. Interestingly, in the OSA-03, OSA-05 and OSA-06 cell lines, a combined treatment with ATRA and MTX significantly enhanced the mineralization in comparison with the untreated control by 21–28 %. The greatest increase in mineralization with the combined treatment was found in the OSA-06 cell line (Fig. 6e).

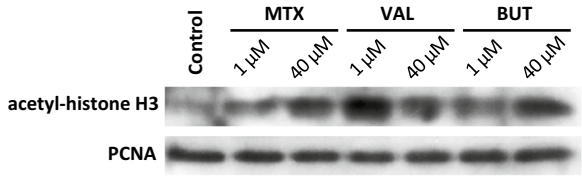

Fig. 4 Effect of MTX on histone H3 acetylation in OSA-06 cells. Cells were incubated with 1 or 40 μM MTX, VAL or BUT. At day 3, nuclear protein extracts were harvested and immunoblotted by anti-acetyl-histone H3 antibody. PCNA served as a loading control

Discussion

For decades, MTX was a commonly used therapy in osteosarcoma patients [19]. MTX interferes with folate metabolism but its other antineoplastic effects are still being discovered, and these effects can be helpful in the development of new strategies for osteosarcoma treatment [20]. The principal goals of this study were to analyze the non-DHFR-mediated effects of MTX in cell lines derived from osteosarcomas and to determine whether MTX acts as an epigenetic modifier in terms of DNA demethylation, histone acetylation, subsequent changes in gene expression and induced cell differentiation. The Saos-2 osteosarcoma cell line was chosen as the reference cell line for this study, and it was compared with five other cell lines that were derived in our laboratory from biopsy samples taken from patients suffering with osteosarcoma [21].

The MTT assay indicated that Saos-2 cells were very sensitive to MTX treatment, which showed a strong cytotoxic effect in these cells at 0.1 μM. This observation is in full accordance with our previous study [22] and with results obtained by other research groups studying the sensitivity of Saos-2 cells to MTX [23]. All five OSA cell lines, which were derived from diagnostic biopsies of primary tumors without any previous neoadjuvant chemotherapy, were significantly more resistant to the DHFR-mediated effect of MTX than Saos-2 cell line. The resistance of the OSA cell lines is surprising when we consider that 40 μM MTX is comparable with the peak of the MTX plasma concentration achieved during high dose-MTX treatments of pediatric hematological malignancies. In osteosarcomas, the peak MTX levels are approximately 1000 μM but rapidly decline within hours. Altogether, these results show that lower levels of MTX could not fully inhibit DHFR and nucleotide biosynthesis in all OSA cell lines despite prolonged exposure [24]. Furthermore, all OSA cells showed a low doubling time in comparison with Saos-2 cells that could diminish the proliferation-dependent cytotoxicity of MTX [25]. Other possible mechanisms of MTX resistance are an augmented drug efflux, impaired intracellular polyglutamation or alterations in the activity of target enzymes [6].

Because we did not observe any profound negative DHFR-mediated impact of MTX on cell proliferation in almost all of the cell lines included in this study, we continued with experiments that focused on other possible non-DHFR-mediated effects of MTX on osteosarcoma cells. MTX decreases the concentration of 5-methyltetrahydrofolate [26, 27] and reduces MAT expression and activity [13], which can further affect methylation in treated cells. 5-methyltetrahydrofolate and homocysteine are two important molecules in methionine biosynthesis [28]. Methionine reacts with ATP, and SAM is formed as a product. This key reaction is catalyzed by MAT. A methyl group from SAM is enzymatically transferred to the 5-position of cytosine to generate 5-methylcytosine in genomic DNA. Our data demonstrate that MTX significantly decreased 5-methylcytosine levels in genomic DNA and induce global genomic DNA demethylation. Surprisingly, significant DNA demethylation was observed in almost all of the cell lines used in our experiments.

Due to the similar structure of MTX and known histone deacetylase inhibitors, e.g., butyrate and trichostatin A, MTX can inhibit histone deacetylase activity and induce histone H3 acetylation [12]. Nevertheless, the five cell lines in our study including Saos-2 showed a poor response to MTX in this aspect. Only the OSA-06 cell line has a higher level of acetyl histone H3 after MTX treatment. Therefore, OSA-06 cells were further analyzed by western blotting to confirm this effect and the results showed that MTX increased the level of acetylated histone H3 in this cell line. As expected, most of cell lines showed a significant increase in the amount of acetylated histone H3 after treatment with BUT or VAL.

In contrast, MTX changed the methylation status of DNA in almost all of the studied cell lines. This finding led us to explore two important issues: (i) alterations of expression of the selected genes in MTX-treated cells and (ii) effect of MTX on differentiation in osteosarcoma cells after a combined treatment with ATRA because ATRA is a widely used inducer of differentiation in osteosarcoma cells [15, 29, 30].

Both of these aspects are important and mutually interconnected. Inducing differentiation of tumor cells by retinoids seems to be a very promising strategy, but it can be complicated by the resistance of tumor cells [16, 31–33]. The regulation of cell differentiation by retinoids is mediated by two types of nuclear receptors: retinoic acid receptors (RAR) and retinoid X receptors (RXR). DNA methylation patterns could affect the normal course of the expression of genes involved in cell differentiation [34]. For instance, *RARB* is methylated in many breast

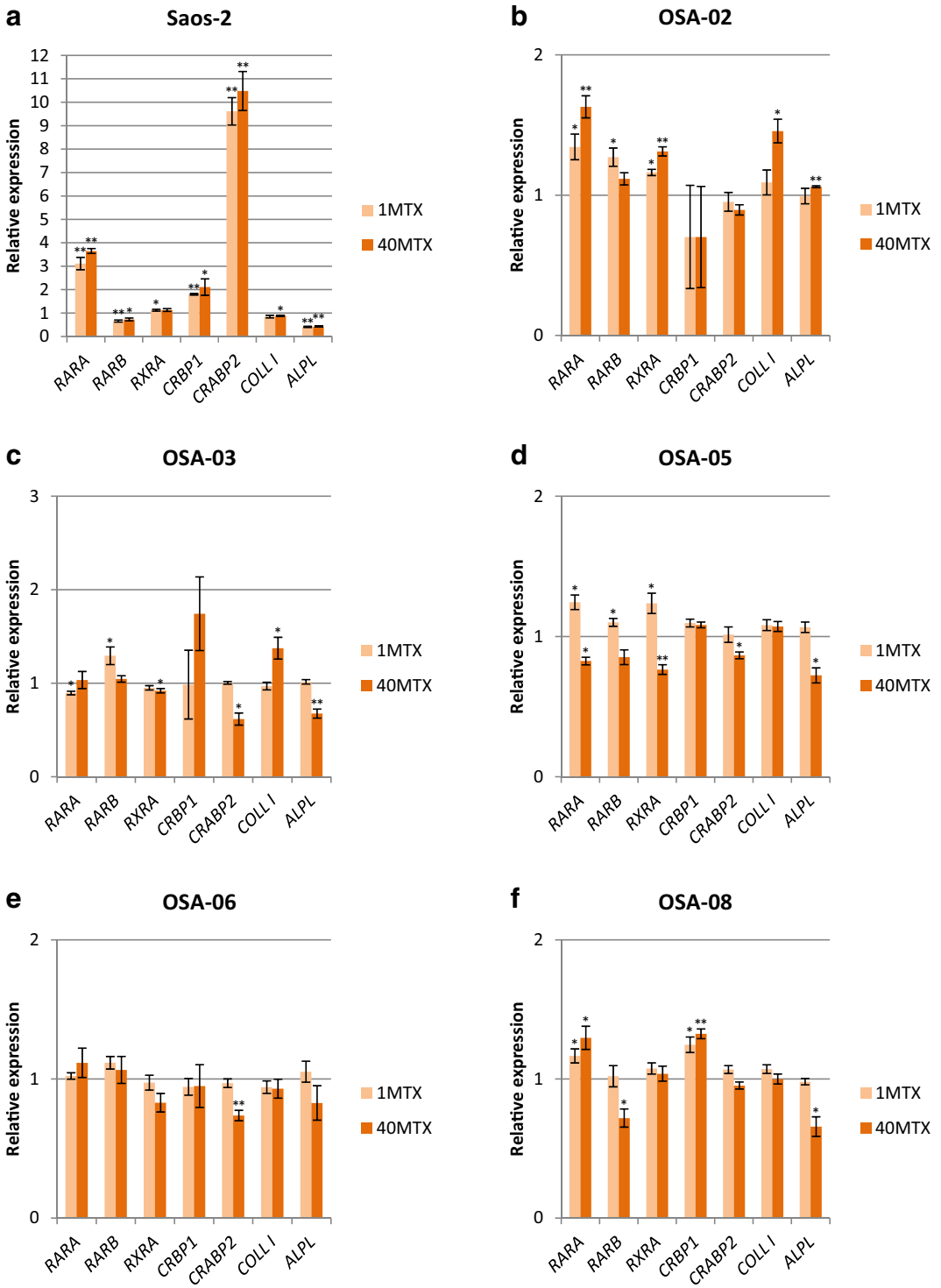

Fig. 5 Changes in expression of differentiation-related genes in osteosarcoma cell lines after treatment with MTX. The relative expression of selected genes in Saos-2 (**a**), OSA-02 (**b**), OSA-03 (**c**), OSA-05 (**d**), OSA-06 (**e**) and OSA-08 (**f**) cells measured using RT-qPCR at day 3 of incubation with 1 μM MTX (1MTX) or with 40 μM MTX (40MTX). The levels of relative gene expression are presented as fold changes compared to the levels detected in control samples. The data represent the mean ± SD. Experiments were repeated three times. *$P < 0.05$, **$P < 0.01$, indicate significant differences from the respective control groups

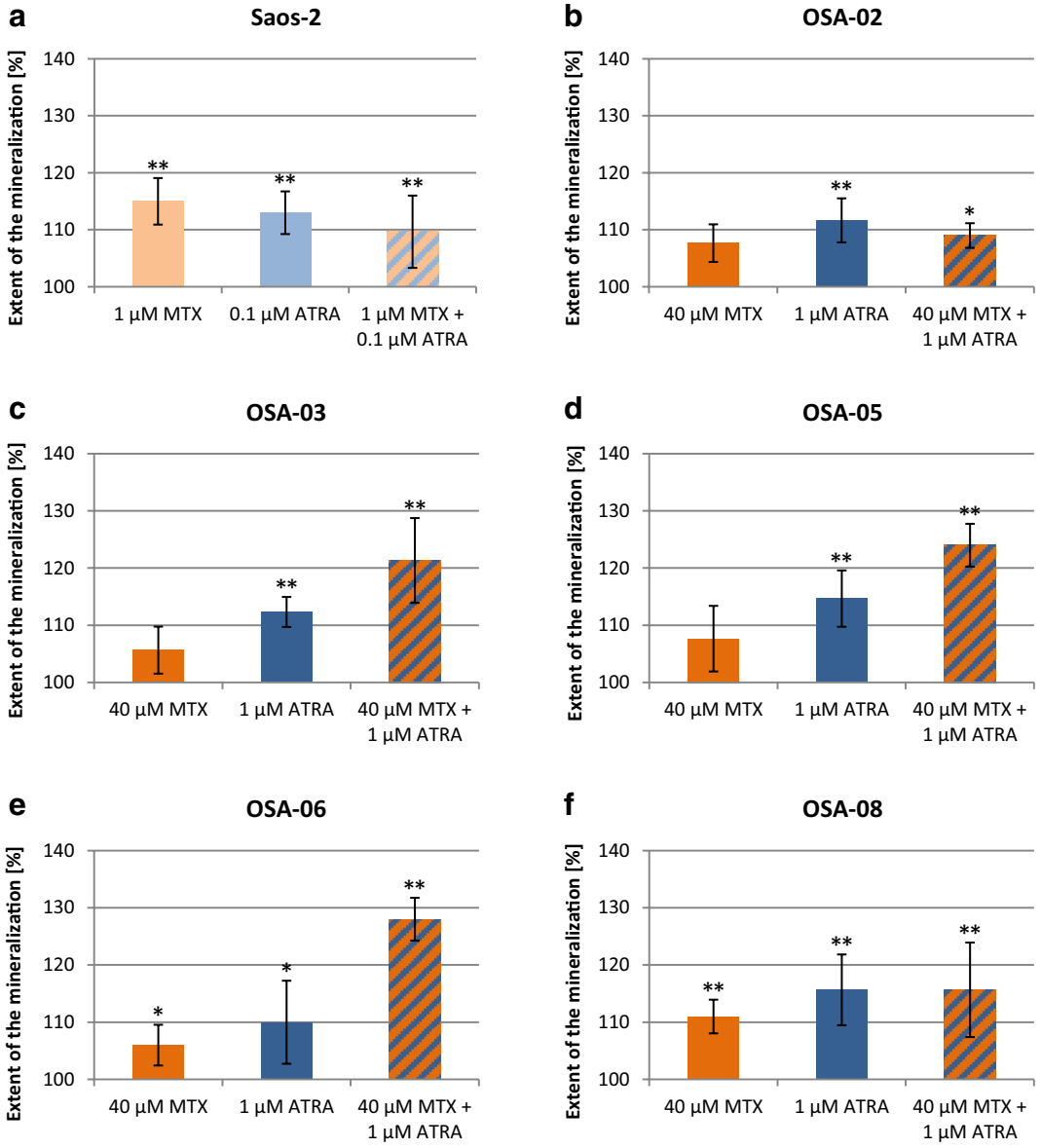

Fig. 6 Changes in matrix mineralization in osteosarcoma cell lines after treatment with MTX. Saos-2 (**a**), OSA-02 (**b**), OSA-03 (**c**), OSA-05 (**d**), OSA-06 (**e**) and OSA-08 (**f**) cell lines treated with MTX and/or ATRA were measured using staining with Alizarin Red S at day 21 of incubation. The extent of mineralization is presented as a percentage change compared to the levels found in untreated control cells. Untreated controls were set as 100 %. The data represent the mean ± SD. Experiments were repeated three times. *$P < 0.05$, **$P < 0.01$, indicate significant differences from the respective control groups

cancer cell lines and treatment of these cell lines with a demethylating agent can restore inducibility of *RARB* by ATRA [35]. Other studies have demonstrated that the *RARB* promoter is hypermethylated in colorectal and lung carcinomas and that this methylation could account for the *RARB* downregulation [18, 36].

At first, we studied whether MTX could modulate the expression of genes involved in retinoid/ATRA metabolism and signaling and whether MTX alone could induce differentiation in osteosarcoma cells. After treatment with MTX, we observed that the *RARA* was significantly highly expressed in Saos-2 and OSA-02 cells. Another interesting observation was the significantly increased expression of *CRABP2* in Saos-2 cells. *CRABP2* encodes the cytosol-to-nuclear shuttling protein, which facilitates the binding of retinoic acid to its receptor and the transfer of this complex to the nucleus. Furthermore, the expression *CRBP1*, which encodes the carrier protein

involved in the transport of retinol from liver storage site to the peripheral tissue was also significantly elevated in Saos-2 cells as well as in OSA-08 cells.

Regarding osteogenic differentiation, we examined the expression of known osteogenic differentiation markers, i.e., collagen type I (*COLLI*) and alkaline phosphatase (*ALPL*) [30]. Increase in *COLLI* expression is typical in the early stages of differentiation whereas levels of *ALPL* usually increase during the process of mineralization, i.e., during the late stages of induced differentiation [37]. Nevertheless, we did not observe a marked increase in expression of these markers.

Because the expression of some differentiation-related genes was modulated after 3 days of MTX treatment, we decided to evaluate a long time course of osteogenic differentiation using mineralization measured by Alizarin Red S staining [30]. MTX and ATRA alone increased the extent of matrix mineralization in all cell lines but ATRA was apparently more effective. Interestingly, MTX alone was able to induce cell differentiation effectively in the Saos-2 cell line; this finding is in accordance with previously published results on choriocarcinoma cells [38]. Our data also demonstrated that a combined treatment with ATRA and MTX enhanced matrix mineralization most greatly in the OSA-03, OSA-05 and OSA-06 cell lines, so the combined administration of MTX and retinoids could be effective in differentiation therapy of some osteosarcomas.

Conclusions

To summarize, our study represents the first complex analysis of the non-DHFR-mediated effects of MTX on cell lines derived from osteosarcomas. We showed that MTX treatment significantly decreased the proliferation activity in the Saos-2 reference cell line, but all five patient-derived OSA cell lines were much less sensitive to MTX action. These results suggest that all OSA cell lines were not sensitive to the DHFR-mediated effects of MTX at concentrations used. More importantly, our results provide the evidence for non-DHFR-mediated effects of MTX in both Saos-2 and OSA cell lines. MTX could act as an epigenetic modifier because (1) it induced significant DNA demethylation in almost all of the studied osteosarcoma cells and (2) it increased the global acetylation of histone H3 in OSA-06 cells. Our findings also demonstrated the modulation of the expression of differentiation-related genes by MTX at certain concentrations. The most important result of our study showed that ATRA-induced cell differentiation might be enhanced by the combined treatment of cells with MTX; this implies new possibilities in administration of these drugs in clinical practice.

Methods

Cell culture

The Saos-2 cell line (No. HTB-85) was purchased from the American Type Culture Collection (Manassas, VA, USA). The OSA-02, OSA-03, OSA-05, OSA-06 and OSA-08 cell lines were derived in our laboratory from tumor samples obtained from patients surgically treated for osteosarcoma as previously described [21]. A description of the cell lines included in this study and their responses to MTX is provided in Table 1. The Research Ethics Committee of the School of Medicine (Masaryk University, Brno, Czech Republic) approved the study protocol and a written statement of informed consent was obtained from each patient or his/her legal guardian.

Cells were grown in Dulbecco's modified Eagle's medium (DMEM) supplemented with 10 % (Saos-2) or 20 % (OSA-02, OSA-03, OSA-05, OSA-06 and OSA-08) fetal bovine serum, 100 IU/ml penicillin, 100 mg/ml streptomycin, and 2 mM glutamine (all purchased from GE Healthcare Europe GmbH, Freiburg, Germany). Cell culture was performed under standard conditions at 37 °C in a humidified atmosphere containing 5 % CO_2.

Chemicals

MTX (Sigma-Aldrich, St. Louis, MO, USA) was prepared as a stock solution at a concentration of 20 mM in 1 M NaOH (Sigma) and stored at −20 °C under light-free conditions. BUT and VAL (both from Sigma) were prepared as stock solutions at concentrations of 50 mM in sterile PBS and 5AZA (Sigma) was prepared as a stock solution at a concentration of 1 mM in sterile PBS. All three stock solutions were prepared freshly for each use. ATRA (Sigma) was prepared as a stock solution at concentration of 100 mM in DMSO (Sigma) and stored at −20 °C under light-free conditions.

For the determination of proliferation activity, seven different concentrations of MTX ranging from 0.0001 to 100 μM were tested. For all other experiments, concentrations of 1 and 40 μM MTX were used. 5AZA, VAL and BUT served as positive controls and were used at the same concentration as MTX, i.e., 1 and 40 μM.

In experiments on matrix mineralization, 1 μM ATRA was used as in previously published experiments concerning the ATRA-induced differentiation of osteosarcoma cells [30]. For the treatment of Saos-2 cells lower concentrations (i.e., 1 μM MTX and 0.1 μM ATRA) were used due to the previously reported sensitivity of these cells [30].

MTT assay

To evaluate cell proliferation, the MTT assay was used to detect the activity of mitochondrial dehydrogenases in

Table 1 Description of the cell lines and characterization of their responses to MTX

Cell line	Gender	Age	Tumor type	Time of biopsy	DNA demethylation	Increased histone H3 acetylation	MTX + ATRA enhanced differentiation
Saos-2	F	11	N/A	N/A	Y	N	N
OSA-02	M	21	HGCC	DG	N	N	N
OSA-03	M	15	HGCC	DG	Y	N	Y
OSA-05	M	9	T	DG	Y	N	Y
OSA-06	F	16	O	DG	Y	Y	Y
OSA-08	M	10	O	DG	Y	N	N

Gender: *M* male, *F* female; Age at the time of diagnosis: years; Tumor type: *HGCC* high grade conventional-chondroblastic, *T* teleangiectatic, *O* osteoblastic, *N/A* information not available; Time of biopsy: *DG* diagnostic, *N/A* information not available; Responses to MTX, i.e. DNA demethylation, histone H3 acetylation; enhanced matrix mineralization: *Y* yes, *N* no

living cells. 96-well plates were seeded with 1×10^4 cells per well in 200 µl of culture medium, and the cells were allowed to adhere overnight. The medium was removed and fresh medium containing the selected concentrations of chemicals described above or a control medium was added. The plates were incubated under standard conditions. To evaluate changes in cell proliferation, the medium was removed and replaced with 200 µl of fresh DMEM containing 3-[4,5-dimethylthiazol-2-yl]-2,5-diphenyltetrazolium bromide (MTT) at 0.5 mg per ml. The plates were then incubated at 37 °C for 2.5 h. The medium was carefully removed, and the formazan crystals were dissolved in 200 µl of DMSO. The absorbance with a reference absorbance at 620 nm was measured at 570 nm using a Sunrise Absorbance Reader (Tecan, Männedorf, Switzerland).

DNA methylation analysis

Total DNA was extracted using a DNeasy Blood & Tissue Kit (Qiagen, Hilden, Germany), and its concentration and purity was determined spectrophotometrically. Levels of 5-methylcytosine were detected using a 5-mC DNA ELISA Kit (Zymo Research Corporation, Irvine, CA, USA) according to the manufacturer's instructions. The absorbance was measured at 450 nm with the Sunrise Absorbance Reader.

Global histone H3 acetylation

For the specific measurement of global histone H3 acetylation, an EpiQuik Global Histone H3 Acetylation Assay Kit (Epigentek Group Inc., Farmingdale, NY, USA) was used according to the manufacturer's instructions. The absorbance was measured at 450 nm using the Sunrise Absorbance Reader.

RT-qPCR

The relative expression levels of selected genes were studied using RT-qPCR. Total RNA was extracted using the GenElute™ Mammalian Total RNA Miniprep kit (Sigma), and its concentration and integrity was determined spectrophotometrically. For all samples, equal amounts of RNA (i.e., 25 ng of RNA per 1 µl of total reaction volume) were reverse transcribed into cDNA using M-MLV (Top-Bio, Prague, Czech Republic). RT-qPCR was carried out in 10 µl using KAPA SYBR® FAST qPCR Kit (Kapa Biosystems, Wilmington, MA, USA) and analyzed using 7500 Fast Real-Time PCR System and 7500 Software v. 2.0.6 (both Life Technologies, Carlsbad, CA, USA). Changes in the transcript levels were calculated using Cq values standardized to a housekeeping gene (*HSP90AB1*), used as an endogenous reference gene control. Primers used for retinoic acid receptor alpha (*RARA*), retinoic acid receptor beta (*RARB*), retinoid X receptor alpha (*RXRA*), retinol binding protein 1 (*RBP1*), cellular retinoic acid binding protein 2 (*CRABP2*), collagen type I (*COLL I*), alkaline phosphatase (*ALPL*) and heat shock protein (*HSP90AB1*) are described in Table 2.

Table 2 Sequences of the primers used for qPCR

Gene	Primer sequence	Product length (bp)
RARA	F: 5′-CGACCGAAACAAGAAGAAGAAGG-3′ R: 5′-TTCTGAGCTGTTGTTCGTAGTGT-3′	166
RARB	F: 5′-TGATGGAGTTGGGTGGACTT-3′ R: 5′-GCTTGGGACGAGTTCCTCAG-3′	288
RXRA	F: 5′-CTCAATGGCGTCCTCAAGGT-3′ R: 5′-CACTCCATAGTGCTTGCCTGA-3′	111
RBP1	F: 5′-TGACCGCAAGTGCATGACAA-3′ R: 5′-GACCACACCTTCCACTCTCA-3′	142
CRABP2	F: 5′-TGCTGAGGAAGATTGCTGTG-3′ R: 5′-CCCATTTCACCAGGCTCTTA-3′	183
COLL I	F: 5′-CAGACTGGCAACCTCAAGAA-3′ R: 5′-GGAGGTCTTGGTGGTTTTGT-3′	180
ALPL	F: 5′-CCACGTCTTCACATTTGGTG-3′ R: 5′-AGACTGCGCCTGGTAGTTGT-3′	196
HSP90AB1	F: 5′-CGCATGAAGGAGACACAGAA-3′ R: 5′-TCCCATCAAATTCCTTGAGC-3′	169

Western blot analysis

Nuclear protein extracts were harvested using NE-PER™ Nuclear and Cytoplasmic Extraction Reagents (Life Technologies, Carlsbad, CA, USA) according to the manufacturer's instructions. Total proteins (15 μg) were loaded onto 10 % polyacrylamide gels, electrophoresed, and blotted on polyvinylidene difluoride membrane (Bio-Rad Laboratories, Munich, Germany). The membranes were blocked with 5 % nonfat dry milk in PBS with 0.1 % Tween-20 (Sigma) and incubated overnight either with rabbit polyclonal anti-acetyl-Histone H3 (Ac-Lys^9) (No. H9286, Sigma, dilution 1:1000) or with mouse monoclonal anti-Proliferating Cell Nuclear Antigen (anti-PCNA) (No. P8825, clone PC10, Sigma, dilution 1:3000). Anti-mouse IgG antibody peroxidase conjugate (No. A9917, Sigma, dilution 1:10,000) or anti-rabbit IgG HRP-linked antibody (No. 7074, Cell Signaling Technology, Danvers, MA, USA, dilution 1:2000) was used as the secondary antibodies. ECL-Plus detection was performed according to the manufacturer's instructions (GE Healthcare, Little Chalfont, UK).

Alizarin Red S staining

Levels of extracellular matrix mineralization were evaluated using Alizarin Red S staining, which detects calcium compounds both in tissue sections and in vitro. The cells were seeded onto 12-well plates at concentrations of 1×10^4 (Saos-2 cell line) or 5×10^3 (all OSA cell lines) cells per well and were cultivated in the presence or absence of ATRA and/or MTX for 21 days. The cultivation medium with these substances was renewed every 7 days. After 21 days of incubation, the medium was removed, the cells were washed with PBS and fixed with 3 % paraformaldehyde in PBS at room temperature for 20 min. Subsequently, the cells were incubated with 2 % Alizarin Red S (Sigma) at room temperature for 45 min. Thereafter, the cells were washed five times with deionized water and then with 70 % ethanol for 30 s. Red Alizarin dye was then dissolved via incubation with 100 mM cetylpyridinium chloride (Sigma) at 50 °C for 60 min. The absorbance was measured at 450 nm also using the Sunrise Absorbance Reader.

Statistical analysis

The quantitative data are shown as mean ± SD of three independent experiments. Data from MTT assays were analyzed using two-way ANOVA followed by the Scheffé post hoc test. $P < 0.01$ was considered significant. The other data were analyzed using Student's t test. $P < 0.05$ (two-sides) were considered statistically significant.

Abbreviations

AICAR transformylase: phosphoribosylaminoimidazolecarboxamide formyltransferase; 5AZA: 5-aza-2′-deoxycytidine; ATRA: all-*trans* retinoic acid; BUT: sodium butyrate; DHFR: dihydrofolate reductase; MAT: methionine adenosyltransferase; MTT: (3-(4,5-dimethylthiazol-2-yl)-2,5-diphenyltetrazolium bromide; MTX: methotrexate; PCNA: proliferating cell nuclear antigen; SAM: S-adenosylmethionine; TS: thymidylate synthase; VAL: sodium valproate.

Authors' contributions

MS carried out the experiments, analyzed the results and drafted the manuscript. JN designed this study, participated in analysis of results and in manuscript preparation. JS conceived and coordinated this study and participated in manuscript preparation. RV participated in the analysis of results and drafted the manuscript. All authors read and approved the final manuscript.

Author details

[1] Laboratory of Tumor Biology, Department of Experimental Biology, Faculty of Science, Masaryk University, Kotlarska 2, 611 37 Brno, Czech Republic. [2] Department of Pediatric Oncology, University Hospital Brno and Faculty of Medicine, Masaryk University, Cernopolni 9, 613 00 Brno, Czech Republic.

Acknowledgements

This study was supported by the grant IGA MZCR NT14327-3. The authors thank Dr. Jan Skoda and Dr. Petr Chlapek for skillful technical assistance.

Competing interests

The authors declare that they have no competing interests.

Received: 21 October 2015 Accepted: 12 February 2016
Published online: 29 February 2016

References

1. Hattinger CM, Fanelli M, Tavanti E, Vella S, Ferrari S, Picci P, et al. Advances in emerging drugs for osteosarcoma. Expert Opin Emerg Drugs. 2015;20:495–514.
2. Sterba J, Dusek L, Demlova R, Valik D. Pretreatment plasma folate modulates the pharmacodynamic effect of high-dose methotrexate in children with acute lymphoblastic leukemia and non-Hodgkin lymphoma: "folate overrescue" concept revisited. Clin Chem. 2006;52:692–700.
3. Sterba J, Valik D, Bajciova V. High-dose methotrexate in pediatric oncology—back to bench from bedside for a while? J Pediatr Hematol Oncol. 2009;31:151–2.
4. Cutolo M, Sulli A, Pizzorni C, Seriolo B, Straub RH. Anti-inflammatory mechanisms of methotrexate in rheumatoid arthritis. Ann Rheum Dis. 2001;60:729–35.
5. Tian H, Cronstein BN. Understanding the mechanisms of action of methotrexate: implications for the treatment of rheumatoid arthritis. Bull NYU Hosp Jt Dis. 2007;65:168–73.
6. Fotoohi AK, Albertioni F. Mechanisms of antifolate resistance and methotrexate efficacy in leukemia cells. Leuk Lymphoma. 2008;49:410–26.
7. McGuire JJ. Anticancer antifolates: current status and future directions. Curr Pharm Des. 2003;9:2593–613.
8. Singh R, Fouladi-Nashta AA, Li D, Halliday N, Barrett DA, Sinclair KD. Methotrexate induced differentiation in colon cancer cells is primarily due to purine deprivation. J Cell Biochem. 2006;99:146–55.
9. Seitz M, Zwicker M, Loetscher P. Effects of methotrexate on differentiation of monocytes and production of cytokine inhibitors by monocytes. Arthritis Rheum. 1998;41:2032–8.
10. Hatse S, Naesens L, De Clercq E, Balzarini J. Potent differentiation-inducing properties of the antiretroviral agent 9-(2-phosphonylmethoxyethyl) adenine (PMEA) in the rat choriocarcinoma (RCHO) tumor cell model. Biochem Pharmacol. 1998;56:851–9.
11. Wu J, Wood GS. Reduction of Fas/CD95 promoter methylation, upregulation of Fas protein, and enhancement of sensitivity to apoptosis in cutaneous T-cell lymphoma. Arch Dermatol. 2011;147:443–9.

12. Yang PM, Lin JH, Huang WY, Lin YC, Yeh SH, Chen CC. Inhibition of histone deacetylase activity is a novel function of the antifolate drug methotrexate. Biochem Biophys Res Commun. 2010;391:1396–9.
13. Wang YC, Chiang EP. Low-dose methotrexate inhibits methionine S-adenosyltransferase in vitro and in vivo. Mol Med. 2012;18:423–32.
14. Garattini E, Terao M. Cytodifferentiation: a novel approach to cancer treatment and prevention. Curr Opin Pharmacol. 2001;1:358–63.
15. Zhang L, Zhou Q, Zhang N, Li W, Ying M, Ding W, et al. E2F1 impairs all-trans retinoic acid-induced osteogenic differentiation of osteosarcoma via promoting ubiquitination-mediated degradation of RARα. Cell Cycle. 2014;13:1277–87.
16. Garattini E, Gianni M, Terao M. Retinoids as differentiating agents in oncology: a network of interactions with intracellular pathways as the basis for rational therapeutic combinations. Curr Pharm Des. 2007;13:1375–400.
17. Diede SJ, Guenthoer J, Geng LN, Mahoney SE, Marotta M, Olson JM, et al. DNA methylation of developmental genes in pediatric medulloblastomas identified by denaturation analysis of methylation differences. Proc Natl Acad Sci. 2010;107:234–9.
18. Virmani AK, Rathi A, Zöchbauer-Müller S, Sacchi N, Fukuyama Y, Bryant D, et al. Promoter methylation and silencing of the retinoic acid receptor-beta gene in lung carcinomas. J Natl Cancer Inst. 2000;92:1303–7.
19. Jaffe N, Gorlick R. High-dose methotrexate in osteosarcoma: let the questions surcease-time for final acceptance. J Clin Oncol. 2008;26:4365–6.
20. Hagner N, Joerger M. Cancer chemotherapy: targeting folic acid synthesis. Cancer Manag Res. 2010;2:293–301.
21. Veselska R, Hermanova M, Loja T, Chlapek P, Zambo I, Vesely K, et al. Nestin expression in osteosarcomas and derivation of nestin/CD133 positive osteosarcoma cell lines. BMC Cancer. 2008;8:300.
22. Neradil J, Pavlasova G, Sramek M, Kyr M, Veselska R, Sterba J. DHFR-mediated effects of methotrexate in medulloblastoma and osteosarcoma cells: the same outcome of treatment with different doses in sensitive cell lines. Oncol Rep. 2015;33:2169–75.
23. Wang JJ, Li GJ. Relationship between RFC gene expression and intracellular drug concentration in methotrexate-resistant osteosarcoma cells. Genet Mol Res. 2014;13:5313–21.
24. Rihacek M, Pilatova K, Sterba J, Pilny R, Valik D. New indings in methotrexate pharmacology—diagnostic possibilities and impact on clinical care. Klin Onkol. 2015;28:163–70.
25. Bastian L, Einsiedel HG, Henze G, Seeger K, Shalapour S. The sequence of application of methotrexate and histone deacetylase inhibitors determines either a synergistic or an antagonistic response in childhood acute lymphoblastic leukemia cells. Leukemia. 2011;25:359–61.
26. Vezmar S, Schüsseler P, Becker A, Bode U, Jaehde U. Methotrexate-associated alterations of the folate and methyl-transfer pathway in the CSF of ALL patients with and without symptoms of neurotoxicity. Pediatr Blood Cancer. 2009;52:26–32.
27. Kao TT, Lee GH, Fu CC, Chen BH, Chen LT, Fu TF. Methotrexate-induced decrease in embryonic 5-methyl-tetrahydrofolate is irreversible with leucovorin supplementation. Zebrafish. 2013;10:326–37.
28. Locasale JW. Serine, glycine and one-carbon units: cancer metabolism in full circle. Nat Rev Cancer. 2013;13:572–83.
29. Yang QJ, Zhou LY, Mu YQ, Zhou QX, Luo JY, Cheng L, et al. All-trans retinoic acid inhibits tumor growth of human osteosarcoma by activating Smad signaling-induced osteogenic differentiation. Int J Oncol. 2012;41:153–60.
30. Krzyzankova M, Chovanova S, Chlapek P, Radsetoulal M, Neradil J, Zitterbart K, et al. LOX/COX inhibitors enhance the antineoplastic effects of all-trans retinoic acid in osteosarcoma cell lines. Tumour Biol. 2014;35:7617–27.
31. Patatanian E, Thompson DF. Retinoic acid syndrome: a review. J Clin Pharm Ther. 2008;33:331–8.
32. Cruz FD, Matushansky I. Solid tumor differentiation therapy—is it possible? Oncotarget. 2012;3:559–67.
33. Tomita A, Kiyoi H, Naoe T. Mechanisms of action and resistance to all-trans retinoic acid (ATRA) and arsenic trioxide (As2O3) in acute promyelocytic leukemia. Int J Hematol. 2013;97:717–25.
34. Crider KS, Yang TP, Berry RJ, Bailey LB. Folate and DNA methylation: a review of molecular mechanisms and the evidence for folate's role. Adv Nutr. 2012;3:21–38.
35. Widschwendter M, Berger J, Hermann M, Müller HM, Amberger A, Zeschnigk M, et al. Methylation and silencing of the retinoic acid receptor-beta2 gene in breast cancer. J Natl Cancer Inst. 2000;92:826–32.
36. Hayashi K, Yokozaki H, Goodison S, Oue N, Suzuki T, Lotan R, et al. Inactivation of retinoic acid receptor beta by promoter CpG hypermethylation in gastric cancer. Differentiation. 2001;68:13–21.
37. Aubin JE, Liu F, Malaval L, Gupta AK. Osteoblast and chondroblast differentiation. Bone. 1995;17(2):77–83.
38. Hatse S, De Clercq E, Balzarini J. Role of antimetabolites of purine and pyrimidine nucleotide metabolism in tumor cell differentiation. Biochem Pharmacol. 1999;58:539–55.

Tumor Biol. (2016) 37:9535–9548
DOI 10.1007/s13277-016-4837-0

ORIGINAL ARTICLE

Cancer stem cell markers in pediatric sarcomas: Sox2 is associated with tumorigenicity in immunodeficient mice

Jan Skoda[1,2,3] · Alena Nunukova[1] · Tomas Loja[1] · Iva Zambo[4] · Jakub Neradil[1,2] · Peter Mudry[2] · Karel Zitterbart[2] · Marketa Hermanova[4] · Ales Hampl[5] · Jaroslav Sterba[2] · Renata Veselska[1,2,3]

Received: 5 October 2015 / Accepted: 11 January 2016 / Published online: 20 January 2016

Abstract The three most frequent pediatric sarcomas, i.e., Ewing's sarcoma, osteosarcoma, and rhabdomyosarcoma, were examined in this study: three cell lines derived from three primary tumor samples were analyzed from each of these tumor types. Detailed comparative analysis of the expression of three putative cancer stem cell markers related to sarcomas—ABCG2, CD133, and nestin—was performed on both primary tumor tissues and corresponding cell lines. The obtained results showed that the frequency of ABCG2-positive and CD133-positive cells was predominantly increased in the respective cell lines but that the high levels of nestin expression were reduced in both osteosarcomas and rhabdomyosarcomas under in vitro conditions. These findings suggest the selection advantage of cells expressing ABCG2 or CD133, but the functional tests in NOD/SCID gamma mice did not confirm the tumorigenic potential of cells harboring this phenotype. Subsequent analysis of the expression of common stem cell markers revealed an evident relationship between the expression of the transcription factor Sox2 and the tumorigenicity of the cell lines in immunodeficient mice: the Sox2 levels were highest in the two cell lines that were demonstrated as tumorigenic. Furthermore, Sox2-positive cells were found in the respective primary tumors and all xenograft tumors showed apparent accumulation of these cells. All of these findings support our conclusion that regardless of the expression of ABCG2, CD133 and nestin, only cells displaying increased Sox2 expression are directly involved in tumor initiation and growth; therefore, these cells fit the definition of the cancer stem cell phenotype.

Keywords Cancer stem cells · Pediatric sarcomas · Markers · Tumorigenicity · Sox2

✉ Renata Veselska
veselska@sci.muni.cz

[1] Department of Experimental Biology, School of Science, Masaryk University, Brno, Czech Republic

[2] Department of Pediatric Oncology, University Hospital Brno and School of Medicine, Masaryk University, Brno, Czech Republic

[3] International Clinical Research Center, St. Anne's University Hospital Brno, Brno, Czech Republic

[4] 1st Institute of Pathologic Anatomy, St. Anne's University Hospital and School of Medicine, Masaryk University, Brno, Czech Republic

[5] Department of Histology and Embryology, School of Medicine, Masaryk University, Brno, Czech Republic

Introduction

Malignancies are the second most frequent cause of death (after injuries) in children under the age of 15 worldwide. For this reason, one of the main goals in pediatric oncology is to understand the biological features of cancers that typically appear during childhood because prompt and precise diagnosis together with specific and effective treatment may lead to a complete cure or to a marked prolongation of life expectancy among these patients.

In this context, cancer stem cells (CSCs) represent a very important research topic in pediatric oncology. In heterogeneous tumor tissue, only CSCs are able to initiate tumor growth after grafting into immunodeficient mice. Therefore, CSCs are undoubtedly key drivers of tumor initiation, progression, metastasizing, and treatment failure [1–3]. Thus, a detailed understanding of the characteristics of particular tumor types and biological features of CSCs may be of great importance for the development of new effective antineoplastic therapies designed specifically for children [4, 5].

Pediatric sarcomas represent a very heterogeneous group of tumors with varying molecular, pathological, and clinical features: osteosarcoma, Ewing's sarcoma, and rhabdomyosarcoma are the most frequent of them. In addition to common stem cell markers, such as Oct3/4, Sox2, and Nanog, special attention is paid to the identification of additional markers that enable the positive detection of CSCs in these tumors. A combination of the cell surface antigens prominin-1 (CD133) and ABCG2 (CD338) together with the intermediate filament protein nestin is the marker expression profile most frequently discussed as a CSC phenotype specific to sarcomas [6–9].

Despite the publication of several studies aimed at the identification and characterization of CSCs using established cell lines and standardized functional assays, little is known about the "previous step" of cancer stem cell biology: which cell subpopulations expressing putative CSC markers predominate after successful derivation of a cell line from a tumor sample. For this reason, our study focused on a detailed comparative analysis of the expression of the most frequently discussed putative CSC markers in pediatric sarcomas, i.e., ABCG2, CD133, and nestin, in both primary tumor tissues and their respective derived cell lines. Three most common pediatric sarcomas, i.e., osteosarcoma, rhabdomyosarcoma, and Ewing's sarcoma, were included in this study: three cell lines derived from three primary tumor samples were analyzed for each of these tumor types. This experimental design provided an important opportunity to compare the pattern of the expression of the markers mentioned above in nine tumor samples paired with nine cell lines. Additionally, in both the cell lines and the tumor samples, special attention was paid to the intracellular localization of CD133 because this characteristic may be relevant to the biological features of tumor cells [10, 11]. Furthermore, all cell lines were tested for tumorigenicity in NOD/SCID mice, and the resulting xenograft tumors were analyzed.

Materials and methods

Tumor samples and primary cell lines

Nine tumor samples collected from patients suffering from pediatric sarcoma and nine corresponding cell lines derived from these tumors were included in this study: a brief description of the cohort is provided in Table 1. The OSA-05 and NSTS-11 cell lines were originally described in our previous studies [12, 13]; all other cell lines were derived using the same procedure to generate primary cultures [14]. The cell lines were maintained under standard conditions as described previously [13]. The Research Ethics Committee of the School of Science (Masaryk University) approved the study protocol, and a written statement of informed consent was obtained from each participant or his/her legal guardian prior to participation in this study.

Immunohistochemistry

Immunohistochemical (IHC) detection was performed on formalin-fixed paraffin-embedded (FFPE) samples of primary or xenograft tumors. The 4 μm thick tissue sections were applied to positively charged slides, deparaffinized in xylene, and rehydrated using a graded alcohol series. For nestin and CD133, antigen retrieval was performed in a calibrated Pascal pressure chamber (Dako, Glostrup, Denmark) by heating the sections in Tris/EDTA buffer (DAKO) at pH 9.0 for 40 min at 97 °C. For ABCG2, the sections were not subjected to any pretreatment. Endogenous peroxidase activity was quenched by incubating the sections in 3 % hydrogen peroxide in methanol for 20 min, followed by incubation at room temperature (RT) with a primary antibody (Table 2). For nestin and ABCG2, the Vectastain Elite ABC kit and the streptavidin-biotin horseradish peroxidase (HRP) detection method were

Table 1 Description of patient cohort, corresponding cell lines, and xenograft tumors

Tumor sample	Gender	Age	Diagnosis	Time of biopsy	Primary cell line	Xenograft tumors		
1	M	17	EWS	DG	ESFT-03	–		
2	M	2	EWS	DG	ESFT-04	–		
3	M	25	EWS/PNET	DG	ESFT-09	–		
4	M	9	OS teleangiectatic	DG	OSA-05	–		
5	F	16	C-OS osteoblastic	DG	OSA-06	–		
6	F	6	C-OS	DG	OSA-13	LTB17	LTB18	LTB19
7	F	16	RMS embryonal	NACHT	NSTS-11	LTB1	LTB2	LTB3
8	F	6	RMS alveolar	DG	NSTS-22	–		
9	M	8	RMS alveolar	PROG	NSTS-28	–		

Gender: *M* male, *F* female. Age at the time of diagnosis: years. Diagnosis: *EWS* Ewing's sarcoma, *PNET* primitive neuroectodermal tumor, *OS* osteosarcoma, *C-OS* conventional osteosarcoma, *RMS* rhabdomyosarcoma. Time of biopsy: *DG* diagnostic, *NACHT* after neo-adjuvant chemotherapy, *PROG* progression of the disease

Table 2 Antibodies and primers used in this study

Primary antibodies						
Antigen	Type/host	Clone (catalog no.)	Manufacturer	Dilution		
				IHC	IF	WB
ABCG2	Polyclonal/Rb	– (bs-0662R)	Bioss	1:400	–	–
ABCG2	Monoclonal/Mo	5D3	BD Pharmingen	–	1:50	–
ALDH1	Monoclonal/Mo	44/ALDH	BD Biosciences	–	–	1:1000
CD133	Monoclonal/Mo	17A6.1	Millipore	1:100	1:100	–
Nanog	Polyclonal/Rb	– (ab21624)	Abcam	–	–	1:100
Nestin	Monoclonal/Mo	10C2	Millipore	1:200	1:100	–
Oct4	Polyclonal/Rb	– (ab19857)	Abcam	–	–	1:500
Sox2	Monoclonal/Rb	EPR3131	Abcam	1:100	1:10	–
Sox2	Monoclonal/Rb	D6D9	Cell Signaling	–	–	1:500
Sox2	Polyclonal/Rb	– (ab137385)	Abcam	–	–	1:1000
α-tubulin	Monoclonal/Mo	TU-01	Exbio	–	1:100	1:500
β-actin	Monoclonal/Mo	AC-15	Sigma	–	–	1:10,000
Secondary antibodies						
Host	Specificity	Conjugate	Manufacturer	Dilution		
				IHC	IF	WB
Goat	anti-Rb IgG	Alexa Fluor 488	Life Technologies	–	1:200	–
Goat	anti-Mo IgG	Alexa Fluor 488	Life Technologies	–	1:200	–
Goat	anti-Rb IgG	HRP	Cell Signaling	–	–	1:5000
Horse	anti-Mo IgG	HRP	Cell Signaling	–	–	1:5000
Primers						
Gene	Gene symbol	Primer sequence				
ABCG2	*ABCG2*	F: 5′-TCACTACTTCCTTCCTTACCCCT-3′ R: 5′-ACAGAAACACAACACTTGGCTG-3′				
CD133	*PROM1*	F: 5′-CCATTGACTTCTTGGTGCTGT-3′ R: 5′-TGGAGTTACGCAGGTTTCTCT-3′				
Nestin	*NES*	F: 5′-AGTGATGCCCCTTCACCTTG-3′ R: 5′-GCTCGCTCTCTACTTTCCCC-3′				
Oct4	*POU5F1*	F: 5′-GCAAAGCAGAAACCCTCGT-3′ R: 5′-ACACTCGGACCACATCCTTC-3′				
Nanog	*NANOG*	F: 5′-AATACCTCAGCCTCCAGCAGAT-3′ R: 5′-TGCGTCACACCATTGCTATTCTTC-3′				
Sox2	*SOX2*	F: 5′-TCCCATCACCCACAGCAAATGA-3′ R: 5′-TTTCTTGTCGGCATCGCGGTTT -3′				
Aldehyde dehydrogenase	*ALDH1A1*	F: 5′- GTCAAAGGCTTCCTGCCCTA-3′ R: 5′- GGTTCTGATAGAGCACTTGGCT-3′				
Heat shock protein HSP 90-beta	*HSP90AB1*	F: 5′-CGCATGAAGGAGACACAGAA-3′ R: 5′-TCCCATCAAATTCCTTGAGC-3′				

Rb rabbit, *Mo* mouse, *HRP* horseradish peroxidase, *F* forward primer, *R* reverse primer

used (Vector Laboratories, Burlingame, CA, USA). For CD133, EnVision+ Dual Link system-HRP without avidin or biotin was applied for detection (Dako). For Sox2, the EXPOSE Rabbit-specific HRP/DAB detection kit (Abcam) was used. 3,3′-diaminobenzidine (DAB) was used as a chromogen. Positive controls were obtained by staining sections of glioblastoma multiforme or breast carcinoma; nestin- or CD133-positive endothelial cells in tumor tissue samples were used as internal positive controls. For Sox2, sections of fetal lung tissue were used as a positive control. Negative controls were prepared by incubating samples in the absence of a primary antibody. Evaluation of all IHC staining results was performed using an Olympus BX51 microscope and an Olympus DR72 camera with uniform settings. All immunostained slides were evaluated at ×400 magnification independently by two observers (IZ and MH). The percentage of positive tumor cells (TC) and the

average intensity of immunostaining (i.e., immunoreactivity, IR) were assessed in at least five discrete foci of neoplastic infiltration.

Immunofluorescence

Indirect immunofluorescence (IF) was performed as previously described [13]. The primary and secondary antibodies used in the experiments are listed in Table 2; mouse monoclonal anti-α-tubulin served as a positive control. An Olympus BX-51 microscope was used for sample evaluation; micrographs were captured using an Olympus DP72 CCD camera and analyzed using the Cell^P imaging system (Olympus). At least 200 cells were evaluated in total within discrete areas of each sample, and the samples were prepared from at least three independent passages of all examined cell lines. The mean percentage of cells showing positivity for the examined antigen and the IR for the antigen were determined. Finally, for each cell line, the total immunoscores were calculated for individual antigens as described previously [15]. The immunoscore values were classified as low (≥100), middle (101–200), or high (201–300).

Western blotting and immunodetection

We also used a previously described procedure [13] to analyze expression of Sox2, Oct4, Nanog, and aldehyde dehydrogenase 1 (ALDH1) in sarcoma cell lines. The primary and secondary antibodies used are listed in Table 2; mouse monoclonal anti-α-tubulin or mouse monoclonal anti-β-actin served as a loading control.

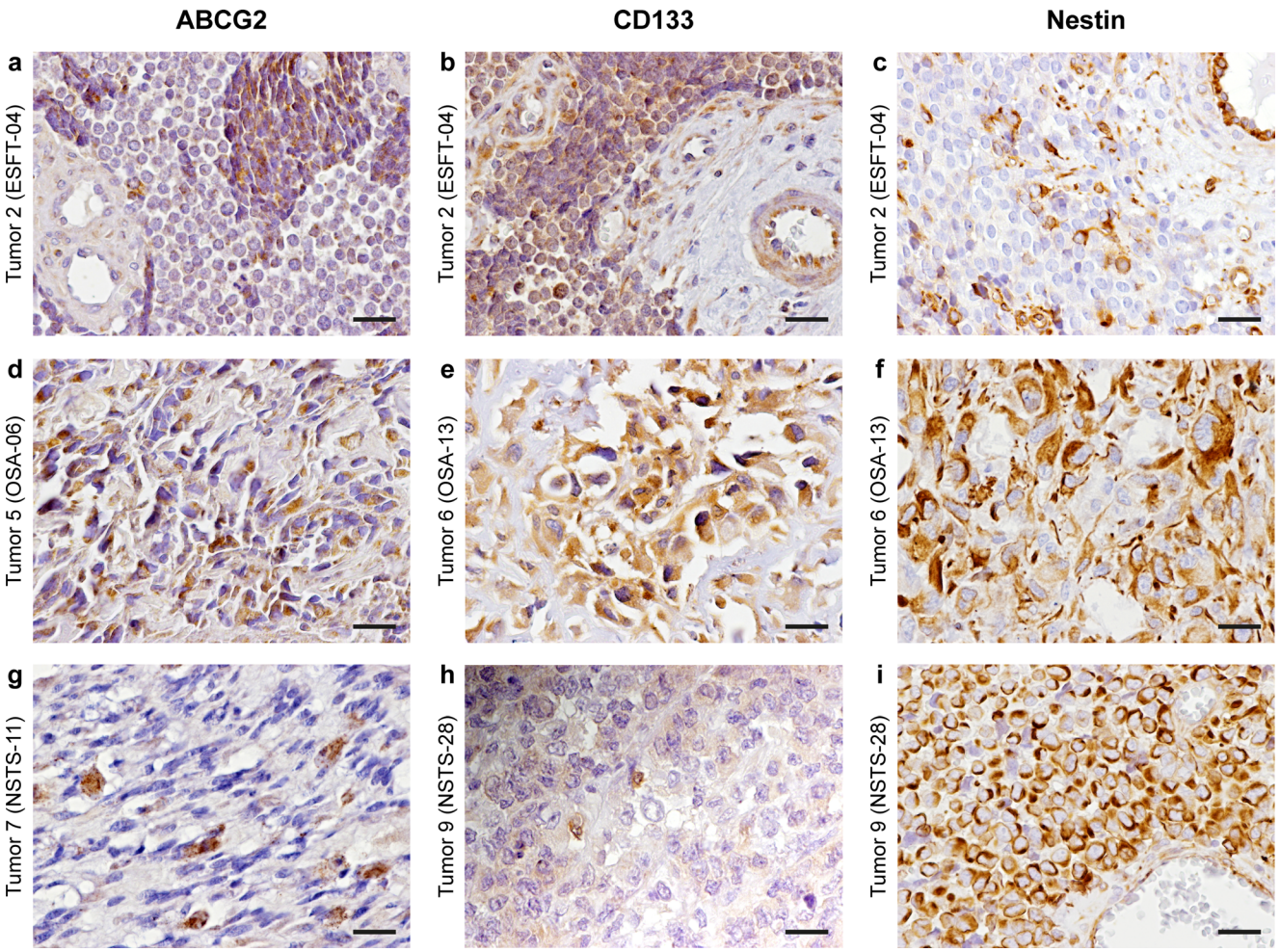

Fig. 1 Expression of ABCG2, CD133 and nestin in tumor tissues as detected by IHC. Ewing's sarcoma (**a**–**c**), osteosarcoma (**d**–**f**), and rhabdomyosarcoma (**g**–**i**) tissue samples were analyzed. Tumor sample and corresponding cell line (in *brackets*) are indicated. *Scale bars*, 50 μm

Real-time quantitative reverse transcription PCR (qRT-PCR)

For qRT-PCR of sarcoma cell lines, total RNA was extracted and reverse transcribed as previously described [13]. Quantitative PCR was performed in a volume of 10 μl using the KAPA SYBR® FAST qPCR Kit (Kapa Biosystems, Wilmington, MA, USA) and 7500 Fast Real-Time PCR System (Applied Biosystems, Foster City, CA, USA). The data were analyzed by 7500 Software v. 2.0.6 (Applied Biosystems) and relative quantification (RQ) of gene expression were calculated using $2^{-\Delta\Delta CT}$ method [16]; heat shock protein gene (*HSP90AB1*) was used as the endogenous reference control and ESFT-03 cell line served as the arbitrary calibrator. The primer sequences used are listed in Table 2.

In vivo tumorigenicity assay

Enzymatically dissociated cell suspensions of all nine primary cell lines were each injected subcutaneously into three 8-week-old female NOD/SCID gamma mice at a concentration of 1×10^6 cells (for Ewing's sarcoma and osteosarcoma cell lines) or 3×10^5 cells (for rhabdomyosarcoma cell lines) per 100 μl. The mice were examined every 3 days for the presence of subcutaneous tumors. After the appearance of a tumor, the mice were sacrificed, and the tumor tissue was dissected. This study was approved by the Institutional Animal Care and Use Committee of Masaryk University and was registered by the Ministry of Agriculture of the Czech Republic as required by national legislation. Each tumor was divided into two equal portions: one portion was processed for primary culture [14], and the second portion was fixed in 10 % buffered formalin

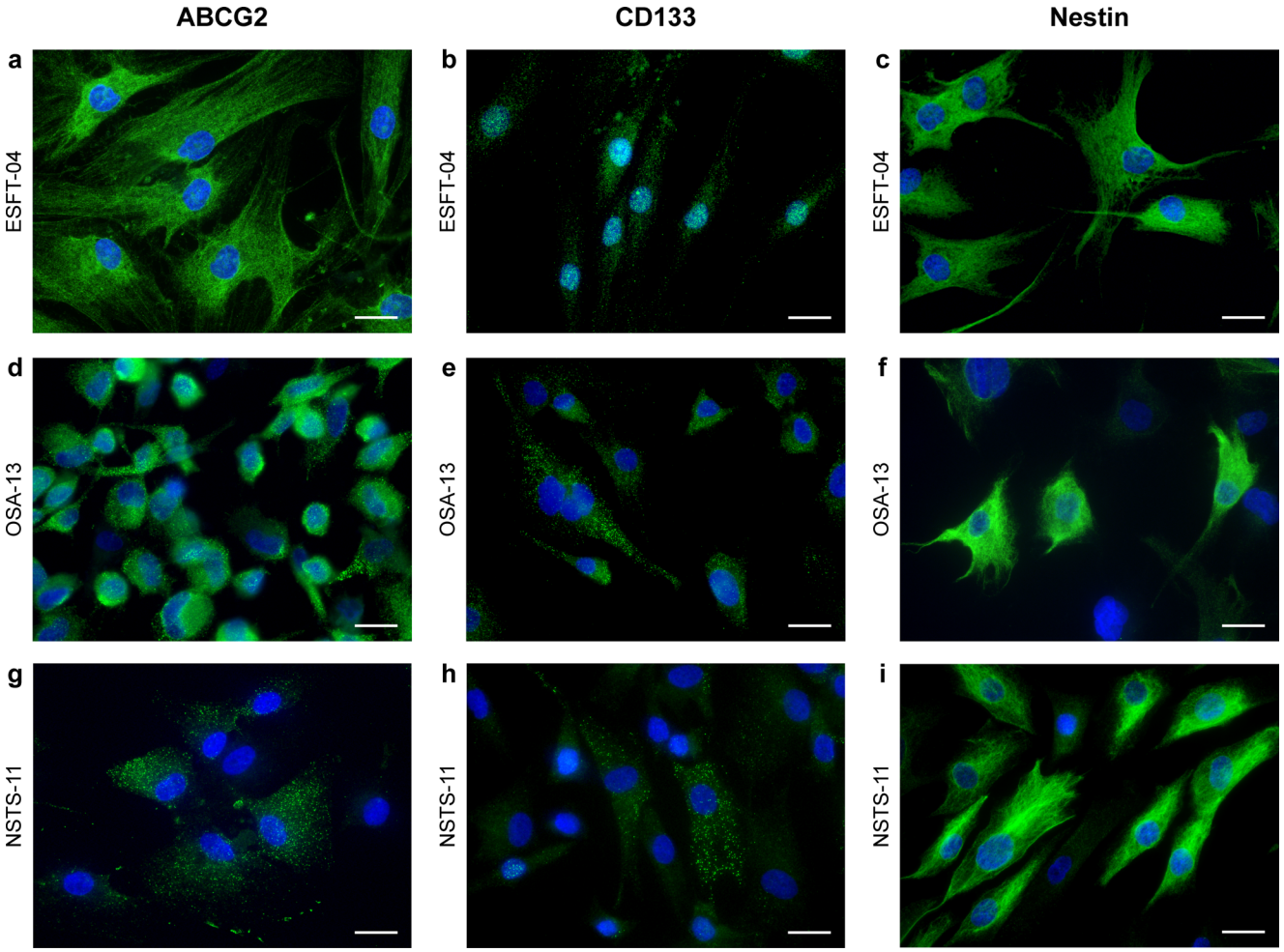

Fig. 2 Expression of ABCG2, CD133 and nestin in sarcoma cell lines as detected by IF. Ewing's sarcoma (**a**–**c**), osteosarcoma (**d**–**f**), and rhabdomyosarcoma (**g**–**i**) cell lines were analyzed. Each marker was visualized by indirect immunofluorescence using Alexa 488-conjugated secondary antibody (*green*); nuclei were counterstained with DAPI (*blue*). *Scale bars*, 25 μm

Table 3 Analysis of ABCG2, CD133, and nestin expression in tumor samples and corresponding cell lines

Tumor sample	Cell line	ABCG2				CD133				Nestin			
		IHC (tumor)		IF (cell line)		IHC (tumor)		IF (cell line)		IHC (tumor)		IF (cell line)	
		% TC	IR	% PC	I-sc	% TC	IR TC	% PC	I-sc	% TC	IR TC	% PC	I-sc
Ewing's sarcoma													
1	ESFT-03	+/−	+	93 %	201.00	+	+	67 %	106.00	−	−	45 %	83.00
2	ESFT-04	+	+	95 %	235.00	+++	+	97 %	174.00	+	++	65 %	131.00
3	ESFT-09	++	++	92 %	197.00	+++	+	70 %	115.00	−	−	53 %	98.00
Osteosarcoma													
4	OSA-05	+/−	+	98 %	249.09	+++	++	56 %	99.90	+++	+++	51 %	93.50
5	OSA-06	+++	++	97 %	231.58	+++	++	86 %	149.87	+++	+++	94 %	230.00
6	OSA-13[a]	+/−	+	86 %	199.25	+++	++	94 %	215.65	+++	+++	74 %	160.00
Rhabdomyosarcoma													
7	NSTS-11[a]	+/−	++	50 %	82.32	++	+	51 %	88.52	+++	+++	67 %	141.67
8	NSTS-22	+	+	47 %	72.00	+	+	50 %	94.09	+++	+++	65 %	164.79
9	NSTS-28	+/−	++	44 %	69.55	+++	+	54 %	100.08	+++	+++	61 %	101.77

The percentage of positive tumor cells (% TC) was categorized into five levels as follows: − (0 %), +/− (1–5 %), + (6–20 %), ++ (21–50 %), and +++ (51–100 %). The immunoreactivity of tumor cells (IR TC) was graded as − (none), + (weak), ++ (medium), and +++ (strong). For cell lines, the mean percentage of cell positive for the respective antigen (% PC) is given. Immunoscores (I-sc) were determined by multiplying the percentage of positive cells by the respective immunoreactivity

IHC immunohistochemistry, *IF* immunofluorescence

[a] Primary cell lines proved to be tumorigenic in NOD/SCID gamma mice

for 24 h, routinely processed for histological examination and embedded in paraffin. Tissue sections of FFPE samples were stained with hematoxylin-eosin and examined. Alternatively, IHC detection was performed as previously described.

Results

In general, comparison of the results from IHC staining of the primary tumor samples (Fig. 1) and from IF of the corresponding cell lines (Fig. 2) showed a selection of cells expressing ABCG2, CD133 and nestin under in vitro conditions. All cell lines included in this study showed at least approximately 50 % positive cells for each of these markers, although the respective immunoscore values varied from low to high (Table 3).

ABCG2 was found relatively rarely and at a low intensity in all tumor samples independent of the sarcoma type (Table 3, Fig. 1a, d, g), although the Ewing's sarcoma (Fig. 2a) and osteosarcoma (Fig. 2d) cell lines showed strong expression of this molecule in almost all cells. However, in the rhabdomyosarcoma cell lines (Fig. 2g), only approximately half of the cells were positive for ABCG2 and ABCG2 IR was scored as middle (Table 3).

CD133 was more frequently detected in the tumor samples of all sarcoma types, but the intensity of immunostaining was weak in Ewing's sarcomas and rhabdomyosarcomas and was middle in osteosarcomas (Table 3, Fig. 1b, e, h). In all examined cell lines, the frequency of CD133-positive cells was greater than 50 %, and the IR appeared to be higher than that in the primary tumors (Table 3, Fig. 2b, e, h). The atypical nuclear localization of CD133 was observed in some tumor samples and in all cell lines at various frequencies (Table 4, Fig. 3a–c), but the most surprising result was in the ESFT-04 cell line, in which absolute nuclear positivity for CD133 was observed (Fig. 3d, e). These cells clearly exhibited a strong selection advantage because nuclear positivity for CD133 was found only sporadically in the corresponding primary tumor tissue (Fig. 3f).

Quite different results were achieved for nestin: although it was expressed very intensively in all osteosarcoma and rhabdomyosarcoma tumor samples (Table 3, Fig. 1f, i), one Ewing's sarcoma tumor sample showed a markedly low proportion of nestin-positive cells (Fig. 1c), and the other two Ewing's sarcoma tumor samples were nestin-negative (Table 3). In contrast, cell lines, including those derived from Ewing's sarcomas, contained more than 50 % nestin-positive cells and displayed medium or high IR (Table 3, Fig. 2c, f, i).

In all cell lines, the expression of ABCG2, CD133 and nestin was further examined at the transcriptional level by qRT-PCR (Fig. 4a). For nestin, the mRNA levels nearly completely correlated with the immunoscore as calculated

Table 4 Analysis of the subcellular localization of CD133 in tumor samples and corresponding cell lines

Tumor sample	Cell line	Localization	IHC (tumor)		IF (cell line)	
			% TC	IR TC	% PC	I-sc
Ewing's sarcoma						
1	ESFT-03	Me | Cy	− | +	− | +	67.00	106.00
		Nu	−	−	11.20[b]	11.20
2	ESFT-04	Me | Cy	− | +++	− | +	97.00	155.00
		Nu	+/−	+	97.00[b]	232.00
3	ESFT-09	Me | Cy	− | +++	− | +	70.00	115.00
		Nu	−	−	53.00[b]	53.00
Osteosarcoma						
4	OSA-05	Me | Cy	+ | +++	++ | ++	56.00	99.90
		Nu	++	+	10.66[b]	10.66
5	OSA-06	Me | Cy	+/− | +++	+ | ++	86.00	149.87
		Nu	+/−	+	16.91[b]	16.91
6	OSA-13[a]	Me | Cy	+++	++	94.00	215.65
		Nu	−	−	50.33[b]	50.33
Rhabdomyosarcoma						
7	NSTS-11[a]	Me | Cy	− | ++	− | +	46.40	83.92
		Nu	−	−	4.60	13.80
8	NSTS-22	Me | Cy	− | +	− | +	44.00	88.09
		Nu	+/−	+	6.00	18.00
9	NSTS-28	Me | Cy	− | +++	− | +	48.80	94.88
		Nu	−	−	5.20	15.60

Localization of CD133 was classified as membranous (Me), cytoplasmic (Cy) or nuclear (Nu). The percentage of positive tumor cells (% TC) was categorized into five levels: − (0 %), +/− (1–5 %), + (6–20 %), ++ (21–50 %), and +++ (51–100 %). The immunoreactivity of tumor cells (IR TC) was graded as − (none), + (weak), ++ (medium), and +++ (strong). For cell lines, the mean percentage of cell positive for the membranous / cytoplasmic or nuclear localization (% PC) is given. Immunoscores (I-sc) were determined by multiplying the percentage of positive cells by the respective immunoreactivity

IHC immunohistochemistry, *IF* immunofluorescence

[a] Primary cell lines proved to be tumorigenic in NOD/SCID gamma mice

[b] Cells were not exclusively positive for nuclear localization but represented a subset of membranous/cytoplasmic positive cells

for individual cell lines. However, no such trends were observed for ABCG2 or CD133.

To detect a possible relationship between the expression of these markers and tumorigenic potential, all cell lines were tested using an in vivo tumorigenicity assay. Surprisingly, only two cell lines—OSA-13 and NSTS-11—were able to form tumors in immunodeficient mice (Table 3, Fig. 5a–c, g–i). Furthermore, the detected tumorigenicity of these cell lines did not correspond to any comparable change in the expression of the markers described above or to the atypical nuclear localization of CD133 (Table 4). Only qRT-PCR showed increased transcriptional levels of ABCG2 and CD133; this pattern was not observed at the protein levels, as detected by IF (Fig. 4a, Table 3).

For this reason, we performed additional qRT-PCR experiments to evaluate the levels of common stem cell markers (Oct4, Nanog, Sox2, and ALDH1) to identify possible changes associated with the tumorigenicity of OSA-13 and NSTS-11 cell lines. Among these markers, only Sox2 showed elevated mRNA levels in the tumorigenic cell lines but not in the other cell lines (Fig. 4b, Table 5). Further analysis at the protein level showed identical results: Sox2 was highly expressed exclusively in the two tumorigenic cell lines as detected by Western blotting, whereas no differences in expression of Oct4, Nanog and ALDH1 were observed between tumorigenic and non-tumorigenic cell lines (Fig. 4c). Furthermore, IF analysis showed the highest immunoscores of Sox2 in the two tumorigenic cell lines (Table 5, Fig. 6d–f), and the expression of Sox2 was validated by Western blotting using two independent antibodies (Fig. 6g).

In the last step of our study, we analyzed all primary tumor samples and all xenograft tumors for Sox2 expression via IHC staining. Among the primary tumors, the

highest proportion of Sox2-positive cells was found in the tumor sample from which the tumorigenic NSTS-11 cell line was derived, and these Sox2-positive cells were typically accumulated in small distinct clusters or striations (Fig. 6c). A rare incidence of Sox2-positive cells was identified in two additional tumor samples, but their corresponding cell lines were non-tumorigenic (Table 5). Finally, IHC analysis of all xenograft rhabdomyosarcoma and osteosarcoma tumors showed a marked increase in the frequency of Sox2-positive cells in all xenograft rhabdomyosarcoma and osteosarcoma tumors (Fig. 5d–f, j–l) compared with the corresponding primary tumor samples.

Discussion

The initial aim of our study was to analyze the changes in the expression of ABCG2, CD133, and nestin as putative CSC markers in pediatric sarcomas, in both primary tumors and corresponding cell lines derived from these tumors. We intended to elucidate the selection process for these three markers during the derivation process under in vitro conditions because the findings published in this field bring to date had reported partly contradictory results [6].

ABCG2, a plasma membrane ATP-binding cassette (ABC) transporter responsible for the multidrug resistance of tumor cells, was reported to be a specific marker of CSCs in osteosarcoma cell lines, as only this ABC transporter family member was detected in sarcospheres formed during a functional assay of the CSCs [17, 18]. However, the expression of other ABC transporters was described in several osteosarcoma and Ewing's sarcoma cell lines, specifically in side populations (SPs) detected within these cell lines [19, 20]. Our results are in accordance with these findings: although ABCG2 expression was weak and infrequent in the primary tumors, the immunoscore for ABCG2 was markedly increased in all six cell lines derived from Ewing's sarcoma or osteosarcoma. In contrast, the expression of ABCG2 remained weak in all three rhabdomyosarcoma cell lines under in vitro conditions. Other research groups also reported the low expression of ABCG2 in rhabdomyosarcomas [21]; however, increased ABCG2 immunoreactivity was found in the embryonal subtype compared with the alveolar subtype of rhabdomyosarcoma [22].

CD133 is a pentaspan transmembrane glycoprotein with unclear biological functions. The AC133, i.e., glycosylated epitope of CD133 is widely discussed to be a putative "universal" marker of CSCs in various human malignancies [23]. Among our nine tumor samples, six of them showed a high frequency of CD133-positive cells, but CD133 IR was only weak to medium in all samples. Nevertheless, these cells apparently maintain their selection advantage under in vitro conditions because all cell lines contained at least 50 % CD133-positive cells and because the immunoscore values were middle or high. These results are in accordance with previously published findings on rhabdomyosarcomas as well as on rhabdomyosarcoma and osteosarcoma cell lines [12, 13, 24]. Conversely, only low levels (up to 7.8 %) of CD133-positive cells were reported in four cell lines derived from

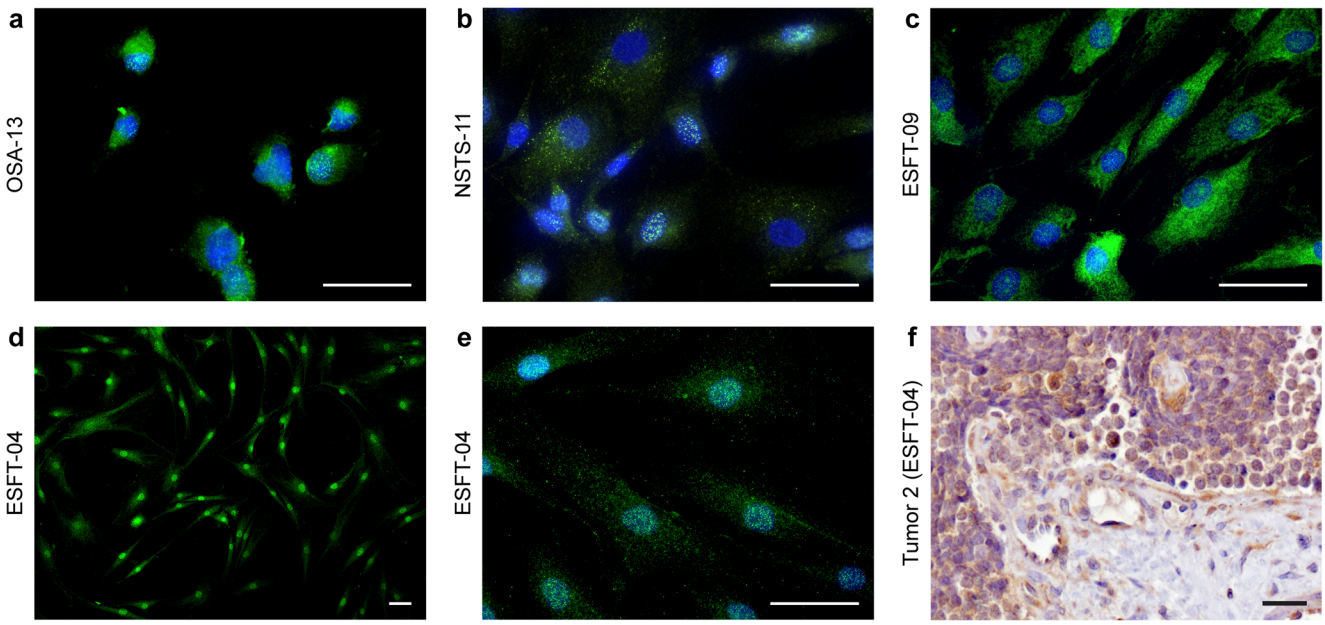

Fig. 3 Alterations in the CD133 subcellular localization in sarcoma cell lines and tumor tissues. (**a**–**e**) IF revealed nuclear localization of CD133 (*green*) in cell lines derived from all three types of sarcoma; nuclei were counterstained with DAPI (*blue*). (**d**–**e**) Nuclear positivity was detected absolutely in the ESFT-04 cell line but sporadically in the corresponding tumor (**f**). *Scale bars*, 50 μm

osteosarcomas and chondrosarcomas and in the corresponding primary tumors [25]. This discrepancy could be explained by either the use of different antibodies for CD133 detection or by variances in the subcellular localization of CD133.

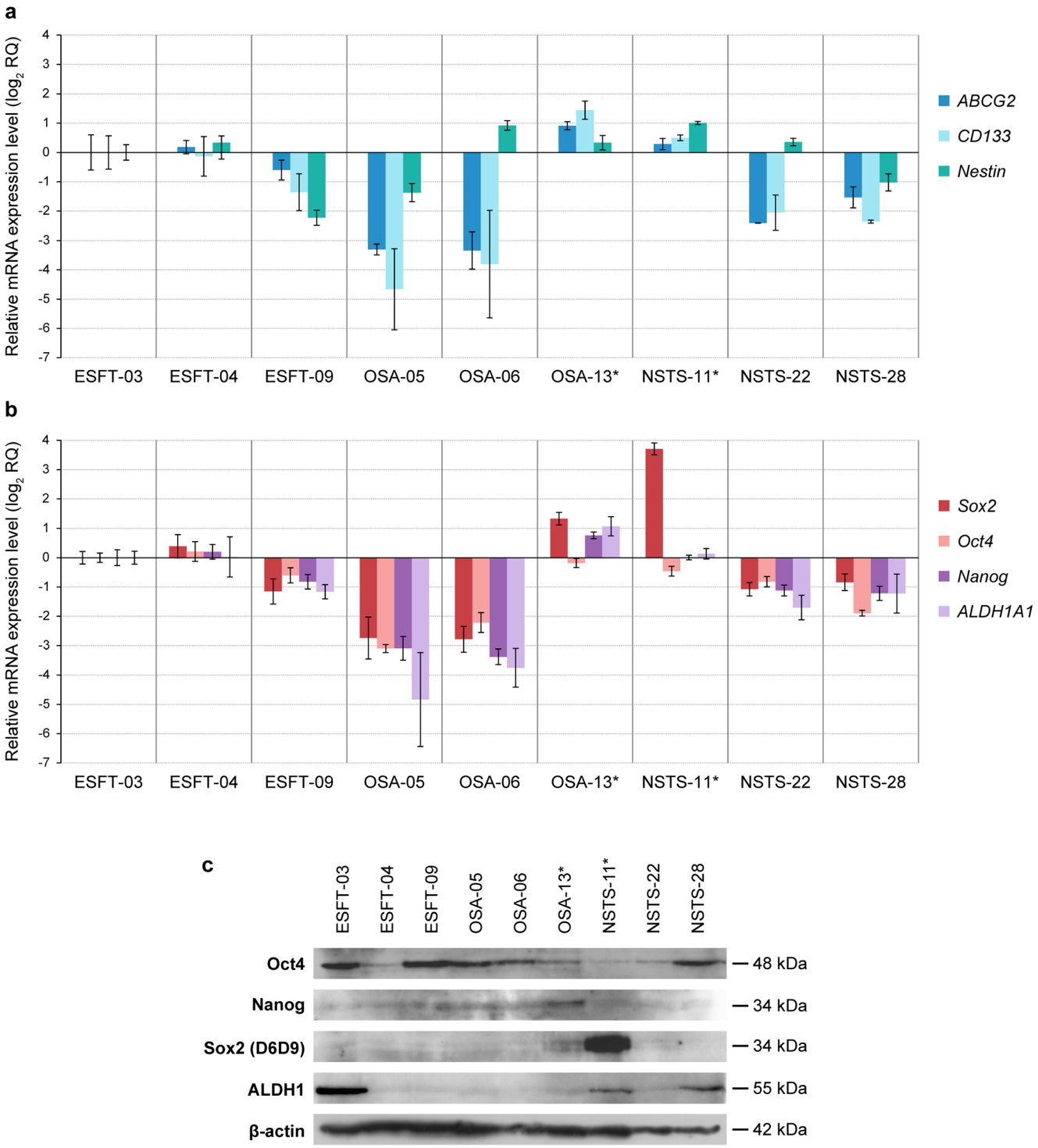

Fig. 4 qRT-PCR and Western blot analysis of CSCs markers expression in sarcoma cell lines. Gene expression levels of sarcoma-specific CSC markers (**a**) and common stem cell markers (**b**) were determined using qRT-PCR. Only tumorigenic cell lines (indicated by *asterisks*) but not non-tumorigenic cell lines expressed Sox2 at mRNA level. The ESFT-03 cell line served as the arbitrary calibrator; the data are presented in log2 scale. The *error bars* indicate the calculated maximum (RQMax) and minimum (RQMin) expression levels that represent the standard error of the mean expression level (RQ value). (**c**) Western blotting of common stem cell markers confirmed upregulation of Sox2 exclusively in tumorigenic cell lines (indicated by *asterisks*). β-actin served as a loading control

Based on other recent studies, CD133 is also clearly detectable in the cytoplasm of tumor cells, where it could be involved in signal transduction, specifically in the canonical Wnt pathway or the PI3K/Akt pathway [26–29]. Very recently, the nuclear localization of CD133 in a stable proportion of cells in rhabdomyosarcoma cell lines was clearly established [11]. For this reason, we considered cells displaying apparent cytoplasmic and/or nuclear positivity for CD133 as CD133-positive; thus, the frequency of these cells must be higher than the reported frequency of CD133-positive cells as detected by flow cytometry. Nevertheless, our results clearly showed that neither cytoplasmic nor nuclear localization of CD133 is clearly associated with the tumorigenic potential of these cells: the tumorigenic NSTS-11 cell line contained only up to 5 % of cells displaying nuclear positivity for CD133, whereas the non-tumorigenic ESFT-04 cell line displayed nuclear positivity for CD133 in nearly all cells.

Nestin, a class VI intermediate filament protein, is widely described as an important marker of CSCs, especially in tumors of neurogenic origin [9, 30]. However, our previous

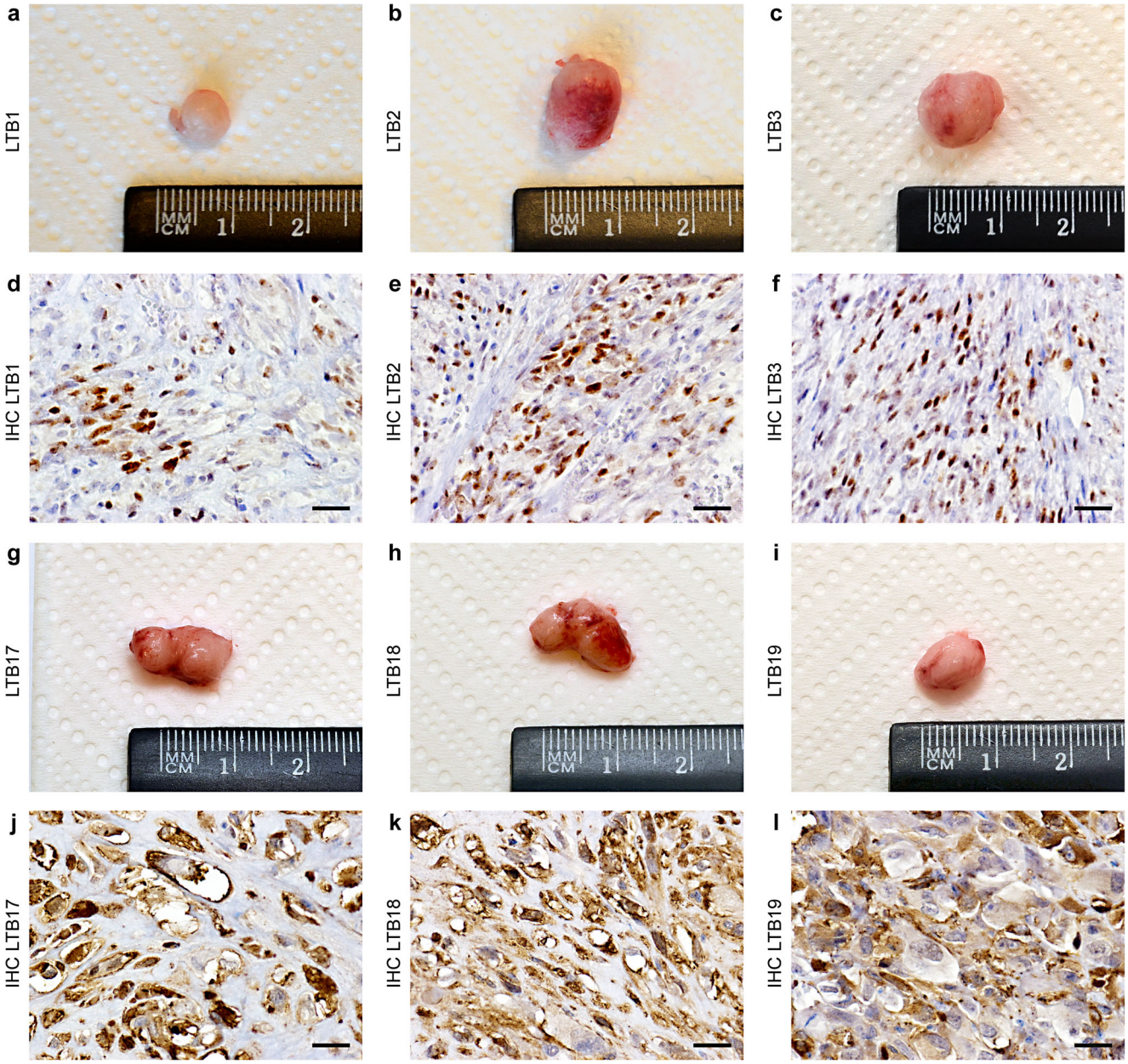

Fig. 5 In vivo tumorigenicity assay and IHC analysis of Sox2 expression in the resulting xenograft tumors. Only NSTS-11 (**a**–**c**) and OSA-13 (**g**–**i**) cells formed xenograft tumors in NOD/SCID gamma mice. (**d**–**f**, **j**–**l**) Markedly enhanced Sox2 expression was detected in xenograft tumors by IHC. *Scale bars*, 50 μm

Table 5 Analysis of Sox2 expression in tumor samples and corresponding cell lines

Tumor sample	IHC − tumor		Primary cell line	IF − cell line	
	% TC	IR TC		% PC	I-sc
Ewing's sarcoma					
1	−	−	ESFT-03	95.00 %	95.00
2	+/−	+	ESFT-04	94.00 %	94.00
3	−	−	ESFT-09	94.00 %	94.00
Osteosarcoma					
4	−	−	OSA-05	71.00 %	71.00
5	−	−	OSA-06	78.00 %	78.00
6	−	−	OSA-13[a]	94.00 %	145.00
Rhabdomyosarcoma					
7	+	+	NSTS-11[a]	76.00 %	146.00
8	−	−	NSTS-22	25.00 %	25.00
9	+/−	+	NSTS-28	10.00 %	10.00

The percentage of tumor cells (% TC) positive for Sox2 was categorized into five levels: − (0 %), +/− (1–5 %), + (6–20 %), ++ (21–50 %), and +++ (51–100 %). The immunoreactivity of tumor cells (IR TC) was graded as − (none), + (weak), ++ (medium), and +++ (strong). For IF analysis, the mean percentage of cell positive for the Sox2 (% PC) is given. Immunoscores (I-sc) were determined by multiplying the percentage of positive cells by the respective immunoreactivity

IHC immunohistochemistry, *IF* immunofluorescence

[a] Primary cell lines proved to be tumorigenic in NOD/SCID gamma mice

studies reported a variable proportion of nestin expression in high-risk osteosarcomas and corresponding cell lines, although high levels of nestin tended to indicate a worse clinical outcome in these patients [12, 31]. In contrast, rhabdomyosarcoma primary tumors showed high levels of nestin expression, but cell lines derived from these tumors contained only up to 10 % of nestin-positive cells [13]. Our recent results showed strong expression of nestin in tumor tissue of both osteosarcomas and rhabdomyosarcomas, but cell lines derived from these tumors were primarily assigned a middle immunoscore. Furthermore, nestin expression appears not to be associated with the tumorigenicity of these cell lines. These findings are in accordance with the previously published studies on bone sarcoma cell lines, in which no clear relationship between nestin expression and sarcosphere-forming capacity was found [17, 25]. The weak or absent expression of nestin in Ewing's sarcomas is also in agreement with other studies of this tumor type, which have reported negativity for nestin or low expression levels of nestin [32, 33]. However, another research group found 54 % positivity for nestin in tumor samples from their cohort [24].

In summary, our results showed that the frequency of putative CSC markers apparently changed after explantation of the tumor tissues and their transfer to cell cultures. Although the frequency of cells positive for ABCG2 and CD133 predominantly increased in the respective cell lines, the high levels of nestin expression were reduced in both osteosarcomas and rhabdomyosarcomas under in vitro conditions. These findings suggest the selection advantage of cells expressing ABCG2 or CD133, but the in vivo functional tests did not confirm the tumorigenic potential of the cells harboring this phenotype.

In contrast, the most important finding of our study was the evident relationship between the expression of the transcription factor Sox2, as demonstrated by qRT-PCR and Western blot analysis, and the tumorigenicity of the OSA-13 and NSTS-11 cell lines. To confirm this interesting result at the protein level, we performed further analysis of Sox2 expression in cell lines via IF. Similarly, the Sox2 levels were highest in the two tumorigenic cell lines, although the immunoscore values did not display the same profile as the qRT-PCR results. Subsequent analysis of Sox2 expression in primary tumors via IHC staining confirmed the presence of Sox2-positive cells in the tumor from which the NSTS-11 cell line was derived. Interestingly, these Sox2-positive cells tended to be accumulated in small areas of the tumor tissue. This finding implies morphological similarity among a stem cell niche. Moreover, IHC analysis of the xenograft tumors showed a substantial increase in the frequency of Sox2-positive cells in all tissue samples.

Our findings are in full accordance with the results reported for human and murine osteosarcoma cell lines [34]. Increased Sox2 levels were also detected in sarcospheres derived from osteosarcoma [35] and rhabdomyosarcoma cell lines [36], although the correlation of Sox2 expression with tumorigenic potential was not reported in these studies. Other recent studies showed that Sox2 expression is required for self-renewal and tumorigenicity of CSCs in other tumor types, including glioblastoma [37, 38], melanoma [39], ovarian carcinoma [40], cervical carcinoma [41], prostatic carcinoma [42], lung carcinoma [43, 44], and squamous-cell carcinoma of the skin [45, 46]. Finally, the involvement of Sox2 in sarcoma tumorigenesis was indirectly illustrated via the targeting of Sox2 by miR-126, which acts as a tumor suppressor in osteosarcomas [47].

All of these findings support our conclusion that cells displaying elevated expression of Sox2 are key mediators of sarcoma tumorigenesis. Although the experimental data on these tumor types remain limited, our results provide the first evidence that increased Sox2 expression is associated with the tumorigenic potential of not only osteosarcomas but also rhabdomyosarcomas. Regardless of the expression of ABCG2, CD133, and nestin, only cell lines displaying increased Sox2 expression were tumorigenic, and the xenograft tumors showed apparent accumulation of Sox2-positive cells.

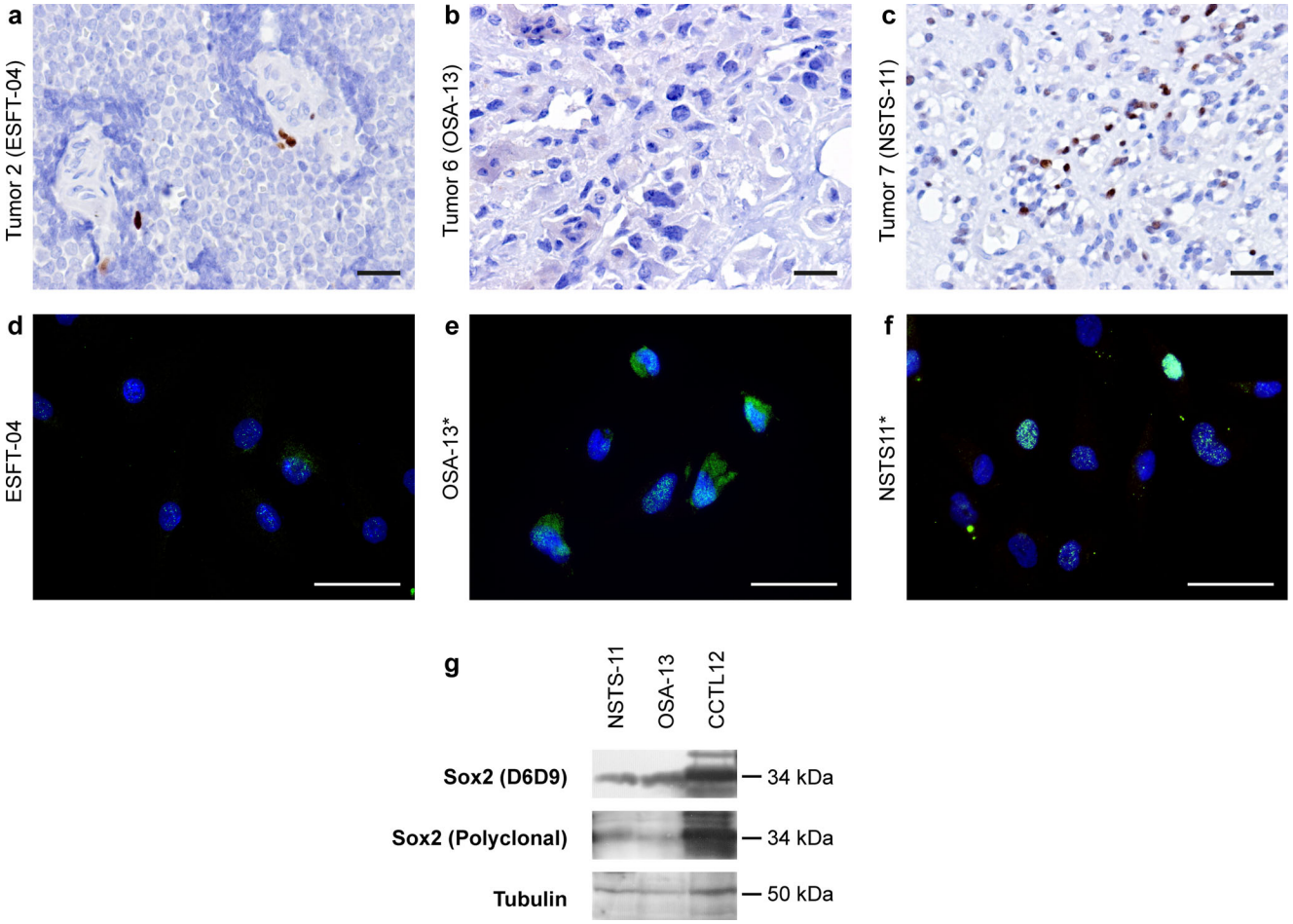

Fig. 6 Expression of Sox2 in sarcomas and derived cell lines. **a**–**c** IHC analysis revealed the presence of Sox2-positive cells in tumor tissues; corresponding cell lines are indicated in brackets. **d**–**f** Elevated Sox2 expression was detected using IF in tumorigenic cell lines (indicated by *asterisk*). **g** Western blotting using two different antibodies confirmed the expression of Sox2 in tumorigenic cell lines as detected by IF. Protein lysate of human embryonic stem cell line CCTL-12 [48] was used as positive control. *Scale bars*, 50 μm

Taken together, sarcoma cells displaying high levels of Sox2 are undoubtedly directly involved in tumor initiation and growth; therefore, these cells fit the definition of the CSC phenotype. Thus, the Sox2 pathway could be considered as a target for new anticancer drugs or immunotherapies based on up-to-date approaches such as chimeric antigen receptors or dendritic cell vaccines.

Acknowledgments The authors thank Johana Maresova, Marcela Vesela, and Dr. Jan Verner for their skillful technical assistance. This study was supported by the project no. NT13443-4 from the Internal Grant Agency of the Czech Ministry of Healthcare, by the project no. LQ1605 from the National Program of Sustainability II, and by the European Regional Development Fund—Project CEB no. CZ.1.07/2.3.00/20.0183.

Compliance with ethical standards The Research Ethics Committee of the School of Science (Masaryk University) approved the study protocol, and a written statement of informed consent was obtained from each participant or his/her legal guardian prior to participation in this study. This study was approved by the Institutional Animal Care and Use Committee of Masaryk University and was registered by the Ministry of Agriculture of the Czech Republic as required by national legislation.

Conflicts of interest None

References

1. Lasky 3rd JL, Choe M, Nakano I. Cancer stem cells in pediatric brain tumors. Curr Stem Cell Res Ther. 2009;4:298–305.
2. Friedman GK, Gillespie GY. Cancer stem cells and pediatric solid tumors. Cancers (Basel). 2011;3:298–318.
3. Manoranjan B, Venugopal C, McFarlane N, Doble BW, Dunn SE, Scheinemann K, et al. Medulloblastoma stem cells: modeling tumor heterogeneity. Cancer Lett. 2013;338:23–31.
4. Soltanian S, Matin MM. Cancer stem cells and cancer therapy. Tumour Biol. 2011;32:425–40.
5. Friedman GK, Cassady KA, Beierle EA, Markert JM, Gillespie GY. Targeting pediatric cancer stem cells with oncolytic virotherapy. Pediatr Res. 2012;71:500–10.

6. Veselska R, Skoda J, Neradil J. Detection of cancer stem cell markers in sarcomas. Klin Onkol. 2012;25:2S16–20.
7. Dela Cruz FS. Cancer stem cells in pediatric sarcomas. Front Oncol. 2013;3:168.
8. Satheesha S, Schafer BW. Cancer stem cells in pediatric sarcomas. In: Hayat MA, editor. Stem cells and cancer stem cells. Dordrecht: Springer; 2014. p. 111–26.
9. Neradil J, Veselska R. Nestin as a marker of cancer stem cells. Cancer Sci. 2015;106:803–11.
10. Huang M, Zhu H, Feng J, Ni S, Huang J. High CD133 expression in the nucleus and cytoplasm predicts poor prognosis in non-small cell lung cancer. Dis Markers. 2015;2015:986095.
11. Nunukova A, Neradil J, Skoda J, Jaros J, Hampl A, Sterba J, et al. Atypical nuclear localization of CD133 plasma membrane glycoprotein in rhabdomyosarcoma cell lines. Int J Mol Med. 2015;36:65–72.
12. Veselska R, Hermanova M, Loja T, Chlapek P, Zambo I, Vesely K, et al. Nestin expression in osteosarcomas and derivation of nestin/CD133 positive osteosarcoma cell lines. BMC Cancer. 2008;8:300.
13. Sana J, Zambo I, Skoda J, Neradil J, Chlapek P, Hermanova M, et al. CD133 expression and identification of CD133/nestin positive cells in rhabdomyosarcomas and rhabdomyosarcoma cell lines. Anal Cell Pathol. 2011;34:303–18.
14. Veselska R, Kuglik P, Cejpek P, Svachova H, Neradil J, Loja T, et al. Nestin expression in the cell lines derived from glioblastoma multiforme. BMC Cancer. 2006;6:32.
15. Mikulenkova E, Neradil J, Zitterbart K, Sterba J, Veselska R. Overexpression of the ΔNp73 isoform is associated with centrosome amplification in brain tumor cell lines. Tumour Biol. 2015;36:7483–91.
16. Livak KJ, Schmittgen TD. Analysis of relative gene expression data using real-time quantitative PCR and the $2^{-\Delta\Delta CT}$ method. Methods. 2001;25:402–8.
17. Saini V, Hose CD, Monks A, Nagashima K, Han B, Newton DL, et al. Identification of CBX3 and ABCA5 as putative biomarkers for tumor stem cells in osteosarcoma. PLoS One. 2012;7, e41401.
18. Martins-Neves SR, Lopes AO, do Carmo A, Paiva AA, Simões PC, Abrunhosa AJ, et al. Therapeutic implications of an enriched cancer stem-like cell population in a human osteosarcoma cell line. BMC Cancer. 2012;12:139.
19. Di Fiore R, Santulli A, Ferrante RD, Giuliano M, De Blasio A, Messina C, et al. Identification and expansion of human osteosarcoma-cancer-stem cells by long-term 3-aminobenzamide treatment. J Cell Physiol. 2009;219:301–13.
20. Yang M, Zhang R, Yan M, Ye Z, Liang W, Luo Z. Detection and characterization of side population in Ewing's sarcoma SK-ES-1 cells in vitro. Biochem Biophys Res Commun. 2010;391:1062–6.
21. Pituch-Noworolska A, Zaremba M, Wieczorek A. Expression of proteins associated with therapy resistance in rhabdomyosarcoma and neuroblastoma tumour cells. Pol J Pathol. 2009;60:168–73.
22. Oda Y, Kohashi K, Yamamoto H, Tamiya S, Kohno K, Kuwano M, et al. Different expression profiles of Y-box-binding protein-1 and multidrug resistance-associated proteins between alveolar and embryonal rhabdomyosarcoma. Cancer Sci. 2008;99:726–32.
23. Grosse-Gehling P, Fargeas CA, Dittfeld C, Garbe Y, Alison MR, Corbeil D, et al. CD133 as a biomarker for putative cancer stem cells in solid tumours: limitations, problems and challenges. J Pathol. 2013;229:355–78.
24. Sadikovic B, Graham C, Ho M, Zielenska M, Somers GR. Immunohistochemical expression and cluster analysis of mesenchymal and neural stem cell-associated proteins in pediatric soft tissue sarcomas. Pediatr Dev Pathol. 2011;14:259–72.
25. Tirino V, Desiderio V, Paino F, De Rosa A, Papaccio F, Fazioli F, et al. Human primary bone sarcomas contain CD133+ cancer stem cells displaying high tumorigenicity in vivo. FASEB J. 2011;25:2022–30.
26. Takenobu H, Shimozato O, Nakamura T, Ochiai H, Yamaguchi Y, Ohira M, et al. CD133 suppresses neuroblastoma cell differentiation via signal pathway modification. Oncogene. 2011;30:97–105.
27. Mak AB, Nixon AM, Kittanakom S, Stewart JM, Chen GI, Curak J, et al. Regulation of CD133 by HDAC6 promotes β-catenin signaling to suppress cancer cell differentiation. Cell Rep. 2012;2:951–63.
28. Wei Y, Jiang Y, Zou F, Liu Y, Wang S, Xu N, et al. Activation of PI3K/Akt pathway by CD133-p85 interaction promotes tumorigenic capacity of glioma stem cells. Proc Natl Acad Sci U S A. 2013;110:6829–34.
29. Shimozato O, Waraya M, Nakashima K, Souda H, Takiguchi N, Yamamoto H, et al. Receptor-type protein tyrosine phosphatase κ directly dephosphorylates CD133 and regulates downstream AKT activation. Oncogene. 2014;34:1949–60.
30. Krupkova Jr O, Loja T, Zambo I, Veselska R. Nestin expression in human tumors and tumor cell lines. Neoplasma. 2010;57:291–8.
31. Zambo I, Hermanova M, Adamkova Krakorova D, Mudry P, Zitterbart K, Kyr M, et al. Nestin expression in high-grade osteosarcomas and its clinical significance. Oncol Rep. 2012;27:1592–8.
32. Olsen SH, Thomas DG, Lucas DR. Cluster analysis of immunohistochemical profiles in synovial sarcoma, malignant peripheral nerve sheath tumor, and Ewing sarcoma. Mod Pathol. 2006;19:659–68.
33. Murphy AJ, Viero S, Ho M, Thorner PS. Diagnostic utility of nestin expression in pediatric tumors in the region of the kidney. Appl Immunohistochem Mol Morphol. 2009;17:517–23.
34. Basu-Roy U, Seo E, Ramanathapuram L, Rapp TB, Perry JA, Orkin SH, et al. Sox2 maintains self renewal of tumor-initiating cells in osteosarcomas. Oncogene. 2012;31:2270–82.
35. Honoki K, Fujii H, Kubo A, Kido A, Mori T, Tanaka Y, et al. Possible involvement of stem-like populations with elevated ALDH1 in sarcomas for chemotherapeutic drug resistance. Oncol Rep. 2010;24:501–5.
36. Walter D, Satheesha S, Albrecht P, Bornhauser BC, D'Alessandro V, Oesch SM, et al. CD133 positive embryonal rhabdomyosarcoma stem-like cell population is enriched in rhabdospheres. PLoS One. 2011;6, e19506.
37. Gangemi RM, Griffero F, Marubbi D, Perera M, Capra MC, Malatesta P, et al. SOX2 silencing in glioblastoma tumor-initiating cells causes stop of proliferation and loss of tumorigenicity. Stem Cells. 2009;27:40–8.
38. Ikushima H, Todo T, Ino Y, Takahashi M, Saito N, Miyazawa K, et al. Glioma-initiating cells retain their tumorigenicity through integration of the Sox axis and Oct4 protein. J Biol Chem. 2011;286:41434–41.
39. Santini R, Pietrobono S, Pandolfi S, Montagnani V, D'Amico M, Penachioni JY, et al. SOX2 regulates self-renewal and tumorigenicity of human melanoma-initiating cells. Oncogene. 2014;33:4697–708.
40. Bareiss PM, Paczulla A, Wang H, Schairer R, Wiehr S, Kohlhofer U, et al. SOX2 expression associates with stem cell state in human ovarian carcinoma. Cancer Res. 2013;73:5544–55.
41. Liu XF, Yang WT, Xu R, Liu JT, Zheng PS. Cervical cancer cells with positive Sox2 expression exhibit the properties of cancer stem cells. PLoS One. 2014;9, e87092.
42. Rybak AP, Tang D. SOX2 plays a critical role in EGFR-mediated self-renewal of human prostate cancer stem-like cells. Cell Signal. 2013;25:2734–42.
43. Nakatsugawa M, Takahashi A, Hirohashi Y, Torigoe T, Inoda S, Murase M, et al. SOX2 is overexpressed in stem-like cells of human lung adenocarcinoma and augments the tumorigenicity. Lab Invest. 2011;91:1796–804.
44. Chou YT, Lee CC, Hsiao SH, Lin SE, Lin SC, Chung CH, et al. The emerging role of SOX2 in cell proliferation and survival and its crosstalk with oncogenic signaling in lung cancer. Stem Cells. 2013;31:2607–19.

45. Boumahdi S, Driessens G, Lapouge G, Rorive S, Nassar D, Le Mercier M, et al. SOX2 controls tumour initiation and cancer stem-cell functions in squamous-cell carcinoma. Nature. 2014;511:246–50.
46. Siegle JM, Basin A, Sastre-Perona A, Yonekubo Y, Brown J, Sennett R, et al. SOX2 is a cancer-specific regulator of tumour initiating potential in cutaneous squamous cell carcinoma. Nat Commun. 2014;5:4511.
47. Yang C, Hou C, Zhang H, Wang D, Ma Y, Zhang Y, et al. miR-126 functions as a tumor suppressor in osteosarcoma by targeting Sox2. Int J Mol Sci. 2013;15:423–37.
48. Adewumi O, Aflatoonian B, Ahrlund-Richter L, Amit M, Andrews PW, Beighton G, et al. Characterization of human embryonic stem cell lines by the International Stem Cell Initiative. Nat Biotechnol. 2007;25:803–16.

Profil aktivace receptorových tyrozinkináz a mitogenem aktivovaných proteinkináz v terapii Maffucciho syndromu

Profile of Activation of Tyrosine Kinases and MAP Kinases in Therapy of Maffucci Syndrome

Melichárková K.[1], Neradil J.[2,3], Múdry P.[1], Zitterbart K.[1,3], Obermannová R.[3,5], Skotáková J.[4], Veselská R.[1,2], Štěrba J.[1,3]

[1] Klinika dětské onkologie LF MU a FN Brno
[2] Laboratoř nádorové biologie, Ústav experimentální biologie, PřF MU, Brno
[3] Regionální centrum aplikované molekulární onkologie, Masarykův onkologický ústav, Brno
[4] Klinika dětské radiologie LF MU a FN Brno
[5] Klinika komplexní onkologické péče, Masarykův onkologický ústav, Brno

Souhrn

Východiska: Maffucciho syndrom je vzácné kongenitální nehereditární onemocnění charakterizované přítomností mnohočetných hemangiomů a enchondromů s tendencí k malignímu zvratu. Kauzální terapie neexistuje a léčba je zaměřena na řešení komplikací. Stanovení vhodného postupu je komplikované a často je nutná multioborová spolupráce v péči o tyto pacienty. ***Případ:*** Autoři prezentují případ 20leté pacientky s Maffucciho syndromem. V průběhu života se u ní objevily mnohočetné enchondromy i progredující hemangiomy, které postupem času působily řadu komplikací jako např. omezení hybnosti, poruchy růstu, bolesti, fluidothorax nebo ascites. Byl vyšetřen profil fosforylace vybraných tyrozinových kináz a MAP kináz z progredujících ložisek hemangiomů, což vedlo ke změně léčebné strategie reflektující výsledky vyšetření. Personalizovaná léčba nasazená na základě profilu fosforylace kináz vedla ke klinicky významné léčebné odpovědi trvající šest měsíců.

Klíčová slova

enchondromatóza – hemangiom – protein-tyrozinkinázy – MAP kinázový signální systém – individualizovaná medicína – Maffucciho syndrom

Summary

Background: Maffucci syndrome is a rare congenital non-hereditary disease characterized by multiple hemangiomas and enchondromas, which may progress into malignancy. The causal therapy does not exist, and therapy is aimed at complications. The determination of appropriate therapy is complicated, and a multidisciplinary approach is often essential. ***Case:*** Authors are presenting the case of a 20-year-old patient with Maffucci syndrome. During her life, multiple enchondromas and progressing hemangiomas have been revealed and they have caused many complications, such as limited movement, growth failure, pain, fluidothorax and ascites. A profile of phosphorylation of selected tyrosine kinases and MAP kinases from progressing hemangioma was performed and with consideration of the result, it led to change of treatment strategy with encouraging clinical response lasting for six months.

Key words

enchondromatosis – hemangioma – receptor protein-tyrosine kinases – MAP kinases signaling system – individualized medicine – Maffucci syndrome

Práce byla podpořena Evropským fondem pro regionální rozvoj a státním rozpočtem České republiky OP VaVpI – RECAMO, CZ.1.05/2.1.00/03.0101, projektem CEB, OPVK CZ.1.07/2.3.00/20.0183 a projektem MUNI/A/1552/2014.

This study was supported by the European Regional Development Fund and the State Budget of the Czech Republic – RECAMO, CZ.1.05./2.1.00/03.0101, by the project CEB, OP VK CZ.1.07/2.3.00/20.0183 and by the project MUNI/A/1552/2014.

Autoři deklarují, že v souvislosti s předmětem studie nemají žádné komerční zájmy.

The authors declare they have no potential conflicts of interest concerning drugs, products, or services used in the study.

Redakční rada potvrzuje, že rukopis práce splnil ICMJE kritéria pro publikace zasílané do biomedicínských časopisů.

The Editorial Board declares that the manuscript met the ICMJE "uniform requirements" for biomedical papers.

MUDr. Kristýna Melichárková
Klinika dětské onkologie
LF MU a FN Brno
Černopolní 9
613 00 Brno
e-mail:
kristyna.melicharkova@fnbrno.cz

Obdrženo/Submitted: 18. 4. 2015
Přijato/Accepted: 26. 6. 2015

http://dx.doi.org/10.14735/amko20152S47

Úvod

Maffucciho syndrom je vzácné kongenitální nehereditární onemocnění, které patří spolu s Ollierovou chorobou mezi enchondromatózy. Toto onemocnění je charakterizováno přítomností četných hemangiomů a enchondromů, které mají tendenci k malignímu zvratu až u 40 % pacientů [1]. Standardní léčebná doporučení, která by ovlivňovala přirozený průběh vzniku a progrese mnohočetných enchondromů a hemangiomů, nejsou k dispozici a doporučuje se jen symptomatická a podpůrná léčba [2,3].

Případ

Dvacetiletá mladá žena byla sledována již od kojeneckého věku pro přítomnost mnohočetných enchondromů na končetinách, genua vara a poruchu kostního růstu s těžkou růstovou retardací. Její stav vyžadoval opakované korekční ortopedické výkony. Ve dvou letech věku se u ní objevil myelodysplastický syndrom, který se následně rozvinul do RAEB (refractory anemia with excess blasts) s nutností terapie dle protokolu pro akutní myeloidní leukemii zahrnující i alogenní transplantaci kostní dřeně.

Ve věku šesti let se u ní začaly objevovat postupně progredující hemangiomy na rukou (obr. 1), proto bylo při podezření na Maffucciho syndrom provedeno celkové přešetření. Výsledky potvrdily přítomnost chondromu/enchondromu pravé sfenoidální kosti o velikosti 3,4 × 2,5 × 1,7 cm. V rámci základní nemoci docházelo k postupné progresi histologicky vřetenobuněčných hemangiomů na pažích a vzniku nových lézí na nohou i v parenchymových orgánech, proto bylo tři roky po transplantaci kostní dřeně doporučeno zahájit léčbu nízce dávkovanou chemoterapií. Byla zvolena terapie vincristin 1,5 mg/m^2/týden + cyklofosfamid 300 mg/m^2/à 3 týdny, avšak vzhledem ke špatné toleranci již vysoce předléčené pacientky bylo nutné tuto léčbu po šesti měsících přerušit.

Stav se postupně dále zhoršoval, objevilo se nové ložisko hemangiomu na játrech 4,8 × 3,8 cm a další ložiska na hrudníku a horních končetinách. Proběhl pokus o ovlivnění těchto ložisek kortikoterapií, a to metylprednisolonem 30 mg/kg/den D1, D3 a D5, 20 mg/kg/den D6 a v dávce 10 mg/kg/den D7 a dále navázáno prednizonem 4 mg/kg/den po 2 týdny [4]. Výsledkem této terapie byla v nejlepším případě smíšená odpověď. V průběhu léčby proběhly pokusy o ovlivnění ložisek zářením, laserem i chirurgickými korekcemi.

Od 18 let se pacientka potýkala s opakovaným chylózním fluidothoraxem a přítomností chylózní ascitické tekutiny v důsledku aktivity hemangiomů. Tento stav vyžadoval opakované punkce

Obr. 1. Fotografie levé ruky (zdroj: archiv KDO) a RTG snímek levé ruky (zdroj: archiv KDR).

ascitu, v průměru 2 l ascitické tekutiny každé dva týdny. Byl nasazen bevacizumab 10 mg/kg/à 2 týdny, po osmi měsících terapie bylo dosaženo pouze stacionárního stavu s pokračující potřebou punkcí ascitu i fluidothoraxu. V této době byla změněna léčba na sirolimus 1 mg/den a paclitaxel 12,5 mg/m^2/ /à 1 týden [5]. Tato terapie byla podávána šest měsíců s nutností redukce paclitaxelu na 50 % dávky pro hematologickou toxicitu. Výsledek byl pouze stacionární stav.

Nově byl vyšetřen profil fosforylace receptorových tyrozinkináz (RTK) a MAP kináz (mitogen-activated protein kinases) z ložiska na patě a dle těchto výsledků byla terapie upravena na sunitinib 12,5 mg/den a taxol 5,5 mg/týden. Mimo těchto léků měla dívka v dlouhodobé medikaci také β-blokátory z kardiologické indikace, u nichž některé práce poukazují na jejich antineoplastický potenciál [6]. Po nasazení této personalizované terapie došlo postupně k prodlužování intervalů pro evakuace ascitu či chylothoraxu, s periodou čtyř měsíců bez potřeby evakuace, což mělo významný dopad na kvalitu života pacientky. Po čtyřech měsících od poslední evakuace ascitu se i přes nasazenou léčbu obnovila potřeba evakuace chylothoraxu s potřebou opakovaných chirurgických intervencí a tedy i s přerušováním, až vysazením antineoplastické medikace na dobu téměř tří měsíců. V průběhu významně redukované či vysazené antineoplastické léčby progredovala potřeba chirurgické derivace chylu charakteru jahodového mléka. Pacientka zemřela náhlou smrtí na akutní krvácení do dutiny břišní v důsledku spontánní ruptury jaterního hemangioendotheliomu tři měsíce po deeskalaci antineoplastické terapie, devět měsíců po zahájení personalizované terapie.

Metodika a výsledky

Pro detekci fosforylace RTK byl použit Human Phospho-RTK Array Kit (R&D Systems) umožňující současné stanovení fosforylace 49 kináz z 16 receptorových rodin, přičemž u člověka bylo zatím popsáno 58 RTK rozdělených do 20 rodin v závislosti na podobnosti proteinové struktury receptorů [7]. Princip metody detekce spočívá v nanesení proteinového lyzátu na nitrocelulózovou membránu, na níž jsou ve dvojicích bodů imobilizovány specifické protilátky proti dané kináze. Fosforylované i nefosforylované formy proteinu se na protilátku naváží v ekvimolárním poměru a v následujícím kroku jsou pouze fosforylované formy proteinu označeny protilátkou proti fosforylovanému tyrozinu konjugovanou s peroxidázou. Po aplikaci chemiluminiscenčního substrátu na membránu lze luminiscenci detekovat na filmu nebo pomocí chemiluminiscenčního skeneru.

Fosforylační status MAP kináz a vybraných serin/treoninových kináz a dalších signálních molekul byl analyzován pomocí Human Phospho-MAPK Array Kit (R&D Systems) umožňující současné stanovení fosforylace 26 kináz včetně zástupců tří hlavních rodin (ERK, JNK a p38). Princip metody je podobný jako v předchozím v případě, s tou výjimkou, že pro odlišení fosforylovaných a nefosforylovaných forem kináz je použito specifických protilátek přímo proti fosforylovaným formám kináz konjugovaných s biotinem. Na biotin se následně naváže streptavidin konjugovaný s peroxidázou, jež aktivuje chemiluminiscenční substrát.

Zmražený vzorek tkáně byl rozdělen na dvě části a lyzáty pro obě analýzy byly připraveny dle pokynů výrobce, následně bylo použito 300 µg celkového proteinu pro každou z analýz. Míra fosforylace jednotlivých proteinů byla denzitometricky kvantifikována softwarem ImageJ, z duplikátů byl vypočítán průměr a od něj odečtena hodnota pozadí. Data byla normalizována vztažením k maximální hodnotě dosažené na každé z použitých membrán.

Fosforylace RTK byla výrazná především u receptoru pro epidermální růstový faktor (EGFR), inzulinového receptoru (InsR) a obou variant receptoru pro růstový faktor krevních destiček (platelet derived growth factor – PDGFRα a PRGFRβ) (graf 1A, C).

V rámci analýzy fosforylace MAP kináz byla zaznamenána vysoká míra fosforylace ERK1 a ERK2 a částečně i kinázy p38γ. Dále byla aktivována kináza Akt-2, jež patří do rodiny nejvýznamnějších signálních molekul serin/treoninových kináz Akt. Jedním z nejvíce fosforylovaných proteinů, jenž může být fosforylačním cílem v případě aktivace kináz rodiny p38 [8], byl HSP27 (graf 1B, D).

Diskuze

Maffucciho syndrom patří mezi velmi vzácná onemocnění a manifestuje se v 78 % před začátkem puberty [9]. Je charakterizován přítomností enchondromů, mnohočetných hemangiomů a vzácně také lymfangiomů. Standardní terapie neexistuje a výběr vhodné strategie může být velmi svízelný. Enchondromy vznikají nejčastěji v oblasti dlouhých kostí dolních končetin, nohy a ruky [9]. V případě, že omezují funkčnost končetiny, ovlivňují normální růst nebo působí bolest, je přistoupeno k chirurgickému řešení. Hemangiomy jsou benigní cévní tumory, které mohou vznikat prakticky kdekoliv v těle, v rámci tohoto onemocnění mohou postupně progredovat a výrazně omezovat kvalitu života postiženého jedince. V literatuře jsou popsány případy, u nichž bylo úspěšně využito antiangiogenní terapie k ovlivnění hemangiomů u těchto pacientů [5].

V případě této pacientky bylo těžké vybrat vhodnou léčebnou strategii, mimo jiné především z důvodu komorbidit a rozsahu jejího onemocnění. Bylo vyzkoušeno několik, dříve v literatuře popsaných, léčebných modalit, avšak výsledky léčby byly dosti nepřesvědčivé. V rámci snahy nalézt vhodný terapeutický cíl na úrovni proteinů, který by odrážel skutečnou aktivitu v patologických buňkách, byl vyšetřen profil fosforylace RTK a navazujících signálních drah. Tato diagnostická metoda se jeví jako slibný prostředek, který by mohl umožnit podávání cílené biologické léčby pacientům s prokázanou aktivací signální dráhy na úrovni proteinů. Tento postup by v konečném důsledku mohl zlepšit výsledky léčby, snížit množství komplikací a celkově snížit náklady na léčbu vlastního onemocnění, které mohou být při empirickém podávání takovýchto léků dosti vysoké.

Na základě výsledků naší analýzy byl do léčebného schématu přidán sunitinib v kombinaci s paclitaxelem. Sunitinib je multikinázový inhibitor, který cílí pře-

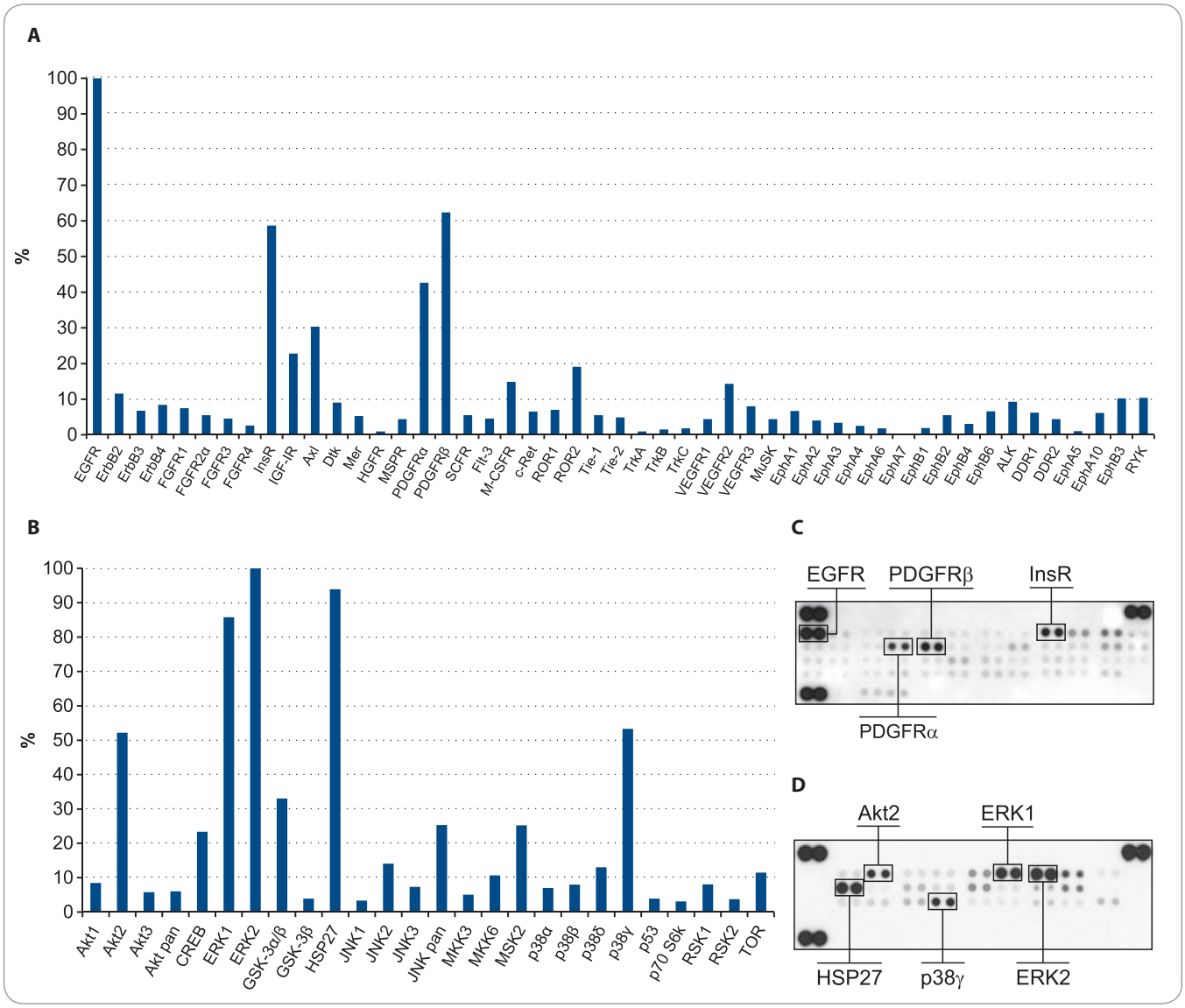

Graf 1. Profil fosforylace receptorových tyrozinkináz (RTK), MAP kináz a vybraných cytoplazmatických proteinů ve vzorku hemangiomu odebraného pacientce s Maffucciho syndromem.

A. Denzitometrická analýza fosforylace RTK. B. Denzitometrická analýza fosforylace MAPK a vybraných cytoplazmatických proteinů. C. Proteinová array s označenými RTK, jež vykazují nejvyšší hodnotu denzity. D. Proteinová array s označenými MAPK a vybranými cytoplazmatickými proteiny, jež vykazují nejvyšší hodnotu denzity.

devším proti receptoru pro růstový faktor krevních destiček (PDGFR) a proti receptoru pro cévní endoteliální růstový faktor (vascular endothelial growth factor – VEGFR), čímž ovlivňuje angiogenezi a buněčnou proliferaci. FDA (Food and Drug Administration – Úřad pro kontrolu léčiv) jej oficiálně schválila k léčbě GIST, renálního karcinomu a neuroendokrinních tumorů pankreatu, avšak pro silný antiangiogenní potenciál byl výhodný i pro naše účely. Paclitaxel je alkaloid, který blokuje depolymerizaci mikrotubulů dělícího vřeténka a je používán pro léčbu řady malignit. Při metronomickém dávkování a v kombinaci s dalšími léky prokázal významný antiangiogenní potenciál [10]. Prezentovaná kazuistika dokumentuje obtížnost péče o pacienty s Maffucciho syndromem, kdy interpretace klinického průběhu posledních týdnů a vysvětlení úmrtí pacientky zůstává spekulativní.

Závěr

Terapie vzácných onemocnění je nesnadná. Neexistují ověřené postupy a většina poznatků o takových stavech je známa pouze z kazuistik. Velké randomizované klinické studie fáze III zde nikdy nebudou k dispozici, přestože je systém registrací a úhrad zdravotních pojišťoven vyžaduje i v těchto případech. Vyšetření signálních drah aktivovaných RTK by mohlo do budoucna přispět k sestavování individualizované léčby tam, kde standardní léčba není známa anebo není dostatečně účinná, jako jsou vzácná, refrakterní nebo některá pokročilá nádorová onemocnění dětského

věku. Vytváření a následná realizace personalizovaných léčebných postupů vyžadují komplexní, multioborovou spolupráci a pečlivé vyvažovaní rizik a event. přínosů takových postupů.

Literatura

1. Verdegaal SH, Bovee JV, Pansuriya TC et al. Incidence, predictive factors, and prognosis of chondrosarcoma in patients with Ollier disease and Maffucci syndrome: an international multicenter study of 161 patients. Oncologist 2011; 16(12): 1771–1779. doi: 10.1634/theoncologist.2011-0200.

2. Lissa F, Argente J, Antunes G et al. Maffucci syndrome and soft tissue sarcoma: a case report. Int Semin Surg Oncol 2009; 6(1): 2. doi: 10.1186/1477-7800-6-2.

3. Lin PP, Moussallem CD, Deavers MT. Secondary chondrosarcoma. J Am Acad Orthop Surg 2010; 18(10): 608–615.

4. Park EA, Seo JW, Lee SW et al. Infantile hemangioendothelioma treated with high dose methylprednisolone pulse therapy. J Korean Med Sci 2001; 16(1): 127–129.

5. Riou S, Morelon E, Guibaud L et al. Efficacy of rapamycin for refractory hemangioendotheliomas in Maffucci's syndrome. J Clin Oncol 2012; 30(23): e213–e215. doi: 10.1200/JCO.2012.41.7287.

6. Pasquier E, Street J, Pouchy C et al. β-blockers increase response to chemotherapy via direct antitumour and anti-angiogenic mechanisms in neuroblastoma. Br J Cancer 2013; 108(12): 2485–2494. doi: 10.1038/bjc.2013.205.

7. Lewis RJ, Ketcham AS. Maffucci's syndrome: functional and neoplastic significance. Case report and review of the literature. J Bone Joint Surg Am 1973; 55(7): 1465–1479.

8. Lemmon MA, Schlessinger J. Cell signaling by receptor tyrosine kinases. Cell 2010; 141(7): 1117–1134.

9. Dorion S, Landry J. Activation of the mitogen-activated protein kinase pathways by heat shock. Cell Stress Chaperones 2002; 7(2): 200–206.

10. Pasquier E, Tuset MP, Street J et al. Concentration- and schedule-dependent effects of chemotherapy on the angiogenic potential and drug sensitivity of vascular endothelial cells. Angiogenesis 2013; 16(2): 373–386. doi: 10.1007/s10456-012-9321-x.

Atypical nuclear localization of CD133 plasma membrane glycoprotein in rhabdomyosarcoma cell lines

ALENA NUNUKOVA[1], JAKUB NERADIL[1,2], JAN SKODA[1,3], JOSEF JAROS[4], ALES HAMPL[4], JAROSLAV STERBA[2,3] and RENATA VESELSKA[1,3]

[1]Department of Experimental Biology, Faculty of Science, Masaryk University; [2]Regional Centre for Applied Molecular Oncology, Masaryk Memorial Cancer Institute; [3]Department of Pediatric Oncology, University Hospital Brno; [4]Department of Histology and Embryology, Faculty of Medicine, Masaryk University, 61137 Brno, Czech Republic

Received February 5, 2015; Accepted April 27, 2015

DOI: 10.3892/ijmm.2015.2210

Abstract. CD133 (also known as prominin-1) is a cell surface glycoprotein that is widely used for the identification of stem cells. Furthermore, its glycosylated epitope, AC133, has recently been discussed as a marker of cancer stem cells in various human malignancies. During our recent experiments on rhabdomyosarcomas (RMS), we unexpectedly identified an atypical nuclear localization of CD133 in a relatively stable subset of cells in five RMS cell lines established in our laboratory. To the best of our knowledge, this atypical localization of CD133 has not yet been proven or analyzed in detail in cancer cells. In the present study, we verified the nuclear localization of CD133 in RMS cells using three independent anti-CD133 antibodies, including both rabbit polyclonal and mouse monoclonal antibodies. Indirect immunofluorescence and confocal microscopy followed by software cross-section analysis, transmission electron microscopy and cell fractionation with immunoblotting were also employed, and all the results undeniably confirmed the presence of CD133 in the nuclei of stable minor subpopulations of all five RMS cell lines. The proportion of cells showing an exclusive nuclear localization of CD133 ranged from 3.4 to 7.5%, with only minor differences observed among the individual anti-CD133 antibodies. Although the role of CD133 in the cell nucleus remains unclear, these results clearly indicate that this atypical nuclear localization of CD133 in a minor subpopulation of cancer cells is a common phenomenon in RMS cell lines.

Correspondence to: Professor Renata Veselska, Department of Experimental Biology, Faculty of Science, Masaryk University, Kotlarska 2, 61137 Brno, Czech Republic
E-mail: veselska@sci.muni.cz

Abbreviations: BSA, bovine serum albumin; CSCs, cancer stem cells; DMEM, Dulbecco's modified Eagle's medium; FISH, fluorescence *in situ* hybridization; HRP, horseradish peroxidase; NSCLC, non-small cell lung cancer; PBS, phosphate-buffered saline; PVDF, polyvinylidene difluoride; RMS, rhabdomyosarcoma; SDS, sodium dodecyl sulfate; TBS, Tris-buffered saline; TEM, transmission electron microscopy

Key words: CD133, prominin-1, rhabdomyosarcoma, cell nuclei, immunodetection

Introduction

CD133 (also known as prominin-1) is a glycoprotein that is typically localized to the plasma membrane. The molecule consists of five transmembrane domains, two large extracellular loops, an extracellular N-terminus and an intracellular C-terminus. Eight potential glycosylation sites have been identified within the extracellular domains, with four per loop. Human CD133 is encoded by the *PROM1* gene, which is located in chromosomal region 4p15.32. At least seven CD133 isoforms resulting from alternative splicing have been described in humans (1,2).

CD133 is widely used to identify stem cells, and its glycosylated epitope, AC133, has recently been discussed as a marker of cancer stem cells (CSCs) in various human malignancies (2-4). In our previous studies, we identified CD133-positive cells that presented typical membrane positivity in two of the most common types of pediatric sarcomas, osteosarcoma (5) and rhabdomyosarcoma (RMS) (6). The expression of CD133 in these two solid tumors, as well as the tumorigenicity of CD133-positive cells, has been confirmed by other research groups (7-10). Therefore, CD133 is currently accepted as one of the markers of a CSC phenotype in pediatric sarcomas, including RMS (11-13).

During our recent study aimed at the analysis of CSC markers in pediatric sarcomas, we noted a surprising result: a stable subset of cells in each of five RMS cell lines examined exhibited an exclusive nuclear localization of CD133 (these data are published in this article). To date, a similar localization of this antigen has been described only in one case report of breast cancer (14) and in a large study on lung cancer (15) using immunohistochemical methods, nevertheless, without any verification or systematic description. For this reason, in this study, we sought to analyze this interesting phenomenon in detail using three independent anti-CD133 commercial antibodies (Fig. 1).

Materials and methods

Cell culture. Five cell lines derived from pediatric patients with RMS were included in this study: NSTS-8, NSTS-9, NSTS-11, NSTS-22 and NSTS-28. The first three cell lines were described in our previous study (6), and the last two were derived using the same procedure to generate primary cultures (16). All cell lines were authenticated by the immunodetection of MyoD, and the subtype was distinguished using *FKHR* break detection by fluorescence *in situ* hybridization (FISH). Authentication using MyoD detection was performed in the same passages as the experiments; FISH analysis of the *FKHR* break was completed up to passage 10. The cell lines were maintained in Dulbecco's modified Eagle's medium (DMEM) supplemented with 20% fetal calf serum, 2 mM glutamine, 100 IU/ml penicillin and 100 μg/ml streptomycin (all purchased from GE Healthcare Europe GmbH, Freiburg, Germany). The cells were maintained under standard conditions at 37˚C in a humified atmosphere containing 5% CO_2 and were subcultured once or twice per week. The Research Ethics Committee of the School of Science (Masaryk University, Brno, Czech Republic) approved the study protocol, and a written statement of informed consent was obtained from each participant or his/her legal guardian prior to participation in this study. A brief description of the cohort of patients included in this study is provided in Table I.

Indirect immunofluorescence. The cells were cultivated on coverslips in Petri dishes for one day and then rinsed with phosphate-buffered saline (PBS) and fixed with 3% paraformaldehyde (Sigma-Aldrich, St. Louis, MO, USA) at room temperature for 20 min. After washing again with PBS, non-specific binding was blocked with 3% bovine serum albumin (BSA; Sigma-Aldrich) in PBS for 10 min. The cells were then incubated with primary antibody at 37˚C for 60 min, washed three times in PBS and then incubated with the corresponding secondary antibody at 37˚C for 45 min. Rabbit polyclonal anti-CD133 (Cat. no. ab19898, dilution 1:70; Abcam, Cambridge, UK), mouse monoclonal anti-CD133 (clone 17A6.1, Cat. no. MAB4399, dilution 1:100; Millipore, Billerica, MA, USA), mouse monoclonal anti-AC133 (clone AC133, Cat. no. 130-090-422, dilution 1:4; Miltenyi Biotec, Bergisch Gladbach, Germany), and mouse monoclonal anti-α-tubulin antibody (clone: TU-01, Cat. no. 11-250, dilution 1:100; Exbio, Vestec, Czech Republic), which served as a control, were used as the primary antibodies. Anti-rabbit Alexa Fluor 488 (Cat. no. A11008, dilution 1:200) and anti-mouse Alexa Fluor 488 antibody (Cat. no. A11001, dilution 1:200) (both from Invitrogen, Paisley, UK) were used as the secondary antibodies. After a final wash with PBS, the cell nuclei were counterstained with 0.05% Hoechst 33342 (Life Technologies, Carlsbad, CA, USA) for 10 min, and the coverslips were mounted using Dako fluorescence mounting medium (Dako, Glostrup, Denmark). An Olympus BX-51 microscope was used for sample evaluation; micrographs were captured using an Olympus DP72 CCD camera and analyzed using the Cell P imaging system (Olympus, Tokyo, Japan). At least 200 cells were evaluated overall within discrete areas of each sample, and the samples were prepared from at least three independent passages of all examined cell lines. The mean percentages of cells showing exclusive nuclear CD133 localization were determined for entire samples of individual cell lines. For the detailed examination of CD133 nuclear localization, the same protocol for indirect immunofluorescence was employed, and the specimens were then examined using an Olympus FluoView-500 confocal imaging system combined with an inverted Olympus IX-81 microscope. The images were recorded using an Olympus DP70 CCD camera and analyzed using analySIS FIVE software (Soft Imaging System GmbH, Muenster, Germany) and an Olympus FluoView Confocal Laser Scanning Microscope System 4.3.

Transmission electron microscopy (TEM). To perform the immunodetection of CD133 in ultrathin sections, the cells grown on coverslips were rinsed with PBS and fixed in 3% paraformaldehyde (Sigma-Aldrich) and 0.1% glutaraldehyde (AppliChem GmbH, Darmstadt, Germany) in PBS at room temperature for 60 min. Following a PBS rinse and dehydration, the cells were embedded in LR White medium (Polysciences Inc., London, UK). The labeling of the ultrathin sections was performed on grids. CD133 was detected using mouse monoclonal anti-CD133 antibody (dilution 1:25; Millipore) and a gold particle-conjugated secondary antibody (anti-mouse IgG 20 nm gold, Cat. no. ab27242, dilution 1:40; Abcam). Ultrathin sections incubated without primary antibody or with the TU-01 primary monoclonal antibody against α-tubulin (dilution 1:200; Exbio) were used as controls. Following immunodetection, the specimens were contrasted with 2.5% uranyl acetate (PLIVA-Lachema, Brno, Czech Republic) for 10 min and with Reynolds solution (Sigma-Aldrich) for 6 min at room temperature. The specimens were then observed under a Morgagni 268(D) transmission electron microscope (FEI Co., Hillsboro, OR, USA). The images were captured using an Olympus Veleta TEM CCD camera and analyzed using iTEM Olympus Soft Imaging Solution (Olympus).

Immunoblot analysis. To analyze the nuclear and cytoplasmic fractions, a Nuclear Protein Extraction kit (Thermo Fisher Scientific, Rockford, IL, USA) was used according to the manufacturer's instructions. A 20 μl sample of protein extract was loaded onto an 8% sodium dodecyl sulfate (SDS)-polyacrylamide gel and separated by electrophoresis. Subsequently, the proteins were transferred onto polyvinylidene difluoride (PVDF) membranes (Bio-Rad Laboratories, Hercules, CA, USA), blocked in 5% non-fat milk at room temperature for 60 min, and incubated with primary antibodies, rabbit polyclonal anti-CD133 (Abcam), mouse monoclonal anti-α-tubulin (Exbio), or rabbit monoclonal anti-lamin B2 antibody (clone: D8P3U, Cat. no. 12255S; Cell Signaling Technology, Danvers, MA, USA) at a 1:1,000 dilution overnight at 4˚C. Anti-α-tubulin and anti-lamin B2 served as the controls for the purity of the cytoplasmic and nuclear cell fractions, respectively. After washing with Tris-buffered saline (TBS)-Tween-20, the membranes were incubated with the corresponding horseradish peroxidase (HRP)-conjugated secondary antibodies anti-mouse IgG-HRP (cat. no. A9917, dilution 1:5,000; Sigma-Aldrich) and anti-rabbit IgG-HRP antibodies (cat. no. 7074, dilution 1:5,000; Cell Signaling Technology) at room temperature for 60 min. Signal detection was performed using ECL Prime Western Blotting Detection

Table I. Description of patients from whom tumor samples were obtained to establish the rhabdomyosarcoma cell lines and the results concerning the mean percentage of cells with an exclusive nuclear localization of CD133.

					Mean percentage of cells with exclusive nuclear localization of CD133		
Cell line	Gender	Age (years)	RMS type	No. of passages analyzed	Anti-CD133 antibody (rabbit polyclonal)	Anti-CD133 antibody (mouse monoclonal)	Anti-AC133 antibody (mouse monoclonal)
NSTS-8	F	21	A	15-18	4.6	6.1	3.4
NSTS-9	M	17	A	13-18	4.6	5.2	4.1
NSTS-11	F	16	E	11-19	3.8	4.6	6.6
NSTS-22	F	5	A	11-15	4.0	6.0	6.4
NSTS-28	M	8	A	12-16	4.1	5.2	7.5

M, male; F, female; RMS, rhabdomyosarcoma. Tumor type: A, alveolar; E, embryonal.

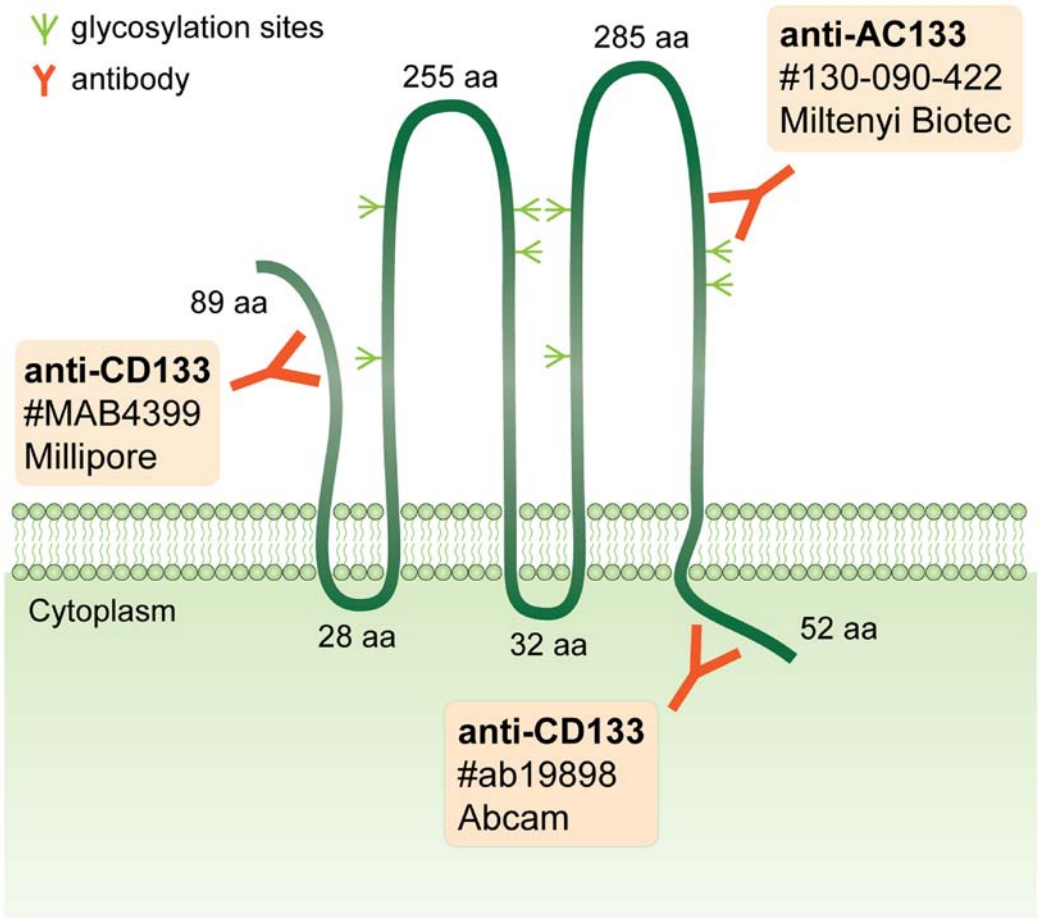

Figure 1. Overview of epitopes of the anti-CD133 and anti-AC133 antibodies used in this study. For each antibody, the catalogue number and manufacturer are indicated. Potential glycosylation sites, as well as length of the N-terminal region, the intracellular and extracellular loops and the C-terminal region of CD133 are depicted.

Reagent (GE Healthcare) according to the manufacturer's instructions.

Results

For all five RMS cell lines examined in this study, we performed a detailed analysis of the presence of cells with nuclear CD133 positivity using indirect immunofluorescence with three independent anti-CD133 antibodies (Fig. 1). A subset of cells showed only nuclear CD133 positivity, i.e., no detectable membrane or cytoplasmic positive signal. The results were markedly similar in all five cell lines analyzed, regardless of the primary antibody utilized, and the proportion ranged from 3.4 to 7.5%, with only minor differences observed among the

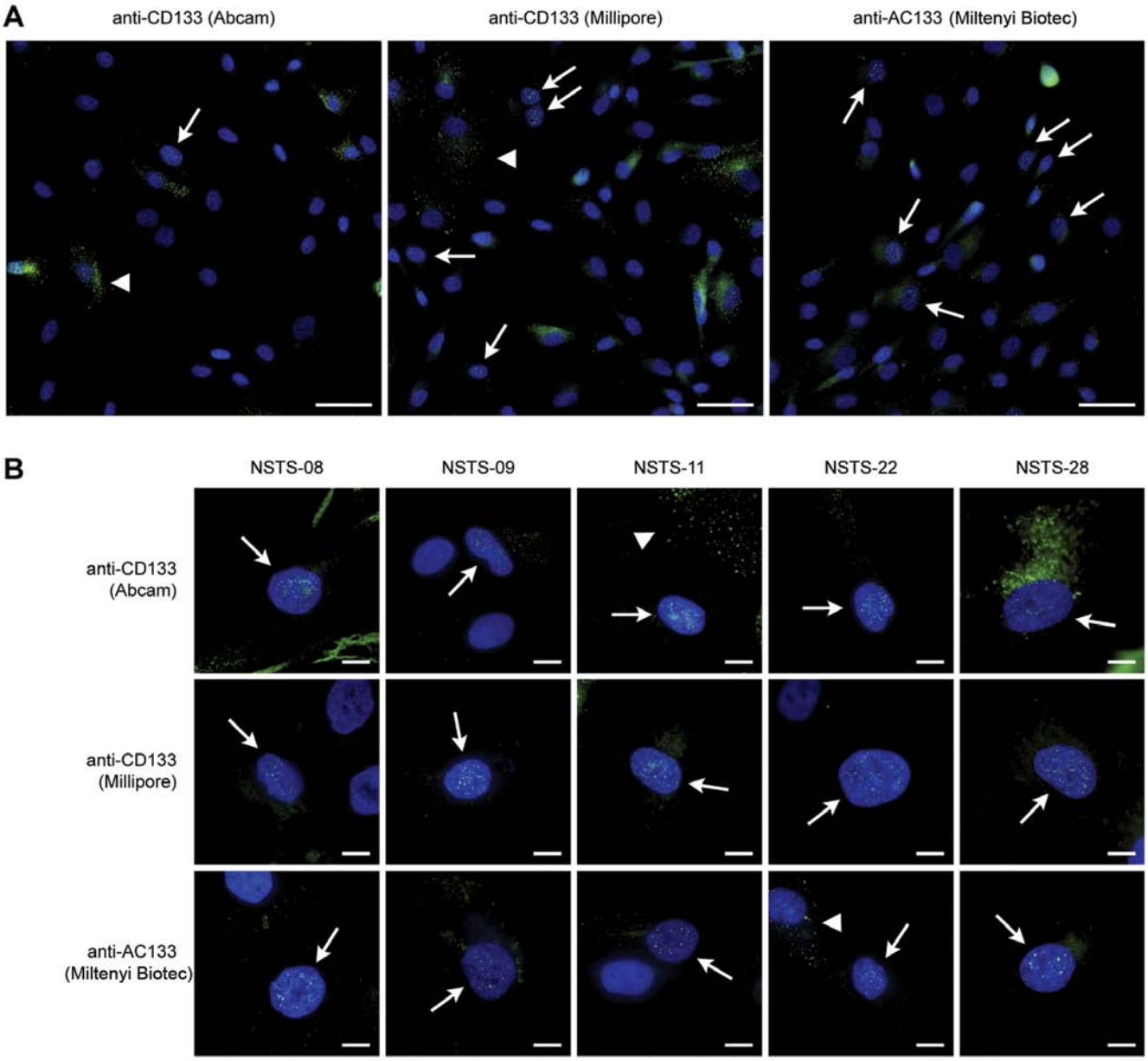

Figure 2. Nuclear localization of CD133 in rhabdomyosarcoma cells. (A) Example of the frequency of cells with CD133 nuclear positivity in the NSTS-11 cell line, as detected using three independent primary antibodies. Cells with exclusive nuclear positivity for CD133 are indicated by arrows; cells with the typical membrane positivity are indicated by arrowheads. (B) Details of cells that exhibited exclusive nuclear positivity for CD133 in all five rhabdomyosarcoma cell lines. CD133 was stained by indirect immunofluorescence using Alexa Fluor 488-labeled secondary antibodies (green), and the nuclei were counterstained with Hoechst 33342 (blue). Scale bars, (A) 50 μm and (B) 10 μm.

individual anti-CD133 antibodies (Fig. 2A and Table I). We also performed a detailed morphological analysis of the cells that exhibited exclusive nuclear positivity for CD133 (Fig. 2B); as can be seen on these micrographs, the pattern of CD133 nuclear positivity was markedly similar in all of the cell lines.

To confirm the presence of CD133 in the nuclei of the RMS cells visualized using indirect immunofluorescence, we employed confocal microscopy and software cross-section analysis through these CD133-positive nuclei (Fig. 3). As is apparent from the results, the localization of the fluorescence signal for CD133 was detected within the cell nuclei both on the software cross-sections (Fig. 3B) and on the plot diagrams of the fluorescence intensity (Fig. 3D).

Furthermore, we also used immunogold labeling with TEM to verify the localization of CD133 in the nuclei of the RMS cells. To avoid any artifacts associated with this methodological approach, the accumulation of three or more gold particles together was considered to indicate a positive signal. The results clearly indicated the presence of CD133 in both the nuclei and nucleoli (Fig. 4A and B).

These results are all completely consistent with the microscopic observations described above (Fig. 2): the software cross-sections also showed clear, punctuate signals for CD133 within the nucleus (Fig. 3B and D), i.e., no diffuse positivity throughout the entire nucleus was observed. Nevertheless, the TEM micrographs also showed the presence of CD133

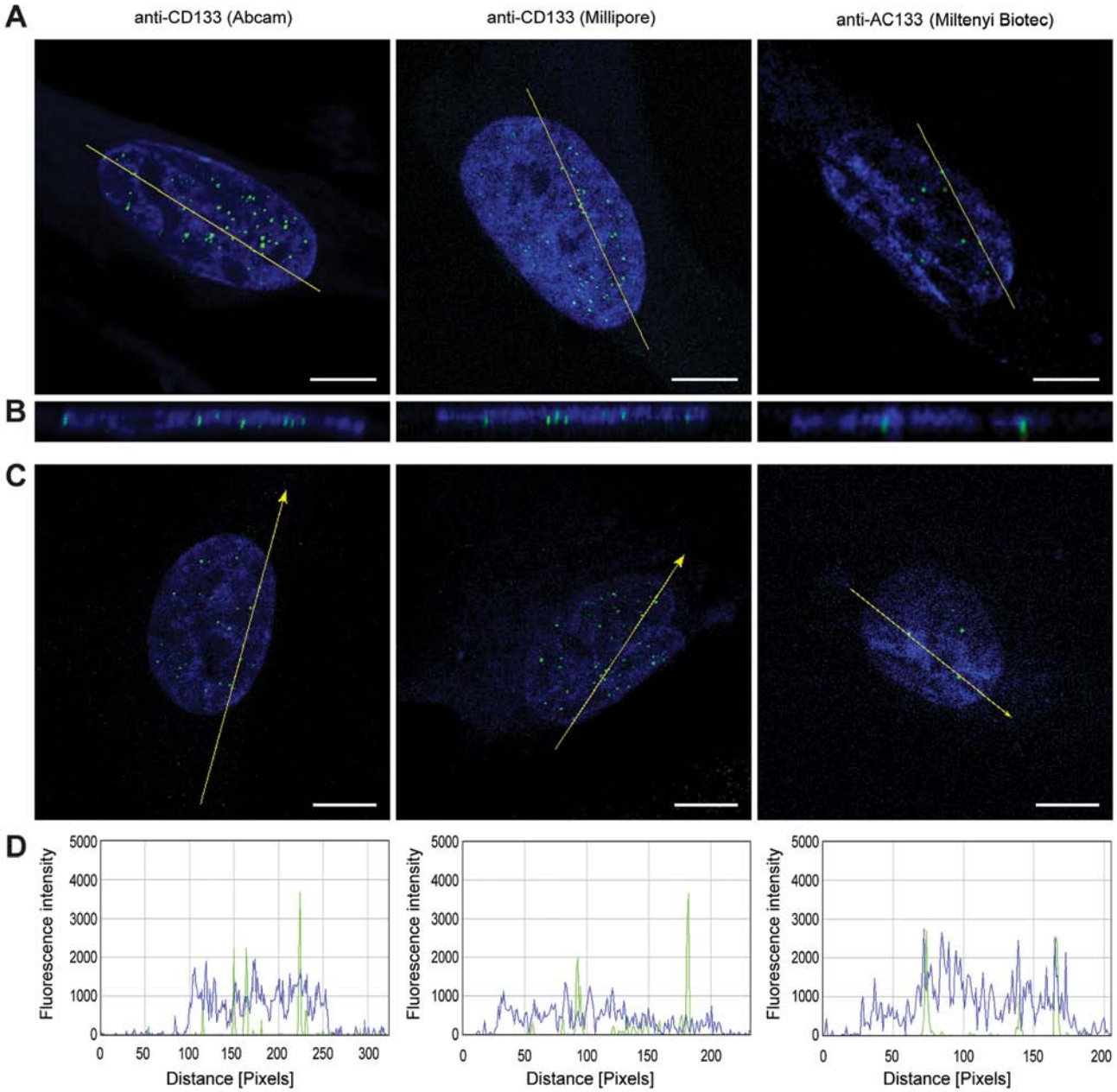

Figure 3. Confocal microscopy analysis of CD133-positive cell nuclei. (A) The planes of software cross-sections through the CD133-positive nuclei are highlighted by simple yellow lines. (B) The cross-sections at these yellow lines are shown at the bottom. (C) The yellow arrows indicate lines drawn across individual CD133-positive nuclei in the confocal image; (D) matching plots reporting the fluorescence intensity according to these arrows are given below. CD133 was stained by indirect immunofluorescence using Alexa Fluor 488-labeled secondary antibodies (green), and nuclei were counterstained with Hoechst 33342 (blue). Scale bars, 5 μm.

in the nucleoli (Fig. 4B), and this observation corresponds with the diffuse positivity for CD133 observed in some of the nucleoli (Fig. 2B). In addition to cells with the typical membrane positivity or exclusive nuclear positivity for CD133, we also sporadically noted clusters of positive signals in the cytoplasm near the cell nucleus or very close to the nuclear envelope (Fig. 4B).

Final confirmation of the results achieved through microscopic methods was carried out by immunoblot analysis of the cytoplasmic and nuclear fractions of all five RMS cell lines. The presence of CD133-specific bands of various intensities was detected in all nuclear fractions, in addition to the strong CD133-specific bands in the cytoplasmic fractions (Fig. 4C). The purity of both subcellular fractions was confirmed by the presence/absence of α-tubulin and lamin B2. These results are completely in accordance with our other findings (reported above) achieved by indirect immunofluorescence and TEM, i.e., in all five RMS cell lines, the presence of a small subpopulation of cells with CD133 in the nucleus was revealed.

Discussion

As described above, we unexpectedly identified an atypical nuclear localization of CD133 in a relatively stable subset of cells in five RMS cell lines established in our laboratory. To date, this atypical localization of CD133 was described in one

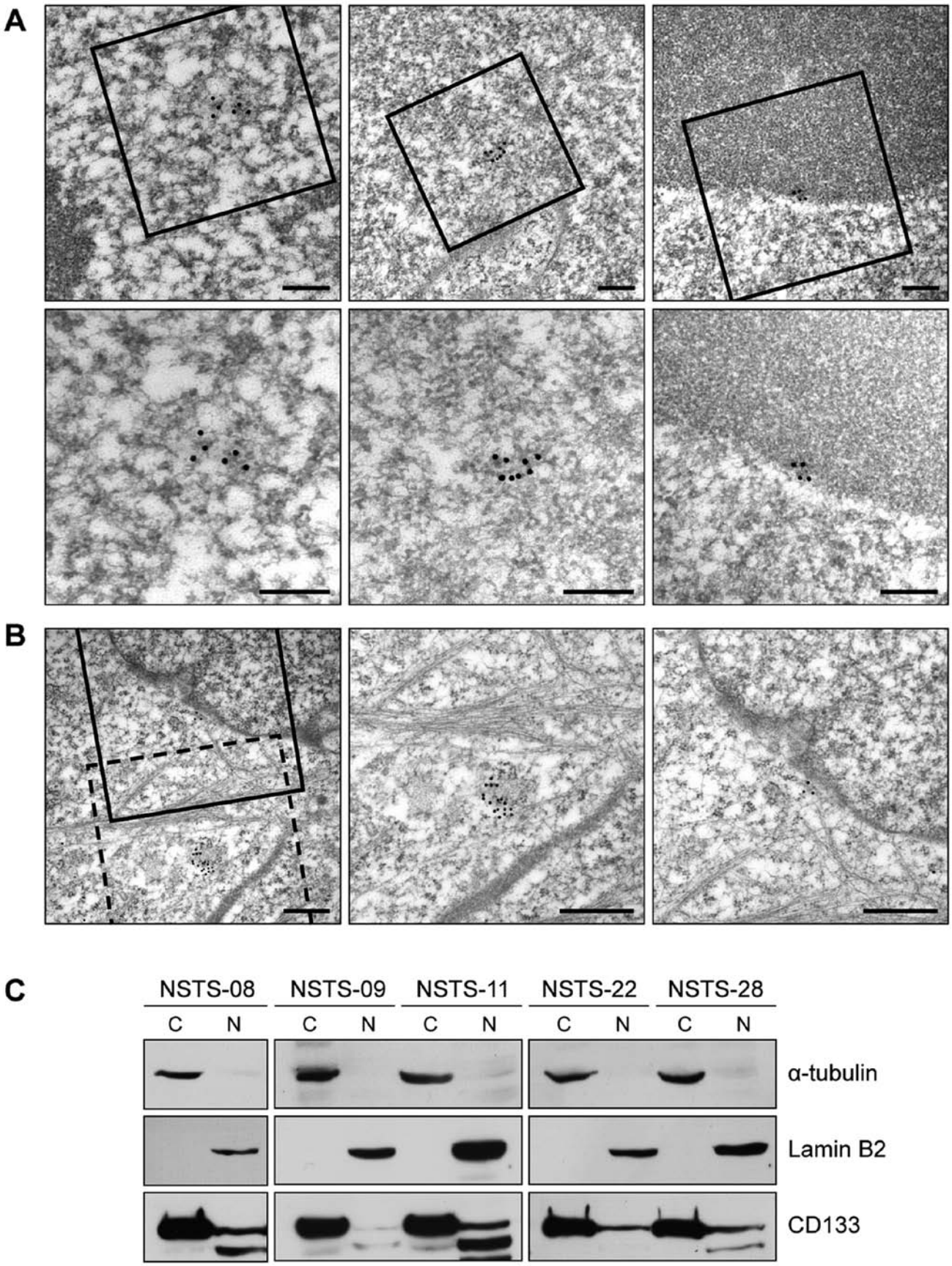

Figure 4. Detection of CD133 in the nuclei of rhabdomyosarcoma cells using transmission electron microscopy and immunoblot analysis. (A) Presence of CD133 in cell nuclei and nucleoli; more detailed images of the positive signal for CD133 in the highlighted square areas are presented on the bottom row. (B) The presence of CD133 in the cytoplasm near the nucleus (dashed square) and very close to the nuclear envelope (solid square). More detailed images of the positive signal for CD133 in the highlighted square areas, as indicated above, are shown on the right side. Representative labeling of CD133 in NSTS-28 cells is shown; CD133 was detected using 20 nm gold particles. Scale bars: (A) 250 nm and (B) 500 nm. (C) Nuclear/cytoplasmic fractionation followed by immunoblotting was performed using a rabbit polyclonal anti-CD133 primary antibody; α-tubulin and lamin B2 were used to confirm the purity of the fractions.

case report on breast cancer (14) and in a large study of prognostic markers on lung cancer (15) using immunohistochemical methods. Nevertheless, published data on CD133 expression in human cancer cells are partly inconsistent, possibly due to different analytical tools, as well as methodological limitations and pitfalls (2). For this reason, results obtained by immunohistochemistry or flow cytometry must be confirmed with alternative antibodies and should be complemented by the utilization of different detection methods of either protein or transcript (2). Furthermore, the glycosylation of CD133 epitopes in relation to the CSC phenotype should be also taken into account, particularly if the antibodies against AC133 epitope are commercially available (17).

In this study, we verified the nuclear localization of CD133 in RMS cells using three independent anti-CD133 antibodies, including both rabbit polyclonal and mouse monoclonal antibodies (Fig. 1). Indirect immunofluorescence and confocal microscopy followed by software cross-section analysis, TEM and cell fractionation with immunoblotting were also employed, and all the results undeniably confirmed the presence of CD133 in the nuclei of stable minor subpopulations of all five RMS cell lines.

These results strongly support the hypothesis that a stable subpopulation of cells with nuclear positivity for CD133 is a common phenomenon in RMS cell lines. Surprisingly, and to the best of our knowledge, similar results have not been reported to date for RMS cells. Although certain micrographs from our previous study showed cells with an accumulation of fluorescent signal for CD133 in the nucleus (6), we assumed that this finding was an artifact resulting from the use of a rabbit polyclonal antibody against CD133, (which was the only anti-CD133 antibody available at the time), although we had never detected similar nuclear positivity for CD133 in osteosarcoma or glioblastoma cell lines using the same antibody (5,18). Other authors investigating CD133 expression in RMS and RMS cell lines have not described the pattern of CD133 positivity in detail, and no micrographs of the individual cells are available in their published articles (9,10).

Very recently, one publication has mentioned the nuclear localization of CD133 in triple-negative breast cancer cells as revealed by immunohistochemistry; nevertheless, this study is a case report based on only one simple descriptive method and therefore does not include any continuing systematic analysis of this apparently interesting finding. Moreover, two of three methods listed in this article, quantitative RT-PCR and flow cytometry, are not suitable for identifying the cell surface, cytoplasmic or nuclear localization of any protein (14).

To date, another study concerning the possible value of CD133 as a prognostic indicator of survival in patients with non-small cell lung cancer (NSCLC) was just published. These interesting results suggest that CD133 expression in the nucleus of NSCLC cells was related to tumor diameter, tumor differentiation and the TNM stage. Kaplan-Meier survival and Cox regression analyses revealed that a high CD133 expression in the nucleus, as well as in the cytoplasm also predicted the poor prognosis of NSCLC (15).

As mentioned above, in addition to cells with the typical membrane positivity or exclusive nuclear positivity for CD133, clusters of positive signals in the cytoplasm near the cell nucleus or very close to the nuclear envelope were also sporadically noted. This finding is in accordance with our previously published observations of sporadic cytoplasmic positivity for CD133 in RMS cells (6), as well as with the deposition of CD133 in cytoplasmic vesicles that has been described in osteosarcoma (19) and the recently suggested mechanism of CD133 internalization and trafficking into lysosomes through interactions between CD133 and the histone deacetylase HDAC6 (20).

Taken together, our results undeniably confirmed the presence of CD133 in the cell nuclei of stable minor subpopulations in RMS cell lines. These results, although surprising and novel, were achieved through three independent methods using three independent antibodies purchased from three separate suppliers.

Nevertheless, the main question of what is the exact role of CD133 in the nucleus of RMS cells remains unanswered. In a previous study on breast cancer, the authors suggested that CD133 in the nucleus may act as transcriptional regulator and is most likely associated with a poor prognosis; however, this conclusion is largely speculative in this case report (14). By contrast, the most recent findings on NSCLC undoubtedly proved the association of nuclear positivity for CD133 poor prognosis in these patients (15).

Although a similar function of another type of surface molecule internalized into the cell nucleus, receptor tyrosine kinases, has been reported (21-23), CD133 belongs to a distinct class of cell membrane proteins, and the analogies to this process are therefore limited. Furthermore, recent studies also discuss the involvement of internalized CD133 in cell signaling pathways, such as the canonical Wnt pathway (20), or report an association between CD133 and the PI3K/Akt pathway (24-26). Regardless, the elucidation of the possible role of CD133 in the nucleus of cancer cells should be based on detailed descriptions of the localization and interactions of CD133 with other molecules in the cell nucleus. These experiments will be the focus of our upcoming study on this interesting phenomenon.

Acknowledgements

This study was supported by grant IGA NT13443-4 of the Ministry of Healthcare of the Czech Republic. We thank Johana Maresova and Dobromila Klemova for their skilful technical assistance.

References

1. Corbeil D, Karbanová J, Fargeas CA and Jászai J: Prominin-1 (CD133): Molecular and cellular features across species. Adv Exp Med Biol 777: 3-24, 2013.
2. Grosse-Gehling P, Fargeas CA, Dittfeld C, Garbe Y, Alison MR, Corbeil D and Kunz-Schughart LA: CD133 as a biomarker for putative cancer stem cells in solid tumours: Limitations, problems and challenges. J Pathol 229: 355-378, 2013.
3. Friedman GK and Gillespie GY: Cancer stem cells and pediatric solid tumors. Cancers (Basel) 3: 298-318, 2011.
4. Xia P: Surface markers of cancer stem cells in solid tumors. Curr Stem Cell Res Ther 9: 102-111, 2014.
5. Veselska R, Hermanova M, Loja T, Chlapek P, Zambo I, Vesely K, Zitterbart K and Sterba J: Nestin expression in osteosarcomas and derivation of nestin/CD133 positive osteosarcoma cell lines. BMC Cancer 8: 300, 2008.
6. Sana J, Zambo I, Skoda J, Neradil J, Chlapek P, Hermanova M, Mudry P, Vasikova A, Zitterbart K, Hampl A, *et al*: CD133 expression and identification of CD133/nestin positive cells in rhabdomyosarcomas and rhabdomyosarcoma cell lines. Anal Cell Pathol (Amst) 34: 303-318, 2011.

7. Di Fiore R, Santulli A, Ferrante RD, Giuliano M, De Blasio A, Messina C, Pirozzi G, Tirino V, Tesoriere G and Vento R: Identification and expansion of human osteosarcoma-cancer-stem cells by long-term 3-aminobenzamide treatment. J Cell Physiol 219: 301-313, 2009.
8. Tirino V, Desiderio V, Paino F, De Rosa A, Papaccio F, Fazioli F, Pirozzi G and Papaccio G: Human primary bone sarcomas contain CD133$^+$ cancer stem cells displaying high tumorigenicity in vivo. FASEB J 25: 2022-2030, 2011.
9. Walter D, Satheesha S, Albrecht P, Bornhauser BC, D'Alessandro V, Oesch SM, Rehrauer H, Leuschner I, Koscielniak E, Gengler C, *et al*; CWS Study Group: CD133 positive embryonal rhabdomyosarcoma stem-like cell population is enriched in rhabdospheres. PLoS One 6: e19506, 2011.
10. Pressey JG, Haas MC, Pressey CS, Kelly VM, Parker JN, Gillespie GY and Friedman GK: CD133 marks a myogenically primitive subpopulation in rhabdomyosarcoma cell lines that are relatively chemoresistant but sensitive to mutant HSV. Pediatr Blood Cancer 60: 45-52, 2013.
11. Veselska R, Skoda J and Neradil J: Detection of cancer stem cell markers in sarcomas. Klin Onkol 25: 2S16-2S20, 2012.
12. Dela Cruz FS: Cancer stem cells in pediatric sarcomas. Front Oncol 3: 168, 2013.
13. Satheesha S and Schafer BW: Cancer stem cells in pediatric sarcomas. In: Stem Cells and Cancer Stem Cells. Hayat MA (ed). Springer, Dordrecht, pp111-126, 2014.
14. Cantile M, Collina F, D'Aiuto M, Rinaldo M, Pirozzi G, Borsellino C, Franco R, Botti G and Di Bonito M: Nuclear localization of cancer stem cell marker CD133 in triple-negative breast cancer: A case report. Tumori 99: e245-e250, 2013.
15. Huang M, Zhu H, Feng J, Ni S and Huang J: High CD133 expression in the nucleus and cytoplasm predicts poor prognosis in non-small cell lung cancer. Dis Markers 2015: 986095, 2015.
16. Veselska R, Kuglik P, Cejpek P, Svachova H, Neradil J, Loja T and Relichova J: Nestin expression in the cell lines derived from glioblastoma multiforme. BMC Cancer 6: 32, 2006.
17. Bidlingmaier S, Zhu X and Liu B: The utility and limitations of glycosylated human CD133 epitopes in defining cancer stem cells. J Mol Med Berl 86: 1025-1032, 2008.
18. Loja T, Chlapek P, Kuglik P, Pesakova M, Oltova A, Cejpek P and Veselska R: Characterization of a GM7 glioblastoma cell line showing CD133 positivity and both cytoplasmic and nuclear localization of nestin. Oncol Rep 21: 119-127, 2009.
19. Tirino V, Desiderio V, d'Aquino R, De Francesco F, Pirozzi G, Graziano A, Galderisi U, Cavaliere C, De Rosa A, Papaccio G and Giordano A: Detection and characterization of CD133$^+$ cancer stem cells in human solid tumours. PLoS One 3: e3469, 2008.
20. Mak AB, Nixon AM, Kittanakom S, Stewart JM, Chen GI, Curak J, Gingras AC, Mazitschek R, Neel BG, Stagljar I and Moffat J: Regulation of CD133 by HDAC6 promotes β-catenin signaling to suppress cancer cell differentiation. Cell Rep 2: 951-963, 2012.
21. Wang SC and Hung MC: Nuclear translocation of the epidermal growth factor receptor family membrane tyrosine kinase receptors. Clin Cancer Res 15: 6484-6489, 2009.
22. Mills IG: Nuclear translocation and functions of growth factor receptors. Semin Cell Dev Biol 23: 165-171, 2012.
23. Carpenter G and Liao HJ: Receptor tyrosine kinases in the nucleus. Cold Spring Harb Perspect Biol 5: a008979, 2013.
24. Takenobu H, Shimozato O, Nakamura T, Ochiai H, Yamaguchi Y, Ohira M, Nakagawara A and Kamijo T: CD133 suppresses neuroblastoma cell differentiation via signal pathway modification. Oncogene 30: 97-105, 2011.
25. Wei Y, Jiang Y, Zou F, Liu Y, Wang S, Xu N, Xu W, Cui C, Xing Y, Liu Y, *et al*: Activation of PI3K/Akt pathway by CD133-p85 interaction promotes tumorigenic capacity of glioma stem cells. Proc Natl Acad Sci USA 110: 6829-6834, 2013.
26. Shimozato O, Waraya M, Nakashima K, Souda H, Takiguchi N, Yamamoto H, Takenobu H, Uehara H, Ikeda E, Matsushita S, *et al*: Receptor-type protein tyrosine phosphatase κ directly dephosphorylates CD133 and regulates downstream AKT activation. Oncogene 34: 1949-1960 2014.

Cancer Science
Japanese Cancer Association JCA
Open Access

Review Article

Nestin as a marker of cancer stem cells

Jakub Neradil[1,2] and Renata Veselska[1,3]

[1]Laboratory of Tumor Biology, Department of Experimental Biology, School of Science, Masaryk University, Brno; [2]Regional Centre for Applied Molecular Oncology, Masaryk Memorial Cancer Institute, Brno; [3]Department of Pediatric Oncology, University Hospital Brno and School of Medicine, Masaryk University, Brno, Czech Republic

Key words

Cancer stem cells, cytoskeleton, intermediate filaments, nestin, tumor markers

Correspondence
Renata Veselska, Department of Experimental Biology, School of Science, Masaryk University, Kotlarska 11, 61137 Brno, Czech Republic.
Tel: +420-549-49-7905; Fax: +420-549-49-5533;
E-mail: veselska@sci.muni.cz

Funding Information
Czech Ministry of Healthcare; European Regional Development Fund; State Budget of the Czech Republic.

Received January 19, 2015; Revised April 14, 2015; Accepted April 27, 2015

Cancer Sci **106** (2015) 803–811

doi: 10.1111/cas.12691

The crucial role of cancer stem cells (CSCs) in the pathology of malignant diseases has been extensively studied during the last decade. Nestin, a class VI intermediate filament protein, was originally detected in neural stem cells during development. Its expression has also been reported in different tissues under various pathological conditions. Specifically, nestin has been shown to be expressed in transformed cells of various human malignancies, and a correlation between its expression and the clinical course of some diseases has been proved. Furthermore, the coexpression of nestin with other stem cell markers was described as a CSC phenotype that was subsequently verified using tumorigenicity assays. The primary aim of this review is to summarize the recent findings regarding nestin expression in CSCs, its possible role in CSC phenotypes, particularly with respect to capacity for self-renewal, and its utility as a putative marker of CSCs.

The role of cancer stem cells (CSCs) in the pathology of malignant diseases has been extensively studied during the last decade. At present, it is widely accepted that CSCs participate in the processes of tumor initiation, progression, metastasis, and relapse.[1,2] The intermediate filament (IF) protein nestin is an extensively studied marker of neural stem cells that is a putative marker of the CSC phenotype, as its expression has been identified in many human malignancies.[3,4] The primary aim of this review is to summarize the recent findings in this interesting field of tumor biology.

Characteristics and Detection of CSCs

Cancer stem cells are defined as a small subpopulation of undifferentiated cells in tumor tissue that are characterized by their capacity for self-renewal and differentiation into various lineages and clones that generate tumor masses. Due to their ability to form a continuously growing tumor, the synonymous terms "tumor-initiating" or "tumorigenic" have been used to describe these cells.[5,6]

Published reports suggest three primary hypotheses regarding the origin of CSCs. The first hypothesis is that CSCs develop from tissue-specific adult stem cells, which show the same capacity for self-renewal and differentiation and survive in the organism for an extended period, rendering these cells as vulnerable to the accumulation of oncogenic mutations. Furthermore, CSCs showed similar primitive phenotypes, such as the expression of specific stem cell markers.[7] The second hypothesis for the origin of CSCs is based on the transformation and dedifferentiation of mature or differentiating cells, which have been reported to reacquire stem cell properties as a consequence of transforming mutations.[8] The third hypothesis is that CSCs and, consequentially, tumorigenesis originate as a result of an "aberrant deposit" of embryonic stem cells in developing tissues during ontogenesis.[1]

Cancer stem cells are typically characterized based on the presence and/or absence of several cellular markers, a combination of which is specific for the CSC phenotype in a respective tumor. These markers include cell surface or membranous proteins (CD15, CD24, CD44, CD133, CXCR4, NCAM, and ABC transporters), cytoplasmic proteins (nestin, Musashi-1, and aldehyde dehydrogenase) or nuclear proteins (Sox-2, Oct3/4, and Nanog) that carry out various structural or metabolic functions in the cell.

The immunodetection of CSC markers on the cell surface has facilitated the identification and isolation of selected CSC subpopulations using appropriate sorting methods (FACS or magnetic-activated cell sorting (MACS)). Other frequently used methods for the isolation of CSCs are based on the functional characteristics of CSCs, for example, the expression of cell adhesion molecules, cytoprotective enzymes, and membrane transporters.[9] These characteristics can be identified using standardized *in vitro* functional assays: detection of the side population, sphere formation assays, and clonogenicity assays, for example. However, *in vivo* tumorigenicity assays using immunodeficient mice represent the gold standard for

the detection of CSCs because this method provides direct evidence of self-renewal and of tumor-forming capacities in an organism. A positive result on this test is considered to confirm the CSC phenotype in the observed cell population.[5]

Characterization of Nestin

Nestin (neuronal stem cell protein) was originally identified using the Rat-401 monoclonal mouse antibody in 1985. This antibody displayed specificity to an antigen that was transiently expressed in specific regions of the developing central nervous system (CNS) and in non-neuronal cells in the peripheral nervous system.[10] Subsequent analysis led to the classification of nestin as a class VI IF protein.[11]

In general, IF represent one of the three main components of cytoskeleton in animal cells. In contrast to microtubules and actin filaments, which consist exclusively of highly conserved globular proteins tubulin and actin, respectively, IF proteins are fibrous and their expression is tissue- or cell-specific. All IF proteins exhibit the same structural organization: a central α-helical rod domain flanked by N- and C-terminal tail domains;[12] therefore, IF are homopolymers or heteropolymers formed of two or more IF proteins. Intermediate filament proteins are classified according their structure and localization as follows: classes I and II encompass acidic and basic cytokeratins; class III embraces vimentin, desmin, glial fibrillary acidic protein, syncoilin, and peripherin; class IV consists of neurofilaments and α-internexin; class V of lamins; and class VI of nestin and synemin.[13] Intermediate filaments are responsible for mechanical integrity of the cell, they serve as an integrating scaffold for other cytoskeletal components and for some organelles. They are also involved in formation of tissue architecture and in the process of tissue regeneration.[14]

The human nestin gene (Fig. 1) is located on the long (q) arm of chromosome 1 at position 23.1. Its promoter resides in a 5′-non-translated region containing two Sp-1-binding sites and lacks a functional TATA box.[15] The nestin gene consists of four exons separated by three introns. Enhancer elements were found in the first and second introns.[16] The enhancer located in the first intron specifically increases nestin expression in myogenic precursors; the mechanism underlying this regulation is likely based on the presence of two E-boxes within the enhancer sequence, to which the transcription factor MyoD cooperatively binds.[17] The second intron contains two neural precursor-specific enhancers, identified as a pan-CNS enhancer and a midbrain-specific enhancer, both of which contain at least two regulatory elements.[18] These two enhancer elements represent binding sites for different types of regulatory molecules, for example, nuclear hormone receptors and transcription factors belonging to the SOX or POU family.[18,19] The expression of the nestin gene is also regulated by epigenetic mechanisms, that is, DNA methylation and histone acetylation. Specifically, histone acetylation appears to be the preferred mechanism of nestin regulation during neural differentiation.[20]

The human nestin protein (Fig. 2) consists of 1621 amino acids and displays a predicted molecular weight of 177.4 kDa. However, nestin is typically detected by Western blotting at a higher apparent molecular weight, ranging from 200 to 240 kDa. This difference can be explained by the presence of multiple phosphorylation sites and glycosylated side chains.[21] The structure of the nestin protein is similar to that of other IF proteins: a conserved 306-amino acid α-helical rod domain, which forms the protein core, 7-amino acid N-terminal and 1308-amino acid C-terminal tail domains. Within the rod domain, helical coils play an important role in dimerization and consecutive filament formation. Previous studies have suggested that nestin is able to form heterodimers only with other IF proteins, most favorably with vimentin.[18,22]

Nestin Expression in Transformed Cells

Nestin expression in the developing and adult human organism under both physiological and pathological conditions has been well described.[4,23–25] Although nestin is primarily regarded as a marker of neural stem/progenitor cells, its expression has also been shown in various embryonic cells and tissues, including skeletal muscle, cardiac muscle, umbilical cord blood cells, Sertoli and interstitial testicular cells, odontoblasts, hair follicle sheath cells, hepatic cells, and renal progenitors.[23] In adults, nestin-positive cells are localized to tissue/organ-specific sites, where they serve as a quiescent resource of cells capable of proliferation, differentiation, and migration after their re-activation.[23] The re-expression or upregulation of nestin was observed in various tissues during reparation processes after several types of injury, including the following: in

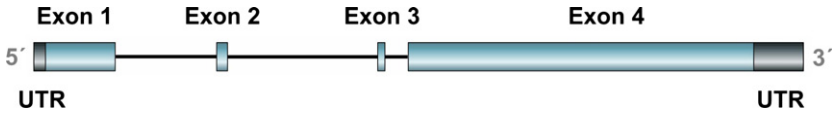

Fig. 1. Exon/intron structure of the human nestin gene. Four exons are depicted in cyan color. The 5′-UTR (black) is located within the first exon; similarly, the 3′-UTR (black) is located within the fourth exon.

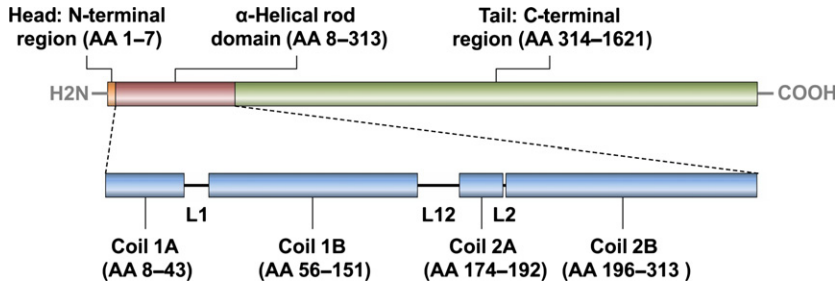

Fig. 2. Domain structure of the human nestin protein. Three domains are depicted: "head" located in the N-terminal region (orange), α-helical rod domain (red), and "tail" in the C-terminal region (green). The rod domain consists of four coils (blue) separated by three linkers (L1, L12, and L2). Numbers of amino acids (AA) in the individual domains and coils are given in brackets.

reactive astrocytes after CNS damage,[26] during the fibrotic response to ischemic heart disease,[27] and in the context of mesangial cell repopulation after induced nephritis.[28] Special attention has been paid to the detailed analyses of nestin expression in many types of human malignancies because nestin may serve as an important diagnostic or prognostic marker.

Increased nestin expression is typical for tumors generated from undifferentiated precursor cells or immature progenitors, which rapidly proliferate during neurogenesis.[29] Although these precursor cells replace nestin with other IF proteins during neuronal differentiation, nestin expression can be transiently re-activated in transformed cells.[25]

In our previous detailed review, we summarized the current understanding of nestin expression in cancer cells and vascular endothelial cells from various types of solid tumors.[24] Unsurprisingly, nestin was detected in neuroectodermal neuroepithelial tumors, including tumors of astrocytic, oligodendroglial, oligoastrocytic, ependymal, embryonic, neuronal, and mixed neuronal-glial origin. Furthermore, nestin expression was found in mesenchymal tumors (e.g. osteosarcoma, rhabdomyosarcoma, gastrointestinal stromal tumor), germ cell tumors (e.g. embryonal carcinoma, germinoma, choriocarcinoma, yolk sac tumor), and epithelial tumors (e.g. pancreatic adenocarcinoma, breast carcinoma, ovarian carcinoma, lung carcinoma).[24,25,30,31]

In some tumor types, increased nestin expression correlates with the tumor grade and indicates an immature and invasive phenotype of transformed cells.[32] Moreover, a correlation between the levels of nestin expression in tumor tissue and the clinical course of the disease was reported for breast carcinoma, ovarian carcinoma, gastrointestinal tumors, germ cell tumors, osteosarcoma, ependymoma, and melanoma.[33–39] Thus, nestin expression is considered to serve as a prognostic marker in these cancer types; however, its prognostic value should be verified in large cohorts of the patients. In contrast, no such relationship was found for pancreatic adenocarcinoma.[40,41] Interestingly, the use of nestin as a predictive marker of a poor response to conventional therapy and to novel therapeutic agents was recently reported for multiple myeloma.[42]

The evidence regarding nestin expression in hematological malignancies is limited to a small number of studies of multiple myeloma. Nestin mRNA was detected in NCAM-positive cells of human myeloma cell lines and in primary myeloma cells.[43] The nestin protein was immunodetected in mature plasma cells from multiple myeloma patients and in myeloma cell lines.[44] Furthermore, an association between increased nestin expression and the pathogenesis of multiple myeloma has been reported.[42]

Nestin as a Putative Marker of CSCs

At present, there is no consensus concerning a "universal" marker for the identification of CSCs in various tumor types.[9] Clearly, a tumor-specific CSC phenotype should be characterized by the co-expression of several markers, both intracellular and surface-associated. As mentioned above, one putative CSC marker is nestin, which is often co-expressed with other stem cell markers (Table 1), such as CD133, Oct3/4 and Sox-2 (Fig. 3).

Identification of nestin in CSCs of neurogenic tumors. The first study of nestin in CSCs revealed its expression in brain tumor stem cells (BTSCs) isolated from different types of human CNS tumors (medulloblastoma, astrocytoma, ependymoma, and ganglioglioma). All of these CSC populations were formed nestin-positive spheres, which were subsequently grown *in vitro*. However, nestin was downregulated during the induced differentiation of BTSCs. Moreover, BTSCs isolated from glioblastoma or medulloblastoma initiated tumor growth in the brains of NOD/SCID mice.[29,45] Detailed analyses of cell lines derived from other types of pediatric brain tumors (i.e., ependymoma, medulloblastoma, glioma, and primitive neuroectodermal tumors) revealed that the number of nestin-positive CSCs is increased in spheres exhibiting a CSC phenotype based on functional assays. Furthermore, sphere-derived cells showed a higher capacity for multilineage differentiation and greater resistance to etoposide than monolayer-derived cells.[46] Other evidence of increased nestin expression in spheres was described using glioblastoma and medulloblastoma cell lines[47,48] and cells derived from peripheral nerve sheath tumor.[49] This increase in nestin expression due to sphere formation appears to be a common phenomenon associated with the stemness of cells within the sphere. The studies mentioned above reported the co-expression of nestin with CD133 or both CD133 and Sox-2 as a common CSC phenotype in tumors of neurogenic origin.[29,46–49]

Nestin-positive cells in xenografts from human astrocytoma- and glioblastoma-derived CSCs showed significant co-expression of proliferating cell nuclear antigen (PCNA) indicating proliferation activity of these cells, as well as co-expression of vascular cell adhesion molecule-1, which may affect cell migration and spreading.[50]

In glioma-prone mice with nestin-GFP tagged transgene expressed both in neural stem cells and in relatively quiescent glioma cells, re-initiation of cell division and growth of nestin-positive glioma cells were observed after eradication of proliferating tumor cells by temozolomide.[51] These results are in accordance with cancer stem cell theory concerning relapses after conventional chemotherapy aimed at proliferating tumor cells.

Furthermore, neural stem cells and "more stem-like glioma-initiating cells" showed similar biological features as well as gene expression profiles, particularly enrichment of Ca^{2+} signaling genes. High expression of Ca^{2+} channels (i.e., AMPA-selective glutamate receptor 1) correlated with expression of nestin and brain lipid-binding protein as well as with sensitivity to Ca^{2+} channel blockers in glioma-initiating cells. Nestin, together with brain lipid-binding protein and glutamate receptor 1, are thus considered a novel combination of glioma CSC markers and the enhanced sensitivity to Ca^{2+} could be included in functional tests of glioma CSCs.[52]

Identification of nestin in CSCs from mesenchymal tumors. Surprisingly, the coexpression of nestin with CD133, which was originally described as the CSC phenotype in neurogenic tumors, was also found in tumors of mesenchymal origin. The first evidence of nestin-/CD133-positive cells in rhabdomyosarcoma samples and cell lines (Fig. 3a) was followed by verification of their tumorigenic potential based on functional assays.[53] The same group also described the presence of nestin-/CD133-positive cells in osteosarcoma cell lines based on immunodetection and predicted the coexpression of these markers as a putative CSC phenotype.[54] An additional study of osteosarcoma, chondrosarcoma, and fibrosarcoma cell lines indicated that nestin mRNA is expressed in sphere-forming subpopulations; however, adherent subpopulations of the same cell lines were identified as nestin-negative.[55] Alternatively, one study of established osteosarcoma cell lines reported contrasting results: the same pattern of nestin expression (i.e.,

Table 1. Overview of known cancer stem cell (CSC) phenotypes in various human solid tumors and functional assays used for their identification

Tumor type	Phenotype of CSCs	Functional assays		References
		In vitro	*In vivo*	
Neurogenic tumors				
Medulloblastoma	Nestin, CD133	Neurospheres, differentiation assay	Xenograft formation	(29,45)
	Nestin, Sox2, CD133	Neurospheres, differentiation assay, drug resistance	Xenograft formation	(46)
	Nestin, Sox2, CD133, β-catenin	Medullospheres		(47)
Ependymoma	Nestin, CD133	Neurospheres, differentiation assay		(29)
	Nestin, Sox2, CD133	Neurospheres, differentiation assay, drug resistance	Xenograft formation	(46)
Glioma	Nestin, CD133	Neurospheres, differentiation assay	Xenograft formation	(29,45)
	Nestin, Sox2, CD133	Neurospheres, differentiation assay, drug resistance	Xenograft formation	(46)
Glioblastoma	Nestin, CD133, Musashi-1, Sox2	Neurospheres, differentiation assay, clonogenic assay	Xenograft formation	(48)
CNS primitive neuroectodermal tumor	Nestin, Sox2, CD133	Neurospheres, differentiation assay, drug resistance	Xenograft formation	(46)
Malignant peripheral nerve sheath tumors	CD133, Oct4, nestin, NGFR (CD271)	Spheres, differentiation assay	Xenograft formation	(49)
Mesenchymal tumors				
Rhabdomyosarcoma	Nestin, CD133	Clonogenic assay	Xenograft formation	(53)
Osteosarcoma	Nestin, CD133			(54)
	CD133, Oct3/4, Sox2, Nanog, nestin	Sarcospheres, clonogenic test, *in vitro* tumorigenic assay, side population, differentiation assay		(55)
	ABCA5, CBX3, ABCG2, ALDH	Spheres, clonogenic test, drug resistance	Xenograft formation	(56)
Chondrosarcoma	CD133, Oct3/4, Sox2, Nanog, nestin	Sarcospheres, clonogenic test, *in vitro* tumorigenic assay, side population, differentiation assay	Xenograft formation	(55)
Fibrosarcoma	CD133, Oct3/4, Sox2, Nanog, nestin	Sarcospheres, clonogenic test, *in vitro* tumorigenic assay, side population	Xenograft formation	(55)

Table 1 (Continued)

Tumor type	Phenotype of CSCs	Functional assays		References
		In vitro	*In vivo*	
Epithelial tumors				
Ovarian carcinoma	Nestin, Oct4, Nanog	Spheroids, differentiation assay	Xenograft formation	(57)
	Nestin, Nanog, Oct4, Sox2, ABCG2, CD133, CD117	Spheres, drug resistance	Xenograft formation	(58)
	Nestin, Oct4, Nanog, Sox2, Bmi-1, CD133, CD44, CD24, ALDH1, CD117, ABCG2	Spheroids, drug resistance	Xenograft formation	(59)
Oral squamous cell carcinoma	Nestin, CD133, Oct4, Nanog, ABCG2, CD117	Spheres, soft-agar assay, differentiation assay	Xenograft formation	(60)
Prostate carcinoma	CD49b, CD49f, CD44, deltaNp63, nestin, CD133, Nanog, Oct-4, Bmi-1, Jagged-1, Hes-1, Patched, Smoothened, CD201	Prostaspheres, clonogenic assay		(61)
	CD117, ABCG2, Nanog, Oct4, Sox2, nestin, CD133	Drug resistance	Xenograft formation	(62)
Gallbladder carcinoma	CD133, nestin, Oct4, Nanog	Spheres, drug resistance, differentiation assay	Xenograft formation	(63)
Non-small-cell lung cancer	Nestin, CD133			(64)
Lung cancers	CD44, CD90, Nanog, Oct4	Spheres, irradiation resistance, clonogenic assay	Xenograft formation	(65)
Colon cancer	Nestin, Bmi1	Spheres, soft agar colony formation assay, invasion assay, drug resistance		(68)
Breast cancer	CD44, Oct4, nestin, $CD24^{-}$	Mammospheres		(69)
	CD44, ESA, nestin, $CD24^{-}$	Mammospheres, invasion assay	Xenograft formation	(70)
	Nanog, Oct3/4, nestin, Sox2, CD34			(71)
Gastric adenocarcinoma	Nestin, CD44			(72)
Pancreatic ductal adenocarcinoma	ALDH1A1, ABCG2, nestin	Spheres, invasion assay, side population,		(74)
	CD133, CD44, Oct4, nestin	Drug resistance	Xenograft formation	(76)

CNS, central nervous system.

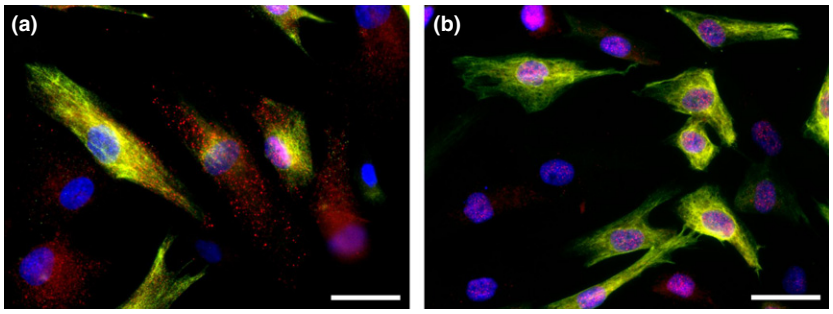

Fig. 3. Co-expression of nestin and other putative cancer stem cells markers in the NSTS-11 rhabdomyosarcoma cell line. Representative double labeling for nestin and CD133 (a) and for nestin and Oct4 (b). CD133 (a) and Oct4 (b) were stained by indirect immunofluorescence using Alexa 568-labeled secondary antibody (red); nestin (a, b) was stained by the same method using Alexa 488-labeled secondary antibody (green); nuclei were counterstained with DAPI (blue). Bar = 25 μm.

downregulation of nestin in adherent cells) was found in spheres and adherent populations of CHA59 cells based on real-time PCR and Western blotting, whereas a reverse pattern (i.e., downregulation of nestin in sarcospheres) was described in the HuO9 cell line.[56] Interestingly, both spheres and adherent cells were detected as nestin-negative in the Saos-2 cell line,[56] but strong nestin expression was previously identified in the same cell line based on immunofluorescence.[54]

Identification of nestin in CSCs from epithelial tumors. Cells coexpressing CD133 and nestin (a putative CSC phenotype) were also found in several types of epithelial tumors.

Early studies of ovarian adenocarcinoma, including high-grade serous ovarian carcinoma, identified a population of self-renewing CSCs that grew as sphere-forming clusters. Furthermore, these cells were tumorigenic *in vivo*, showing increased chemoresistance and expressed CSC markers, including nestin.[57–59]

Cultivation of oral squamous cell carcinoma cells in defined serum-free medium led to the formation of spheres enriched with cells exhibiting CSC phenotypes, including high expression of nestin and other stem cell markers (i.e., CD133, Oct-4, and Nanog), differentiation capacity, enhanced migratory capacity, and tumorigenicity. However, nestin was also found in sphere-like bodies of basal cells that showed limited proliferation potential and reduced expression of self-renewal genes.[60]

Similarly, stem-like prostate cancer cells expressing typical stem cell markers, such as Nanog, Oct4, Sox-2, CD133, and nestin, were isolated from prostate tumor tissue[61] and from a prostate cancer cell line.[62] In the first study, the obtained "prostaspheres" were maintained *in vitro*.[61] The second study verified the proposed chemoresistance and tumorigenicity of these prostatic CSCs.[62] Additionally, CSCs were obtained from human gallbladder carcinoma through sphere formation, and the expression of nestin, CD133, Oct-4, and Nanog was identified in these cells.[63]

Nestin/CD133-positive cells were also detected in paraffin blocks of 121 non-small-cell lung cancer samples based on immunohistochemistry and immunofluorescence; the co-localization of these two markers was detected in 17% of the samples, although the double-stained cells represented <1% of all positive cells. The authors concluded that CD133/nestin-positivity may serve as a marker of lung CSCs.[64] Other relevant studies did not refer to nestin expression in lung CSCs[65,66] and only mentioned the effect of nestin on cell proliferation.[67]

Treatment of an HCT-117 colon cancer cell line or primary colon cancer cells with interleukin-1β promoted sphere formation, upregulated the typical stemness markers nestin and Bmi1, and increased drug resistance. Moreover, the observed self-renewal status was accompanied by epithelial-mesenchymal transition (EMT), the upregulation of the EMT activator Zeb1, and the downregulation or loss of E-cadherin expression.[68]

Breast CSCs are typically isolated according to their ESA+/CD44+/CD24- phenotype. Interestingly, these cells also express Oct-4 and nestin and display increased tumorigenicity through the formation of mammospheres under *in vitro* conditions.[69] The high expression of nestin is associated with a 100-fold increase in tumorigenicity in comparison with cells showing weak nestin expression and ESA+/CD44+/CD24- phenotype. Conversely, knockdown of nestin in breast CSCs led to cell cycle arrest, apoptosis induction, repression of cell migration, and inhibition of spontaneous EMT. On a molecular level, silencing of nestin disrupted Wnt/β-catenin activation, which is an important signaling pathway in breast CSCs.[70] Furthermore, Oct-4/nestin-positivity in cancer tissues has been associated with younger age, malignant tumor grades, lymph node metastasis, and shorter survival.[69,70] Co-expression of nestin with other established stem cell markers (e.g., Oct3/4 or Sox-2) was shown in circulating breast cancer cells.[71]

A correlation between the expression of nestin and CD44 was recently found in gastric adenocarcinoma; this study provided the first evidence of the nestin+/CD44+ phenotype in this type of tumor.[72] In pancreatic ductal adenocarcinoma (PDAC), the expression of nestin as a putative marker of CSCs has recently been discussed.[73,74] High levels of nestin together with ALDH1A1 and ABCG2 were detected in metastatic cells from human PDAC injected into NOG mice; moreover, these cells showed typical features of CSCs such as sphere formation and tumorigenicity. Downregulation of nestin by shRNA in these cells resulted in decreased capacity of both sphere formation *in vitro* and metastasizing *in vivo*.[74] Nestin modulates nestin-positive cell invasion, EMT, and metastasis during the progression of PDAC. It was also shown that nestin expression in PDAC cells is regulated by the transforming growth factor-β1/Smad pathway: nestin expression is induced in a Smad4-dependent manner and under hypoxic conditions.[75] Nestin was also detected in spheres together with CD133 and CD44,[73] and the recently isolated Panc-1 stem-like cell line demonstrated coexpression of CD133, CD44, Oct4, and nestin.[76] In contrast, no significant correlation between the CD133 and nestin expression patterns has been detected in PDAC tumor samples,[41] and nestin expression did not correlate with the clinical course of PDAC.[40]

What is the Role of Nestin in CSCs?

In some tumor types, nestin expression correlates with aggressive growth, metastasis, and poor prognosis.[25] Nevertheless, the role of nestin in transformed cells, especially CSCs, aside from its participation in cytoskeleton formation, remains unclear.

One primary hypothesis for the role of nestin in CSCs arose from an *in vivo* experiment: nestin knockout mice showed embryonic lethality and a reduced number of neuronal stem cells. Moreover, the remaining neuronal stem cells exhibited decreased self-renewal capacity and increased cell death, with no apparent defects in proliferation, differentiation, or cytoskeletal integrity.[77] A proposed relationship between nestin expression and self-renewal is supported by the previous finding that the nestin promoter is activated by Notch, which binds to the second intron enhancer element of the nestin gene. The combined activation of Notch and KRAS led to the proliferation of nestin/PCNA-positive cells in lesions along the subventricular zone of mice, suggesting that these lesions may represent premalignant stages of tumorigenesis and that nestin/PCNA-positive cells may exhibit CSC phenotypes.[78]

It has been shown in neuroblastoma cells that E-box sequences in the regulatory second intron of the nestin gene are specific regions to which N-myc transcription factors can bind. Furthermore, an increase in N-myc protein levels subsequently enhances nestin expression and cell proliferation and motility.[79] In addition, N-myc regulates the expression of several genes that encode stem-related factors, including lif, klf2, klf4, and lin28b.[80] Thus, nestin unequivocally belongs to the group of stemness genes regulated by N-myc.

An additional mouse study indicated that nestin-positive CSCs localized to the perivascular niche of medulloblastoma tumor tissue and exhibited radioresistance through the

activation of the AKT/PI3K and p53 signaling pathways. These characteristics are in contrast to those of the rest of the tumor mass, which undergoes apoptosis. In medulloblastoma displaying extensive nodularity, the loss of the *PTEN* gene in combination with Sonic hedgehog overexpression induced the formation of tumors from nestin-positive progenitor cells. Furthermore, the activation of the AKT signaling pathway using ionizing irradiation led to the proliferation of nestin-positive CSCs, whereas the majority of cells in the tumor mass were differentiated.[81]

A cytoprotective function of nestin was shown in neuronal stem cells, as overexpression of nestin inhibited oxidant-induced apoptosis, including the activity of cyclin-dependent kinase 5, which serves as an important regulator of neuronal development and function.[82] However, this mechanism of nestin activity has not been demonstrated in CSCs.

The functions of many proteins are regulated by their cellular localization. Nestin is predominantly localized to the cytoplasm, where it participates in the formation of IFs as integral components of the cytoskeleton in animal cells. However, based on confocal microscopy and immunodetection using ultrathin sections by transmission electron microscopy, strong nestin signals were detected in the nuclei of the GM7 glioblastoma cell line;[83] this cell line was later characterized as positive for both nestin and CD133.[84] Subsequently, the nuclear localization of nestin was found in two neuroblastoma cell lines and in one medulloblastoma cell line out of a total of 11 neurogenic patient-derived cell lines. These results suggest that this phenomenon is not particularly rare in transformed cells. However, the percentage of cells displaying nestin-positive nuclei was approximately 10% in these cell lines, suggesting that these cells show no great advantage in clonal selection.[85] A role for nestin in the nucleus is not yet clear, although previous cross-linking experiments revealed that nestin binds to DNA in N-myc-amplified N-type neuroblastoma cell lines.[79]

Recently, nestin was found on the cell surface of 14 glioma stem cell lines, and the positivity for nestin at the cell surface ranged from 1.4% to 70%. Isolated nestin-positive cells showed increased sphere-forming capacity and sphere size. The authors proposed that surface nestin underwent post-translational modification by γ-secretase and that, after plasma membrane exposure, nestin may be used as a marker for the isolation and characterization of CSCs in glioblastoma.[86] Surface nestin was originally identified in murine glioma stem cells (GSCs) and it was reported as a ~60-kDa N-terminal isotype of nestin. Surface nestin was detectable with GSC-targeting peptide with selective binding affinity to undifferentiated GSCs. Glioma stem cell-targeting peptide conjugated with fluorochrome is able to undergo internalization and its colocalization with nestin-positive GSCs was observed both in a glioma cell population maintained *in vitro* as well as in a murine glioblastoma model *in vivo*.[87] Surface nestin thus seems to be a suitable target molecule for identification of CSCs in some types of brain tumors, especially in gliomas. In addition to the detection methods described above, the application of specific mAb against the N-terminal part of the nestin molecule or of GSC-targeting peptide could also be used for eradication of these cells because peptide- and antibody-based radiopharmaceuticals or cytotoxic conjugates are discussed as very promising strategies in cancer treatment.[88–90]

In conclusion, nestin is undoubtedly a putative CSC marker of both neurogenic tumors and tumors of epithelial or mesenchymal origin. The coexpression of nestin with other CSC markers, particularly CD133, Oct3/4, and Sox-2, should be considered as a specific CSC phenotype; however, the verification of this phenotype using functional assays is required for each tumor type. Some experimental results suggest that nestin expression is closely associated with self-renewal capacity, although the detailed mechanisms underlying this relationship remain unclear.

Acknowledgments

The authors thank Alena Nunukova for skillful technical assistance. This study was supported by grants from the Internal Grant Agency of the Czech Ministry of Healthcare (no. NT13443-4), the European Regional Development Fund, and the State Budget of the Czech Republic (RECAMO CZ.1.05./2.1.00/03.0101 and CEB OP VK CZ.1.07/2.3.00/20.0183).

Disclosure Statement

The authors have no conflict of interests.

References

1 Ratajczak MZ. Cancer stem cells – normal stem cells "Jedi" that went over to the "dark side". *Folia Histochem Cytobiol* 2005; **43**: 175–81.
2 Fábián A, Barok M, Vereb G, Szöllosi J. Die hard: are cancer stem cells the Bruce Willises of tumor biology? *Cytometry A* 2009; **75**: 67–74.
3 Friedman GK, Gillespie GY. Cancer stem cells and pediatric solid tumors. *Cancers (Basal)* 2011; **3**: 298–318.
4 Matsuda Y, Hagio M, Ishiwata T. Nestin: a novel angiogenesis marker and possible target for tumor angiogenesis. *World J Gastroenterol* 2013; **19**: 42–8.
5 Clarke MF, Dick JE, Dirks PB *et al.* Cancer stem cells–perspectives on current status and future directions: AACR Workshop on cancer stem cells. *Cancer Res* 2006; **66**: 9339–44.
6 Neuzil J, Stantic M, Zobalova R *et al.* Tumour-initiating cells vs. cancer 'stem' cells and CD133: what's in the name? *Biochem Biophys Res Commun* 2007; **355**: 855–9.
7 McDonald SA, Graham TA, Schier S, Wright NA, Alison MR. Stem cells and solid cancers. *Virchows Arch* 2009; **455**: 1–13.
8 Foreman KE, Rizzo P, Osipo C, Miele L. The Cancer Stem Cell Hypothesis. In: Bagley RG, Teicher BA, eds. *Stem Cells and Cancer (Cancer Drug Discovery)*. New York: Humana Press, 2009; 3–14.
9 Alison MR, Lim SM, Nicholson LJ. Cancer stem cells: problems for therapy? *J Pathol* 2011; **223**: 147–61.
10 Hockfield S, McKay RD. Identification of major cell classes in the developing mammalian nervous system. *J Neurosci* 1985; **5**: 3310–28.
11 Lendahl U, Zimmerman LB, McKay RD. CNS stem cells express a new class of intermediate filament protein. *Cell* 1990; **60**: 585–95.
12 Herrmann H, Strelkov SV, Burkhard P, Aebi U. Intermediate filaments: primary determinants of cell architecture and plasticity. *J Clin Invest* 2009; **119**: 1772–83.
13 Leduc C, Etienne-Manneville S. Intermediate filaments in cell migration and invasion: the unusual suspects. *Curr Opin Cell Biol* 2015; **32**: 102–12.
14 Dey P, Togra J, Mitra S. Intermediate filament: structure, function, and applications in cytology. *Diagn Cytopathol* 2014; **42**: 628–35.
15 Cheng L, Jin Z, Liu L *et al.* Characterization and promoter analysis of the mouse nestin gene. *FEBS Lett* 2004; **565**: 195–202.
16 Zimmerman L, Parr B, Lendahl U *et al.* Independent regulatory elements in the nestin gene direct transgene expression to neural stem cells or muscle precursors. *Neuron* 1994; **12**: 11–24.
17 Zhong H, Jin Z, Chen Y *et al.* First intron of nestin gene regulates its expression during C2C12 myoblast differentiation. *Acta Biochim Biophys Sin* 2008; **40**: 526–32.
18 Michalczyk K, Ziman M. Nestin structure and predicted function in cellular cytoskeletal organisation. *Histol Histopathol* 2005; **20**: 665–71.
19 Tanaka S, Kamachi Y, Tanouchi A, Hamada H, Jing N, Kondoh H. Interplay of SOX and POU factors in regulation of the Nestin gene in neural primordial cells. *Mol Cell Biol* 2004; **24**: 8834–46.

20 Han DW, Do JT, Araúzo-Bravo MJ *et al.* Epigenetic hierarchy governing Nestin expression. *Stem Cells* 2009; **27**: 1088–97.
21 Messam CA, Hou J, Major EO. Coexpression of nestin in neural and glial cells in the developing human CNS defined by a human-specific anti-nestin antibody. *Exp Neurol* 2000; **161**: 585–96.
22 Herrmann H, Aebi U. Intermediate filaments and their associates: multi-talented structural elements specifying cytoarchitecture and cytodynamics. *Curr Opin Cell Biol* 2000; **12**: 79–90.
23 Wiese C, Rolletschek A, Kania G *et al.* Nestin expression – a property of multi-lineage progenitor cells? *Cell Mol Life Sci* 2004; **61**: 2510–22.
24 Krupkova O Jr, Loja T, Zambo I, Veselska R. Nestin expression in human tumors and tumor cell lines. *Neoplasma* 2010; **57**: 291–8.
25 Ishiwata T, Matsuda Y, Naito Z. Nestin in gastrointestinal and other cancers: effects on cells and tumor angiogenesis. *World J Gastroenterol* 2011; **17**: 409–18.
26 Gilyarov AV. Nestin in central nervous system cells. *Neurosci Behav Physiol* 2008; **38**: 165–9.
27 Calderone A. Nestin+ cells and healing the infarcted heart. *Am J Physiol Heart Circ Physiol* 2012; **302**: H1–9.
28 Daniel C, Albrecht H, Lüdke A, Hugo C. Nestin expression in repopulating mesangial cells promotes their proliferation. *Lab Invest* 2008; **88**: 387–97.
29 Singh SK, Clarke ID, Terasaki M *et al.* Identification of a cancer stem cell in human brain tumors. *Cancer Res* 2003; **63**: 5821–8.
30 Veselska R, Skoda J, Neradil J. Detection of cancer stem cell markers in sarcomas. *Klin Onkol* 2012; **25**: 2S16–20.
31 Sterlacci W, Savic S, Fiegl M, Obermann E, Tzankov A. Putative stem cell markers in non-small-cell lung cancer: a clinicopathologic characterization. *J Thorac Oncol* 2014; **9**: 41–9.
32 Ehrmann J, Kolár Z, Mokry J. Nestin as a diagnostic and prognostic marker: immunohistochemical analysis of its expression in different tumours. *J Clin Pathol* 2005; **58**: 222–3.
33 Kolar Z, Ehrmann J Jr, Turashvili G, Bouchal J, Mokry J. A novel myoepithelial/progenitor cell marker in the breast? *Virchows Arch* 2007; **450**: 607–9.
34 He QZ, Luo XZ, Zhou Q *et al.* Expression of nestin in ovarian serous cancer and its clinicopathologic significance. *Eur Rev Med Pharmacol Sci* 2013; **17**: 2896–901.
35 Parfitt JR, McLean CA, Joseph MG, Streutker CJ, Al-Haddad S, Driman DK. Granular cell tumours of the gastrointestinal tract: expression of nestin and clinicopathological evaluation of 11 patients. *Histopathology* 2006; **48**: 424–30.
36 Sakurada K, Saino M, Mouri W, Sato A, Kitanaka C, Kayama T. Nestin expression in central nervous system germ cell tumors. *Neurosurg Rev* 2008; **31**: 173–6.
37 Zambo I, Hermanova M, Adamkova Krakorova D *et al.* Nestin expression in high-grade osteosarcomas and its clinical significance. *Oncol Rep* 2012; **27**: 1592–8.
38 Nambirajan A, Sharma MC, Gupta RK, Suri V, Singh M, Sarkar C. Study of stem cell marker nestin and its correlation with vascular endothelial growth factor and microvascular density in ependymomas. *Neuropathol Appl Neurobiol* 2014; **40**: 714–25.
39 Sabet MN, Rakhshan A, Erfani E, Madjd Z. Co-expression of putative cancer stem cell markers, CD133 and nestin, in skin tumors. *Asian Pac J Cancer Prev* 2014; **15**: 8161–9.
40 Lenz J, Karasek P, Jarkovsky J *et al.* Clinicopathological correlations of nestin expression in surgically resectable pancreatic cancer including an analysis of perineural invasion. *J Gastrointestin Liver Dis* 2011; **20**: 389–96.
41 Kim HS, Yoo SY, Kim KT, Park JT, Kim HJ, Kim JC. Expression of the stem cell markers CD133 and nestin in pancreatic ductal adenocarcinoma and clinical relevance. *Int J Clin Exp Pathol* 2012; **5**: 754–61.
42 Svachova H, Kryukov F, Kryukova E *et al.* Nestin expression throughout multistep pathogenesis of multiple myeloma. *Br J Haematol* 2014; **164**: 701–9.
43 Liu S, Otsuyama K, Ma Z *et al.* Induction of multilineage markers in human myeloma cells and their down-regulation by interleukin 6. *Int J Hematol* 2007; **85**: 49–58.
44 Svachova H, Pour L, Sana J, Kovarova L, Raja KR, Hajek R. Stem cell marker nestin is expressed in plasma cells of multiple myeloma patients. *Leuk Res* 2011; **35**: 1008–13.
45 Singh SK, Hawkins C, Clarke ID *et al.* Identification of human brain tumour initiating cells. *Nature* 2004; **432**: 396–401.
46 Hussein D, Punjaruk W, Storer LC *et al.* Pediatric brain tumor cancer stem cells: cell cycle dynamics, DNA repair, and etoposide extrusion. *Neuro Oncol* 2011; **13**: 70–83.
47 Zanini C, Ercole E, Mandili G *et al.* Medullospheres from DAOY, UW228 and ONS-76 cells: increased stem cell population and proteomic modifications. *PLoS One* 2013; **8**: e63748.
48 Iacopino F, Angelucci C, Piacentini R *et al.* Isolation of cancer stem cells from three human glioblastoma cell lines: characterization of two selected clones. *PLoS One* 2014; **9**: e105166.
49 Spyra M, Kluwe L, Hagel C *et al.* Cancer stem cell-like cells derived from malignant peripheral nerve sheath tumors. *PLoS One* 2011; **6**: e21099.
50 Zarnescu O, Brehar FM, Bleotu C, Gorgan RM. Co-localization of PCNA, VCAM-1 and caspase-3 with nestin in xenografts derived from human anaplastic astrocytoma and glioblastoma multiforme tumor spheres. *Micron* 2011; **42**: 793–800.
51 Chen J, Li Y, Yu TS *et al.* A restricted cell population propagates glioblastoma growth after chemotherapy. *Nature* 2012; **488**: 522–6.
52 Wee S, Niklasson M, Marinescu VD *et al.* Selective calcium sensitivity in immature glioma cancer stem cells. *PLoS One* 2014; **9**: e115698.
53 Sana J, Zambo I, Skoda J *et al.* CD133 expression and identification of CD133/nestin positive cells in rhabdomyosarcomas and rhabdomyosarcoma cell lines. *Anal Cell Pathol* 2011; **34**: 303–18.
54 Veselska R, Hermanova M, Loja T *et al.* Nestin expression in osteosarcomas and derivation of nestin/CD133 positive osteosarcoma cell lines. *BMC Cancer* 2008; **8**: 300.
55 Tirino V, Desiderio V, Paino F *et al.* Human primary bone sarcomas contain CD133 + cancer stem cells displaying high tumorigenicity in vivo. *FASEB J* 2011; **25**: 2022–30.
56 Saini V, Hose CD, Monks A *et al.* Identification of CBX3 and ABCA5 as putative biomarkers for tumor stem cells in osteosarcoma. *PLoS One* 2012; **7**: e41401.
57 Bapat SA, Mali AM, Koppikar CB, Kurrey NK. Stem and progenitor-like cells contribute to the aggressive behavior of human epithelial ovarian cancer. *Cancer Res* 2005; **65**: 3025–9.
58 Ma L, Lai D, Liu T, Cheng W, Guo L. Cancer stem-like cells can be isolated with drug selection in human ovarian cancer cell line SKOV3. *Acta Biochim Biophys Sin* 2010; **42**: 593–602.
59 He QZ, Luo XZ, Wang K *et al.* Isolation and characterization of cancer stem cells from high-grade serous ovarian carcinomas. *Cell Physiol Biochem* 2014; **33**: 173–84.
60 Chiou SH, Yu CC, Huang CY *et al.* Positive correlations of Oct-4 and Nanog in oral cancer stem-like cells and high-grade oral squamous cell carcinoma. *Clin Cancer Res* 2008; **14**: 4085–95.
61 Guzmán-Ramírez N, Völler M, Wetterwald A *et al.* In vitro propagation and characterization of neoplastic stem/progenitor-like cells from human prostate cancer tissue. *Prostate* 2009; **69**: 1683–93.
62 Liu T, Xu F, Du X *et al.* Establishment and characterization of multi-drug resistant, prostate carcinoma-initiating stem-like cells from human prostate cancer cell lines 22RV1. *Mol Cell Biochem* 2010; **340**: 265–73.
63 Shi CJ, Gao J, Wang M *et al.* CD133(+) gallbladder carcinoma cells exhibit self-renewal ability and tumorigenicity. *World J Gastroenterol* 2011; **17**: 2965–71.
64 Janikova M, Skarda J, Dziechciarkova M *et al.* Identification of CD133+/nestin+ putative cancer stem cells in non-small cell lung cancer. *Biomed Pap Med Fac Univ Palacky Olomouc Czech Repub* 2010; **154**: 321–6.
65 Wang P, Gao Q, Suo Z *et al.* Identification and characterization of cells with cancer stem cell properties in human primary lung cancer cell lines. *PLoS One* 2013; **8**: e57020.
66 Alamgeer M, Peacock CD, Matsui W, Ganju V, Watkins DN. Cancer stem cells in lung cancer: evidence and controversies. *Respirology* 2013; **18**: 757–64.
67 Takakuwa O, Maeno K, Kunii E *et al.* Involvement of intermediate filament nestin in cell growth of small-cell lung cancer. *Lung Cancer* 2013; **81**: 174–9.
68 Li Y, Wang L, Pappan L, Galliher-Beckley A, Shi J. IL-1β promotes stemness and invasiveness of colon cancer cells through Zeb1 activation. *Mol Cancer* 2012; **11**: 87.
69 Liu C, Cao X, Zhang Y *et al.* Co-expression of Oct-4 and Nestin in human breast cancers. *Mol Biol Rep* 2012; **39**: 5875–81.
70 Zhao Z, Lu P, Zhang H *et al.* Nestin positively regulates the Wnt/β-catenin pathway and the proliferation, survival and invasiveness of breast cancer stem cells. *Breast Cancer Res* 2014; **16**: 408.
71 Apostolou P, Toloudi M, Chatziioannou M, Ioannou E, Papasotiriou I. Cancer stem cells stemness transcription factors expression correlates with breast cancer disease stage. *Curr Stem Cell Res Ther* 2012; **7**: 415–9.
72 Dhingra S, Feng W, Brown RE *et al.* Clinicopathologic significance of putative stem cell markers, CD44 and nestin, in gastric adenocarcinoma. *Int J Clin Exp Pathol* 2011; **4**: 733–41.
73 Matsuda Y, Yoshimura H, Naito Z, Ishiwata T. The roles and molecular mechanisms of nestin expression in cancer with a focus on pancreatic cancer. *J Carcinog Mutagen* 2013; **S9**: 002.
74 Matsuda Y, Yoshimura H, Ueda J, Naito Z, Korc M, Ishiwata T. Nestin delineates pancreatic cancer stem cells in metastatic foci of NOD/Shi-scid IL2Rγ(null) (NOG) mice. *Am J Pathol* 2014; **184**: 674–85.
75 Su HT, Weng CC, Hsiao PJ *et al.* Stem cell marker nestin is critical for TGF beta1-mediated tumor progression in pancreatic cancer. *Mol Cancer Res* 2013; **11**: 768–79.

76 Wang D, Zhu H, Zhu Y *et al.* CD133(+)/CD44(+)/Oct4(+)/Nestin(+) stem-like cells isolated from Panc-1 cell line may contribute to multi-resistance and metastasis of pancreatic cancer. *Acta Histochem* 2013; **115**: 349–56.
77 Park D, Xiang AP, Mao FF *et al.* Nestin is required for the proper self-renewal of neural stem cells. *Stem Cells* 2010; **28**: 2162–71.
78 Shih AH, Holland EC. Notch signaling enhances nestin expression in gliomas. *Neoplasia* 2006; **8**: 1072–82.
79 Thomas SK, Messam CA, Spengler BA, Biedler JL, Ross RA. Nestin is a potential mediator of malignancy in human neuroblastoma cells. *J Biol Chem* 2004; **279**: 27994–9.
80 Cotterman R, Knoepfler PS. N-Myc regulates expression of pluripotency genes in neuroblastoma including lif, klf2, klf4, and lin28b. *PLoS One* 2009; **4**: e5799.
81 Hambardzumyan D, Becher OJ, Holland EC. Cancer stem cells and survival pathways. *Cell Cycle* 2008; **7**: 1371–8.
82 Sahlgren CM, Pallari HM, He T, Chou YH, Goldman RD, Eriksson JE. A nestin scaffold links Cdk5/p35 signaling to oxidant-induced cell death. *EMBO J* 2006; **25**: 4808–19.
83 Veselska R, Kuglik P, Cejpek P *et al.* Nestin expression in the cell lines derived from glioblastoma multiforme. *BMC Cancer* 2006; **6**: 32.
84 Loja T, Chlapek P, Kuglik P *et al.* Characterization of a GM7 glioblastoma cell line showing CD133 positivity and both cytoplasmic and nuclear localization of nestin. *Oncol Rep* 2009; **21**: 119–27.
85 Krupkova O Jr, Loja T, Redova M *et al.* Analysis of nuclear nestin localization in cell lines derived from neurogenic tumors. *Tumour Biol* 2011; **32**: 631–9.
86 Jin X, Jin X, Jung JE, Beck S, Kim H. Cell surface Nestin is a biomarker for glioma stem cells. *Biochem Biophys Res Commun* 2013; **433**: 496–501.
87 Beck S, Jin X, Yin J *et al.* Identification of a peptide that interacts with Nestin protein expressed in brain cancer stem cells. *Biomaterials* 2011; **32**: 8518–28.
88 Okarvi SM. Peptide-based radiopharmaceuticals and cytotoxic conjugates: potential tools against cancer. *Cancer Treat Rev* 2008; **34**: 13–26.
89 Brown KC. Peptidic tumor targeting agents: the road from phage display peptide selections to clinical applications. *Curr Pharm Des* 2010; **16**: 1040–54.
90 Kraeber-Bodéré F, Rousseau C, Bodet-Milin C *et al.* Tumor immunotargeting using innovative radionuclides. *Int J Mol Sci* 2015; **16**: 3932–54.

DHFR-mediated effects of methotrexate in medulloblastoma and osteosarcoma cells: The same outcome of treatment with different doses in sensitive cell lines

JAKUB NERADIL[1,2], GABRIELA PAVLASOVA[1], MARTIN SRAMEK[1,3], MICHAL KYR[3], RENATA VESELSKA[1,3] and JAROSLAV STERBA[2,3]

[1]Department of Experimental Biology, School of Science, Masaryk University;
[2]Regional Centre for Applied Molecular Oncology, Masaryk Memorial Cancer Institute;
[3]Department of Pediatric Oncology, University Hospital Brno and School of Medicine, Masaryk University, Brno, Czech Republic

Received November 19, 2014; Accepted January 21, 2015

DOI: 10.3892/or.2015.3819

Abstract. Although methotrexate (MTX) is the most well-known antifolate included in many standard therapeutic regimens, substantial toxicity limits its wider use, particularly in pediatric oncology. Our study focused on a detailed analysis of MTX effects in cell lines derived from two types of pediatric solid tumors: medulloblastoma and osteosarcoma. The main aim of this study was to analyze the effects of treatment with MTX at concentrations comparable to MTX plasma levels in patients treated with high-dose or low-dose MTX. The results showed that treatment with MTX significantly decreased proliferation activity, inhibited the cell cycle at S-phase and induced apoptosis in Daoy and Saos-2 reference cell lines, which were found to be MTX-sensitive. Furthermore, no difference in these effects was observed following treatment with various doses of MTX ranging from 1 to 40 μM. These findings suggest the possibility of achieving the same outcome with the application of low-dose MTX, an extremely important result, particularly for clinical practice. Another important aspect of treatment with high-dose MTX in clinical practice is the administration of leucovorin (LV) as an antidote to reduce MTX toxicity in normal cells. For this reason, the combined application of MTX and LV was also included in our experiments; however, this application of MTX together with LV did not elicit any detectable effect. The expression analysis of genes involved in the mechanisms of resistance to MTX was a final component of our study, and the results helped us to elucidate the mechanisms of the various responses to MTX among the cell lines included in our study.

Correspondence to: Dr Jakub Neradil, Laboratory of Tumor Biology, Department of Experimental Biology, School of Science, Masaryk University, 611 37 Brno, Czech Republic
E-mail: jneradil@sci.muni.cz

Abbreviations: DHFR, dihydrofolate reductase; FPGH, folylpolyglutamate hydrolase; FPGS, folylpolyglutamate synthetase; LV, leucovorin; MTX, methotrexate; RCF, reduced folate carrier; THF, tetrahydrofolate; TYMS, thymidylate synthase

Key words: methotrexate, leucovorin, osteosarcoma, resistance, antifolate, medulloblastoma

Introduction

Methotrexate (MTX) is the most widely known antifolate successfully used in oncology for a long time. MTX is particularly effective in the treatment of acute lymphoblastic leukemia, non-Hodgkin lymphoma, breast carcinoma, lung carcinoma, osteosarcoma, choriocarcinoma, and some neuroectodermal tumors (1). Although MTX has been included in therapeutic protocols for more than 60 years, its dosage as well as administration schedules are still being optimized.

The most important effect of MTX is based on the inhibition of dihydrofolate reductase (DHFR), which blocks the reduction of folic acid and, consequently, folic acid metabolism. When the concentration of MTX exceeds the binding capacity of DHFR, all available molecules of tetrahydrofolate (THF) are gradually depleted in the cell, and the synthesis of purine and pyrimidine precursors, which are necessary for synthesis of nucleic acids, is reduced (2).

Although MTX is included in many standard therapeutic regimens, its substantial toxicity limits its wider use, particularly in pediatric oncology. The cytotoxic effects of high-dose MTX (HD-MTX) on normal somatic cells could be reduced by the administration of an antidote, with the most frequent being leucovorin (LV). Another possibility of an MTX schedule is the repeated administration of low-dose MTX (LD-MTX) without LV (3,4).

Nevertheless, there is a fear in clinical practice that HD-MTX chemotherapy can induce drug resistance, resulting in a reduced treatment effect (5). The primary and the most frequent mechanism of resistance to MTX is caused by defects in reduced folate carrier (RCF)-mediated transport, which are caused by mutations in the *RCF* gene or by the downregulation of its expression (6). Other well-described mechanisms of MTX resistance include the overexpression

of DHFR or thymidylate synthase (TYMS) or mutations in genes encoding these enzymes, decreasing their affinity for antifolates. Another important aspect in resistance to MTX is defective polyglutamylation, which substantially reduces the cytotoxicity of MTX. Reductions in MTX polyglutamylation usually result from the decreased expression of folylpolyglutamate synthetase (FPGS) or from inactivating mutations in the *FPGS* gene, as well as from the increased expression of folylpolyglutamate hydrolase (FPGH) (7).

Our study focused on a detailed analysis of MTX effects in cell lines derived from two types of pediatric solid tumors, medulloblastoma and osteosarcoma, which were chosen on the basis of their different histogenetic origin and because MTX is typically included in therapeutic protocols for both. The main aim of this study was to analyze the effects of treatment with MTX at concentrations comparable to the MTX plasma levels in patients treated with high-dose or low-dose MTX. Furthermore, an extremely important part of the treatment with high-dose MTX in clinical practice is the administration of LV as an antidote to reduce MTX toxicity in normal cells. Thus, the combined application of MTX and LV was also included in our experiments. An analysis of the expression of genes involved in the mechanisms of resistance to MTX was the final component of our study; the results helped us to elucidate the mechanisms of the various responses to MTX among the examined cell lines.

Materials and methods

Cell lines. Two reference cell lines and two cell lines derived in our laboratory were used in this study. Daoy (ATCC HTB-186™) medulloblastoma and Saos-2 (ATCC HTB-85™) osteosarcoma cell lines were purchased from the American Type Culture Collection (Manassas, VA, USA). MBL-02 is an in-house cell line derived previously from a biopsy sample obtained from a 7-year-old girl suffering from desmoplastic medulloblastoma (8). The OSA-08 cell line was newly derived from a biopsy sample obtained from an 11-year-old boy surgically treated for conventional osteosarcoma. The Research Ethics Committee of the School of Medicine (Masaryk University, Brno, Czech Republic) approved the study protocol, and a written statement of informed consent was obtained from each patient or his/her legal guardian.

Cell culture. Cells were grown in Dulbecco's modified Eagle's medium (DMEM) supplemented with 10% (Daoy and Saos-2) or 20% (MBL-02 and OSA-08) fetal bovine serum, 100 IU/ml penicillin, 100 mg/ml streptomycin, and 2 mM glutamine. In addition, the medium for the Daoy cells also contained 1% nonessential amino acids (all cell culture reagents were purchased from PAA, Linz, Austria). Experiments with leucovorin (LV) application were performed in folate-free DMEM (both reagents were purchased from Sigma-Aldrich, St. Louis, MO, USA). Cell culture was performed under standard conditions at 37˚C in a humidified atmosphere containing 5% CO_2.

Chemicals. MTX (Sigma) was prepared as a stock solution at a concentration of 20 mM in 1 M NaOH (Sigma). This stock solution was diluted in DMEM or folate-free DMEM to obtain the final concentrations used in the experiments. For determination of the IC_{50} value, 7 different concentrations of MTX ranging from $1x10^{-4}$ to $1x10^{2}$ μM were tested. For all other experiments, concentrations of 0.1, 1, 10 and 40 μM MTX were used; these concentrations are in the range of MTX plasma levels reached in patients suffering from cancer. The maximum used concentration of MTX, i.e., 40 μM, is comparable with the peak of the MTX plasma concentration achieved during HD-MTX treatment of pediatric solid tumors (4). LV was dissolved in deionized water to prepare a 1 mM stock solution. LV at final concentrations of 10 and 100 nM was prepared in folate-free DMEM.

Table I. Sequences of the primers used for RT-PCR.

Gene	Primer sequences	Product (bp)
RFC1	F: 5'-GCGGGCTTCGTGAAGATC-3' R: 5'-CTGGAACTGCTTGCGGAC-3'	330
DHFR	F: 5'-CAGAACATGGGCATCGGCAAGAACG-3' R: 5'-AAACAGAACTGCCACCAACTATCCA-3'	328
TYMS	F: 5'-CGGGAGACATGGGCCTCGGT-3' R: 5'-GCATCCAGCCCAACCCCTAA-3'	353
FPGS	F: 5'-CACTGGGACGAAGGGGAA-3' R: 5'-GTCATAAGCCCCGCCAAT-3'	322
FPGH	F: 5'-AAAGTACTTGGAGTCTGCAGGTGC-3' R: 5'-TGCAATTGACCTCCAGTGAAGTTCA-3'	327
HSP90AB1	F: 5'-CGCATGAAGGAGACACAGAA-3' R: 5'-TCCCATCAAATTCCTTGAGC-3'	169

MTT assay. To evaluate cell proliferation, an MTT assay to detect the activity of mitochondrial dehydrogenases in living cells was used; 96-well plates were seeded with $1x10^{4}$ cells/well in 200 μl of culture medium, and the cells were allowed to adhere overnight. The medium was then removed and a new medium containing the selected concentrations of MTX described above or control MTX-free medium was added. The plates were incubated under standard conditions, and LV at the chosen concentrations was added after 42 h. To evaluate changes in cell proliferation, medium with reagents was removed and replaced by 200 μl of DMEM containing 3-[4,5-dimethylthiazol-2-yl]-2,5-diphenyltetrazolium bromide (MTT) at 0.5 mg/ml. The plates were then incubated at 37˚C for 2.5 h. Subsequently, the medium was carefully removed, and the formazan crystals were dissolved in 200 μl of DMSO. The absorbance at 570 nm with a reference absorbance at 620 nm was measured using the Sunrise Absorbance Reader (Tecan, Männedorf, Switzerland).

RT-PCR. Differences in the expression of MTX resistance-related genes in the cell lines under standard conditions were evaluated using RT-PCR. Total RNA was extracted using the GenElute™ Mammalian Total RNA Miniprep kit (Sigma), and its concentration and integrity were determined spectrophotometrically. For all samples, equal amounts of RNA (i.e.,

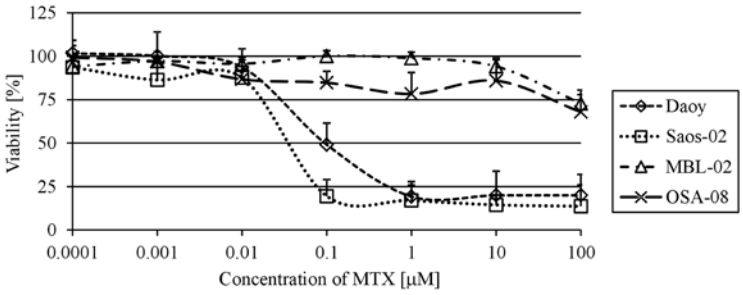

Figure 1. Dose-response curves and IC_{50} values of MTX. Cells were incubated with different doses of MTX for 6 days. Cell viability was analyzed using the MTT assay. Data are presented as the means + standard deviations. x-axis, doses of MTX in μM. y-axis, percentage of viability relative to the untreated cells. MTX, methotrexate.

25 ng of RNA per 1 μl of total reaction volume) were reverse transcribed into cDNA using M-MLV (Top-Bio, Prague, Czech Republic) and oligo dT (Qiagen, Hilden, Germany) priming. PCR was carried out in 25 μl reactions containing 12.5 μl of PPP master mix, 0.5 μl of PCR enhancer (both from Top-Bio), 0.5 μM of each primer and 5 μl of diluted cDNA. The primers used for *RFC1*, *DHFR*, *TYMS*, *FPGS*, *FPGH* and *HSP90AB1* are described in Table I. A total of 10 μl of the PCR product was loaded onto a 2% agarose gel stained with Midori Green (Nippon Genetics, Dueren, Germany) and examined after electrophoresis. The optical density was stained and quantified using ImageJ software (9). The data were normalized to *HSP90AB1* expression.

Flow cytometry. To evaluate changes in the cell cycle, $1.2x10^5$ cells were seeded in 25 cm^2 Petri dishes and allowed to attach overnight. The cells were then treated with MTX for 3 or 6 days. Both the detached and adherent cells were harvested together, fixed with 70% ethanol and stained with Vindelov's solution [0.01 M Tris, 10 μg/ml RNase, 50 μg/ml PI and 1 mM NaCl (all from Sigma)] at 37˚C for 30 min.

To quantify the rate of apoptosis, $1x10^6$ cells were seeded in 75 cm^2 Petri dishes and allowed to attach overnight. The cells were treated with MTX for 1 or 3 days. Both the detached and adherent cells were harvested together, fixed with 3% paraformaldehyde (Sigma) at room temperature for 30 min, permeabilized in 0.2% Triton X-100 (Sigma) for 1 min, and incubated with 2% BSA (PAA) for 10 min to block nonspecific antibody binding. The cells were then treated with a rabbit polyclonal anti-cleaved caspase-3 (Asp-175) primary antibody (dilution 1:250, cat. no. 9661; Cell Signaling Technology, Beverly, MA, USA) at 37˚C for 60 min. After washing with PBS twice, goat anti-rabbit IgG conjugated with Alexa Fluor® 488 (dilution 1:300, cat. no. A-11008; Life Technologies, Carlsbad, CA, USA) was applied at 37˚C for 45 min.

The BD FACSVerse™ flow cytometer with BD FACSuite software (Beckton Dickinson, San Jose, CA, USA) was employed to analyze both the cell cycle and frequency of caspase-3-positive cells at the intervals specified above. Ten thousand events per sample were evaluated in all experiments.

Results

Determination of MTX IC_{50}. To confirm that the Daoy and Saos-2 reference cell lines are useful models for the examination of the MTX effects on medulloblastoma and osteosarcoma cells, the IC_{50} values were first determined. Using the MTT assay, we analyzed cell viability at day 6 of MTX treatment in a range of MTX concentrations from $1x10^{-4}$ to $1x10^2$ μM. Both of these cell lines showed a very similar IC_{50} value: $9.5x10^{-2}$ μM for Daoy cells and $3.5x10^{-2}$ μM for Saos-2 cells (Fig. 1). In contrast, neither the MBL-02 medulloblastoma nor the OSA-08 osteosarcoma patient-derived cell lines reached the IC_{50} value within the concentrations of MTX used. The highest concentration of MTX used for experiments with the reference cell lines, i.e., 100 μM, only led to 27 and 32% decreases in viability when compared with the untreated MBL-02 and OSA-08 cells, respectively.

Effect of MTX and 'leucovorin rescue' treatment on cell proliferation. To analyze the effects of MTX on cell proliferation, concentrations corresponding to MTX plasma levels were used. Daoy (Fig. 2A) and Saos-2 (Fig. 2D) cell lines showed evident cytostatic effects at day 6 of treatment with MTX at all the chosen concentrations. For Saos-2 cells, no statistically significant differences were observed among all the different MTX treatments. It was also apparent that treatment with 0.1 μM MTX decreased the proliferation of Daoy cells to a significantly lesser extent than the other MTX concentrations. Both the MBL-02 and OSA-08 patient-derived cell lines did not show any marked decrease in the number of viable cells within the concentration interval from 0.1 to 40 μM. Nevertheless, the MBL-02 medulloblastoma cell line (Fig. 2G) appeared to be more sensitive than the OSA-08 osteosarcoma cell line in terms of cell viability (Fig. 2J).

To determine whether the application of LV influences the observed cytostatic effects of MTX, we added LV at two different concentrations, 10 and 100 nM, to the cultivation medium at 42 h after treatment with MTX. The application of 10 nM LV resulted in a slight but statistically significant increase in the proliferation activity of Daoy (Fig. 2B) and Saos-2 (Fig. 2E) cells pretreated with 0.1 μM MTX. In contrast, the use of an elevated concentration of LV, i.e., 100 nM, caused a statistically significant increase in proliferation activity and an inhibition of MTX action in both cell lines pretreated with 0.1 μM MTX (Fig. 2C and F). The cytostatic effects of higher concentrations of MTX were not affected by LV in these cell lines, and the MTX-pretreated in-house cell lines did not respond to the application of LV (Fig. 2H, I, K and L).

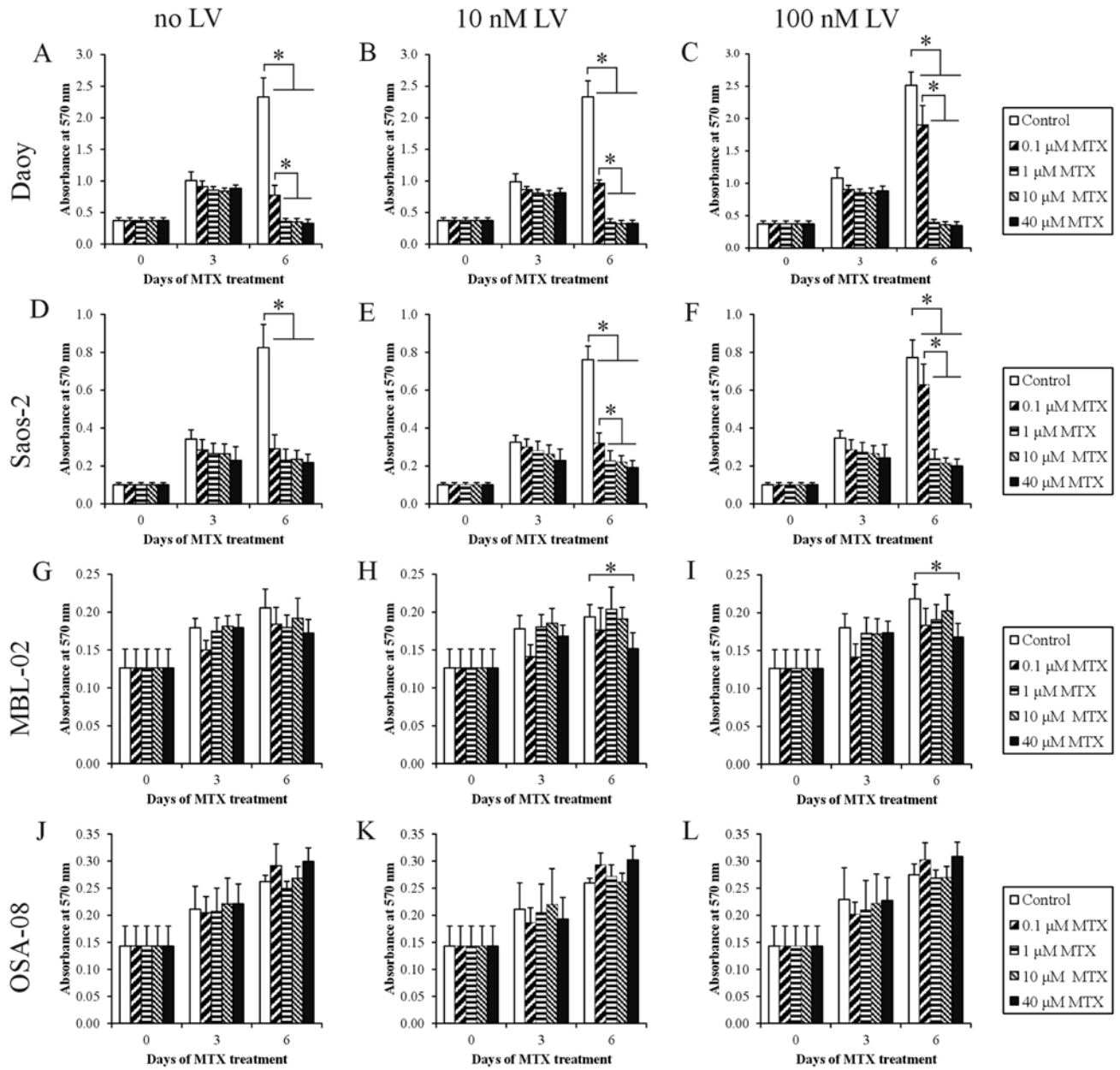

Figure 2. Cell viability after treatment with MTX in combination with LV. Cell viability was measured using the MTT assay before treatment and at day 3 and 6 of incubation with MTX. LV was administered 42 h after the initial treatment with MTX. x-axis, days of treatment. y-axis, absorbance measured at 570 nm. The data represent the means + SEM and were analyzed using ANOVA followed by the Fisher-LSD post-hoc test ($^{*}p<0.05$, significant difference between two treatments). MTX, methotrexate; LV, leucovorin.

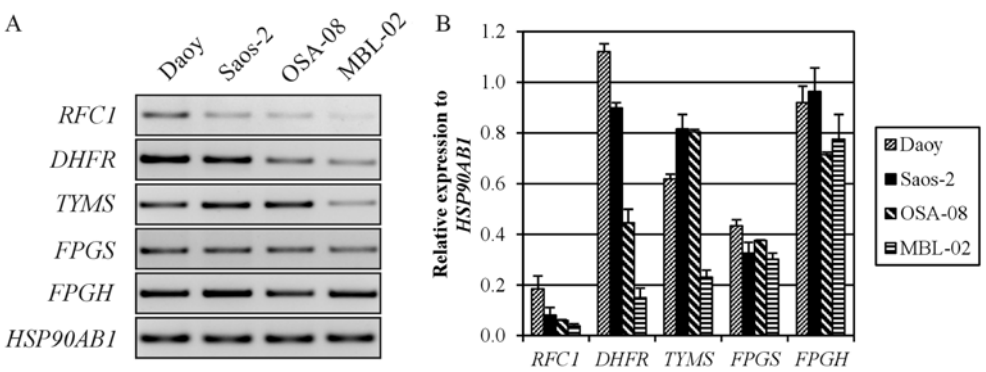

Figure 3. Analysis of gene expression of MTX resistance-related genes. (A) Representative agarose gel. (B) PCR analysis of the mRNA expression of MTX resistance-related genes. The expression of selected genes was quantified using densitometry and was related to the expression of the HSP90AB1 housekeeping gene. x-axis, MTX resistance-related genes. y-axis, expression of the selected genes as related to HSP90AB1. MTX, methotrexate.

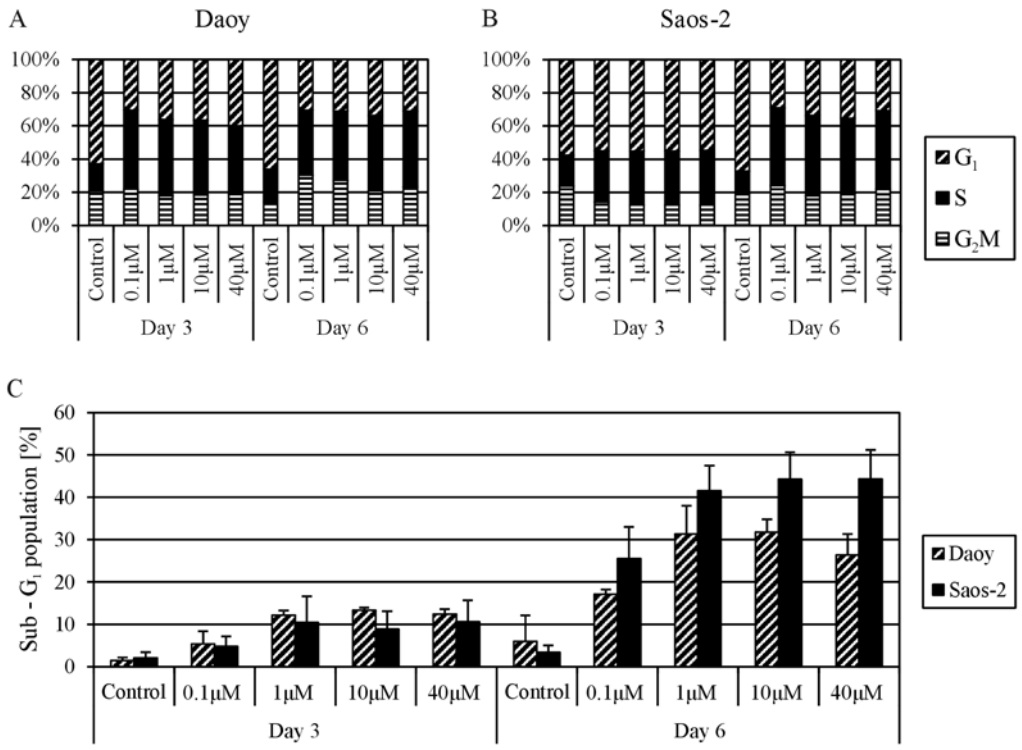

Figure 4. (A and B) Flow cytometric analysis of the cell cycle in Daoy and Saos-2 cells following MTX treatment. Cells were analyzed at day 3 and 6 of incubation with MTX. (C) The percentage of the sub-G_1 population was evaluated at the same time points. x-axis, doses of MTX and days of treatment (A-C). y-axis, percentage of cells in specific phases of the cell cycle (A and B); percentage of cells in sub-G_1 phase (C). MTX, methotrexate.

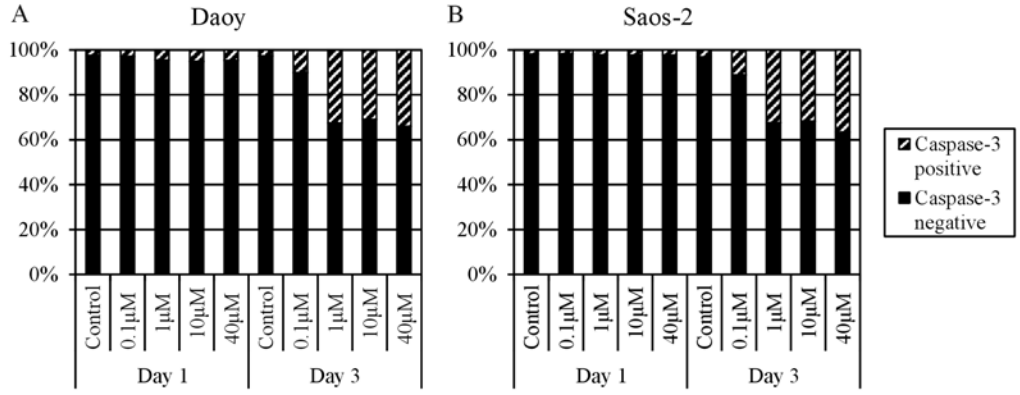

Figure 5. Flow cytometric analysis of caspase-3 positivity in (A) Daoy and (B) Saos-2 cells following MTX treatment. Cells were analyzed at day 1 and 3 of incubation. x-axis, doses of MTX and days of treatment. y-axis, percentage of caspase-3-positive/negative cells in the cell populations. MTX, methotrexate.

Expression of MTX resistance-related genes. To understand the strong differences in MTX toxicity between our in-house cell lines (MBL-02 and OSA-08) and the reference cell lines obtained from ATCC (Daoy and Saos-2), we examined the expression of genes involved in the resistance of tumor cells to MTX (Fig. 3). For this RT-PCR expression analysis, we chose genes encoding the main membrane transporter of MTX, i.e., RFC, two key enzyme targets for MTX, i.e., DHFR and TYMS, and two enzymes catalyzing the glutamylation of MTX, i.e., FPGS and FPGH. The Daoy medulloblastoma cells showed higher relative expression of the *RFC1*, *DHFR* and *TYMS* genes, whereas the expression of these genes was very weak in the MBL-02 medulloblastoma cells. In contrast, both osteosarcoma cell lines displayed similar expression levels of MTX resistance-related genes, with the exception of *DHFR*, the expression level of which was also decreased in the OSA-08 cells.

Effect of MTX on the cell cycle and cell death. Based on the results of previous experiments, both MTX-responding cell lines, i.e., the Daoy and Saos-2 lines, were chosen for cell cycle analysis. The cells were treated with different concentrations of MTX, and the proportions of cells in sub-G_1, G_1, S and G_2/M phases were determined using flow cytometry at day 3 and 6 of treatment with MTX. All MTX concentrations had the same effect on the distribution of the cell cycle phases; an increase

in cells in the S phase was accompanied by a decrease in cells in the G_1 phase in the treated cell lines compared with the untreated controls. Importantly, this phenomenon was noted sooner in the Daoy cells, at day 3 of MTX treatment (Fig. 4A), but was partially delayed in the Saos-2 cells (Fig. 4B). The analysis of the sub-G_1 population revealed cytotoxic effects of MTX on both cell lines (Fig. 4C). The population of cells with reduced DNA content markedly increased at day 6 of treatment. Furthermore, this trend was more apparent in the Saos-2 cells; the sub-G_1 population was >40% in the Saos-2 cells and ~30% in the Daoy cells. The cytotoxic effect of MTX at concentrations ranging from 1 to 40 μM was nearly the same in both cell lines.

To prove whether the increase in the sub-G_1 proportion after MTX treatment is caused by apoptosis induction, the MTX-treated cell populations were labeled with an anti-active caspase-3 antibody at day 1 and 3 of MTX application. Both cell lines showed a >30% increase in caspase-3-positive cells at day 3 of treatment with 1, 10 or 40 μM MTX. In contrast, treatment with 0.1 μM MTX led to a 7-8% increase in caspase-3-positive cells in comparison to the control cells (Fig. 5).

Discussion

At present, the standard protocol for cancer treatment with MTX includes the application of HD-MTX, defined as >1 g/m^2 of body surface, in combination with leucovorin, which enables reaching high plasma concentrations with enhanced anticancer and cytotoxic effects (10). 'Leucovorin rescue' is administered in a specific time schedule after treatment with MTX, usually from 24 to 42 h, to protect non-cancerous proliferating cells from the side effects of MTX. Nevertheless, the toxicity of MTX may induce myelosuppression, mucositis, nephrotoxicity, hepatotoxicity, and, in severe cases, multi-organ failure (11). Although MTX has long been an integral part of many therapeutic regimens, a definite agreement in regards to MTX dosage and timetables and/or LV treatment is still lacking (12).

The main aim of this study was to analyze the effects of MTX on cell lines derived from two types of pediatric solid tumors, medulloblastoma and osteosarcoma, and to determine how these cell lines respond to doses of MTX that correspond to concentrations in a patient's plasma during administration in clinical practice.

Daoy medulloblastoma and Saos-2 osteosarcoma cell lines were chosen as reference cell lines for this study and were compared to two other cell lines that were derived in our laboratory from these tumors. The Saos-2 osteosarcoma cells were apparently more sensitive to treatment with MTX than the Daoy cells, as revealed by determination of the IC_{50} value (Fig. 1); however, the IC_{50} value obtained for both of these cell lines was within a similar range of concentrations, i.e., 10^{-8} M MTX. These results are in accordance with those obtained by other research groups (5,13). The negative effect of MTX on cell proliferation was clearly evident at day 6 of treatment (Fig. 1) and importantly was in the same concentration range, from 1 to 40 μM, for both of these cell lines. In contrast, only a slight cytotoxic effect of 0.1 μM MTX was able to be reverted by LV (Fig. 2). This finding can be explained by an incomplete inhibition of DHFR by a concentration lower than 1 μM of MTX, as described by Assaraf *et al* (14) on the basis of computational simulation.

Both of our in-house cell lines, i.e., MBL-02 medulloblastoma and OSA-08 osteosarcoma cell lines, appeared to be strongly resistant to MTX; 100 μM MTX did not induce a 50% inhibitory effect in these cells. One of the possible explanations for this difference is the low proliferation rate of these tumor cells in comparison with the reference cell lines (15). No observable effect of LV in these cell lines could be explained by the same mechanisms since treatment with MTX is targeted to quickly proliferating tumor cells.

Other possible specific mechanisms of resistance include impaired transmembrane uptake, alterations in the expression or activity of target enzymes, or impaired intracellular polyglutamylation as a determining process of drug efficacy (6). The *RFC1* gene, which encodes the transmembrane solute carrier and is considered to be a main MTX transporting pathway to the cytoplasm (16), was only expressed weakly in our in-house cell lines (Fig. 3). Consequently, the low levels of RCF may have caused a decrease in MTX intracellular availability. Conversely, high levels of *DHFR* expression were detected in both the Daoy and Saos-2 cells compared with these levels in the in-house cell lines (Fig. 3). On the one hand, increased levels of DHFR have been commonly observed in cells exhibiting an MTX-resistant phenotype (17). On the other hand, this key enzyme involved in the *de novo* synthesis of purine and pyrimidine precursors plays a critical role in cell growth and proliferation, and its high expression in rapidly proliferating cells is thus expected (2,18). Although the expression levels of *TYMS* in both osteosarcoma cell lines were identical, marked differences in the expression of this gene were detected between the medulloblastoma cell lines, with higher levels of *TYMS* found in Daoy cells with higher proliferation activity (Fig. 3). The product of the *TYMS* gene catalyzes dUMP conversion into dTMP and thus provides the sole source of deoxythymidylate for DNA biosynthesis (6). In fact, ectopic TYMS expression has been shown to promote cell proliferation *in vitro*, and the high expression of TYMS in tumor tissue is also associated with poor clinical outcome in some types of cancers (19). Another mechanism of resistance to MTX affects the ratio of FPGS/FPGH since polyglutamylated MTX has a substantially longer half-life than monoglutamated MTX (20). Nevertheless, all four cell lines showed similar expression levels of both *FPGS* and *FPGH* (Fig. 3); thus, the differences in MTX effects on cell proliferation were not caused by changes in MTX polyglutamylation.

The flow cytometric analysis of the MTX-sensitive cell lines, i.e., Daoy and Saos-2 cells, clearly confirmed the two main effects of MTX on tumor cells that are responsible for its ability to restrict cell proliferation. First, the cell cycle was arrested in S-phase due to the depletion of nucleotide precursors; our results showed apparent MTX-induced cell cycle arrest in S-phase (Fig. 4). Similar findings were previously described for cell lines derived from adrenocortical carcinoma (21), glioblastoma (22) and lung carcinoma (23). Notably, we did not observe any significant differences in the effects of the MTX concentrations ranging from 0.1 to 40 μM on the distribution of cell cycle phases (Fig. 4). Secondly, the induction of cell death detected as the sub-G_1 fraction following treatment with MTX

was also involved in proliferation failure (Fig. 4). Furthermore, we noted a marked difference between treatment with 0.1 μM MTX and the treatments with other concentrations (Fig. 4), and these results were in accordance with those achieved by the detection of activated caspase-3-positive cells (Fig. 5). Caspase-3-dependent/p53-independent apoptosis induced by MTX was previously described in MCF-7 breast carcinoma cells (24). The apoptosis induced in the Saos-2 and Daoy cells was also p53-independent since Saos-2 cells do not express p53 (25) and the C242F mutation in the *TP53* gene, which disables the transactivation function of the p53 protein, was proven in Daoy cells (26,27),

To summarize, our results showed that treatment with MTX significantly decreased proliferation activity, inhibited the cell cycle at S-phase and induced apoptosis in the Daoy and Saos-2 reference cell lines. Such effects apparently belong to the DHFR-mediated mechanism of MTX action and are based on the depletion of purine and pyrimidine precursors necessary for the biosynthesis of nucleic acids. Importantly, we noted no difference in these effects after treatment with various doses of MTX ranging from 1 to 40 μM. These findings suggest the possibility of achieving the same outcome with the application of low-dose MTX, which is an extremely important result, particularly for clinical practice, and may explain the lack of clinical advantage of HD-MTX in children with advanced lymphoblastic lymphomas vs. low doses (28). Moreover, the combined application of MTX together with LV did not produce any detectable effect, with exception of a partial reduction in MTX toxicity after the use of the lowest concentration of MTX, i.e., 0.1 μM.

Acknowledgements

The present study was supported by the grant IGA MZCR NT14327-3.

References

1. Takimoto CH: New Antifolates: Pharmacology and Clinical Applications. Oncologist 1: 68-81, 1996.
2. Neradil J, Pavlasova G and Veselska R: New mechanisms for an old drug; DHFR- and non-DHFR-mediated effects of methotrexate in cancer cells. Klin Onkol 25: 2S87-2S92, 2012.
3. Sterba J, Valík D, Bajciová V, Kadlecová V, Gregorová V and Mendelová D: High-dose methotrexate and/or leucovorin rescue for the treatment of children with lymphoblastic malignancies: do we really know why, when and how? Neoplasma 52: 456-463, 2005.
4. Sterba J, Dusek L, Demlova R and Valik D: Pretreatment plasma folate modulates the pharmacodynamic effect of high-dose methotrexate in children with acute lymphoblastic leukemia and non-Hodgkin lymphoma: 'folate overrescue' concept revisited. Clin Chem 52: 692-700, 2006.
5. Wang JJ and Li GJ: Relationship between RFC gene expression and intracellular drug concentration in methotrexate-resistant osteosarcoma cells. Genet Mol Res 13: 5313-5321, 2014.
6. Fotoohi AK and Albertioni F: Mechanisms of antifolate resistance and methotrexate efficacy in leukemia cells. Leuk Lymphoma 49: 410-426, 2008.
7. Assaraf YG: Molecular basis of antifolate resistance. Cancer Metastasis Rev 26: 153-181, 2007.
8. Veselska R, Neradil J, Nekulova M, Dobrucka L, Vojtesek B, Sterba J and Zitterbart K: Intracellular distribution of the ΔNp73 protein isoform in medulloblastoma cells: a study with newly generated rabbit polyclonal antibodies. Histol Histopathol 28: 913-924, 2013.
9. Schneider CA, Rasband WS and Eliceiri KW: NIH Image to ImageJ: 25 years of image analysis. Nat Methods 9: 671-675, 2012.
10. Holmboe L, Andersen AM, Mørkrid L, Slørdal L and Hall KS: High dose methotrexate chemotherapy: pharmacokinetics, folate and toxicity in osteosarcoma patients. Br J Clin Pharmacol 73: 106-114, 2012.
11. Rahiem Ahmed YAA and Hasan Y: Prevention and management of high dose methotrexate toxicity. J Cancer Sci Ther 5: 106-112, 2013.
12. Cohen IJ1 and Wolff JE: How long can folinic acid rescue be delayed after high-dose methotrexate without toxicity? Pediatr Blood Cancer 61: 7-10, 2014.
13. Najim N, Podmore ID, McGown A and Estlin EJ: Methionine restriction reduces the chemosensitivity of central nervous system tumour cell lines. Anticancer Res 29: 3103-3108, 2009.
14. Assaraf YG, Ifergan I, Kadry WN and Pinter RY: Computer modelling of antifolate inhibition of folate metabolism using hybrid functional petri nets. J Theor Biol 240: 637-647, 2006.
15. Bastian L, Einsiedel HG, Henze G, Seeger K and Shalapour S: The sequence of application of methotrexate and histone deacetylase inhibitors determines either a synergistic or an antagonistic response in childhood acute lymphoblastic leukemia cells. Leukemia 25: 359-361, 2011.
16. Huang Y: Pharmacogenetics/genomics of membrane transporters in cancer chemotherapy. Cancer Metastasis Rev 26: 183-201, 2007.
17. Yoon SA, Choi JR, Kim JO, Shin JY, Zhang X and Kang JH: Influence of reduced folate carrier and dihydrofolate reductase genes on methotrexate-induced cytotoxicity. Cancer Res Treat 42: 163-171, 2010.
18. Nazki FH, Sameer AS and Ganaie BA: Folate: metabolism, genes, polymorphisms and the associated diseases. Gene 533: 11-20, 2014.
19. Furuta E, Okuda H, Kobayashi A and Watabe K: Metabolic genes in cancer: their roles in tumor progression and clinical implications. Biochim Biophys Acta 1805: 141-152, 2010.
20. Rots MG, Willey JC, Jansen G, van Zantwijk CH, Noordhuis P, DeMuth JP, Kuiper E, Veerman AJ, Pieters R and Peters GJ: mRNA expression levels of methotrexate resistance-related proteins in childhood leukemia as determined by a standardized competitive template-based RT-PCR method. Leukemia 14: 2166-2175, 2000.
21. Nilubol N, Zhang L, Shen M, Zhang YQ, He M, Austin CP and Kebebew E: Four clinically utilized drugs were identified and validated for treatment of adrenocortical cancer using quantitative high-throughput screening. J Transl Med 10: 198, 2012.
22. Capelôa T, Caramelo F, Fontes-Ribeiro C, Gomes C and Silva AP: Role of methamphetamine on glioblastoma cytotoxicity induced by Doxorubicin and methotrexate. Neurotox Res 26: 216-227, 2014.
23. Yan KH, Lee LM, Hsieh MC, Yan MD, Yao CJ, Chang PY, Chen TL, Chang HY, Cheng AL, Lai GM and Chuang SE: Aspirin antagonizes the cytotoxic effect of methotrexate in lung cancer cells. Oncol Rep 30: 1497-1505, 2013.
24. Hattangadi DK, DeMasters GA, Walker TD, Jones KR, Di X, Newsham IF and Gewirtz DA: Influence of p53 and caspase 3 activity on cell death and senescence in response to methotrexate in the breast tumor cell. Biochem Pharmacol 68: 1699-1708, 2004.
25. Hellwinkel OJ, Müller J, Pollmann A and Kabisch H: Osteosarcoma cell lines display variable individual reactions on wildtype p53 and Rb tumour-suppressor transgenes. J Gene Med 7: 407-419, 2005.
26. Jordan JJ, Inga A, Conway K, Edmiston S, Carey LA, Wu L and Resnick MA: Altered-function p53 missense mutations identified in breast cancers can have subtle effects on transactivation. Mol Cancer Res 8: 701-716, 2010.
27. Künkele A, De Preter K, Heukamp L, Thor T, Pajtler KW, Hartmann W, Mittelbronn M, Grotzer MA, Deubzer HE, Speleman F, Schramm A, Eggert A and Schulte JH: Pharmacological activation of the p53 pathway by nutlin-3 exerts anti-tumoral effects in medulloblastomas. Neuro Oncol 14: 859-869, 2012.
28. Termuhlen AM, Smith LM, Perkins SL, Lones M, Finlay JL, Weinstein H, Gross TG and Abromowitch M: Disseminated lymphoblastic lymphoma in children and adolescents: results of the COG A5971 trial: a report from the Children's Oncology Group. Br J Haematol 162: 792-801, 2013.

CANCER CELL INTERNATIONAL

PRIMARY RESEARCH Open Access

The ATRA-induced differentiation of medulloblastoma cells is enhanced with LOX/COX inhibitors: an analysis of gene expression

Petr Chlapek[1], Jakub Neradil[1,3], Martina Redova[1], Karel Zitterbart[1,2], Jaroslav Sterba[2,3] and Renata Veselska[1,2*]

Abstract

Background: A detailed analysis of the expression of 440 cancer-related genes was performed after the combined treatment of medulloblastoma cells with all-*trans* retinoic acid (ATRA) and inhibitors of lipoxygenases (LOX) and cyclooxygenases (COX). The combinations of retinoids and celecoxib as a COX-2 inhibitor were reported to be effective in some regimens of metronomic therapy of relapsed solid tumors with poor prognosis. Our previous findings on neuroblastoma cells using expression profiling showed that LOX/COX inhibitors have the capability of enhancing the differentiating action of ATRA. Presented study focused on the continuation of our previous work to confirm the possibility of enhancing ATRA-induced cell differentiation in these cell lines via the application of LOX/COX inhibitors. This study provides more detailed information concerning the mechanisms of the enhancement of the ATRA-induced differentiation of medulloblastoma cells.

Methods: The Daoy and D283 Med medulloblastoma cell lines were chosen for this study. Caffeic acid (an inhibitor of 5-LOX) and celecoxib (an inhibitor on COX-2) were used in combined treatment with ATRA. The expression profiling was performed using Human Cancer Oligo GEArray membranes, and the most promising results were verified using RT-PCR.

Results: The expression profiling of the selected cancer-related genes clearly confirmed that the differentiating effects of ATRA should be enhanced via its combined administration with caffeic acid or celecoxib. This effect was detected in both cell lines. An increased expression of the genes that encoded the proteins participating in induced differentiation and cytoskeleton remodeling was detected in both cell lines in a concentration-dependent manner. This effect was also observed for the *CDKN1A* gene encoding the p21 protein, which is an important regulator of the cell cycle, and for the genes encoding proteins that are associated with proteasome activity. Furthermore, our results showed that D283 Med cells are significantly more sensitive to treatment with ATRA alone than Daoy cells.

Conclusions: The obtained results on medulloblastoma cell lines are in accordance with our previous findings on neuroblastoma cells and confirm our hypothesis concerning the common mechanism of the enhancement of ATRA-induced cell differentiation in various types of pediatric solid tumors.

Keywords: All-*trans* retinoic acid, Caffeic acid, Celecoxib, Medullobastoma, LOX and COX inhibitors

* Correspondence: veselska@sci.muni.cz
[1]Department of Experimental Biology - Laboratory of Tumor Biology, School of Science, Masaryk University, Kotlarska 2, 611 37 Brno, Czech Republic
[2]Department of Pediatric Oncology, University Hospital Brno and School of Medicine, Masaryk University, Cernopolni 9, 613 00 Brno, Czech Republic
Full list of author information is available at the end of the article

Background

Medulloblastoma (MBL), an embryonal neuroectodermal tumor of the cerebellum, is the most common type of malignant brain tumor in children. Although recent advances in MBL therapy have led to a dramatic increase in survival rate, the mortality rate is currently approximately 20–40% [1]. Moreover, MBL survivors are often affected by treatment-related side effects such as growth hormone deficiency, gonadal alterations, hypo- or hyperthyroidism, and long-term cognitive, neuropsychological and academic impairments, etc. New approaches are thus needed to improve the survival rate and to reduce the negative side effects of MBL treatment [2].

The induced differentiation of tumor cells has become a promising strategy in modern antineoplastic therapy. Retinoids, which are derivatives of vitamin A, are the most frequently used group of cell differentiation inducers. The regulation of relevant cell signaling pathways via retinoids is based on the activation of two groups of nuclear receptors, RAR and RXR [3,4]. These activated receptors can influence the transcription either directly by binding to the DNA or indirectly by interacting with other transcription factors [5,6].

In general, retinoids play an important role in cell proliferation and differentiation, and their efficacy in the treatment of various types of tumor cells has been described both *in vivo* and *in vitro* [7-11]. However, the toxicity of and intrinsic or acquired resistance to retinoids substantially limit their use in clinical protocols [12].

Therefore, special attention has been paid to treating cancer cells with a combination of retinoids and other compounds that may enhance or prolong their antineoplastic effects. The enhancing effects of these modulators were described in several clinical trials focused on the treatment of leukemia [13-16]; they were also demonstrated under *in vitro* conditions using tumor cells of a neurogenic origin [17-20].

To date, many studies on various cancer cell lines have reported the additive or synergistic effects of combined treatment with retinoids and inhibitors of lipoxygenases (LOX) [21-24] or cyclooxygenases (COX) [25-27]. The molecular mechanisms of this modulation remain unknown, but the published data suggest the inhibition of the retinoid degradation pathways [28] or the cooperation of compounds that are utilized in cell signaling inhibition (through the PI3K/Akt pathway) or the induction of the mitochondrial apoptotic pathway [25].

Our previous studies were also focused on how to enhance the differentiation effect of all-*trans* retinoic acid (ATRA) through its combination with LOX/COX inhibitors in neuroblastoma cell lines [20,29]. In these experiments, we used caffeic acid (CA) as an inhibitor of 5-LOX and celecoxib (CX) as an inhibitor of COX-2. Our results clearly confirmed that the ATRA-induced differentiation of neuroblastoma cells can be enhanced via the combined application of these inhibitors [20,29]. Furthermore, data from the expression profiling of the treated cells showed an increase in the expression of the genes involved in the process of retinoid-induced neuronal differentiation, especially in cytoskeleton remodeling after combined treatment [20].

To verify these findings, we used a different type of neurogenic tumor cells, i.e. established medulloblastoma cell lines but the same experimental design for the treatment of these cells. Our new data from the gene expression profiling of medulloblastoma cells also demonstrated the capability of CA or CX to enhance the cell differentiation induced via ATRA.

Methods

Cell lines and cell culture

Daoy (ATCC HTB-186™) and D283 Med (ATCC HTB-185™) medulloblastoma cell lines were used in this study. These cell lines were chosen according their different origin (primary tumor vs. metastatic site) and their different biological features as described by supplier in the documentation to cover known heterogeneity in this disease. Both of these cell lines are widely used in medulloblastoma research. These cell lines were maintained in Dulbecco's modified Eagle's medium (DMEM)/Ham's F-12 medium mixture (1:1) supplemented with 20% fetal calf serum, 1% non-essential amino acids, 2 mM L-glutamine, 100 $IU.ml^{-1}$ penicillin, and 100 $mg.ml^{-1}$ streptomycin (all purchased from PAA Laboratories, Linz, Austria). Cell culture was performed under standard conditions at 37°C in a humidified atmosphere containing 5% CO_2. Both of these cell lines were subcultured 1–2 times weekly. The Research Ethics Committee of the University Hospital Brno approved the study protocol.

Chemicals

ATRA (Sigma-Aldrich, St. Louis, MO, USA), CA (Sigma), and CX (LKT Laboratories, St. Paul, MN, USA) were prepared as stock solutions at concentrations of 100 mM in dimethyl sulfoxide (DMSO) (Sigma). For experiments, these stock solutions were diluted in fresh cell culture medium to obtain final concentrations as follow: 0.05 and 0.1 μM of ATRA for the treatment of D283 Med cells, 1 and 10 μM of ATRA for the treatment of Daoy cells, 13 and 52 μM of CA, as well as 10 and 50 μM of CX for the treatment of both cell lines.

Experimental design

The experimental design was the same as that in our previous studies [20,29]: the cell populations were treated with ATRA alone or with ATRA and an inhibitor (CA or CX) at the concentrations mentioned above. The concentrations of ATRA and inhibitors were chosen on the basis

of previously published data, and they corresponded to the plasma levels obtained using these compounds therapeutically [23,30-33]. However, lower concentrations of 0.05 and 0.1 μM ATRA were used for treating the D283 Med cells due to the predominant cytotoxic effect on the cell populations at higher concentrations [34]. In all experiments, the cells were seeded into Petri dishes or culture flasks 24 h prior to the treatment. Untreated cells were used as controls in all experiments.

Expression profiling

The total RNA of the treated cell populations was isolated using the GenElute™ Mammalian Total RNA Miniprep Kit (Sigma), and its concentration and integrity were determined using a spectrophotometer. This isolation of RNA was performed at day 3 after treatment. The conversion of the experimental RNA into cDNA and its further transcription and biotin-UTP labeling was performed using TrueLabeling-AMP™ 2.0 cRNA (SABiosciences, Frederick, MD, USA). After purification with the SuperArray ArrayGrade cRNA Cleanup Kit, the labeled target cRNA was hybridized to Human Cancer OHS-802 Oligo GEArray membranes that profile 440 genes (both SABiosciences). The expression levels of each gene were detected via chemiluminescence using the alkaline phosphatase-conjugated streptavidin substrate. The membranes were then recorded using the MultiImage™ II Light Cabinet DE- 500 (Alpha Innotech, CA, USA). The image data were processed and analyzed using the GEArray Expression Analysis Suite software (SABiosciences) with background subtraction. All data were standardized as a ratio of the gene expression intensity to the mean expression intensity of the selected *HSP90AB1* housekeeping gene, which was chosen using the GeNorm [35] and NormFinder [36] software tools. Standardized spot intensity ratios (treated/control samples) were calculated and data filtering criteria were as follows: genes with ratio higher than 2 were rated as upregulated and genes with ratio lower than 0.5 were rated as downregulated. The expression of the specific gene was evaluated as changed if the same trend of change, i.e. upregulation or downregulation was detected at least in four experimental variants (of six in total) regardless the concentrations used for treatment. Cluster analyses were performed using the GEArray Expression Analysis Suite software according to the design of the experiments, i.e., separately for each cell line and inhibitor type. DAVID software tool [37] was used for primary detection of relevant pathways.

RT-PCR

The changes in the expression of the two selected candidate genes were evaluated using RT-PCR. The RNA was isolated as described above. A total of 0.25 μg RNA was then reverse transcribed using M-MLV reverse transcriptase (Top-Bio, Prague, Czech Republic) according to the manufacturer's protocol. RT-PCR was performed on 4 μl cDNA using Taq DNA polymerase 1.1 (Top-Bio) with human primers for the *CDKN1A* and *GDF15* candidate genes as well as the *HSP90AB1* housekeeping gene (Table 1) in 20 μl of the reaction volume. The PCR reaction was performed with denaturation at 94°C for 4 min, annealing at 60°C for 30 s, and elongation at 72°C for 1 min (35 cycles for all primers) (Table 1). A total of 10 μl of the PCR product was loaded on the 1% agarose gel and examined using electrophoresis. The optical density was stained and quantified using ImageJ software [38], and the data were normalized to *HSP90AB1* expression.

Results

The present study was focused on a detailed analysis of Daoy and D283 Med medulloblastoma cells after the combined application of ATRA and LOX/COX inhibitors. CA as the specific inhibitor of 5-LOX and CX as the specific inhibitor of COX-2 were used in these experiments. The changes in the expression of cancer-related genes were evaluated using expression profiling. Furthermore, a detailed analysis of the expression of five candidate genes was performed using RT-PCR to verify the microarray results. We used the same experimental design as our previous studies on neuroblastoma cells [20,29].

In Daoy cells, changes in the expression of 80 cancer-related genes were detected after combined treatment with ATRA and inhibitors (Figure 1A). A total of 29 of these genes demonstrated changed expressions after combinations of ATRA and CA as well as of ATRA and CX. The expressions of another 29 genes were changed only after the combined treatment of ATRA and CA. A total of 22 different genes showed changes in expression after undergoing combined treatment with ATRA and CX (Figure 1A).

In D283 Med cells, the expressions of 37 genes were changed (Figure 1B). Of these, 22 showed changes after combined treatment with ATRA and CA as well as with ATRA and CX. Changes in the expression of another 11 genes were identified after treatment with ATRA and CA only. Similarly, the expressions of 4 different genes were changed after treatment with ATRA and CX only (Figure 1B).

Table 1 Sequences of primers used for RT-PCR

Gene	Primer sequence	Product
CDKN1A	F: 5′ TTA GCA GCG GAA CAA GGA GT 3′	225 bp
	R: 5′ GCC GAG AGA AAA CAG TCC AG 3′	
GDF15	F: 5′ CTC CAG ATT CCG AGA GTT GC 3′	169 bp
	R: 5′ AGA GAT ACG CAG GTG CAG GT 3′	
HSP90AB1	F: 5′ CGC ATG AAG GAG ACA CAG AA 3′	169 bp
	R: 5′ TCC CAT CAA ATT CCT TGA GC 3′	

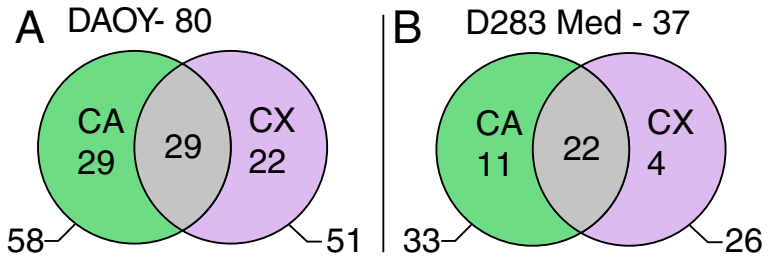

Figure 1 Summary of detected changes in the expression of 440 cancer-related genes after the combined treatment of the Daoy (A) and D283 Med (B) cell lines. The black circles indicate the total number of genes with changed expression after combinations of ATRA with CA or CX. The green areas indicate the number of genes with changed expression after combined treatment with ATRA and CA only. Similarly, the violet areas indicate the number of genes with changed expression after combined treatment with ATRA and CA only. The gray overlays indicate the number of genes that demonstrated changed expressions after treatment with ATRA in both combinations; i.e., with CA as well as with CX.

The data achieved via expression profiling are presented after cluster analysis, which grouped the genes or gene groups by the type of changes in their expressions (Figure 2). Based on this analysis, three typical patterns of changes in gene expression are described:

(i.) Genes with strong concentration-dependent changes in their expressions. This pattern was typical in the I.A, II.A, III.A, and IV.A groups, in which the upregulation of gene expression was detected. This concentration-dependent pattern was also detected in the groups with downregulated gene expressions, i.e., in the I.E., II.D, III.D, and IV.C groups.

(ii.) Genes for which the expression was upregulated (groups I.B and II.C) or downregulated (group III.C) after treatment with lower concentrations of reagents. The use of higher concentrations had no or minimal influence on the expression of these genes.

(iii.) Genes with changes in their expressions after treatment with higher concentrations of reagents only. This pattern was characteristic in the II.B and III.B groups; however, such trends were also obvious in the I.A and IV.A groups.

Similarities in the gene expression changes are summarized in Table 2 and Table 3. The genes with changed expression in a particular cell line after combined treatment with ATRA and both inhibitors (CA or CX) are given: 8 genes were upregulated and 8 genes were downregulated in the Daoy cells; 16 genes were upregulated and 3 were downregulated in the D283 Med cells (Table 2). Two of these genes, *GDF15* and *UBE2L6*, were upregulated in both cell lines after all types of combined treatment (Table 2). Changes in gene expression after the same type of combined treatment (ATRA with CA or ATRA with CX) were identified in both cell lines; 2 of the genes were upregulated and 1 was downregulated after treatment with ATRA and CA, while 8 were upregulated and 1 was downregulated after treatment with ATRA and CX (Table 3).

The analysis of the detected changes in gene expressions showed a concentration-dependent increase in the expression of genes known to be involved in the process of retinoid-induced differentiation and especially of the genes generally associated with the regulation of the cell cycle, of genes involved in mitochondrial metabolism, etc. The observed changes in the expressions of two selected candidate genes - *GDF15* (Figure 3) and *CDKN1A* (Figure 4) - were subsequently verified via RT-PCR.

Discussion

At present, retinoids (powerful inducers of cell differentiation) have become a part of many therapeutic regimens in pediatric oncology, especially in the treatment of solid tumors of neurogenic origin [39-43]. In our previous experiments, we demonstrated the enhancement of the ATRA-induced differentiation of neuroblastoma cells via the combined application of LOX/COX inhibitors [20,29].

In our present study, we profiled the expression of 440 cancer-related genes in medulloblastoma cells after the same type of combined treatment (see above). Our results clearly confirmed our previous finding that ATRA-induced cell differentiation is enhanced via combined treatment with CA (inhibitor of 5-LOX) or with CX (inhibitor of COX-2) because the expression of the genes involved in the process of induced differentiation is increased in a concentration-dependent manner. A comparison of two established medulloblastoma cell lines showed a higher sensitivity in Daoy cells (compared with D283 Med cells) to the combined treatment with ATRA and inhibitors; nevertheless, our pilot experiments indicated that D283 Med cells were apparently more sensitive to the ATRA alone [34,44]. The same difference in sensitivity of Daoy and D283 Med cell lines to the ATRA was already described and the higher sensitivity of D283 Med cells is explained by expression of OTX2, a transcription factor,

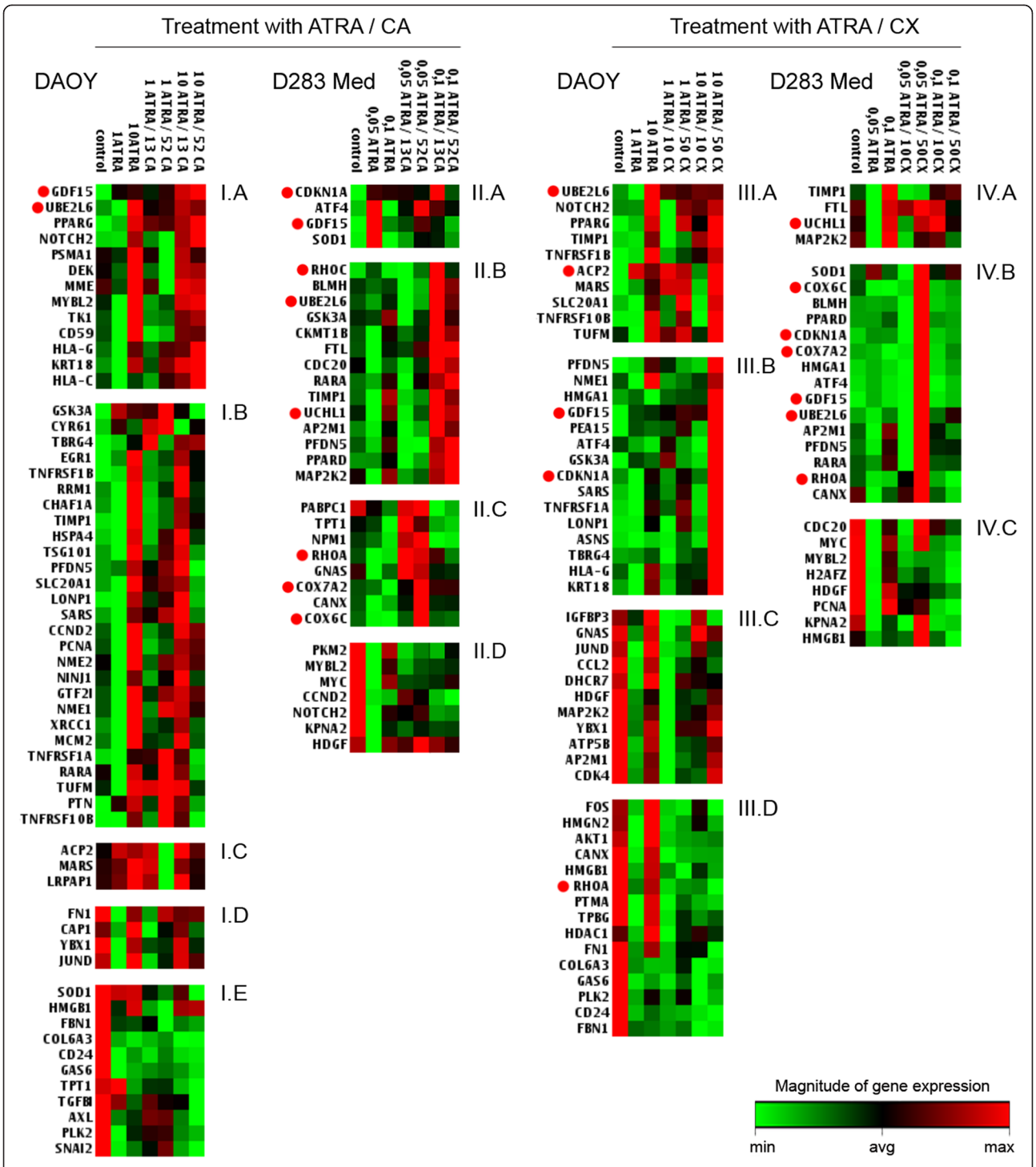

Figure 2 Results of gene cluster analysis after the expression profiling of treated cells. The genes were clustered according to the type of changes in the expression in the respective cell line (Daoy or D283 Med) after the combined treatment with ATRA and inhibitors (CA or CX). The cells were treated with ATRA alone or in combination with CA (an inhibitor of 5-LOX) or CX (an inhibitor of COX-2); numbers indicate the concentration in μM. The green color at the farthest left end of the color scale corresponds to the minimal value; the red color at the farthest right end of the color scale corresponds to the maximal value; the black color in the middle corresponds to the average value. Each of the other values corresponds to a certain color according to its magnitude. The colors are assigned according to the value of the particular gene expression in all samples in the respective experimental variant (I, II, III or IV). Genes discussed in the text in detail are highlighted by red dots.

Table 2 Genes with changed expression in a particular cell line (Daoy or D283 Med) after combined treatment with ATRA and both inhibitors (CA or CX)

Daoy cell line	
Upregulated:	*ACP2,* ***GDF15****, HLA-G, KRT18, MARS, NOTCH2, PPARG,* ***UBE2L6***
Downregulated:	*CD24, COL6A3, FBN1, GAS6, HMGB1, JUND, PLK2, YBX1*
D283 Med cell line	
Upregulated:	*AP2M1, ATF4, BLMH, CANX, CDKN1A, COX6C, COX7A2, FTL,* ***GDF15****, MAP2K2, PFDN5, PPARD, RARA, RHOA, SOD1, TIMP1,* ***UBE2L6****, UCHL1*
Downregulated:	*KPNA2, MYBL2, MYC*

The genes that were influenced via the combinations of both inhibitors are typed in bold.

which was reported as a suppressor of neuronal differentiation in medulloblastoma cells [45].

The three patterns of changes in gene expression described here were very similar to our previous results on neuroblastoma cells [20]. In terms of the individual genes, we noted significant changes in the expression of the *GDF15*, *RHOA*, and *RHOC* genes. Although the expression of the *GDF15* gene was enhanced in both cell lines via combined treatment with ATRA and both inhibitors (Figures 2 and 3), changes in the expression of the *RHOA* and *RHOC* genes were detected in the D283 Med cells only (Figure 2). These two genes are members of the Rho GTPases family and are known to participate in cytoskeleton rearrangement and regulation processes such as changes in cell morphology during cell differentiation, proliferation and motility [46,47]. This finding is in accordance with our pilot study in which the decrease in proliferation activity and in the formation of multicellular aggregates was reported after the combined treatment (using CA or CX) of D283 Med cells [44].

The protein encoded by the *GDF15* gene is an important regulator of cell differentiation during embryonal development, especially in neural tissues [48]. This protein also has other important functions in the regulation of immune response or response to stress factors [49], and some studies have described its role as a paracrine mediator in the p53 cell signaling pathway that can inhibit cell proliferation and induce apoptosis [50,51]. Furthermore, the expression of *GDF15* correlated with the amount of the p21 protein that was encoded by the *CDKN1A* gene [50,51]. Although the overexpression of *GDF15* was detected in both cell lines after combined treatment with both inhibitors (Tables 2 and 3), we observed some differences between these cell lines. The expression of *GDF15* increased in Daoy cells in a concentration-dependent manner (Figures 2 and 3A), but the changes in *GDF15* expression in D283 Med cells were not so obvious (Figures 2 and 3B).

As mentioned above, some previous studies have demonstrated a correlation between the expressions of the *GDF15* and *CDKN1A* genes [50,51]. The *CDKN1A* gene encodes the p21 protein, which serves as an important regulator of the cell cycle progression via the inhibition of cyclin-dependent kinases. In our experiments, the expression of *CDKN1A* was enhanced in both cell lines after combined treatment with ATRA and CX, whereas the combination of ATRA and CA did not show a similar effect (Table 3, Figure 4). The increase in *CDKN1A* expression after treatment with retinoids was described in many human malignancies under *in vivo* and *in vitro* conditions: acute promyelocytic leukemia [52], acute T-lymphoblastic leukemia [53], pre-B lymphoma [54], hepatoblastoma [55,56], and neuroblastoma [57-60]. Our *in vitro* data confirmed these findings (especially in D283 Med cells) and also clearly showed that this effect of ATRA can be enhanced through its combined administration with CX (Figure 4B).

Furthermore, we detected the upregulated expression of the *UBE2L6* gene, which encodes a member of the E2 ubiquitin-conjugating enzyme family in both cell lines after combined treatment with both inhibitors (Tables 2 and 3). The overexpression of the *ACP2* gene encoding a beta-subunit of lysosomal acid phosphatase was observed in Daoy cells after combined treatment with both inhibitors (Table 2). The upregulated expression of both of these genes indicated an increased activity of proteasome in the treated cells. Higher proteasome activity was reported in breast carcinoma cells [61] as well as in acute promyelocytic leukemia cells [62,63] after treatment with retinoids. However, the relationship between retinoids and proteasome activity should be associated with resistance to retinoids [64]. This mechanism of resistance to retinoids, i.e., the increased activity of proteasome in Daoy cells, could be one of the possible explanations for the differing sensitivity demonstrated by these cell lines to ATRA treatment, as reported in our pilot study [44]. This hypothesis is also supported by the fact that the upregulation of the *UCHL1* gene encoding a deubiquitinating

Table 3 Genes with changed expression detected after the same type of combined treatment (ATRA with CA or ATRA with CX) in both cell lines (Daoy and D283 Med)

ATRA/CA	
Upregulated:	***GDF15, UBE2L6***
Downregulated:	*CCND2*
ATRA/CX	
Upregulated:	*ATF4, CDKN1A,* ***GDF15****, HMGA1, HMGB1, PFDN5, TIMP1,* ***UBE2L6***
Downregulated:	*AP2M1*

The genes that were influenced via the combinations of both inhibitors are typed in bold.

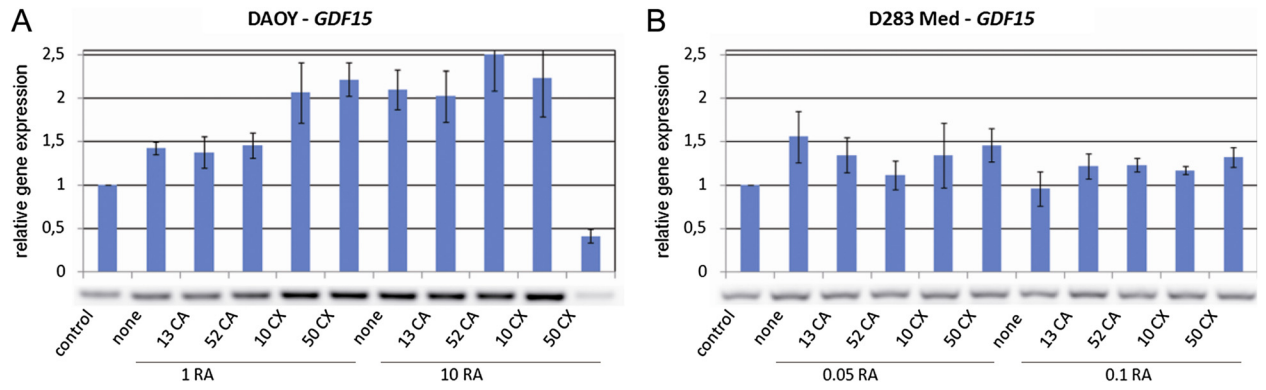

Figure 3 Changes in the expression of the *GDF15* gene in Daoy (A) and D283 Med (B) cells analyzed using RT-PCR. The cells were treated with ATRA alone or in combination with CA (an inhibitor of 5-LOX) or CX (an inhibitor of COX-2); numbers indicate the concentrations of these compounds in μM. Respective numerical data from densitometry for three independent experiments are shown in the graphs: X-axis, treatment condition; Y-axis, relative gene expression. The data represent the means ± SD; they were normalized to the expression of the *HSP90AB1* housekeeping gene and were related to the untreated control cells. Representative electrophoresis is presented for each cell line.

enzyme was detected in more sensitive D283 Med cells after combined treatment with both inhibitors (Table 2). Moreover, the protein encoded by this gene was found solely in mature neurons [65]; its increased expression in D283 Med, which is apparently enhanced via a combined treatment with ATRA and inhibitors, should indicate the neuronal differentiation of D283 Med after experimental treatment.

Higher sensitivity of D283 Med cells to the ATRA-induced neuronal differentiation is also indicated by the overexpression of two genes encoding subunits of cytochrome C oxidase, *COX6C* and *COX7A2*, after both types of combined treatment (Table 2). An increased mitochondrial activity after treatment with retinoids was reported in neuroblastoma cell lines [66], and it was demonstrated that more differentiated neuronal cells exhibit higher oxygen consumption rates as well as metabolic rates [67]. These findings thus support the presumed neuronal differentiation of D283 Med cells treated with ATRA and the capability of CA and CX to enhance this effect. Furthermore, a similar upregulation of these two genes was previously detected in neuroblastoma cell lines after the same type of experimental treatment [20].

The presented results are closely connected to our previously published studies reporting encouraging treatment responses to metronomic therapy in children suffering from some types of relapsed solid tumors with poor prognosis [42,43,68]. In these protocols, retinoids are administered in combination with celecoxib (as an anti-angiogenic agent) and several cytotoxic agents. The usefulness of this type of metronomic therapy was also demonstrated in patients with MBL [43,69,70]. In

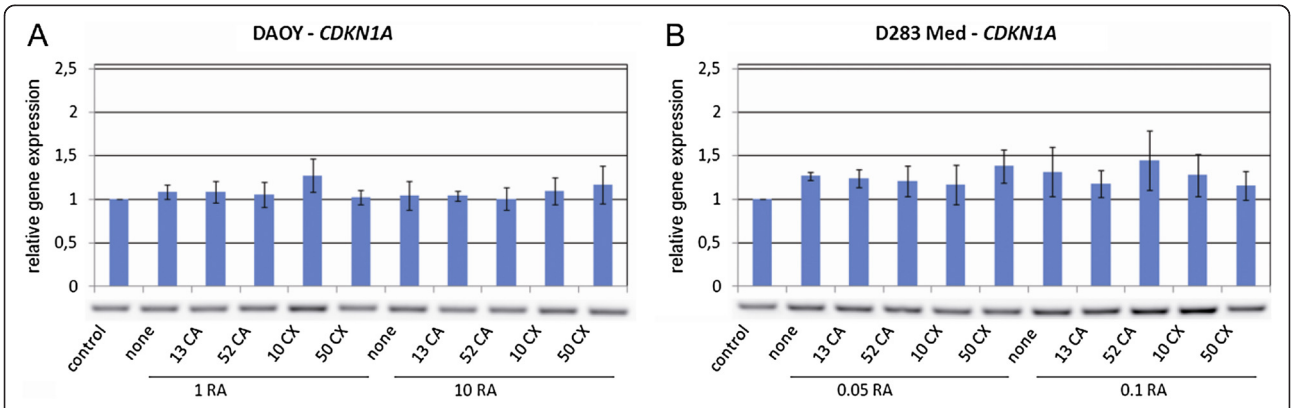

Figure 4 Changes in the expression of the *CDKN1A* gene in Daoy (A) and D283 Med (B) cells analyzed using RT-PCR. The cells were treated with ATRA alone or in combination with CA (an inhibitor of 5-LOX) or CX (an inhibitor of COX-2); numbers indicate the concentrations of these compounds in μM. Respective numerical data from densitometry for three independent experiments are shown in the graphs: X-axis, treatment condition; Y-axis, relative gene expression. The data represent the means ± SD; they were normalized to the expression of the *HSP90AB1* housekeeping gene and were related to the untreated control cells. Representative electrophoresis is presented for each cell line.

light of this, our experimental data clearly demonstrated that the combined administration of retinoids and celecoxib should also be beneficial in enhancing tumor cell differentiation. Furthermore, a very similar effect could be achieved through the dietary uptake of plant phenolic compounds including caffeic acid [71,72].

Conclusion

To summarize, our results on two established medulloblastoma cell lines – Daoy and D283 Med – confirmed our previous findings in leukemia and neuroblastoma cells that the differentiating effects of ATRA should be enhanced in its combined administration with caffeic acid (an inhibitor of 5-LOX) or celecoxib (an inhibitor of COX-2). This effect was apparently achieved in both cell lines via the increased expression of genes encoding proteins participating in inducing the differentiation and cytoskeleton remodeling (GDF-15, Rho GTPases) or the p21 protein, which is an important regulator of the cell cycle and of proteins associated with proteasome activity. Furthermore, our results showed an important difference between the established MBL cell lines: the Daoy cells showed the same sensitivity as the cell lines that were derived from other types of pediatric solid tumors, but the D283 Med cells were significantly more sensitive to the treatment with ATRA alone (this effect was further enhanced via combined treatment with LOX/COX inhibitors). To clarify detailed mechanisms of such difference, additional experiments concerning more cell lines derived from various MBL subtypes are needed. Nevertheless, the obtained results confirmed our initial hypothesis regarding the common mechanism of enhancement in ATRA-induced cell differentiation in various types of pediatric solid tumors.

Abbreviations

ATRA: All-trans retinoic acid; COX-2: Cyclooxygenase 2; DMEM: Dulbecco's modified Eagle's medium; DMSO: Dimethyl sulfoxide; 5-LOX: 5-lipoxygenase; MBL: Medulloblastoma.

Competing interests

The authors declare that they have no competing interests.

Authors' contributions

PC carried out the experiments with the cell lines, performed the expression profiling and RT-PCR and drafted the manuscript. JN participated in manuscript preparation and the experiments concerning RT-PCR and expression profiling and also in manuscript preparation. MR participated in the experiments with the cell lines. KZ participated in the analysis of results and in manuscript preparation. JS coordinated this study and participated in manuscript preparation. RV conceived the study, participated in the analysis of results and drafted the manuscript. All authors read and approved the final manuscript.

Acknowledgements

This study was supported by grant IGA NR9341-3/2007, by the European Regional Development Fund, as well as by the State Budget of the Czech Republic – project RECAMO CZ.1.05/2.1.00/03.0101 and the project CEB CZ.1.07/2.3.00/20.0183. We are grateful to Mrs. Johana Maresova for her technical assistance.

Author details

[1]Department of Experimental Biology - Laboratory of Tumor Biology, School of Science, Masaryk University, Kotlarska 2, 611 37 Brno, Czech Republic. [2]Department of Pediatric Oncology, University Hospital Brno and School of Medicine, Masaryk University, Cernopolni 9, 613 00 Brno, Czech Republic. [3]Masaryk Memorial Cancer Institute, Zluty kopec 7, 656 53 Brno, Czech Republic.

Received: 27 February 2014 Accepted: 5 June 2014
Published: 13 June 2014

References

1. Gerber NU, Mynarek M, von Hoff K, Friedrich C, Resch A, Rutkowski S: **Recent developments and current concepts in medulloblastoma.** *Cancer Treat Rev* 2014, **40:**356–365.
2. Massimino M, Giangaspero F, Garre ML, Gandola L, Poggi G, Biassoni V, Gatta G, Rutkowski S: **Childhood medulloblastoma.** *Crit Rev Oncol Hematol* 2011, **79:**65–83.
3. Dragnev KH, Petty WJ, Dmitrovsky E: **Retinoid targets in cancer therapy and chemoprevention.** *Cancer Biol Ther* 2003, **2:**S150–S156.
4. Brtko J, Dvorak Z: **Role of retinoids, rexinoids and thyroid hormone in the expression of cytochrome p450 enzymes.** *Curr Drug Metab* 2011, **12:**71–88.
5. Dedieu S, Lefebvre P: **Retinoids interfere with the AP1 signalling pathway in human breast cancer cells.** *Cell Signal* 2006, **18:**889–898.
6. Masia S, Alvarez S, de Lera AR, Barettino D: **Rapid, nongenomic actions of retinoic acid on phosphatidylinositol-3-kinase signaling pathway mediated by the retinoic acid receptor.** *Mol Endocrinol* 2007, **21:**2391–2402.
7. Cruz FD, Matushansky I: **Solid tumor differentiation therapy - is it possible?** *Oncotarget* 2012, **3:**559–567.
8. Hallahan AR, Pritchard JI, Chandraratna RA, Ellenbogen RG, Geyer JR, Overland RP, Strand AD, Tapscott SJ, Olson JM: **BMP-2 mediates retinoid-induced apoptosis in medulloblastoma cells through a paracrine effect.** *Nat Med* 2003, **9:**1033–1038.
9. Garattini E, Gianni M, Terao M: **Retinoids as differentiating agents in oncology: a network of interactions with intracellular pathways as the basis for rational therapeutic combinations.** *Curr Pharm Des* 2007, **13:**1375–1400.
10. Andres D, Keyser BM, Petrali J, Benton B, Hubbard KS, McNutt PM, Ray R: **Morphological and functional differentiation in BE(2)-M17 human neuroblastoma cells by treatment with Trans-retinoic acid.** *BMC Neurosci* 2013, **14:**49.
11. Maurer BJ, Kang MH, Villablanca JG, Janeba J, Groshen S, Matthay KK, Sondel PM, Maris JM, Jackson HA, Goodarzian F, Shimada H, Czarnecki S, Hasenauer B, Reynolds CP, Marachelian A: **Phase I trial of fenretinide delivered orally in a novel organized lipid complex in patients with relapsed/refractory neuroblastoma: a report from the New Approaches to Neuroblastoma Therapy (NANT) consortium.** *Pediatr Blood Cancer* 2013, **60:**1801–1808.
12. Patatanian E, Thompson DF: **Retinoic acid syndrome: a review.** *J Clin Pharm Ther* 2008, **33:**331–338.
13. Kuendgen A, Gattermann N: **Valproic acid for the treatment of myeloid malignancies.** *Cancer* 2007, **110:**943–954.
14. Tomita A, Kiyoi H, Naoe T: **Mechanisms of action and resistance to all-trans retinoic acid (ATRA) and arsenic trioxide (As2O 3) in acute promyelocytic leukemia.** *Int J Hematol* 2013, **97:**717–725.
15. Nowak D, Stewart D, Koeffler HP: **Differentiation therapy of leukemia: 3 decades of development.** *Blood* 2009, **113:**3655–3665.
16. Lo-Coco F, Avvisati G, Vignetti M, Thiede C, Orlando SM, Iacobelli S, Ferrara F, Fazi P, Cicconi L, di Bona E, Specchia G, Sica S, Divona M, Levis A, Fiedler W, Cerqui E, Breccia M, Fioritoni G, Salih HR, Cazzola M, Melillo L, Carella AM, Brandts CH, Morra E, von Lilienfeld-Toal M, Hertenstein B, Wattad M, Lübbert M, Hänel M, Schmitz N, *et al*: **Retinoic acid and arsenic trioxide for acute promyelocytic leukemia.** *N Engl J Med* 2013, **369:**111–121.
17. Haque A, Banik NL, Ray SK: **Emerging role of combination of all-trans retinoic acid and interferon-gamma as chemoimmunotherapy in the management of human glioblastoma.** *Neurochem Res* 2007, **32:**2203–2209.
18. De los Santos M, Zambrano A, Aranda A: **Combined effects of retinoic acid and histone deacetylase inhibitors on human neuroblastoma SH-SY5Y cells.** *Mol Cancer Ther* 2007, **6:**1425–1432.
19. Frumm SM, Fan ZP, Ross KN, Duvall JR, Gupta S, VerPlank L, Suh BC, Holson E, Wagner FF, Smith WB, Paranal RM, Bassil CF, Qi J, Roti G, Kung AL, Bradner JE, Tolliday N, Stegmaier K: **Selective HDAC1/HDAC2 inhibitors induce neuroblastoma differentiation.** *Chem Biol* 2013, **20:**713–725.

20. Chlapek P, Redova M, Zitterbart K, Hermanova M, Sterba J, Veselska R: **Enhancement of ATRA-induced differentiation of neuroblastoma cells with LOX/COX inhibitors: an expression profiling study.** *J Exp Clin Cancer Res* 2010, **29:**45.
21. Avis I, Martinez A, Tauler J, Zudaire E, Mayburd A, Abu-Ghazaleh R, Ondrey F, Mulshine JL: **Inhibitors of the arachidonic acid pathway and peroxisome proliferator-activated receptor ligands have superadditive effects on lung cancer growth inhibition.** *Cancer Res* 2005, **65:**4181–4190.
22. Kuo HC, Kuo WH, Lee YJ, Wang CJ, Tseng TH: **Enhancement of caffeic acid phenethyl ester on all-trans retinoic acid-induced differentiation in human leukemia HL-60 cells.** *Toxicol Appl Pharmacol* 2006, **216:**80–88.
23. Veselska R, Zitterbart K, Auer J, Neradil J: **Differentiation of HL-60 myeloid leukemia cells induced by all-trans retinoic acid is enhanced in combination with caffeic acid.** *Int J Mol Med* 2004, **14:**305–310.
24. Bell E, Ponthan F, Whitworth C, Westermann F, Thomas H, Redfern CP: **Cell Survival Signalling through PPARdelta and Arachidonic Acid Metabolites in Neuroblastoma.** *PLoS One* 2013, **8:**e68859.
25. Schroeder CP, Kadara H, Lotan D, Woo JK, Lee HY, Hong WK, Lotan R: **Involvement of mitochondrial and Akt signaling pathways in augmented apoptosis induced by a combination of low doses of celecoxib and N-(4-hydroxyphenyl) retinamide in premalignant human bronchial epithelial cells.** *Cancer Res* 2006, **66:**9762–9770.
26. Simeone AM, Li YJ, Broemeling LD, Johnson MM, Tuna M, Tari AM: **Cyclooxygenase-2 is essential for HER2/neu to suppress N- (4-hydroxyphenyl) retinamide apoptotic effects in breast cancer cells.** *Cancer Res* 2004, **64:**1224–1228.
27. Liu JP, Wei HB, Zheng ZH, Guo WP, Fang JF: **Celecoxib increases retinoid sensitivity in human colon cancer cell lines.** *Cell Mol Biol Lett* 2010, **15:**440–450.
28. Soda M, Hu D, Endo S, Takemura M, Li J, Wada R, Ifuku S, Zhao HT, El-Kabbani O, Ohta S, Yamamura K, Toyooka N, Hara A, Matsunaga T: **Design, synthesis and evaluation of caffeic acid phenethyl ester-based inhibitors targeting a selectivity pocket in the active site of human aldo-keto reductase 1B10.** *Eur J Med Chem* 2012, **48:**321–329.
29. Redova M, Chlapek P, Loja T, Zitterbart K, Hermanova M, Sterba J, Veselska R: **Influence of LOX/COX inhibitors on cell differentiation induced by all-trans retinoic acid in neuroblastoma cell lines.** *Int J Mol Med* 2010, **25:**271–280.
30. Nardini M, Scaccini C, Packer L, Virgili F: **In vitro inhibition of the activity of phosphorylase kinase, protein kinase C and protein kinase A by caffeic acid and a procyanidin-rich pine bark (Pinus marittima) extract.** *Biochim Biophys Acta* 2000, **1474:**219–225.
31. Dandekar DS, Lopez M, Carey RI, Lokeshwar BL: **Cyclooxygenase-2 inhibitor celecoxib augments chemotherapeutic drug-induced apoptosis by enhancing activation of caspase-3 and −9 in prostate cancer cells.** *Int J Cancer* 2005, **115:**484–492.
32. Kang KB, Zhu C, Yong SK, Gao Q, Wong MC: **Enhanced sensitivity of celecoxib in human glioblastoma cells: Induction of DNA damage leading to p53-dependent G1 cell cycle arrest and autophagy.** *Mol Cancer* 2009, **8:**66.
33. Graff J, Skarke C, Klinkhardt U, Watzer B, Harder S, Seyberth H, Geisslinger G, Nusing RM: **Effects of selective COX-2 inhibition on prostanoids and platelet physiology in young healthy volunteers.** *J Thromb Haemost* 2007, **5:**2376–2385.
34. Gumireddy K, Sutton LN, Phillips PC, Reddy CD: **All-*trans*-retinoic acid-induced apoptosis in human medulloblastoma: activation of caspase-3/poly(ADPribose) polymerase 1 pathway.** *Clin Cancer Res* 2003, **9:**4052–4059.
35. Vandesompele J, de Preter K, Pattyn F, Poppe B, van Roy N, de Paepe A, Speleman F: **Accurate normalization of real-time quantitative RT-PCR data by geometric averaging of multiple internal control genes.** *Genome Biol* 2002, **3:**RESEARCH0034.
36. Andersen CL, Jensen JL, Orntoft TF: **Normalization of real-time quantitative reverse transcription-PCR data: a model-based variance estimation approach to identify genes suited for normalization, applied to bladder and colon cancer data sets.** *Cancer Res* 2004, **64:**5245–5250.
37. Huang DW, Sherman BT, Lempicki RA: **Systematic and integrative analysis of large gene lists using DAVID bioinformatics resources.** *Nat Protoc* 2009, **4:**44–57.
38. Schneider CA, Rasband WS, Eliceiri KW: **NIH Image to ImageJ: 25 years of image analysis.** *Nat Methods* 2012, **9:**671–675.
39. Reynolds CP, Lemons RS: **Retinoid therapy of childhood cancer.** *Hematol Oncol Clin North Am* 2001, **15:**867–910.
40. Reynolds CP, Matthay KK, Villablanca JG, Maurer BJ: **Retinoid therapy of high-risk neuroblastoma.** *Cancer Lett* 2003, **197:**185–192.
41. Sterba J: **Contemporary therapeutic options for children with high risk neuroblastoma.** *Neoplasma* 2002, **49:**133–140.
42. Sterba J, Valik D, Mudry P, Kepak T, Pavelka Z, Bajciova V, Zitterbart K, Kadlecova V, Mazanek P: **Combined biodifferentiating and antiangiogenic oral metronomic therapy is feasible and effective in relapsed solid tumors in children: single-center pilot study.** *Onkologie* 2006, **29:**308–313.
43. Zapletalova D, Andre N, Deak L, Kyr M, Bajciova V, Mudry P, Dubska L, Demlova R, Pavelka Z, Zitterbart K, Skotakova J, Husek K, Martincekova A, Mazanek P, Kepak T, Doubek M, Kutnikova L, Valik D, Sterba J: **Metronomic chemotherapy with the COMBAT regimen in advanced pediatric malignancies: a multicenter experience.** *Oncology* 2012, **82:**249–260.
44. Redova M: **Enhancement of differentiation inductors' effect on the solid tumors model *in vitro*.** In *PhD thesis.* Masaryk University, Department of Experimental Biology; Brno 2010.
45. Bai RY, Staedtke V, Lidov HG, Eberhart CG, Riggins GJ: **OTX2 represses myogenic and neuronal differentiation in medulloblastoma cells.** *Cancer Res* 2012, **72:**5988–6001.
46. David M, Petit D, Bertoglio J: **Cell cycle regulation of Rho signaling pathways.** *Cell Cycle* 2012, **11:**3003–3010.
47. Bustelo XR, Sauzeau V, Berenjeno IM: **GTP-binding proteins of the Rho/Rac family: regulation, effectors and functions in vivo.** *Bioessays* 2007, **29:**356–370.
48. Strelau J, Strzelczyk A, Rusu P, Bendner G, Wiese S, Diella F, Altick AL, von Bartheld CS, Klein R, Sendtner M, Unsicker K: **Progressive postnatal motoneuron loss in mice lacking GDF-15.** *J Neurosci* 2009, **29:**13640–13648.
49. Mimeault M, Batra SK: **Divergent molecular mechanisms underlying the pleiotropic functions of macrophage inhibitory cytokine-1 in cancer.** *J Cell Physiol* 2010, **224:**626–635.
50. Li PX, Wong J, Ayed A, Ngo D, Brade AM, Arrowsmith C, Austin RC, Klamut HJ: **Placental transforming growth factor-beta is a downstream mediator of the growth arrest and apoptotic response of tumor cells to DNA damage and p53 overexpression.** *J Biol Chem* 2000, **275:**20127–20135.
51. Yang H, Filipovic Z, Brown D, Breit SN, Vassilev LT: **Macrophage inhibitory cytokine-1: a novel biomarker for p53 pathway activation.** *Mol Cancer Ther* 2003, **2:**1023–1029.
52. Ryningen A, Stapnes C, Paulsen K, Lassalle P, Gjertsen BT, Bruserud O: **In vivo biological effects of ATRA in the treatment of AML.** *Expert Opin Investig Drugs* 2008, **17:**1623–1633.
53. Luo P, Lin M, Chen Y, Yang B, He Q: **Function of retinoid acid receptor alpha and p21 in all-trans-retinoic acid-induced acute T-lymphoblastic leukemia apoptosis.** *Leuk Lymphoma* 2009, **50:**1183–1189.
54. Bao GC, Wang JG, Jong A: **Increased p21 expression and complex formation with cyclin E/CDK2 in retinoid-induced pre-B lymphoma cell apoptosis.** *FEBS Lett* 2006, **580:**3687–3693.
55. Lim JS, Park SH, Jang KL: **All-trans retinoic acid induces cellular senescence by up-regulating levels of p16 and p21 via promoter hypomethylation.** *Biochem Biophys Res Commun* 2011, **412:**500–505.
56. Park SH, Lim JS, Jang KL: **All-trans retinoic acid induces cellular senescence via upregulation of p16, p21, and p27.** *Cancer Lett* 2011, **310:**232–239.
57. Wainwright LJ, Lasorella A, Iavarone A: **Distinct mechanisms of cell cycle arrest control the decision between differentiation and senescence in human neuroblastoma cells.** *Proc Natl Acad Sci U S A* 2001, **98:**9396–9400.
58. Liu Y, Encinas M, Comella JX, Aldea M, Gallego C: **Basic helix-loop-helix proteins bind to TrkB and p21(Cip1) promoters linking differentiation and cell cycle arrest in neuroblastoma cells.** *Mol Cell Biol* 2004, **24:**2662–2672.
59. Marzinke MA, Clagett-Dame M: **The all-trans retinoic acid (atRA)-regulated gene Calmin (Clmn) regulates cell cycle exit and neurite outgrowth in murine neuroblastoma (Neuro2a) cells.** *Exp Cell Res* 2012, **318:**85–93.
60. Qiao J, Paul P, Lee S, Qiao L, Josifi E, Tiao JR, Chung DH: **PI3K/AKT and ERK regulate retinoic acid-induced neuroblastoma cellular differentiation.** *Biochem Biophys Res Commun* 2012, **424:**421–426.
61. Son SH, Yu E, Ahn Y, Choi EK, Lee H, Choi J: **Retinoic acid attenuates promyelocytic leukemia protein-induced cell death in breast cancer cells by activation of the ubiquitin-proteasome pathway.** *Cancer Lett* 2007, **247:**213–223.
62. Isakson P, Bjoras M, Boe SO, Simonsen A: **Autophagy contributes to therapy-induced degradation of the PML/RARA oncoprotein.** *Blood* 2010, **116:**2324–2331.

63. Trocoli A, Mathieu J, Priault M, Reiffers J, Souquere S, Pierron G, Besancon F, Djavaheri-Mergny M: **ATRA-induced upregulation of Beclin 1 prolongs the life span of differentiated acute promyelocytic leukemia cells.** *Autophagy* 2011, **7:**1108–1114.
64. Ferry C, Gaouar S, Fischer B, Boeglin M, Paul N, Samarut E, Piskunov A, Pankotai-Bodo G, Brino L, Rochette-Egly C: **Cullin 3 mediates SRC-3 ubiquitination and degradation to control the retinoic acid response.** *Proc Natl Acad Sci U S A* 2011, **108:**20603–20608.
65. Day IN, Thompson RJ: **UCHL1 (PGP 9.5): neuronal biomarker and ubiquitin system protein.** *Prog Neurobiol* 2010, **90:**327–362.
66. Schneider L, Giordano S, Zelickson BR, SJ M, AB G, Ouyang X, Fineberg N, Darley-Usmar VM, Zhang J: **Differentiation of SH-SY5Y cells to a neuronal phenotype changes cellular bioenergetics and the response to oxidative stress.** *Free Radic Biol Med* 2011, **51:**2007–2017.
67. Xun Z, Lee DY, Lim J, Canaria CA, Barnebey A, Yanonne SM, McMurray CT: **Retinoic acid-induced differentiation increases the rate of oxygen consumption and enhances the spare respiratory capacity of mitochondria in SH-SY5Y cells.** *Mech Ageing Dev* 2012, **133:**176–185.
68. Malik PS, Raina V, Andre N: **Metronomics as maintenance treatment in oncology: time for chemo-switch.** *Front Oncol* 2014. epub ahead of print, doi: 10.3389/fonc.2014.00076.
69. Choi LMR, Rood B, Kamani N, La Fond D, Packer RJ, Santi MR, MacDonald TJ: **Feasibility of metronomic maintenance chemotherapy following high-dose chemotherapy for malignant central nervous system tumors.** *Pediatr Blood Cancer* 2008, **50:**970–975.
70. Sterba J, Pavelka Z, Andre N, Ventruba J, Skotakova J, Bajciova V, Bronisova D, Dubska L, Valik D: **Second complete remission of relapsed medulloblastoma induced by metronomic chemotherapy.** *Pediatr Blood Cancer* 2010, **54:**616–617.
71. Jaganathan SK, Mandal M: **Antiproliferative effects of honey and of its polyphenols: a review.** *J Biomed Biotechnol* 2009, **2009:**830616.
72. Korkina LG: **Phenylpropanoids as naturally occurring antioxidants: from plant defense to human health.** *Cell Mol Biol (Noisy-le-Grand)* 2007, **53:**15–25.

doi:10.1186/1475-2867-14-51
Cite this article as: Chlapek *et al.*: The ATRA-induced differentiation of medulloblastoma cells is enhanced with LOX/COX inhibitors: an analysis of gene expression. *Cancer Cell International* 2014 **14**:51.

Funkční testy pro detekci nádorových kmenových buněk

Functional Assays for Detection of Cancer Stem Cells

Škoda J.[1,2], Neradil J.[1,3], Veselská R.[1,2]

[1] Laboratoř nádorové biologie, Ústav experimentální biologie, Přírodovědecká fakulta MU, Brno
[2] Klinika dětské onkologie LF MU a FN Brno
[3] Regionální centrum aplikované molekulární onkologie, Masarykův onkologický ústav, Brno

Souhrn
Nádorové kmenové buňky (cancer stem cells – CSCs) jsou považovány za populaci buněk, která odpovídá za iniciaci a progresi nádoru, účastní se procesu metastazování a je možnou příčinou získané lékové rezistence a rekurence nádorů. CSCs disponují schopností sebeobnovy a mají tumorigenní potenciál. Funkční testy, které umožňují detekovat zmiňované vlastnosti, jsou hlavním nástrojem pro identifikaci nádorových kmenových buněk. Tento článek přináší ucelený přehled *in vivo* a *in vitro* metod využívaných pro průkaz CSCs s důrazem na recentně zaváděné techniky detekce CSCs. Mezi nejčastěji prováděné funkční testy patří test tumorigenicity *in vivo*, testy tvorby sfér (sphere formation assay) a kolonií (colony-forming unit assay) a rovněž detekce tzv. vedlejší populace (side population). Dále jsou popsány metody zadržování detekční značky (label-retention assay) a test aktivity aldehyddehydrogenázy.

Klíčová slova
nádorové kmenové buňky – funkční testy – tumorigenicita – nádorové sféry – tvorba kolonií – vedlejší populace buněk – aldehyddehydrogenáza

Summary
Cancer stem cells (CSCs) are considered to be a population of tumor cells, which are responsible for tumor initiation and progression. They are also involved in metastasizing and may be a possible cause of multidrug resistance and tumor recurrence. CSCs possess the ability to self-renew and show a tumorigenic potential. Functional assays, which enable the detection of these properties, represent the main tool for identification of CSCs. This article summarizes both *in vitro* and *in vivo* methods used to identify the CSCs with emphasis on recently employed techniques of CSCs detection. *In vivo* tumorigenicity assay, sphere formation assay and colony-forming unit assay belong to the most commonly used functional assays. Further, label-retention assay and aldehyde dehydrogenase activity assay are described in this article.

Key words
cancer stem cells – functional assays – tumorigenicity – tumor spheres – colony-forming unit assay – side population cells – aldehyde dehydrogenase

Práce byla podpořena grantem IGA MZ ČR NT13443-4 a Evropským fondem pro regionální rozvoj a státním rozpočtem České republiky OP VaVpI – RECAMO, CZ.1.05/2.1.00/03.0101 a projektem CEB, OP VK CZ.1.07/2.3.00/20.0183.

The study was supported by grant of Internal Grant Agency of the Czech Ministry of Health No. NT13443-4 and by the European Regional Development Fund and the State Budget of the Czech Republic – RECAMO, CZ.1.05/2.1.00/03.0101 and by the project CEB, OP VK CZ.1.07/2.3.00/20.0183.

Autoři deklarují, že v souvislosti s předmětem studie nemají žádné komerční zájmy.

The authors declare they have no potential conflicts of interest concerning drugs, products, or services used in the study.

Redakční rada potvrzuje, že rukopis práce splnil ICMJE kritéria pro publikace zasílané do biomedicínských časopisů.

The Editorial Board declares that the manuscript met the ICMJE "uniform requirements" for biomedical papers.

Mgr. Jan Škoda
Laboratoř nádorové biologie
Ústav experimentální biologie
Přírodovědecká fakulta MU
Kotlářská 2
611 37 Brno
e-mail: janskoda@sci.muni.cz

Obdrženo/Submitted: 16. 1. 2014
Přijato/Accepted: 4. 4. 2014

Úvod

Nádorové kmenové buňky (cancer stem cells – CSCs) jsou definovány jako subpopulace buněk nádoru, které jsou schopny sebeobnovy a mají potenciál diferencovat do všech typů nádorových buněk tvořících masu daného nádoru [1]. Dle tohoto modelu odpovídají CSCs za iniciaci a kontinuální růst nádoru a jsou také příčinou vysoké buněčné heterogenity, se kterou se u mnoha typů nádorů setkáváme [2]. Navíc již v řadě studií bylo prokázáno, že CSCs (podobně jako jiné druhy kmenových buněk) disponují zvýšenou odolností proti chemoterapii a radioterapii [3–5]. Z toho lze usuzovat, že právě CSCs by mohly být příčinou často se vyskytující získané lékové rezistence a rekurence nádorů, které představují v současnosti největší problém v léčbě nádorových onemocnění. Zatímco dosavadní léčba nádorů se zaměřuje především na redukci celkové masy nádoru, limitem v dlouhodobém vyléčení nemoci mohou být právě rezistentní CSCs, jež v určitém čase po terapii dají vzniknout nové populaci nádorových buněk – často již rezistentních k původní léčbě. Zejména v posledním desetiletí proto CSCs představují významnou oblast výzkumu nádorových onemocnění a recentní studie přinášejí slibné výsledky, kdy kombinovaná léčba zaměřující se mj. na CSCs vede k lepší léčebné odpovědi [3].

Základ modelu CSCs lze dohledat již v roce 1855, kdy Rudolf Virchow představil teorii, podle které nádory vznikají z nezralých buněk [6]. Termín „nádorové kmenové buňky" byl však použit až v roce 1959 pro popis nepočetné populace buněk, jež byly rezistentní k chemoterapii a nacházely se u nich odlišné chromozomální změny v porovnání s ostatními buňkami nádoru [7]. Následné transplantační experimenty *in vivo* a klonogenní testy *in vitro* provedené v 70. letech minulého století potvrdily, že nádory mohou vznikat ze vzácně se vyskytujících buněk, které mají schopnost sebeobnovy a jsou schopny rekapitulovat buněčnou heterogenitu původního nádoru. S rozvojem technik průtokové cytometrie a s přispěním poznatků o biologii kmenových buněk bylo možné izolovat CSCs z nádorové tkáně na základě specifických povrchových markerů, často shodných s těmi, které se využívají pro identifikaci adultních kmenových buněk. Tímto přístupem byly CSCs nejprve identifikovány u hematoonkologických malignit [8], později u karcinomu prsu [9] a poté u celé řady dalších solidních nádorů [10]. V současné době je sortování buněk na základě povrchových markerů obecně uplatňovaným přístupem při výzkumu CSCs. Specifita markerů CSCs se však může mezi jednotlivými typy nádorů lišit a je nezbytné ověřit, zda izolovaná populace buněk disponuje základními vlastnostmi CSCs – schopností sebeobnovy a tumorigeneze. Pro tyto účely se využívají funkční testy, které lze dle metodického přístupu rozdělit na testy *in vivo* a *in vitro*. V následujících kapitolách bude podán přehled těchto metod.

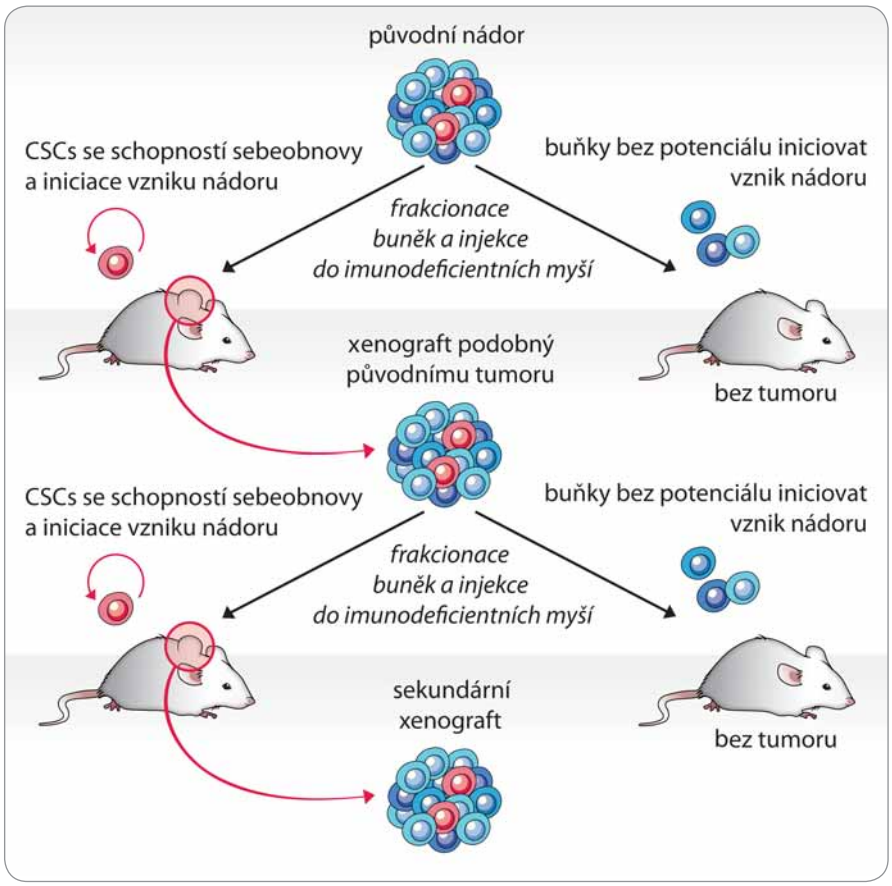

Obr. 1. Schéma testu tumorigenicity.

Průkaz fenotypu CSCs je proveden opakovanou transplantací izolovaných buněčných populací, které jsou schopny po injikaci do imunodeficientní myši vytvořit nádor.

Funkční testy CSCs *in vivo*

Test tumorigenicity

Test tumorigenicity představuje dosud nejlepší funkční test fenotypu CSCs, kterým lze současně ověřit schopnost sebeobnovy i schopnost vytvořit nádor, jenž rekapituluje buněčnou heterogenitu nádoru původního, a to přímo v prostředí *in vivo*. Principem testu je opakovaná transplantace testovaných buněk do zvířecího modelu, nejčastěji myši imunodeficientního kmene – typicky NOD/SCID (nonobese diabetic/severe combined immunodeficiency) (obr. 1) [1]. Dle původu a homogenity testované populace buněk bývá do vhodného místa myši injikováno 100 až několik miliónů buněk [9,11,12]. Injikace se obvykle provádí subkutánně, ale buňky lze transplantovat i do jednotlivých orgánů – mozku [11,13], svalu [12] či prsní žlázy [14]. Myši jsou poté průběžně kontrolovány a v případě nálezu nádoru nebo po uplynutí stanovené doby jsou usmrceny (obr. 2A). Schopnost tumorigeneze je hodnocena na základě

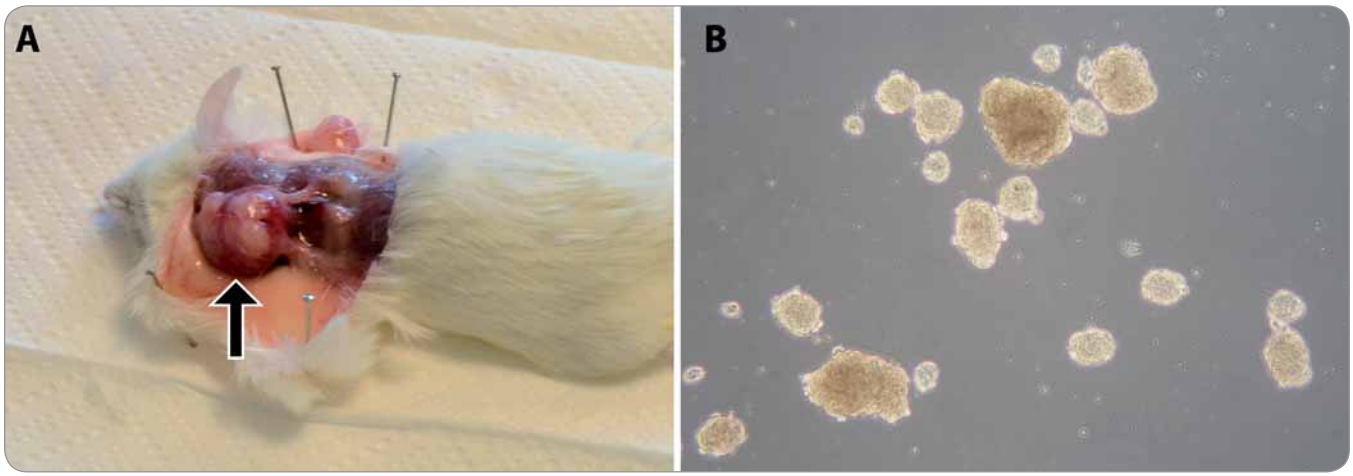

Obr. 2. Ukázky našich výsledků funkčních testů CSCs u rabdomyosarkomu a osteosarkomu.

A. Xenograftový nádor v podkoží myši kmene NOD/SCID/IL2Rγ$_{null}$ po injikaci rabdomyosarkomových buněk. Šipka označuje lokalizaci nádoru. B. Sarkosféry vytvořené z osteosarkomové linie OSA-02.

poměru počtu zvířat, u kterých se vyvinul nádor, k počtu celkově injikovaných. Mezi další kritéria hodnocení pak patří velikost nádoru, doba do nálezu tumoru a počet injikovaných buněk. Schopnost sebeobnovy je však potřeba dále ověřit opakovanou izolací CSCs z xenograftového nádoru a jejich transplantací do dalšího zvířete (obr. 1) [1].

Ve většině prvotních prací prokazujících přítomnost nepočetné populace CSCs u různých typů nádorů byly pro test tumorigenicity využívány NOD/SCID myši. V posledních letech ale byly publikovány práce, které ukázaly, že tumorigenicita testovaných buněk (a tedy i senzitivita testu) může být výrazně zvýšena použitím více imunodeficientních transgenních myších kmenů NOD/SCID/IL2Rγ$_{null}$, NOD/ShiLtSz-scid/IL2Rγ$_{null}$ (NSG) a NOD/ShiJic-scid/IL2Rγ$_{null}$ (NOG), nesoucích mutaci v genu pro řetězec gama receptoru pro interleukin-2 [15]. Použitím NSG myší se u maligního melanomu zvýšilo vypočítané zastoupení CSCs z původně publikovaných 0,0001 % na 25 %, přičemž nádory u myší vznikaly již při injikaci jediné buňky [16]. Podobně došlo ke zvýšení tumorigenicity u leukemických kmenových buněk [17]. Ačkoliv u některých solidních nádorů, např. adenokarcinomu pankreatu, nebyla pozorována změna ve frekvenci výskytu CSCs [18], využití NSG myší obecně zkrátilo dobu do prvního nálezu nádoru. Právě časová náročnost testu tumorigenicity, kdy od injekce testovaných buněk do vytvoření nádoru uplyne často i několik měsíců, je jedna z nevýhod tohoto testu. CSCs mohou během této doby projít řadou genetických a epigenetických změn, což znesnadňuje interpretaci výsledků testu [1]. Využití více imunodeficientních kmenů myší, NSG a NOG, se proto jeví jako vhodná optimalizace testu.

Další limit testu tumorigenicity může představovat mikroprostředí v místě transplantace a způsob injikace buněk. Je známo, že kmenové buňky jsou do značné míry závislé na produkci signálů od okolního stromatu [19]. Při experimentech, kdy byly do myší injikovány smíšené populace nádorových buněk a fibroblastů asociovaných s nádorem (cancer-associated fibroblasts), došlo ke zvýšení agresivity a velikosti nádoru [20]. Kombinace nádorových buněk s normálními diploidními fibroblasty měla po transplantaci do myši efekt opačný. Výsledky některých studií ukazují, že i samotné nádorové stroma ovlivňuje okolní buňky a původně nenádorové buňky umístěné do jeho blízkosti se pravděpodobně v důsledku genetických či epigenetických změn stávají tumorigenními [21–24]. Míra tumorigenicity může být také zvýšena přidáním mitoticky inaktivovaných podpůrných buněk (feeder cells) nebo Matrigelu™, který obsahuje proteiny extracelulární matrix [1,16,25,26].

Potřeba sledovat interakce CSCs a mikroprostředí *in vivo* vedla v posledních letech k rozvoji specializovaných metod založených na intravitální mikroskopii a multifotonovém zobrazování [27]. Pomocí těchto metod je možné v čase a při rozlišení jednotlivých buněk pozorovat buňky exprimující fluorescenční protein přímo v myši bez nutnosti jejího usmrcení či narušení příslušné tkáně. To mimo jiné umožňuje sledování původu buněk (lineage tracing), což pomáhá lépe pochopit dynamiku tumorigeneze. V recentních studiích byly fluorescenčně značené nádorové buňky získány dvěma způsoby: 1. využitím transgenních kmenů myší, které spontánně vytvářejí nádory a zároveň v buňkách obsahují fluorescenční protein s regulovatelnou expresí [28–30], nebo 2. pomocí transdukce izolovaných buněk příslušnou fluorescenční značkou a jejich xenotransplantací do imunodeficientní myši [31]. Právě tento druhý přístup, kdy je možné izolovanou populaci CSCs značit fluorescenčním proteinem, injikovat do myši (případně i společně s dalšími odlišně značenými populacemi buněk) a sledovat v čase, by se v budoucnu mohl stát optimálním rozšířením klasického testu CSCs *in vivo*.

Funkční testy CSCs *in vitro*

Oproti metodám *in vivo* jsou *in vitro* testy fenotypu CSCs výhodné zejména z důvodu menší časové a finanční ná-

ročnosti. I přesto je nutné výsledky získané *in vitro* ověřit testem *in vivo*. Dobře navržený funkční test *in vitro* by měl mít dostatečnou specifitu a citlivost pro detekci nízce zastoupené populace CSCs a zároveň by měl umožňovat kvantitativní hodnocení. Mezi nejčastěji využívané funkční testy *in vitro* patří: 1. test tvorby buněčných sfér (sphere formation assay), 2. test tvorby kolonií (colony-forming unit – CFU assay), označovaný též jako klonogenní test, 3. detekce vedlejší populace (side population – SP analysis), 4. test zadržování detekční značky v buňce (label-retention assay) a 5. test aktivity aldehyddehydrogenázy [1,32].

Test tvorby buněčných sfér

Průkaz schopnosti původně jednotlivých buněk dělit se a vytvářet sféry – tedy kulovité shluky buněk – umožňuje kvantifikovat aktivitu a sebeobnovu CSCs (obr. 2B) [33]. Test je prováděn v médiu s definovaným obsahem růstových faktorů, aby se minimalizovalo působení externích buněčných signálů, a za neadherentních podmínek kvůli ověření nezávislosti na adherenci k substrátu. Pro ověření sebeobnovy CSCs je nutné sféry opakovaně pasážovat – sféry jsou enzymaticky převedeny na suspenzi jednotlivých buněk a opětovně kultivovány za definovaných podmínek [34,35]. Dle počtu zformovaných sfér v druhé a dalších generacích lze určit nejen schopnost sebeobnovy, ale také klonogenity příslušných buněk.

Buněčné sféry byly odvozeny z celé řady nádorů a často bývají nazývány dle tkáňového původu nebo názvu nádoru (uvedeno v závorce): neuronální nádory (neurosféry) [13,36], karcinom prsu (mamosféry) [14], rabdomyosarkom (rabdosféry) [12], osteosarkom (sarkosféry) [37,38], karcinom tlustého střeva (kolonosféry) [39], karcinom prostaty (prostasféry) [40] a hepatom (hepatosféry) [41].

Nevýhodou počátečních experimentů prováděných v tekutém médiu byla skutečnost, že mohlo docházet k agregaci buněk, a sféry tak mohly vznikat z více než jedné buňky, přičemž tento aspekt je ale zásadním kritériem pro hodnocení testu. Uvedený problém lze překonat použitím semisolidního média, které omezuje pohyb buněk a tím i jejich možnou agregaci [37,38].

Obdobu testu tvorby sfér představuje test tvorby kolonií z jednobuněčné suspenze v měkkém agaru (soft agar colony-forming assay), v němž je také ověřována schopnost sebeobnovy, tumorigenity a klonogenity CSCs [37,40]. Dělením jednotlivých buněk dochází v agaru ke vzniku trojrozměrných buněčných kolonií.

Test tvorby kolonií

Princip této metody je podobný jako u předchozího testu. Suspenze jednotlivých buněk izolované populace se vyseje na kultivační misku a po určité době se vyhodnotí počet kolonií (obvykle musí být tvořeny více než 30–70 buňkami) [41–44]. Kultivace však probíhá za adherentních podmínek v médiu s přídavkem séra. Povrch kultivačních misek může být případně potažen Matrigelem™ [41].

V minulém roce byl publikován postup, který test tvorby kolonií do značné míry automatizuje [44]. Buňky byly tříděny metodou FACS (fluorescence-activated cell sorting, třídění buněk pomocí fluorescence) na základě exprese povrchových markerů CSCs a jednotlivě automaticky vysety do 96jamkových nebo 384jamkových mikrotitračních destiček. Tento přístup výrazně zkracuje časovou a manuální náročnost testu a díky použití vícejamkových destiček umožňuje velmi rychlé kvantitativní hodnocení, např. fluorescenčním skenovacím cytometrem [45].

Detekce vedlejší populace

Vedlejší populace (side population – SP) je definována jako populace buněk, která je schopna z cytoplazmy vylučovat fluorescenční barvivo Hoechst 33342 [46]. Tento fluorochrom s emisním maximem 460 nm (modrá barva spektra) má schopnost vázat se na DNA a v tomto stavu lze navíc detekovat emisi i v červené části spektra. Toho se využívá při průtokové cytometrii, případně při FACS, kdy SP vykazuje výrazně nižší fluorescenci v červeném spektru oproti modrému spektru.

K vypuzování fluorescenčního barviva dochází aktivitou membránových proteinů spadajících do rodiny ABC (ATP-binding cassette) transportérů, které jsou mimo jiné odpovědné za transport xenobiotik [46,47]. V souvislosti s CSCs je z této skupiny nejčastěji zkoumaný protein ABCG2, jehož zvýšená exprese je považována za možnou příčinu rezistence CSCs k chemoterapeutikům [47,48]. Při detekci nebo izolaci CSCs na základě SP je proto nezbytné provést kontrolní experiment s využitím některého z inhibitorů ABCG2 proteinu – nejčastěji se používají verapamil [49] nebo fumitremorgin C [50].

Určitou nevýhodou detekce SP fluorochromem Hoechst 33342 je nutnost použití excitačního UV laseru (355 nm), který nebývá v základní konfiguraci obvykle používaných průtokových cytometrů. Jako alternativu k barvivu Hoechst 33342 lze použít rhodamin 123 (Rho123), který je vylučován stejným typem membránového transportéru a jeho excitace se provádí pomocí základního modrého laseru (488 nm) [38].

Test zadržování detekční značky

Další *in vitro* metodou pro identifikaci CSCs izolovaných ze solidních nádorů je test schopnosti zadržování detekční značky v buňce (label-retention assay) [51–53]. V literatuře lze najít pod označením „label-retention assay" dvě metody značení buněk.

Původní metoda vychází z hypotézy existence „nesmrtelného řetězce" (immortal strand hypothesis) a jejím cílem je průkaz kmenových buněk pomocí značení mateřského řetězce DNA H3-thymidinem nebo bromdeoxyuridinem [51,54]. Testované buňky jsou nejprve označeny některým z těchto prekurzorů a po několika buněčných děleních je u nich detekována intenzita signálu. Během asymetrického dělení by měly kmenové buňky zadržovat značený mateřský („nesmrtelný") řetězec a do dceřiné buňky by měl být předáván pouze nově vzniklý neznačený řetězec. Jiným vysvětlením pro zadržování detekční značky by mohl být prodloužený buněčný cyklus CSCs oproti ostatním buňkám nádoru. U buněk, které nemají vlastnosti CSCs, by mělo jejich dělením docházet k rozředění značených řetězců v populaci dceřiných buněk [55].

Druhá z metod označovaných jako „label-retention assay" využívá stabilní značení buněk fluorochromy [52,56]. Při buněčném dělení dochází k rovnoměrnému rozdělení těchto flurochromů do dceřiných buněk, a tedy ke snížení fluorescence jednotlivých buněk na polovinu. Po určitém počtu dělení (obvykle 8–10) dojde ke snížení intenzity fluorescence na úroveň neznačených buněk. Hodnocením fluorescence jednotlivých buněk lze potom určit míru proliferace dané populace buněk. Pro značení buněk je využíváno fluorescenční barvivo CFSE (carboxyfluorescein diacetate succinimidylester), které volně prostupuje přes plazmatickou membránu a kovalentně se váže na proteiny v buňkách, nebo sondy PKH26 a DiI, jež se vážou na plazmatickou membránu. Na základě vysoké fluorescence v důsledku prodlouženého buněčného cyklu byla pomocí této metody detekována populace buněk, která vykazuje další znaky typické pro CSCs, jako je zvýšená schopnost tvorby kolonií, tumorigeneze *in vivo* a exprese markerů kmenových buněk [57].

Test aktivity aldehyddehydrogenázy

Exprese aldehyddehydrogenázy (ALDH) je specifická pro kmenové buňky, a je proto využívána jako jeden z jejich markerů [58]. Měření aktivity ALDH pomocí štěpení specifického substrátu patří mezi funkční testy fenotypu CSCs [59]. Substrát označovaný jako BAAA (BODIPY aminoacetaldehyde) proniká difuzí do buňky, kde je štěpen pomocí ALDH na BAA (BODIPY amino acetate) a dochází tak k emisi fluorescence, která může být kvantifikována pomocí průtokové cytometrie. Buňky s vysokou intenzitou fluorescence (a tedy vysokou aktivitou ALDH) jsou považovány za CSCs. V současnosti existuje komerčně dostupný systém pro detekci aktivity ALDH pod označením Aldefluor™.

Závěr

Funkční testy pro detekci buněk s fenotypem CSCs představují nepostradatelnou součást aktuálního výzkumu nádorových onemocnění. Metodické přístupy, které byly pro účely detekce CSCs vyvinuty, jsou postupně využívány i pro výzkum léčiv cílených na CSCs stejně jako pro vývoj protinádorových léčiv obecně. Nádorové sféry představují lepší model solidního nádoru v podmínkách *in vitro* než buňky pěstované jako monolayer. Automatizovaná příprava kolonií umožňuje vysoce efektivně testovat a kvantifikovat účinky léčiv. Sledování původu buněk u transgenních kmenů myší může v budoucnu ukázat, které populace buněk jsou v organizmu použitou léčbou ovlivněny. Lze očekávat, že při dalším vývoji funkčních testů CSCs bude snaha lépe postihnout i vliv nádorového mikroprostředí na funkci CSCs a testy budou rozšiřovány o metody sledování původu buněk, které pomohou charakterizovat interakce CSCs a ostatních buněk nádoru.

Literatura

1. Clarke MF, Dick JE, Dirks PB et al. Cancer stem cells – perspectives on current status and future directions: AACR workshop on cancer stem cells. Cancer Res 2006; 66(19): 9339–9344.
2. Magee JA, Piskounova E, Morrison SJ. Cancer stem cells: impact, heterogeneity, and uncertainty. Cancer Cell 2012; 21(3): 283–296. doi: 10.1016/j.ccr.2012.03.003.
3. Vidal SJ, Rodriguez-Bravo V, Galsky M et al. Targeting cancer stem cells to suppress acquired chemotherapy resistance. Oncogene 2013; 10: 1–13. doi: 10.1038/onc.2013.411.
4. Baumann M, Krause M, Hill R. Exploring the role of cancer stem cells in radioresistance. Nat Rev Cancer 2008; 8(7): 545–554. doi: 10.1038/nrc2419.
5. Hittelman WN, Liao Y, Wang L et al. Are cancer stem cells radioresistant? Future Oncol 2010; 6(10): 1563–1576. doi: 10.2217/fon.10.121.
6. Cogle CR. Cancer stem cells: historical perspectives and lessons from leukemia. In: Alison AL (ed.). Cancer stem cells in solid tumors. Springer 2011: 3–11.
7. Welte Y, Adjaye J, Lehrach HR et al. Cancer stem cells in solid tumors: elusive or illusive? Cell Commun Signal 2010; 8(1): 6. doi: 10.1186/1478-811X-8-6.
8. Bonnet D, Dick JE. Human acute myeloid leukemia is organized as a hierarchy that originates from a primitive hematopoietic cell. Nat Med 1997; 3(7): 730–737.
9. Al-Hajj M, Wicha MS, Benito-Hernandez A et al. Prospective identification of tumorigenic breast cancer cells. Proc Natl Acad Sci USA 2003; 100(7): 3983–3988.
10. Beck B, Blanpain C. Unravelling cancer stem cell potential. Nat Rev Cancer 2013; 13(10): 727–738. doi: 10.1038/nrc3597.
11. Singh SK, Hawkins C, Clarke ID et al. Identification of human brain tumour initiating cells. Nature 2004; 432(7015): 396–401.
12. Walter D, Satheesha S, Albrecht P et al. CD133 positive embryonal rhabdomyosarcoma stem-like cell population is enriched in rhabdospheres. PLoS One 2011; 6(5): e19506. doi: 10.1371/journal.pone.0019506.
13. Hemmati HD, Nakano I, Lazareff JA et al. Cancerous stem cells can arise from pediatric brain tumors. Proc Natl Acad Sci USA 2003; 100(25): 15178–15183.
14. Ponti D, Costa A, Zaffaroni N et al. Isolation and in vitro propagation of tumorigenic breast cancer cells with stem/progenitor cell properties. Cancer Res 2005; 65(13): 5506–5011.
15. McDermott SP, Eppert K, Lechman ER et al. Comparison of human cord blood engraftment between immunocompromised mouse strains. Blood 2010; 116(2): 193–200. doi: 10.1182/blood-2010-02-271841.
16. Quintana E, Shackleton M, Sabel MS et al. Efficient tumour formation by single human melanoma cells. Nature 2008; 456(7222): 593–598. doi: 10.1038/nature07567.
17. Agliano A, Martin-Padura I, Mancuso P et al. Human acute leukemia cells injected in NOD/LtSz-scid/IL-2Rgamma null mice generate a faster and more efficient disease compared to other NOD/scid-related strains. Int J Cancer 2008; 123(9): 2222–2227. doi: 10.1002/ijc.23772.
18. Ishizawa K, Rasheed ZA, Karisch R et al. Tumor-initiating cells are rare in many human tumors. Cell Stem Cell 2010; 7(3): 279–282. doi: 10.1016/j.stem.2010.08.009.
19. Scadden DT. The stem-cell niche as an entity of action. Nature 2006; 441: 1075–1079.
20. Orimo A, Gupta PB, Sgroi DC et al. Stromal fibroblasts present in invasive human breast carcinomas promote tumor growth and angiogenesis through elevated SDF-1/CXCL12 secretion. Cell 2005; 121(3): 335–348.
21. Olumi AF, Grossfeld GD, Hayward SW et al. Carcinoma-associated fibroblasts direct tumor progression of initiated human prostatic epithelium. Cancer Res 1999; 59(19): 5002–5011.
22. Tzukerman M, Skorecki K. A novel experimental platform for investigating tumorigenesis and anti-cancer therapy in a human microenvironment derived from embryonic stem cells. Discov Med 2003, 3(19): 51–54.
23. Micke P, Ostman A. Tumour-stroma interaction: cancer-associated fibroblasts as novel targets in anti-cancer therapy? Lung Cancer 2004; 45 (Suppl 2): 163–175.
24. Fabris VT, Sahores A, Vanzulli SI et al. Inoculated mammary carcinoma-associated fibroblasts: contribution to hormone independent tumor growth. BMC Cancer 2010; 10: 293. doi: 10.1186/1471-2407-10-293.
25. Yeung TM, Gandhi SC, Wilding JL et al. Cancer stem cells from colorectal cancer-derived cell lines. Proc Natl Acad Sci USA 2010; 107(8): 3722–3727. doi: 10.1073/pnas.0911135107.
26. Di Fiore R, Guercio A, Puleio R et al. Modeling human osteosarcoma in mice through 3AB-OS cancer stem cell xenografts. J Cell Biochem 2012; 113(11): 3380–3392. doi: 10.1002/jcb.24214.
27. Wyckoff J, Gligorijevic B, Entenberg D et al. High-resolution multiphoton imaging of tumors in vivo. Cold Spring Harb Protoc 2011; 2011(10): 1167–1184. doi: 10.1101/pdb.top065904.
28. Chen J, Li Y, Yu TS et al. A restricted cell population propagates glioblastoma growth after chemotherapy. Nature 2012; 488(7412): 522–526. doi: 10.1038/nature11287.
29. Driessens G, Beck B, Caauwe A et al. Defining the mode of tumour growth by clonal analysis. Nature 2012; 488(7412): 527–530. doi: 10.1038/nature11344.
30. Zomer A, Ellenbroek SI, Ritsma L et al. Intravital imaging of cancer stem cell plasticity in mammary tumors. Stem Cells 2013; 31(3): 602–606. doi: 10.1002/stem.1296.
31. Lathia JD, Gallagher J, Myers JT et al. Direct in vivo evidence for tumor propagation by glioblastoma cancer stem cells. PLoS One 2011; 6(9): e24807. doi: 10.1371/journal.pone.0024807.
32. Alison MR, Lim SM, Nicholson LJ. Cancer stem cells: problems for therapy? J Pathol 2011; 223(2): 147–161. doi: 10.1002/path.2793.
33. Shaw FL, Harrison H, Spence K et al. A detailed mammosphere assay protocol for the quantification of breast stem cell activity. J Mammary Gland Biol Neoplasia 2012; 17(2): 111–117. doi: 10.1007/s10911-012-9255-3.
34. Reynolds BA, Weiss S. Generation of neurons and astrocytes from isolated cells of the adult mammalian central nervous system. Science 1992; 255(5052): 1707–1710.
35. Dontu G, Wicha MS. Survival of mammary stem cells in suspension culture: implications for stem cell biology

and neoplasia. J Mammary Gland Biol Neoplasia 2005; 10(1): 75–86.
36. Singh SK, Clarke ID, Terasaki M et al. Identification of a cancer stem cell in human brain tumors. Cancer Res 2003; 63(18): 5821–5828.
37. Tirino V, Desiderio V, d'Aquino R et al. Detection and characterization of CD133+ cancer stem cells in human solid tumours. PLoS One 2008; 3(10): e3469. doi: 10.1371/journal.pone.0003469.
38. Di Fiore R, Santulli A, Ferrante R et al. Identification and expansion of human osteosarcoma-cancer-stem cells by long-term 3-aminobenzamide treatment. J Cell Physiol 2009; 219(2): 301–313. doi: 10.1002/jcp.21667.
39. Kanwar SS, Yu Y, Nautiyal J et al. The Wnt/beta-catenin pathway regulates growth and maintenance of colonospheres. Mol Cancer 2010; 9: 212. doi: 10.1186/1476-4598-9-212.
40. Lee EK, Cho H, Kim CW. Proteomic analysis of cancer stem cells in human prostate cancer cells. Biochem Biophys Res Commun 2011; 412(2): 279–285. doi: 10.1016/j.bbrc.2011.07.083.
41. Cao L, Zhou Y, Zhai B et al. Sphere-forming cell subpopulations with cancer stem cell properties in human hepatoma cell lines. BMC Gastroenterol 2011; 11: 71. doi: 10.1186/1471-230X-11-71.
42. Ye J, Wu D, Shen J et al. Enrichment of colorectal cancer stem cells through epithelial-mesenchymal transition via CDH1 knockdown. Mol Med Rep 2012; 6(3): 507–512. doi: 10.3892/mmr.2012.938.
43. Yang M, Yan M, Zhang R et al. Side population cells isolated from human osteosarcoma are enriched with tumor-initiating cells. Cancer Sci 2011; 102(10): 1774–1781. doi: 10.1111/j.1349-7006.2011.02028.x.
44. Fedr R, Pernicová Z, Slabáková E et al. Automatic cell cloning assay for determining the clonogenic capacity of cancer and cancer stem-like cells. Cytometry A 2013; 83(5): 472–482. doi: 10.1002/cyto.a.22273.
45. Wylie PG, Bowen WP. Determination of cell colony formation in a high-content screening assay. Clin Lab Med 2007; 27(1): 193–199.
46. Bunting KD. ABC transporters as phenotypic markers and functional regulators of stem cells. Stem Cells 2002; 20(1): 11–20.
47. Dean M. ABC transporters, drug resistance, and cancer stem cells. J Mammary Gland Biol Neoplasia 2009; 14(1): 3–9. doi: 10.1007/s10911-009-9109-9.
48. Veselska R, Skoda J, Neradil J. Detection of cancer stem cell markers in sarcomas. Klin Onkol 2012; 25 (Suppl 2): 2S16–2S20.
49. Mayol JF, Loeuillet C, Hérodin F et al. Characterisation of normal and cancer stem cells: one experimental paradigm for two kinds of stem cells. Bioessays 2009; 31(9): 993–1001. doi: 10.1002/bies.200900041.
50. Hiraga T, Ito S, Nakamura H. Side population in MDA-MB-231 human breast cancer cells exhibits cancer stem cell-like properties without higher bone-metastatic potential. Oncol Rep 2011; 25(1): 289–296.
51. Fillmore CM, Kuperwasser C. Human breast cancer cell lines contain stem-like cells that self-renew, give rise to phenotypically diverse progeny and survive chemotherapy. Breast Cancer Res 2008; 10(2): R25. doi: 10.1186/bcr1982.
52. Dembinski JL, Krauss S. Characterization and functional analysis of a slow cycling stem cell-like subpopulation in pancreas adenocarcinoma. Clin Exp Metastasis 2009; 26(7): 611–623. doi: 10.1007/s10585-009-9260-0.
53. Roesch A, Fukunaga-Kalabis M, Schmidt EC et al. A temporarily distinct subpopulation of slow-cycling melanoma cells is required for continuous tumor growth. Cell 2010; 141(4): 583–594. doi: 10.1016/j.cell.2010.04.020.
54. McDonald SA, Graham TA, Schier S et al. Stem cells and solid cancers. Virchows Arch 2009; 455(1): 1–13. doi: 10.1007/s00428-009-0783-1.
55. Lee JT, Herlyn M. Old disease, new culprit: tumor stem cells in cancer. J Cell Physiol 2007; 213(3): 603–609.
56. Deleyrolle LP, Harding A, Cato K et al. Evidence for label-retaining tumour-initiating cells in human glioblastoma. Brain 2011; 134(Pt 5): 1331–1343. doi: 10.1093/brain/awr081.
57. Willan PM, Farnie G. Application of stem cell assays for the characterization of cancer stem cells. In: Allan AL (ed.). Cancer stem cells in solid tumors. Springer 2011: 259–282.
58. Alison MR, Murphy G, Leedham S. Stem cells and cancer: a deadly mix. Cell Tissue Res 2008; 331(1): 109–124.
59. Storms RW, Trujillo AP, Springer JB et al. Isolation of primitive human hematopoietic progenitors on the basis of aldehyde dehydrogenase activity. Proc Natl Acad Sci USA 1999; 96(16): 9118–9123.

Tumor Biol. (2014) 35:7617–7627
DOI 10.1007/s13277-014-2019-5

RESEARCH ARTICLE

LOX/COX inhibitors enhance the antineoplastic effects of all-*trans* retinoic acid in osteosarcoma cell lines

Miroslava Krzyzankova · Silvia Chovanova · Petr Chlapek · Matej Radsetoulal · Jakub Neradil · Karel Zitterbart · Jaroslav Sterba · Renata Veselska

Received: 14 January 2014 / Accepted: 23 April 2014 / Published online: 6 May 2014

Abstract The induced differentiation of tumor cells into mature phenotypes is a promising strategy in cancer therapy. In this study, the effects of combined treatment with all-*trans* retinoic acid (ATRA) and lipoxygenase/cyclooxygenase inhibitors were examined in two osteosarcoma cell lines, Saos-2 and OSA-01. Caffeic acid and celecoxib were used as inhibitors of 5-lipoxygenase and of cyclooxygenase-2, respectively. Changes in the cell proliferation, matrix mineralization, and occurrence of differentiation markers were evaluated in treated cell populations at intervals. The results confirmed the capability of caffeic acid to enhance the antiproliferative effect of ATRA in both cell lines. In contrast, celecoxib showed the same effect in Saos-2 cells only. Furthermore, the extension of matrix mineralization was observed after combined treatment with ATRA and celecoxib or caffeic acid. The increased expression of osteogenic differentiation markers was observed in both cell lines after the combined application of ATRA and inhibitors. The obtained results clearly demonstrate the capability of lipoxygenase/cyclooxygenase inhibitors to enhance the antiproliferative and differentiating effect of ATRA in osteosarcoma cells, although some of these effects are specific and depend on the biological features of the respective tumor or cell line.

Keywords Osteosarcoma · All-*trans* retinoic acid · Caffeic acid · Celecoxib · Osteogenic differentiation

M. Krzyzankova · S. Chovanova · P. Chlapek · M. Radsetoulal · J. Neradil · K. Zitterbart · R. Veselska (✉)
Laboratory of Tumor Biology, Department of Experimental Biology, School of Science, Masaryk University, Kotlarska 2, 611 37 Brno, Czech Republic
e-mail: veselska@sci.muni.cz

K. Zitterbart · J. Sterba · R. Veselska
Department of Pediatric Oncology, University Hospital Brno and School of Medicine, Masaryk University, Cernopolni 9, 613 00 Brno, Czech Republic

S. Chovanova · J. Neradil · J. Sterba
Masaryk Memorial Cancer Institute, Zluty kopec 7, 656 53 Brno, Czech Republic

Introduction

Osteosarcoma is the most common primary bone malignancy in children and adolescents [1]. Osteosarcoma has a higher incidence in males (5.4/1 million person-years) than in females (4.0/1 million person-years) [2] with a peak in the second decade of life, which is related to growth acceleration [3].

The present therapeutic strategies for osteosarcoma include neoadjuvant chemotherapy followed by surgical resection and subsequent adjuvant chemotherapy. Cisplatin, doxorubicin, high-dose methotrexate, and ifosfamide are the most effective compounds used in osteosarcoma protocols [3]. Combined treatment consisting of surgical resection and of chemotherapy improved the 5-year survival rate for patients with non-metastatic disease from 25 % to approximately 60 % [4]. In contrast, the survival of patients with metastatic osteosarcoma is approximately 10–30 % [5]. Therefore, new therapeutic approaches are needed.

Currently, the combination of the classical chemotherapeutics mentioned above with new types of biological therapy targeting cell proliferation, angiogenesis, or apoptosis shows promising effects both in preclinical testing and phase I and II clinical trials [5].

Moreover, the efficacy of some therapeutic agents can be enhanced by their combination with other compounds. The typical example is all-*trans* retinoic acid (ATRA) and its derivatives, which can induce cell differentiation and

apoptosis in many types of hematological malignancies as well as in solid tumors including osteosarcoma [6–9].

The main disadvantage of retinoid usage is their short intracellular availability and the occurrence of resistance [10]. Therefore, how to enhance the therapeutic effect of retinoids is being investigated. Synergistic effects were observed after the combined application of retinoids with vitamin D3 [11, 12], curcumin, vitamin E [13], bile acids [14], interferon gamma [15], or arsenic trioxide [16, 17].

Lipoxygenases and cyclooxygenases are enzymes that are involved in the arachidonic acid degradation pathway. Some final products of this pathway, namely prostaglandins and leukotriens, should participate in the catabolism of retinoic acid, both directly by catalysis of its deactivation or indirectly by regulation of the activity of RA receptors [18–20]. The use of inhibitors of these metabolic pathways can thus prolong the intracellular availability of ATRA. Several studies showing the enhancement of antineoplastic effects of ATRA via its combined application with caffeic acid (CA), which is an inhibitor of 5-lipoxygenase (5-LOX), or with celecoxib (CX), which is an inhibitor of cyclooxygenase-2 (COX-2), have been performed by our research group using cell lines derived from leukemia [21] and neurogenic tumors [22, 23].

In this study, we confirmed that CA and CX can be used to enhance the antineoplastic effects of ATRA in osteosarcoma cell lines.

Materials and methods

Cell culture

The Saos-2 cell line (Cat. no. HTB-85) was purchased from the American Type Culture Collection (Manassas, VA, USA). OSA-01 is an in-house cell line derived previously from a biopsy sample taken from a 13-year-old girl surgically treated for osteosarcoma [24]. The cells were grown in DMEM supplemented with 10 % (Saos-2) or 20 % (OSA-01) fetal bovine serum, antibiotics, and 2 mM glutamine under standard conditions at 37 °C in 5 % CO_2 and a humidified atmosphere. All cell culture reagents were purchased from PAA (Linz, Austria).

Chemicals

ATRA, CX, and CA were purchased from Sigma-Aldrich (St. Louis, USA). These reagents were dissolved in dimethyl sulfoxide (Sigma-Aldrich) to prepare stock solutions of 100 mM (ATRA, CX) and 130 mM (CA). Reagents and solutions were stored at −20 °C under light-free conditions.

Induction of cell differentiation

Stock solutions were diluted in fresh cell culture medium to obtain final concentrations of 0.1 and 1 μM ATRA (for experiments with Saos-2 cells), 1 and 10 μM ATRA (for experiments with OSA-01 cells), of 13 and 52 μM CA and of 10 and 50 μM CX. The concentrations of CA and CX were chosen according the previously published studies and represent levels in blood plasma [21, 23, 25, 26]. Cells were seeded in concentrations described below and allowed to adhere overnight. Untreated cells were used as a control.

MTT assay

For the evaluation of cell proliferation, the MTT assay for the detection of the activity of mitochondrial dehydrogenases in living cells was used. 96-well plates were seeded with 10,000 (Saos-2) or 5,000 (OSA-01) cells/well in 200 μl culture medium, and the cells were allowed to adhere overnight. The culture medium was then removed, and the medium containing the appropriate concentrations of ATRA, CA, and CX and their combinations or control solvents was added and the cells were incubated under standard conditions. To evaluate the changes in cell proliferation, the culture medium with reagents was removed and replaced by 200 μl of the new medium containing 3-[4,5-dimethylthiazol-2-yl]-2,5-diphenyltetrazolium bromide (MTT) in a concentration of 0.5 mg/ml and incubated for 2.5 h at 37 °C. Subsequently, the culture medium was carefully removed, and formazan crystals were dissolved in 200 μl of DMSO. The absorbance at 570 nm with a reference at 620 nm was measured using the Sunrise Absorbance Reader (Tecan, Männedorf, Switzerland) at days 2 and 6 after treatment. Each experiment was performed in triplicate. Dose reduction indexes (DRI, Table 1) and combination indexes (CI, Table 2) were calculated according method described by Chou [27].

Alizarin Red S staining

The level of extracellular matrix mineralization was evaluated using Alizarin Red S staining, which detects calcium compounds both in tissue sections and under in vitro conditions. The cells were cultivated in 12-well plates (10,000 (Saos-2) and 5,000 (OSA-01) cells/well) with the presence or absence of ATRA in combination with CA or CX for 21 days. A cultivation medium with these substances was renewed every 7 days. After 21 days of incubation, the medium was removed; the cells were washed with PBS and fixed with 3 % paraformaldehyde in PBS for 20 min at RT. Subsequently, the cells were incubated with 2 % Alizarin Red S (Sigma-Aldrich) for 45 min at RT. Thereafter, the cells were washed five times with deionized water and then with 70 % ethanol for 30 s. Red Alizarin dye was then dissolved via incubation with 100 mM

Table 1 Dose reduction indexes (DRI) for different concentrations of ATRA and CA or CX

	ATRA 0.1 μM	ATRA 1 μM	ATRA 10 μM	CA 13 μM	CA 52 μM	CX 10 μM	CX 50 μM
Saos-2	5.83	30.61	–	3.00	0.75	1.33	1.56
OSA-01	–	8.30	2.11	4.44	1.40	0.22	0.25

DRI value determines how many -fold the dose of each drug in a synergistic combination may be reduced at a given effect level compared with the doses of each drug alone. DRI were calculated according method described by Chou [27]

cetylpyridinium chloride (Sigma-Aldrich) for 60 min at 50 °C [28]. The absorbance was measured at 450 nm and was compared with the results of the MTT assay, which was performed simultaneously on the same cell populations. Each experiment was performed in triplicate.

Evaluation of cell morphology

Control or treated cells growing on glass coverslips were rinsed in PBS, fixed in methanol to PBS mixture (1:1) for 2 min at RT and then in methanol only for 10 min at RT. The cells were subsequently dried, stained with an undiluted Giemsa stain for 2 min and with Giemsa diluted in water (1:4) for 2 min at RT. Specimens were finally rinsed in water, dried, and mounted onto glass slides.

RT-PCR

The expression of cell differentiation markers was evaluated using RT-PCR. RNA was isolated using the Gene Elute Mammalian Total RNA Miniprep Kit (Sigma-Aldrich). A total of 0.25 μg RNA was then reverse transcribed using M-MLV reverse transcriptase (Top-Bio, Prague, Czech Republic) according to the manufacturer's protocol. RT-PCR was performed on 4 μl cDNA using Taq DNA polymerase 1.1 (Top-Bio) with human primers for bone morphogenic protein-2 (*BMP-2*) collagen type I (*COLL I*), alkaline phosphatase (*ALPL*), osteocalcin (*OCN*), osteopontin (*OPN*), and heat shock protein (*HSP90AB1*) (Table 3) in 20 μl of the reaction volume. The PCR reaction was performed with denaturation at 94 °C for 4 min, annealing at 62 °C for 30 s, elongation at 72 °C for 1 min, and with denaturation at 94 °C for 60 s for 25 cycles for *HSP90AB1* and 30 cycles for the other primers (Table 3). A total of 7 μl of the PCR product was loaded on the 1 % agarose gel with addition of Midori Green Advance (NIPPON Genetics EUROPE GmbH, Germany) and examined using electrophoresis. The Midori Green-stained gels were documented using UVIdoc-HD5 system (Uvitec, UK), the optical density of bands was quantified using ImageJ software [29], and the data were normalized to *HSP90AB1* expression.

Table 2 Combination indexes (CI) for different concentrations of ATRA and CA or CX

		CA 13 μM	CA 52 μM	CX 10 μM	CX 50 μM
Saos-2	ATRA 0.1 μM	0.505 (+++)	1.505 (−−−)	0.924 (±)	0.813 (+)
	ATRA 1 μM	0.366 (+++)	1.366 (−−−)	0.785 (++)	0.674 (+++)
OSA-01	ATRA	0.345	0.834	4.665	4.120
	1 μM	(+++)	(++)	(−−−−)	(−−−−)
	ATRA	0.699	1.188	5.019	4.474
	10 μM	(++)	(−)	(−−−−)	(−−−−)

The combination indexes indicate synergism (+++, CI 0.3–0.7), moderate synergism (++, CI 0.7–0.85), slight synergism (+, CI 0.85–0.90), nearly additive effect (±, CI 0.90–1.10), slight antagonism (−, CI 1.10–1.20), moderate antagonism (−−, CI 1.20–1.45), antagonism (−−−, CI 1.45–3.3), strong antagonism (−−−−, CI 3.3–10). CI were calculated according method described by Chou [27]

Immunoblotting

Protein lysates were loaded onto 10 or 12 % polyacrylamide gels, electrophoresed, and blotted on polyvinylidene difluoride membrane (Bio-Rad Laboratories, Munich, Germany). The membranes were blocked with 5 % nonfat milk in PBS with 0.1 % Tween 20, incubated either with mouse monoclonal anti-osteopontin (clone OPN46, Sigma-Aldrich; dilution 1:500), mouse polyclonal anti-alkaline phosphatase (anti-ALPL) (No. SAB1405448, Sigma-Aldrich;

Table 3 Sequences of primers used for RT-PCR

Gene	Primer sequence	Product
BMP-2	F: 5′CCC AGC GTG AAA AGA GAG AC 3′ R: 5′GAG ACC GCA GTC CGT CTA AG 3′	168 bp
COLL I	F: 5′CAG ACT GGC AAC CTC AAG AA 3′ R: 5′ GGA GGT CTT GGT GGT TTT GT 3′	180 bp
ALPL	F: 5′CCA CGT CTT CAC ATT TGG TG 3′ R: 5′AGA CTG CGC CTG GTA GTT GT 3′	196 bp
OCN	F: 5′GAG GGC AGC GAG GTA GTG AA 3′ R: 5′ TCC TGA AAG CCG ATG TGG TC 3′	152 bp
OPN	F: 5′GCC GAG GTG ATA GTG TGG TT 3′ R: 5′ GTG GGT TTC AGC ACT CTG GT 3′	242 bp
HSP90AB1	F: 5′ CGC ATG AAG GAG ACA CAG AA 3′ R: 5′ TCC CAT CAA ATT CCT TGA GC 3′	169 bp

dilution 1:1,000), rabbit polyclonal anti-COX-2 (No. 100-401-226, Rockland Immunochemicals, Gilbertsville, PA, USA; dilution 1:5,000), or mouse monoclonal β-actin (clone AC-15, Sigma-Aldrich; 1:5,000) primary antibodies. Anti-mouse IgG antibody peroxidase conjugate (No. A9917, Sigma-Aldrich, dilution 1:10,000) or anti-rabbit IgG antibody peroxidase conjugate (No. A2074, Sigma-Aldrich, dilution 1:5,000) was used as secondary antibodies. ECL-Plus detection was performed according to the manufacturer's instructions (GE Healthcare, Little Chalfont, UK).

Results

Cell proliferation

A treatment with ATRA alone in all concentrations reduced the proliferation in both cell lines in the range between 90 and 56 % of the respective control value (Fig. 1).

CA alone reduced the proliferation activity of both cell lines to approximately 80 % after 6 days of treatment (Fig. 1a, c), with the exception of Saos-2 cells treated with 52 μM CA, in which the reduction was markedly stronger (Fig. 1a). The combined treatment with ATRA and CA significantly enhanced the inhibitory effect of ATRA in both cell lines and at all concentrations (Fig. 1a, c). Calculated CI confirmed synergistic effect of the combinations of ATRA with 13 μM CA in both cell lines (Table 2).

CX alone, especially at a concentration of 50 μM, showed a strong inhibitory effect in the Saos-2 cell line (Fig. 1b). In contrast, the inhibition of the cell proliferation of OSA-01 cells by CX was slight regardless of the CX concentration (Fig. 1d).

The combined application of ATRA and CX caused significantly enhanced inhibitory effects that were dose-dependent in Saos-2 cells (Fig. 1b). CI also confirmed synergistic effect of these combinations in Saos-2 cells (Table 2). Nevertheless, similar effects in OSA-01 cells were not observed, and the inhibition of cell proliferation after combined treatment with ATRA and CX was minimal (Fig. 1d).

Matrix mineralization and cell morphology

Both cell lines formed calcium-positive nodules after 21 days of cultivation in control cell populations as well as in all experimental variants (Fig. 2a). The inhibitors alone showed no effect on mineralization if compared with the untreated control cells (Fig. 2b–e).

ATRA alone enhanced the extent of the mineralization by approximately 10–20 % in both the Saos-2 and OSA-01 cell lines (Fig. 2b–e). In the Saos-2 cells, this increase was significant (Fig. 2b, c). The combination of ATRA with CA has no additional effect on the amount of calcium sediments in both cell lines compared with ATRA (Fig. 2b, d). A similar situation was also detected after the treatment of OSA-01 cells with ATRA and CX (Fig. 2e); however, this combined treatment could enhance the mineralization in Saos-2 cells. This effect was not statistically significant (Fig. 2c).

Interestingly, the combined treatment with ATRA and CA significantly enhanced the mineralization in the OSA-01 cell

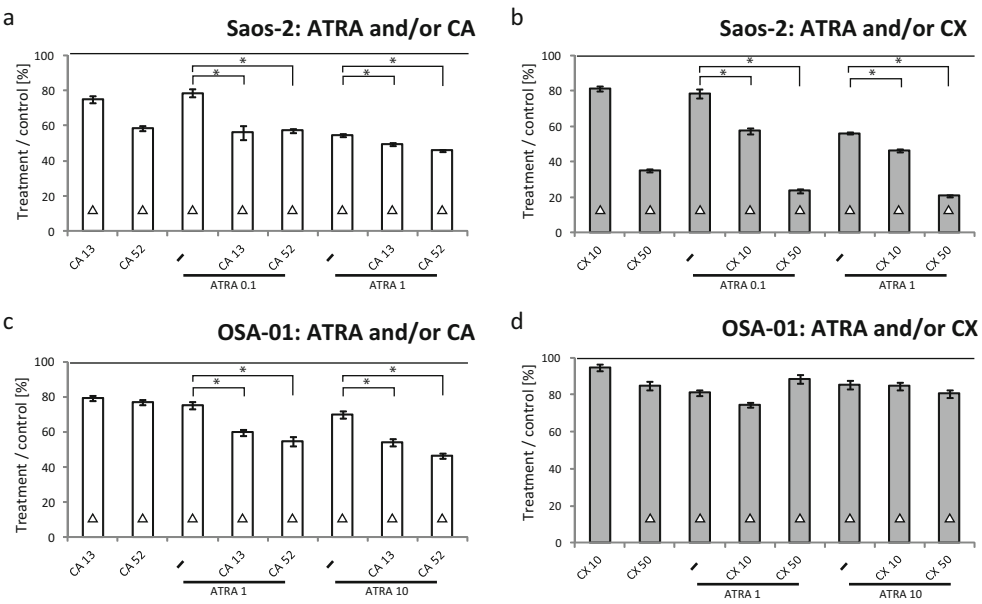

Fig. 1 Proliferation activity of the Saos-2 (**a**, **b**) and OSA-01 (**c**, **d**) cell lines treated with ATRA in combination with CA (**a**, **c**) or CX (**b**, **d**) as measured using the MTT assay after 6 days of incubation. *X-axis*, treatment condition; *Y-axis*, relative cell number (ratio of treatment/control) in percentages. The data represent the means± SEM and were analyzed using one-way ANOVA followed by the Scheffé post hoc test. (* indicates a significant difference between two treatments, Δ indicates a significant difference to the control, $p<0.05$)

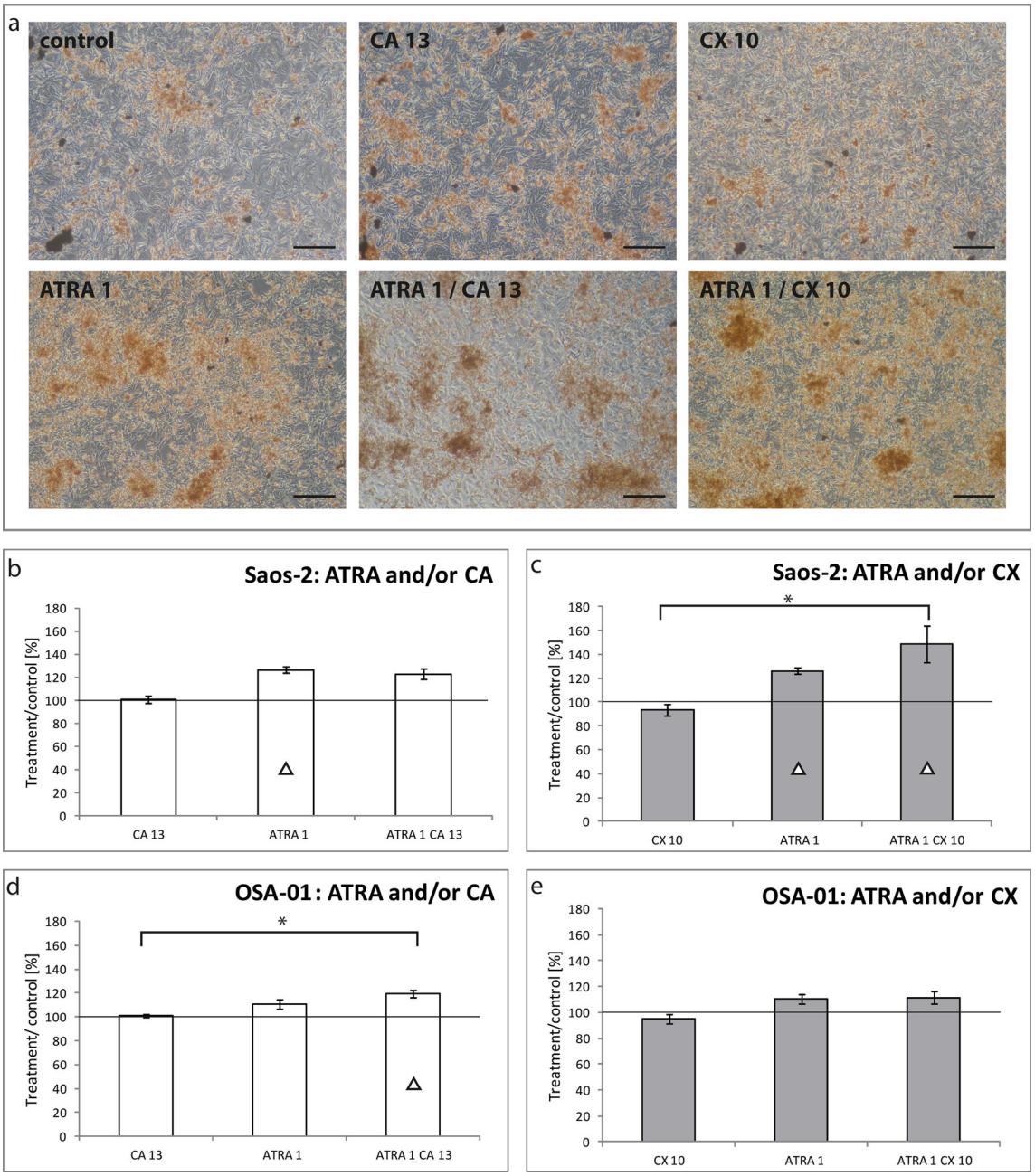

Fig. 2 Matrix mineralization in Saos-2 (**a**–**c**) and OSA-01 (**d**, **e**) cell lines treated with ATRA in combination with CA (**b**, **d**) or CX (**c**, **e**) as measured via staining with Alizarin Red S after 21 days of incubation. Examples of the staining of Saos-2 cells with Alizarin Red S after 21 days of various treatments; bar=200 μm (**a**). Quantification of the matrix mineralization in the Saos-2 (**b**, **c**) and OSA-01 (**d**, **e**) cell lines via staining with Alizarin Red S compared with the mitochondrial activity evaluated using the MTT assay. *X-axis*, treatment condition; *Y-axis*, ratio of Alizarin Red S/MTT compared with the control in percentages. The data represent the means±SEM and were analyzed using one-way ANOVA followed by the Scheffé post hoc test. (* indicates a significant difference between two treatments, Δ indicates a significant difference to the control, $p<0.05$)

line compared with the application of CA only even though ATRA alone did not (Fig. 2d).

In contrast, we did not observe any marked changes in cell morphology during these experiments. Saos-2 cells treated with ATRA-alone or in combinations with inhibitors-only showed the slightly increased tendency to form small islet sheets and the cells became spindle-like shape (Fig. 3a). Control OSA-01 cells showed a polygonal morphology with many protrusions and tend to overgrowth at confluence. Experimental treatment with ATRA alone or in combinations with inhibitors led to the apparent decrease in cell number in the cell culture and the cells are well spread (Fig. 3b).

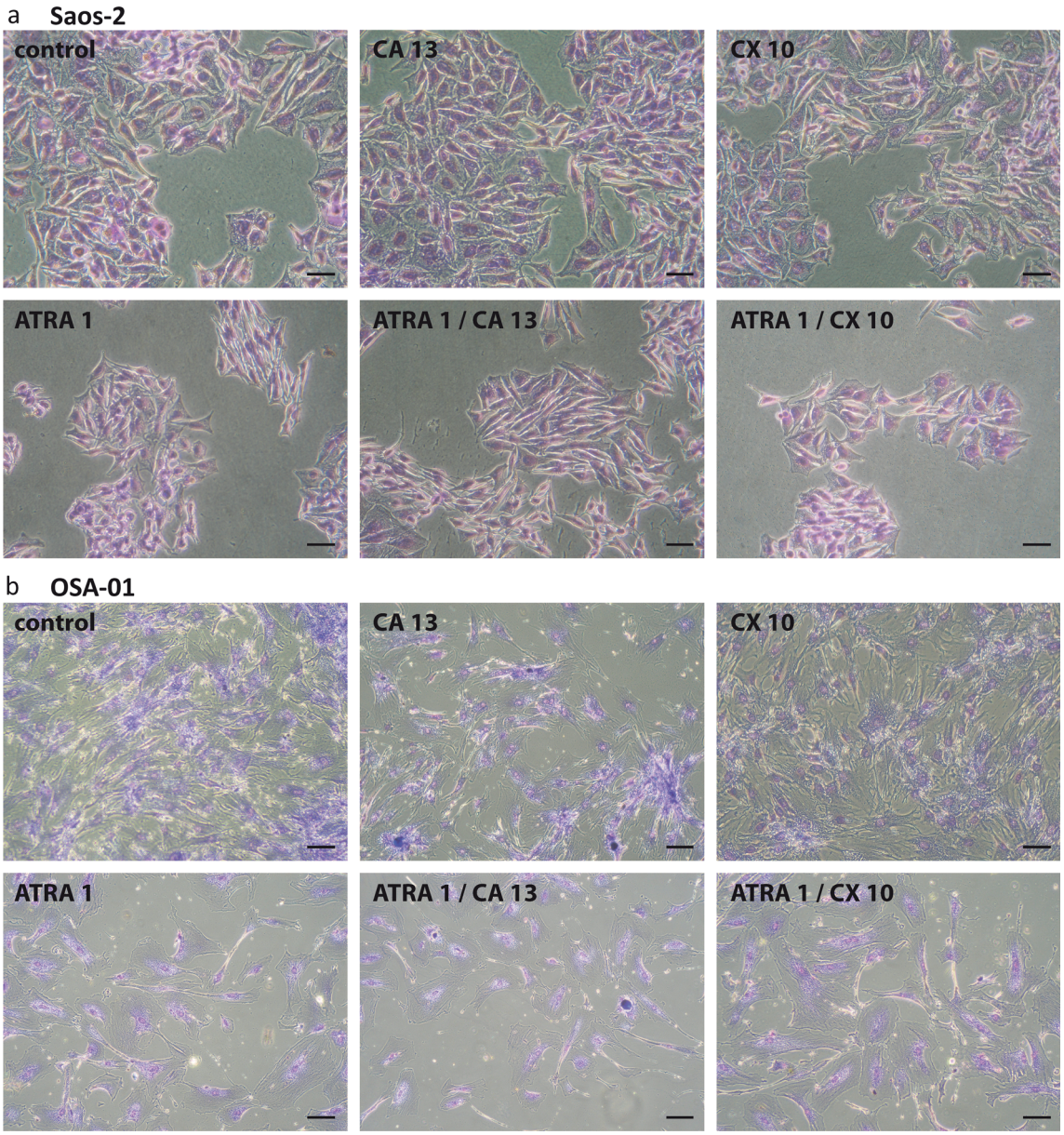

Fig. 3 Morphology of Saos-2 (**a**) and OSA-01 (**b**) cells, control or treated with ATRA in combination with CA or CX as visualized via Giemsa staining after 7 (Saos-2) or 21 (OSA-01) days of incubation; bar=50 μm

Induced cell differentiation

The expression of genes encoding known osteogenic differentiation markers was evaluated using RT-PCR after 7 days of treatment with ATRA, CA, and CX or their combinations both in Saos-2 (Fig. 4) and OSA-01 cells (Fig. 5). The course of induced differentiation was evaluated using markers typical for early, middle, and late phase of osteogenic differentiation. *BMP-2* is involved in the induction of differentiation, while *ALPL* and *COLL I* represent the middle stage of differentiation. For the late stage of differentiation, expressions of *OPN* and *OCN* were evaluated.

The expression of all middle- or late-phase differentiation markers incubated with CA alone did not change or slightly enhanced in the cell lines (Figs. 4b–f and 5b–f) when compared with control levels.

In Saos-2 cells, CA alone did not increase the expression of markers of the early or middle stages of differentiation (Fig. 4b–d), but the expression of *OPN* was enhanced (Fig. 4f). In contrast, the application of CA alone led to a slight increase in *BMP-2*, *ALPL*, and *OPN* gene expressions in OSA-01 cells (Fig. 5b, c, f). Conversely, immunoblotting showed an increase in ALPL expression in Saos-2 cells and osteopontin in OSA-01 cells (Fig. 6).

Surprisingly, CX alone markedly increased the expressions of both *COLL I* and *OPN* in Saos-2 cells (Fig. 4d, f), as well as

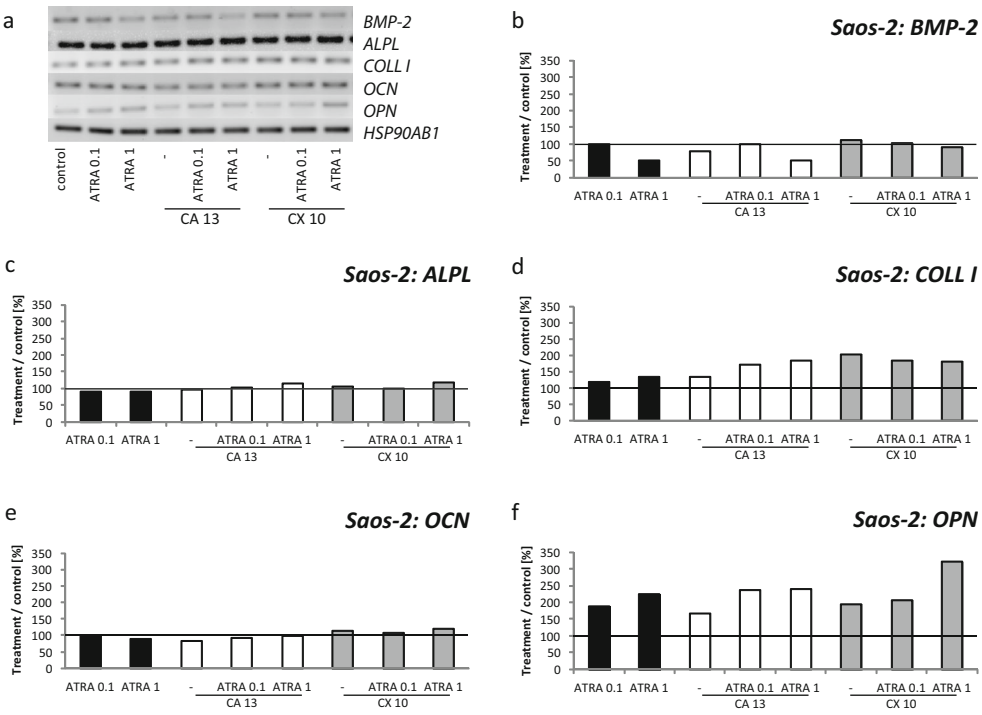

Fig. 4 Course of the osteogenic differentiation in the Saos-2 cell line treated with ATRA in combination with CA or CX as analyzed using RT-PCR. Representative electrophoresis (**a**) and the evaluation of the mRNA expression of *BMP-2* (**b**), *ALPL* (**c**), *COLL I* (**d**), *OCN* (**e**) and *OPN* (**f**). The expressions were quantified using densitometry and were compared with the expression of *HSP90AB1*

the expression of *OCN* in OSA-01 cells (Fig. 5e). Furthermore, the expressions of *BMP-2* and *OPN* were also slightly enhanced in OSA-01 cells after treatment with CX alone (Fig. 5b, f). Nevertheless, this change of osteopontin expression was not detectable at protein levels in Saos-2 cells but this effect was observed in OSA-01 cells (Fig. 6).

Treatment with ATRA alone enhanced the expressions of the middle and late differentiation markers *COLL I* and *OPN* in Saos-2 cells (Fig. 4d, f). The expression of *BMP-2* was strongly enhanced after incubation with ATRA alone in the OSA-01 cells (Fig. 5b). On the protein levels, the increase in expression of osteopontin was detected in both cell lines, whereas of ALPL in Saos-2 cells only (Fig. 6).

The combined treatment with ATRA and CA considerably enhanced the expression of *COLL I* and *OPN* in the Saos-2

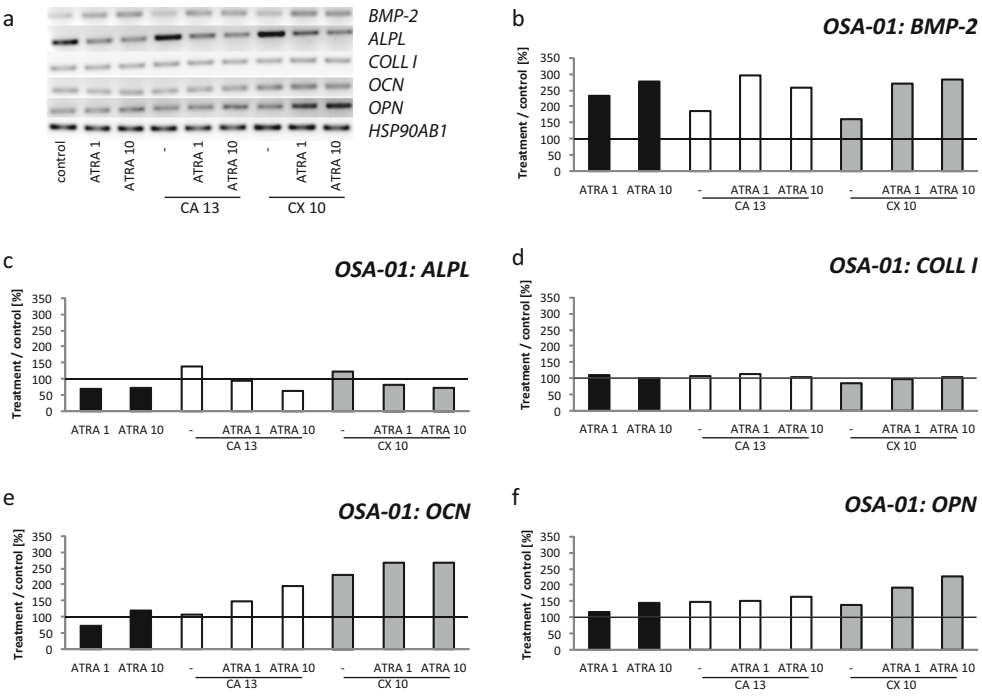

Fig. 5 Course of the osteogenic differentiation in the OSA-01 cell line treated with ATRA in combination with CA or CX as analyzed using RT-PCR. Representative electrophoresis (**a**) and the evaluation of mRNA expression of *BMP-2* (**b**), *ALPL* (**c**), *COLL I* (**d**), *OCN* (**e**), and *OPN* (**f**). The expressions were quantified using densitometry and were compared with the expression of *HSP90AB1*

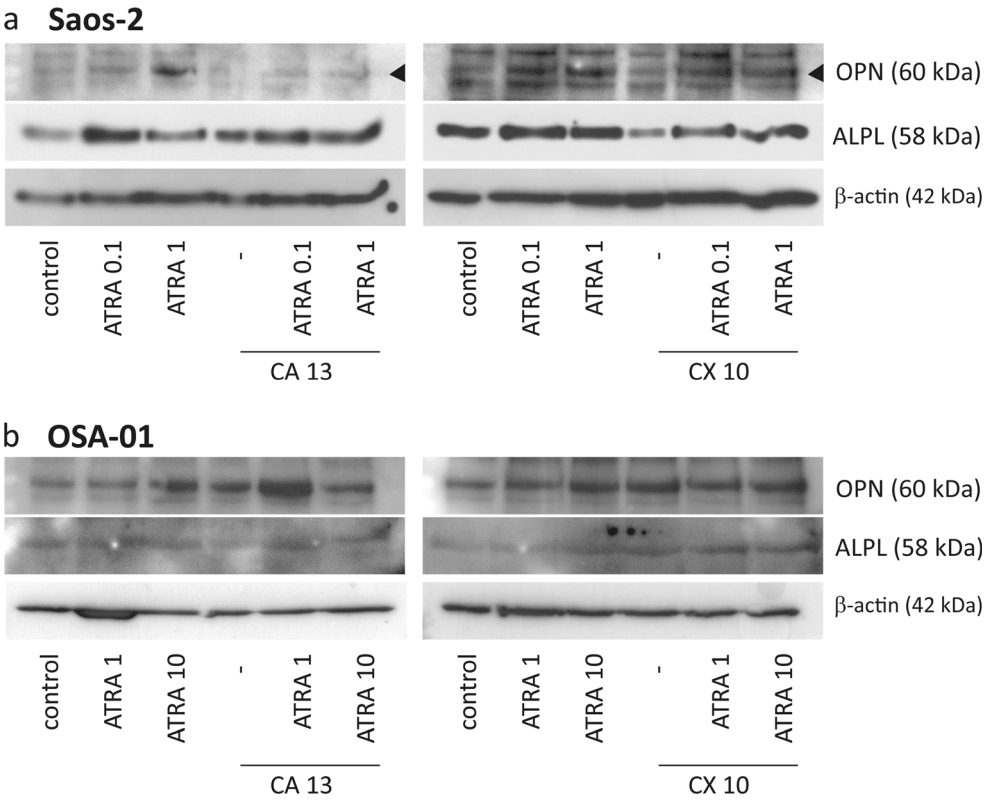

Fig. 6 Immunoblot analysis of the osteopontin (OPN) and alkaline phosphatase (ALPL) in Saos-2 (**a**) and OSA-01 (**b**) cells, control or treated with ATRA in combination with CA or CX after 7 days of incubation. β-actin served as a loading control

cells (Fig. 4d, f). In the OSA-01 cells, the enhanced expression of *BMP-2* and *OCN* was detected after combined treatment with lower concentrations of ATRA and CA (Fig. 5b, e). In contrast, the increase in osteopontin expression was detected namely in OSA-01 cells, while enhanced levels of ALPL were noted in both cell lines (Fig. 6).

Combined application of ATRA and CX increased the effect of ATRA alone in terms of the *OPN* expression in Saos-2 cells (Fig. 4f) and *BMP-2* (in combination with a lower concentration of ATRA), *OCN*, and *OPN* expressions in the OSA-01 cells (Fig. 5b, e, f). The very similar changes in osteopontin and ALPL were detected in both cell lines with immunoblotting (Fig. 6).

Discussion

At present, patients suffering from osteosarcoma experience high rates of morbidity and mortality with poor prognosis in cases of metastatic disease despite multiagent cytotoxic chemotherapy and surgery [1, 30, 31]. Therefore, new strategies in osteosarcoma treatment, especially biological therapies, are needed.

One example of these novel approaches is the COMBAT therapeutic protocol, which was originally designed for pediatric patients with relapsed and/or high-risk solid tumors [32]. According to this protocol, low doses of cytotoxic (etoposide, temozolomide) and anti-angiogenic (celecoxib) agents, as well as differentiation inducers (retinoids, vitamin D3 and its derivatives) and other biologicals are administered in the metronomic regimen. More tailored versions of COMBAT protocol were also reported as feasible and effective treatment options for patients with refractory tumors including sarcomas [33].

Based on this clinical experience with the COMBAT protocol as well as on our previous findings that antineoplastic effects of retinoids are enhanced through their combination with 5-lipoxygenase/cyclooxygenase-2 (LOX/COX) inhibitors in neurogenic tumors [22, 23] and leukemias [21], we decided to perform the analogical study to include osteosarcoma cells.

Our results clearly demonstrated that CA as the inhibitor of 5-LOX and CX as the inhibitor of COX-2 can be used to enhance the antiproliferative effects of ATRA on both of the osteosarcoma cell lines included in this study. These observations were the same as our previously reported findings on leukemic and neuroblastoma cells after a combined treatment with ATRA and LOX/COX inhibitors [21, 23].

ATRA alone also induced recognizable growth inhibition against the control at a concentration given above for both osteosarcoma cell lines; these results are in accordance with those obtained by Yang and colleagues [9].

Some authors also showed a significant inhibition of proliferation activity in other established osteosarcoma cell lines,

MG-63 and U2OS, via treatment with the same concentration of CX that was used in one of our previous studies [34, 35]. It was also demonstrated that the inhibition of cell proliferation after the treatment with CX involves Wnt/β-catenin and P13K/Akt pathways in the MG63 osteosarcoma cell line [35, 36].

This result appears to be important because CX is administered to reach the same concentration in the plasma of patients in treatment protocols primarily for its antiangiogenic effect, and the inhibition of tumor cell proliferation could be beneficial. Nevertheless, our results showed the inhibition of cell proliferation in the Saos-2 cell line but not in the OSA-01 cells. As we mentioned above, the OSA-01 cell line represents the in-house cell line that was derived from tumor tissue taken from a 13-years-old girl suffering from localized high-grade osteosarcoma. The girl was initially treated according the EURAMOS international protocol. Nevertheless, the tumor showed a poor response to the neoadjuvant chemotherapy, and the course of the disease was very aggressive despite subsequent treatments in which immunomodulation and metronomic therapies were included. The patient died 4.5 years after diagnosis. Thus, we assume that the difference in the antiproliferative effect of CX between the Saos-2 and OSA-01 cell lines can be explained by different growth parameters in these two cell lines. It is known that COX-2 promotes proliferation, migration, and invasion in the other human osteosarcoma cell line, U2OS [34]. Furthermore, high levels of COX-2 were reported to be associated with a worse response to chemotherapy [37] and metastases [38] in osteosarcomas. These findings are in accordance with the biological features of the tumor from which the OSA-01 cell line was derived; an overexpression of the COX-2 was found in tumor tissue. Furthermore, the overexpression of the COX-2 was confirmed in OSA-01 cells by immunoblotting (Fig. 7).

CA alone is known to inhibit cell proliferation in human hepatoma cell lines [39]. Our results also confirm a significant inhibition of cell proliferation in both of the osteosarcoma cell lines. In contrast, an increase in proliferation activity by CA was described in human lung cancer cell lines; this effect was pursued via the NF-kappa B signaling pathway [40].

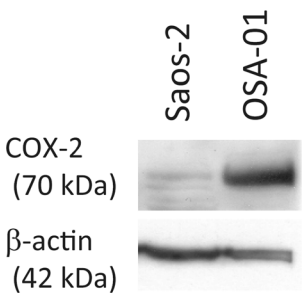

Fig. 7 Immunoblot analysis of the COX-2 in untreated Saos-2 and OSA-01 cells. β-actin served as a loading control

In our study, we also investigated how to enhance the ATRA-induced cell differentiation using a combined treatment with LOX/COX inhibitors. The capability of ATRA to induce osteogenic differentiation was formerly described using stem cells derived from human periodontal ligaments [41]. ATRA-induced osteogenic differentiation was also demonstrated in the 143B human osteosarcoma cell line [9]. According to these two studies, we decided to evaluate the course of osteogenic differentiation by measuring the matrix mineralization after Alizarin Red staining as well as through the detection of the selected differentiation markers using RT-PCR. BMP-2 is known to be involved in the induction of osteogenic differentiation [42]. The expression of Coll I is also typical for the early stages of the differentiation. Levels of ALPL usually increase during the process of mineralization. OPN and OCN are recognized to be markers of late osteogenic differentiation; OPN appears prior to OCN [43].

In light of this course of differentiation, we observed that Saos-2 cells achieved later stages of osteogenic differentiation within an interval of 7 days in which an enhanced expression of *COLL I* and *OPN*, as well as a decrease in *BMP-2* expressions were noted after treatment with ATRA. In contrast, OSA-01 cells were found to be in the early differentiation stage at the same interval with upregulated *BMP-2* and partial *OPN* expression. The enhancement of the differentiation effect of ATRA in combination with CA or CX was observed in both cell lines, confirming our previous findings on neuroblastoma cells [22, 23]. Our results on osteosarcoma cells also demonstrated that the effect of CX appears to be more effective than that of CA.

To conclude, our results provide the first evidence that the antineoplastic effects of ATRA, i.e., the inhibition of cell proliferation activity and induced differentiation, can be enhanced through its combined application with LOX/COX inhibitors not only in neurogenic tumor cells but also in osteosarcoma cells, although some of these effects are cell line-specific. These findings support our previous statement that the therapeutic usage of retinoid in combination with COX inhibitor has strong biological rationale and that the dietary uptake of the natural phenolic compounds including caffeic acid (for example, honey, apple juice, grapes, and some vegetables) may also potentiate the cell differentiation induced by retinoids [22]. Nevertheless, further studies focusing on the molecular mechanisms of the modulation of ATRA actions in osteosarcoma cells are needed.

Acknowledgments The project is funded from the SoMoPro (South Moravian Programme for distinguished researchers) programme. Research leading to these results has received a financial contribution from the European Community within the Seventh Framework Programme (FP/2007-2013) under Grant Agreement No229603. The research is

also co-financed by the South Moravian Region, by the European Regional Development Fund and the State Budget of the Czech Republic-project RECAMO CZ.1.05/2.1.00/03.0101, and by the project CEB CZ.1.07/2.3.00/20.0183. We are grateful to Mrs. Johana Maresova for her technical assistance.

Conflicts of interest None.

References

1. Amankwah EK, Conley AP, Reed DR. Epidemiology and therapies for metastatic sarcoma. Clin Epidemiol. 2013;5:147–62.
2. Ottaviani G, Jaffe N. The epidemiology of osteosarcoma. Cancer Treat Res. 2009;152:3–13.
3. Gorlick R, Janeway K, Lessnick S, Randall RL, Marina N. COG Bone Tumor Committee. Children's Oncology Group's 2013 blueprint for research: bone tumors. Pediatr Blood Cancer. 2013;60:1009–15.
4. Caudill JS, Arndt CA. Diagnosis and management of bone malignancy in adolescence. Adolesc Med State Art Rev. 2007;18:62–78.
5. Sampson VB, Gorlick R, Kamara D, Anders Kolb E. A review of targeted therapies evaluated by the pediatric preclinical testing program for osteosarcoma. Front Oncol. 2013;3:132.
6. Hong SH, Kadosawa T, Mochizuki M, Matsunaga S, Nishimura R, Sasaki N. Effect of all-trans and 9-cis retinoic acid on growth and metastasis of xenotransplanted canine osteosarcoma cells in athymic mice. Am J Vet Res. 2000;61:1241–4.
7. He BC, Chen L, Zuo GW, Zhang W, Bi Y, Huang J, et al. Synergistic antitumor effect of the activated PPARγ and retinoid receptors on human osteosarcoma. Clin Cancer Res. 2010;16:2235–45.
8. Dozza B, Papi A, Lucarelli E, Scotlandi K, Pierini M, Tresca G, et al. Cell growth inhibition and apoptotic effect of the rexinoid 6-OH-11-O-hydroxyphenantrene on human osteosarcoma and mesenchymal stem cells. In Vitro Toxicol. 2012;26:142–9.
9. Yang QJ, Zhou LY, Mu YQ, Zhou QX, Luo JY, Cheng L, et al. All-trans retinoic acid inhibits tumor growth of human osteosarcoma by activating Smad signaling-induced osteogenic differentiation. Int J Oncol. 2012;41:153–60.
10. Montesinos P, Sanz MA. The differentiation syndrome in patients with acute promyelocytic leukemia: experience of the pethema group and review of the literature. Mediterr J Hematol Infect Dis. 2011;3:e2011059.
11. Verlinden L, Verstuyf A, Mathieu C, Tan BK, Bouillon R. Differentiation induction of HL60 cells by 1,25(OH)2D3, all trans retinoic acid, rTGF-beta2 and their combinations. J Steroid Biochem Mol Biol. 1997;60:87–97.
12. James S, Williams M, Newland A, Colston K. Leukemia cell differentiation: cellular and molecular interactions of retinoids and vitamin D. Gen Pharmacol. 1999;32:143–54.
13. Sokoloski JA, Sartorelli AC. Induction of the differentiation of HL-60 promyelocytic leukemia cells by nonsteroidal anti-inflammatory agents in combination with low levels of vitamin D3. Leuk Res. 1998;22:153–61.
14. Zimber A, Chedeville A, Abita JP, Barbu V, Gespach C. Functional interactions between bile acids, all-*trans* retinoic acid, and 1,25-dihydroxy-vitamin D3 on monocytic differentiation and *myeloblastin* gene down-regulation in HL60 and THP-1 human leukemia cells. Cancer Res. 2000;60:672–8.
15. Haque A, Das A, Hajiaghamohseni L, Younger A, Banik N, Ray S. Induction of apoptosis and immune response by all-trans retinoic acid plus interferon-gamma in human malignant glioblastoma T98G and U87MG cells. Cancer Immunol Immunother. 2007;56:615–25.
16. Chen G, Zhu J, Shi X, Ni J, Zhong H, Si G, et al. In vitro studies on cellular and molecular mechanisms of arsenic trioxide (As2O3) in the treatment of acute promyelocytic leukemia: As2O3 induces NB4 cell apoptosis with downregulation of Bcl-2 expression and modulation of PML-RAR alpha/PML proteins. Blood. 1996;88:1052–61.
17. Hu J, Liu YF, Wu CF, Xu F, Shen ZX, Zhu YM, et al. Long-term efficacy and safety of all-trans retinoic acid/arsenic trioxide-based therapy in newly diagnosed acute promyelocytic leukemia. Proc Natl Acad Sci U S A. 2009;106:3342–7.
18. Nadin L, Murray M. Arachidonic acid-mediated cooxidation of all-trans-retinoic acid in microsomal fractions from human liver. Br J Pharmacol. 2000;131:851–7.
19. Avis I, Martínez A, Tauler J, Zudaire E, Mayburd A, Abu-Ghazaleh R, et al. Inhibitors of the arachidonic acid pathway and peroxisome proliferator-activated receptor ligands have superadditive effects on lung cancer growth inhibition. Cancer Res. 2005;65:4181–90.
20. Bell E, Ponthan F, Whitworth C, Westermann F, Thomas H, Redfern CPF. Cell survival signalling through PPARδ and arachidonic acid metabolites in neuroblastoma. PLoS ONE. 2013;8:e68859.
21. Veselska R, Zitterbart K, Auer J, Neradil J. Differentiation of HL-60 myeloid leukemia cells induced by all-trans retinoic acid is enhanced in combination with caffeic acid. Int J Mol Med. 2004;14:305–10.
22. Chlapek P, Redova M, Zitterbart K, Hermanova M, Sterba J, Veselska R. Enhancement of ATRA-induced differentiation of neuroblastoma cells with LOX/COX inhibitors: an expression profiling study. J Exp Clin Cancer Res. 2010;29:45.
23. Redova M, Chlapek P, Loja T, Zitterbart K, Hermanova M, Sterba J, et al. Influence of LOX/COX inhibitors on cell differentiation induced by all-trans retinoic acid in neuroblastoma cell lines. Int J Mol Med. 2010;25:271–80.
24. Veselska R, Hermanova M, Loja T, Chlapek P, Zambo I, Vesely K, et al. Nestin expression in osteosarcomas and derivation of nestin/CD133 positive osteosarcoma cell lines. BMC Cancer. 2008;8:300.
25. Nardini M, Scaccini C, Packer L, Virgili F. In vitro inhibition of the activity of phosphorylase kinase, protein kinase C and protein kinase A by caffeic acid and a procyanidin-rich pine bark (*Pinus marittima*) extract. Biochim Biophys Acta. 2000;1474:219–25.
26. Dandekar DS, Lopez M, Carey RI, Lokeshwar BL. Cyclooxygenase-2 inhibitor celecoxib augments chemotherapeutic drug-induced apoptosis by enhancing activation of caspase-3 and -9 in prostate cancer cells. Int J Cancer. 2005;115:484–92.
27. Chou TC. Theoretical basis, experimental design, and computerized simulation of synergism and antagonism in drug combination studies. Pharmacol Rev. 2006;58:621–81.
28. Muthusami S, Senthilkumar K, Vignesh C, Ilangovan R, Stanley J, Selvamurugan N, et al. Effects of Cissus quadrangularis on the proliferation, differentiation and matrix mineralization of human osteoblast like SaOS-2 cells. J Cell Biochem. 2011;112:1035–45.
29. Schneider CA, Rasband WS, Eliceiri KW. NIH Image to ImageJ: 25 years of image analysis. Nat Methods. 2012;9:671–5.
30. O'Day K, Gorlick R. Novel therapeutic agents for osteosarcoma. Expert Rev Anticancer Ther. 2009;9:511–23.
31. Dela Cruz FS. Cancer stem cells in pediatric sarcomas. Front Oncol. 2013;3:168.
32. Sterba J, Valik D, Mudry P, Kepak T, Pavelka Z, Bajciova V, et al. Combined biodifferentiating and antiangiogenic oral metronomic therapy is feasible and effective in relapsed solid tumors in children: single-center pilot study. Onkologie. 2006;29:308–13.
33. Zapletalova D, Andre N, Deak L, Kyr M, Bajciova V, Mudry P, et al. Metronomic chemotherapy with the COMBAT regimen in advanced pediatric malignancies: a multicenter experience. Oncology. 2012;82:249–60.
34. Lee EJ, Choi EM, Kim SR, Park JH, Kim H, Ha KS, et al. Cyclooxygenase-2 promotes cell proliferation, migration and invasion in U2OS human osteosarcoma cells. Exp Mol Med. 2007;39:469–76.

35. Xia J-J, Pei L-B, Zhuang J-P, Ji Y, Xu G-P, Zhang Z-P, et al. Celecoxib inhibits β-catenin-dependent survival of the human osteosarcoma MG-63 cell line. J Int Med Res. 2010;38:1294–304.
36. Liu B, Qu L, Yang Z, Tao H. Cyclooxygenase-2 inhibitors induce anoikis in osteosarcoma via PI3K/Akt pathway. Med Hypotheses. 2012;79:98–100.
37. Masi L, Recenti R, Silvestri S, Pinzani P, Pepi M, Paglierani M, et al. Expression of cyclooxygenase-2 in osteosarcoma of bone. Appl Immunohistochem Mol Morphol. 2007;15:70–6.
38. Jiao G, Ren T, Lu Q, Sun Y, Lou Z, Peng X, et al. Prognostic significance of cyclooxygenase-2 in osteosarcoma: a meta-analysis. Tumour Biol. 2013;34:2489–95.
39. Guerriero E, Sorice A, Capone F, Costantini S, Palladino P, D'ischia M, et al. Effects of lipoic acid, caffeic acid and a synthesized lipoyl-caffeic conjugate on human hepatoma cell lines. Molecules. 2011;16:6365–77.
40. Lin CL, Chen RF, Chen JY, Chu YC, Wang HM, Chou HL, et al. Protective effect of caffeic acid on paclitaxel induced anti-proliferation and apoptosis of lung cancer cells involves NF-κB pathway. Int J Mol Sci. 2012;13:6236–45.
41. Chadipiralla K, Yochim JM, Bahuleyan B, Huang CY, Garcia-Godoy F, Murray PE, et al. Osteogenic differentiation of stem cells derived from human periodontal ligaments and pulp of human exfoliated deciduous teeth. Cell Tissue Res. 2010;340:323–33.
42. Susperregui AR, Vinals F, Ho PW, Gillespie MT, Martin TJ, Ventura F. BMP-2 regulation of PTHrP and osteoclastogenic factors during osteoblast differentiation of C2C12 cells. J Cell Physiol. 2008;216:144–52.
43. Aubin JE, Liu F, Malaval L, Gupta AK. Osteoblast and chondroblast differentiation. Bone. 1995;17:77S–83S.

EGFR signaling in the HGG-02 glioblastoma cell line with an unusual loss of EGFR gene copy

JAN SKODA[1,2], JAKUB NERADIL[1,3], KAREL ZITTERBART[2], JAROSLAV STERBA[2,3] and RENATA VESELSKA[1,2]

[1]Laboratory of Tumor Biology, Department of Experimental Biology, Faculty of Science, Masaryk University, Brno;
[2]Department of Pediatric Oncology, University Hospital Brno and Faculty of Medicine, Masaryk University, Brno;
[3]Masaryk Memorial Cancer Institute, Brno, Czech Republic

Received September 11, 2013; Accepted October 24, 2013

DOI: 10.3892/or.2013.2864

Abstract. Epidermal growth factor receptor (*EGFR*) gene amplification and the overexpression of EGFR are described as common features of glioblastoma multiforme (GBM). Nevertheless, we previously reported the loss of *EGFR* gene copy in a GBM specimen from a patient with an unusually favorable course of the disease, and the HGG-02 cell line with this aberration was successfully derived from this tumor. Here, we present a detailed analysis of changes in gene expression and cell signaling in the HGG-02 cell line; the GM7 reference cell line with a standard EGFR gene copy number derived from a very aggressive GBM was used as a control. We confirmed the downregulation of EGFR expression and signaling in HGG-02 cells using different methods (RTK analysis, gene profiling and RT-PCR). Other changes that may have contributed to the non-aggressive phenotype of the primary tumor were identified, including the downregulated phosphorylation of the Axl and Trk receptors, as well as increased activity of JNK and p38 kinases. Notably, differences in PDGF signaling were detected in both of these cell lines; HGG-02 cells preferentially expressed and signaled through PDGFRα, and PDGFRβ was strongly overexpressed and phosphorylated in the GM7 reference cell line. Using expression profiling of cancer-related genes, we revealed the specific profile of HGG-02 cells that included upregulated tumor-suppressors as well as downregulated genes associated with the extracellular matrix. This study represents the first comprehensive analysis of gene expression and cell signaling in glioblastoma cells with lower *EGFR* gene dosage. As indicated by our results, the TAM receptors, Trk receptors and PDGFRs need to be investigated further since their regulation appears to be important for glioblastoma biological features as well as the clinical course of the disease.

Correspondence to: Professor Renata Veselska, Laboratory of Tumor Biology, Department of Experimental Biology, Faculty of Science, Masaryk University, Kotlarska 2, 611 37 Brno, Czech Republic
E-mail: veselska@sci.muni.cz

Key words: glioblastoma multiforme, epidermal growth factor receptor signaling, PDGFR, TAM receptors, receptor tyrosine kinase, mitogen-activated protein kinase

Introduction

The epidermal growth factor receptor (EGFR) is a member of the EGFR receptor tyrosine kinase (RTK) family, together with ErB2/Neu/HER2, Erb3/HER3 and ErbB4/HER4 (1). Activating ligands of these receptors include epidermal growth factor (EGF), transforming growth factor α (TGF-α), epiregulin, neuregulins and amphiregulin. Binding of the ligands to the extracellular domain of EGFR RTKs causes the formation of homodimers or heterodimers, cross-activation of tyrosine kinase domains and autophosphorylation. These events result in the stimulation of intracellular signaling cascades, including the phosphatidylinositol-3 kinase (PI3K)/Akt and mitogen-activated protein kinase (MAPK) cascades. Although EGFR signaling is essential for normal tissue development and homeostasis, the abnormal activity of EGFR RTK members plays a key role in tumor initiation and progression (2).

Glioblastoma multiforme (GBM) is the most frequent and malignant neoplasm of the human nervous system. Despite current therapies, the prognosis for patients with GBMs remains poor, with a median survival time that ranges from 8.8 months (patients <50 years of age) to 1.8 months (patients >80 years of age) (3,4). *EGFR* gene amplification and EGFR overexpression are common features of GBM; however, they are rare in low-grade gliomas, which suggests a causal role of aberrant EGFR signaling in the pathogenesis of GBM (5). The amplification of *EGFR* is present in 35-70% of cases, typically in primary *de novo* GBM (4,6,7).

In our previous study, we reported the unusual loss of *EGFR* gene copy in GBM obtained from a patient with an unusually favorable course of the disease who experienced a survival of 5.5 years between diagnosis and death (8). Here, we present further detailed analysis of the HGG-02 cell line derived from this tumor when compared with the GM7 reference cell line that contains a standard *EGFR* gene copy number (9).

Materials and methods

Cell lines and cell culture. The HGG-02 (8) and GM7 (9) established glioblastoma cell lines were used in the present study. Cell cultures were maintained in DMEM supplemented with 20% fetal calf serum, 2 mM glutamine and antibiotics (100 IU/ml of penicillin and 100 μg/ml of streptomycin) (PAA

Laboratories, Linz, Austria) under standard conditions at 37˚C in an atmosphere of 95% air and 5% CO_2. The cells were subcultivated once a week. Where indicated, the cells were starved in serum-free media.

RT-PCR. For RT-PCR, total RNA was extracted with the GenElute™ Mammalian Total RNA Miniprep kit (Sigma-Aldrich, St. Louis, MO, USA). For all samples, equal amounts of RNA (25 ng of RNA/1 μl of total reaction content) were reverse transcribed into cDNA using M-MLV (Top-Bio, Prague, Czech Republic) and oligo-dT (Qiagen Inc., Valencia, CA, USA) priming. Primers for EGFR, ErbB2, ErbB3, ErbB4, TGF-α, EGF, epiregulin (EREG), neuroglycan C (NGC), NRG-1, NRG-2, PDGFRα, PDGFRβ, PDGFA, PDGFB, HSP90AB1 and GAPDH were used as described in Table I.

Phospho-RTK array analysis. The Human Phospho-RTK Array kit (R&D Systems, Minneapolis, MN, USA) was used to determine the relative levels of tyrosine phosphorylation of 42 distinct RTKs according to the manufacturer's protocol. The arrays were incubated with 450 μg of protein lysate. The levels of phosphorylation were quantified using ImageJ software and normalized to phosphotyrosine positive-control spots.

Phospho-MAPK array analysis. For the detection of the phosphorylation status of MAPKs and other serine/threonine kinases, the Human Phospho-MAPK Array kit (R&D Systems) was used according to the manufacturer's protocol, and 250 μg of protein lysate was used for each array. The arrays were analyzed using ImageJ software, and the levels of phosphorylation were normalized to positive control spots.

Expression profiling. Total RNA was extracted with the GenElute™ Mammalian Total RNA Miniprep kit, and the samples were assessed spectrophotometrically. Purified biotin-labeled cRNA was generated using the Oligo GEArray® Reagent kit and was hybridized to the OHS-802 Oligo GEArray® Human Cancer Microarray, which profiles 440 genes related to cancer, in accordance with the manufacturer's instructions (SABiosciences, Frederick, MD, USA). The GEArray Expression Analysis Suite software (SABiosciences) was used for data analyses.

Results

EGFR and EGFRvIII mRNA status. As our previous findings suggested that the loss of the *EGFR* gene copy may have contributed to the unusually prolonged survival in a GBM patient (8), we continued a study of this case with a more detailed analysis of EGFR expression and dysregulation of cell signaling pathways in HGG-02 cells derived from the corresponding primary tumor tissue. Using RT-PCR, we assessed the EGFR status at the mRNA level in the HGG-02 and GM7 cell lines. HGG-02 cells showed significantly (2.24-fold) lower expression of EGFR when compared to the GM7 cells derived from a glioblastoma with a standard *EGFR* gene copy number. Relative expression levels of EGFR in HGG-02 and GM7 were 0.38 and 0.85, respectively (Fig. 1). Furthermore, we examined the presence of the most common mutant form of EGFR, i.e., EGFRvIII. HGG-02 and GM7 cells did not express

Table I. Primer sequences used for RT-PCR.

Gene symbol	Gene full name	Forward primer	Reverse primer	Size (bp)
EGFR	Epidermal growth factor receptor	5'-AGAAAGGCAGCCACCAAATTAGCC-3'	5'-TTCCTGGCTAGTCGGTGTAAACGT-3'	304
ErbB2	V-erb-b2 erythroblastic leukemia viral oncogene homolog 2	5'-CCTGAATATGTGAACCAGC-3'	5'-ACCTCTTGATGCCAGCAGAA-3'	440
ErbB3	V-erb-b2 erythroblastic leukemia viral oncogene homolog 3	5'-GGGTATGAAGAGATGAGAGC-3'	5'-TCAAGAGCCTGAGAGGAA-3'	496
ErbB4	V-erb-b2 erythroblastic leukemia viral oncogene homolog 4	5'-TACCGAGATGGAGGTTTTGC-3'	5'-GTTGGCAAAGGTGTTGAGGT-3'	447
TGF-α	Transforming growth factor α	5'-CCTGCTGCCCGCCCGCCGT-3'	5'-GCTGGCAGCCACCACGGCCA-3'	305
EGF	Epidermal growth factor	5'-TGCCAACTGGGGGTGCACAG-3'	5'-CTGCCCGTGGCCAGCGTGGC-3'	339
EREG	Epiregulin	5'-TCCAGTGTCAGAGGGACACA-3'	5'-GGTTGTGGACGGTTAAAAA-3'	488
NGC	Neuroglycan C	5'-CCCCACCACATCCTTTTATG-3'	5'-GGGGAGCACTAGGATCATCA-3'	680
NRG-1	Neuregulin 1	5'-GACCTCTACTTCTCGTGACA-3'	5'-TCCAATCTGTTAGCAATGTG-3'	256
NRG-2	Neuregulin 2	5'-CGTTGGTAAAGGTGCTGGAC-3'	5'-ACGCAATAGGACTTGGCTGT-3'	586
PDGFRα	Platelet-derived growth factor receptor α	5'-TCCCGAGACTCCTGTAACCT-3'	5'-TTCACTTCTCCAGGGTAAGTC-3'	300
PDGFRβ	Platelet-derived growth factor receptor β	5'- AGGTGTCATCCATCAACGTCT-3'	5'-CTCTCACTTAGCTCCAGCAC-3'	646
PDGFA	Platelet-derived growth factor α polypeptide	5'-TGCCCATTCGGAGGAAGAGA-3'	5'-TTGGCCACCTTGACGCTGC-3'	223
PDGFB	Platelet-derived growth factor β polypeptide	5'-TTGGACCTGAACATGACCCG-3'	5'-ACGTTGCGGTTGTTGCAGCA-3'	239
HSP90AB1	Heat shock protein 90 kDa α (cytosolic), class B member 1	5'-CGCATGAAGGAGACACAGAA-3'	5'-TCCCATCAAATTCCTTGAGC-3'	169
GAPDH	Glyceraldehyde-3-phosphate dehydrogenase	5'-AGCCACATCGCTCAGACACC-3'	5'-GTACTCAGCGCCAGCATCG-3'	302

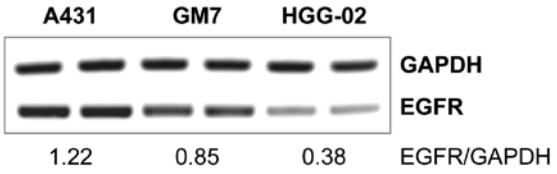

Figure 1. Expression status of EGFR in the HGG-02 and GM7 cell lines detected using semi-quantitative RT-PCR. Reduced expression of EGFR in HGG-02 cells was observed. The expression levels of EGFR were quantified with ImageJ software and normalized to the expression of the housekeeping gene, glyceraldehyde 3-phosphate dehydrogenase (GAPDH). Each sample was loaded in duplicate; EGFR/GAPDH ratios are noted. The A431 cell line served as the positive control; the GM7 cell line was derived from a glioblastoma with a standard EGFR gene copy number. EGFR, epidermal growth factor receptor.

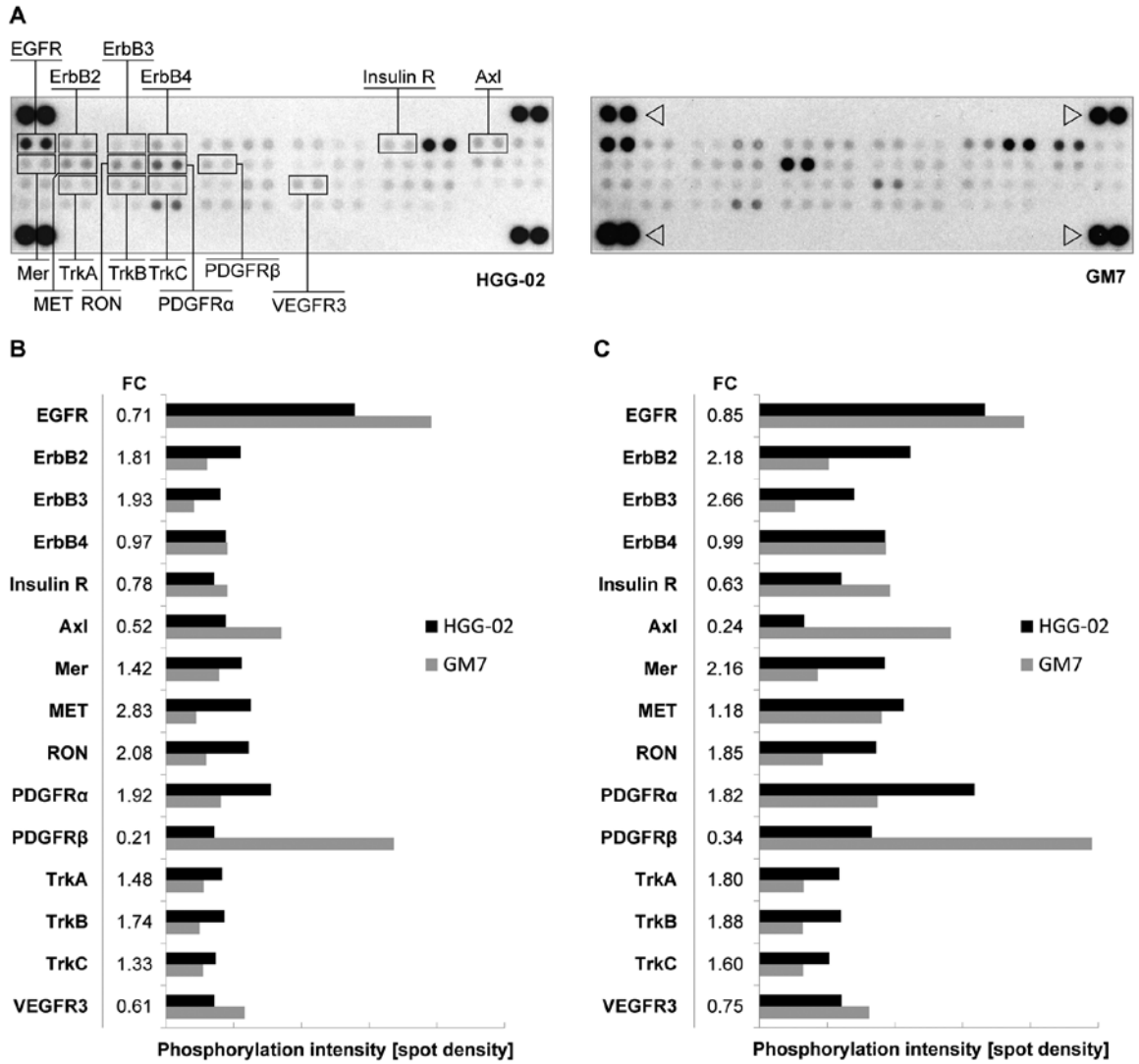

Figure 2. Phospho-RTK array in the HGG-02 cells demonstrates the downregulation of EGFR in comparison with the GM7 reference cell line. (A) Simultaneous detection of the phosphorylation status of 42 RTKs in the HGG-02 and GM7 cell lines using a human phospho-RTK array. Relevant receptors are noted. Phosphotyrosine-positive control spots are marked with an arrowhead. (B) In comparison with the GM7 cell line, HGG-02 cells exhibited downregulation of the EGFR, PDGFRβ, Axl, VEGFR3 and insulin receptors. PDGFRα, Mer, MET, RON, TrkA, TrkB and TrkC were upregulated. The level of phosphorylation was quantified using ImageJ software and normalized to phosphotyrosine-positive control spots. (C) The phosphorylation status after a 24-h serum-free cultivation. Note the overall higher phosphorylation levels and changes in ErbB2, ErbB3, Axl and Mer phosphorylation between the cell lines in comparison with the serum-containing conditions. FC, phosphorylation fold-change values of the HGG-02 cell line when compared to the GM7 reference cell line. RTK, receptor tyrosine kinase; EGFR, epidermal growth factor receptor.

the EGFRvIII variant (data not shown). These results support the hypothesis that the decreased EGFR mRNA expression in HGG-02 cells was caused by the lower *EGFR* gene dosage.

RTK signaling. As EGFR-downstream pathways may be activated and modulated by other RTKs aside from EGFR family receptors, we performed human phospho-RTK arrays to explore the phosphorylation status of 42 RTKs in the HGG-02 cells (Fig. 2A). Consistent with our previous data, we detected lower levels of phosphorylated EGFR in the HGG-02 cell line, which was in contrast with the GM7 cells (Fig. 2B). However, HGG-02 cells showed higher levels of ErbB2 and ErbB3

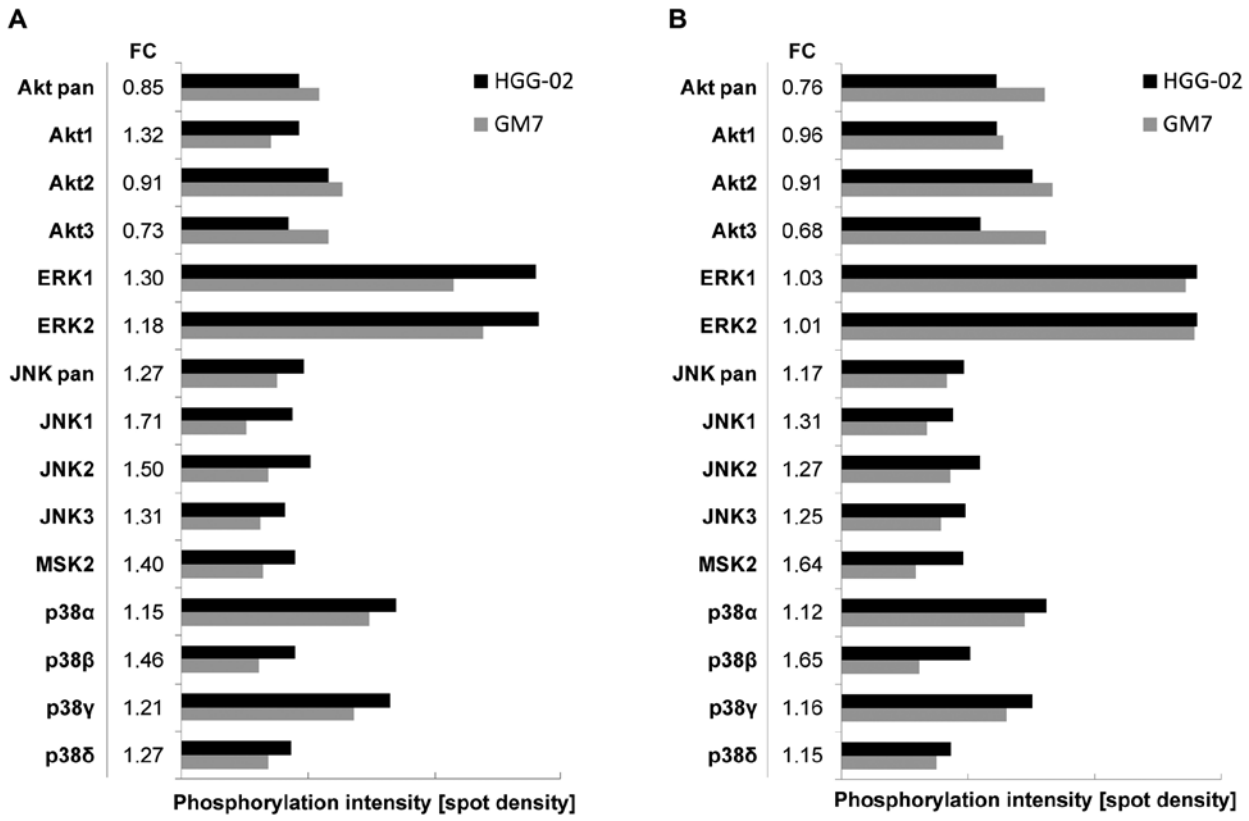

Figure 3. Phosphorylation status of MAPK in the HGG-02 and GM7 cell lines in (A) serum-containing and (B) serum-free conditions detected using phospho-MAPK arrays. The levels of phosphorylation were quantified using ImageJ software and were normalized to phosphotyrosine-positive control spots. FC, phosphorylation fold-change values of the HGG-02 cell line when compared to the GM7 reference cell line. MAPK, mitogen-activated protein kinase.

activation. ErbB4, another receptor of the EGFR family, did not show a significant difference in the phosphorylation state between these two cell lines.

In addition, we identified the downregulation of the phosphorylation of the PDGFRβ, Axl, VEGFR3 and insulin receptors as well as the upregulation of the phosphorylation of PDGFRα, MET, RON, Mer, TrkA, TrkB and TrkC in the HGG-02 cells (Fig. 2B).

To eliminate the influence of serum (which contains growth factors, hormones and other components) on the phosphorylation status of RTKs, we performed phospho-RTK arrays simultaneously using the cell lines after a 24-h serum-free cultivation. Notably, the serum-free conditions did not markedly change the phosphorylation status in the HGG-02 and GM7 cells; however, the overall level of phosphorylation was higher when compared to the serum-containing conditions (Fig. 2C). In the serum-free conditions, increased upregulation of Mer, ErbB2 and ErbB3 as well as downregulation of Axl were detected.

Signaling of MAPK and other serine/threonine kinases. To examine RTK downstream pathways activated in the HGG-02 cells, we employed phospho-MAPK arrays. We also performed the phospho-MAPK arrays on cells cultivated under serum-containing and serum-free conditions, as described above. An Akt pan-specific antibody revealed an overall diminished level of signaling through the Akt pathway in the HGG-02 cells when compared to the GM7 cells in the serum-containing and serum-free conditions (Fig. 3). However, differences in the phosphorylation levels of Akt1, Akt2 and Akt3 kinases were observed. Akt1 was more phosphorylated in the HGG-02 cells in the serum-containing but not in the serum-free conditions, whereas the levels of Akt2 and Akt3 phosphorylation were decreased regardless of the conditions. In addition, we detected an upregulation of signaling through the p38 pathway, JNK pathway and MSK2 in the HGG-02 cells. ERK1 and ERK2 signaling was also slightly elevated in the HGG-02 cells but only under the serum-containing conditions (Fig. 3A).

Expression of the EGFR and PDGFR families and their ligands. The results of the phospho-RTK arrays obtained under serum-free conditions indicated the presence of constitutively active receptor tyrosine-kinase pathways in the HGG-02 and GM7 cell lines. To investigate this possibility, we performed RT-PCR of the receptors in the EGFR and PDGFR families and their respective ligands after cultivation of the cells under serum-containing and serum-free conditions (Fig. 4).

As expected, expression of EGFR was decreased in the HGG-02 cells and did not significantly vary with time or under serum-free conditions. Although there was no difference in the expression of ErbB2, ErbB3 expression was higher under serum-free conditions and increased with time in both cell lines. ErbB4 expression was detected in the HGG-02 cells only and was stronger in the serum-free conditions. These patterns of expression were observable for its ligand

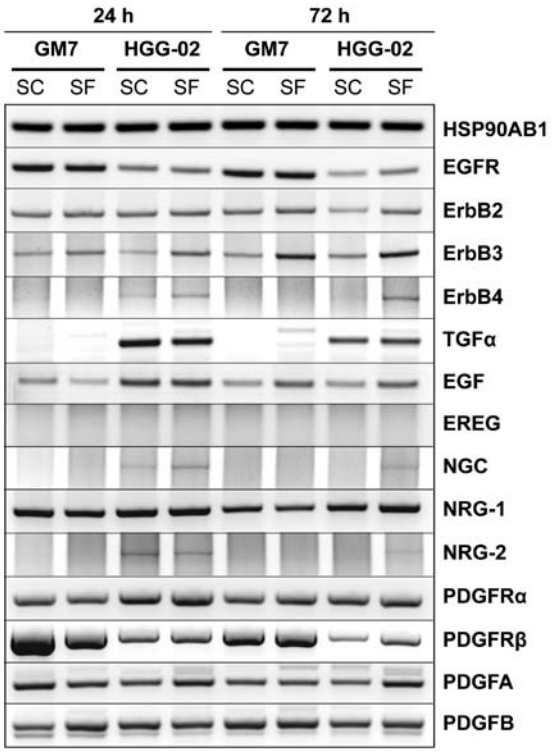

Figure 4. Expression of the receptors of the EGFR and the PDGFR families and their respective ligands using RT-PCR. The expression was analyzed after a 24- and 72-h culture in serum-containing and serum-free conditions. The housekeeping gene HSP90AB1 served as a control. SC, serum-containing conditions; SF, serum-free conditions.

NRG-2 and for the ErbB3-specific ligand NGC. In contrast to the low levels of EGFR mRNA, strong expression of the EGFR-specific ligand TGF-α was observed in the HGG-02 cells but not in the GM7 cells. EGF, the second EGFR-specific ligand, was also upregulated in the HGG-02 cells. Nevertheless, after 72 h of cultivation, the expression of EGF did not differ between cell lines and was higher in the serum-free conditions. Finally, the expression of NRG-1 increased in the HGG-02 cells after 72 h of cultivation, and EREG was not expressed in any of the samples.

We observed an apparent downregulation of PDGFRβ in the HGG-02 cells. In contrast, the expression of PDGFRα was slightly increased when compared with that in the GM7 cells. However, there were no obvious trends in the expression of the ligands for these receptors, including PDGFA and PDGFB.

Cancer-related gene expression. Gene expression profiling affirmed a decrease in EGFR expression at the mRNA level in the HGG-02 cells. Out of the 440 investigated genes, the HGG-02 expression profile revealed the upregulation of 108 genes (FC of 2-38.8) and downregulation of 10 genes (FC of 0.2-0.44) in comparison with the GM7 cells. Functional clustering showed that most of the upregulated genes are involved in the cell cycle, signaling pathways induced by growth factors, focal adhesions and apoptosis (Table II). The downregulated genes encode proteins responsible for organizing the extracellular matrix (ECM) or interacting with the ECM.

The 17 genes that were upregulated in the HGG-02 cells more than 5-fold were CDKN2A, TFAP2C, IGFBP3, CDKN2B, FRZB, SRPX and Siva1. The downregulated genes included COL6A3, COL1A1, DCN, FN1, FBN1 and GDF15.

Discussion

Despite many advances in the treatment of GBM, the outcomes of patients with this tumor remain poor. Previously, we reported the case of a patient with GBM with a mild clinical course and a loss of *EGFR* gene copy (8). As both of these aspects are uncommon in GBMs, we performed a detailed analysis of the HGG-02 cell line that was derived from this patient's tumor to understand the cancer regulatory pathways that may have contributed to the favorable clinical course in this case. As control cells, the reference GM7 cell line that was derived from a highly aggressive tumor type and showed a standard *EGFR* gene copy number (9) was used.

Using RT-PCR, a phospho-RTK array and expression profiling, we confirmed the downregulation of EGFR expression and signaling in HGG-02 cells. However, this downregulated signaling did not affect the downstream MAPKs, ERK1 or ERK2 and was possibly compensated for by the activation of the ErbB2 and ErbB3 receptors. These results are in agreement with another study that recently reported the compensatory activation of ErbB2 and ErbB3 receptors in GBM deprived of EGFR signaling, which suggests an intrinsic mechanism of GBM resistance to EGFR-targeted therapy (10). RT-PCR analysis revealed weak but detectable ErbB4 expression in the HGG-02 cells, while ErbB4 expression was not detected in the GM7 reference cell line. In contrast, the ErbB4 phosphorylation status was the same in these two cell lines, and we assume that this discrepancy may point to the previously questioned correlation of RNA and protein levels (11). However, the RT-PCR results of EGFR family-related ligands showed a strong elevation in TGF-α, which was accompanied by an increased expression of EGF in the HGG-02 cells. Previous studies have suggested that EGFR and its ligands EGF and TGF-α play an important role in the autocrine/paracrine loop and support cell proliferation in human gliomas (12,13). Nevertheless, considering that the HGG-02 cells acquired the loss of *EGFR* gene copy and the phospho-RTK array revealed a downregulation in EGFR signaling, we assume that the HGG-02 cells and the respective tumor do not represent EGFR-driven GBM.

Apart from the EGFR family, we identified changes in the phosphorylation of 11 other RTKs, including Axl. The phosphorylation of Axl was significantly reduced in comparison with the GM7 cells. This reduction was even more obvious under serum-free conditions, which suggests the constitutive activation of Axl in the GM7 reference cell line. Previous studies have found that Axl is constitutively phosphorylated in many glioma cell lines and that the downstream MAPK and PI3K pathways are activated (14). Moreover, Axl overexpression has been reported as a frequent event in human gliomas and is correlated with a poor prognosis in these patients (15). Therefore, the downregulation of Axl phosphorylation in HGG-02 cells may indicate a less aggressive phenotype of the respective tumor. Nevertheless, in the HGG-02 cells, we detected an upregulation of signaling through Mer, another member of the TAM family of RTKs (16). Recently, 2 independent studies demonstrated that Mer promotes invasion,

Table II. Functional clustering of the molecular or biochemical pathways associated with genes that were differentially expressed in the HGG-02 cell line when compared to the GM7 cell line.

Molecular or biochemical pathway	No. of deregulated genes	Percentage of deregulated genes	P-value
Upregulated gene expression (>2-fold change vs. GM7)			
Pathways in cancer	20	19.05	<0.001
Cell cycle	12	11.43	<0.001
MAPK signaling pathway	12	11.43	<0.001
Glioma	8	7.62	<0.001
Focal adhesions	8	7.62	0.017
Neurotrophin signaling pathway	7	6.67	0.006
p53 signaling pathway	6	5.71	0.002
Apoptosis	6	5.71	0.006
T cell receptor signaling pathway	6	5.71	0.014
B cell receptor signaling pathway	5	4.76	0.017
Toll-like receptor signaling pathway	5	4.76	0.045
Downregulated gene expression (<0.5-fold change vs. GM7)			
ECM-receptor interactions	3	30.00	0.004
Focal adhesions	3	30.00	0.021

MAPK, mitogen-activated protein kinase; ECM, extracellular matrix.

protects cells from apoptosis in GBM and has a similar function to Axl (17,18). However, the reduction in Axl phosphorylation in the HGG-02 cells was ~2-fold greater than Mer upregulation. Overall, these results suggest that Axl and Mer play an important role in the aggressiveness of GBM and emphasize the need for further research of the TAM receptor tyrosine kinases in GBM.

Recently, it has been observed that MET, an HGF receptor, is activated during EGFR-targeted therapy resistance, and various studies have suggested that silencing EGFR is compensated by MET signaling in these cases (19). In accordance with these observations, we detected an upregulation of signaling through MET in the HGG-02 cells, which may partially compensate for the downregulation of EGFR signaling caused by the loss of *EGFR* gene copy. MET overexpression has been associated with a shorter survival time and poor response (20), and it has been suggested that MET activation is required for the acquisition of the glioblastoma cancer stem cell phenotype (21). Furthermore, upregulated phosphorylation of RON, the MSP receptor, may indicate another compensatory mechanism in HGG-02 cells. Eckerich *et al* reported that although RON signaling showed no mitogenic effect on GBM cells, it can induce glioma cell migration (22). However, these findings are in contrast with the unusually non-aggressive phenotype of the HGG-02 tumor, and we hypothesize that the activation of MET and RON signaling is not strong enough to overcome the loss of *EGFR* gene copy number in this case.

Nevertheless, HGG-02 cells exhibited increased phosphorylation of Trk receptors. It is well established that Trk receptors support the survival and differentiation of the nervous system; however, there is growing evidence that the Trk family can also induce or enhance cell death in certain tumor types, primarily in pediatric tumors of neural origin (23). It has been shown that expression of TrkA and TrkC correlates with a favorable outcome in neuroblastoma and medulloblastoma patients. In GBM, immunoreactivity for TrkA was shown to be inversely associated with the grade of malignancy (24). Moreover, TrkA overexpression was found to induce autophagic cell death that was mediated through the JNK pathway (25,26). Therefore, we hypothesized that elevated signaling through Trk receptors and JNK MAPKs in HGG-02 cells contributed to the non-aggressive phenotype of the primary tumor.

Notably, we also detected an apparent difference in PDGF signaling in both of the cell lines studied. Whereas HGG-02 cells preferentially signaled through PDGFRα, PDGFRβ was strongly phosphorylated in the GM7 reference cell line. Moreover, these results, which were obtained using the phospho-RTK array, corresponded with the results obtained by RT-PCR. Using RT-PCR, we detected PDGFRβ overexpression in the GM7 cells, whereas PDGFRα was overexpressed in the HGG-02 cells. Expression of PDGFs and PDGFRs has been observed even in low-grade gliomas, which suggests that this pathway possibly represents an early oncogenic event in gliomagenesis (27,28). According to previous studies, PDGFRα is overexpressed in GBM cells, whereas PDGFRβ is detected in adjacent vascular cells (27). However, a recent study interrogated the proposed role of PDGFRs in intratumoral GBM heterogeneity (29). Kim *et al* found that expression of PDGFRβ, but not PDGFRα, was strongly associated with the glioblastoma stem cell (GSC) phenotype. Moreover, targeting PDGFRβ decreased GSC self-renewal, survival, tumor growth and invasion. Using *in silico* survival analysis, the authors noted that PDGFRβ indicated a poor prognosis, whereas PDGFRα was a positive prognostic marker. Together, these data support our observation in HGG-02 cells. Higher expression and signaling activity of PDGFRα, instead of PDGFRβ, may indicate the presence of a limited number of GSCs in the HGG-02 cell line when compared with the GM7 reference cell

line derived from an aggressive tumor type. While our data stress the importance of PDGF signaling in GBM with respect to the distinct effects of PDGFRα and PDGFRβ in gliomagenesis, we strongly encourage further research of these RTKs in GBM biology.

We identified increased signaling through the p38 and JNK pathways in HGG-02 cells. It is known that p38 kinase activation is associated with anti-proliferative functions and plays a role in the induction of apoptosis (30). Moreover, recent studies have shown that p38 kinase activation is necessary for GBM cell death initiated by various anticancer agents (31-33). Furthermore, we detected increased signaling through the JNK kinases, which are also involved in apoptosis, and their activation is required for UV-induced apoptosis (30,34). As previously noted, the JNK pathway can also mediate TrkA-induced autophagic cell death (25,26). Overall, the increased activation of the p38 and JNK pathways, with regard to anti-proliferative and apoptotic functions, may represent the less aggressive characteristics of the HGG-02 cell line.

Although gene expression profiling detected changes in the expression of 118 genes, analysis of the most upregulated and downregulated genes in the HGG-02 cells revealed a specific expression profile of HGG-02 cells that may reflect the non-aggressive phenotype of this tumor. Seven of the 17 highly upregulated genes in the HGG-02 cells represent well accepted or potential tumor suppressors, including CDKN2A (35,36), TFAP2C (37), IGFBP3 (38), CDKN2B (36), FRZB (39), SRPX (40) and Siva1 (41). However, the downregulated genes involved genes associated with the ECM, including COL6A3, COL1A1, DCN, FN1 and FBN1. These genes have been proposed to play an important role in controlling and facilitating the motility of glioma cells (42). For example, COL6A3 was found to correlate with glioma grade (43). Apart from the ECM-related genes, we detected significantly lower expression of GDF15 in the HGG-02 cells. Recent studies revealed that GDF15 contributes to the proliferation and immune escape of malignant gliomas (44,45). This finding is in agreement with its low expression in the HGG-02 cell line that was derived from the unusually non-aggressive GBM.

In conclusion, the detailed analysis of the HGG-02 cell line confirmed the unusually reduced EGFR signaling and indicated several other targets that may contribute to the non-aggressive phenotype of the respective tumor. As suggested by our results, TAM receptors, Trk receptors and PDGFRs need to be further investigated since these proteins may play an important role in GBM biology, gliomagenesis and patient outcome.

Acknowledgements

The present study was supported by the European Regional Development Fund and the State Budget of the Czech Republic (RECAMO, CZ.1.05/2.1.00/03.0101) and OP VK CZ.1.07/2.3.00/20.0183.

References

1. Linggi B and Carpenter G: ErbB receptors: new insights on mechanisms and biology. Trends Cell Biol 16: 649-656, 2006.
2. Yarden Y and Sliwkowski MX: Untangling the ErbB signalling network. Nat Rev Mol Cell Biol 2: 127-137, 2001.
3. Ohgaki H and Kleihues P: Population-based studies on incidence, survival rates, and genetic alterations in astrocytic and oligodendroglial gliomas. J Neuropathol Exp Neurol 64: 479-489, 2005.
4. Ohgaki H and Kleihues P: Genetic pathways to primary and secondary glioblastoma. Am J Pathol 170: 1445-1453, 2007.
5. Hatanpaa KJ, Burma S, Zhao D and Habib AA: Epidermal growth factor receptor in glioma: signal transduction, neuropathology, imaging, and radioresistance. Neoplasia 12: 675-684, 2010.
6. Lopez-Gines C, Gil-Benso R, Ferrer-Luna R, *et al*: New pattern of *EGFR* amplification in glioblastoma and the relationship of gene copy number with gene expression profile. Mod Pathol 23: 856-865, 2010.
7. Bredel M, Scholtens DM, Yadav AK, *et al*: *NFKBIA* deletion in glioblastomas. N Engl J Med 364: 627-637, 2011.
8. Veselska R, Skoda J, Loja T, *et al*: An unusual loss of *EGFR* gene copy in glioblastoma multiforme in a child: a case report and analysis of a successfully derived HGG-02 cell line. Childs Nerv Syst 26: 841-846, 2010.
9. Loja T, Chlapek P, Kuglik P, Pesakova M, Oltova A, Cejpek P and Veselska R: Characterization of a GM7 glioblastoma cell line showing CD133 positivity and both cytoplasmic and nuclear localization of nestin. Oncol Rep 21: 119-127, 2009.
10. Clark PA, Iida M, Treisman DM, *et al*: Activation of multiple ERBB family receptors mediates glioblastoma cancer stem-like cell resistance to EGFR-targeted inhibition. Neoplasia 14: 420-428, 2012.
11. Gry M, Rimini R, Strömberg S, Asplund A, Pontén F, Uhlén M and Nilsson P: Correlations between RNA and protein expression profiles in 23 human cell lines. BMC Genomics 10: 365, 2009.
12. Tang P, Steck PA and Yung WK: The autocrine loop of TGF-α/EGFR and brain tumors. J Neurooncol 35: 303-314, 1997.
13. Ekstrand AJ, James CD, Cavenee WK, Seliger B, Pettersson RF and Collins VP: Genes for epidermal growth factor receptor, transforming growth factor α, and epidermal growth factor and their expression in human gliomas in vivo. Cancer Res 51: 2164-2172, 1991.
14. Stommel JM, Kimmelman AC, Ying H, *et al*: Coactivation of receptor tyrosine kinases affects the response of tumor cells to targeted therapies. Science 318: 287-290, 2007.
15. Hutterer M, Knyazev P, Abate A, *et al*: Axl and growth arrest-specific gene 6 are frequently overexpressed in human gliomas and predict poor prognosis in patients with glioblastoma multiforme. Clin Cancer Res 14: 130-138, 2008.
16. Linger RM, Keating AK, Earp HS and Graham DK: TAM receptor tyrosine kinases: biologic functions, signaling, and potential therapeutic targeting in human cancer. Adv Cancer Res 100: 35-83, 2008.
17. Rogers AE, Le JP, Sather S, Pernu BM, Graham DK, Pierce AM and Keating AK: Mer receptor tyrosine kinase inhibition impedes glioblastoma multiforme migration and alters cellular morphology. Oncogene 31: 4171-4181, 2012.
18. Wang Y, Moncayo G, Morin P Jr, *et al*: Mer receptor tyrosine kinase promotes invasion and survival in glioblastoma multiforme. Oncogene 32: 872-882, 2013.
19. Velpula KK, Dasari VR, Asuthkar S, Gorantla B and Tsung AJ: EGFR and c-Met cross talk in glioblastoma and its regulation by human cord blood stem cells. Transl Oncol 5: 379-392, 2012.
20. Kong DS, Song SY, Kim DH, *et al*: Prognostic significance of c-Met expression in glioblastomas. Cancer 115: 140-148, 2009.
21. Joo KM, Jin J, Kim E, *et al*: MET signaling regulates glioblastoma stem cells. Cancer Res 72: 3828-3838, 2012.
22. Eckerich C, Schulte A, Martens T, Zapf S, Westphal M and Lamszus K: RON receptor tyrosine kinase in human gliomas: expression, function, and identification of a novel soluble splice variant. J Neurochem 109: 969-980, 2009.
23. Harel L, Costa B and Fainzilber M: On the death Trk. Dev Neurobiol 70: 298-303, 2010.
24. Wadhwa S, Nag TC, Jindal A, Kushwaha R, Mahapatra AK and Sarkar C: Expression of the neurotrophin receptors Trk A and Trk B in adult human astrocytoma and glioblastoma. J Biosci 28: 181-188, 2003.
25. Hansen K, Wagner B, Hamel W, Schweizer M, Haag F, Westphal M and Lamszus K: Autophagic cell death induced by TrkA receptor activation in human glioblastoma cells. J Neurochem 103: 259-275, 2007.
26. Dadakhujaev S, Noh HS, Jung EJ, Hah YS, Kim CJ and Kim DR: The reduced catalase expression in TrkA-induced cells leads to autophagic cell death via ROS accumulation. Exp Cell Res 314: 3094-3106, 2008.

27. Hermanson M, Funa K, Hartman M, Claesson-Welsh L, Heldin CH, Westermark B and Nistér M: Platelet-derived growth factor and its receptors in human glioma tissue: expression of messenger RNA and protein suggests the presence of autocrine and paracrine loops. Cancer Res 52: 3213-3219, 1992.
28. Maher EA, Furnari FB, Bachoo RM, Rowitch DH, Louis DN, Cavenee WK and DePinho RA: Malignant glioma: genetics and biology of a grave matter. Genes Dev 15: 1311-1333, 2001.
29. Kim Y, Kim E, Wu Q, *et al*: Platelet-derived growth factor receptors differentially inform intertumoral and intratumoral heterogeneity. Genes Dev 26: 1247-1262, 2012.
30. Wagner EF and Nebreda AR: Signal integration by JNK and p38 MAPK pathways in cancer development. Nat Rev Cancer 9: 537-549, 2009.
31. Amantini C, Mosca M, Nabissi M, *et al*: Capsaicin-induced apoptosis of glioma cells is mediated by TRPV1 vanilloid receptor and requires p38 MAPK activation. J Neurochem 102: 977-990, 2007.
32. Yao YQ, Ding X, Jia YC, Huang CX, Wang YZ and Xu YH: Anti-tumor effect of β-elemene in glioblastoma cells depends on p38 MAPK activation. Cancer Lett 264: 127-134, 2008.
33. Das A, Banik NL and Ray SK: Flavonoids activated caspases for apoptosis in human glioblastoma T98G and U87MG cells but not in human normal astrocytes. Cancer 116: 164-176, 2010.
34. Dhanasekaran DN and Reddy EP: JNK signaling in apoptosis. Oncogene 27: 6245-6251, 2008.
35. Liu W, Lv G, Li Y, Li L and Wang B: Downregulation of CDKN2A and suppression of cyclin D1 gene expressions in malignant gliomas. J Exp Clin Cancer Res 30: 76, 2011.
36. Feng J, Kim ST, Liu W, *et al*: An integrated analysis of germline and somatic, genetic and epigenetic alterations at 9p21.3 in glioblastoma. Cancer 118: 232-240, 2012.
37. Gabriely G, Yi M, Narayan RS, *et al*: Human glioma growth is controlled by microRNA-10b. Cancer Res 71: 3563-3572, 2011.
38. Wu C, Liu X, Wang Y, *et al*: Insulin-like factor binding protein-3 promotes the G1 cell cycle arrest in several cancer cell lines. Gene 512: 127-133, 2013.
39. Zi X, Guo Y, Simoneau AR, Hope C, Xie J, Holcombe RF and Hoang BH: Expression of Frzb/secreted Frizzled-related protein 3, a secreted Wnt antagonist, in human androgen-independent prostate cancer PC-3 cells suppresses tumor growth and cellular invasiveness. Cancer Res 65: 9762-9770, 2005.
40. Tambe Y, Isono T, Haraguchi S, Yoshioka-Yamashita A, Yutsudo M and Inoue H: A novel apoptotic pathway induced by the *drs* tumor suppressor gene. Oncogene 23: 2977-2987, 2004.
41. Li N, Jiang P, Du W, *et al*: Siva1 suppresses epithelial-mesenchymal transition and metastasis of tumor cells by inhibiting stathmin and stabilizing microtubules. Proc Natl Acad Sci USA 108: 12851-12856, 2011.
42. Mahesparan R, Tysnes BB, Read TA, Enger PO, Bjerkvig R and Lund-Johansen M: Extracellular matrix-induced cell migration from glioblastoma biopsy specimens in vitro. Acta Neuropathol 97: 231-239, 1999.
43. Fujita A, Sato JR, Festa F, *et al*: Identification of *COL6A1* as a differentially expressed gene in human astrocytomas. Genet Mol Res 7: 371-378, 2008.
44. Wu A, Wei J, Kong LY, *et al*: Glioma cancer stem cells induce immunosuppressive macrophages/microglia. Neuro Oncol 12: 1113-1125, 2010.
45. Roth P, Junker M, Tritschler I, *et al*: GDF-15 contributes to proliferation and immune escape of malignant gliomas. Clin Cancer Res 16: 3851-3859, 2010.

New Mechanisms for an Old Drug; DHFR- and non-DHFR-mediated Effects of Methotrexate in Cancer Cells

Nové možnosti starého léku: DHFR- a non-DHFR-mediované účinky metotrexátu na nádorové buňky

Neradil J.[1,2], Pavlasova G.[1], Veselska R.[1,3]

[1] Laboratory of Tumor Biology, Department of Experimental Biology, School of Science, Masaryk University, Brno, Czech Republic
[2] Regional Centre for Applied Molecular Oncology, Masaryk Memorial Cancer Institute, Brno, Czech Republic
[3] Department of Pediatric Oncology, University Hospital Brno and School of Medicine, Masaryk University, Brno, Czech Republic

Summary
Methotrexate, a structural analogue of folic acid, is one of the most frequently used chemotherapeutics, especially in haematological malignancies, various solid tumours and also inflammatory disorders. Methotrexate interferes with folate metabolism, mainly by inhibition of dihydrofolate reductase, resulting in the suppression of purine and pyrimidine precursor synthesis. The depletion of nucleic acid precursors seems to be responsible for the cytostatic, cytotoxic and differentiation effects of methotrexate. Methylation of biomolecules represents another folate-dependent pathway that is also affected by methotrexate. Furthermore, methotrexate is able to modify metabolic pathways and cellular processes independently of folate metabolism. Based on the similar structure of methotrexate and of functional groups of certain histone deacetylase inhibitors, the ability of methotrexate to inhibit histone deacetylases was predicted and consequently verified. Recently published findings also suggest that methotrexate affects glyoxalase and antioxidant systems. Although methotrexate has been used as a folate metabolism antagonist in anticancer therapy for more than 60 years, the identification of its' other molecular targets in cellular metabolism still continues.

Key words
methotrexate – folate metabolism – dihydrofolate reductase – methylation – histone deacetylase inhibitors – glyoxalase system – oxidative stress

Souhrn
Metotrexát, strukturální analog kyseliny listové, je jedním z nejčastěji používaných chemoterapeutik především pro léčbu hematoonkologických onemocnění, solidních nádorů, ale také některých autoimunitních poruch. Primárně metotrexát narušuje folátový metabolizmus inhibicí dihydrofolátreduktázy, což má za následek potlačení syntézy pyrimidinových a purinových prekurzorů. Nedostatek stavebních kamenů nukleových kyselin se pak odráží v cytostatickém, cytotoxickém a diferenciačním efektu metotrexátu. Mezi další procesy, které jsou ovlivněny inhibicí folátového metabolizmu, patří metylace biomolekul, především proteinů a DNA. Metotrexát však působí na metabolické dráhy a buněčné procesy i nezávisle na metabolizmu folátů. Na základě podobnosti struktury metotrexátu a funkčních skupin některých inhibitorů histondeacetyláz bylo predikováno a poté i experimentálně potvrzeno, že metotrexát má schopnost inhibovat histondeacetylázy. Dále byla prokázána schopnost metotrexátu účinně ovlivňovat glyoxalázový a antioxidační systém. I když je metotrexát používán jako folátový antagonista v protinádorové terapii více než 60 let, odhalování jeho dalších cílů působení na molekulární i buněčné úrovni stále pokračuje.

Klíčová slova
metotrexát – folátový metabolizmus – dihydrofolátreduktáza – metylace – inhibitory histondeacetylázy – glyoxalázový systém – oxidativní stres

This study was supported by European Regional Development Fund and the State Budget of the Czech Republic for RECAMO (CZ.1.05./2.1.00/03.0101) and by internal project of Masaryk University No. MUNI/C/0803/2011.

Práce byla podpořena Evropským fondem pro regionální rozvoj a státním rozpočtem České republiky (OP VaVpI – RECAMO, CZ.1.05/2.1.00/03.0101) a interním projektem Masarykovy univerzity MUNI/C/0803/2011.

The authors declare they have no potential conflicts of interest concerning drugs, products, or services used in the study.

Autoři deklarují, že v souvislosti s předmětem studie nemají žádné komerční zájmy.

The Editorial Board declares that the manuscript met the ICMJE "uniform requirements" for biomedical papers.

Redakční rada potvrzuje, že rukopis práce splnil ICMJE kritéria pro publikace zasílané do biomedicínských časopisů.

Jakub Neradil, RNDr., Ph.D.
Laboratory of Tumor Biology
Institute of Experimental Biology
School of Science
Masaryk University
Kotlarska 2
611 37 Brno
Czech Republic
e-mail: jneradil@sci.muni.cz

Submitted/Obdrženo: 1. 10. 2012
Accepted/Přijato: 6. 11. 2012

Introduction

Methotrexate (MTX; amethopterin; 4-amino-10-methylfolic acid), a structural analogue of folic acid, is one of the most frequent chemotherapeutic drugs [1]. MTX is used in the treatment of haematological malignancies, various types of solid tumours and also of inflammatory disorders. This large group of MTX-treated diseases includes leukaemia, breast cancer, colorectal cancer, head and neck cancer, lymphoma, osteogenic sarcoma, urothelial cancer, choriocarcinoma, psoriasis and rheumatoid arthritis [2]. This review is focused on the various mechanisms of MTX action at the cellular level.

Folate Metabolism

The main biochemical function of folate, especially of its reduced form tetrahydrofolate (THF), is to serve as a co-factor/ /co-enzyme and to transfer one-carbon groups. THF acts as a donor of these groups in several interconnected metabolic pathways in the cytoplasm (Fig. 1). Three of one-carbon substituted THF derivatives are associated with crucial metabolic pathways: 5-methyl THF, which is required for synthesis of methionine; 5,10-methylene THF, which is essential for the synthesis of deoxythymidylate (dTMP), a pyrimidine component of DNA; and 10-formyl THF, which serves as co-factor for purine synthesis [3,4].

MTX as Inhibitor of Nucleotide Biosynthesis

The enzyme dihydrofolate reductase (DHFR) is the key intracellular target of MTX in folate metabolism. DHFR catalyses the reduction of folate to THF in two steps. The inhibition of DHFR by MTX is competitive with dihydrofolate (DHF) and results in THF depletion, leading to the inhibition of purine and pyrimidine precursor synthesis [5].

The lack of 5,10-methylene THF is a cause of the reduced synthesis of pyrimidine precursors, because thymidylate synthase (TS) is not able to catalyse methylation of dUMP to dTMP without 5,10-methylene THF. Moreover, TS is directly blocked by MTX and by un-metabolised dihydrofolate [6]. A severe lack of dTTP can lead to the phenomenon called "thymineless stress" followed by "thymineless death" due to the inhibition of DNA synthesis. Preceding thymineless death, a large increase in dUTP concentration and its incorporation into DNA instead of dTTP can be found. Activation of the DNA excision repair pathway is the next step; however, this process cannot run correctly and apoptosis is induced by DNA damage [7]. Alternatively, changes in the ratio of intracellular concentrations of the nucleotides (i.e. nucleotide pool imbalance) are also able to trigger the mitochondrial pathway of apoptosis [8]. Nevertheless, other studies show that numerous homologous recombinations resulting from single--strand breaks in DNA are responsible for the cell death [9].

Purine precursor biosynthesis is also partially indirectly inhibited by deficiency of another folate co-factor, 10-formyl THF. However, it is primarily inhibited directly by the excessive levels of DHF in a cell [10], because during the inhibition of DHFR, the intracellular concentration of 10-formyl THF is maintained up to 80% [11]. In addition, MTX is also a direct inhibitor of AICAR transformylase (ATIC) [12] and GAR transformylase (GART) [13], two pivotal enzymes responsible for purine precursor synthesis. Unlike DHFR, the inhibition of ATIC and GART is markedly improved by polyglutamylation of MTX as MTX polyglutamates are more potent inhibitors – polyglutamy-

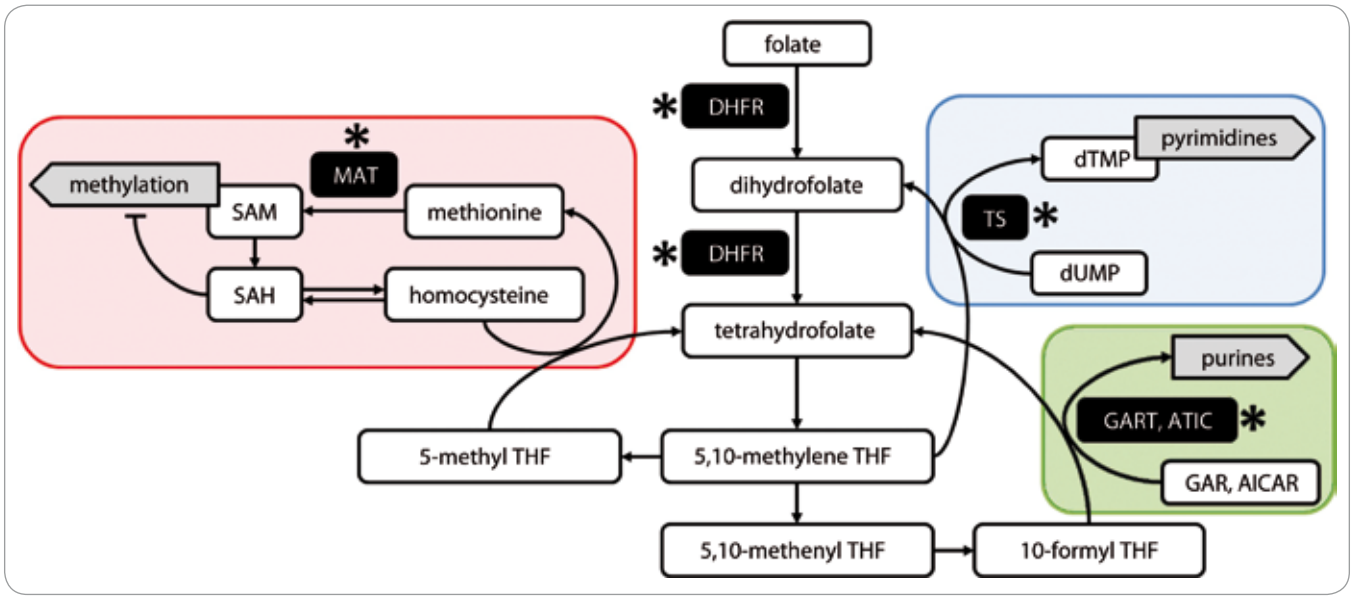

Fig. 1. Folate metabolism. Schematic picture of three main folate-dependent pathways: methylation of biomolecules (red area), thymidylate synthesis (blue area) and synthesis of purines (green area). The spots of MTX-intervention are indicated by asterisks. Abbreviations: AICAR – 5-aminoimidazole-4-carboxamide ribonucleoside; ATIC – AICAR transformylase; DHFR – dihydrofolate reductase; GAR – glycinamide ribonucleotide; GART – GAR transformylase; MAT – methionine S-adenosyltransferase; SAM – S-adenosyl methionine; SAH – S-adenosyl homocysteine; THF – tetrahydrofolate; TS – thymidylate synthase.

lated MTX provides a stronger bond with enzymes [12,14].

MTX as Inducer of Cell Death

The previous data show that the inhibition of dTMP synthesis and *de novo* purine synthesis, either directly or as a result of the inhibition of DHFR, is the main reason for MTX-induced cell death. The proportion of the inhibition effect of purine or pyrimidine precursor synthesis on cell death may differ among various cell types, as well as between two main ways of cell death – apoptosis and necrosis [15]. Apoptosis is probably initiated during the S-phase of the cell cycle when DNA is synthesised [6], because a blockade of transition from G1 to S phase prevents MTX-induced apoptosis [16].

Surprisingly, MTX can also induce apoptosis in post-mitotic cells, in which DNA replication does not occur. For example, this phenomenon was described in post-mitotic pulmonary artery endothelial cells [17], or in rodent cortical neurons [18]. Kruman et al [18] found that MTX induces cell cycle re-entry in neurons; it was confirmed by the incorporation of BrdU (5-bromo-2'-deoxyuridine) into newly synthesised DNA. Subsequently, affected cells can undergo apoptosis. The same effect was shown by homocysteine (Hcy), which additionally increased expression of p53 and cdc25 required for a progression from G1 to the S phase.

MTX as Inducer of Differentiation

Besides the cytostatic and cytotoxic effects of MTX, there was also described a differentiation effect of this compound. MTX was found to be a potent differentiation inducer in HL-60 human promyelocytic leukaemia cells [19], LA-N-1 human neuroblastoma cells [20], human neonatal foreskin keratinocytes [21], U937 human monocytic cells [22], human and rat choriocarcinoma cells [23,24], HT29 colon cancer cells [25], A549 adenocarcinoma cells [26], human APL (acute promyelocytic leukaemia) and ALL (acute lymphoblastic leukaemia) cell lines, and patients' ALL blasts [27].

The cause of the induced differentiation is not still fully understood. In some cases, differentiating effects of MTX result from thymine nucleotide depletion, because the addition of thymidine is able to prevent MTX-induced differentiation [28]. On the contrary, cell differentiation arises apparently due to the deprivation of purines in HT29 human colon cancer cells [25].

In both cases, the differentiating effect of MTX is linked to the nucleotide precursor synthesis arrest. This phenomenon was also observed in mouse [29] and human [30] embryonic stem cells, when they were intravitreally transplanted to induce neuronal differentiation in murine retinas. Furthermore, intravitreally or intraperitoneally administered MTX decreased proliferative activity and tumourigenic potential of transplanted embryonic stem cells and it also induced neuronal differentiation.

MTX as Inhibitor of Methylation of Biomolecules

One of the important folate metabolites is 5-methyl THF, which is – together with homocysteine – necessary for the endogenous synthesis of methionine. Methionine reacts with ATP and S-adenosyl methionine (SAM) is formed. SAM functions as donor of methyl groups for protein methylation (including histones), cytosine bases in DNA (CpG islands), neurotransmitters, phospholipids and other small molecules [31]. MTX decreases the level of 5-methyl THF in a cell via the functional suppression of DHFR [32,33]. Moreover, MTX directly inhibits the expression and activity of the methionine S-adenosyltransferase (MAT), which is a key enzyme catalysing the synthesis of SAM from methionine [34].

At the molecular level, Ras protein was identified to be a subject of MTX-induced hypomethylation [35]. Ras hypomethylation results in the mis-localisation of this protein from the plasma membrane to the cytoplasm, as well as a decrease of activation of ERK and AKT kinases that play a significant role in cell proliferation and differentiation. However, the inhibition of Ras methylation by MTX is not direct. It is caused by the suppression of isoprenylcysteine carboxyl methyltransferase, which is the enzyme blocked by S-adenosyl homocysteine (SAH). SAH arises in a reversible reaction from homocysteine, which cannot be methylated to methionine due to the inhibition of folate metabolism.

MTX also acts as a demethylating agent in highly methylated cutaneous T-cell lymphoma (CTCL) lines and in circulating tumour cells from a patient with leukemic CTCL [36]. In these cells, MTX reduced the methylation of CpG islands in the Fas promoter leading to its higher expression and increased sensitivity to Fas-mediated apoptosis.

Generally, the reduction of DNA methylation after the treatment with MTX usually occurs in intensively rapidly proliferating cells, such as during physiological processes of embryonic development, haematopoiesis and tissue regeneration, but also in transformed cells. In case of an insufficient pool of methyl donors, hemimethylated spots arise in DNA after mitotic division and after the next cycle there are no methyl templates on both strands of DNA of daughter cells. This process can lead to the loss of DNA methylation patterns and consequently to changes in gene expression [37].

Based on the findings mentioned above, MTX is considered to be a methylation inhibitor that could be used in the treatment of cancers with a specific DNA methylation pattern. Hypermethylated CpG sites in genes (and/or their promoters) regulating tissue development, differentiation and tumourigenesis were described in rhabdomyosarcoma [38], medulloblastoma [39], glioma [40,41] and other human cancers [42].

MTX as Inhibitor of Histone Deacetylases (HDAC)

Due to the similar structure of MTX and of functional groups of certain HDAC inhibitors (HDACi), it was predicted that MTX may have the ability to inhibit HDAC [43]. Some known HDACi, such as trichostatin (TSA) and suberoylanilide hydroxamic acid (SAHA) contain a hydrophobic group (benzyl) in their molecule. This group is connected by a short spacer (aliphatic group) with a functional group (hydroxamic acid) that acts as a chelator of Zn ion in the active site of zinc-dependent HDAC [44,45]. In con-

trast to TSA and SAHA, butyrate, the smallest HDACi, consists of 3-carbon chain linked to a carboxyl group.

MTX contains a pteridine ring, which is the hydrophobic group. Additionally, the residue of p-aminobenzoic acid is structurally similar to the TSA and SAHA. Furthermore, the end of the MTX molecule contains the residue of butyrate. It was demonstrated by computer modelling that MTX is able to bind into the binding site of HDAC homolog (HDAC-like protein) and to interact with the zinc ion and the surrounding structures of this protein. The inhibition of HDAC was also shown under *in vitro* conditions in cell lines derived from lung cancer, cervical or stomach cancer; an increase in the acetylation status of histone H3 was also described in these cell lines [43].

In addition to the acetylation of histone H3, MTX has the ability to induce the acetylation of p53 protein at residues Lys373/382 [46]. However, this posttranslational modification was not observed if other HDACi were applied. Simultaneously with the acetylation, MTX induced the phosphorylation of p53 protein at Ser15 that leads to the accumulation and increasing stability of p53 protein because acetylated sites are used in the process of its ubiquitination. HDAC-inhibiting activity of MTX resulted in down-regulation of the histone-lysine N-methyltransferase (EZH2), which is the catalytic core protein in the Polycomb Repressor Complex 2 (PRC2). PRC2 catalyses the addition of three methyl groups to Lys27 of histone 3 and mediates gene silencing of the tumour suppressor genes [47]. The epigenetic suppression of EZH2 expression by MTX resulted in the increasing expression of E-cadherin, which participates in the reduced cell migration and restricts a neoplastic transformation of epithelial cells [46].

Although the application of HDACi is a promising strategy to counter epigenetic changes associated with tumourigenesis [48,49], combination of these compounds with MTX has a different effect depending on the inhibitor type. For example, SAHA and sodium butyrate (NaBu) seem to be suitable HDACi for combination with MTX in ALL cell lines. These inhibitors increase both the cytotoxicity of MTX and the induction of apoptosis by modulation of the expression of enzymes involved in folate metabolism. After treatment with NaBu or SAHA, DHFR and TS expression decreased and the expression of the folylpoly-γ-glutamate synthetase (FPGS) was enhanced [50]. FPGS is the key enzyme which links glutamate residues to MTX and prevents MTX exclusion from the cell and increases its efficiency [4].

Nevertheless, the main problem of combined treatment with HDACi and MTX seems to be the sequence of their administration because the effects can be opposite [51,52]. Some HDACi (e.g. valproate or MS275) can even enhance the resistance of cells to MTX by up-regulation of thymidylate synthase expression; it was demonstrated in mouse choroid plexus carcinoma cell lines [53].

MTX as Inhibitor of the Glyoxalase System

Recently, it was also found that MTX affects the glyoxalase system. This three-step metabolic pathway is localised in the cytoplasm and it is considered to be the main pathway of methylglyoxal detoxification. Methylglyoxal, a secondary product of glycolysis or lipid peroxidation, is converted to D-lactate via the intermediate S-d-lactoylglutathione. The glyoxalase system consists of two enzymes, glyoxalase 1 (Glo1) and glyoxalase 2 (Glo2) and a catalytic amount of reduced glutathione [54].

Enhanced activity or expression of Glo1 was described as a marker of many human neoplasias. This metabolic change is associated with increased invasiveness, metastatic potential and multidrug resistance [54]. Moreover, amplification of the gene encoding Glo1 was identified in some types of primary solid tumours [55].

Bartyik et al [1] showed that MTX inhibits Glo1 *in vitro*; confirmed indirectly by detection of decrease in plasma D-lactate following MTX treatment in ALL patients. Inhibition of Glo1 elevates the intracellular methylglyoxal level that causes glycation of biomolecules [56,57], production of ROS, or genotoxic damage in tumour cells [58,59]. All these changes can lead to the enhancement of antitumor effects of MTX.

Thus, the glyoxalase system, namely the Glo1 enzyme, represents another target of the anti-neoplastic actions of MTX and expands the range of MTX effects on various metabolic pathways.

MTX as Inductor of Oxidative Stress

Several studies have confirmed the role of oxidative stress in the cytotoxic effect of MTX [60–62]. It was demonstrated that some NAD(P)H-dependent dehydrogenases, namely 2-oxoglutarate, iso-citrate, malate and pyruvate dehydrogenases, are inhibited by MTX [63]. Inhibition of these enzymes can induce a decrease in the NADPH levels; NADPH is required to reduce oxidised glutathione (GSSG) to the reduced form (GSH). GSH acts as cytoplasmic antioxidant and its MTX-induced decrease leads to a reduced effectiveness of the antioxidant defence system [64]. At the tissue level, a decline of GSH, superoxide dismutase and catalase activities were observed after MTX application in rat cerebellum [65].

Association of MTX-induced apoptosis and MTX-induced ROS generation was depicted in HL-60 and Jurkat T human leukaemia cells [2]. Cell death was mediated by the mitochondrial pathway accompanied with a disruption of the mitochondrial membrane potential and subsequent activation of caspases. Another study showed that MTX activates JNK kinase through production of ROS resulting in induction of pro-apoptotic target genes and increased sensitivity to apoptosis [66].

Conclusion

Recent promising strategies in cancer treatment are based on the administration of drugs in combination and with different modes of action (cytostatics, differentiation inducers and angiogenic growth factors) [67] or on the new compounds affecting multiple, sometimes unrelated, cancer cell targets [68], because drugs designed exclusively against individual molecular targets usually cannot combat complex diseases such as cancer [69].

Although MTX has been used as a folate metabolism antagonist in cancer

therapy for more than 60 years, identification of the whole spectrum of its' molecular targets in cellular metabolism still continues. MTX inhibits not only synthesis of nucleotides and methylation of biomolecules, but also negatively regulates acetylation of histones, glyoxalase metabolism and antioxidant systems. Interventions in all of these metabolic pathways can induce changes in gene expression and consequently can lead to differentiation or cell death of cancer cells.

References

1. Bartyik K, Turi S, Orosz F et al. Methotrexate inhibits the glyoxalase system in vivo in children with acute lymphoid leukaemia. Eur J Cancer 2004; 40(15): 2287–2292.
2. Huang CC, Hsu PC, Hung YC et al. Ornithine decarboxylase prevents methotrexate-induced apoptosis by reducing intracellular reactive oxygen species production. Apoptosis 2005; 10(4): 895–907.
3. Lamprecht SA, Lipkin M. Chemoprevention of colon cancer by calcium, vitamin D and folate: molecular mechanisms. Nat Rev Cancer 2003; 3(8): 601–614.
4. Assaraf YG. Molecular basis of antifolate resistance. Cancer Metastasis Rev 2007; 26(1): 153–181.
5. Fotoohi AK, Albertioni F. Mechanisms of antifolate resistance and methotrexate efficacy in leukemia cells. Leuk Lymphoma 2008; 49(3): 410–426.
6. Genestier L, Paillot R, Quemeneur L et al. Mechanisms of action of methotrexate. Immunopharmacology 2000; 47(2–3): 247–257.
7. Webley SD, Welsh SJ, Jackman AL et al. The ability to accumulate deoxyuridine triphosphate and cellular response to thymidylate synthase (TS) inhibition. Br J Cancer 2001; 85(3): 446–452.
8. Muñoz-Pinedo C, Robledo G, López-Rivas A. Thymidylate synthase inhibition triggers glucose-dependent apoptosis in p53-negative leukemic cells. FEBS Lett 2004; 570(1–3): 205–210.
9. Waldman BC, Wang Y, Kilaru K et al. Induction of intrachromosomal homologous recombination in human cells by raltitrexed, an inhibitor of thymidylate synthase. DNA Repair 2008; 7(10): 1624–1635.
10. Allegra CJ, Hoang K, Yeh GC et al. Evidence for direct inhibition of de novo purine synthesis in human MCF-7 breast cells as a principal mode of metabolic inhibition by methotrexate. J Biol Chem 1987; 262(28): 13520–13526.
11. Allegra CJ, Fine RL, Drake JC et al. The effect of methotrexate on intracellular folate pools in human MCF-7 breast cancer cells. Evidence for direct inhibition of purine synthesis. J Biol Chem 1986; 261(14): 6478–6485.
12. Allegra CJ, Drake JC, Jolivet J et al. Inhibition of phosphoribosylaminoimidazolecarboxamide transformylase by methotrexate and dihydrofolic acid polyglutamates. Proc Natl Acad Sci U S A 1985; 82(15): 4881–4885.
13. Baggott JE, Morgan SL, Vaughn WH. Differences in methotrexate and 7-hydroxymethotrexate inhibition of folate-dependent enzymes of purine nucleotide biosynthesis. Biochem J 1994; 300(3): 627–629.
14. Allegra CJ, Chabner BA, Drake JC et al. Enhanced inhibition of thymidylate synthase by methotrexate polyglutamates. J Biol Chem 1985; 260(17): 9720–9726.
15. McGuire JJ. Anticancer antifolates: current status and future directions. Curr Pharm Des 2003; 9(31): 2593–2613.
16. Genestier L, Paillot R, Fournel S et al. Immunosuppressive properties of methotrexate: apoptosis and clonal deletion of activated peripheral T cells. J Clin Invest 1998; 102(2): 322–328.
17. Merkle CJ, Moore IM, Penton BS et al. Methotrexate causes apoptosis in postmitotic endothelial cells. Biol Res Nurs 2000; 2(1): 5–14.
18. Kruman II, Wersto RP, Cardozo-Pelaez F et al. Cell cycle activation linked to neuronal cell death initiated by DNA damage. Neuron 2004; 41(4): 549–561.
19. Bodner AJ, Ting RC, Gallo RC. Induction of differentiation of human promyelocytic leukemia cells (HL-60) by nucleosides and methotrexate. J Natl Cancer Inst 1981; 67(5): 1025–1030.
20. Ross SA, Jones CS, De Luca LM. Retinoic acid and methotrexate specifically increase PHA-E-lectin binding to a 67-kDa glycoprotein in LA-N-1 human neuroblastoma cells. Int J Cancer 1995; 62(3): 303–308.
21. Schwartz PM, Barnett SK, Atillasoy ES et al. Methotrexate induces differentiation of human keratinocytes. Proc Natl Acad Sci U S A 1992; 89(2): 594–598.
22. Seitz M, Zwicker M, Loetscher P. Effects of methotrexate on differentiation of monocytes and production of cytokine inhibitors by monocytes. Arthritis Rheum 1998; 41(11): 2032–2038.
23. Hatse S, Naesens L, De Clercq E et al. Potent differentiation-inducing properties of the antiretroviral agent 9-(2-phosphonylmethoxyethyl) adenine (PMEA) in the rat choriocarcinoma (RCHO) tumor cell model. Biochem Pharmacol 1998; 56(7): 851–859.
24. Hohn HP, Linke M, Denker HW. Adhesion of trophoblast to uterine epithelium as related to the state of trophoblast differentiation: in vitro studies using cell lines. Mol Reprod Dev 2000; 57(2): 135–145.
25. Singh R, Fouladi-Nashta AA, Li D et al. Methotrexate induced differentiation in colon cancer cells is primarily due to purine deprivation. J Cell Biochem 2006; 99(1): 146–155.
26. Serra JM, Gutiérrez A, Alemany R et al. Inhibition of c-Myc down-regulation by sustained extracellular signal-regulated kinase activation prevents the antimetabolite methotrexate- and gemcitabine-induced differentiation in non-small-cell lung cancer cells. Mol Pharmacol 2008; 73(6): 1679–1687.
27. Lin TL, Vala MS, Barber JP et al. Induction of acute lymphocytic leukemia differentiation by maintenance therapy. Leukemia 2007; 21(9): 1915–1920.
28. Hatse S, De Clercq E, Balzarini J. Role of antimetabolites of purine and pyrimidine nucleotide metabolism in tumor cell differentiation. Biochem Pharmacol 1999; 58(4): 539–555.
29. Hara A, Niwa M, Kumada M et al. Intraocular injection of folate antagonist methotrexate induces neuronal differentiation of embryonic stem cells transplanted in the adult mouse retina. Brain Res 2006; 1085(1): 33–42.
30. Hara A, Taguchi A, Aoki H et al. Folate antagonist, methotrexate induces neuronal differentiation of human embryonic stem cells transplanted into nude mouse retina. Neurosci Lett 2010; 477(3): 138–143.
31. Stover PJ. One-carbon metabolism-genome interactions in folate-associated pathologies. J Nutr 2009; 139(12): 2402–2405.
32. Vezmar S, Schüsseler P, Becker A et al. Methotrexate-associated alterations of the folate and methyl-transfer pathway in the CSF of ALL patients with and without symptoms of neurotoxicity. Pediatr Blood Cancer 2009; 52(1): 26–32.
33. Li M, Hu SL, Shen ZJ et al. High-performance capillary electrophoretic method for the quantification of global DNA methylation: application to methotrexate-resistant cells. Anal Biochem 2009; 387(1): 71–75.
34. Wang YC, Chiang EP. Low-dose methotrexate inhibits methionine S-adenosyltransferase in vitro and in vivo. Mol Med 2012; 18(1): 423–432.
35. Winter-Vann AM, Kamen BA, Bergo MO et al. Targeting Ras signaling through inhibition of carboxyl methylation: an unexpected property of methotrexate. Proc Natl Acad Sci U S A 2003; 100(11): 6529–6534.
36. Wu J, Wood GS. Reduction of Fas/CD95 promoter methylation, upregulation of Fas protein, and enhancement of sensitivity to apoptosis in cutaneous T-cell lymphoma. Arch Dermatol 2011; 147(4): 443–449.
37. Salbaum JM, Kappen C. Genetic and epigenomic footprints of folate. Prog Mol Biol Transl Sci 2012; 108: 129–158.
38. Mahoney SE, Yao Z, Keyes CC et al. Genome-wide DNA methylation studies suggest distinct DNA methylation patterns in pediatric embryonal and alveolar rhabdomyosarcomas. Epigenetics 2012; 7(4): 400–408.
39. Diede SJ, Guenthoer J, Geng LN et al. DNA methylation of developmental genes in pediatric medulloblastomas identified by denaturation analysis of methylation differences. Proc Natl Acad Sci U S A 2010; 107(1): 234–239.
40. Restrepo A, Smith CA, Agnihotri S et al. Epigenetic regulation of glial fibrillary acidic protein by DNA methylation in human malignant gliomas. Neuro Oncol 2011; 13(1): 42–50.
41. Hill VK, Underhill-Day N, Krex D et al. Epigenetic inactivation of the RASSF10 candidate tumor suppressor gene is a frequent and an early event in gliomagenesis. Oncogene 2011; 30(8): 978–989.
42. Esteller M. CpG island hypermethylation and tumor suppressor genes: a booming present, a brighter future. Oncogene 2002; 21(35): 5427–5440.
43. Yang PM, Lin JH, Huang WY et al. Inhibition of histone deacetylase activity is a novel function of the antifolate drug methotrexate. Biochem Biophys Res Commun 2010; 391(3): 1396–1399.
44. Xu WS, Parmigiani RB, Marks PA. Histone deacetylase inhibitors: molecular mechanisms of action. Oncogene 2007; 26(37): 5541–5552.
45. Marks PA, Xu WS. Histone deacetylase inhibitors: Potential in cancer therapy. J Cell Biochem 2009; 107(4): 600–608.
46. Huang WY, Yang PM, Chang YF et al. Methotrexate induces apoptosis through p53/p21-dependent pathway and increases E-cadherin expression through downregulation of HDAC/EZH2. Biochem Pharmacol 2011; 81(4): 510–517.
47. Chang CJ, Hung MC. The role of EZH2 in tumour progression. Br J Cancer 2012; 106(2): 243–247.
48. Bolden JE, Peart MJ, Johnstone RW. Anticancer activities of histone deacetylase inhibitors. Nat Rev Drug Discov 2006; 5(9): 769–784.
49. Dell'Aversana C, Lepore I, Altucci L. HDAC modulation and cell death in the clinic. Exp Cell Res 2012; 318(11): 1229–1244.
50. Leclerc GJ, Mou C, Leclerc GM et al. Histone deacetylase inhibitors induce FPGS mRNA expression and intracellular accumulation of long-chain methotrexate polyglutamates in childhood acute lymphoblastic leukemia: implications for combination therapy. Leukemia 2010; 24(3): 552–562.
51. Einsiedel HG, Kawan L, Eckert C et al. Histone deacetylase inhibitors have antitumor activity in two NOD/SCID mouse models of B-cell precursor childhood acute lymphoblastic leukemia. Leukemia 2006; 20(8): 1435–1436.
52. Bastian L, Einsiedel HG, Henze G et al. The sequence of application of methotrexate and histone deacetylase inhibitors determines either a synergistic or an antagonistic response in childhood acute lymphoblastic leukemia cells. Leukemia 2011; 25(2): 359–361.
53. Prasad P, Vasquez H, Das CM et al. Histone acetylation resulting in resistance to methotrexate in choroid plexus cells. J Neurooncol 2009; 91(3): 279–286.
54. Thornalley PJ, Rabbani N. Glyoxalase in tumourigenesis and multidrug resistance. Semin Cell Dev Biol 2011; 22(3): 318–325.
55. Santarius T, Bignell GR, Greenman CD et al. GLO1-A novel amplified gene in human cancer. Genes Chromosomes Cancer 2010; 49(8): 711–725.

56. Suji G, Sivakami S. DNA damage during glycation of lysine by methylglyoxal: assessment of vitamins in preventing damage. Amino Acids 2007; 33(4): 615–621.
57. Pepper ED, Farrell MJ, Nord G et al. Antiglycation effects of carnosine and other compounds on the long--term survival of Escherichia coli. Appl Environ Microbiol 2010; 76(24): 7925–7930.
58. Kalapos MP. The tandem of free radicals and methylglyoxal. Chem Biol Interact 2008; 171(3): 251–271.
59. Koizumi K, Nakayama M, Zhu WJ et al. Characteristic effects of methylglyoxal and its degraded product formate on viability of human histiocytes: a possible detoxification pathway of methylglyoxal. Biochem Biophys Res Commun 2011; 407(2): 426–431.
60. Uzar E, Koyuncuoglu HR, Uz E et al. The activities of antioxidant enzymes and the level of malondialdehyde in cerebellum of rats subjected to methotrexate: protective effect of caffeic acid phenethyl ester. Mol Cell Biochem 2006; 291(1–2): 63–68.
61. Miketova P, Kaemingk K, Hockenberry M et al. Oxidative changes in cerebral spinal fluid phosphatidylcholine during treatment for acute lymphoblastic leukemia. Biol Res Nurs 2005; 6(3): 187–195.
62. Jahovic N, Cevik H, Sehirli AO et al. Melatonin prevents methotrexate-induced hepatorenal oxidative injury in rats. J Pineal Res 2003; 34(4): 282–287.
63. Caetano NN, Campello AP, Carnieri EG et al. Effect of methotrexate (MTX) on NAD(P)+ dehydrogenases of HeLa cells: malic enzyme, 2-oxoglutarate and isocitrate dehydrogenases. Cell Biochem Funct 1997; 15(4): 259–264.
64. Babiak RM, Campello AP, Carnieri EG et al. Methotrexate: pentose cycle and oxidative stress. Cell Biochem Funct 1998; 16(4): 283–293.
65. Vardi N, Parlakpinar H, Ates B. Beneficial effects of chlorogenic acid on methotrexate-induced cerebellar Purkinje cell damage in rats. J Chem Neuroanat 2012; 43(1): 43–47.
66. Spurlock CF 3rd, Aune ZT, Tossberg JT et al. Increased sensitivity to apoptosis induced by methotrexate is mediated by JNK. Arthritis Rheum 2011; 63(9): 2606–2616.
67. Zapletalova D, André N, Deak L et al. Metronomic chemotherapy with the COMBAT regimen in advanced pediatric malignancies: a multicenter experience. Oncology 2012; 82(5): 249–260.
68. Carrasco MP, Enyedy EA, Krupenko NI et al. Novel folate-hydroxamate based antimetabolites: synthesis and biological evaluation. Med Chem 2011; 7(4): 265–274.
69. Zimmermann GR, Lehár J, Keith CT. Multi-target therapeutics: when the whole is greater than the sum of the parts. Drug Discov Today 2007; 12(1–2): 34–42.

Detection of Cancer Stem Cell Markers in Sarcomas

Detekce nádorových kmenových buněk v sarkomech

Veselska R.[1,2], Skoda J.[1,2], Neradil J.[1,3]

[1] Laboratory of Tumor Biology, Department of Experimental Biology, School of Science, Masaryk University, Brno, Czech Republic
[2] Department of Pediatric Oncology, University Hospital Brno and School of Medicine, Masaryk University, Brno, Czech Republic
[3] Regional Centre for Applied Molecular Oncology, Masaryk Memorial Cancer Institute, Brno, Czech Republic

Summary
The identification of cancer stem cell markers represents one of the very relevant research topics because cancer stem cells play important roles in tumour initiation and progression, as well as during metastasis formation and in relapse of the disease. This article summarises recent knowledge on well-known and putative cancer stem cell markers in various types of bone and soft-tissue sarcomas. Special attention is paid to the detection of CD133, ABC transporters, nestin and aldehyde dehydrogenase that have been intensively studied both in tumour tissues and in sarcoma cell lines during the past few years. Finally, an overview is given of the possible CSC phenotypes provided by functional assays of tumourigenicity.

Key words
cancer stem cells – osteosarcoma– rhabdomyosarcoma – CD133 – ABC transporters – nestin – aldehyde dehydrogenase – tumourigenicity

Souhrn
Identifikace nádorových kmenových buněk v současnosti představuje jednu z nejdůležitějších oblastí výzkumu, neboť nádorové kmenové buňky hrají důležitou úlohu v iniciaci a progresi nádoru, stejně jako v procesech metastazování a relapsu onemocnění. Tento článek shrnuje současné poznatky o známých i předpokládaných markerech nádorových kmenových buněk v různých typech sarkomů kostí i měkkých tkání. Zvláštní pozornost je věnována detekci CD133, ABC transportérů, nestinu a aldehyddehydrogenázy, které byly v posledních letech intenzivně zkoumány jak v nádorové tkáni, tak v sarkomových buněčných liniích. V závěru článku je uveden přehled možných fenotypů nádorových kmenových buněk, které byly prokázány funkčními testy tumorigenicity.

Klíčová slova
nádorové kmenové buňky – osteosarkom – rabdomyosarkom – CD133 – ABC transportéry – nestin – aldehyddehydrogenáza – tumorigenicita

The study was supported by grant of Internal Grant Agency of the Czech Ministry of Health No. NT13443-4 and by the European Regional Development Fund and the State Budget of the Czech Republic (RECAMO; CZ.1.05./2.1.00/03.0101).

Práce byla podpořena grantem IGA MZ ČR NT13443-4 a Evropským fondem pro regionální rozvoj a státním rozpočtem České republiky (OP VaVpI – RECAMO, CZ.1.05/2.1.00/03.0101).

The authors declare they have no potential conflicts of interest concerning drugs, products, or services used in the study.

Autoři deklarují, že v souvislosti s předmětem studie nemají žádné komerční zájmy.

The Editorial Board declares that the manuscript met the ICMJE "uniform requirements" for biomedical papers.

Redakční rada potvrzuje, že rukopis práce splnil ICMJE kritéria pro publikace zasílané do biomedicínských časopisů.

Renata Veselska, Assoc. Prof. RNDr., Ph.D., M.Sc.
Laboratory of Tumor Biology
Institute of Experimental Biology
School of Science, Masaryk University
Kotlarska 2
611 37 Brno
Czech Republic
e-mail: veselska@sci.muni.cz

Submitted/Obdrženo: 2. 10. 2012
Accepted/Přijato: 7. 11. 2012

Introduction

At present, a theory concerning the role of cancer stem cells (CSCs) – sometimes termed tumour-initiating cells (TICs) – in initiation and progression of cancer is widely accepted. CSCs undoubtedly play an important role in the processes of tumour initiation and progression, as well as during metastasis formation and relapse of the disease [1,2]. Thus, a detailed understanding of the characteristics of CSCs in particular tumour types may play a key role in the development of new effective antineoplastic therapies because, in heterogeneous tumour tissue, only CSCs are supposed to initiate tumour growth after grafting into immunodeficient mice [3,4]. In this context, the biological features of CSCs represent one of the very important research topics in tumour biology and experimental oncology. Although a lot of papers concerning CSCs were published during past few years, especially in haematological malignancies, neurogenic tumours and most frequent carcinomas, relatively few studies have focused on the identification of CSCs in sarcomas. Therefore, the main aim of this paper is to summarise up-to-date knowledge on the identification of well-known and potential cancer stem cell markers in various types of human sarcomas.

Detection of Cancer Stem Cell Markers in Sarcomas

In general, detection of specific markers of CSCs can be performed in tissue sections from selected types of sarcomas can be followed by detection of the same markers in the corresponding cell lines derived from samples of the respective tumour tissues. The identification of CSC markers in tumour tissues enables us to determine the frequency of cells expressing individual markers as well as levels of co-expression of these markers; an exploratory analysis of CSC markers in relation to clinical characteristics of the cohort can be also performed using these data. Cell lines derived from the respective tumours can be used to determine the proportion of cells showing the CSC phenotype and then for cell sorting based on differences in expression of these markers. Subsequently, the sorted cell populations are analysed by functional assays of the tumourigenic potential both *in vitro* (colony forming assay, sphere formation assay, invasion assay) and *in vivo* (tumourigenicity in immunodeficient mice).

Methodological approaches to the identification of expression of individual stem cell markers or their combinations in both sarcoma tissue and sarcoma cell lines are based on the detection of the mRNA in question (RT-PCR or real-time PCR) or on immunodetection of the respective protein (immunohistochemistry – IHC; immunofluorescence – IF; western blotting – WB; flow cytometry – FC; fluorescence activated cell sorting – FACS).

Furthermore, expression profiling can also be employed to identify differences in expression of genes participating in regulatory pathways in tumour cells. The results obtained should be compared with those from tissue sections as well as with the data concerning the clinical course of the disease in the respective patients to help us to determine the clinical importance of the examined individual marker or cell phenotype. Other potential markers of CSCs can also be selected on the basis of the obtained expression profiles compared with clinical data.

In addition to commonly known stem cell markers (Oct3/4, Sox2, Nanog, etc.), special attention is paid to finding specific markers that enable us to detect CSCs positively in specific types of sarcomas [5]. As given in the subheadings below, expression of the widely accepted and putative markers of CSCs is intensively studied both in tumour tissues and cell lines derived from various types of bone and soft-tissue sarcomas. The following overview is focused particularly on CSC markers that were identified in sarcomas by more than one research group. The last subheading is dedicated to describe possible CSCs phenotypes (i.e. combinations of various CSCs markers) as identified in various sarcomas by functional assays of tumourigenicity.

CD133 (Prominin-1)

CD133 glycoprotein (also known as prominin-1) is a cell surface antigen with five transmembrane domains. CD133 and namely its AC133 epitope are widely discussed to be putative "universal" markers of CSCs in various human malignancies; however, its biological function still remains unclear [6].

Expression of CD133 was detected using real-time PCR and FC in Saos-2 reference osteosarcoma cell line for the first time [7]. This finding in the same cell line was later confirmed using IF; strong expression of CD133 was also reported in four other in-house osteosarcoma cell lines [8]. CD133-positive side population was further confirmed by FACS in Saos-2, U2OS and MG-63 osteosarcoma cell lines; all these cell populations were simultaneously positive also for Ki-67 that is expressed in proliferating cells only [9]. The next study of this research group confirmed a CD133 positive subpopulation in primary cultures of 21 sarcomas (two osteosarcomas, six chondrosarcomas, one osteochondrosarcoma, four fibrosarcomas, three synovial sarcomas, three liposarcomas, one leiomyosarcoma and one chordoma), as well as in HT1080 reference fibrosarcoma cell line using FACS [10]. From all of these primary cultures, two osteosarcoma and two chondrosarcoma cell lines were successfully established; all of them show only low levels (up to 7.8%, similarly to those in primary tumors) of CD133 expression, as detected by FACS. Moreover, sorted CD133-positive cell populations were able to regenerate the original not-sorted cell populations, i.e. the mixture of CD133-positive and CD133-negative cells [10]. Strong expression of CD133 was also found in 3AB-OS osteosarcoma cell line by employment of IF, FC and RT-PCR, which was reported as a new in-house cancer stem-like cell line. In contrast, the above mentioned MG-63 osteosarcoma cell line was described as CD133-negative by this research group [11]. Most recently, CD133 expression was identified in monolayers of Saos-2, CHA59 and HuO9 osteosarcoma cell lines but significantly decreased in spheres formed from Saos-2 and CHA59 cells; in HuO9 sarcospheres CD133 expression remains at the same levels as in monolayer [12].

The clinical relevance of the CD133 expression in osteosarcoma tumour tissue

was recently reported in a cohort of 70 patients diagnosed with primary osteosarcoma. CD133 expression was found in 46 (65.7%) tumours and correlated positively with the occurrence of lung metastases [13]. Interestingly, CD133 expression in MG-63 cells was also analysed in this study using FACS and WB and this cell line was found to express CD133, in accordance with results given by Tirino and colleagues [9] but in contrast to the results by DiFiore and colleagues [11].

In synovial sarcomas, strong expression of CD133 was originally found using IHC in five samples and in three cell lines derived from these tumours [14]. In rhabdomyosarcomas, CD133 was originally detected using IHC and IF in ten FFPE samples of rhabdomyosarcoma tissue. Moreover, the same study reported CD133 expression also in five in-house cell lines derived from these tumours, demonstrated using IF, FC and WB [15]. Another study showed strong CD133 expression in five cell lines derived from embryonal rhabdomyosarcomas as well as in rhabdospheres formed from these cell lines using real-time PCR, IF, FC and WB [16]. Another five rhabdomyosarcoma cell lines (both embryonal and alveolar) were then analysed for CD133 expression by FACS and isolated CD133-positive subpopulations were obtained from all of these cell lines [17]. Results achieved using FC also indicate an increase in CD133 expression in rhabdomyosarcoma cell populations during culture and IF showed both membranous and cytoplasmic localisations of this molecule [15]; a similar finding was previously reported in an osteosarcoma cell line and this effect should be explained by deposition of CD133 into cytoplasmic vesicles, as identified by confocal microscopy [9].

ABC Transporters

ATP-binding cassette (ABC) transporters are found in the plasma membrane of numerous cell types giving them protection against xenobiotics. Their expression in transformed cells determines the multidrug-resistance (MDR) phenotype because they can actively exclude antineoplastic agents from the cytoplasm and the same mechanism is considered to cause the resistance of CSCs to chemotherapy [18].

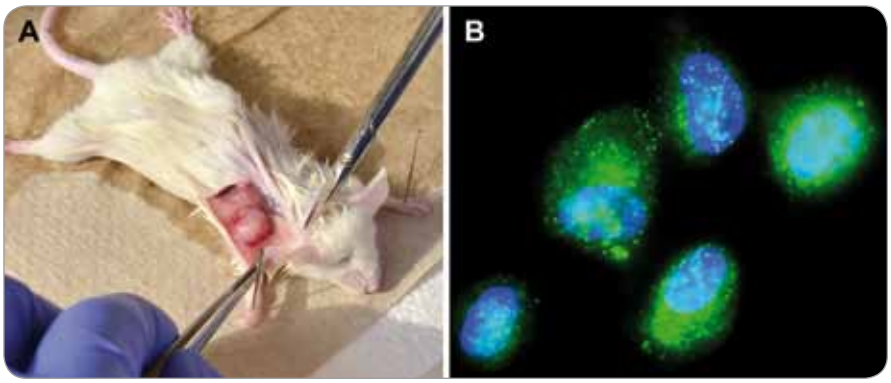

Fig. 1. Examples of our results on identification of CSCs in rhabdomyosarcomas. A. Subcutaneous xenograft tumour in NOD/SCID mice injected with NSTS-11 embryonal rhabdomyosarcoma cells. B. Expression of CD133 (green) as detected by indirect immunofluorescence in NSTS-11 cell line; counterstaining: DAPI (blue). Original magnification: 1,000×.

Results concerning expression of ABC transporters in sarcomas seem to be partly controversial. Strong expression of ABCG2 transporter was detected by FACS in Saos-2, U2OS and MG-63 osteosarcoma cell lines at the first time [9]. Surprisingly, one of these cell lines, Saos-2 cell line used as reference cell line in another study, was previously found ABCG2 negative by quantitative real-time RT-PCR analysis as well as by FC [7]. Furthermore, both MG-63 osteosarcoma cell line and 3AB-OS in-house osteosarcoma cell line were reported as ABCG2 positive using IF, FC and RT-PCR. In contrast, expression of ABCB1 transporter was found only in MG-63 cell line but not in 3AB-OS cell line in the same study [11].

Saos-2 cell line, as well as two other osteosarcoma cell lines, CHA59 and HuO9, were recently analysed for the expression of selected ABC transporters in detail using transcriptome and proteome analysis, real-time PCR and FACS. In this study, expression of four ABC transporters – ABCA5, ABCB1, ABCC1 and ABCG2 – was found in all three cell lines, but some marked differences were identified if expression in monolayers and in sarcospheres were compared. Nevertheless, only ABCG2 transporter showed a significant increase in sarcospheres of all three examined cell lines compared with the respective monolayers [12].

The up-regulation of ABCG2 was also shown in side population of MHF2003 malignant fibrous histiocytoma cell line using expression profiling [19].

Nestin

Nestin (= neuronal stem cell protein) belongs to class VI of the intermediate filaments. This protein is expressed primarily in nervous tissue during embryonic development and especially in neuronal stem cells. Nevertheless, nestin expression has also been detected in various types of human solid tumours, as well as in the corresponding established cell lines. Co-expression of nestin together with other stem cell markers, namely CD133, is discussed to be a possible marker of cancer stem cells [20].

The first study concerning nestin in sarcomas showed expression in samples of various paediatric rhabdomyosarcomas (sixteen embryonal rhabdomyosarcomas, six alveolar rhabdomyosarcomas, five pleomorphic rhabdomyosarcomas, one spindle cell rhabdomyosarcoma, one dense rhabdomyosarcoma and two embryonal sarcomas) using IHC [21]. In contrast, the same study did not find nestin in one sample of fibrosarcoma and in two samples of Ewing's sarcoma [21]. The presence of nestin in ten samples both of embryonal and alveolar rhabdomayosarcomas; as well as in five rhabdomyosarcoma cell lines derived from these tumours was later confirmed by IHC and/or IF with another anti-nestin antibody [15].

Regarding bone sarcomas, nestin was originally detected in all eighteen samples of osteosarcoma (fourteen osteoblastic osteosarcomas, three chondroblastic osteosarcomas and one teleangiectatic osteosarcoma) using IHC, as well as in three osteosarcoma cell lines derived from these tumours using IF [8]. A subsequent study of the same research group aimed to determine the prognostic value of nestin expression in 45 high-grade osteosarcomas but the results were partly controversial. Although nestin-positive tumour cells were detected in all of the examined FFPE samples using both IHC and IF, the proportion of positive neoplastic cells varied in individual samples. Moreover, high levels of nestin as measured by IF were significantly associated with worse clinical outcomes and the similar results achieved with IHC also showed a trend to shorter patient survival rates but these results did not reach statistical significance. Therefore nestin does not seem to be a powerful prognostic marker in high-grade osteosarcomas [22].

Nestin expression was also detected by RT-PCR in sphere-forming cell subpopulations of two osteosarcoma and two chondrosarcoma in-house cell lines, as well as the HT1080 fibrosarcoma reference cell line. In contrast, adherent cell populations of the same cell lines were obviously nestin negative [10]. Similar results were obtained by analysis of spheres and adherent populations of CHA59 cells by real-time PCR and WB. A reverse pattern of nestin expression (i.e. down-regulation of nestin in sarcospheres) was described in HuO9 cell line. Surprisingly, both spheres and adherent cell populations were found to be nestin negative in Saos-2 cells [12].

Aldehyde Dehydrogenase

Aldehyde dehydrogenase (ALDH) is the enzyme catalysing the oxidation of intracellular aldehydes in many cell types. High ALDH activities were detected in neuronal and haematopoietic stem cells as well as in CSCs of some human solid tumours, especially carcinomas [23].

Four human osteosarcoma cell lines – Saos-2, MG-63, HuO9, and OS99-1 – showed high levels of ALDH in cell subpopulations that substantially differ in size among these cell lines: whereas they were minor in Saos-2, MG-63, and HuO9 cell lines, OS99-1 contained about 45% of cells with high ADLH activities as detected by FC [24]. Surprisingly, a significant decrease in total number of cells with high levels of ALDH was found in OS99-1 xenografts grown in NOD/SCID mice but these cells were much more tumourigenic if compared to those with low activities of ALDH [24]. In contrast, very low activities of ALDH were identified both in Saos-2 and HuO9 cell lines (mentioned above as ALDH positive) by another research group. Nevertheless, ALDH activities were higher in spheres of CHA59 cells compared with adherent population of this same cell line [12]. CSCs exhibiting high levels of ALDH and characterised by marked chemoresistance were also identified in Ewing's sarcoma. This cell subpopulation was also successfully tested as tumourigenic using clonogenicity assay, sphere formation assay and in NOD/SCID mice [25].

Other Putative Markers of CSCs in Sarcomas

In addition to the four markers discussed above, some other molecules have been proposed as putative markers of CSCs in various sarcoma types. Nevertheless, the most important results were achieved using osteosarcoma cell lines. For example, overexpression of MET oncogene is involved in regulation of self-renewal and cell differentiation [26]. Double positivity for both CD117 (c-kit) and Stro-1 (a marker of osteogenic progenitors in bone marrow) is also considered to indicate a tumourigenic phenotype in osteosarcoma cells [27]. Furthermore, the previous study as well as other findings suggest the CXCR4 chemokine receptor to be one of the putative CSCs markers in this tumour type [13,27].

Possible CSCs Phenotypes in Sarcomas Identified by Functional Assays

Cell subpopulations isolated from two osteosarcoma and two chondrosarcoma in-house cell lines, as well as the HT1080 fibrosarcoma reference cell line, were analysed in detail using sphere-formation assay and tumourigenic assay in NOD/SCID mice [10]. Strong expressions of CD44 and CD29 cell surface antigens, as well as expression of Oct3/4, Nanog, Sox2 and nestin, were found in all CD133-positive cell populations capable of forming spheres and to induce tumour xenografts. These cell populations were also able to differentiate into mesenchymal lineages, such as osteoblasts and adipocytes [10].

The 3AB-OS cells belonging to another osteosarcoma in-house cell line were identified as CD133 and ABCG2 positive, with strong expression of stem cell markers Oct3/4, Nanog, nucleostemin, hTERT and several apoptosis inhibitors. Both MG-63 and 3AB-OS cell lines were capable of sarcosphere formation, but these spheres differed in number and volume during growth [11]. Although the previous study reported the MG-63 cell line to be CD133 negative, He et al successfully isolated a CD133-positive subpopulation from this cell line; this subpopulation was identified as positive for Oct4, Nanog and CXCR4, and showed increased migration and invasive potential [13]. Similarly, a cell subpopulation characterised by high ALDH activity was positive for Oct3/4, Nanog and Sox2 [24].

The sarcospheres rich in CSCs isolated from Saos-2, CHA59 and HuO9 osteosarcoma cell lines were shown to be positive for ABCG2 transporter and chromobox protein homolog 3 (CBX3); this phenotype was accompanied by decreased expression of CD24, CD44 and CD326 compared with monolayer culture [12].

In rhabdomyosarcomas, Sana et al showed using functional assays that NSTS-11 in-house cell line positive for CD133, nestin, nucleostemin and Oct3/4 is able to form colonies *in vitro* and tumour xenografts in NOD/SCID mice [15]. Similarly, a tumourigenic potential of rhabdomyosarcoma cell populations forming rhabdospheres *in vitro* was proved; CD133, Oct4, Nanog, c-Myc, Pax3 and Sox2 stem cell markers were up-regulated in these cell populations [16].

CD133-positive subpopulations isolated from RD and RH30 rhabdomyosarcoma cell lines were shown to be myo-

genically primitive cells with enhanced ability to form colonies. Interestingly, both of these cell lines were identified as resistant to chemotherapy but sensitive to genetically engineered HSV oncolytic virotherapy [17].

Moreover, Walter et al found by expression profiling that tumourigenic populations of rhabdomyosarcoma cells showed apparently more similarities with neuronal stem cells compared with expression profiles of haematopoietic or mesenchymal stem cells [16]. These findings are in accordance with all published results of Veselska and colleagues that found CD133/nestin positive cell populations – previously described as typical cancer stem cell phenotype in neurogenic tumours [28,29] – in both osteosarcoma [8] and rhabdomyosarcoma [15] cell lines.

Conclusion

To conclude, the findings on various types of sarcoma cells as summarised above suggest that putative CSCs markers such as CD133, ABC transporters, nestin and ALDH are of importance also in sarcoma cells. Nevertheless, despite published results especially on various osteosarcoma and rhabdomyosarcoma cell lines, the characteristic phenotype of CSCs allowing their unambiguous identification for diagnostic or therapeutic purposes remains unclear.

References

1. Ratajczak MZ. Cancer stem cells – normal stem cells „Jedi" that went over to the „dark side". Folia Histochem Cytobiol 2005; 43(4): 175–181.

2. Fábián A, Barok M, Vereb G et al. Die hard: are cancer stem cells the Bruce Willises of tumor biology? Cytometry A. 2009; 75(1): 67–74.

3. Garvalov BK, Acker T. Cancer stem cells: a new framework for the design of tumor therapies. J Mol Med (Berl) 2011; 89(2): 95–107.

4. Scatena R, Bottoni P, Pontoglio A et al. Cancer stem cells: An innovative therapeutic approach. In: Scatena R, Mordente A, Giardina B (eds). Advances in Cancer Stem Cell Biology. Springer 2012: 239–266.

5. Siclari VA, Qin L. Targeting the osteosarcoma cancer stem cell. J Orthop Surg Res 2010; 5(1): 78–87.

6. Grosse-Gehling P, Fargeas CA, Dittfeld C et al. CD133 as a biomarker for putative cancer stem cells in solid tumours: limitations, problems and challenges. J Pathol. DOI: 10.1002/path.4086. Epub ahead of print 2012.

7. Olempska M, Eisenach PA, Ammerpohl O et al. Detection of tumor stem cell markers in pancreatic carcinoma cell lines. Hepatobiliary Pancreat Dis Int 2007; 6(1): 92–97.

8. Veselska R, Hermanova M, Loja T et al. Nestin expression in osteosarcomas and derivation of nestin/ /CD133 positive osteosarcoma cell. BMC Cancer 2008; 8: 300.

9. Tirino V, Desiderio V, d'Aquino R et al. Detection and characterization of CD133+ cancer stem cells in human solid tumours. PLoS One 2008; 3: e3469.

10. Tirino V, Desiderio V, Paino F et al. Human primary bone sarcomas contain CD133+ cancer stem cells displaying high tumorigenicity in vivo. FASEB J 2011; 25(6): 2022–2030.

11. Di Fiore R, Santulli A, Ferrante RD et al. Identification and expansion of human osteosarcoma-cancer-stem cells by long-term 3-aminobenzamide treatment. J Cell Physiol 2009; 219(2): 301–313.

12. Saini V, Hose CD, Monks A et al. Identification of CBX3 and ABCA5 as putative biomarkers for tumor stem cells in osteosarcoma. PLoS One 2012; 7: e41401.

13. He A, Qi W, Huang Y et al. CD133 expression predicts lung metastasis and poor prognosis in osteosarcoma patients: A clinical and experimental study. Exp Therap Med 2012; 4(3): 435–441.

14. Terry J, Nielsen T. Expression of CD133 in synovial sarcoma. Appl Immunohistochem Mol Morphol 2010; 18(2): 159–165.

15. Sana J, Zambo I, Skoda J et al. CD133 expression and identification of CD133/nestin positive cells in rhabdomyosarcomas and rhabdomyosarcoma cell lines. Anal Cell Pathol (Amst) 2011; 34(6): 303–318.

16. Walter D, Satheesha S, Albrecht P et al. CD133 positive embryonal rhabdomyosarcoma stem-like cell population is enriched in rhabdospheres. PLoS One 2011; 6: e19506.

17. Pressey JG, Haas MC, Pressey CS et al. CD133 marks a myogenically primitive subpopulation in rhabdomyosarcoma cell lines that are relatively chemoresistant but sensitive to mutant HSV. Pediatr Blood Cancer. DOI: 10.1002/pbc 24117. Epub ahead of print 2012.

18. Dean M. ABC transporters, drug resistance, and cancer stem cells. J Mammary Gland Biol Neoplasia 2009; 14(1): 3–9.

19. Murase M, Kano M, Tsukahara T et al. Side population cells have the characteristics of cancer stem-like cells/ /cancer-initiating cells in bone sarcomas. Br J Cancer 2009; 101(8): 1425–1432.

20. Krupkova O Jr, Loja T, Zambo I et al. Nestin expression in human tumors and tumor cell lines. Neoplasma 2010; 57(4): 291–298.

21. Kobayashi M, Sjöberg G, Söderhäll S et al. Pediatric rhabdomyosarcomas express the intermediate filament nestin. Pediatr Res 1998; 43(3): 386–392.

22. Zambo I, Hermanova M, Adamkova Krakorova D et al. Nestin expression in high-grade osteosarcomas and its clinical significance. Oncol Rep 2012; 27(5): 1592–1598.

23. Adhikari AS, Agarwal N, Iwakuma T. Metastatic potential of tumor-initiating cells in solid tumors. Front Biosci 2011; 16: 1927–1938.

24. Wang L, Park P, Zhang H et al. Prospective identification of tumorigenic osteosarcoma cancer stem cells in OS99-1 cells based on high aldehyde dehydrogenase activity. Int J Cancer 2011; 128(2): 294–303.

25. Awad O, Yustein JT, Shah P et al. High ALDH activity identifies chemotherapy-resistant Ewing's sarcoma stem cells that retain sensitivity to EWS-Fli1 inhibition. PLoS One 2010; 5: e13943.

26. Dani N, Olivero M, Mareschi K et al. The MET oncogene transforms human primary bone-derived cells into osteosarcomas by targeting committed osteo-progenitors. J Bone Miner Res 2012; 27(6): 1322–1334.

27. Adhikari AS, Agarwal N, Wood BM et al. CD117 and Stro-1 identify osteosarcoma tumor-initiating cells associated with metastasis and drug resistance. Cancer Res 2010; 70(11): 4602–4612.

28. Zhang M, Song T, Yang L et al. Nestin and CD133: Valuable stem cell-specific markers for determining clinical outcome of glioma patients. J Exp Clin Cancer Res 2008; 27: 85.

29. Dell'Albani P, Pellitteri R, Tricarichi EM et al. Markers of stem cells in gliomas. In: Hayat MA (ed.). Tumors of the Central Nervous System. Vol. 1. Springer 2011: 175–190.

Analytical Cellular Pathology 34 (2011) 303–318
DOI 10.3233/ACP-2011-0018
IOS Press

CD133 expression and identification of CD133/nestin positive cells in rhabdomyosarcomas and rhabdomyosarcoma cell lines

Jiri Sana[a,1], Iva Zambo[b,1], Jan Skoda[a,c], Jakub Neradil[a,c], Petr Chlapek[a,c], Marketa Hermanova[b], Peter Mudry[c], Alzbeta Vasikova[d], Karel Zitterbart[c], Ales Hampl[e], Jaroslav Sterba[c] and Renata Veselska[a,c,*]

[a]*Laboratory of Tumor Biology and Genetics, Department of Experimental Biology, School of Science, Masaryk University, Brno, Czech Republic*
[b]*1st Institute of Pathologic Anatomy, St. Anne's University Hospital and School of Medicine, Masaryk University, Brno, Czech Republic*
[c]*Department of Pediatric Oncology, University Hospital Brno and School of Medicine, Masaryk University, Brno, Czech Republic*
[d]*Center of Molecular Biology and Gene Therapy, Department of Internal Medicine - Hematooncology, University Hospital Brno and School of Medicine, Masaryk University, Brno, Czech Republic*
[e]*Department of Histology and Embryology, School of Medicine, Masaryk University, Brno, Czech Republic*

Received: January 4, 2011
Accepted: June 26, 2011

Abstract. *Background*: Co-expression of CD133, cell surface glycoprotein, and nestin, an intermediate filament protein, was determined to be a marker of neural stem cells and of cancer stem cells in neurogenic tumors.

Methods: We examined the expression of CD133 and nestin in ten tumor tissue samples taken from patients with rhabdomyosarcomas and in five rhabdomyosarcoma cell lines. Immunohistochemistry and immunofluorescence were used to examine FFPE tumor tissue samples. Cell lines were analyzed by immunofluorescence, immunoblotting, flow cytometry, and RT-PCR. Functional assays (clonogenic *in vitro* assay and tumorigenic *in vivo* assay) were also performed using these cell lines.

Results: CD133 and nestin were detected in all 10 tumor tissue samples and in all 5 cell lines; however, the frequency of CD133+, Nes+, and CD133+/Nes+ cells, as well as the intensity of fluorescence varied in individual samples or cell lines. The expression of CD133 and nestin was subsequently confirmed in all cell lines by immunoblotting. Furthermore, we observed an increasing expression of CD133 in relation to the cultivation. All cell lines were positive for Oct3/4 and nucleostemin; NSTS-11 cells were also able to form xenograft tumors in mice.

Conclusion: Our results represent the first evidence of CD133 expression in rhabdomyosarcoma tissue and in rhabdomyosarcoma cell lines. In addition, the co-expression of CD133 and nestin as well as results of the functional assays suggest a possible presence of cancer cells with a stem-like phenotype in these tumors.

Keywords: Rhabdomyosarcoma, CD133, nestin, cancer stem cells, stem cell related markers

[1] Both authors contributed equally to this work.

*Corresponding author: Renata Veselska, Laboratory of Tumor Biology and Genetics, Department of Experimental Biology, School of Science, Masaryk University, Kotlarska 2, 611 37 Brno, Czech Republic. Tel.: +420 549 49 7905; Fax: +420 549 49 5533; E-mail: veselska@sci.muni.cz.

1. Introduction

CD133 (also known as prominin-1) was originally described in two independent studies as a plasma membrane glycoprotein in mouse neuroepithelial stem cells and as an antigenic marker expressed on the CD34+ population of hematopoietic stem cells in humans [21, 44]. This molecule contains five-transmembrane domains, two large glycosylated extracellular loops, an extracellular N-terminus, and an intracellular C-terminus [21, 44, 46]. CD133 localizes to microvilli and other protrusions of the apical plasma membrane in various cell types [6, 44]. Although the biological function of CD133 is still not known, the above-mentioned localization indicates that CD133 may act as an organizer of plasma membrane protrusions and affect cell polarity as well as interactions with nearby cells and with the extracellular matrix [5, 6, 9].

In humans, this protein is encoded by a gene on locus 4p15.32. The molecular weight of CD133 ranges from 89 to 120 kDa, depending on its glycosylation status [12, 13, 32]. However, truncated forms of CD133 with a lower molecular weight have been described recently [26, 41].

CD133, usually in combination with other specific markers, is widely used to identify stem cells in various human tissues, such as bone marrow [21, 46], CNS [40], prostate [29], or kidney [31]. Immunodetection has also showed that CD133 is frequently expressed in many types of human tumors and tumor cell lines; it was detected in cells from neurogenic tumors [33, 34], prostate carcinomas [4], hepatocellular carcinomas [35], renal carcinomas [3], colorectal carcinomas [28], melanomas [23], pancreatic adenocarcinomas [16], lung carcinomas [11], ovarian carcinomas [14], osteosarcomas [42], endometrial carcinomas [30], acute lymphoblastic leukemias [7], and synovial sarcomas [36].

At present, co-expression of glycosylated CD133 and nestin, a class VI intermediate filament protein, is considered to be a marker of cancer stem cells (CSCs) or tumor initiating cells (TICs). This was experimentally proven in glioblastoma multiforme [19, 27] and in melanoma [23]. Furthermore, the co-expression of CD133 and nestin was also shown in medulloblastomas [33], pilocytic astrocytomas [33], oligoastrocytomas [45], and in osteosarcomas [42].

Here, we present our results regarding CD133 and nestin expression in ten tumor tissue samples taken from patients with rhabdomyosarcomas and in five cell lines derived from these tumors.

2. Material and methods

2.1. Tumor samples

Ten samples of rhabdomyosarcoma tissues were included in this study. These samples were taken from seven patients (5 males, 2 females; age range: 2–21 years old). Formalin-fixed and paraffin-embedded (FFPE) surgical samples of neoplastic tissues were retrieved from the files of the Department of Pathology, University Hospital Brno, Czech Republic, and of the Department of Oncological and Experimental Pathology, Masaryk Memorial Cancer Institute, Brno, Czech Republic. Histological sections stained with hematoxylin-eosin (H-E) were reviewed by two pathologists (IZ and MH), and representative tissue blocks were selected for immunohistochemical and immunofluorescence analysis. Cell lines were derived from respective biopsy samples that were taken from patients surgically treated for rhabdomyosarcoma; all samples for cell cultures were coded and processed in the laboratory in an anonymous manner. The Research Ethics Committee of the University Hospital Brno approved the study protocol, and a written statement of informed consent was obtained from each participant prior to their participation in this study. A description of the cohort of patients included in this study is provided in Table 1.

2.2. PCR analysis of the tumor samples

Reverse transcriptase (RT) two-step nested PCR for fusion transcript PAX3-FKHR and one-step RT-PCR for fusion transcript PAX7-FKHR were used according to published methods [1, 37]. Briefly, extraction of total RNA from a patient's tumor samples was performed using an RNeasy Mini Kit (Qiagen, Hilden, Germany) according to the instruction manual. An initial amount of 1 μg RNA was used for reverse transcription using random hexamers and MuLV reverse transcriptase (Applied Biosystems, Foster City, CA, USA). PCR products were electrophoresed on a 2% agarose gel and visualized after ethidium bromide staining. For all positive assays, the PCR product was confirmed by standard direct nucleotide sequencing.

2.3. Cell cultures

Starting with primary cultures, fresh specimens of tumor tissue were processed as described previously

Table 1
Description of patient cohort and characterization of analyzed tumors

Tumor sample	Gender	Age	Tumor type	Time of biopsy	Translocation in tumor tissue	Cell line	Translocation in cell line
1	M	13	A	DG	positive PAX3/FKHR	-	-
2	M	17	A	DG	positive PAX3/FKHR	NSTS-09	21.3%
3	F	16	E	NACHT	negative PAX3,PAX7/FKHR	NSTS-11	2.7%
4	M	7	E	DG	negative PAX3,PAX7/FKHR	-	-
5	F	2	E	DG	negative PAX3,PAX7/FKHR	NSTS-12	2.3%
6	M	2	A	DG	positive PAX3/FKHR	-	-
7a	F	21	A	DG	positive PAX3/FKHR	NSTS-08	22.3%
7b				NACHT	not available	NSTS-10	20.3%
7c				PROG	positive PAX3/FKHR	-	-
7d				PROG	not available	-	-

Notes: Gender: M, male; F, female. Age at the time of diagnosis: years. Tumor type: A, alveolar; E, embryonal. Time of biopsy: DG, diagnostic; NACHT, after neo-adjuvant chemotherapy; PROG, progression of the disease. Translocation in tumor tissue: translocation *PAX3/PAX7-FKHR* as detected by RT-PCR analysis. Translocation in cell line: *FKHR* break of as detected by FISH analysis.

[42, 43]. The primary cultures were maintained in DMEM supplemented with 20% fetal calf serum, 2 mM glutamine, and antibiotics: 100 IU/ml penicillin and 100 μg/ml streptomycin (all purchased from PAA Laboratories, Linz, Austria) and cultivated under standard conditions at 37°C in an atmosphere of 95% air : 5% CO_2. Once the specimen pieces had attached, the volume of the medium was gradually increased to 5 ml over the next 48 hours. As soon as the outgrowing cells covered approximately 60% of the surface, they were trypsinized, diluted, and transferred into a new flask. A similar procedure was used for further subcultivations of all cell lines that were derived from the primary cultures.

2.4. FISH analysis of the cell lines

Using Poseidon^{TM} probes ON FKHR Break (Kreatech Diagnostics, Amsterdam, Netherlands), we examined all the above described rhabdomyosarcoma cell lines. For FISH analysis, cell suspensions were hypotonized with 75 mM KCl and fixed in methanol/acetic acid (3 : 1, vol:vol). Cell suspensions were spread onto microscopic slides and chemically aged in 2 × SSC for 30 min at 37°C. The slides were then dehydrated in 70%, 80%, and 96% ethanol for 2 min each and air-dried. Codenaturation was performed for 5 min at 75°C, and following hybridization, was allowed to proceed overnight at 37°C. Hybridized slides were then washed sequentially in 0.5 × SSC for 3 min at 75°C and 2 × SSC for 1 min at room temperature and were mounted in DAPI Counterstain (Kreatech). An Olympus BX-61 microscope was used for FISH evaluation. Micrographs were captured by Vosskühler 1300D CCD camera and analyzed using Lucia 4.80 - KARYO/FISH/CGH software (Laboratory Imaging, Prague, Czech Republic). At least 150, but most often 300, interphase nuclei were scored for *FKHR* (13q14) gene status.

2.5. FFPE immunohistochemistry

Immunohistochemical detection of both nestin and CD133 was performed on 4 μm thick tissue sections applied to positively charged slides. The sections were deparaffinized in xylene and rehydrated through a graded alcohol series. Antigen retrieval was performed in a Pascal calibrated pressure chamber (DAKO, Glostrup, Denmark) by heating the sections in modified citrate buffer (DAKO) at pH 6.1 (CD133 IHC) or in Tris/EDTA buffer (DAKO) at pH 9.0 (nestin IHC) for 40 min at 97ºC. Endogenous peroxidase activity was quenched in 3% hydrogen peroxide in methanol for 10 min, followed by incubation at room temperature with a rabbit polyclonal antibody against CD133 (No. ab19898, dilution 1 : 200, Abcam, Cambridge, UK) for 60 min or a mouse monoclonal antibody against nestin (clone 10C2, dilution 1 : 200, Millipore, Billerica, MA, USA) for 90 min. A streptavidin-biotin peroxidase detection system was used according to the manufacturer's instructions (Vectastain Ellite ABC Kit, Vector Laboratories, Burlingame, CA, USA); 3,3′-diaminobenzidine was used as a chromogen (DAB, DAKO). Slides were counterstained with Gill's hematoxylin. Tissue sections of glioblastoma multiforme served as external positive controls for the anti-nestin

antibody; Nes+ or CD133+ endothelial cells in rhabdomyosarcoma tissue samples were used as internal positive controls. Negative controls were prepared by incubating samples without primary antibody. Evaluation of immunohistochemical results was performed using a uniform microscope and camera setting (Olympus BX51 microscope and DP70 camera).

2.6. Evaluation of FFPE immunohistochemistry

For CD133, only specific membranous positivity was scored; however, cytoplasmic immunopositivity was observed in a variable proportion of tumor cells in all examined samples (see explanation in discussion). For nestin, cytoplasmic immunostaining was regarded as positive. The intensity of staining and the percentages of positive tumor cells (TC) were evaluated by two pathologists (IZ and MH) independently, using a light microscope at × 400 magnification. At least five discrete foci of neoplastic infiltration were analyzed, and the average staining intensity and the percentage of CD133+ or Nes+ cells of the entire covered area were determined. The percentage of CD133+ or Nes+ TC was categorized into four levels: ± (<2% CD133+ or Nes+ TC), + (2–10% CD133+ or Nes+ TC), ++ (11–50% CD133+ or Nes+ TC), and +++ (51–100% CD133+ or Nes+ TC). The intensity of immunostaining was graded as very weak (±), weak (+), medium (++), and strong (+++). The intensity of immunostaining was also evaluated in endothelial cells, which were used as an internal positive control.

2.7. FFPE immunofluorescence

After deparaffinization and rehydration of the tissue sections, antigen retrieval was carried out under same conditions as mentioned above. Rabbit polyclonal anti-CD133 antibody (No. ab19898, dilution 1 : 50, Abcam) or mouse monoclonal anti-nestin antibody (clone 10C2, dilution 1 : 200, Millipore) were used as primary antibodies. Tissue sections were incubated with primary antibodies at room temperature for 30 min or 90 min, respectively. Then appropriate secondary antibodies, i.e., goat anti-rabbit antibody conjugated with TRITC (No. TI-1000, dilution 1 : 100, Vector) or goat anti-mouse antibody conjugated with FITC (No. AP124F, dilution 1 : 50, Millipore) were applied for 45 min or 60 min, respectively. Subsequently, slides were mounted with mounting medium (No. S3025, Faramount Aqueous Mounting Medium, DAKO). A uniform microscope and camera setting (Nikon Eclipse 80i microscope and DS-Fi1 camera) was used for the evaluation of immunofluorescence results. Micrographs were analyzed using NIS-Elements BR 3.0 software (Laboratory Imaging).

2.8. Evaluation of FFPE immunofluorescence

Both for CD133 and nestin, the frequency of clearly positive cells (membranous positivity for CD133 and cytoplasmic positivity for nestin) was determined as follows: + (sporadically positive TC), ++ (dispersedly positive TC) and +++ (abundant positive TC). In CD133 immunofluorescence, weak cytoplasmic positivity was observed in sporadic TC in all examined cases. The slides were evaluated by two pathologists (IZ and MH) independently, using a fluorescent microscope at × 400 magnification.

2.9. Immunofluorescence of cell lines

To immunostain for CD133 and nestin, cell suspensions at a concentration of 10^4 cells per ml were seeded on glass coverslips and grown under standard conditions for 24 h. Cells were then washed in PBS, fixed with 3% para-formaldehyde (Sigma-Aldrich, St. Louis, USA) in PBS for 20 min at room temperature. The cells were subsequently washed in PBS and incubated for 10 min with 2% BSA (PAA) to block nonspecific binding of the secondary antibodies. CD133 and nestin were visualized by indirect immunofluorescence. Rabbit polyclonal anti-CD133 antibody (No. ab19898, dilution 1 : 100, Abcam) and mouse monoclonal human-specific anti-nestin antibody (clone 10C2, dilution 1 : 200, Millipore) were used as primary antibodies. The cells were treated with primary antibodies at 37°C for 1 h and washed three times in PBS. Corresponding secondary antibodies, i.e., anti-rabbit antibody conjugated with TRITC (No. T6778, dilution 1 : 160, Sigma) or anti-mouse antibody conjugated with FITC (No. F8521, dilution 1 : 160, Sigma), were applied under the same conditions. Finally, the cells were mounted onto glass slides in Vectashield mounting medium containing DAPI (Vector). The cells were observed using an Olympus BX-61 fluorescence microscope. Micrographs were captured with a CCD camera COHU 4910 and ana-

lyzed using Lucia 4.80 software – KARYO/FISH/CGH (Laboratory Imaging, Prague, Czech Republic).

2.10. Evaluation of immunofluorescence on cell lines

The percentage and intensity of immunostaining (immunoreactivity) of CD133+ or Nes+ cells were evaluated at discrete areas of each sample. The samples were prepared from several various passages of all examined cell lines. The average percentage of positive cells and the intensity of immunostaining were determined for entire samples of individual cell lines. The percentage of CD133+ or Nes+ cells was categorized into six levels: (+), ∼1% CD133+ or Nes+ cells; +, 1–10% CD133+ or Nes+ cells; +(+), ∼10% CD133+ or Nes+ cells; ++, 10–50% CD133+ or Nes+ cells; ++(+), ∼50% CD133+ or Nes+ cells; +++, >50% CD133+ or Nes+ cells. The intensity of immunostaining (immunoreactivity) was categorized into three levels: +, weak; ++, medium; +++, strong.

2.11. Flow cytometry

Cell suspensions at identical concentrations were seeded onto Petri dishes (60 cm^2) and grown under standard conditions. Evaluation of CD133 expression was performed from the second to the sixth day of cultivation at 24 h intervals. For CD133 and isotype control cell surface indirect immunostaining, cells were detached using 1 mM EDTA (PAA), fixed with 3% para-formaldehyde (Sigma) in PBS overnight at 4°C and then washed in PBS. The cells were treated either with rabbit polyclonal anti-CD133 primary antibody (No. ab19898, Abcam) or rabbit polyclonal isotype control (No. ab37416, Abcam) at 6 μg/ml for 40 min at 4°C and washed in PBS. Anti-rabbit IgG conjugated with FITC (No. F9887, dilution 1 : 160, Sigma) was applied as a secondary antibody under the same conditions. Cytometric analysis was performed using a FACS Canto™ II (BD Biosciences). Ten thousand events per sample were evaluated using WinMDI 2.8 software. After completion of the flow cytometric analysis, the remaining cell suspensions were mounted onto glass slides and observed using a Nikon Eclipse 80i fluorescence microscope in combination with a DS-Fi1 camera. Micrographs were taken at 24 h intervals using the same microscope and camera settings.

2.12. Immunoblotting

Whole-cell extracts were loaded onto polyacrylamide gels, electrophoresed, and blotted onto polyvinylidene difluoride membranes (Bio-Rad Laboratories GmbH, Germany). The membranes were blocked with 5% nonfat milk in PBS with 0.1% Tween 20 (PBS-T), then incubated either with rabbit polyclonal anti-CD133 primary antibody (No. ab19898, Abcam), mouse monoclonal anti-nestin primary antibody (clone 10C2, Millipore) or mouse monoclonal anti-alpha tubulin primary antibody (clone TU-01, Exbio, Prague, Czech Republic) diluted 1 : 1000 in blocking solution at 4°C overnight. After rinsing with PBS-T, the membranes were incubated with corresponding secondary antibodies at room temperature for 45 min; i.e., anti-mouse IgG antibody peroxidase conjugate (No. A9917, Sigma) or anti-rabbit IgG antibody peroxidase conjugate (No. A2074, Sigma) diluted 1 : 5000. Each step was followed by at least three 10-min washes in PBS-T. ECL-Plus detection was performed according to the manufacturer's instructions (Amersham, GE Healthcare, UK).

2.13. PCR analysis of the cell lines

For RT-PCR, total RNA was extracted with GenElute™ Mammalian Total RNA Miniprep Kit (Sigma-Aldrich). For all samples, equal amounts of RNA (25 ng of RNA per 1 μl of total reaction content) was reverse transcribed into cDNA using M-MLV (Top-Bio, Prague, Czech Republic) and oligo-dT (Qiagen) priming. PCR was carried out in 50 μl reactions containing 0,5 μM of each primer and 10 μl of diluted cDNA. Following primer sequences were used: Oct3/4, 5′-GCAAAGCAGAAACCCTCGT-3′ (forward) and 5′-ACACTCGGACCACATCCTTC-3′ (reverse); Nucleostemin, 5′-TGCGAAGTCCAGCAA GTATTG-3′ (forward) and 5′-AATGAGGCACCTGT CCACTC-3′ (reverse); GAPDH, 5′-AGCCACATCGC TCAGACACC-3′ (forward) and 5′-GTACTCAGCGC CAGCATCG-3′ (reverse). PCR conditions include a first step of 4 minutes at 94°C, a second step of 30 cycles of 30 seconds at 94°C, 30 seconds annealing step at 60°C, 45 seconds at 72°C and a final step of 5 minutes at 72°C. Final products were examined by gel electrophoresis on 1% agarose.

2.14. Clonogenicity assay in vitro

The cells were trypsinized, single cells were manually transferred with a micropipette under microscope into separate wells of 96-well microtiter plates and were cultivated under standard conditions (see 2.3. for details). A capability of cells to proliferate and to form colonies was examined every two days for two weeks and documented using an Olympus CKX41 inverted microscope in combination with an Olympus SP-350 camera.

2.15. Tumorigenicity assay in vivo

Enzymaticaly dissociated cell suspension of NSTS-11 cells at concentration of 1.5×10^6 cells per 100 µl was injected subcutaneously in three 8-week-old female NOD/SCID mice. The mice were examined every three days for the presence of subcutaneous tumors. After appearance of the tumors, the mice were sacrificed and tumor tissue was collected. Each tumor was dissected into two equal parts: one of them was processed for primary culture (see 2.3.), the second was fixed in 10% buffered formalin for 24 hours, routinely processed for histological examination and embedded in paraffin. Tissue sections of FFPE samples were stained with H-E and examined. Immunohistochemical analysis was performed (see 2.5. and 2.6. for details). Monoclonal mouse anti-human desmin (clone D33, dilution 1 : 100, DAKO), monoclonal mouse anti-human muscle actin (clone HHF35, dilution 1 : 50, DAKO) and polyclonal rabbit anti-human myoglobin (dilution 1 : 500, Novocastra Lab., Newcastle upon Tyne, UK) were employed to confirm myogenic differentiation of xenograft tumors. For desmin IHC, antigen retrieval was performed in a Pascal calibrated pressure chamber (DAKO) by heating the section in modified citrate buffer at pH 6.1. Myoglobin and muscle actin IHC was performed without antigen retrieval. The incubation time for all these primary antibodies was 60 minutes. A peroxidase conjugated polymer detection system was used for desmin, muscle actin and myoglobin detection (EnVision™ + Dual Link, HRP rabbit/mouse, DAKO), 3,3′-diaminobenzidine was used as a chromogen (DAB, DAKO). Detection of nestin and CD133 in xenograft tumors was performed as described above (see 2.5. and 2.6. for details).

3. Results

3.1. CD133 and nestin detection in the rhabdomyosarcoma tumor tissue

The results of nestin and CD133 expression in rhabdomyosarcomas by immunohistochemical (IHC) and immunofluorescence (IF) detection are summarized in Table 2.

Table 2
Immunohistochemical and immunofluorescence analysis of CD133 and nestin expression in rhabdomyosarcomas

Tumor sample	Tumor type	IF CD133	IHC CD133			IF Nestin	IHC Nestin		
			% TC	IR TC	IR EC		% TC	IR TC	IR EC
1	A	+	±	+++	+++	+++	+++	+	+
2	A	+	±	+++	++	+++	++	+	++
3	E	+	±	+	++	+	++	+	+
4	E	+	+	+	++	+	++	++	++
5	E	+	±	++	+++	++	+++	+	±
6	A	+	±	+++	+++	+++	+++	+	+
7a		+	±	++	+++	++	+++	++	±
7b		+	±	++	+++	++	+++	++	++
	A								
7c		+	±	+++	+++	+++	+++	+	+
7d		+	±	++	+++	++	+++	+	+

Notes: Expression of CD133 and nestin was examined on formaline-fixed, paraffin embedded tissue samples of rhabdomyosarcomas using both immunofluorescence (IF) and immunohistochemistry (IHC). Evaluation of IF: + (sporadically positive TC), ++ (dispersedly positive TC) and +++ (abundant positive TC). Evaluation of IHC: % TC, percentage of nestin-positive or CD133-positive tumor cells (±, <2%; +, 2–10%; ++, 11–50%; +++, 51–100%). IR TC, intensity of immunostaining (immunoreactivity) in tumor cells (±, very weak; +, weak; ++, medium; +++, strong). IR EC, intensity of immunostaining (immunoreactivity) in endothelial cells (±, very weak; +, weak; ++, medium; +++, strong). Tumor type: A, rhabdomyosarcoma, alveolar type; E, rhabdomyosarcoma, embryonal type.

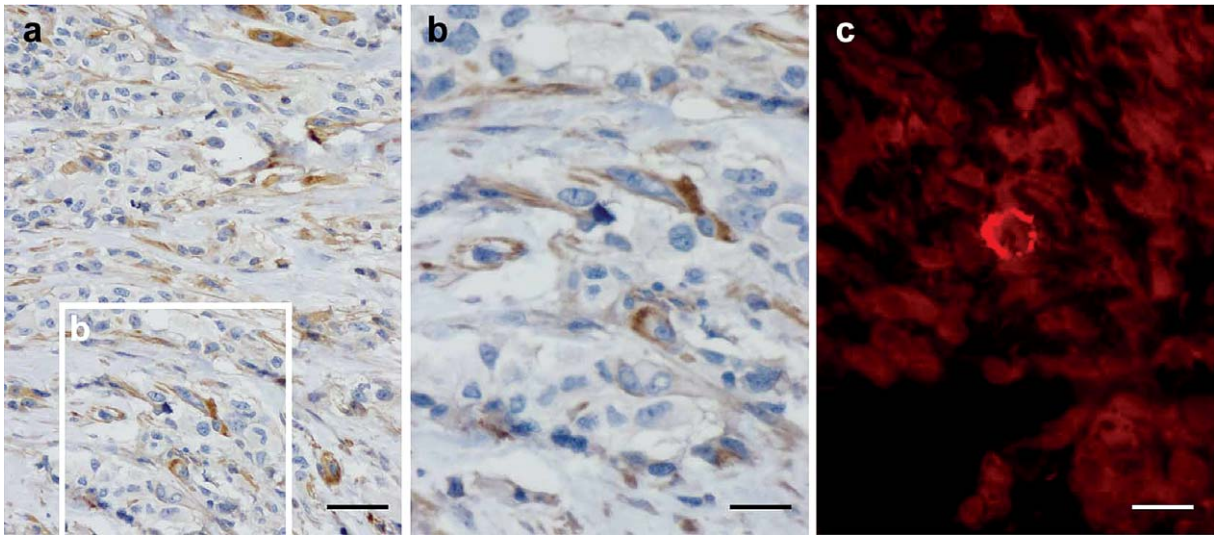

Fig. 1. Immunohistochemical and immunofluorescence analysis of CD133 expression in rhabdomyosarcomas tissues. Both IHC (a, b) and IF (c) revealed membranous CD133 positivity in only small number of tumor cells. Nonspecific cytoplasmic positivity was revealed in a significant proportion of tumor cells (a, b). Immunohistochemistry with Gill's hematoxylin counterstain (a, b); indirect immunofluorescence using TRITC-labeled secondary antibody (c). Bars, 100 μm (a), 50 μm (b), 50 μm (c).

In all examined cases, IF detection of membranous CD133 positivity was revealed in only a few tumor cells dispersed throughout the tumor tissues (Fig. 1c). Both CD133 IHC (Fig. 1b) and IF revealed not only membranous positivity in sporadic tumor cells, but also a nonspecific cytoplasmic positivity in a variable proportion of tumor cells (Fig. 1a).

Nestin expression was identified using both IHC and IF in all examined tumor samples (Fig. 2). The intensity of cytoplasmic IHC staining varied from strong (Fig. 2a) to weak (Fig. 2b). Similarly, the frequency of positive tumor cells revealed both by IHC and IF ranged from a strong, diffuse positivity (Fig. 2a and c) to a sporadic, medium to weak cytoplasmic nestin immunostaining in a subset of tumor cells (Fig. 2b and d).

3.2. *Expression of CD133 and nestin in rhabdomyosarcoma cell lines*

CD133 was observed in the form of a clear, membranous signal in all five newly derived rhabdomyosarcoma cell lines using indirect immunofluorescence (Table 3, Fig. 3). However, the percentage and the intensity of immunostaining (immunoreactivity) of CD133+ cells varied among individual cell lines (Table 3, Fig. 3c and d). The presence of CD133 was subsequently verified using immunoblotting, and a 75-kDa band specific for CD133 was detected in all five cell lines examined (Fig. 4a).

Furthermore, using the NSTS-11 cell line, we experimentally determined that CD133 expression in cell populations seeded at the same concentrations increased over the course of a six-day cultivation (Fig. 5). Using a fluorescence microscope, we observed an increase of CD133+ fluorescence intensity in individual cells (Fig. 5a). The same results were also achieved by immunoblotting (Fig. 5b). Using flow cytometry, approximately a 193 percent increase in CD133 fluorescence intensity (FI) was noted from day 2 to day 6 in the cell populations (Fig. 5c).

Similar to CD133, nestin was observed in all examined cell lines, and both the percentage and the intensity of immunostaining of Nes+ cells varied among individual cell lines (Table 3, Fig. 3). Using immunoblotting, we confirmed that nestin is present in all five cell lines, and the specific bands detected were 300 kDa, 270 kDa and 100 kDa (Fig. 4b). Nevertheless, Nes+ cells only represent minor subpopulations, and the level of immunostaining was lower, compared to CD133+ cells (Table 3). Additionally, all Nes+ cells expressed CD133, but not all CD133+ cells expressed nestin (Fig. 3c and d). In contrast to the changes in CD133 expression mentioned above, expression of

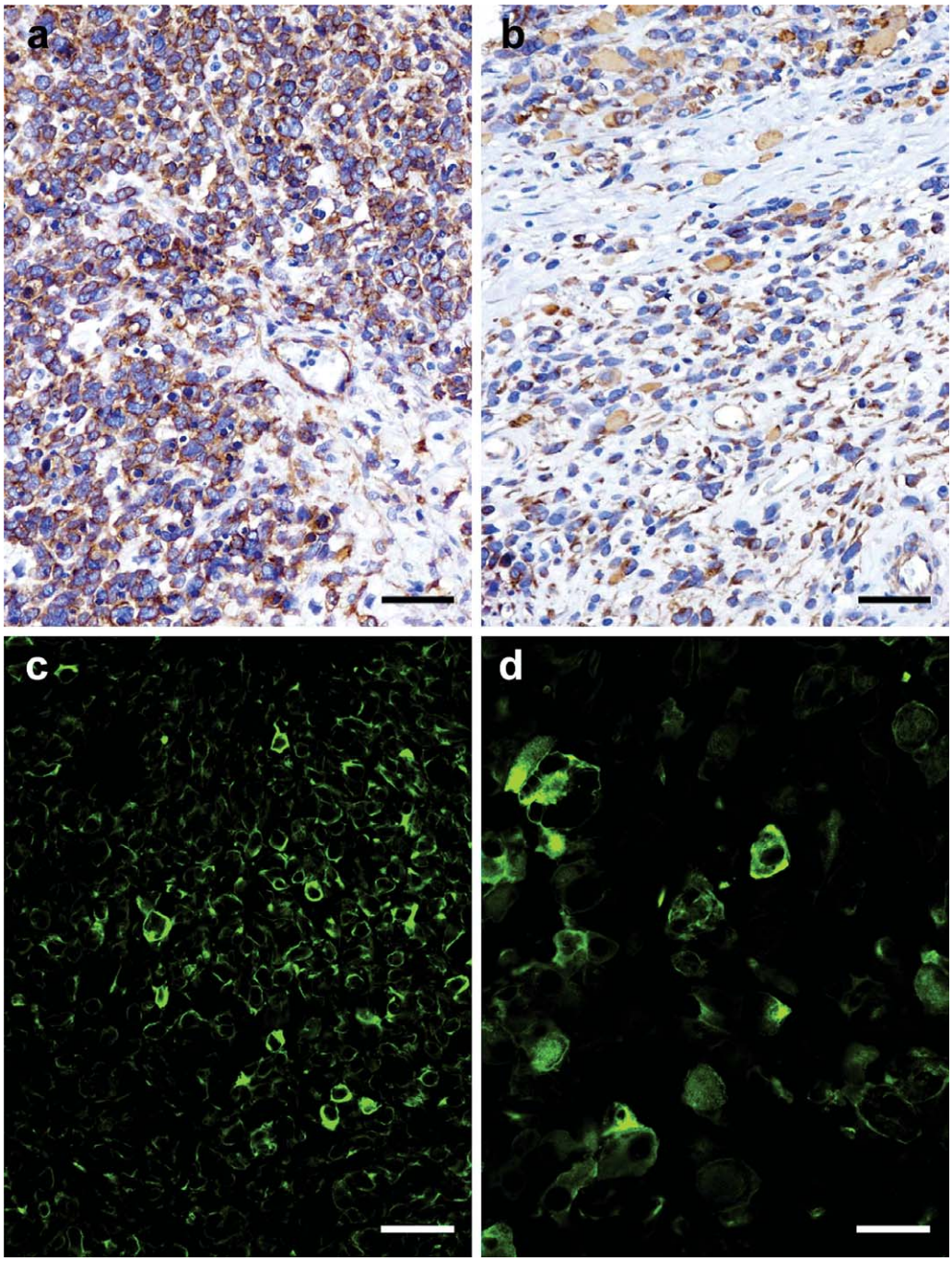

Fig. 2. Immunohistochemical and immunofluorescence analysis of nestin expression in rhabdomyosarcomas tissues. Strong, diffuse cytoplasmic positivity in the majority of tumor cells with an internal positive control of Nes+ endothelial cells; sample 8 (a). Medium cytoplasmic nestin immunostaining in a subset of dispersed tumor cells; sample 7 (b). Nestin expression in a significant proportion of tumor cells; sample 8 (c). Nestin expression in individual tumor cells; sample 4 (d). Immunohistochemistry with Gill's hematoxylin counterstain (a, b); indirect immunofluorescence using FITC-labeled secondary antibody (c, d). Bars, 100 μm (a, b, c), 50 μm (d).

Table 3
Expression of CD133 and nestin in the rhabdomyosarcoma cell lines

Cell line	Tumor type	CD133		Nestin	
		% TC	IR TC	% TC	IR TC
NSTS-08	A	+++	++	+	+
NSTS-09	A	++(+)	+++	+(+)	++
NSTS-10	A	+++	++	+(+)	++
NSTS-11	E	++	++/+++	+(+)	+
NSTS-12	E	+++	++/+++	(+)	+

Notes: Expression of CD133 and nestin in cell lines was examined using indirect immunofluorescence method. % TC, percentage of CD133/nestin positive tumor cells: (+), ∼1%; +, 1–10%; +(+), ∼10%; ++, 10–50%; ++(+), ∼50%; +++, >50%. IR TC, intensity of immunostaining (immunoreactivity) in tumor cells: +, weak; ++, medium; +++, strong. Tumor type: A, rhabdomyosarcoma, alveolar type; E, rhabdomyosarcoma, embryonal type.

nestin in cell populations was not altered during the cultivation.

3.3. Detection of CD133 and nestin in different samples from the same patient

As mentioned in Table 1, four FFPE tissue samples and two derived cell lines were obtained from the same patient suffering from rhabdomyosarcoma during the progression of the disease. This situation gave us the unique opportunity to analyze possible changes in CD133 and nestin expression in tumor tissue of the same patient in relation to the clinical course of the disease and to the applied therapy.

A 21-year-old woman was diagnosed with alveolar rhabdomyosarcoma of the left forearm and regional axillary lymph nodes, IRS stage III (tumor sample No. 7a, NSTS-08 cell line). She was treated according to protocol "EpSSG RMS 2005" very high risk arm with systemic chemotherapy of ifosfamide, vincristine, actinomycin D, and doxorubicin. After three initial courses, the patient was re-evaluated by PET and MRI imaging and determined to have a stable disease response. The tumor was inoperable without mutilating surgery, but amputation was rejected by the patient. Locoregional marginal surgery was performed, and she achieved 1st complete remission (tumor sample No. 7b, NSTS-10 cell line). Despite a second line of chemotherapy with irinotecan and vincristine, radiotherapy and metronomic antiangiogenic therapy, she relapsed in the regional lymph nodes on her shoulder (tumor sample No. 7c); her event-free survival was 13 months. Salvage chemotherapy with topotecan and carboplatin was administered, but again, stable disease was found upon imaging. Following resection (tumor sample No. 7d) and radiotherapy, she achieved a 2nd complete remission. Several months later, she was diagnosed with a 3rd locoregional relapse on her shoulder; her event-free survival was 7 months. After a discussion with the patient, a dendritic cell vaccine against PAX3/FKHR protein was prepared. Meanwhile, concomitant chemotherapy with irinotecan, vincristine, and temodal, and radiotherapy were administered. Amputation was not accepted by the patient, despite a poor prognosis for survival. Unfortunately, the patient was diagnosed with metastatic relapse in the bones and bone marrow nine months later. As an experimental approach, a dendritic cell vaccine was applied together with palliative radiotherapy to a pathologic fracture of the vertebra. Currently, the experimental treatment with vincristine, cyclophosphamide, bevacizumab, sirolimus and valproate was administered. The overall survival of this patient is 39 months, and her prognosis remains very poor; such patients usually survive no more than three years after diagnosis.

Analysis of CD133 and nestin expression in all four tumor samples taken from this patient at various stages of the disease (see above) showed a sporadic occurrence of CD133+ cells with relatively strong immunoreactivity and a high proportion of Nes+ cells with medium to weak immunoreactivity. The frequency both of CD133+ and Nes+ cells did not change significantly during the course of the disease (Table 2).

The cell lines derived from the primary tumor (NSTS-08 cell line) and from the tumor tissue after the first chemotherapy treatment (NSTS-10 cell line) also showed the very same frequency of CD133+ and/or Nes+ cells; and the immunoreactivity for both of these markers was stable in both of these cell lines (Table 3).

3.4. Expression of stem cell markers in rhabdomyosarcoma cell lines

To confirm the presence of cells with stem cell related markers in rhabdomyosarcoma cell lines, we employed RT-PCR for detection of Oct3/4 (POU5F1) and nucleostemin (GNL3) that are considered to be markers of the embryonic stem cells. All five cell lines were identified as positive for both of these markers (Fig. 6); however, their expression partly differed among cell lines: a strong expression of Oct3/4 was

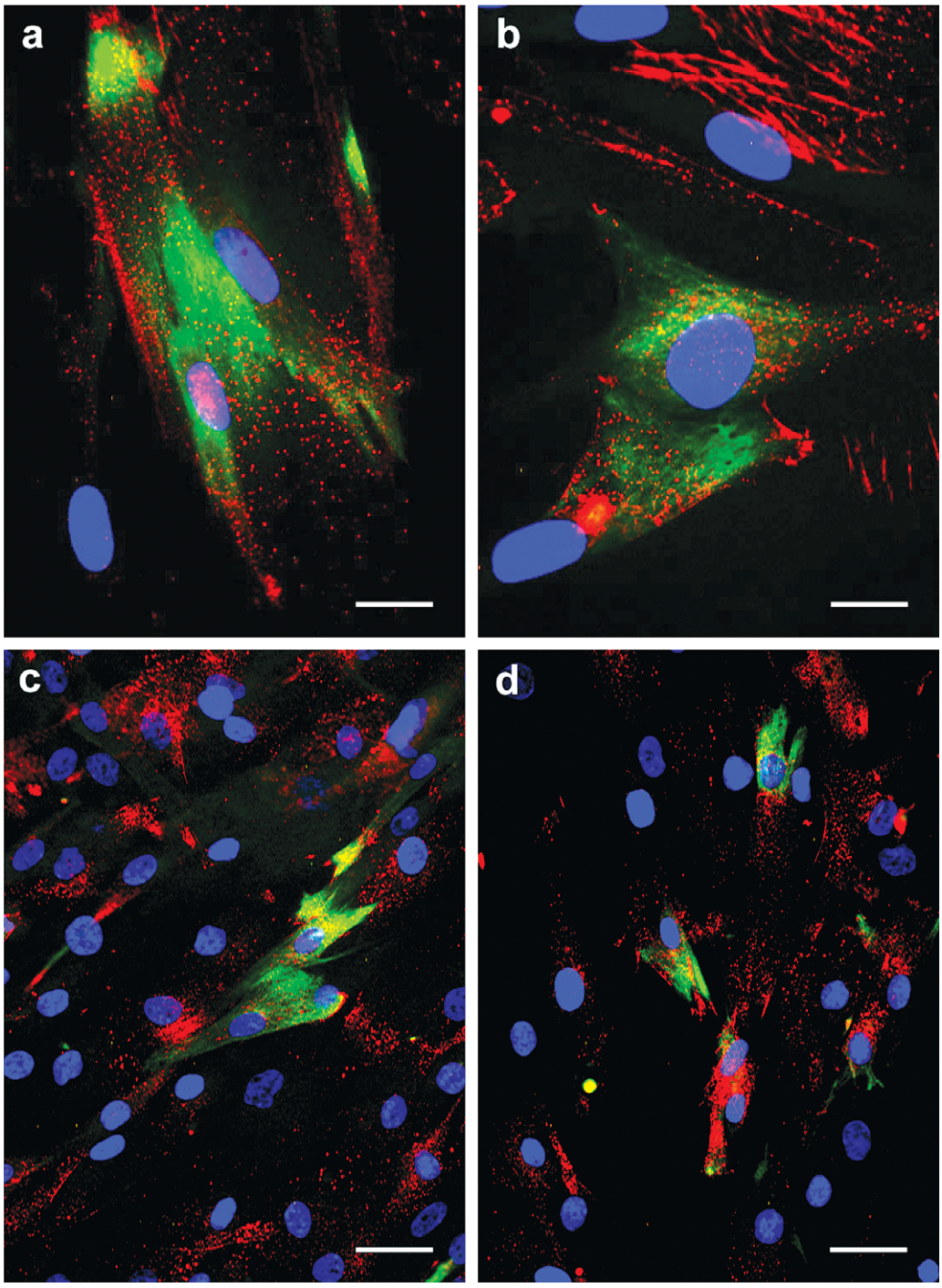

Fig. 3. Expression of CD133 and nestin in rhabdomyosarcoma cell lines. Representative double labeling for CD133 and nestin in NSTS-9 (a, b) and NSTS-8 (c, d) rhabdomyosarcoma cell lines. CD133 showed predominantly membranous positivity, visible as a dotted CD133 signal (red) on the cell surface (a-d). Invaginations of plasma membrane accumulating CD133 signals (red) led to the stripped pattern in a small subset of cells (b). CD133 (red) and nestin (green) stained by indirect immunofluorescence using TRITC-labeled secondary antibody and FITC-labeled secondary antibody, respectively; counterstaining with DAPI. Bars, 25 μm (a, b), 50 μm (c, d).

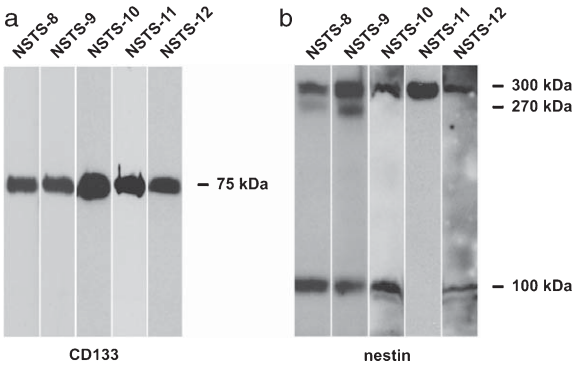

Fig. 4. Immunoblot analysis of the CD133 and nestin expression in rhabdomyosarcoma cell lines. Analysis of the CD133 expression in all five rhabdomyosarcoma cell lines (a). Analysis of the nestin expression in all five rhabdomyosarcoma cell lines (b).

identified in NSTS-8, NSTS-9, and NSTS-12 cell lines, a medium in NSTS-10 and a low expression in NSTS-11, while a medium expression of nucleostemin was detected in all cell lines with exception of NSTS-10 that showed only low level of nucleostemin expression (Fig. 6).

3.5. Functional assays using NSTS-11 cells

To confirm the presence of cells with cancer stem cell phenotype in our cell lines, we performed preliminary functional assays on NSTS-11 cell line. Clonogenicity *in vitro* assay showed that 5 to 10 % of isolated cells were able under standard *in vitro* conditions to form colonies containing more than 50 cells (Fig.7).

Furthermore, the tumorigenicity *in vivo* assay clearly confirmed the ability of NSTS-11 cells to originate xenograft tumors in NOD/SCID mice (Fig. 8). All three mice injected with NSTS-11 cell suspensions developed subcutaneous tumors in the same positions (Fig. 8a-c) within 12 weeks after injection. The diameter of all three tumors was about 10 mm (Fig. 8 d-f). Histological examination of all these xenograft tumors showed neoplastic highly mitotically active proliferation of undifferentiated dominantly spindle-shaped cells admixed with number of round, strap- or tadpole-shaped eosinophilic rhabdomyoblasts in a partially myxoid stroma (Fig. 8g-i). Moreover, the cross-striation of several cells has been displayed in all examined tumor samples. Histopathological findings correlate with the diagnosis of embryonal rhabdomyosarcoma. Myogenic differentiation was additionally proved immunohistochemically in all three xenograft tumors (Table 4).

4. Discussion

The focus of our study was on the detection of CD133 and nestin in rhabdomyosarcoma cells. Ten samples of rhabdomyosarcoma tumor tissue and five cell lines derived from these tumors were examined using immunodetection methods; RT-PCR and functional assays were also employed to analyze the cell lines. Expression of both CD133 and nestin was microscopically determined in all tissue samples and cell lines; in the cell lines, these finding were confirmed by immunoblotting. Cells with distinct membranous positivity for CD133 occurred only sporadically in tumor tissues, although the proportion of Nes+ cells was markedly higher in the same tissues. In contrast, all five rhabdomyosarcoma cell lines showed an increased frequency of CD133+ cells, only some of which were concurrently Nes+. Above all, our research provides the first evidence of CD133 expression in rhabdomyosarcomas.

CD133 glycoprotein is considered to be a marker of the CSC phenotype in many kinds of tumors, usually in combination with other cell surface or intracellular molecules; for example: with nestin in CNS tumors [9, 24, 33, 34, 47], with CD44 in hepatocellular carcinomas [20, 48] and in colon carcinomas [15], with CD44 and $\alpha_1\beta_2^{hi}$ in prostate carcinomas [4], and with ABCG2 in pancreatic adenocarcinomas [25] and in osteosarcomas [10]. Nevertheless, expression of CD133 alone was also reported as a CSC phenotype in colon carcinomas [28], in non-small-cell lung carcinomas [2, 38], in ovarian carcinomas [8] and in endometrial carcinomas [30].

The detection of cells showing membranous positivity for CD133 that were only sporadically dispersed in rhabdomyosarcoma tumor tissues suggests that these cells may act as CSCs/TICs in this tumor type. In cell lines derived from the same tumors, we noted a markedly higher proportion of CD133+ cells; this difference may be explained by clonal selection for this phenotype under *in vitro* conditions. Since our results are the first evidence of CD133 expression in rhabdomyosarcoma cells, we verified these findings by immunoblotting cell lysates from five rhabdomyosarcoma cell lines examined in this study. Immunoblot results undoubtedly showed the CD133 expression;

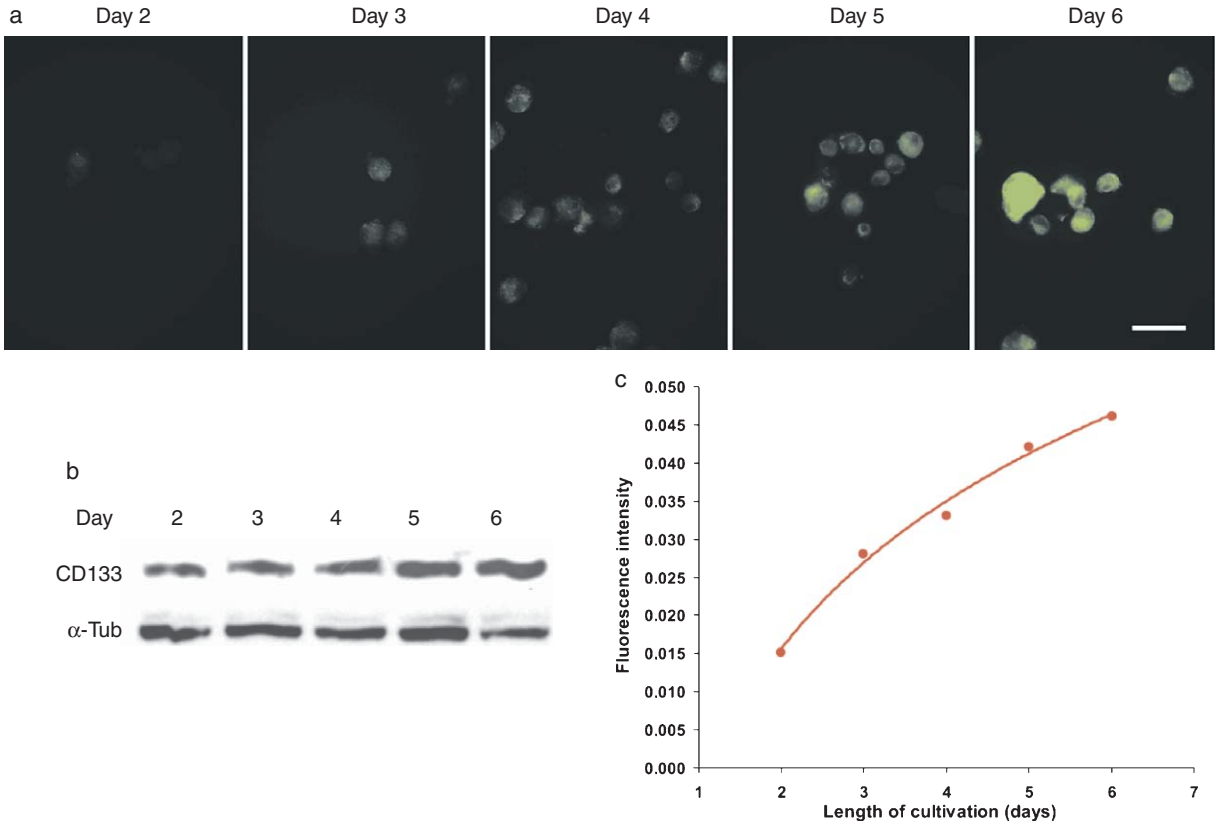

Fig. 5. CD133 expression changes in the rhabdomyosarcoma cell line NSTS-11 during a six-day cultivation. Cell suspensions were stained against CD133 (green) by indirect immunofluorescence using a FITC-labeled secondary antibody and were simultaneously analyzed using a fluorescence microscope; bar 50 μm (a) and by flow-cytometry (c). Fluorescence intensity (FI) is calculated as a quotient of difference; FITC-A *log* $_{CD133}$ median fluorescence intensity (MFI) with FITC-A *log* $_{Iso}$ MFI, and FSC-A where: FITC-A *log* $_{CD133}$ is calculated as the mean ($n = 2$) of medians FITC-A *log* in samples immunostained with rabbit polyclonal anti-CD133 primary antibody, FITC-A *log* $_{Iso}$ is calculated as a mean ($n = 2$) of medians FITC-A *log* in samples immunostained with rabbit polyclonal isotype control, FSC-A is calculated as a mean ($n = 4$) of medians FSC-A above mentioned all samples. FI = (FITC-A *log* $_{CD133}$ – FITC-A *log* $_{Iso}$) / FSC-A. Immunoblot analysis of the CD133 expression changes during a six-day cultivation (b). Alpha-tubulin (α-Tub) served as a loading control.

a specific 75-kDa band was detected in all cell lines, suggesting the presence of a truncated form of CD133 that was described by two independent studies [26, 41].

During the *in vitro* experiments, we also noted increased fluorescence in individual CD133+ cells in relation to a prolonged cultivation time. For this reason, we measured the cell populations seeded at the same concentrations and at the same time. By flow cytometry, we confirmed a substantial increase in fluorescence of the whole cell population during a six-day cultivation; non-specific fluorescence and the average size of individual cells was taken into account in this experiment. In parallel, we used a fluorescence microscope to confirm the increase of CD133 labeling in individual cells. Moreover, these microscopic observations suggest not only membranous, but also cytoplasmic localization of CD133 molecules. These findings are in agreement with another study on osteosarcoma

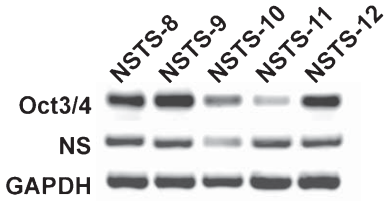

Fig. 6. RT-PCR analysis of stemness markers in rhabdomyosarcoma cell lines. Expression of Oct3/4 and nucleostemin was analyzed in all five of these cell lines; GAPDH served as a control.

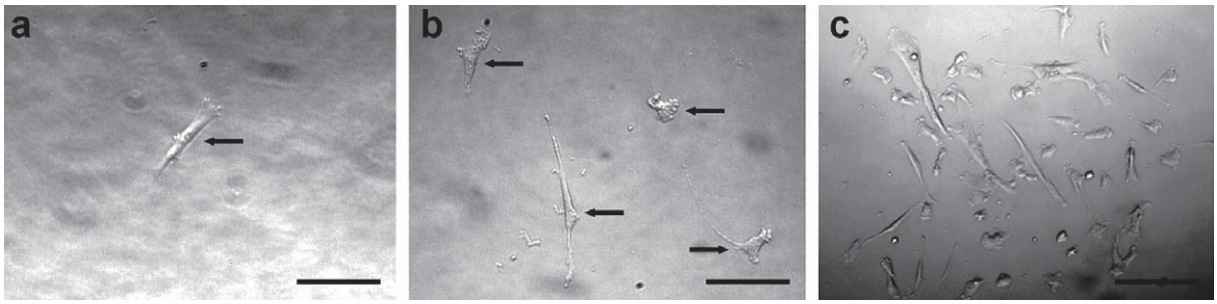

Fig. 7. Clonogenicity assay *in vitro* using NSTS-11 cell line. During two weeks of cultivation, single isolated cells (7a) were able to proliferate (7b) and to form colonies containing more than 50 cells (7c). Bars, 100 μm (a, b), 200 μm (c).

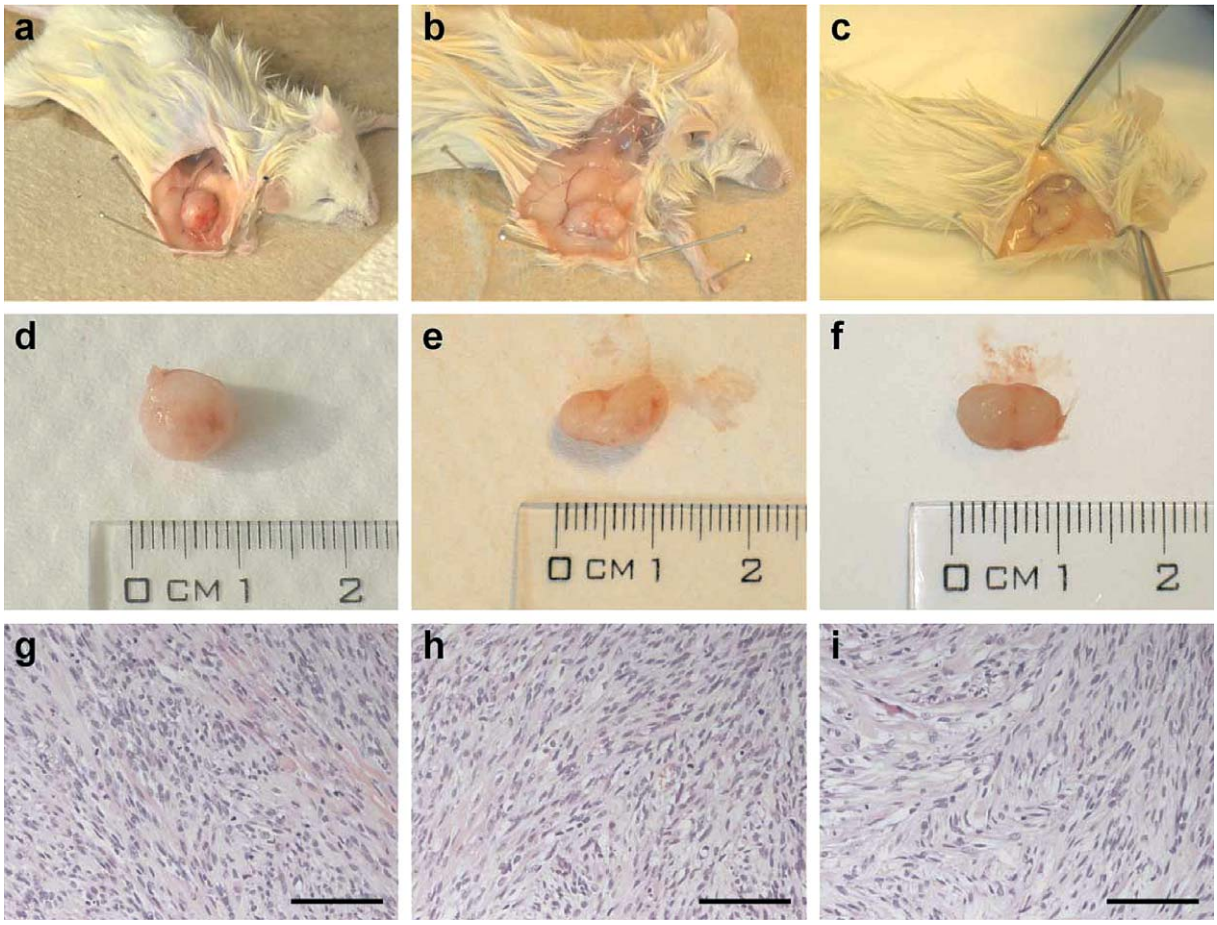

Fig. 8. Tumorigenicity *in vivo* assay using NSTS-11 cell line. Subcutaneous xenograft tumors in NOD/SCID mice at 81–84 days after injection of NSTS-11 cells (8a-c). Size of all three tumors was about 10 mm in diameter (8d-f). Histological examination of these tumors showed a pattern corresponding to the diagnosis of embryonal rhabdomyosarcoma; bars, 200 μm (8g-i).

cells, in which the deposition of CD133 into cytoplasmic vesicles was visualized by confocal microscopy [39].

Based on our previous study of osteosarcoma cell lines, in which the co-expression of CD133 and nestin was described in sarcomas for the first time [42], we

Table 4
Immunohistochemical analysis of NSTS-11 xenograft tumors in mice

Tumor	Myoglobin	Desmin	Muscle actin	Nestin	CD133
M3A138	++	++	++	+++	±
M3B138	+	++	++	+++	±
M3C138	+	++	++	+++	±

Notes: Expression of myogenic differentiation markers (myoglobin, desmin, muscle actin), CD133 and nestin was examined on formalin-fixed, paraffin embedded tissue samples of xenograft tumors using immunohistochemistry (IHC). Evaluation of IHC: percentage of positive tumor cells (±, <2%; +, 2–10%; ++, 11–50%; +++, 51–100%).

also examined the rhabdomyosarcoma samples and derived cell lines for the detection of this intermediate filament protein. Although nestin expression was reported in many tumor types including sarcomas [18], and nestin was originally described in rhabdomyosarcoma cells twelve years ago [17], there is no published work describing a possible co-expression of nestin and CD133 in rhabdomyosarcomas.

Our microscopy results confirmed that nestin is expressed in all our rhabdomyosarcoma samples as well as in all the derived rhabdomyosarcoma cell lines. Immunoblotting was employed to verify nestin expression in the examined cell lines; 300 kDa, 270 kDa and 100 kDa specific bands were detected in all of them. The 300 kDa and 270 kDa bands correspond to post-translationally-modified forms of nestin; the 100 kDa band is probably nestin that has been cleaved by lysate cryoconservation, as reported by the antibody manufacturer.

More interestingly, the expression pattern of nestin was inversely correlated to that of CD133; we detected a relatively high proportion of Nes+ cells in tumor tissues together with a sporadic occurrence of CD133+ cells, whereas CD133+ cells predominated the cell populations of all examined cell lines, including Nes+ cells, under *in vitro* conditions. Furthermore, all Nes+ cells in the cultures showed positivity for CD133 simultaneously; i.e. their phenotype was CD133+/Nes+, while CD133-/Nes+ cells were never been detected in the cell cultures.

Taken together, the sporadic occurrence of CD133+ cells (with distinct membranous positivity) in tumor tissues and a minor proportion of CD133+/Nes+ in cell cultures suggest that these cancer cells with expression of stem cell related markers may represent a CSCs/TICs phenotype in rhabdomyosarcomas. Positivity of all five examined cell lines for Oct3/4 and nucleostemin that are required for maintaining stem cell state [10] is in accordance with this idea. The hypothesis on CSCs/TICs phenotype is also partially supported by CD133 and nestin detection in different tumor samples taken from the same patient at various stages of the disease. The relatively stable frequency of CD133+ cells in tumor samples during cancer progression in this patient may indicate a resistance of these cells to the applied chemotherapy. Similarly, the presence of these cells in sample No.3 that was taken after neoadjuvant chemotherapy also suggests their CSCs/TICs phenotype.

Moreover, results of preliminary functional assays using our rhabdomyosarcoma cell lines also suggest the presence of a CSCs/TICs fraction in these cell lines. Nevertheless, further detailed functional studies of CD133+/Nes+ rhabdomyosarcoma cells are required to confirm their possible CSCs/TICs phenotype.

To summarize, the most important result of our study is the first evidence of CD133 expression in rhabdomyosarcomas and the corresponding rhabdomyosarcoma cell lines. Using immunodetection methods, we confirmed the expression of CD133 and nestin in all examined tumor samples and in all cell lines derived from them. The low incidence of CD133+ cells in tumor tissues and of CD133+/Nes+ cells in cultures as well as results of preliminary functional assays suggest a possible stem-like phenotype of cells showing co-expression of these markers. We also showed increasing expression of CD133 in rhabdomyosarcoma cells and probable accumulation of this glycoprotein in cytoplasmic vesicles during cultivation. Our results represent the first important step toward the forthcoming studies on CSCs/TICs detection in rhabdomyosarcomas.

Acknowledgments

The authors would like to thank Mrs. Hana Rychtecka, Mrs. Marcela Vesela, Mrs. Johana Maresova and Dr. Jan Verner for their skillful technical assistance. We are grateful to Dr. Rudolf Nenutil for providing tumor samples from the files of the Department of Oncological and Experimental Pathology, Masaryk Memorial Cancer Institute (Brno, Czech Republic). We also thank Professor Roman Hajek for providing the flow cytometry facilities and Dr. Ivana Buresova for her assistance in perform-

ing flow cytometry. This study was supported by grants VZ MSM 0021622415, VZ MSM 0021622430, IGA MZCR NR/9125-4 2006, MUNI/A/0091/2009, MUNI/A/1012/2009, MUNI/A/0950/2010 and GACR 204/08/H054.

References

[1] F.G. Barr, J. Chatten, C.M. D'Cruz, A.E. Wilson, L.E. Nauta, L.M. Nycum, J.A. Biegel and R.B. Womer, Molecular assays for chromosomal translocations in the diagnosis of pediatric soft tissue sarcomas, *JAMA* **273** (1995), 553–557.

[2] G. Bertolini, L. Roz, P. Perego, M. Tortoreto, E. Fontanella, L. Gatti, G. Pratesi, A. Fabbri, F. Andriani, S. Tinelli, E. Roz, R. Caserini, S. Lo Vullo, T. Camerini, L. Mariani, D. Delia, E. Calabrò, U. Pastorino and G. Sozzi, Highly tumorigenic lung cancer CD133+ cells display stem-like features and are spared by cisplatin treatment, *Proc Natl Acad Sci USA* **106** (2009), 16281–16286.

[3] S. Bruno, B. Bussolati, C. Grange, F. Collino, M.E. Graziano, U. Ferrando and G. Camussi, CD133+ renal progenitor cells contribute to tumor angiogenesis, *Am J Pathol* **169** (2006), 2223–2235.

[4] A.T. Collins, P.A. Berry, C. Hyde, M.J. Stower and N.J. Maitland, Prospective identification of tumorigenic prostate cancer stem cells, *Cancer Res* **65** (2005), 10946–10951.

[5] D. Corbeil, K. Röper, C.A. Fargeas, A. Joester and W.B. Huttner, Prominin: A story of cholesterol, plasma membrane protrusions and human pathology, *Traffic* **2** (2001), 82–91.

[6] D. Corbeil, K. Röper, A. Hellwig, M. Tavian, S. Miraglia, S.M. Watt, P.J. Simmons, B. Peault, D.W. Buck and W.B. Huttner, The human AC133 hematopoietic stem cell antigen is also expressed in epithelial cells and targeted to plasma membrane protrusions, *J Biol Chem* **275** (2000), 5512–5520.

[7] C.V. Cox, P. Diamanti, R.S. Evely, P.R. Kearns and A. Blair, Expression of CD133 on leukemia-initiating cells in childhood ALL, *Blood* **113** (2009), 3287–3296.

[8] M.D. Curley, V.A. Therrien, C.L. Cummings, P.A. Sergent, C.R. Koulouris, A.M. Friel, D.J. Roberts, M.V. Seiden, D.T. Scadden, B.R. Rueda and R. Foster, CD133 expression defines a tumor initiating cell population in primary human ovarian cancer, *Stem Cells* **27** (2009), 2875–2883.

[9] P. Dell'Albani, Stem cell markers in gliomas, *Neurochem Res* **33** (2008), 2407–2415.

[10] R. Di Fiore, A. Santulli, R.D. Ferrante, M. Giuliano, A. De Blasio, C. Messina, G. Pirozzi, V. Tirino, G. Tesoriere and R. Vento, Identification and expansion of human osteosarcoma-cancer-stem cells by long-term 3-aminobenzamide treatment, *J Cell Physiol* **219** (2009), 301–313.

[11] A. Eramo, F. Lotti, G. Sette, E. Pilozzi, M. Biffoni, A. Di Virgilio, C. Conticello, L. Ruco, C. Peschle and R. De Maria, Identification and expansion of the tumorigenic lung cancer stem cell population, *Cell Death Differ* **15** (2008), 504–514.

[12] C.A. Fargeas, W.B. Huttner and D. Corbeil, Nomenclature of prominin-1 (CD133) splice variants - an update, *Tissue Antigens* **69** (2007), 602–606.

[13] C.A. Fargeas, A. Joester, E. Missol-Kolka, A. Hellwig, W.B. Huttner and D. Corbeil, Identification of novel Prominin-1/CD133 splice variants with alternative C-termini and their expression in epididymis and testis, *J Cell Sci* **117** (2004), 4301–4311.

[14] G. Ferrandina, G. Bonanno, L. Pierelli, A. Perillo, A. Procoli, A. Mariotti, M. Corallo, E. Martinelli, S. Rutella, A. Paglia, G. Zannoni, S. Mancuso and G. Scambia, Expression of CD133-1 and CD133-2 in ovarian cancer, *Int J Gynecol Cancer* **18** (2008), 506–514.

[15] N. Haraguchi, M. Ohkuma, H. Sakashita, S. Matsuzaki, F. Tanaka, K. Mimori, Y. Kamohara, H. Inoue and M. Mori, CD133+ CD44+ population efficiently enriches colon cancer initiating cells, *Ann Surg Oncol* **15** (2008), 2927–2933.

[16] H. Immervoll, D. Hoem, P.O. Sakariassen, O.J. Steffensen and A. Molven, Expression of the "stem cell marker" CD133 in pancreas and pancreatic ductal adenocarcinomas, *BMC Cancer* **8** (2008), 48.

[17] M. Kobayashi, G. Sjöberg, S. Söderhäll, U. Lendahl, B. Sandstedt and T. Sejersen, Pediatric rhabdomyosarcomas express the intermediate filament nestin, *Pediatr Res* **43** (1998), 386–392.

[18] O. Krupkova, T. Loja, I. Zambo and R. Veselska, Nestin expression in human tumors and tumor cell lines, *Neoplasma* **57** (2010), 291–298.

[19] G. Liu, X. Yuan, Z. Zeng, P. Tunici, H. Ng, I.R. Abdulkadir, L. Lu, D. Irvin, K.L. Black and J.S. Yu, Analysis of gene expression and chemoresistance of CD133+ cancer stem cells in glioblastoma, *Mol Cancer* **5** (2006), 67.

[20] S. Ma, K.W. Chan, L. Hu, T.K. Lee, J.Y. Wo, I.O. Ng, B.J. Zheng and X.Y. Guan, Identification and characterization of tumorigenic liver cancer stem/progenitor cells, *Gastroenterology* **132** (2007), 2542–2556.

[21] S. Miraglia, W. Godfrey, A.H. Yin, K. Atkins, R. Warnke, J.T. Holden, R.A. Bray, E.K. Waller and D.W. Buck, A novel five-transmembrane hematopoietic stem cell antigen: Isolation, characterization, and molecular cloning, *Blood* **90** (1997), 5013–5021.

[22] E. Monzani, F. Facchetti, E. Galmozzi, E. Corsini, A. Benetti, C. Cavazzin, A. Gritti, A. Piccinini, D. Porro, M. Santinami, G. Invernici, E. Parati, G. Alessandri and C.A. La Porta, Melanoma contains CD133 and ABCG2 positive cells with enhanced tumourigenic potential, *Eur J Cancer* **43** (2007), 935–936.

[23] Y.R. Na, S.H. Seok, D.J. Kim, J.H. Han, T.H. Kim, H. Jung and J.H. Park, Zebrafish embryo extracts promote sphere-forming abilities of human melanoma cell line, *Cancer Sci* **100** (2009), 1429–1433.

[24] J. Neuzil, M. Stantic, R. Zobalova, J. Chladova, X. Wang, L. Prochazka, L. Dong, L. Andera and S.J. Ralph, Tumour-initiating cells vs. cancer 'stem' cells and CD133: What's in the name? *Biochem Biophys Res Commun* **355** (2007), 855–859.

[25] M. Olempska, P.A. Eisenach, O. Ammerpohl, H. Ungefroren, F. Fendrich and H. Kalthoff, Detection of tumor stem cell markers in pancreatic carcinoma cell lines, *Hepatobiliary Pancreat Dis Int* **6** (2007), 92–97.

[26] T.L. Osmond, K.W. Broadley and M.J. McConnell, Glioblastoma cells negative for the anti-CD133 antibody AC133 express a truncated variant of the CD133 protein, *Int J Mol Med* **25** (2010), 883–888.

[27] G.J. Pilkington, Cancer stem cells in the mammalian central nervous system, *Cell Prolif* **38** (2005), 423–433.

[28] L. Ricci-Vitiani, D.G. Lombardi, E. Pilozzi, M. Biffoni, M. Todaro, C. Peschle and R. De Maria, Identification and expansion of human colon cancer-initiating cells, *Nature* **445** (2007), 111–115.

[29] G.D. Richardson, C.N. Robson, S.H. Lang, D.E. Neal, N.J. Maitland and A.T. Collins, CD133 a novel marker for human prostatic epithelial stem cells, *J Cell Sci* **117** (2004), 3539–3545.

[30] S. Rutella, G. Bonanno, A. Procoli, A. Mariotti, M. Corallo, M.G. Prisco, A. Eramo, C. Napoletano, D. Gallo, A. Perillo, M. Nuti, L. Pierelli, U. Testa, G. Scambia and G. Ferrandina, Cells with characteristics of cancer stem/progenitor cells express the CD133 antigen in human endometrial tumors, *Clin Cancer Res* **15** (2009), 4299–4311.

[31] C. Sagrinati, G.S. Netti, B. Mazzinghi, E. Lazzeri, F. Liotta, F. Frosali, E. Ronconi, C. Meini, M. Gacci, R. Squecco, M. Carini, L. Gesualdo, F. Francini, E. Maggi, F. Annunziato, L. Lasagni, M. Serio, S. Romagnani and P. Romagnani, Isolation and characterization of multipotent progenitor cells from the Bowman's capsule of adult human kidneys, *J Am Soc Nephrol* **17** (2006), 2443–2456.

[32] S.V. Shmelkov, R. St Clair, D. Lyden and S. Rafii, AC133/CD133/Prominin-1, *Int J Biochem Cell Biol* **37** (2005), 715–719.

[33] S.K. Singh, I.D. Clarke, M. Terasaki, V.E. Bonn, C. Hawkins, J. Squire and P.B. Dirks, Identification of a cancer stem cell in human brain tumors, *Cancer Res* **63** (2003), 5821–5828.

[34] S.K. Singh, C. Hawkins, I.D. Clarke, J.A. Squire, J. Bayani, T. Hide, R.M. Henkelman, M.D. Cusimano and P.B. Dirks, Identification of human brain tumour initiating cells, *Nature* **432** (2004), 396–401.

[35] A. Suetsugu, M. Nagaki, H. Aoki, T. Motohashi, T. Kunisada and H. Moriwaki, Characterization of CD133+ hepatocellular carcinoma cells as cancer stem/progenitor cells, *Biochem Biophys Res Commun* **351** (2006), 820–824.

[36] J. Terry and T. Nielsen, Expression of CD133 in synovial sarcoma, *Appl Immunohistochem Mol Morphol* **18** (2010), 159–165.

[37] B. Thomson, D. Hawkins, J. Felgenhauer and J.P. Radich, RT-PCR evaluation of peripheral blood, bone marrow and peripheral blood stem cells in children and adolescents undergoing VACIME chemotherapy for Ewing's sarcoma and alveolar rhabdomyosarcoma, *Bone Marrow Transplant* **24** (1999), 527–533.

[38] V. Tirino, R. Camerlingo, R. Franco, D. Malanga, A. La Rocca, G. Viglietto, G. Rocco and G. Pirozzi, The role of CD133 in the identification and characterisation of tumour-initiating cells in non-small-cell lung cancer, *Eur J Cardiothorac Surg* **36** (2009), 446–453.

[39] V. Tirino, V. Desiderio, R. d'Aquino, F. De Francesco, G. Pirozzi, A. Graziano, U. Galderisi, C. Cavaliere, A. De Rosa, G. Papaccio and A. Giordano, Detection and characterization of CD133+ cancer stem cells in human solid tumours, *PLoS One* **3** (2008), e3469.

[40] N. Uchida, D.W. Buck, D. He, M.J. Reitsma, M. Masek, T.V. Phan, A.S. Tsukamoto, F.H. Gage and I.L. Weissman, Direct isolation of human central nervous system stem cells, *Proc Natl Acad Sci USA* **97** (2000), 14720–14725.

[41] D.J. Vander Griend, W.L. Karthaus, S. Dalrymple, A. Meeker, A.M. DeMarzo and J.T. Isaacs, The role of CD133 in normal human prostate stem cells and malignant cancer-initiating cells, *Cancer Res* **68** (2008), 9703–9711.

[42] R. Veselska, M. Hermanova, T. Loja, P. Chlapek, I. Zambo, K. Vesely, K. Zitterbart and J. Sterba, Nestin expression in osteosarcomas and derivation of nestin/CD133 positive osteosarcoma cell lines, *BMC Cancer* **8** (2008), 300.

[43] R. Veselska, P. Kuglik, P. Cejpek, H. Svachova, J. Neradil, T. Loja and J. Relichova, Nestin expression in the cell lines derived from glioblastoma multiforme, *BMC Cancer* **6** (2006), 32.

[44] A. Weigmann, D. Corbeil, A. Hellwig and W.B. Huttner, Prominin, a novel microvillispecific polytopic membrane protein of the apical surface of epithelial cells, is targeted to plasmalemmal protrusions of non-epithelial cells, *Proc Natl Acad Sci USA* **94** (1997), 12425–12430.

[45] L. Yi, Z.H. Zhou, Y.F. Ping, J.H. Chen, X.H. Yao, H. Feng, J.Y. Lu, J.M. Wang and X.W. Bian, Isolation and characterization of stem cell-like precursor cells from primary human anaplastic oligoastrocytoma, *Mod Pathol* **20** (2007), 1061–1068.

[46] A.H. Yin, S. Miraglia, E.D. Zanjani, G. Almeida-Porada, M. Ogawa, A.G. Leary, J. Olweus, J. Kearney and D.W. Buck, AC133, a novel marker for human hematopoietic stem and progenitor cells, *Blood* **90** (1997), 5002–5012.

[47] M. Zhang, T. Song, L. Yang, R. Chen, L. Wu, Z. Yang and J. Fang, Nestin and CD133: Valuable stem cell-specific markers for determining clinical outcome of glioma patients, *J Exp Clin Cancer Res* **27** (2008), 85.

[48] Z. Zhu, X. Hao, M. Yan, M. Yao, C. Ge, J. Gu and J. Li, Cancer stem/progenitor cells are highly enriched in CD133+ CD44+ population in hepatocellular carcinoma, *Int J Cancer* **126** (2010), 2067–2078.

Tumor Biol. (2011) 32:631–639
DOI 10.1007/s13277-011-0162-9

RESEARCH ARTICLE

Analysis of nuclear nestin localization in cell lines derived from neurogenic tumors

Olga Krupkova Jr · Tomas Loja · Martina Redova · Jakub Neradil · Karel Zitterbart · Jaroslav Sterba · Renata Veselska

Received: 2 December 2010 / Accepted: 2 February 2011 / Published online: 22 February 2011

Abstract Nestin is a class VI intermediate filament protein expressed in the cytoplasm of stem and progenitor cells in the mammalian CNS during development. In adults, nestin is present only in a small subset of cells and tissues, including the subventricular zone of the adult mammalian brain, where neurogenesis occurs. Nestin expression has also been detected under such pathological conditions as ischemia, inflammation, and brain injury, as well as in various types of human solid tumors and their corresponding cell lines. Furthermore, nestin was recently found in the nuclei of glioblastoma, neuroblastoma, and angiosarcoma cells and it was proved to interact directly with the nuclear DNA in neuroblastoma cells. Here, we perform the first study of the intracellular distribution of nestin in cell lines derived from neurogenic tumors. Using immunodetection methods, we examined nestin expression in tumor-derived cell lines obtained from 11 patients with neuroblastoma, medulloblastoma, or glioblastoma multiforme. Besides its standard cytoplasmic localization, nestin was present in the nuclei of two neuroblastoma cell lines and one medulloblastoma cell line. Nestin was only present in the nuclei of cells with diffuse cytoplasmic staining for this protein, and the proportion of cells positive for nestin in nuclei, as well as the intensity of staining, varied. The presence of nestin in the nuclei was confirmed by both transmission electron microscopy and Western blotting. Our results indicate that the presence of nestin in the nuclei of tumor cells is not very rare, especially under in vitro conditions.

Keywords Nestin · Intermediate filaments · Cytoskeleton · Glioblastoma multiforme · Neuroblastoma · Medulloblastoma

O. Krupkova Jr · T. Loja · M. Redova · J. Neradil · R. Veselska (✉)
Laboratory of Tumor Biology and Genetics,
Department of Experimental Biology,
Faculty of Science, Masaryk University,
Kotlarska 2,
61137 Brno, Czech Republic
e-mail: veselska@sci.muni.cz

J. Neradil · K. Zitterbart · J. Sterba · R. Veselska
Department of Pediatric Oncology,
Masaryk University and University Hospital Brno,
Cernopolni 9,
61300 Brno, Czech Republic

Introduction

Nestin is a 220–250-kDa protein belonging to class VI of intermediate filaments (IF) commonly expressed in neural stem and progenitor cells within the developing nervous system. During mammalian embryogenesis, nestin is gradually replaced by other IF proteins specific to differentiated cells, such as neurofilaments in neurons and glial fibrillary acidic protein (GFAP) in glial cells [1, 2]. In adult mammals, nestin expression usually indicates a stem or progenitor cell phenotype [3] or a pathological condition. For example, nestin is expressed in nervous tissue after brain damage [3, 4], in post-infarcted myocardium [5], and in many tumor types of various histogenetic origins (see review of Krupkova et al.) [6]. Nestin is also considered to be a cancer stem cell marker in tumors arising from neuroectodermal tissue and is widely used in stem cell and cancer research. A correlation between poor prognosis and the number of nestin-positive cells within tumor tissue has been measured in both astrocytomas [7] and melanomas [8]. In summary, whether in normal or abnormal tissue, nestin expression indicates an undifferentiated state, primitiveness, plasticity, and an increased proliferative potential [3].

At the intracellular level, nestin is detectable as a filamentous network or a diffuse signal in the cytoplasm. Detailed studies of nestin network morphology have indicated asymmetric fibrillar accumulation near the nucleus [9, 10] and depolymerization of nestin-positive filaments during mitosis [10, 11]. Surprisingly, nestin has also been found in the nuclei of glioblastoma multiforme [10, 12], neuroblastoma [13], and angiosarcoma [14] cells. Thomas et al. showed that nestin particularly arises in the nuclei of neuroblastoma cells with *MYCN* amplification, where it interacts directly with the nuclear DNA, suggesting that nestin may be involved in the regulation of gene expression [13]. Nestin is also present in the nuclei of cells in the mouse vomeronasal organ during prenatal development, implying that nestin may play a role in cell maturation as well [15].

Our study focused on the intracellular localization of nestin in 11 cell lines derived from three types of neurogenic tumors: glioblastoma multiforme, medulloblastoma, and neuroblastoma. We found nuclear localization of nestin in three of these cell lines during short-term cultivation and analyzed two of these cell lines in detail.

Materials and methods

Cell lines

Tumor cell lines were derived from biopsy samples collected from patients at the University Hospital Brno, Czech Republic, with their informed consent. This project was approved by the Ethics Committee of the Masaryk University, Brno, Czech Republic. Tumors were histologically characterized according to WHO classification, and primary cultures were established as described previously [10]. Five cell lines derived from glioblastoma multiforme (GM12, GM14, GM20, GM27, GM28), one cell line derived from medulloblastoma (MBL-03), and five cell lines derived from neuroblastoma (NBL-06, NBL-17, NBL-19, NBL-22, NBL-23) were used in this study. All these cell lines were stabilized; i.e., all of them were cultivated for more than six passages, mostly up to passage 20. They were also successfully frozen and thawed at different passages. Histogenetic origin of these cell lines was verified previously by immunofluorescence detection of marker proteins (GFAP, NF160, vimentin, synaptophysin, NSE, S-100, desmin) [16]. Three established cell lines were used as controls: the DAOY medulloblastoma cell line (ATCC HTB-186^{TM}) and the SH-SY5Y neuroblastoma cell line (ECACC 94030304), both with cytoplasmic localization of nestin, and the GM7 glioblastoma cell line with nuclear localization of nestin [12].

Cell culture

Tumor-derived cell lines were maintained in DMEM (PAA Laboratories, Linz, Austria) supplemented with 20% fetal calf serum (FCS; PAA), 2 mM glutamine, 100 IU/ml penicillin (PAA), and 100 μg/ml streptomycin (PAA). The cells were maintained under standard conditions (37°C, atmosphere of 95% air : 5% CO_2) and subcultured one to two times per week. All cell lines were successfully cryopreserved at different passages. The DAOY and SH-SY5Y control cell lines were maintained in DMEM supplemented with 10% FCS, 2 mM glutamine and 2 mM non-essential amino acids (PAA), 100 IU/ml penicillin, and 100 μg/ml streptomycin. Meanwhile, the GM7 control cell line was maintained in DMEM supplemented with 20% FCS, 2 mM glutamine, 100 IU/ml penicillin, and 100 μg/ml streptomycin.

Immunofluorescence

Indirect immunofluorescence was used to visualize cytoskeletal proteins. Cells were cultivated on coverslips in Petri dishes for 1–3 days, according to the cell proliferation rate. The cells were then rinsed with phosphate-buffered saline (PBS), fixed with 3% para-formaldehyde (Sigma Chemical Co., St. Louis, MO, USA) for 20 min at room temperature, and permeabilized in 0.2% Triton X-100 (ICN Biomedicals, Eschwege, Germany) for 1 min. After washing again with PBS, nonspecific binding was blocked by applying 2% bovine serum albumin (BSA; PAA) for 10 min. The cells were then incubated with primary antibody (mouse anti-nestin, cat. n. MAB5326, dilution 1:100; Millipore, Billerica, MA, USA) at 37°C for 60 min, followed by a PBS wash. Next, cells were incubated with FITC-conjugated secondary antibody (anti-mouse IgG FITC, cat. n. F-8521, dilution 1:120; Sigma) at 37°C for 45 min. After rinsing with PBS, coverslips were mounted using Vectashield mounting medium with DAPI (Vector Laboratories, Burlingame, CA, USA). An Olympus BX-61 fluorescence microscope was used for cell evaluation and micrographs were collected using a Vosskühler 1300D CCD camera and analyzed using a Lucia 1.5.9 imaging system (Laboratory Imaging, Prague, Czech Republic). The percentage and intensity of immunostaining (immunoreactivity) of nestin-positive cells were evaluated at discrete areas of each sample. The samples were prepared at least in duplicate from several various passages (from passage 6 to 18) of all examined cell lines. The average percentage of positive cells and the intensity of immunostaining were determined for entire samples of individual cell lines. The intensity of immunostaining (immunoreactivity) was categorized into five levels: −, none; ±, very weak; +, weak; ++, medium; +++, strong. Cells incubated (a) without primary

antibody or (b) with primary monoclonal antibody against α-tubulin (mouse anti-α-tubulin, cat. n. 11–250, dilution 1:200; Exbio, Prague, Czech Republic) were used as controls in all experiments.

Western blot analysis

For total protein analysis, cells were washed with PBS and incubated in lysis buffer containing 50 mM Tris-HCl pH 7.5, 150 mM NaCl, 50 mM NaF, 1 mM EDTA, 10% glycerol (all Sigma), 1% Triton X-100, and protease inhibitors (Roche, Basel, Switzerland) on ice for 5 min. The lysate was then centrifuged at 14,000 RPM for 9 min at 4°C. To obtain nuclear and cytoplasmic fractions, a Nuclear Protein Extraction Kit (Pierce, Rockford, IL, USA) was used according to the manufacturer's instructions. Twenty micrograms of protein extract was loaded onto a 7% SDS-polyacrylamide gel and separated by electrophoresis. Next, proteins were transferred to PVDF membranes (BioRad Laboratories, Hercules, CA, USA), blocked in 5% non-fat milk for 60 min at room temperature, and incubated with primary anti-nestin (cat. n. MAB5326, Millipore) and anti-α-tubulin (cat. n. 11–250, Exbio) monoclonal antibodies diluted 1:1,000 overnight at 4°C; these antibodies were the same as in immunofluorescence experiments. After washing with PBS-T containing 0.5% Tween 20, the membranes were incubated with horseradish peroxidase (HRP)-conjugated secondary antibody (anti-mouse IgG HRP, cat. n. A-9917, dilution 1:5,000; Sigma) for 60 min at room temperature. Signal detection was performed using the ECL Plus chemiluminiscence detection system (Amersham Biosciences, Little Chalfont, UK) according to the manufacturer's instructions.

Transmission electron microscopy

For immunodetection of nestin in ultrathin sections, cells grown on coverslips were washed with PBS and fixed in 2% para-formaldehyde in PBS for 60 min at room temperature. After a PBS rinse and dehydration, the cells were embedded in LR White medium (Polysciences Inc., London, UK). Labeling of the ultrathin sections was performed on grids. Nestin was detected using a monoclonal anti-nestin antibody (cat. n. MAB5326, Millipore) diluted 1:20 and a gold particle-conjugated secondary antibody (anti-mouse IgG Gold, cat. n. G-7652, dilution 1:40; Sigma). After immunodetection, the specimens were contrasted with 2.5% uranyl acetate (Lachema-Pliva, Brno, Czech Republic) for 20 min and with Reynolds' solution (Sigma) for 8 min at room temperature. The specimens were then observed using a Morgagni 268 (D) transmission electron microscope (FEI Company, Hillsboro, OR, USA). Images were captured by a MegaView III CCD camera (Soft Imaging System) and analyzed using AnalySIS software (Soft Imaging System). Ultrathin sections incubated (a) without primary antibody or (b) with primary monoclonal antibody against α-tubulin (cat. n. 11–250, Exbio) were used as controls. Both primary antibodies were the same as in immunofluorescence and Western blot experiments.

Results

Immunofluorescence staining was used to detect nestin in the cytoplasm and nucleus of all cell lines. Analysis of nestin expression in the cytoplasm consisted of detecting the signal type (nestin-positive fibers or diffuse signal), evaluating the signal intensity reached at the control protein tubulin, and counting the number of nestin-positive cells. The presence of nestin in whole cell lysates was confirmed by Western blotting for all cell lines (data not shown). Cell lines with nestin-positive nuclei were further analyzed by nuclear/cytoplasmic fractionation followed by Western blotting, as well as transmission electron microscopy.

Intracellular localization of nestin in tumor-derived cell lines

Using indirect immunofluorescence, nestin expression was verified in all cell lines included in this study and this expression was identified as cell-density independent. However, variability in the signal type, the signal intensity, and the frequency of nestin-positive cells was observed among cell lines (Table 1).

All five newly derived glioblastoma cell lines showed strong cytoplasmic positivity for nestin, with a frequency of nestin-positive cells from 60% to 80% (Fig. 1a, b). Meanwhile, we did not identify any new glioblastoma cell lines positive for nestin in their nuclei. The nuclei of the control GM7 cell line were positive for nestin, as described previously [12].

In the MBL-03 medulloblastoma cell line, nestin was detected in the form of fibers in 40–50% of cells, and these nestin-positive filaments were stained at a high intensity (Fig. 1c, d). Nestin was also present in the nuclei of MBL-03 cells during short-term cultivation, between the second and sixth passage (Fig. 2a, b). However, nestin-positive staining in the nuclei disappeared during long-term cultivation, with nestin only present in the cytoplasm. Finally, in the DAOY control cell line, nestin was detected only in 10% of cells expressing nestin in the cytoplasm.

All five newly derived neuroblastoma cell lines showed a widely variable nestin expression pattern. In the NBL-17 and NBL-23 cell lines, nestin was present exclusively in filaments at a very high (NBL-17 cells) or high (NBL-23 cells) staining intensity. In NBL-22 cells, both nestin-

Table 1 Intracellular localization of nestin in neurogenic tumor cell lines. Nestin expression and localization was detected by indirect immunofluorescence

Cell line	Gender	Age	Nestin in cytoplasm				Nestin in cell nucleus		
			Pattern	IR	% Nes+	WB	IR	% Nes+	WB
Glioblastoma multiforme									
GM7[a]	M	65	Fib/Dif	+	50%	+	±	<10%	+
GM12	M	50	Fib	+++	80%	+	−	−	−
GM14	F	56	Fib	+	60%	+	−	−	−
GM20	F	65	Fib	+++	80%	+	−	−	−
GM27	F	52	Fib	++	80%	+	−	−	−
GM28	F	65	Fib	+++	80%	NA	−	−	−
Medulloblastoma									
DAOY[a]	M	4	Fib	++	10%	+	−	−	−
MBL-03	M	7	Fib/Dif	+++	50%	+	±	50%	NA
Neuroblastoma									
SH-SY5Y[a]	F	4	Fib	+++	80%	+	−	−	−
NBL-06	F	1.5 m	Fib/Dif	+	40%	+	±	<10%	+
NBL-17	M	8	Fib	+++	20%	+	−	−	−
NBL-19	F	4	Fib/Dif	±	20%	+	±	<10%	+
NBL-22	F	11 m	Fib/Dif	±	20%	+	−	−	−
NBL-23	M	6 m	Fib	++	40%	+	−	−	−

M male, *F*, female; age at the time of diagnosis: years or months (m). Pattern of the nestin signal in cytoplasm: *Fib* fibers, *Dif* diffuse, *IR* intensity of immunofluorescence (immunoreactivity) in nestin-positive cells (−, none; ±, very weak; +, weak; ++, medium; +++, strong); *% Nes+* percentage of nestin-positive cells in regard to the intracellular localization of nestin; *WB:* + nestin expression in cytoplasm and/or cell nucleus was confirmed by Western blotting; *NA* data not available

[a] Established cell lines used as a control

positive fibers and a diffuse cytoplasmic signal were observed, but the intensity of the fluorescence signal was moderate, and nestin was detected in only 20–40% of cells (Fig. 1e, f). Interestingly, nestin was also found in the nuclei of two neuroblastoma cell lines, NBL-06 (Fig. 2c, d) and NBL-19 (Fig. 2e, f). We noted that nestin was only present in the nuclei of cells presenting a diffuse signal for nestin in the cytoplasm. In contrast, cells with nestin-positive filaments did not demonstrate nestin localization to the nucleus.

Analysis of nuclear staining for nestin in select neuroblastoma cell lines

In two newly-derived neuroblastoma cell lines exhibiting nestin in the nucleus (NBL-06 and NBL-19), we performed a detailed analysis of nestin nuclear localization using nuclear/cytoplasmic fractionation combined with Western blotting, as well as immunodetection of nestin on ultrathin sections using transmission electron microscopy. As mentioned above, positive nuclear nestin staining was also observed for early passages of the MBL-03 medulloblastoma cell line, while nestin was present in the cytoplasm alone at higher passages, probably due to clonal selection during long-term cultivation. The GM7 glioblastoma cell line, previously shown to have nuclear nestin [12], served as a control for these experiments.

Transmission electron microscopy of ultrathin sections revealed positive staining for nestin in the cytoplasm and nuclei of both the NBL-06 and NBL-19 cell lines (Fig. 3). The immunogold labeling of nestin in the nuclei and nucleoli usually appeared as individual signals (Fig. 3a, c) or small clusters of particles (Fig. 3d), although several medium or large nestin aggregates were present in both the nuclei (Fig. 3e) and nucleoli (Fig. 3f). An accumulation of labeled nestin was also repeatedly noted in the cytoplasm near to the nuclear envelope (Fig. 3b).

The presence of nestin in the nuclei of the NBL-06 and NBL-19 neuroblastoma cell lines was also verified by subcellular fractionation in combination with western blotting (Fig. 4). A nestin-specific band was detected at 250 kDa, mainly in the nuclear fraction of both cell lines. The purity of the nuclear lysate was confirmed by the absence of the cytoplasmic protein tubulin. The presence of an additional 30-kDa nestin-specific band in the cytoplas-

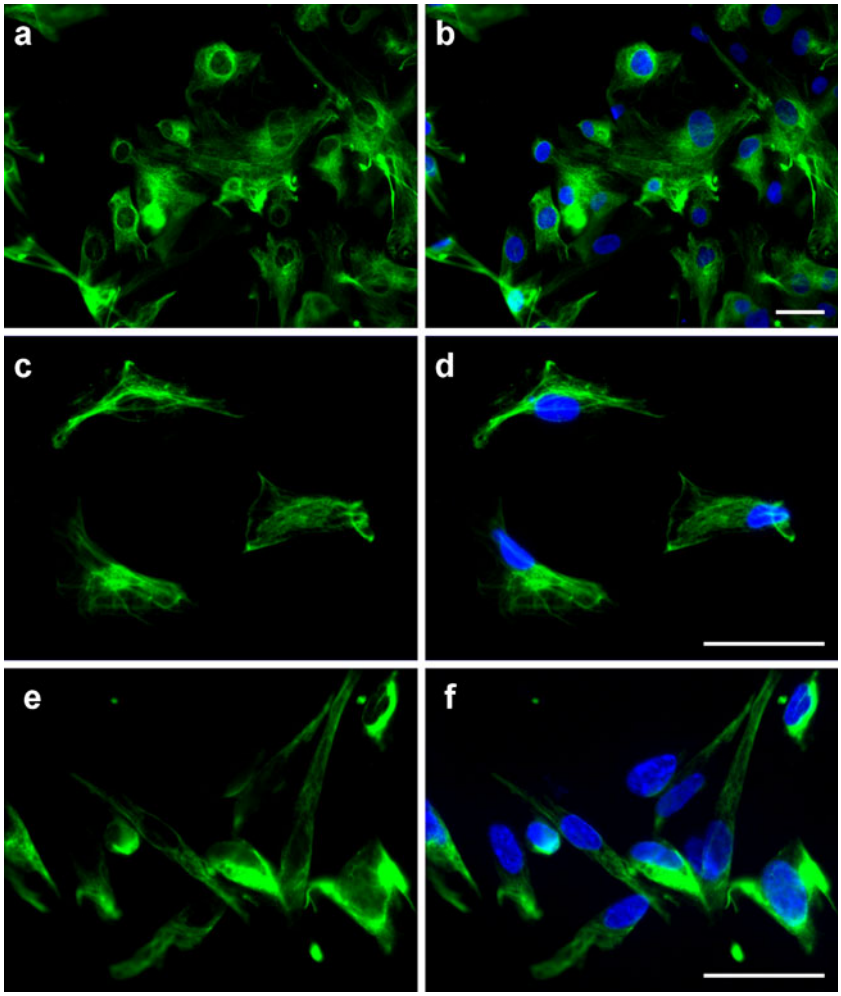

Fig. 1 Nestin expression in cell lines derived from neurogenic tumors. Nestin expression in GM12 glioblastoma cell line (**a**, **b**), MBL-03 medulloblastoma cell line (**c**, **d**), and NBL-17 neuroblastoma cell line (**e**, **f**) is indicated. Nestin-positive filamentous network was detected in the cytoplasm of both the glioblastoma (**a**, **b**) and medulloblastoma (**c**, **d**) cells. In neuroblastoma cells, both nestin-positive fibers and diffuse cytoplasmic signal were found in the minor proportion of cells (**e**, **f**). Nestin was stained by indirect immunofluorescence using FITC-labeled secondary antibody (**a**–**f**, *green*) and nuclei were counterstained with DAPI (**b**, **d**, **f**, *blue*). *Bars* 50 μm

mic fraction may be explained by cleavage of nestin during cell lysis, the reasons for which are unknown. Similarly, the manufacturer of the nestin antibody used in this study reports a nestin-specific band around 60 kDa in whole cell lysates from human cells.

Discussion

To date, nestin expression has been detected in the majority of neuroectodermal tumors [6]. In tumor tissue, nestin is present both in the tumor cells and in the vascular endothelial cells and is often stained at a high intensity, particularly in tumors containing large numbers of undifferentiated precursor and immature progenitor cells. Nestin expression may be a useful prognostic marker, especially in astrocytomas [7, 9, 17, 18] and melanomas [19], because expression in these tumors correlates with an undifferentiated state and a poor prognosis. Since nestin is an IF protein, it is most commonly localized in the cytoplasm, although nestin has been occasionally detected in the nuclei of neuroblastoma [13], glioblastoma multiforme [10, 12], and angiosarcoma cells [14]. However, little is known about this abnormal nuclear localization.

In this study, we performed a detailed analysis of nestin intracellular localization in cell lines derived from three types of neurogenic tumors: glioblastoma multiforme, medulloblastoma, and neuroblastoma. In all of these cell lines, we studied variability in signal type (cytoplasmic versus nuclear), signal intensity, and nestin-positive cell frequency. Not surprisingly, nestin was detected in the cytoplasm of all 11 cell lines of interest, as well as in three control cell lines. The protein was particularly strongly expressed in the cytoplasm of the glioblastoma cell lines, consistent with previous data regarding the prognostic significance of nestin in astrocytic tumors [7, 9, 17, 18]. Interestingly, we noted a larger variability in nestin expression in neuroblastoma cell lines, with low expression in NBL-19 cells derived from a high-risk neuroblastoma and very high expression in NBL-17 cells derived from a low-risk ganglioneuroblastoma. This variability is reflected by conflicting reports in the literature. Thomas et al.

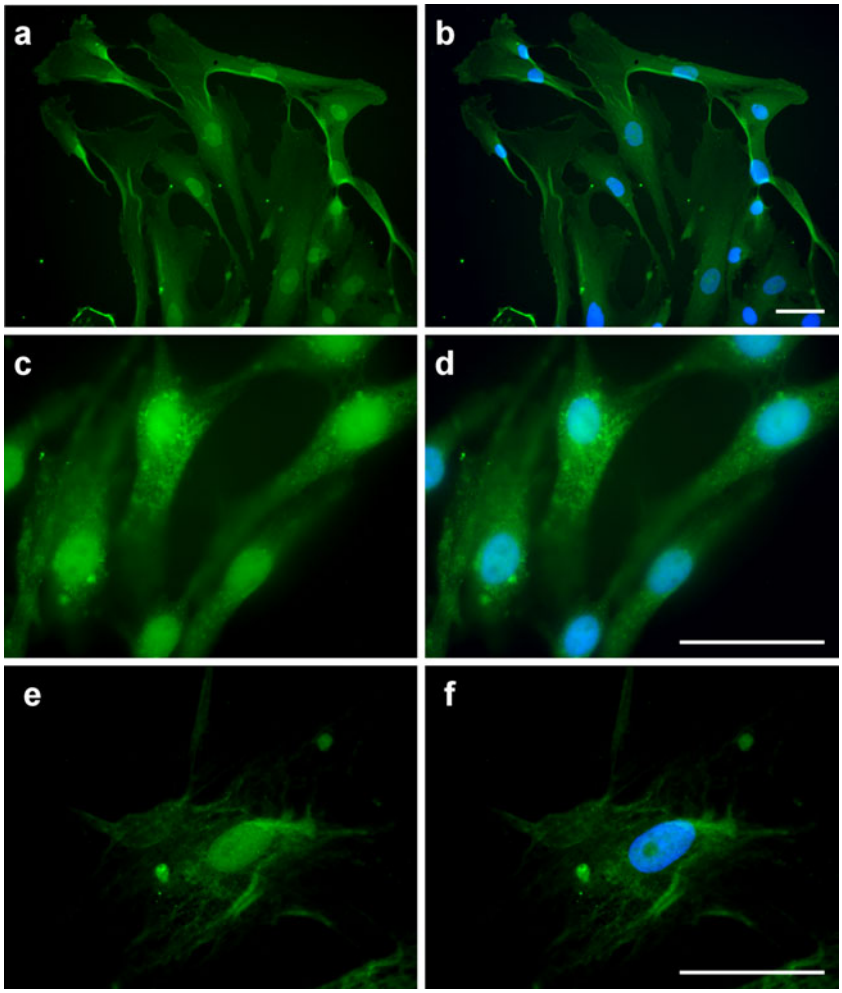

Fig. 2 Nuclear localization of nestin in cell lines derived from neurogenic tumors. Nestin localization in the nuclei of MBL-03 medulloblastoma cells (**a**, **b**), NBL-06 neuroblastoma cells (**c**, **d**), and NBL-19 neuroblastoma cells (**e**, **f**) is indicated. Nestin was only found in the nuclei of cells presenting predominantly a diffuse signal for nestin in the cytoplasm (**a**–**f**). Nestin was stained by indirect immunofluorescence using FITC-labeled secondary antibody (**a-f**, *green*) and nuclei were counterstained with DAPI (**b**, **d**, **f**, *blue*). *Bars* 50 μm

previously observed a correlation between nestin and N-myc expression in neuroblastoma cells and demonstrated that nestin expression is increased by N-myc via the binding of N-myc to the second enhancer of the nestin gene. They concluded that nestin is a potential marker for neuroblastoma prognosis [13]. In contrast, Korja et al. [20] studied 32 paraffin-embedded neuroblastoma sections and observed no correlation between nestin expression and cell proliferation rate, histopathological prognosis, or outcome, with only one of seven N-myc-positive neuroblastomas expressing nestin.

The main aim of this study was a detailed analysis of possible nestin localization in the nuclei of neuroblastoma, medulloblastoma, and glioblastoma cell lines. As described above, we detected nuclear expression of nestin in two neuroblastoma cell lines, NBL-06 and NBL-19, as well as in the MBL-03 medulloblastoma cell line in the early phases of cell culture. However, during long-term cultivation, MBL-03 cells with nestin-positive fibers in the cytoplasm and nestin-negative nuclei clonally overgrew the population with nestin-positive nuclei. The presence of nestin in the nuclei of the neuroblastoma cells was previously confirmed by subcellular fractionation and Western blotting. Additionally, previous work demonstrated that nestin directly interacts with DNA in *MYCN*-amplified cells [13].

The results reported here are consistent with our previous studies on glioblastoma cells [10, 12]: nestin was detected in the nuclei of two cell lines derived from glioblastoma multiforme with the aid of confocal microscopy, transmission electron microscopy, and fractionation accompanied by Western blotting. Using formalin-fixed, paraffin-embedded surgical samples of human neoplastic tissues, nestin has also been observed in the nuclei of some angiosarcoma cells in poorly differentiated angiosarcomas [14].

In both the NBL-06 and NBL-19 cell lines, we noted that nestin is present only in the nuclei of cells containing diffuse nestin signal in the cytoplasm. These results suggest that a high amount of phosphorylated depolymerized nestin in the cytoplasm may facilitate its transport into the nucleus. The nuclear localization of nestin may be due to

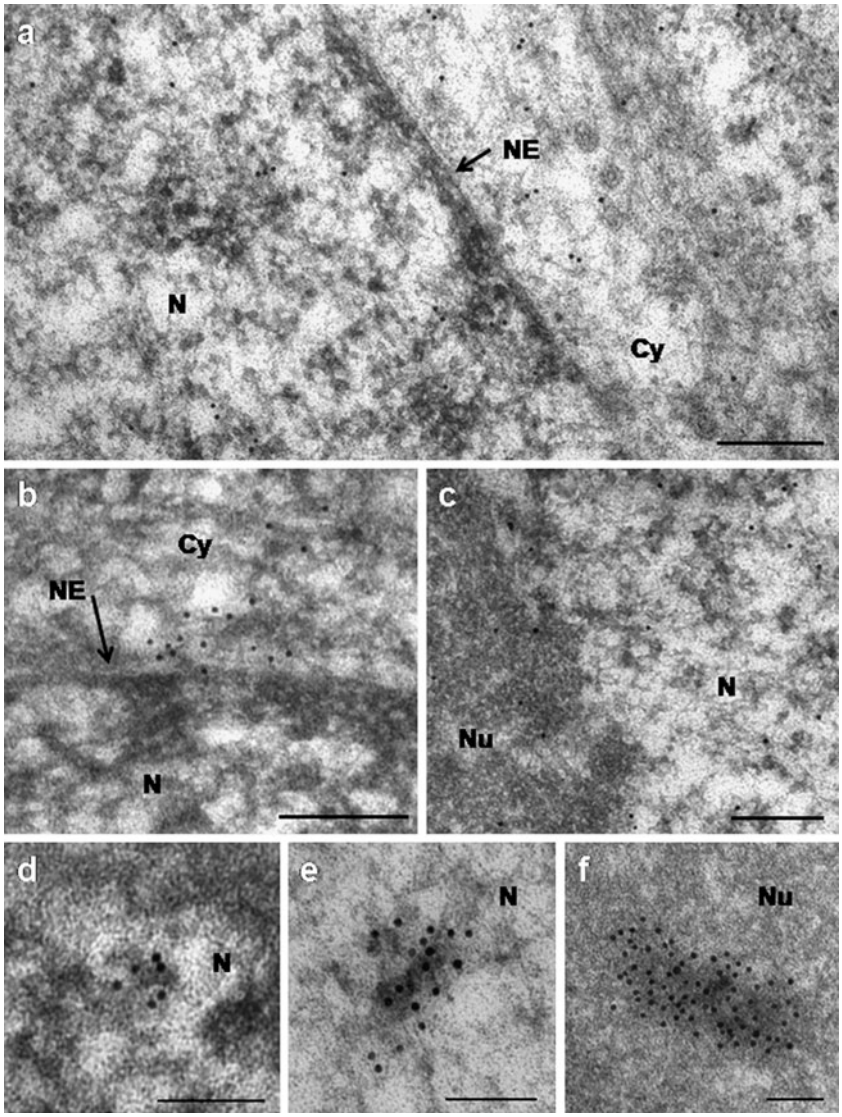

Fig. 3 Detection of nestin in nuclei of neuroblastoma cells by transmission electron microscopy. Nestin presence in nuclei of NBL-06 (**b**, **d**) and NBL-19 (**a**, **c**, **e**, **f**) neuroblastoma cells was clearly confirmed by transmission electron microscopy using immunogold labeling. In both of these cell lines, nestin was detected on ultrathin sections in cytoplasm (**a, b**) as well as in nuclei (**a**–**e**) and nucleoli (**c**, **f**) of examined cells. In addition to individual signals for nestin (**a**, **c**) and small clusters of particles (**d**), several medium (**e**), and large (**f**) nestin aggregates were also present in the nuclei and nucleoli. Accumulation of individual signals for nestin near to the nuclear envelope (**b**) was observed repeatedly. *Cy* cytoplasm, *N* nucleus, *Nu* nucleolus, *NE* nuclear envelope (as indicated by *arrows*). *Bars* 0.2 μm (**a**–**c**); 0.1 μm (**d**–**f**)

a dysfunction in certain signaling pathways or defective nestin structure in tumor cells. Depolymerized nestin may bind to certain proteins containing nuclear localization signals and be co-transported to the nucleus. Interaction partners of nestin include the CDK5 and CDC2 kinases, which regulate nestin assembly and disassembly during mitosis by phosphorylation of its C-terminus. This phosphorylation may regulate nestin's conformation and thus its interactions with other proteins [11, 21, 22], perhaps facilitating the co-transport of nestin into the nucleus.

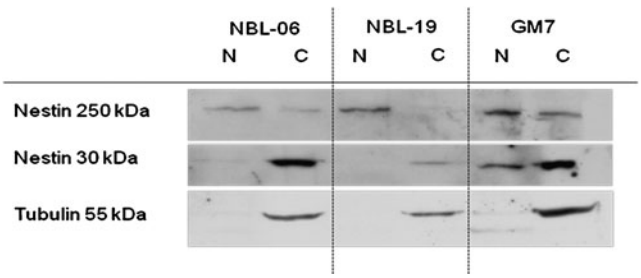

Fig. 4 Western blot analysis of intracellular localization of nestin in neuroblastoma cells. Nuclear/cytoplasmic fractionation followed by Western blotting was performed using NBL-06 and NBL-19 cell lines. GM7 glioblastoma cell line served as a control of nuclear positivity for nestin. Tubulin was used to confirm purity of nuclear fraction

It has been reported that nestin cannot form homodimers due to its extremely short N-terminus, and that wild-type nestin requires vimentin for its polymerization [23]. Additionally, nestin can interact with α-internexin [24] and is important for vimentin depolymerization during mitosis, which is induced by the MPF-specific phosphorylation of the N-terminal domain of vimentin. Hartig et al. supposed that IF proteins not only have cytoplasmic functions, but may also participate in nuclear DNA- and RNA-related events as well [25]. Although IF proteins do not posses classical nuclear localization signals and cannot be transported into the nucleus via nucleopore complexes, they probably can be

co-transported into the nucleus along with single-stranded DNA oligonucleotides, which bind to the N-terminal non-α-helical region [26].

The ancestral gene of the IF protein family was lamin-like, and encoded a nuclear protein. Thus, another possible explanation for IF protein localization to nuclei is their evolutionary origin [1]. The first cytoplasmic IF protein likely arose due to a loss of both the nuclear localization signal and the nuclear membrane-binding isoprenylation signal. The supposed evolutionary origin of the class VI IF nestin is from the neurofilament gene via duplication [1].

IF proteins such as vimentin, desmin, lamin A, and lamin B have been shown to bind to the nuclear matrix attachment regions of genomic DNA in vitro [27, 28]. These findings, as well as results obtained by Thomas et al. [13], support the hypothesis that nestin may have a function in chromatin remodeling and gene regulation.

We detected nuclear localization of nestin in three of 11 newly derived cell lines. This frequency is surprisingly high, indicating that the presence of nestin in the nuclei of tumor cells is not very rare, especially under in vitro conditions. Yet, the frequency of cells with nestin-positive nuclei is at most 10%, suggesting that these cells have no great advantage in clonal selection. The disappearance of such cells during long-term cultivation of the MBL-03 cell line supports this hypothesis. Nevertheless, our study provides a first step toward elucidation of the molecular mechanism of nestin transport to the nucleus and its possible role in gene expression.

Acknowledgments We thank Dobromila Klemova and Johana Maresova for technical assistance. We also acknowledge Barbora Bujokova for confirming nestin expression in the SH-SY5Y cell line. This work was supported by Grant MUNI/A/0090/2009 of the Masaryk University as well as Grants IGA NR/9125-4 of the Ministry of Health of the Czech Republic and VZ MSM0021622415 of the Ministry of Education of the Czech Republic.

Conflicts of interest None

References

1. Dahlstrand J, Zimmerman LB, McKay RD, Lendahl U. Characterization of the human nestin gene reveals a close evolutionary relationship to neurofilaments. J Cell Sci. 1992;103:589–97.
2. Lobo MV, Arenas MI, Alonso FJ, Gomez G, Bazan E, Paino CL, et al. Nestin, a neuroectodermal stem cell marker molecule, is expressed in Leydig cells of the human testis and in some specific cell types from human testicular tumours. Cell Tissue Res. 2004;316:369–76. doi:10.1007/s00441-003-0848-4.
3. Tamagno I, Schiffer D. Nestin expression in reactive astrocytes of human pathology. J Neurooncol. 2006;80:227–33. doi:10.1007/s11060-006-9181-6.
4. Faulkner JR, Herrmann JE, Woo MJ, Tamsey KE, Doan NB, Sofroniew NB. Reactive astrocytes protect tissue and preserve function after spinal cord injury. J Neurosci. 2004;24:2143–55. doi:10.1523/JNEUROSCI.3547-03.2004.
5. Mokry J, Pudil R, Ehrmann J, Cizkova D, Osterreicher J, Filip S, et al. Re-expression of nestin in the myocardium of postinfarcted patients. Virchows Arch. 2008;453:33–41. doi:10.1007/s00428-008-0631-8.
6. Krupkova Jr O, Loja T, Zambo I, Veselska R. Nestin expression in human tumors and tumor cell lines. Neoplasma. 2010;57:291–8. doi:10.4149/neo_2010_04_291.
7. Dahlstrand J, Collins VP, Lendahl U. Expression of the class VI intermediate filament nestin in human central nervous system tumors. Cancer Res. 1992;52:5334–41.
8. Piras F, Perra MT, Murtas D, Minerba L, Floris C, Maxia C, et al. The stem cell marker nestin predicts poor prognosis in human melanoma. Oncol Rep. 2010;23:17–24. doi:10.3892/or_00000601.
9. Sugawara K, Kurihara H, Negishi M, Saito N, Nakazato Y, Sasaki T, et al. Nestin as a marker for proliferative endothelium in gliomas. Lab Invest. 2002;82:345–51.
10. Veselska R, Kuglik P, Cejpek P, Svachova H, Neradil J, Loja T, et al. Nestin expression in the cell lines derived from glioblastoma multiforme. BMC Cancer. 2006;6:32. doi:10.1186/1471-2407-6-32.
11. Sahlgren CM, Mikhailov A, Hellman J, Chou YH, Lendahl U, Goldman RD, et al. Mitotic reorganization of the intermediate filament protein nestin involves phosphorylation by cdc2 kinase. J Biol Chem. 2001;276:16456–63. doi:10.1074/jbc.M009669200.
12. Loja T, Chlapek P, Kuglik P, Pesakova M, Oltova A, Cejpek P, et al. Characterization of a GM7 glioblastoma cell line showing CD133 positivity and both cytoplasmic and nuclear localization of nestin. Oncol Rep. 2009;21:119–27. doi:10.3892/or_00000198.
13. Thomas SK, Messam CA, Spengler BA, Biedler JL, Ross RA. Nestin is a potential mediator of malignancy in human neuroblastoma cells. J Biol Chem. 2004;279:27994–9. doi:10.1074/jbc.M312663200.
14. Yang X, Wu Q, Yu X, Xu CX, Ma BF, Zhang XM, et al. Nestin expression in different tumors and its relevance to malignant grade. J Clin Pathol. 2008;61:467–73. doi:10.1136/jcp.2007.047605.
15. Merigo F, Mucignat-Caretta C, Zancanaro C. Timing of neuronal intermediate filament proteins expression in the mouse vomeronasal organ during pre- and postnatal development. An immunohistochemical study. Chem Senses. 2005;30:707–17. doi:10.1093/chemse/bji063.
16. Loja T. Relationship between histopathological and molecular cytogenetic markers on chosen solid tumors in vitro. Dissertation: Masaryk University; 2008.
17. Ma YH, Mentlein R, Knerlich F, Kruse ML, Mehdorn HM, Held-Feindt J. Expression of stem cell markers in human astrocytomas of different WHO grades. J Neurooncol. 2008;86:31–45. doi:10.1007/s11060-007-9439-7.
18. Ehrmann J, Kolar Z, Mokry J. Nestin as a diagnostic and prognostic marker: immunohistochemical analysis of its expression in different tumours. J Clin Pathol. 2005;58:222–3. doi:10.1136/jcp.2004.021238.
19. Fusi A, Reichelt U, Busse A, Ochsenreither S, Rietz A, Maisel M, et al. Expression of the stem cell markers nestin and CD133 on circulating melanoma cells. J Invest Dermatol. 2010. doi:10.1038/jid.2010.285.
20. Korja M, Finne J, Salmi TT, Kalimo H, Karikoski R, Tanner M, et al. Chromogenic in situ hybridization-detected hotspot MYCN amplification associates with Ki-67 expression and inversely with nestin expression in neuroblastomas. Mod Pathol. 2005;18:1599–605. doi:10.1038/modpathol.3800462.
21. Sahlgren CM, Mikhailov A, Vaittinen S, Pallari HM, Kalimo H, Pant HC, et al. Cdk5 regulates the organization of nestin and its association with p35. Mol Cell Biol. 2003;23:5090–106. doi:10.1128/MCB.23.14.5090-5106.2003.

22. Sahlgren CM, Pallari HM, Chou YH, Goldman RD, Eriksson JE. A nestin scaffold links Cdk5/p35 signaling to oxidant-induced cell death. EMBOJ. 2006;25:4808–19. doi:10.1038/sj.emboj.7601366.
23. Marvin MJ, Dahlstrand J, Lendahl U, McKay RD. A rod end deletion in the intermediate filament protein nestin alters its subcellular localization in neuroepithelial cells of transgenic mice. J Cell Sci. 1998;111:1951–61.
24. Steinert PM, Chou YH, Prahlad V, Parry DA, Marekov LN, Wu KC, et al. A high molecular weight intermediate filament-associated protein in BHK-21 cells is nestin, a type VI intermediate filament protein. Limited co-assembly in vitro to form heteropolymers with type III vimentin and type IV alpha-internexin. J Biol Chem. 1999;274:9881–90.
25. Hartig R, Shoeman RL, Janetzko A, Tolstonog G, Traub P. DNA-mediated transport of the intermediate filament protein vimentin into the nucleus of cultured cells. J Cell Sci. 1998;111:3573–84.
26. Traub P, Mothes E, Shoeman RL, Schroder R, Scherbarth A. Binding of nucleic acids to intermediate filaments of the vimentin type and their effects on filament formation and stability. J Biomol Struct Dyn. 1992;10:505–31.
27. Luderus ME, de Graaf A, Mattia E, den Blaauwen JL, Grande MA, de Jong L, et al. Binding of matrix attachment regions to lamin B1. Cell. 1992;70:949–59.
28. Luderus ME, den Blaauwen JL, de Smit OJ, Compton DA, van Driel R. Binding of matrix attachment regions to lamin polymers involves single-stranded regions and the minor groove. Mol Cell Biol. 1994;14:6297–305.

BMC Cancer

BioMed Central

Research article

Nestin expression in the cell lines derived from glioblastoma multiforme

Renata Veselska*[1], Petr Kuglik[2], Pavel Cejpek[3], Hana Svachova[1], Jakub Neradil[1], Tomas Loja[1] and Jirina Relichova[2]

Address: [1]Cell Culture Laboratory, Department of Biology, School of Medicine, Masaryk University in Brno, Czech Republic, [2]Laboratory of Molecular Cytogenetics, Department of Genetics and Molecular Biology, School of Science, Masaryk University in Brno, Czech Republic and [3]Department of Neurosurgery, School of Medicine, Masaryk University in Brno, Czech Republic

Email: Renata Veselska* - rvesel@med.muni.cz; Petr Kuglik - kugl@sci.muni.cz; Pavel Cejpek - pcejpek@med.muni.cz; Hana Svachova - 43529@mail.muni.cz; Jakub Neradil - jneradil@med.muni.cz; Tomas Loja - tloja@med.muni.cz; Jirina Relichova - reli@sci.muni.cz

* Corresponding author

Published: 02 February 2006

BMC Cancer 2006, **6**:32 doi:10.1186/1471-2407-6-32

Received: 01 July 2005
Accepted: 02 February 2006

This article is available from: http://www.biomedcentral.com/1471-2407/6/32

Abstract

Background: Nestin is a protein belonging to class VI of intermediate filaments that is produced in stem/progenitor cells in the mammalian CNS during development and is consecutively replaced by other intermediate filament proteins (neurofilaments, GFAP). Down-regulated nestin may be re-expressed in the adult organism under certain pathological conditions (brain injury, ischemia, inflammation, neoplastic transformation). Our work focused on a detailed study of the nestin cytoskeleton in cell lines derived from glioblastoma multiforme, because re-expression of nestin together with down-regulation of GFAP has been previously reported in this type of brain tumor.

Methods: Two cell lines were derived from the tumor tissue of patients treated for glioblastoma multiforme. Nestin and other cytoskeletal proteins were visualized using imunocytochemical methods: indirect immunofluorescence and immunogold-labelling.

Results: Using epifluorescence and confocal microscopy, we described the morphology of nestin-positive intermediate filaments in glioblastoma cells of both primary cultures and the derived cell lines, as well as the reorganization of nestin during mitosis. Our most important result came through transmission electron microscopy and provided clear evidence that nestin is present in the cell nucleus.

Conclusion: Detailed information concerning the pattern of the nestin cytoskeleton in glioblastoma cell lines and especially the demonstration of nestin in the nucleus represent an important background for further studies of nestin re-expression in relationship to tumor malignancy and invasive potential.

Background

Nestin was originally described as an antigen of monoclonal antibody RAT401 against embryonic spinal cord [1] and was subsequently identified as a class VI intermediate filament protein [2], which is closely related to the neurofilament branch [3]. Nestin expression has been

proved in both rodent and human neural stem cells in various areas of the developing CNS as well as in immortalized stem cell and precursor cell lines [4-7]. During the development of the mammalian CNS, expression of cytoplasmic intermediate filaments begins with cytokeratins in early embryonic cells, through nestin and vimentin in proliferating neuroepithelium to the neurofilaments and GFAP in differentiated neurons and astrocytes, respectively [3].

In the adult CNS, nestin is expressed only in stem cells of the subventricular zone and to a lesser extent in the choroid plexus [6]. In the normal adult human brain, several morphological types of nestin-positive cells (neuron-like, astrocyte-like, cells with smaller cell bodies and fewer processes) are detectable in different areas of forebrain [8]. Re-expression of down-regulated nestin was demonstrated in reactive astrocytes following certain types of brain injuries. This reversion to the immature phenotype may serve to protect the cells, perhaps by making them less susceptible to the attendant hypoxia that can occur after injury [9]. Similarly, re-induction of nestin has been reported in reactive astrocytes and endothelial cells in cerebral abscesses, this process is probably caused by pathogenic microorganisms inducing inflammatory stress in the tissue [10].

Cell-specific expression of intermediate filament proteins in normal tissue and the differences in this expression in tumors represent an important tool for tumor diagnostics. From this point of view, immunohistochemical and/or immunocytochemical examination of nestin may serve as a useful tool for classification and accurate grading of human malignancies; especially since this protein has been found in many kinds of tumors, predominantly in tumors originating from immature, stem or progenitor cells. Using immunohistochemical staining of paraffin-embedded tissue sections, nestin expression has been detected in brain tumors and tumors derived from CNS tissues, such as, neurocytomas, gangliogliomas, ependymomas, pilocytic astrocytomas, malignant gliomas including glioblastoma multiforme, primitive neuroectodermal tumors (PNETs), medulloblastomas and medulloepitheliomas [4,11-16]. Up-regulation of nestin has also been shown in rhabdomyosarcomas [17], gastrointestinal stromal tumors and interstitial cells of Cajal [18,19], as well as in metastatic melanomas [20].

For detailed studies of intermediate filament protein expression and regulation, several cell lines derived from astrocytic tumors were used [21,22]. The high-grade astrocytomas, i.e. anaplastic astrocytoma (WHO grade III) and glioblastoma multiforme (WHO grade IV), seem to be exceptionally suitable models for the investigation of nestin re-expression and its relationship to the other intermediate filament proteins. Significant changes in these proteins (particularly GFAP and nestin), which are associated with motility and invasiveness, have been described in the astrocytoma cell lines [21]. Other findings suggest that the regulation of GFAP and nestin expression occurs at the transcriptional level [22]. Even though there have been several studies that focused on the detection of nestin in both tumor and normal cells, there are few publications describing the morphology of nestin cytoskeleton in individual human tumor cells. Therefore, the detailed pattern of nestin-containing intermediate filaments as an integral part of cytoskeletal structures is still unclear.

The aim of this study was to investigate, at both the cellular and ultrastructural levels, the nestin cytoskeleton in individual cells of two cell lines derived from glioblastoma multiforme. We characterized the morphology of nestin-positive filaments during the cell cycle, as well as the intracellular distribution of nestin molecules in the cytoplasm and also in the cell nucleus.

Methods

Cell culture

To obtain cell cultures, biopsy samples were taken from patients surgically treated for glioblastoma multiforme. The samples were coded and processed in the laboratory in an anonymous manner. This project has been approved by the Ethics Committee of the University Hospital Brno, Czech Republic.

The specimens were briefly washed in 70% ethanol, followed by two washing in PBS; the specimens were then mechanically chopped into pieces about 2 mm in diameter. After disaggregation, the pieces of tissue were washed three more times in PBS, this time with centrifugation. Next they were seeded into 25 cm^2 cell culture flasks containing 1 ml of complete medium, i.e. in DMEM (PAA Laboratories, Linz, Austria) supplemented with 20% fetal calf serum (PAA), 2 mM glutamine and antibiotics: 100 IU/ml of penicillin and 100 μg/ml of streptomycin (Bio-Whittaker, Inc., Walkersville, MD, USA). The cells were cultivated under standard conditions at 37°C and in an atmosphere of 95% air : 5% CO_2. Once the specimen pieces had attached, the volume of the medium was gradually increased to 5 ml over the next 48 hours. As soon as the outgrowing cells covered about 60% of the surface, they were trypsinized, diluted and transferred into a new flask. A similar procedure was used for further subcultivations of both cell lines, which were derived from the primary cultures.

The expression of intermediate filament proteins and the chromosomal abnormalities were analyzed at passages 3 through 5 for both cell lines; the detailed study of the nestin cytoskeleton morphology using epifluorescence

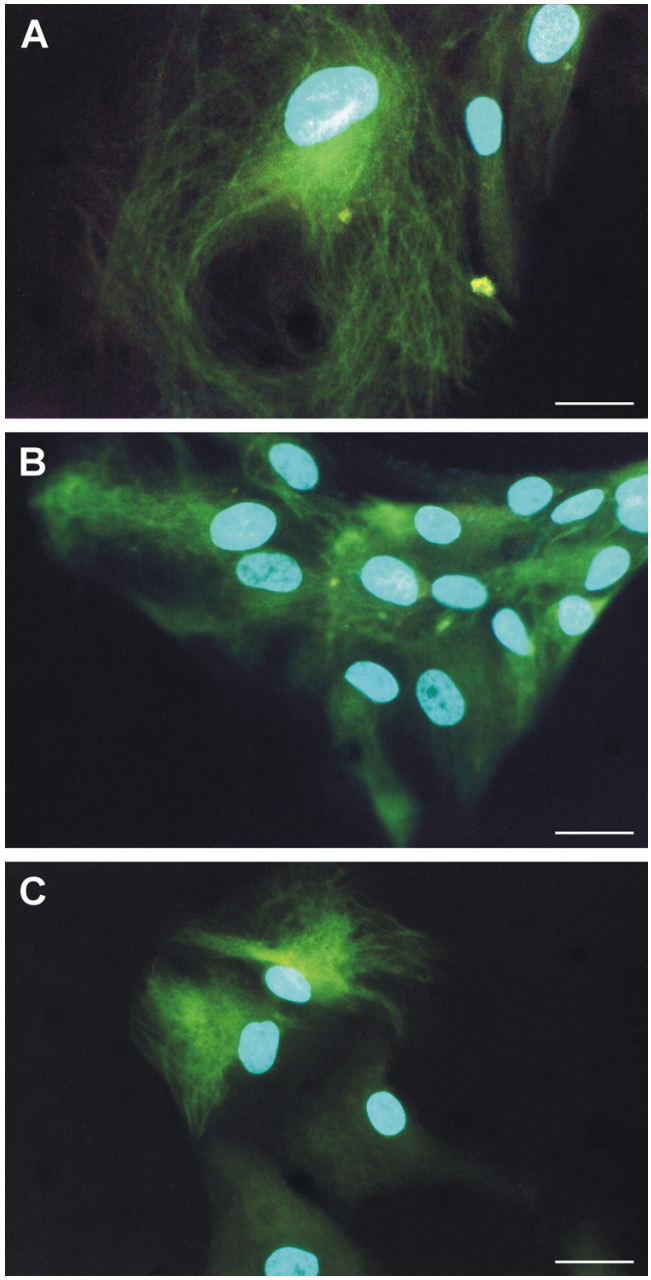

Figure 1
Nestin expression in primary cultures of glioblastoma cells. Nestin-positive intermediate filaments were detected in primary cultures in cells with different morphology – both in giant cells (A) and in smaller cells forming colonies (B). Due to heterogeneity of primary culture, non-tumor cells exhibiting no or very poor signals for nestin were also detectable together with nestin-positive cells (C). Nestin-positive filaments (A–C, green) stained by indirect immunofluorescence using FITC-labeled secondary antibody; nuclei labeled by DAPI (A–C, blue) are shown; bar, 25 μm.

microscopy was carried out between passages 6 and 9. Confocal microscopy and ultrastructural analysis were performed using the GM7 cell line at passages 15 through 22.

For the study of cytoskeletal structures, we used both epifluorescence and transmission electron microscopy. Cell suspensions with a concentration of 10^4 cells/ml were inoculated onto glass coverslips and grown under standard conditions for 24 hours before cytoskeleton staining.

Visualization of cytoskeletal structures

The cells were rinsed in PBS and fixed using 3% para-formaldehyde (Sigma Chemical Co., St. Louis, MO, USA) in PBS for 20 minutes at room temperature. After washing in the same buffer, the cells were permeabilized with a 0.2% solution of Triton X-100 detergent (Sigma) in PBS for 1 minute at room temperature. They were then washed with PBS and incubated for 10 minutes with 2% BSA to block the nonspecific binding of secondary antibodies.

Both cytoskeletal structures, i.e. intermediate filaments and microtubules, were stained by indirect immunofluorescence. To label the intermediate filaments, as our primary antibodies we used mouse monoclonal anti-vimentin antibodies, clones VIM 13.2 and LN-6 (Sigma), mouse monoclonal anti-vimentin antibody (Exbio, Prague, Czech Republic), mouse monoclonal anti-GFAP antibody, clone G-A-5 (Sigma), rabbit polyclonal anti-GFAP antibody (Sigma), and mouse monoclonal human specific anti-nestin antibody (Chemicon International Inc., Temecula, CA, USA). Microtubules were labeled using mouse monoclonal anti-α-tubulin antibody TU-01 (Exbio). All primary antibodies were applied at 37°C for 1 hour. The cells were then rinsed three times in PBS and treated with the corresponding secondary antibodies: anti-mouse antibodies conjugated with FITC or TRITC (Sigma) and/or anti-rabbit antibody conjugated with TRITC (Sigma).

After the labeling procedure was completed, the cells were mounted onto glass slides using Vectashield mounting medium with DAPI (Vector Laboratories, Burlingame, CA, USA). The cells were then observed in a Leitz Laborlux epifluorescence microscope and fluorescence micrographs were recorded with either a Wild Leitz camera or a CCD SB-8 camera. The images were stored using Camera 1.1 software (Dept. of Biology, Masaryk University, Brno, Czech Republic). For the detailed studies of cytoskeleton morphology, we used an Olympus FluoView-500 confocal imaging system in combination with an inverted Olympus IX-81 microscope. Images were recorded using an Olympus DP70 CCD camera. The images were analyzed using analySIS FIVE software (Soft Imaging System

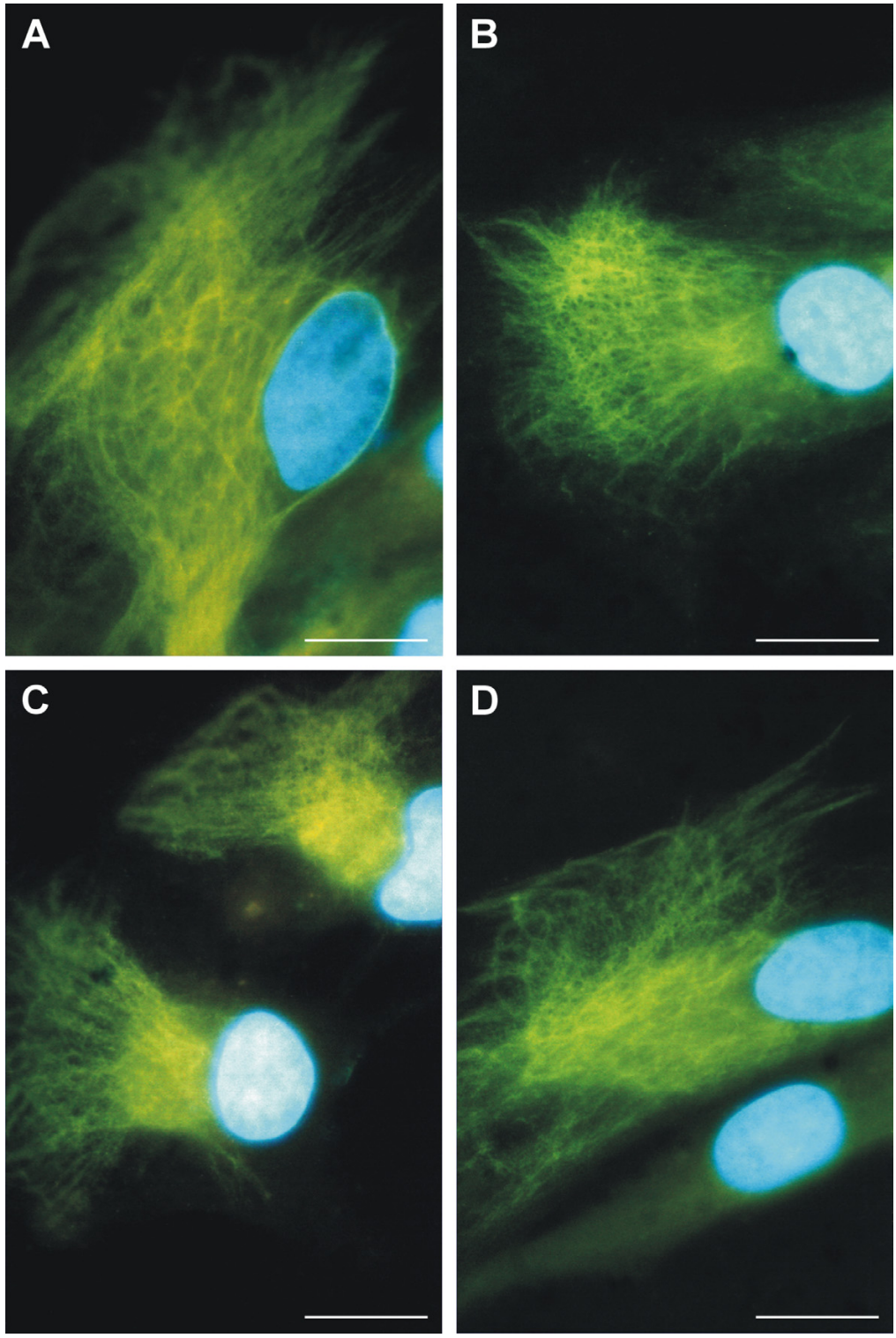

Figure 2
Localization of nestin-positive intermediate filaments in glioblastoma cells. A typical pattern of nestin-positive cytoskeleton in GM7 cells (A–D): the area with dense meshwork of nestin-positive filaments is located near the cell nucleus. Nestin-positive filaments (A–D, green) stained by indirect immunofluorescence using FITC-labeled secondary antibody; nuclei labeled by DAPI (A–D, blue) are shown; bar, 10 μm.

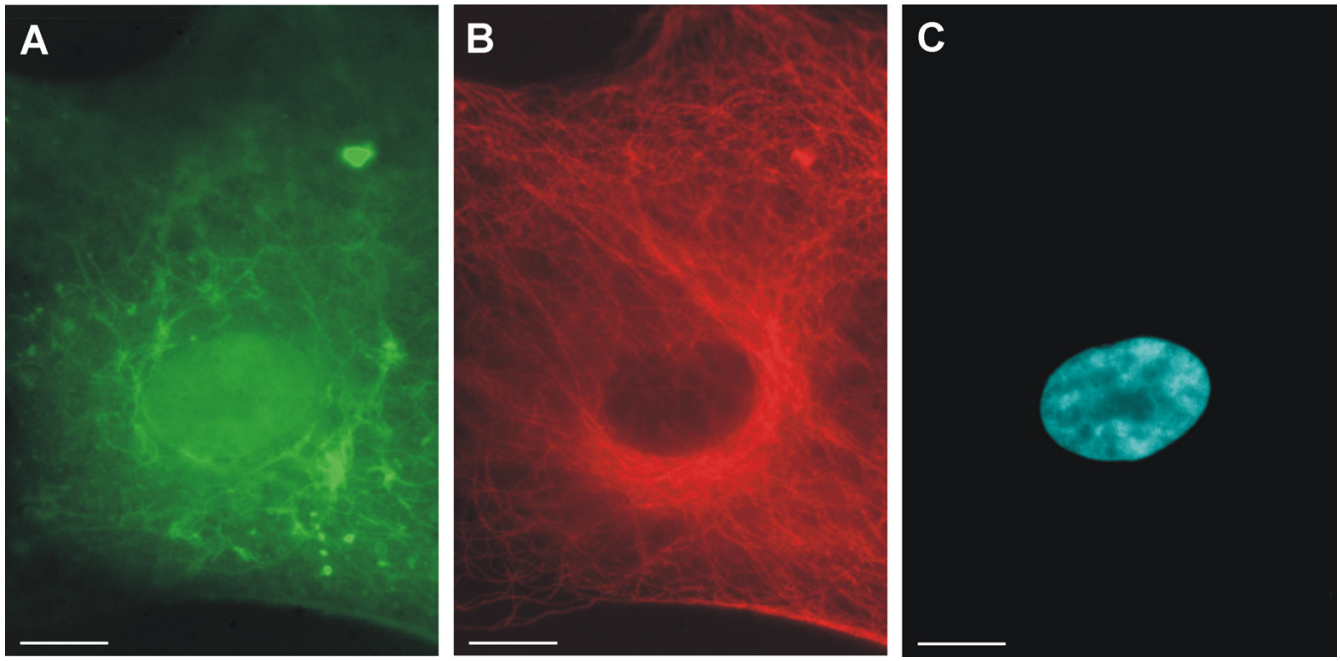

Figure 3
Arrangement of nestin filaments and microtubules in the same cell. Double labeling for both nestin (A) and tubulin (B) in the same cell of GM10 cell line showed no co-localization of nestin filaments with microtubules and confirmed different morphology of these cytoskeletal structures. Nestin-positive filaments (A, green) stained by indirect immunofluorescence using FITC-labeled secondary antibody; microtubules (B, red) stained by the same method using TRITC-labeled secondary antibody; nucleus labeled by DAPI (C, blue) are shown; bar, 10 μm.

GmbH, Muenster, Germany) and the Olympus FluoView Confocal Laser Scanning Microscope System 4.3.

Transmission electron microscopy

For immunodetection of nestin in ultrathin sections, cells were rinsed in PBS and then fixed with 2% para-formaldehyde (Sigma) in PBS for 1 hour at room temperature. After washing in PBS and dehydration, the cells were embedded in LR White (Polysciences Inc., London, UK). Ultrathin sections were labeled on grids and nestin was detected using mouse monoclonal anti-nestin antibody (Chemicon) and anti-mouse gold particle conjugated secondary antibody (Sigma). After immunolabeling, the specimens were contrasted with 2.5% uranyl acetate (Lachema-Pliva, Brno, Czech Republic) for 20 minutes and with Reynolds' solution for 8 minutes at room temperature. The specimens were examined using a Morgagni 268(D) transmission electron microscope (FEI Company, Hillsboro, OR, USA). Images were recorded using a MegaView III CCD camera (Soft Imaging System) and analyzed using Analysis software (Soft Imaging System).

Results

Characterization of cell lines

The tumor character of the derived cell lines was verified by GTG-banding during short-term cultivation – between passages 2 and 4. The GM7 cell line was identified as being near-tetraploid with a large number of structural and numerical abnormalities. The GM10 cell line was described as being near-diploid. The number of chromosomes varied from 43 to 46 and chromosomes 3, 15, 19, 22 and Y were the ones most frequently found to be missing. Genetic changes in both cell lines were also confirmed using FISH and HR-CGH methods (data not shown).

The astrocytic origin of these cell lines was confirmed by indirect immunofluorescence: both vimentin- and GFAP-positive cells were observed. However, the pattern of the cytoskeleton was quite different. While vimentin intermediate filaments, displaying a typical morphology, were detected in a majority of the cells in the culture, only a small proportion of the cells exhibited GFAP-positive filamentous structures. Most of cells in the culture showed only a diffuse, and usually weak, fluorescent signal for GFAP.

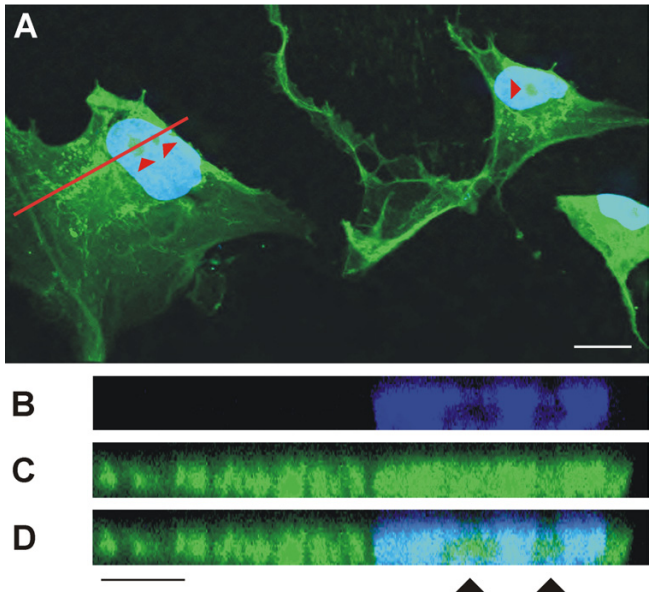

Figure 4
Software cross-section through a cell with nestin-positive nucleus. Nestin occurrence in cell nuclei was confirmed by confocal microscopy using software cross-section (B–D) through the selected cell (A, the plane of software cross-section is highlighted by the red line). The signal for nestin was detected also in the cell nucleus (C). The position of nucleoli is indicated by arrowheads. Nestin (A, C–D, green) stained by indirect immunofluorescence using FITC-labeled secondary antibody; nuclei labeled by DAPI (A–B, D, blue) are shown; bars, 20 μm (A), 10 μm (B–D).

In primary cultures, a different positivity for nestin was detected in the same cell population due to the mixture of various cell types (normal and transformed cells of astrocytic origin, endothelial cells) in the same culture. Transformed astrocytes were usually larger in size when compared to normal cells and, in addition to nestin positivity, abnormalities in nucleus morphology were also detected in these cells (Fig. 1A). Nestin expression and nestin-positive intermediate filament formation were also observed in the smaller cells forming monolayer (Fig. 1B). Nevertheless, nestin expression was very different in this cell population; it varied from no signal or a diffuse signal in the cytoplasm of, presumably, non-tumor cells up to characteristic nestin intermediate filaments as part of the transformed phenotype (Fig. 1C). During short-term cell cultures (between passages 2 and 4), a decreasing number of nestin-negative cells were observed. At passage 5, all cells in the population showed nestin positivity.

Morphology of the nestin cytoskeleton

Cells in the monolayer expressing nestin-positive intermediate filaments usually showed their nuclei in asymmetric positions and the nestin formed a very dense meshwork of intermediate filaments either throughout the cytoplasm (Figure 2A) or only in a specific part of the cell (Figure 2B–D). In both situations, we were able to detect a region in the cytoplasm of each cell, which produced a strong signal for nestin and consisted of a dense meshwork of nestin-positive filaments. The area of this region was approximately the same as that of the nucleus and it was usually located in the vicinity of the nucleus; however, the region was not in the identical position as the cell nucleus (Figure 2A–D).

To investigate a possible co-localization of this asymmetrical positioning of nestin filaments with a higher density of cytoplasmic microtubules in the MTOC region during interphase, a double labeling of both nestin and tubulin was performed. The results showed no co-localization of nestin filaments and microtubules and confirmed a different morphology of these cytoskeletal structures during interphase (Figure 3A–B).

In view of the nestin-positivity of the cell nuclei observed by fluorescence microscopy (Figure 3A), we performed software cross-sections through selected cells using confocal microscopy. The results showed that nestin was not only detectable in the cell nucleus, but also in the nucleoli (Figure 4A,C–D).

In mitotic cells, nestin intermediate filaments were completely depolymerized and as a result, nestin was detectable as a strong diffuse fluorescence in the cytoplasm of the cells (Figure 5A–C).

Ultrastructural distribution of nestin

Following the immunodetection of nestin in ultrathin sections, a strong nestin positivity was observed throughout the cytoplasm of the tumor cells (Figure 6A). The labeling of nestin usually manifested as individual signals or small clusters of particles; filamentous structures were labeled only sporadically (Figure 7A). In keeping with the findings of epifluorescence and confocal microscopy, nestin was distinctly detectable in the cell nucleus (Figure 8A). In addition to individual particles and small clusters of signal, several large nestin aggregates were also detected in the nucleus (Figure 8A–C) and some very short fibers were also noticeable within these aggregates (Figure 8B,C). A special arrangement of short spiral-like fibers was repeatedly found in both the cytoplasm (Figure 6B) and the cell nucleus (Figure 8D–E).

Discussion

Our study was focused on the detection and precise morphological characterization of the nestin cytoskeleton in two cell lines derived from glioblastoma multiforme. Nestin was described twenty years ago [1] and it has since been detected in many cell types, both normal and trans-

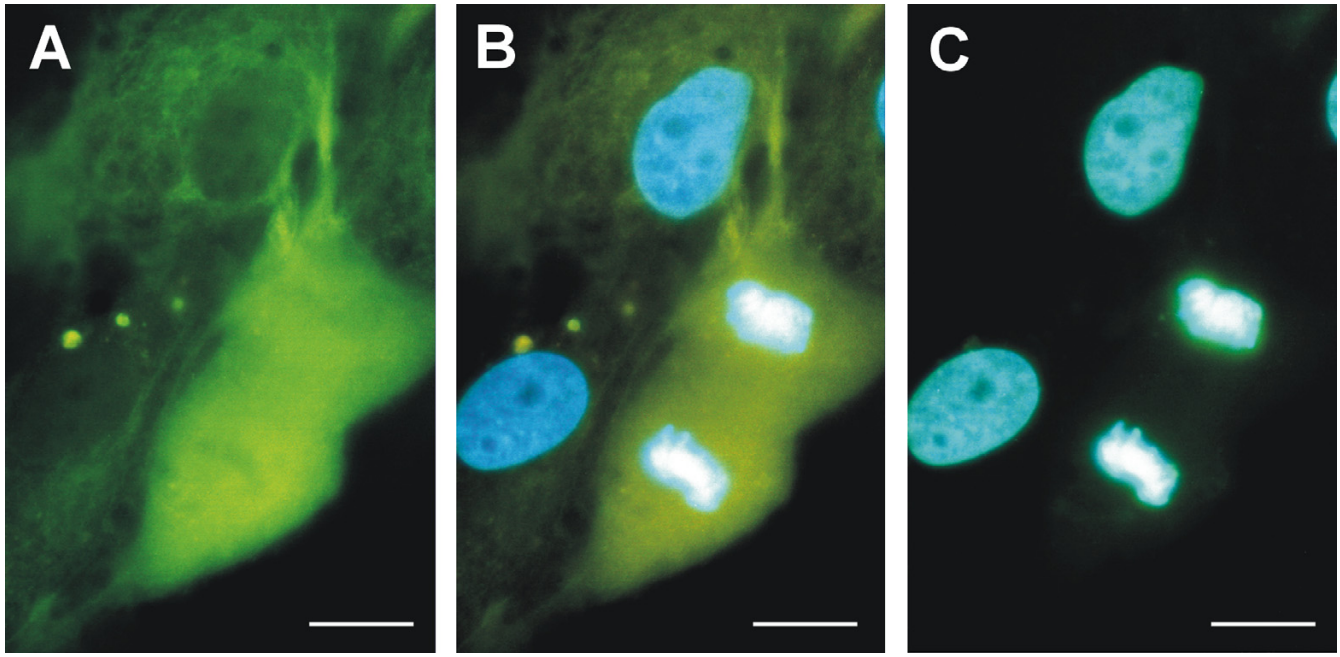

Figure 5
Nestin in the mitotic cell. Nestin-positive intermediate filaments were completely depolymerized and nestin was detectable as a strong diffuse fluorescent signal in the cytoplasm (A–B) of GM10 cell in late anaphase (B–C). Nestin (A–B, green) stained by indirect immunofluorescence using FITC-labeled secondary antibody; nuclei and chromosomes labeled by DAPI (B–C, blue) are shown; bar, 10 μm.

formed and to this time most of the studies involving nestin have been performed in human tissues using standard histological techniques.

The morphological studies of the nestin cytoskeleton have been carried out primarily in rodent cells. An identical arrangement of cytoskeletal structures in the astrocytes of rat hippocampus suggested a co-polymerization of nestin and vimentin or of nestin and GFAP. Nevertheless, the assumed co-polymerized filaments consisting of nestin and vimentin showed a typical pattern of intermediate filaments, while the co-polymerized filaments from nestin and GFAP had a cytoplasmic microtubules-like appearance [23]. Several authors have described a preferential formation of heteropolymers with vimentin and α-internexin. This is explained as being due to the very short N-terminus of the nestin molecule, which is important for protein assembly and its shortend length leads to less stable nestin homodimers [24,25]. Experiments with targeted mutants confirmed heteropolymers made of nestin and vimentin or nestin and GFAP in mouse cells [26-28]. Co-localization of nestin and vimentin or nestin and desmin filaments, which suggests the formation of heteropolymers, has also been described in chinese hamster ovary cells [29] and in the human fetal myoblast cell line [30].

However, there has been little published information concerning the morphology of intermediate filaments containing re-expressed nestin in human tumor cells. Nestin expression in human brain tumors has been detected by immunohistochemical techniques in a number of studies [4,11-16], and nestin positivity has been detected in the processes of tumor cells in tissue sections [31]. If we assume that nestin can polymerize into filaments with only vimentin, then an identical pattern of intermediate filaments in any given cell is to be expected. This situation was reported in the U-373 MG glioblastoma cell line using the same monoclonal anti-nestin antibody as was used in our study; in these experiments, more details were described in the intermediate filament network after nestin detection [32]. Similar findings, describing the astroglial cells of developing rat neocortex [33], showed more intensive staining of the co-localizing intermediate filaments using monoclonal anti-nestin antibody when compared to anti-vimentin and anti-GFAP antibodies.

In contrast, an incomplete co-localization of nestin with intermediate filament bundles containing other intermediate filament proteins (vimentin, GFAP, neurofilament) has been detected in the cell lines derived from PNETs and malignant gliomas [34]. Likewise, in our cell lines, nestin was detected as a distinct network of intermediate filaments, whereas vimentin and especially GFAP showed a

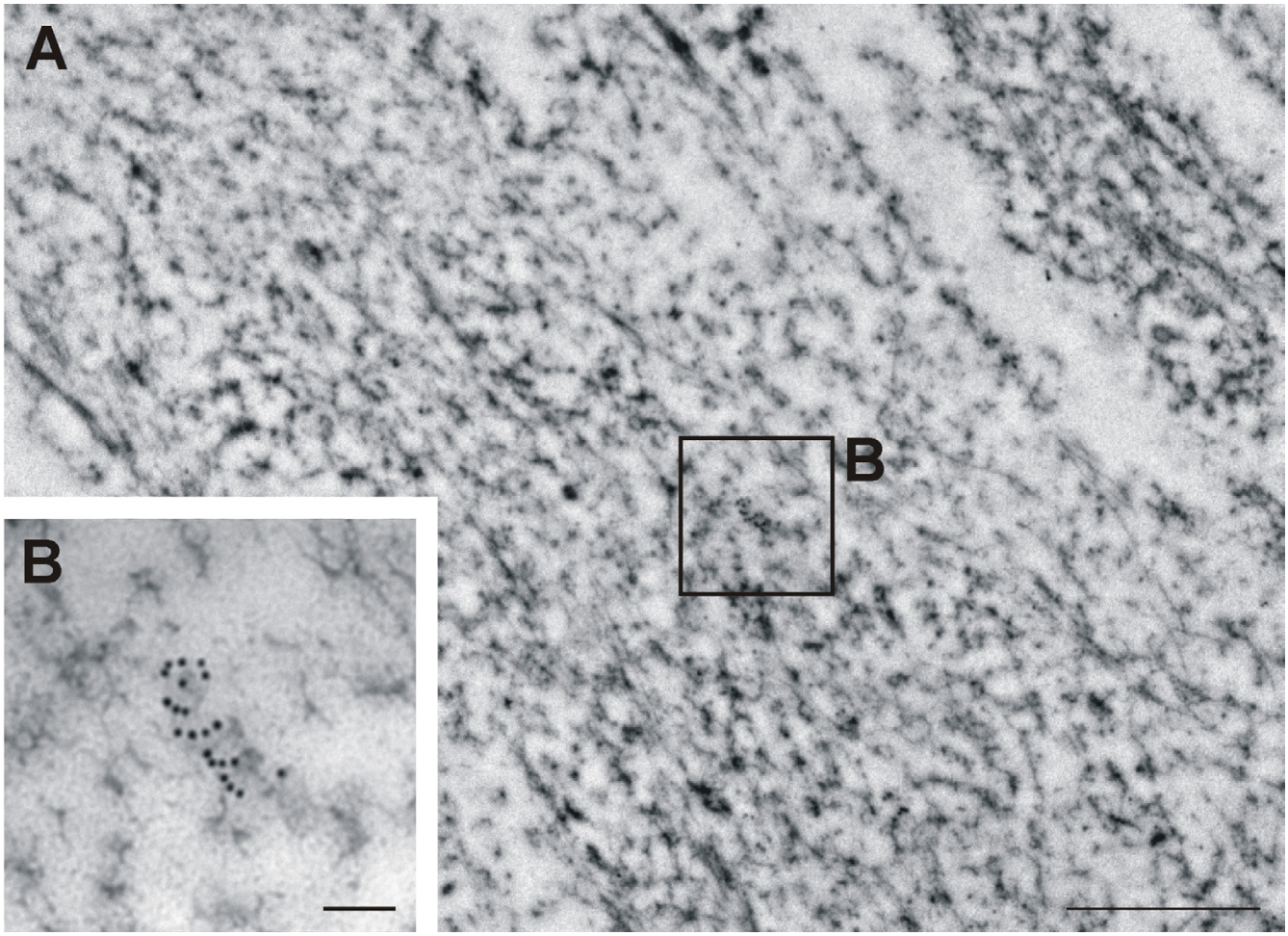

Figure 6
Labeling of nestin in the glioblastoma cells. Strong positivity for nestin was detected in the cytoplasm of GM7 cells (A). A special arrangement into short spiral-like fibers in cytoplasm (B) was found repeatedly in different cells. Nestin was detected using immunogold labeling (A–B); bars, 1 μm (A), 0.1 μm (B).

predominantly diffuse positivity in the cytoplasm. Only vimentin was also detected as a filamentous structure, but this network did not completely co-localize with nestin-positive filaments and it was primarily found surrounding cell nucleus. When the same anti-nestin antibody was used, the pattern of intermediate filament positivity was independent of the anti-vimentin antibodies (all mouse monoclonal, but different clones) or the anti-GFAP antibodies (both mouse monoclonal and rabbit polyclonal) that were used for immunostaining. A reduced GFAP-positivity in high-grade astrocytomas has been reported in several studies [35-37] and experiments carried out on the U-373 MG glioblastoma cell line has confirmed a transcription level regulation of both nestin re-expression and GFAP down-regulation [22]. The possible differences in the pattern of nestin-positive and vimentin-positive filaments may be caused by differences in the antibodies that were used for nestin detection. Co-localization of nestin-positive and vimentin-positive filaments was most often reported when rabbit polyclonal antibody was used for nestin detection [26,27,38], whereas, when the mouse monoclonal antibody was used for nestin detection this, usually, produced a more detailed and distinct nestin cytoskeleton pattern [33,37]. In any event, the specifity of the anti-nestin antibody used for detection has to be taken into account [39].

The typical pattern of nestin filament organization, i.e. the asymmetric position of the nestin-positive region in the cytoplasm near the nucleus, which we observed, has also been detected in U-373 and U-251 human glioma cell lines [32,39]. In another study, the nestin cytoskeleton was described as "button-like" clusters in the cytoplasm of anaplastic oligoastrocytoma cells; unfortunately, it is impossible to compare these findings with our results

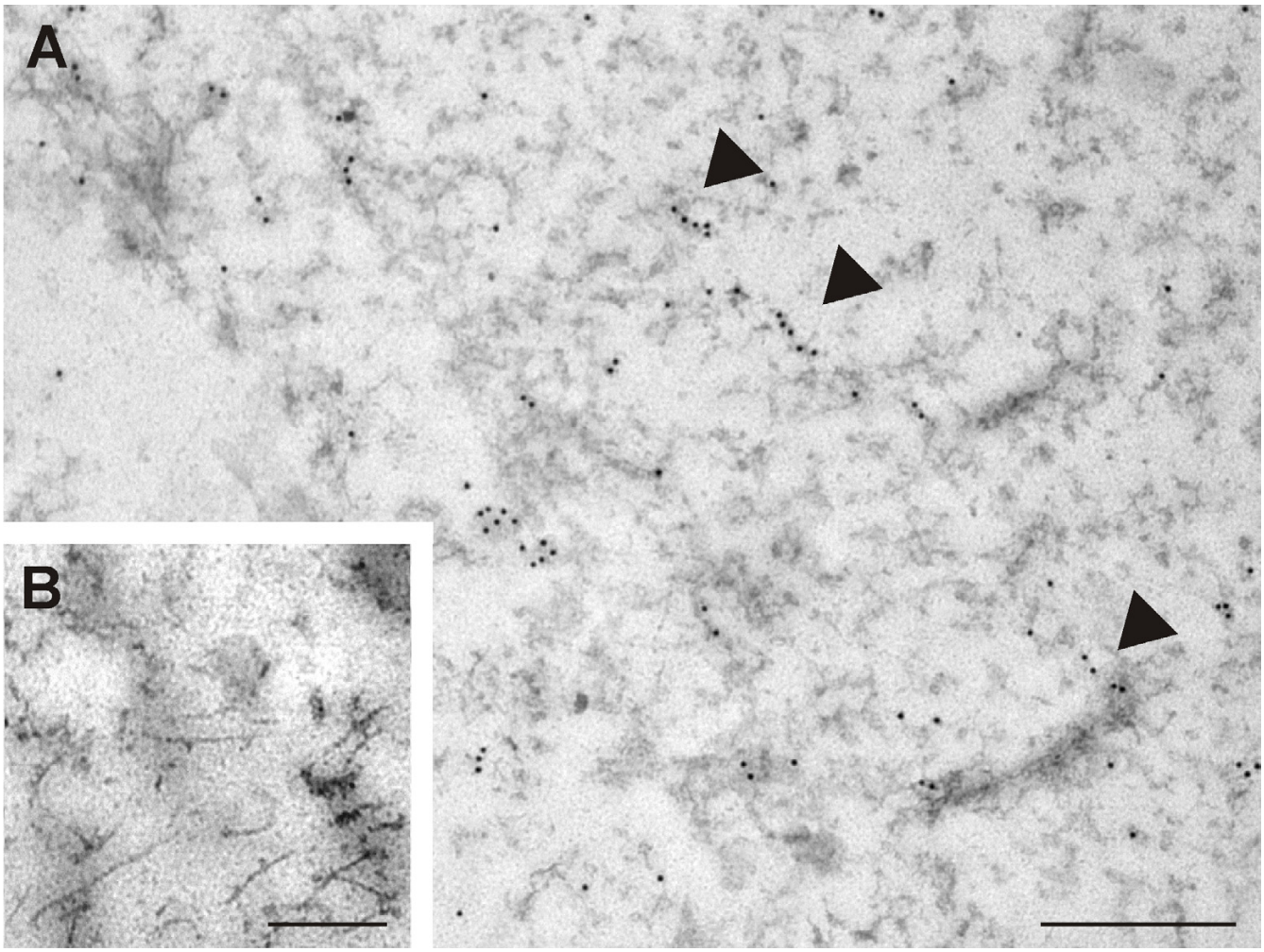

Figure 7
Ultrastructural distribution of nestin in the cytoplasm of glioblastoma cells. Labeling of nestin appeared usually as individual signals or small clusters of particles; filamentous structures (arrowheads) were labeled only sporadically in the cytoplasm of GM7 cells (A). Nestin was detected using immunogold labeling; bar, 1 μm (A). Negative control stained with secondary antibody only: cytoplasm; bar, 0.5 μm (B).

because of the lower magnifications employed compared to the magnifications used in our study [31].

The complete disassembly of the nestin network in mitotic cells, as reported in our experiments, corresponds with the hypothesis that nestin serves as a mediator signal for disassembly of other intermediate filaments during mitosis [29]. Mitotic reorganization of nestin filaments including their partial disassembly has also been detected in the ST15A human neuronal progenitor cell line [40]. Generally speaking, the breakdown of intermediate filaments during mitosis seems to be a common feature of nestin-positive cells [29]. The structural reorganization of the nestin cytoskeleton during the cell cycle is mediated by cdc2 kinase via phosphorylation [40]. Other experiments have confirmed the regulation of nestin organization by phosphorylation on Thr^{316} and Thr^{1495} sites that are specific for cdk5 kinase [38]. In general, low levels of nestin phosphorylation are associated with its assembly into filamentous structures [25].

Without question, the most important finding of our study is the discovery of nestin in the cell nucleus, which was unequivocally demonstrated both by fluorescence microscopy and transmission electron microscopy. Even using indirect immunofluorescence, a diffuse signal for nestin in the position of cell nucleus has also been identified in primary cultures of glioblastoma cells [36]. Another study has demonstrated the presence of nestin in the nucleus of neuroblastoma cells by means of cell fractionation and immunoblotting, and other experiments have showed that nestin binds to nuclear DNA in cell lines

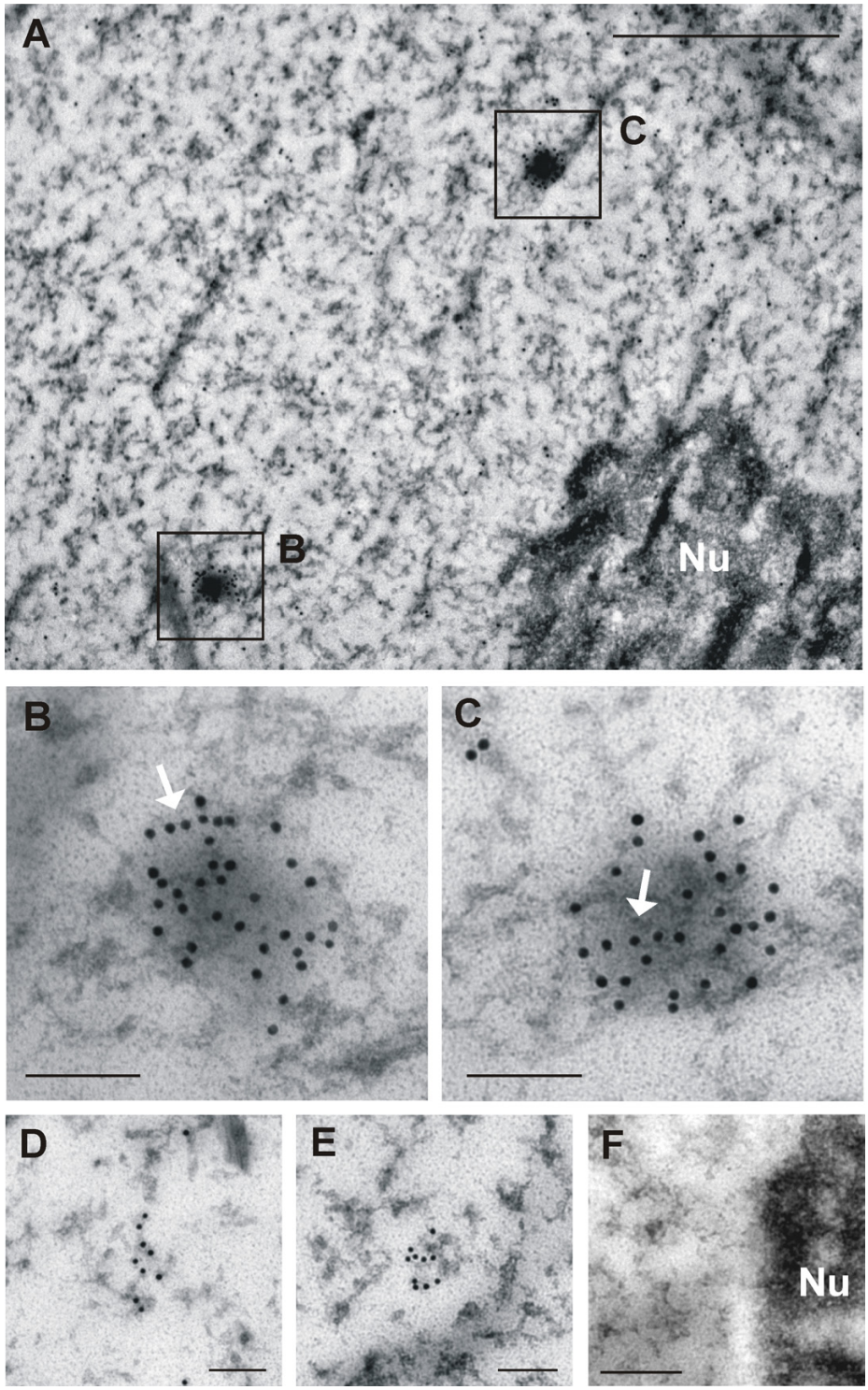

Figure 8

Detection of nestin in the cell nucleus. Labeled nestin was distinctly detectable also in the cell nucleus as individual particles and small clusters of signal (A); several larger nestin aggregates (B–C) were also observed. Arrows indicate very short fibers in these aggregates (B–C). A special arrangement into short spiral-like fibers in cell nucleus (D–E) was found repeatedly in different cells. Nestin was detected using immunogold labeling; bars, 1 μm (A), 0.1 μm (B–E). Negative control stained with secondary antibody only: nucleus and nucleolus (Nu); bar, 0.5 μm (F).

with N-*myc* amplification [41]. Collectively, all these findings suggest that nestin expression in tumor cells is closely related to their dedifferentiated status and increased malignancy. In addition to the role of the cytoskeletal components in cell growth and motility, which is associated with metastatic potential, some proteins of the intermediate filaments identified in the cell nucleus may affect organization of chromatin or they may serve as specific regulators of gene expression [41,42].

Conclusion

Using indirect immunofluorescence, we described the re-expression of nestin and the specific morphology of nestin-positive intermediate filaments in glioblastoma cells. Again, the most significant finding is the evidence of nestin in the cell nucleus, which we detected using transmission electron microscopy and immunogold labelling. Although other studies have suggested that changes in the intermediate filament proteins in brain tumors are associated with tumor malignancy and invasiveness, the role of nestin molecules in the nucleus of tumor cells still remains unclear. A thourough study of nestin in the nucleus of tumor cells on the ultrastructural level in combination with a precise molecular cytogenetic characterization of these cell lines will be a main aim of our future research.

List of abbreviations

BSA, bovine serum albumin; DAPI, 4,6-diamidino-2-phenylindol; DMEM, Dulbecco's modified Eagle's medium; FITC, fluorescein isothiocyanate; GFAP, glial fibrillary acidic protein; MTOC, microtubule-organizing center; PBS, phosphate-buffered saline; PNETs, primitive neuroectodermal tumors; TRITC, tetramethylrhodamine isothiocyanate

Competing interests

The author(s) declare that they have no competing interests.

Authors' contributions

RV conceived the study, carried out the cytoskeleton analysis and drafted the manuscript. PK carried out the cytogenetic analysis and participated in manuscript preparation. PC performed the operations of patients and managed the COST project. HS participated in the immunofluorescence and electron microscopy studies. JN and TL were involved in the electron microscopy study; the former besides took part in the manuscript preparation. JR coordinated this study and managed the VZ project.

Acknowledgements

Authors thank Mrs. Johana Maresova and Mrs. Renata Kupska for their skillful technical assistance and Dipl. Ing. Ladislav Ilkovics (Department of Histology and Embryology, Medical Faculty, Masaryk University in Brno) for his assistance in performing electron microscopy. This study was supported by grants VZ MSM 0021622415 and COST OC B19.001.

References

1. Hockfield S, McKay RD: **Identification of major cell classes in the developing mammalian nervous system.** *J Neurosci* 1985, **5:**3310-3328.
2. Lendahl U, Zimmerman LB, McKay RDG: **CNS stem cells express a new class of intermediate filament protein.** *Cell* 1990, **60:**585-595.
3. Dahlstrand J, Zimmerman LB, McKay RDG, Lendahl U: **Characterization of the human nestin gene reveals a close evolutionary relationship to neurofilaments.** *J Cell Sci* 1992, **103:**589-597.
4. Dahlstrand J, Collins VP, Lendahl U: **Expression of the class VI intermediate filament nestin in human central nervous system tumors.** *Cancer Res* 1992, **52:**5334-5341.
5. Dahlstrand J, Lardelli M, Lendahl U: **Nestin mRNA expression correlates with the central nervous system progenitor cell in many, but not all, regions of developing central nervous system.** *Brain Res Dev Brain Res* 1995, **84:**109-129.
6. Morshead CM, Reynolds BA, Craig CG, McBurney MW, Staines WA, Morassutti D, Weiss S, van der Kooy D: **Neural stem cells in the adult mammalian forebrain: A relatively quiescent subpopulation of subependymal cells.** *Neuron* 1994, **13:**1071-1082.
7. Andressen C, Stöcker E, Klinz FJ, Lenka N, Hescheler J, Fleischmann B, Arnhold S, Addicks K: **Nestin-specific green fluorescent protein specific expression in embryonic stem-cell neural precursor cells used for transplantation.** *Stem Cells* 2001, **19:**419-424.
8. Gu H, Wang S, Messam CA, Yao Z: **Distribution of nestin immunoreactivity in the normal adult human forebrain.** *Brain Res* 2002, **943:**174-180.
9. Krum JM, Rosenstein JM: **Transient coexpression of nestin, GFAP, and vascular endothelial growth factor in mature reactive astroglial following neural grafting or brain wounds.** *Exp Neurol* 1999, **160:**348-360.
10. Ha Y, Choi JU, Yoon DH, Cho YE, Kim TS: **Nestin and small heat shock protein expression on reactive astrocytes and endothelial cells in cerebral abscess.** *Neurosci Res* 2002, **44:**207-212.
11. Smits A, van Grieken D, Hartman M, Lendahl U, Funa K, Nister M: **Coexpression of platelet-derived growth factor alpha and beta receptors on medulloblastomas and other primitive neuroectodermal tumors is consistent with an immature stem cell and neuronal derivation.** *Lab Invest* 1996, **74:**188-198.
12. Khoddami M, Becker LE: **Immunohistochemistry of medulloepithelioma and neural tube.** *Pediatr Pathol Lab Med* 1997, **17:**913-925.
13. Brisson C, Lelong-Rebel I, Mottolese C, Jouvet A, Fevre-Montange M, Saint Pierre G, Rebel G, Belin MF: **Establishment of human tumoral ependymal cell lines and coculture with tubular-like human endothelial cells.** *Int J Oncol* 2002, **21:**775-785.
14. Almqvist PM, Mah R, Lendahl U, Jacobsson B, Hendson G: **Immunohistochemical detection of nestin in pediatric brain tumors.** *J Histochem Cytochem* 2002, **50:**147-158.
15. Duggal N, Hammond RR: **Nestin expression in ganglioglioma.** *Exp Neurol* 2002, **174:**89-95.
16. Kim BJ, Kim SS, Kim YI, Paek SH, Lee YD, Suh-Kim H: **Forskolin promotes astroglial differentiation of human central neurocytoma cells.** *Exp Mol Med* 2004, **36:**52-56.
17. Kobayashi M, Sjöberg G, Söderhäll S, Lendahl U, Sandstedt B, Sejersen T: **Pediatric rhabdomyosarcomas express the intermediate filament nestin.** *Pediatr Res* 1998, **43:**386-392.
18. Tsujimura T, Makiishi-Shimobayashi C, Lundkvist J, Lendahl U, Nakasho K, Sugihara A, Iwasaki T, Mano M, Yamada N, Yamashita K, Toyosaka A, Terada N: **Expression of the intermediate filament nestin in gastrointestinal stromal tumors and interstitial cells of Cajal.** *Am J Pathol* 2001, **158:**817-823.
19. Sarlomo-Rikala M, Tsujimura T, Lendahl U, Miettinen M: **Patterns of nestin and other intermediate filament expression distinguish between gastrointestinal stromal tumors, leiomyomas and schwannomas.** *APMIS* 2002, **110:**499-507.
20. Florenes VA, Holm R, Myklebost O, Lendahl U, Fodstad O: **Expression of the neuroectodermal intermediate filament nestin in human melanomas.** *Cancer Res* 1994, **54:**354-356.

21. Rutka JT, Ivanchuk S, Mondal S, Taylor M, Sakai K, Dirks P, Jun P, Jung S, Becker LE, Ackerley C: **Co-expression of nestin and vimentin intermediate filaments in invasive human astrocytoma cells.** *Int J Dev Neurosci* 1999, **17:**503-515.
22. Zhou R, Skalli O: **TGF-α differentially regulates GFAP, vimentin, and nestin gene expression in U-373 MG glioblastoma cells: Correlation with cell shape and motility.** *Exp Cell Res* 2000, **254:**269-278.
23. Miyaguchi K: **Ultrastructure of intermediate filaments of nestin and vimentin-immunoreactive astrocytes in organotypic slice cultures of hippocampus.** *J Struct Biol* 1997, **120:**61-68.
24. Herrmann H, Aebi U: **Intermediate filaments and their associates: multi-talented structural elements specifying cytoarchitecture and cytodynamics.** *Curr Opin Cell Biol* 2000, **12:**79-90.
25. Michalczyk K, Ziman M: **Nestin structure and predicted function in cellular cytoskeletal organization.** *Histol Histopathol* 2005, **20:**665-671.
26. Pekny M, Eliasson C, Chien CL, Kindblom LG, Liem R, Hamberger A, Betsholtz C: **GFAP-deficient astrocytes are capable of stellation *in vitro* when cocultured with neurons and exhibit a reduced amount of intermediate filaments and an increased cell saturation density.** *Exp Cell Res* 1998, **239:**332-343.
27. Eliasson C, Sahlgren C, Berthold CH, Stakeberg J, Celisi JE, Betsholtz C, Eriksson JE, Pekny M: **Intermediate filament protein partnership in astrocytes.** *J Biol Chem* 1999, **274:**23996-24006.
28. Menet V, Gimenez Ribotta M, Chauvet N, Drian MJ, Lannoy J, Colucci-Guyon E, Privat A: **Inactivation of the glial fibrillary acidic protein gene, but not that of vimentin, improves neuronal survival and neurite growth by modifying adhesion molecule expression.** *J Neurosci* 2001, **21:**6147-6158.
29. Chou YH, Khuon S, Herrmann H, Goldman RD: **Nestin promotes the phosphorylation-dependent disassembly of vimentin intermediate filaments during mitosis.** *Mol Biol Cell* 2003, **14:**1468-1478.
30. Sjoberg G, Jiang WQ, Ringertz NR, Lendahl U, Sejersen T: **Colocalization of nestin and vimentin/desmin in skeletal muscle cells demonstrated by three-dimensional fluorescence digital imaging microscopy.** *Exp Cell Res* 1994, **214:**447-58.
31. Sugawara K, Kurihara H, Negishi M, Saito N, Nakazato Y, Sasaki T, Takeuchi T: **Nestin as a marker for proliferative endothelium in gliomas.** *Lab Invest* 2002, **82:**345-351.
32. Sultana S, Zhou R, Sadagopan MS, Skalli O: **Effects of growth factors and basement membrane proteins on the phenotype of U-373 MG glioblastoma cells as determined by the expression of intermediate filament proteins.** *Am J Pathol* 1998, **153:**1157-1168.
33. Kalman M, Ajtai BM: **A comparison of intermediate filament markers for presumptive astroglia in the developing rat neocortex: immunostaining against nestin reveals more detail, than GFAP or vimentin.** *Int J Dev Neurosci* 2001, **19:**101-108.
34. Tohyama T, Lee VM, Rorke LB, Marvin M, McKay RD, Trojanowski JQ: **Nestin expression in embryonic human neuroepithelium and in human neuroepithelial tumor cells.** *Lab Invest* 1992, **66:**303-313.
35. Branle F, Lefranc F, Camby I, Jeuken J, Geurts-Moespot A, Sprenger S, Sweep F, Kiss R, Salmon I: **Evaluation of the efficiency of chemotherapy in in vivo orthotopic models of human glioma cells with and without 1p19q deletions and in C6 rat orthotopic allografts serving for the evaluation of surgery combined with chemotherapy.** *Cancer* 2002, **95:**641-655.
36. Asklund T, Appelskog IB, Ammerpohl O, Langmoen IA, Dilber MS, Aints A, Ekström TJ, Almqvist PM: **Gap junction-mediated bystander effect in primary cultures of human malignant gliomas with recombinant expression of the HSV *tk* gene.** *Exp Cell Res* 2003, **284:**185-195.
37. Shiras A, Bhosale A, Shepal V, Shukla R, Baburao VS, Prabhakara K, Shastry P: **A unique model system for tumor progression in GBM comprising two developed human neuro-epithelial cell lines with differential transforming potential and coexpressing neuronal and glial markers.** *Neoplasia* 2003, **5:**520-532.
38. Sahlgren CM, Mikhailov A, Vaittinen S, Pallari HM, Kalimo H, Pant HC, Eriksson JE: **Cdk5 regulates the organization of nestin and ist association with p35.** *Mol Cell Biol* 2003, **23:**5090-5106.
39. Messam CA, Hou J, Major EO: **Coexpression of nestin in neural and glial cells in the developing human CNS defined by a human-specific anti-nestin antibody.** *Exp Neurol* 2000, **161:**585-596.
40. Sahlgren CM, Mikhailov A, Hellman J, Chou YH, Lendahl U, Goldman RD, Eriksson JE: **Mitotic reorganization of the intermediate filament protein nestin involves phosphorylation by cdc2 kinase.** *J Biol Chem* 2001, **276:**16456-16463.
41. Thomas SK, Messam CA, Spengler BA, Biedler JL, Ross RA: **Nestin is a potential mediator of malignancy in human neuroblastoma cells.** *J Biol Chem* 2004, **279:**27994-27999.
42. Hartig R, Shoeman RL, Janetzko A, Tolstonog GV, Traub P: **DNA-mediated transport of the intermediate filament protein vimentin into the nucleus of cultured cells.** *J Cell Sci* 1998, **111:**3573-3584.

Pre-publication history

The pre-publication history for this paper can be accessed here:

http://www.biomedcentral.com/1471-2407/6/32/prepub

Differentiation of HL-60 myeloid leukemia cells induced by all-*trans* retinoic acid is enhanced in combination with caffeic acid

RENATA VESELSKÁ[1], KAREL ZITTERBART[1,2], JAN AUER[1,3] and JAKUB NERADIL[1]

[1]Department of Biology, Medical Faculty, Departments of [2]Pediatric Oncology, [3]Internal Hematooncology, University Hospital Brno and Medical Faculty, Masaryk University, Brno, Czech Republic

Received January 19, 2004; Accepted March 15, 2004

Abstract. We investigated a possible enhancement of all-*trans* retinoic acid (ATRA)-induced differentiation of HL-60 human myeloid leukemia cells by caffeic acid (CA), a widely distributed plant phenolic compound. Our results showed that CA, in the concentration of 13 or 52 μM, had no or minimal influence on cell differentiation, whereas the differentiating activity of ATRA was potentiated by CA treatment. We proved, using flow cytometric detection of the CD66b surface molecule, a synergistic effect of CA: at day 10, 18.3% of CD66b-positive cells were detected after treatment with ATRA only, and 33% when CA and ATRA were combined together. NBT-assay confirmed that this additive effect of CA on ATRA-induced differentiation. Proliferating activity as assessed by MTT-assay was generally not affected by CA at given concentrations. However, cell proliferation was significantly reduced by 52 μM CA at 96-h intervals. This effect was markedly enhanced when CA, at both concentrations, and ATRA were combined. The possibility to enhance the differentiation potential of ATRA by CA may improve outcomes in the therapy of acute promyelocytic leukemia.

Correspondence to: Dr Renata Veselská, Cell Culture Laboratory, Department of Biology, Medical Faculty, Masaryk University, Jostova 10, CZ-66243 Brno, Czech Republic
E-mail: rvesel@med.muni.cz

Abbreviations: ANOVA, analysis of variance; APL, acute promyelocytic leukemia; ATRA, all-*trans* retinoic acid; BB, block-buffer; BSA, bovine serum albumin; CA, caffeic acid; DMEM, Dulbecco's modified Eagle's medium; DMSO, dimethyl sulfoxide; FITC, fluorescein isothiocyanate; FS, forward scatter; HBSS, Hanks' balanced salt solution; MTT, 3-[4,5-dimethylthiazol-2-yl]-2,5-diphenyltetrazolium bromide; NBT, nitro blue tetrazolium; NSAIDs, non-steroid anti-inflammatory drugs; $1,25(OH)_2D_3$, 1,25-dihydroxy-vitamin D_3; PBS, phospate buffer saline; SS, side scatter; TPA, 12-*O*-tetradecanoylphorbol-13-acetate

Key words: HL-60 cell line, induced differentiation, acute promyelocytic leukemia, caffeic acid, ATRA

Introduction

Induced differentiation is currently one of the main research topics in the fields of cell and tumor biology, with a special regard to its possible application in clinical oncology. Retinoids play an important role in morphogenesis and differentiation processes, and they are the most frequently reported inductors of differentiation. Retinoic acid and its derivatives induce terminal differentiation of hematopoietic stem cells and progenitor cells (1), neuronal stem cells (2), embryonic stem and carcinoma cell lines (3,4) as well as in cell lines derived from squamous cell carcinoma (5).

All-*trans* retinoic acid (ATRA) is clinically used for the induction of blast differentiation in the treatment of patients with acute promyelocytic leukemia (APL) (6-8). Nevertheless, about 30% of patients treated with ATRA and chemotherapy relapse (9). Therefore, attention has recently been paid to novel differentiation agents and combined induction or enhancement of differentiation effects. For example, an additive differentiation effect was proved in several cell lines when ATRA and 1,25-dihydroxy-vitamin D_3 ($1,25(OH)_2D_3$) were combined (10,11). In cells of the HL-60 myeloid leukemia line, the differentiation effect of $1,25(OH)_2D_3$ could be increased by combined application of non-steroid anti-inflammatory drugs (NSAIDs), anti-oxidant curcumin, vitamin E or ethyl esters of ferulic and caffeic acid (12,13). The enhanced action of ATRA and 12-*O*-tetradecanoylphorbol-13-acetate (TPA) in combination with bile acids was proved in several leukemic cell lines (14). The additive effect was also noted in the combination of ATRA with inhibitors of arachidonic acid metabolism (15,16).

On the basis of these facts, the present study focused on the influence of caffeic acid (3,4-dihydrocinnamic acid, CA) (Fig. 1) on the ATRA-induced differentiation. CA, a phenolic plant compound, exhibits non-specific anti-oxidant effects both *in vivo* and *in vitro* (17-19), as well as specific inhibitory effects on 5-lipoxygenase (20,21) and some protein kinases (22).

The aim of this study was to investigate a possible synergistic effect of CA on differentiation of HL-60 human myeloid leukemia cell lines induced by ATRA treatment. The course of differentiation was studied by detecting the occurrence of functionally mature granulocytes and CD66b-

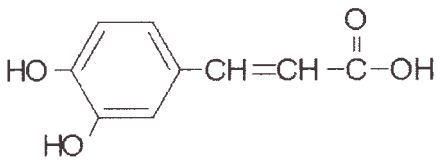

Figure 1. Structure of CA molecule.

expressing cells in ATRA- and/or CA-treated cell populations. The dynamics of early phases of induced differentiation was monitored by measurement of the proliferation activity of differentiating cell populations.

Materials and methods

Cell culture. HL-60 human myeloid leukemia cells were maintained in Dulbecco's modified Eagle's medium (DMEM) (PAA Laboratories GmbH, Linz, Austria) supplemented with 10% fetal calf serum (PAA), 2 mM L-glutamine (PAA), 100 U/ml^{-1} penicillin (BioWhittaker Inc., Walkersville, MD, USA) and 100 mg/ml^{-1} streptomycin (BioWhittaker). Their cultivation was carried out under standard conditions at 37˚C, in the atmosphere of 95% air to 5% CO_2. The cells were sub-cultivated 3 times weekly.

Chemicals. CA (Sigma Chemical Co., St. Louis, MO, USA) was prepared as a stock solution at the concentration of 130 mM in dimethyl sulfoxide (DMSO) (Sigma), ATRA (Sigma) was dissolved in DMSO at the concentration of 10 mM. Both reagents were stored at -20˚C under light-free conditions. For experiments, stock solutions were diluted in a fresh DMEM to obtain final concentrations of 13 μM or 52 μM of CA, and 1 μM of ATRA. Concentrations of CA were chosen on the basis of published data (12,19,21,22). DMSO concentration in medium was maximum 0.05% (v/v), and this concentration of DMSO was found to influence neither cell proliferation nor induced differentiation.

Induction of differentiation. To perform a NBT-assay and flow cytometry measurement, 25 cm^2 cell culture flasks (TPP, Trasadingen, Switzerland) were seeded with the cell suspension at the concentration of 10^6 cells/ml of complete DMEM. ATRA and/or CA were added immediately after the inoculation to achieve the final concentrations listed above. To run an MTT assay, the cell suspension at the concentration of 10^4 cells/ml was seeded into 96-well flat-bottom microtitre plates (TPP) in the volume of 200 μl/well. ATRA and/or CA at given concentrations were added to the cell suspension before inoculation into microtitre plates.

NBT assay. The presence of terminally differentiated granulocytes in a cell population was assessed by the NBT assay. For each experiment, cell populations were incubated in cell culture flasks under standard conditions for 6, 8 or 10 days. At these intervals, 1x10^6 cells were harvested by centrifugation and resuspended in 1.0 ml Hanks' balanced salt solution containing 0.05% (w/w) nitro blue tetrazolium (NBT) (Sigma) and 1.0 μg of TPA (Sigma). The cell suspensions were incubated at 37˚C for 1 h in the dark and were then placed into 96-well flat-bottom microtitre plates in the volume of 100 μl/well. The solution containing NBT was removed by centrifugation and 200 μl of 10% Triton X-100 (Sigma) in 0.1 M HCl (Fluka, Buchs, Switzerland) was added into each well. Cells were then incubated at 37˚C for 30 min in the dark and the absorbance was measured at 570 nm using the Spectra Shell microplate reader (SLT Laborinstrument GmbH, Salzburg, Austria).

Flow cytometry. The expression of CD66b, a maturation and activation marker of granulocytes, was detected by means of indirect immunofluorescence and flow cytometry. Similar to the NBT-assay, cell populations were incubated for 6, 8 or 10 days as described above. Cells (1x10^6) were harvested by centrifugation, washed in PBS at 37˚C, and incubated in a block-buffer, which consisted of 2 mg bovine serum albumin per ml of phosphate buffer saline (PBS), at 37˚C for 5 min and washed twice with ice-cold PBS. The monoclonal antibody to CD66b (Immunotech, Marseille, France) was prepared according to the procedure recommended by the manufacturer. Cells were incubated with this antibody at 4˚C for 90 min, and washed 3 times with ice-cold block-buffer. They were then incubated with swine anti-mouse antibody conjugated to fluorescein isothiocyanate (FITC) (Sigma) at 4˚C for 60 min. After 3 additional washes with ice-cold block-buffer, the cells were fixed with 3.75% para-formaldehyde in PBS with the addition of 0.1% sodium azide. Fluorescence was measured by Coulter Epics XL flow cytometer (Beckman Coulter Inc.). Data from at least 5,000 events per sample were acquired in a list mode and analyzed using WinMDI 2.8 software (Joseph Trotter, Scripps Research Institute, La Jolla, CA, USA). Control studies were performed with the non-binding mouse IgG1 isotype antibody (Immunotech), as well as with the secondary antibody only and with cells incubated in the absence of the FITC-labeled secondary antibody.

MTT assay. The proliferation activity of cell populations, both treated and untreated by CA and/or ATRA, was determined by the MTT assay. For each experiment, cells seeded as described above in 96-well microtitre plates were allowed to grow under standard conditions. The MTT assay was performed immediately after seeding and at the following intervals: 24, 48, 72 and 96 hours. In order to perform the MTT-assay, microtitre plates were centrifuged, the culture medium was removed, and 220 μl of DMEM containing 3-[4,5-dimethylthiazol-2-yl]-2,5-diphenyltetrazolium bromide (MTT) (Sigma) at a final concentration 455 μg/ml of DMEM were added into each well. After the 4-h incubation under standard conditions, the medium with MTT was removed using centrifugation and 200 μl of DMSO were added into each well to solubilize the cells. After the 10-min shaking of microtitre plates, the absorbance was measured at 570 nm using the Spectra Shell microplate reader (SLT).

Statistical analysis. All experiments were repeated independently at least 3 times. Standardized data from NBT and MTT assays were expressed in relative cell numbers (ratio of treatment/control). The results of NBT-assays were analyzed by the non-parametric Kruskal-Wallis test. $P<0.05$ was

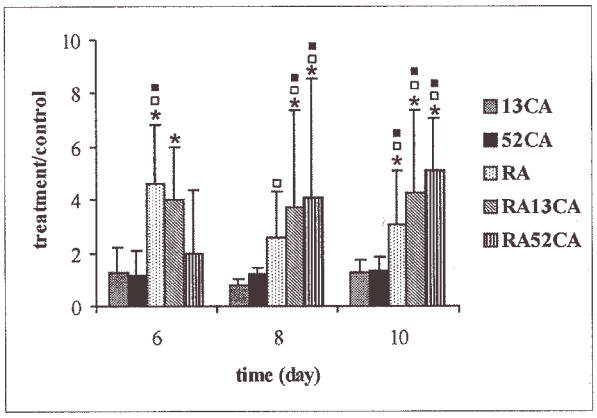

Figure 2. Differentiation into granulocyte stage was measured by NBT-assay. X-axis, time (days); Y-axis, relative cell number (ratio of treatment/control). Each value is the median of 3 independent experiments ± standard deviation. Data were analyzed using Kruskal-Wallis test. (*) significant difference from the control group, (❑), significant difference from 13 μM CA, (■), significant difference from 52 μM CA. P<0.05 was considered significant.

considered significant. Statistically reasonable differences in results of MTT-assays were evaluated by the 2-way ANOVA followed by the Tukey post-hoc test. The statistical analyses were performed by means of Statistica 6 software (StatSoft Inc., Tulsa, OK, USA).

Results

All experiments were designed as studies of the influence of ATRA, CA and their combinations on cell populations. The occurrence of terminally differentiated granulocytes in the cell populations was measured during the prolonged cultivation on day 6, 8 and 10. Proliferation activity of control and treated cell populations was measured during the 96-h cultivation.

Cell differentiation. To detect the cells with mature phenotypes i.e. granulocytes, 2 different methods were used, the NBT-assay, which measures the superoxide-dismutase activity in the terminally differentiated granulocytes after their activation, and the flow-cytometric detection of the cell surface antigen CD66b, which is the marker of the granulocyte stage.

Data from the NBT-assays (Fig. 2) showed that the treatment of HL-60 cells with CA alone in both concentrations had no influence on cell differentiation. In accordance with the known differentiation potential of ATRA, its application led to the significant increase of terminally differentiated granulocytes in a cell population. In addition, ATRA combined with CA, especially at 52 μM concentration, increased the proportion of granulocytes in a cell population in comparison with application of ATRA alone. The tendency of CA to enhance the ATRA-induced differentiation was most obvious on cultivation days 8 and 10, nevertheless, this effect was not statistically significant.

The detection of CD66b antigen expression in cell populations by flow cytometry (Figs. 3 and 4) clearly confirmed the described results of NBT-assays. While the treatment of cell populations with CA alone in both concentrations led only to a moderate increase of CD66b-positive cells, the treatment with ATRA markedly increased their frequency (Fig. 3). Moreover, the combination treatment with ATRA and CA in both concentrations led to a distinctly higher number of CD66b-positive granulocytes in comparison with the application of ATRA alone (Table I). It is also evident on the side scatter versus fluorescence dot plots (Fig. 3) that FITC-positive cells

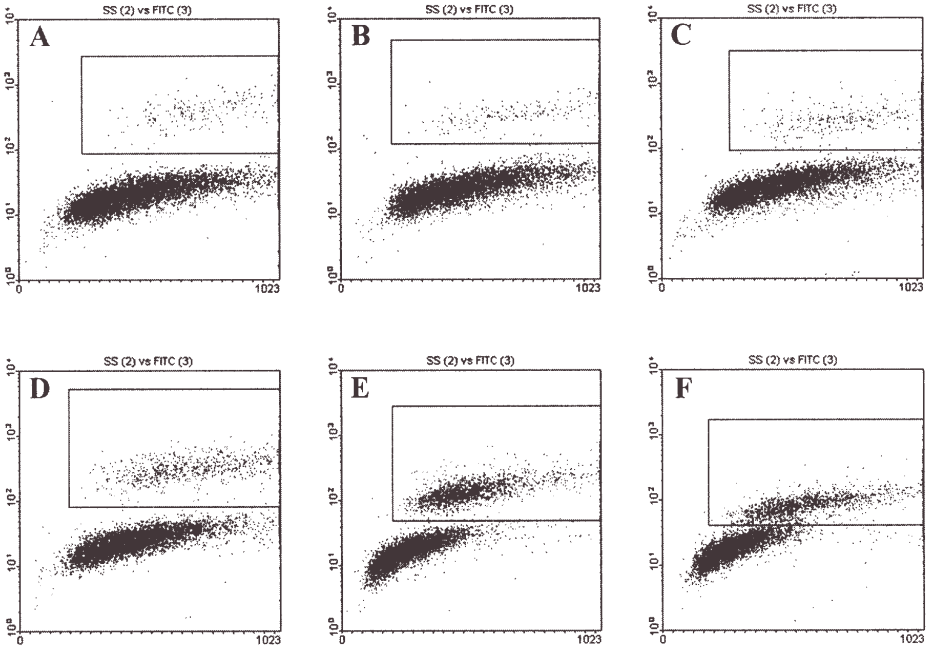

Figure 3. Representative flow cytometric analysis of CD66b expression in cell populations at day 10. X-axis, side scatter (representative of cell granularity); Y-axis, logarithm of fluorescence (representative of CD66b molecule expression). Gates denote CD66b-positive cells. Treatment of the cell populations: (A), control; (B), 13 μM CA; (C), 52 μM CA; (D), 1 μM ATRA; (E), 1 μM ATRA in combination with 13 μM CA; (F), 1 μM ATRA in combination with 52 μM CA.

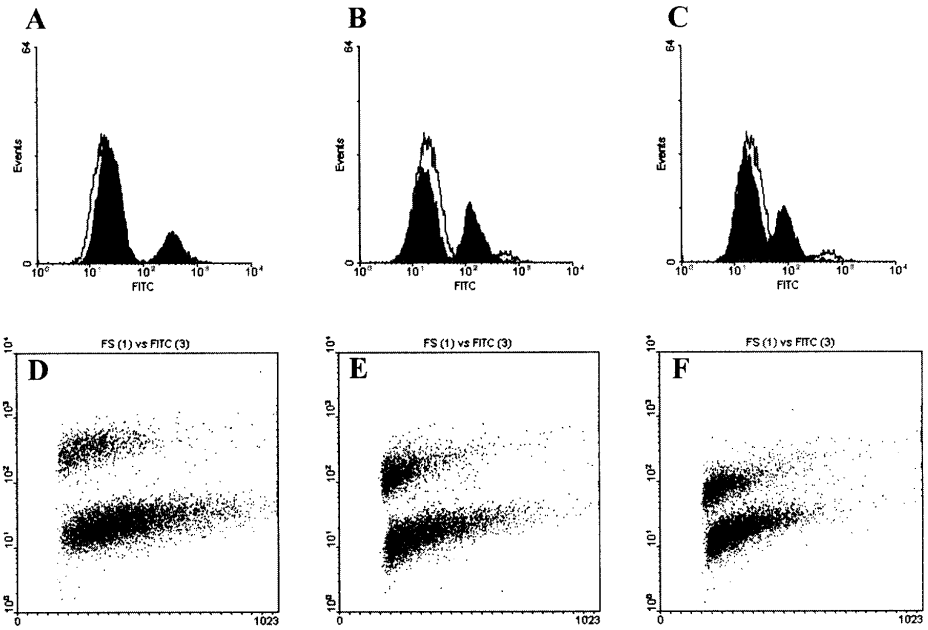

Figure 4. Representative flow cytometric analysis of CD66b expression in cell populations at day 10. Histograms show results for experimental treatment (grey) overlaid with control (colorless): X-axis, logarithm of fluorescence (representative of CD66b molecule expression); Y-axis, number of events. Dot plots: X-axis, forward scatter (representative of cell size); Y-axis, logarithm of fluorescence (representative of CD66b molecule expression). Treatment of the cell populations: (A and D), 1 μM ATRA; (B and E), 1 μM ATRA in combination with 13 μM CA; (C and F), 1 μM ATRA in combination with 52 μM CA.

Table I. Immunophenotypic analysis of CD66b expression on days 6, 8 and 10.

Conditions	Mean percentage of positive cells		
	Day 6	Day 8	Day 10
Control	1.3	2.7	7.3
13 μM CA	2.6	5.1	6.3
52 μM CA	3.0	4.4	10.0
1 μM ATRA	3.9	6.8	18.3
13 μM CA + 1 μM ATRA	10.6	11.1	33.2
52 μM CA + 1 μM ATRA	33.5	36.1	33.3

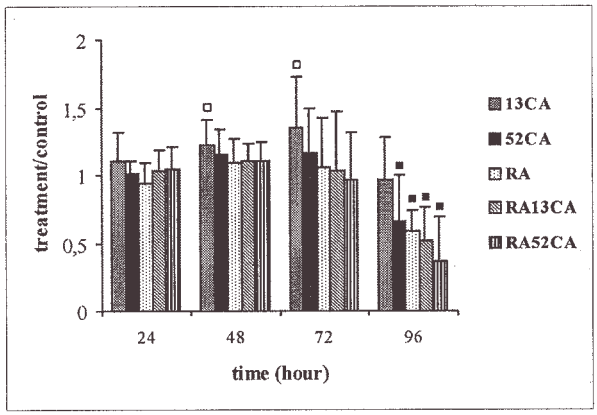

Figure 5. Proliferation activity of differentiating cell populations measured by MTT-assay. X-axis, time (days); Y-axis, relative cell number (ratio of treatment/control). Each value is the median of 3 independent experiments ± standard deviation. Data were analyzed using the two-way ANOVA and the Tukey post-hoc test. (□), significant increase in comparison with control group; (■), significant decrease in comparison with control group. $P<0.05$ was considered significant.

manifest higher granularity than a FITC-negative, undifferentiated cell population. If we compare forward scatter versus fluorescence dot plots and fluorescence histograms (Fig. 4) for cell populations treated with ATRA and CA, it is obvious that the size of CD66b-positive cells is reduced and thus the position of the positive peak is also changed. All these findings confirm the enhancement of ATRA-induced differentiation into the granulocyte stage by the combination of treatment with CA in both concentrations used.

Proliferation activity. The measurement of cell proliferation was carried out by the MTT-assay detecting mitochondrial dehydrogenase activities in live cells. Our findings (Fig. 5) show that the application of CA alone, in either 13 or 52 μM concentrations, generally does not affect the proliferation activity of cell populations in comparison with untreated cells. The 13 μM CA exhibited a moderate stimulating effect at 48 h and 72 h intervals only. The treatment with ATRA alone and its combination with CA led to a reduction of proliferation only at the 96 h interval. A similar effect was noted in the case of treatment with 52 μM CA alone over the same interval.

Discussion

All results achieved by both flow cytometry and NBT-assays confirmed our initial hypothesis on the possible enhancing effects of CA on the ATRA-induced differentiation of HL-60

cells. The flow cytometric analysis was based on the detection of expression of the surface molecule CD66b, which is known as the specific marker of maturation and activation of granulocytes (10). This measurement proved that the proportion of terminally differentiated granulocytes in the cell population was markedly increased if the cells had been treated with ATRA and CA in combination, as compared to those treated with ATRA alone. The treatment with CA increased the CD66b expression only moderately. The use of NBT-assay for the detection of functionally mature granulocytes confirmed the results of flow cytometry. On cultivation days 8 and 10, we detected a tendency of the combination treatment with ATRA and CA to increase the number of activated granulocytes. Moreover, a dose-dependent relationship in cells treated with the combination of ATRA and 13 μM or 52 μM CA was observed by means of both methods.

The possibility to modulate the course of differentiation in HL-60 cells by combining various agents with ATRA was demonstrated in several recent studies. The application of ATRA with the transforming growth factor ß$_2$ led to the higher ability of cells to reduce NBT, although they did not express the CD66b marker. The combined treatment with ATRA and 1,25(OH)$_2$D$_3$ increased both the number of CD66b-positive and NBT-reducing cells in comparison with the cell populations treated with ATRA only (10). Similarly, a positive co-action of bile acids (sodium deoxycholate and sodium chenodeoxycholate) and ATRA was demonstrated by the NBT-assay (14).

It was also clearly shown in the HL-60 cells that the course of induced differentiation could be modulated by the regulation of arachidonic acid metabolism resulting from the inhibition of cyclooxygenases, lipoxygenases or P-450 monooxygenase system (23). In comparison to the application of ATRA alone, MK-886, a 5-lipoxygenase-activating protein inhibitor, significantly increased the frequency of CD11b-positive cells when applied together with ATRA (15). The inhibition of cytochrome P-450 by proadifen also stimulated the ATRA-induced differentiation of HL-60 cells. The course of their differentiation was monitored through the expression of CD11b and NBT positivity (16). A similar effect was demonstrated as a result of the combined application of some NSAIDs, namely indomethacin, and curcumin, with ATRA or 1,25(OH)$_2$D$_3$. Their anti-inflammatory effect is attributed to the inhibition of cyclooxygenase and lipoxygenase activities (12,13,24,25). The same effect was observed, when yomogin, an eudesmane sesquiterpene lactone with anti-inflammatory activity, was applied in combination with ATRA or 1,25 (OH)$_2$D$_3$ (26). Since CA is known as an inhibitor of 5-lipoxygenase (20,21) as well, we can suppose that its enhancing effect on ATRA-induced differentiation observed in our experiments, is caused by the modulation of arachidonic acid pathway of metabolism.

When the cell proliferation activity was measured, a marked growth inhibition was detected in the ATRA and/or CA treated cell populations after 96 h of cultivation. The same inhibitory effect of CA alone or in combination with DMSO was demonstrated in HL-60 cells (21). Similar inhibition of the cell proliferation with the same time course was also detected in HL-60 cells treated with curcumin in combination with ATRA or 1,25(OH)$_2$D$_3$ (25). Caffeic acid phenethyl ester (CAPE) exhibited stronger anti-proliferative effects on HL-60 cells, when compared with CA in our experiments (27-29). This effect of CAPE is ascribed to the fact that CAPE is a more lipophilic compound than CA and enters the HL-60 cells very quickly (12,28). Despite the fact that lipoxygenase inhibitors can induce apoptosis in some systems and inhibit it in others (30), some published data on the HL-60 cell line support the hypothesis on the inhibition of cell proliferation via apoptosis induction by lipoxygenase inhibitors (31), as well as by other inhibitors of arachidonic acid metabolism (32).

The ability of CA to promote the ATRA-induced differentiation of HL-60 cells, which was clearly demonstrated in our experiments, extends the array of its biological effects. CA is a plant phenolic compound from the hydroxycinnamate group. Such compounds are produced as secondary metabolites of the shikimate pathway in a large number of higher plant species (17). CA and its esters are widely distributed in tissues of many plants and their fruit e.g. coffee beans, blueberries and apples (33). In the case of the dietary intake of CA esters, esterases of gut microflora then release CA, free CA can pass through the gut wall and has been found in serum and urine in humans (34,35).

Generally, recent anti-neoplastic strategies include the induced differentiation of tumor cells, among others. Novel compounds that may increase the sensitivity of leukemic cells to ATRA could be useful for a future anti-leukemic differentiation therapy (36). For example, arsenic trioxide applied in combination therapy improved outcomes in patients with APL relapse (9). It was also documented that a normal hematopoiesis was restored in a patient with APL resistant to the combined ATRA and arsenic trioxide therapy. This was achieved via cAMP-triggered enhancement of differentiation during a theophylline treatment (37). Thus, our reported additive effect of the plant phenolic compound, caffeic acid, on differentiation of HL-60 myeloid leukemic cells may offer another alternative in the treatment of APL through the use of differentiation therapy.

Acknowledgements

This work was supported by grant no. 620/2002 FRVS. The authors thank Mrs. Johana Maresova for her skillful technical assistance and Dr Marcela Vlkova (Department of Clinical Immunology and Allergology, University Hospital St. Anna, Brno, Czech Republic) for providing flow cytometry facilities.

References

1. Gottgens B and Green AR: Retinoic acid and the differentiation of lymphohaemopoietic stem cells. Bioessays 17: 187-189, 1995.
2. Wohl CA and Weiss S: Retinoic acid enhances neuronal proliferation and astroglial differentiation in cultures of CNS stem cell-derived precursors. J Neurobiol 37: 281-290, 1998.
3. Rohwedel J, Guan K and Wobus AM: Induction of cellular differentiation by retinoic acid *in vitro*. Cells Tissues Organs 165: 190-202, 1999.
4. Guan K, Chang H, Rolletschek A and Wobus AM: Embryonic stem cell-derived neurogenesis. Retinoic acid induction and lineage selection of neuronal cells. Cell Tissue Res 305: 171-176, 2001.
5. Lotan R: Suppression of squamous cell carcinoma growth and differentiation by retinoids. Cancer Res 54: 1987s-1990s, 1994.
6. Warrell RP, de The H, Wang ZY and Degos L: Acute promyelocytic leukemia. N Engl J Med 329: 177-189, 1993.

7. Lin RJ, Egan DA and Evans RM: Molecular genetics of acute promyelocytic leukemia. Trends Genet 15: 179-184, 1999.
8. Chomienne C, Fenaux P and Degos L: Retinoid differentiation therapy in promyelocytic leukemia. FASEB J 10: 1025-1030, 1996.
9. Douer D: Advances in the treatment of relapsed acute promyelocytic leukemia. Acta Haematol 107: 1-17, 2002.
10. Verlinden L, Verstuyf A, Mathieu C, Tan BK and Bouillon R: Differentiation induction of HL60 cells by $1,25(OH)_2D_3$, all trans retinoic acid, rTGF-$ß_2$ and their combinations. J Steroid Biochem Mol Biol 60: 87-97, 1997.
11. James SY, Williams MA, Newland AC and Colston KW: Leukemia cell differentiation: cellular and molecular interactions of retinoids and vitamin D. Gen Pharmacol 32: 143-154, 1999.
12. Sokoloski JA, Shyam K and Sartorelli AC: Induction of the differentiation of HL-60 promyelocytic leukemia cells by curcumin in combination with low levels of vitamin D_3. Oncol Res 9: 31-39, 1997.
13. Sokoloski JA and Sartorelli AC: Induction of the differentiation of HL-60 promyelocytic leukemia cells by nonsteroidal anti-inflammatory agents in combination with low levels of vitamin D_3. Leuk Res 22: 153-161, 1998.
14. Zimber A, Chedeville A, Abita JP, Barbu V and Gespach C: Functional interactions between bile acids, all-*trans* retinoic acid, and 1,25-dihydroxy-vitamin D_3 on monocytic differentiation and myeloblastin gene down-regulation in HL-60 and THP-1 human leukemia cells. Cancer Res 60: 672-678, 2000.
15. Hofmanová J, Kozubík A, Dusek L and Pacherník J: Inhibitors of lipoxygenase metabolism exert synergistic effects with retinoic acid on differentiation of human leukemia HL-60 cells. Eur J Pharmacol 350: 273-284, 1998.
16. Hofmanová J, Soucek K, Dusek L, Netíková J and Kozubík A: Inhibition of cytochrome P-450 modulates all-trans-retinoic acid-induced differentiation and apoptosis of HL-60 cells. Cancer Detect Prev 24: 325-342, 2000.
17. Rice-Evans CA, Miller NJ and Paganga G: Structure-antioxidant activity relationships of flavonoids and phenolic acids. Free Radic Biol Med 20: 933-956, 1996.
18. Nardini M, Natella F, Gentili V, Di Felice M and Scaccini C: Effect of caffeic acid dietary supplementation on the antioxidant defense system in rat: An *in vivo* study. Arch Biochem Biophys 342: 157-160, 1997.
19. Vieira O, Escargueil-Blanc I, Meilhac O, Basile J-P, Laranjinha J, Almeida L, Salvayre R and Negre-Salvayre A: Effect of dietary phenolic compounds on apoptosis of human cultured endothelial cells induced by oxidized LDL. Br J Pharmacol 123: 565-573, 1998.
20. Koshihara Y, Neichi T, Murota S, Lao A, Fujimoto Y and Tatsuno T: Caffeic acid is a selective inhibitor for leukotriene biosynthesis. Biochim Biophys Acta 792: 92-97, 1984.
21. Miller AM, Kobb SM and McTiernan R: Regulation of HL-60 differentiation by lipoxygenase pathway metabolites *in vitro*. Cancer Res 50: 7257-7260, 1990.
22. Nardini M, Scaccini C, Packer L and Virgili F: *In vitro* inhibition of the activity of phosphorylase kinase, protein kinase C and protein kinase A by caffeic acid and a procyanidin-rich pine bark (*Pinus marittima*) extract. Biochim Biophys Acta 1474: 219-225, 2000.
23. Kozubík A, Hofmanová J, Dusek L and Musilová E: 5-Lipoxygenase inhibitors potentiate effects of TGF-$ß_1$ on the differentiation of human leukemia HL-60 cells. J Leukoc Biol 62: 240-248, 1997.
24. Bunce CM, Mountford JC, French PJ, Mole DJ, Durham J, Michell RH and Brown G: Potentiation of myeloid differentiation by anti-inflammatory agents, by steroids and by retinoic acid involves a single intracellular target probably an enzyme of the aldoketoreductase family. Biochem Biophys Acta 1311: 189-198, 1996.
25. Liu Y, Chang RL, Cui XX, Newmark HL and Conney AH: Synergistic effects of curcumin on all-*trans* retinoic acid- and 1α,25-dihydroxyvitamin D_3-induced differentiation in human promyelocytic leukemia HL-60 cells. Oncol Res 9: 19-29, 1997.
26. Kim SH and Kim TS: Synergistic induction of 1,25-dihydroxyvitamin D(3)- and all-*trans* retinoic acid-induced differentiation of HL-60 leukemia cells by yomogin, a sesquiterpene lactone from *Artemisia princeps*. Planta Med 68: 886-890, 2002.
27. Chen JH, Shao Y, Huang MT, Chin CK and Ho CT: Inhibitory effect of caffeic acid phenethyl ester on human leukemia HL-60 cells. Cancer Lett 108: 211-214, 1996.
28. Chen YJ, Shiao MS, Hsu ML, Tsai TH and Wang SY: Effect of caffeic acid phenethylester, an antioxidant from propolis, on inducing apoptosis in human leukemic HL-60 cells. J Agric Food Chem 49: 5615-5619, 2001.
29. Chen YJ, Shiao MS and Wang SY: The antioxidant caffeic acid phenethyl ester induces apoptosis associated with selective scavening of hydrogen peroxide in human leukemic HL-60 cells. Anticancer Drugs 12: 143-149, 2001.
30. Datta K, Biswal SS and Kehrer JP: The 5-lipoxygenase-activating protein (FLAP) inhibitor, MK886, induces apoptosis independently of FLAP. Biochem J 340: 371-375, 1999.
31. Dittman KH, Mayer C, Rodemann HP, Petrides PE and Denzlinger C: MK-886, a leukotriene biosynthesis inhibitor, induces antiproliferative effect and apoptosis in HL-60 cells. Leuk Res 22: 49-53, 1998.
32. Vondrácek J, Stika J, Soucek K, Minksová K, Bláha L, Hofmanová J and Kozubík A: Inhibitors of arachidonic acid metabolism potentiate tumour necrosis factor-α-induced apoptosis in HL-60 cells. Eur J Pharmacol 424: 1-11, 2001.
33. Clifford NC: Chlorogenic acids and other cinnamates - nature, occurrence and dietary burden. J Sci Food Agric 79: 362-372, 1999.
34. Cremin P, Kasim-Karakas S and Waterhouse AL: LC/ES-MC detection of hydroxycinnamates in human plasma and urine. J Agric Food Chem 49: 1747-1750, 2001.
35. Olthof MR, Hollman PCH and Katan MB: Chlorogenic acid and caffeic acid are absorbed in humans. J Nutr 131: 66-71, 2001.
36. Hirano T, Kizaki M, Kato K, Abe F, Masuda N and Umezawa K: Enhancement of sensitivity by bestatin of acute promyelocytic leukemia NB4 cells to all-*trans* retinoic acid. Leuk Res 26: 1097-1103, 2002.
37. Guillemin MC, Raffoux E, Vitoux D, Kogan S, Soilihi H, Lallemand-Breitenbach V, Zhu J, Janin A, Daniel MT, Gourmel B, Degos L, Dombret H, Lanotte M and De The H: *In vivo* activation of cAMP signaling induces growth arrest and differentiation in acute promyelocytic leukemia. J Exp Med 196: 1373-1380, 2002.